

申 报	系列：教师系列
	教学科研并重型
	专业：动物遗传 育种与繁殖
	职称：教授

业绩成果材料

（申报人的业绩成果材料包括论文、科研项目、获奖以及其他成果等）

单 位（二级单位） 动物科学学院

姓 名 卫恒习

材料核对人：

单位盖章：

核对时间：

华南农业大学制

目 录

一、教学研究业绩

1.教学研究项目:

- 1.1 关于教育部产学研协同育人项目“学生能力培养为目标的动物繁殖学课程改革”的立项合同及有关佐证材料.....1
- 1.2 关于广东省本科高校在线开放课程研究课题“理论与实践一体型《动物繁殖学》在线开放课程建设立项文件.....5
- 1.3 华南农业大学“《动物繁殖学》全英课程教学改革研究与实践”佐证材料.....7

2.编写教材:

- 2.1 十四五规划教材《畜牧概论》第2版.....8
- 2.2 十四五规划教材《实验动物学》.....12
- 2.3 中国科学院教材建设专家委员会规划教材《动物细胞工程》第1版.....16
- 2.4 中国科学院教材建设专家委员会规划教材《动物细胞工程》第2版.....20
- 2.5 《动物繁殖学实验教程》.....24

二、科研项目

1.主持:

- 1.1 关于国家自然科学基金青年项目“猪精液蛋白 OPN 和 CRISP1 表达差异与种公猪繁殖力的相关性及其机制研究”(A 级)的立项通知及有关佐证材料.....28
- 1.2 关于农业农村部种业重大专项 GG 项目(子课题, A 级)立项佐证材料.....37
- 1.3 关于广东省‘珠江人才计划’本土创新科研团队项目(子课题, A 级)的立项合同及有关佐证材料.....55
- 1.4 关于广东省科技计划项目“提高种公猪繁殖能力的相关技术研究集成与示范”(B 级)的立项合同及有关佐证材料.....63
- 1.5 关于广东省科技计划项目“经产母猪新型高效综合繁殖技术研究与示范”(B 级)的立项合同及有关佐证材料.....78
- 1.6 关于广东省基础与应用基础研究项目“断奶母猪 PRL/VI 分泌规律及其对卵泡血管发生的调控作用”(B 级)的立项合同及有关佐证材料.....92

1.7 关于广东省基础与应用基础研究项目“催乳素通过 circSTIP1 靶向 SGK3 调控猪卵泡颗粒细胞增殖的机制研究”（ B 级 ）的立项合同及有关佐证材料.....	102
1.8 关于广东省重点领域研发计划项目“畜禽种质资源高效安全保存与恢复技术体系创新及应用”（子课题， B 级 ）的立项合同及有关佐证材料.....	113
2.主参：	
2.1 关于国家自然科学基金面上项目“种公猪精液蛋白组高通量 iTRAQ 检测及其繁殖性能调控机制研究”（ A 级 ）的立项佐证材料.....	119
2.2 关于国家自然科学基金面上项目“IZUMO2 蛋白提高公猪繁殖性能的机理研究”（ A 级 ）的立项佐证材料.....	130
2.3 关于国家重点研发计划“经产母猪定时输精及批次化繁殖技术研发与示范”（ A 级 ）的立项佐证材料.....	141

三、论文、著作等

1.检索证明.....	147
2.以第一作者发表本专业论文情况	
2.1. Age-Specific Gene Expression Profiles of Rhesus Monkey Ovaries Detected by Microarray Analysis. BioMed research international, 2015 (2015): 625192. (SCI, IF=2.134, 生物学 3 区, B 级)	152
2.2. 猪克隆胚胎激活方法优化与转人溶菌酶基因克隆猪生产. 生物化学与生物物理进展, 2013, 40(1): 72-79. (SCI, IF=0.29)	167
3.以通讯作者发表本专业论文情况	
3.1. Investigation Into the Relationship Between Sperm Cysteine-Rich Secretory Protein 2 (CRISP2) and Sperm Fertilizing Ability and Fertility of Boars. Front Vet Sci. 2021; 8: 653413.(SCI, IF=3.471, 农林科学 2 区, A 级)	175
3.2. PF-05231023 reduces lipid deposition in apolipoprotein E-deficient mice by inhibiting the expression of lipid synthesis genes. Front Vet Sci. 2024; 11:1429639. (SCI, IF=2.9, 农林科学 2 区, A 级)	183
3.3. Semen Protein CRISP3 Promotes Reproductive Performance of Boars through	

Immunomodulation. International Journal of Molecular Sciences. 2024; 25(4):2264. (SCI, IF=4.9, 生物学 3 区, B 级)	198
3.4. Identification of new protein biomarkers associated with the boar fertility using iTRAQ-based quantitative proteomic analysis. International journal of biological macromolecules 2020; 162:50-59. (SCI, IF=6.953, 化学 2 区 TOP, A 级)	213
3.5. Cloprostenol sodium improves reproductive performance of multiparous sows during lactation. Front Vet Sci. 2024; 11:1342930. (SCI, IF=2.9, 农林科学 2 区, A 级)	223
3.6. Epigallocatechin-3-Gallate Promotes the in vitro Maturation and Embryo Development Following IVF of Porcine Oocytes. Drug Des Devel Ther. 2021; 15: 1013-1020. (SCI, IF=4.319, 医学 3 区, B 级)	237
3.7. A novel identified circ-ANKHD1 targets the miR-27a-3p/SFRP1 signaling pathway and modulates the apoptosis of granulosa cells. Environ Sci Pollut Res. 2021; 28(41):57459-57469. (SCI, IF=5.19, 环境与生态学 3 区, B 级)	245
3.8. Perfluorooctanoic acid inhibits the maturation rate of mouse oocytes cultured in vitro by triggering mitochondrial and DNA damage. Birth Defects Res. 2021; 113(14): 1074-1083. (SCI, IF=2.661, 医学 4 区, B 级)	256
3.9. 猪催乳素的真核表达与生物活性验证[J].华南农业大学学报, 2024, 45(02): 179-189. (中文核心, B 级)	266
3.10. 左旋肉碱对猪卵母细胞体外成熟、脂肪代谢和孤雌胚胎发育的影响[J]. 华 南农业大学学报, 2014, 35(6):8-12. (中文核心, B 级)	277

四、科研成果

1.科技奖励证书

1.1 公猪高效繁育关键技术创新与推广应用, 广东省农业技术推广奖二等奖 (2021-2-X12-R02)	283
1.2 种猪高效繁育关键技术创新与推广应用, 广东省农业技术推广奖二等奖 (2022-2-X08-R03)	284

2.知识产权

2.1.专利授权证书：一种鸡精液冷冻组合物、冷冻方法及去甘油方法.....	285
2.2.专利授权证书：一种选育高繁殖性能种公猪的方法.....	286
2.3.专利授权证书：一种与种公猪繁殖性能密切相关的精子蛋白标记 IZUMO2 及其应用.....	288
2.4.专利授权证书：一种与种公猪繁殖性能密切相关的精子蛋白标记 SPACA4 及其应用.....	290
2.5.专利授权证书：一次性便携式抽卵仪.....	292
2.6.专利授权证书：一种畜禽场专用的驱蚊抑菌熏香.....	294
2.7.专利授权证书：一种评定大白公猪受精能力的数学模型及其建立方法.....	296
2.8.专利授权证书：一种评定长白公猪受精能力的数学模型及其建立方法.....	297
2.9.专利授权证书：一种评定杜洛克公猪受精能力的数学模型及其建立方法....	298

五、其他业绩

1.个人荣誉

1.1.校级“教书育人先进个人”证书（2014）	299
1.2.校级“教书育人先进个人”证书（2022）	300
1.3.动科学院“优秀共产党员”（2023）	301
1.4 动科学院“优秀班主任”（2021）	302
1.5 动科学院“服务管理工作先进个人”（2021）	303

2.社会服务

2.1.中国畜牧兽医学会动物繁殖学分会理事证书.....	304
2.2.河源市农村科技特派员证书.....	305
2.3.广东省草食动物产业联盟专家委员会特聘专家证书.....	306
2.4.《华南南农业大学学报》优秀审稿人（2024）	307

教育部产学合作协同育人项目
河北深淵环境科技有限公司

立项证书

项目名称：学生能力培养为目标的动物繁殖学课程改革

项目编号：241001375132333

申报高校：华南农业大学

项目负责人：卫恒习

项目成员：张守全；李莉

该项目入选教育部产学合作协同育人项目 2024 年 7 月批次立项项目。

特发此证！



项目合作协议

甲方：河北深渊环境科技有限公司（企业名称）

联系人：马玥桐

部门：市场部

联系电话：17600870321

通信地址：河北省石家庄市长安区光华路321号

邮政编码：050000

乙方：华南农业大学（高校名称）

联系人：卫恒习

部门：动物科学学院

联系电话：15902067686

通信地址：广东省广州市天河区五山路483号

邮政编码：510642

依据教育部高等教育司发布的《教育部高等教育司关于征集2024年产学合作协同育人项目的函》，甲方申报并入选了“2024年7月产学合作协同育人项目”（以下简称“项目”）。为确保项目顺利实施，根据《教育部产学合作协同育人项目管理办法》，甲乙双方在友好协商的基础上，签署如下项目合作协议。

第一条 乙方接受甲方委托承担的项目名称为《学生能力培养为目标的动物繁殖学课程改革》的教学内容和课程体系改革项目。乙方承担的本项目研究应完成甲方项目指南要求的相关任务，具体包括：

（1）开展课程建设和教学改革工作，结题时提供课程相关配套教学资源（电子版）；

（2）校方根据企业要求，参与课程测试、平台软件设计、测试。

第2条 本项目所产生的全部作品（简称“本项目成果”，包括但不限于：项目研究总结报告、课程体系、在线课程、教学大纲、教学课件、实验方案、教学案例、软硬件作品等）的知识产权归属约定如下：知识产权归甲乙双方共同所有。

第三条 当本项目成果为合作作品时，由乙方负责联系取得其合作者的授

权。

第四条 乙方保证本项目成果的整体或者素材、软件等不侵犯第三方的合法权益。

第五条 本项目建设周期为1年。项目各阶段安排如下：

1、前期准备2024.11——2025.1

成立项目组，明确分工和职责。开展行业调研和需求分析，制定课程改革方案。修订教学大纲和教学计划，编写新教案和教学资料。

2、中期实施2025.2——2025.8

组织教师培训，提高教师的教学能力和科研水平。开展课堂教学改革，实施新的教学方法和教学模式。加强实践教学环节，组织学生参与实验、实习和科研项目。建立和完善学生综合素质评价机制，开展评价工作。

3、后期总结2025.9——2025.11

收集学生反馈和教师评价，对项目实施效果进行评估。撰写项目总结报告，总结经验教训，提出改进建议。展示项目成果和教学改革成效。

第六条 本项目成果的交付时间为：2025年11月，交付方式为：现实交付。

双方约定，按以下标准对项目成果进行验收：

1、学生的综合素质和实际应用能力显著提升。

2、教师的教学能力和科研水平得到提高。

3、《动物繁殖学》课程教学质量和效果显著提升。

4、形成一套可复制、可推广的课程改革模式和经验。

第七条 本项目经费及拨款事宜约定如下：

(1) 本项目经费总额为人民币5万元（大写：伍万元整）。

(2) 项目经费由甲方一次性（一次或分期）支付到乙方指定的账户。具体支付方式及时间：银行电汇。2025年11月前完成支付。

(3) 本项目经费由甲方支付至乙方指定的如下账户：

开户行：中国工商银行广州五山支行

户名：华南农业大学

账号：3602002609000310520

第八条 本协议自签订之日起生效。


第九条 双方应充分、认真地履行本协议。本协议履行过程中如发生争议，双方应友好协商，协商不成时任何一方可将争议提交人民法院依法裁决。

第十条 本协议一式两份，具有同等法律效力，双方各执一份据以履行。本

协议条款如需补充、更改，由双方另行签订补充协议。

甲方（盖章）：河北深溯环境科技有限公司
法定代表人/委托代理人（签字）：



乙方（盖章）：华南农业大学
法定代表人/委托代理人（签字）：



附件1

广东省本科高校在线开放课程指导委员会2022年度研究课题立项名

编号	学校名称	课题类别	课题名称	课题负责人
2022ZXKC051	华南农业大学	一般课题	基于OBE理念的《水力学》在线开放课程建设研究	韦未
2022ZXKC052	华南农业大学	一般课题	AI+在线开放课程学习支持服务创新研究	黄沛杰
2022ZXKC053	华南农业大学	一般课题	在线开放课程支持的一流课程建设创新研究-以省级一流课程《数学建	李朗
2022ZXKC054	华南农业大学	一般课题	在线开放课程驱动高校混合教学变革研究——以融合课程思政的数学	周燕
2022ZXKC055	华南农业大学	一般课题	在线开放课程驱动高校混合教学变革研究	李西明
2022ZXKC056	华南农业大学	一般课题	基于在线开放课程的农业院校课程混合教学设计研究——以《工程热	张烨
2022ZXKC057	华南农业大学	一般课题	基于金融深化改革的《投资学》在线开放课程设计创新研究	董莹
2022ZXKC058	华南农业大学	一般课题	基于OBE的《体育舞蹈》公共课在线开放课程研究	周文英
2022ZXKC059	华南农业大学	一般课题	体育在线开放课程数字化评价与质量保障的研究	姚业戴
2022ZXKC060	华南农业大学	一般课题	在线开放课程驱动高校混合教学变革研究——以《镜前造型与摄影》	米平平
2022ZXKC061	华南农业大学	一般课题	动画专业在线开放课程设计创新研究——以《视听语言》为例	王柯

2022ZXKC062	华南农业大学	重点课题	基于在线开放课程的虚拟教研创新研究——以法庭科学技术虚拟仿真	杜国明
2022ZXKC063	华南农业大学	一般课题	在线开放课程数字化评价与质量保障变革——以模拟法庭课程为例	张艳琼
2022ZXKC064	华南农业大学	一般课题	理论与实践一体型《动物繁殖学》在线开发课程建设	卫恒习
2022ZXKC065	华南农业大学	一般课题	在线开放课程驱动高校混合教学变革研究——以大学英语写作课程思	苏君
2022ZXKC066	华南农业大学	一般课题	在线开放课程驱动高校混合教学变革研究——以《新视野大学英语》	张汉娇
2022ZXKC067	华南农业大学	一般课题	基于SPOC翻转课堂的英语物流课程思政教学模式研究	梁红梅
2022ZXKC068	华南农业大学	重点课题	AI+小程序助力有害生物的普查与图	何晓芳
2022ZXKC069	华南农业大学	重点课题	《生物安全》在线开放课程推动课程思政的实践	程代凤
2022ZXKC070	华南农业大学	一般课题	人工智能技术智慧农业应用导论课程的多模态的数据融合评价教学模	韩宇星
2022ZXKC071	华南农业大学	一般课题	智能分析技术赋能在线课程学习服务研究	徐海涛

结 题 证 明

编号: JXJT20082

我校教师 孟立 主持的校级教学改革项目《《动物繁殖学》
全英课程教学改革研究与实践》(项目编号: JG18122), 经学校
组织验收, 已于2020年12月结题。
特此证明。

华南农业大学本科生院
2020年12月
教务处



高等学校“十四五”农林规划新形态教材

畜牧概论

(第2版)

主 编 蒋思文



内容提要

本教材系统地介绍了畜牧学的基本理论、基本知识和生产现状。教材共十一章，分别为绪论、动物营养与饲料、动物遗传育种与畜禽遗传资源保护利用、畜禽繁殖、畜牧场规划与环境控制、养猪生产、养牛生产、家禽生产、养羊生产、养兔生产和动物福利。本教材将理论与实际相结合，内容详实，配合数字资源内容，增加了本教材的可读性。本教材可以作为高等农业院校动物科学和农学领域相关专业教材或教学参考书，也可供广大畜牧工作者参考。

图书在版编目（CIP）数据

畜牧概论 / 蒋思文主编. --2 版. --北京：高等教育出版社，2023.2

ISBN 978-7-04-059694-6

I. ①畜… II. ①蒋… III. ①畜牧学—高等学校—教材 IV. ①S81

中国版本图书馆 CIP 数据核字（2022）第 257738 号

Xumu Gailun

策划编辑 李光跃 责任编辑 陈亦君 封面设计 杨伟露 责任印制 耿 轩

出版发行 高等教育出版社
社 址 北京市西城区德外大街4号
邮政编码 100120
印 刷 三河市吉祥印务有限公司
开 本 787mm×1092mm 1/16
印 张 21
字 数 450千字
购书热线 010-58581118
咨询电话 400-810-0598

网 址 <http://www.hep.edu.cn>
<http://www.hep.com.cn>
网上订购 <http://www.hepmall.com.cn>
<http://www.hepmall.com>
<http://www.hepmall.cn>
版 次 2006 年 1 月第 1 版
2023 年 2 月第 2 版
印 次 2023 年 2 月第 1 次印刷
定 价 39.90元

本书如有缺页、倒页、脱页等质量问题，请到所购图书销售部门联系调换
版权所有 侵权必究
物 料 号 59694-00



高等学校“十四五”农林规划新形态教材

畜牧概论

(第2版)

主 编 蒋思文(华中农业大学)

副主编 左 波(华中农业大学)

赵兴波(中国农业大学)

康相涛(河南农业大学)

张守全(华南农业大学)

编 者(按姓氏拼音排序)

陈丝宇(佛山科学技术学院)	程泽信(金陵科技学院)	郭爱珍(华中农业大学)
胡 江(甘肃农业大学)	蒋思文(华中农业大学)	康相涛(河南农业大学)
赖松家(四川农业大学)	李 聪(西北农林科技大学)	李东华(河南农业大学)
李家连(华中农业大学)	刘桂琼(华中农业大学)	娄玉杰(吉林农业大学)
罗 军(西北农林科技大学)	毛永江(扬州大学)	彭 健(华中农业大学)
沈水宝(广西大学)	卫恒习(华南农业大学)	魏宏逵(华中农业大学)
徐宁迎(浙江大学)	徐天乐(扬州大学)	尹福泉(广东海洋大学)
张 辉(吉林农业科技学院)	张金枝(浙江大学)	张守全(华南农业大学)
张依裕(贵州大学)	赵兴波(中国农业大学)	赵永聚(西南大学)
仲庆振(吉林农业大学)	左 波(华中农业大学)	

中国教育出版传媒集团
高等教育出版社·北京

绪 论	001	007 第三节 我国畜牧业可持续发展的制约因素
002 第一节 畜牧业的重要意义		
002 一、畜牧业是人类与大自然进行物质交换的重要经济产业		008 一、资源的匮乏对我国畜牧业可持续发展造成了巨大阻碍
002 二、畜牧业是改变膳食结构、提高人民生活水平必不可少的经济产业		008 二、生态环境污染与恶化是畜牧业持续发展面临的严重问题
002 三、畜牧业是吸纳农村剩余劳动力、使农牧民实现小康的重要经济产业		009 三、科学研究和技术推广不力制约了我国畜牧业的可持续发展
003 四、畜牧业促进畜产品加工业的发展		009 四、产业结构不合理,不利于我国畜牧业可持续发展
004 五、畜牧业发达水平是农业现代化程度的标志之一		009 五、畜牧业产业化进程面临困难
004 第二节 我国畜牧业发展的现状		009 六、畜产品安全成为人们关注的焦点之一
005 一、建立畜禽良种繁育体系,提高畜禽生产性能		010 第四节 我国畜牧业可持续发展的趋势和对策
006 二、建设生产基地,带动畜牧业商品生产发展		010 一、加强法制建设
006 三、开发草地资源,发展草地畜牧业		010 二、加强对公众环境保护意识的宣传和教育
006 四、建立畜禽疫病防控体系,保障畜牧业健康发展		011 三、广辟饲料资源,为畜牧业可持续发展奠定基础
006 五、建设和发展饲料工业,推动畜牧业向现代化迈进		011 四、走农牧结合的生态畜牧业发展之路
		012 五、大力推广和应用先进的科学技术
		012 六、加快调整优化畜牧业生产结构



普通高等教育“十四五”规划教材
普通高等学校动物医学类专业系列教材

实验动物学

Laboratory Animal Science

郑振宇 主编



中国农业大学出版社
China Agricultural University Press

第 12 页, 共 307 页

内 容 简 介

本书共十三章,包括绪论;实验动物遗传学及质量控制;实验动物的微生物学与寄生虫学控制;实验动物环境及设施控制;实验动物营养与饲料的质量控制;实验动物的生物学特性及饲养管理;在动物科学和动物医学研究中,实验动物的选择与应用;人类疾病的动物模型;实验动物规范化管理与技术规范;实验动物福利与伦理;动物生物安全实验室设计与管理;动物实验基本技术;动物科学和动物医学中的动物实验方法等内容,每章都有本章简介、思考题和参考文献,供读者参考。

本书内容丰富、系统性强,重点突出,资料新颖,可用作全国高等农林院校本科生和研究生的教材,也可作为实验动物和动物实验技术人员的培训教材以及实验动物科技人员和动物实验人员的实用参考书。

图书在版编目(CIP)数据

实验动物学 / 郑振宇主编. --北京:中国农业大学出版社,2025.2

ISBN 978-7-5655-2933-7

I. ①实… II. ①郑… III. ①实验动物学—高等学校—教材 IV. ①Q95-33

中国国家版本馆 CIP 数据核字(2023)第 009804 号

书 名 实验动物学

Shiyan Dongwuxue

作 者 郑振宇 主编

策划编辑 张 程

责任编辑 石 华 张 程

封面设计 郑 川 李尘工作室

出版发行 中国农业大学出版社

社 址 北京市海淀区圆明园西路2号

邮政编码 100193

电 话 发行部 010-62733489,1190

读者服务部 010-62732336

编辑部 010-62732617,2618

出 版 部 010-62733440

网 址 <http://www.caupress.cn>

E-mail cbsszs@cau.edu.cn

经 销 新华书店

印 刷 天津鑫丰华印务有限公司

版 次 2025年2月第1版 2025年2月第1次印刷

规 格 185 mm×260 mm 16开本 26.25印张 654千字

定 价 79.00元

图书如有质量问题本社发行部负责调换

编 审 人 员

主 编 郑振宇(河南农业大学)

副主编 陈正礼(四川农业大学)

熊家军(华中农业大学)

赵生国(甘肃农业大学)

蒋钦杨(广西大学)

参 编 徐纯柱(东北农业大学)

卫恒习(华南农业大学)

高 明(河北农业大学)

万学瑞(甘肃农业大学)

李 桢(青岛农业大学)

罗启慧(四川农业大学)

林 峰(河南农业大学)

姚 红(河南农业大学)

吴力专(长江大学)

主 审 曲连东(中国农业科学院哈尔滨兽医研究所)

目 录

第一章 绪论	1
第一节 实验动物科学	2
第二节 实验动物科学发展简史	4
第三节 实验动物在畜牧兽医科学研究中的应用现状	9
第四节 实验动物在人类社会中的地位 and 作用	14
第五节 实验动物科学发展趋势	16
第六节 我国实验动物科学的发展目标	18
第七节 发展实验动物科学的主要措施	19
第八节 优秀实验动物站点集锦	20
思考题	23
参考文献	23
第二章 实验动物遗传学及质量控制	25
第一节 实验动物遗传学发展历史	25
第二节 实验动物遗传学分类	27
第三节 近交系动物	28
第四节 封闭群动物	34
第五节 杂交一代动物	37
第六节 实验动物的命名	40
第七节 实验动物遗传监测(质量控制)	43
思考题	46
参考文献	47
第三章 实验动物的微生物学与寄生虫学控制	48
第一节 实验动物的微生物学与寄生虫学等级	48
第二节 普通动物	49
第三节 无特定病原体动物	50
第四节 无菌动物	51
第五节 悉生动物	55
第六节 实验动物微生物学与寄生虫学质量监测	56
思考题	64
参考文献	64



中国科学院教材建设专家委员会规划教材
科学出版社“十二五”规划教材

动物细胞工程

邓 宁 主编



内 容 简 介

本教材是生物技术专业综合素质培养型系列教材之一,涵盖了动物细胞工程的基础知识、基本技术和最新的研究成果。主要内容包括细胞培养、细胞融合、干细胞、基因打靶、胚胎工程、体外受精、细胞核移植和动物克隆等,既有全面的基本理论,又有实用技术。全书共分 11 章,分别为动物细胞工程概论、动物细胞工程基础、动物细胞培养、动物细胞融合、单克隆抗体、干细胞、基因打靶与转基因动物、动物生殖细胞工程、动物胚胎工程、动物染色体工程和鱼类细胞工程。

本书适合作为生命科学、动物科学和海洋科学相关专业的本科、研究生教材和教师参考书。

图书在版编目(CIP)数据

动物细胞工程 / 邓宁主编. —北京:科学出版社,2014. 1

中国科学院教材建设专家委员会规划教材·科学出版社“十二五”规划教材

ISBN 978-7-03-039555-9

I. 动… II. 邓… III. 动物-细胞工程-高等学校-教材 IV. Q952

中国版本图书馆 CIP 数据核字(2014)第 010028 号

责任编辑:李 植 周万源 / 责任校对:张凤琴

责任印制:肖 兴 / 封面设计:范璧合

版权所有,违者必究。未经本社许可,数字图书馆不得使用

科学出版社 出版

北京东黄城根北街 16 号

邮政编码:100717

<http://www.sciencep.com>

骏杰印刷厂 印刷

科学出版社发行 各地新华书店经销

*

2014 年 1 月第 一 版 开本:787×1092 1/16

2014 年 1 月第一次印刷 印张:19 1/2 插页:8

字数:478 000

定价:69.80 元

(如有印装质量问题,我社负责调换)

中国科学院教材建设专家委员会规划教材
科学出版社“十二五”规划教材

动物细胞工程

主 编	邓 宁			
副主编	周 燕	张守全		
编 者	(按姓氏笔画排序)			
	于苗苗	中国海洋大学	陈建华	福建师范大学
	卫恒习	华南农业大学	周 燕	华东理工大学
	王 宏	暨南大学	周世力	江汉大学
	王敏强	烟台大学	赵会敏	广西大学
	邓 宁	暨南大学	唐 勇	暨南大学
	史光华	中国合格评定国家认可中心	唐业刚	武汉生物工程学院
	朱 宏	哈尔滨师范大学	黄金林	扬州大学
	李佳楠	江汉大学	谢 浩	武汉理工大学
	李树锋	东北农业大学	樊廷俊	中国海洋大学
	李登峰	宁波大学	魏 强	西北农林科技大学
	杨志杰	甘肃农业大学	张守全	华南农业大学

(国务院侨务办公室立项)
(彭磷基外招生人才培养改革基金资助)

科 学 出 版 社

北 京

目 录

第一章 动物细胞工程概论	(1)	第六章 干细胞	(140)
第一节 动物细胞工程的研究内容	(1)	第一节 胚胎干细胞	(140)
第二节 动物细胞工程在现代生物技术中的地位 and 作用	(7)	第二节 成体干细胞	(151)
第三节 动物细胞工程的发展历程	(8)	第三节 诱导多能干细胞	(161)
第四节 动物细胞工程的应用与展望	(15)	第四节 组织工程	(164)
第二章 动物细胞工程基础	(19)	第七章 基因打靶与转基因动物 ...	(168)
第一节 动物细胞的结构与功能 ...	(19)	第一节 基因打靶	(168)
第二节 生殖细胞与早期胚胎发育	(24)	第二节 转基因动物的制备	(178)
第三节 动物细胞工程基本研究方法	(32)	第三节 基因打靶技术与转基因动物的应用	(185)
第三章 动物细胞培养	(43)	第八章 动物生殖细胞工程	(190)
第一节 动物细胞体外培养及影响因素	(44)	第一节 精子和卵子的获取	(190)
第二节 动物细胞培养技术	(65)	第二节 X、Y 精子的分离	(197)
第三节 动物细胞培养工程及生物反应器	(84)	第三节 体外受精	(200)
第四章 动物细胞融合	(105)	第四节 显微受精	(215)
第一节 细胞融合的生物学基础与分子机制	(105)	第五节 精子和卵子的冷冻保存	(219)
第二节 动物细胞融合技术	(107)	第九章 动物胚胎工程	(224)
第三节 动物细胞融合技术的应用	(113)	第一节 胚胎移植	(224)
第五章 单克隆抗体	(118)	第二节 胚胎分割	(242)
第一节 单克隆抗体制备基本原理	(119)	第三节 嵌合体动物	(248)
第二节 单克隆抗体制备的基本流程	(120)	第四节 早期胚胎的分子检测 ...	(252)
第三节 新型单克隆抗体技术 ...	(130)	第五节 细胞核移植	(259)
第四节 单克隆抗体的应用	(136)	第十章 动物染色体工程	(268)
参考文献	(305)	第一节 动物多倍染色体技术 ...	(268)
中英文词汇对照	(311)	第二节 雌、雄核发育技术	(272)
		第三节 动物染色体结构的改造	(275)
		第四节 染色体转移技术	(276)
		第五节 人工染色体及应用	(278)
		第十一章 鱼类细胞工程	(284)
		第一节 鱼类细胞培养	(284)
		第二节 鱼类繁殖与育种	(292)
		第三节 转基因鱼	(298)

彩图



中国科学院教材建设专家委员会规划教材
高等院校教材

动物细胞工程

第2版

◎ 主编 邓 宁



科学出版社

第 20 页, 共 307 页

内 容 简 介

《动物细胞工程》(第2版)是一本图文并茂的教材,全书共十一章,内容新颖、丰富,既包含动物细胞工程的基础知识、基本技术,又介绍了一些最新的研究成果。主要包括:动物细胞培养、动物细胞融合、单克隆抗体、干细胞、基因打靶、转基因动物、动物染色体工程、动物生殖细胞工程、动物胚胎工程、细胞核移植与动物克隆等。

本教材以动物细胞工程技术的原理、技术操作及应用为主线,融入最新的科研成果,并对第1版进行了全面的修订,新增了第十一章细胞核移植与动物克隆。其他章节内容也进行了修订、补充和调整。本教材对基本概念、基础知识尽量删繁就简,并审慎引用发展前沿和最新的研究成果,以保持教材内容的准确性,相关知识的科学性和前瞻性。

本教材适合于综合性大学、农业院校、师范院校的生物技术、生物科学、生物工程、动物学、兽医学等相关专业的本科生、研究生使用,也可供相关科研工作者参考。

图书在版编目(CIP)数据

动物细胞工程 / 邓宁主编. — 2版. — 北京:科学出版社, 2021.2
中国科学院教材建设专家委员会规划教材·高等院校教材
ISBN 978-7-03-067841-6

I. ①动… II. ①邓… III. ①动物-细胞工程-高等学校-教材 IV. ①Q952

中国版本图书馆 CIP 数据核字(2020)第 265706 号

责任编辑:张天佐 / 责任校对:贾娜娜
责任印制:赵 博 / 封面设计:陈 敬

科学出版社出版

北京东黄城根北街16号

邮政编码:100717

<http://www.sciencep.com>

天津文林印刷有限公司 印刷

科学出版社发行 各地新华书店经销

*

2014年1月第 一 版 开本:787×1092 1/16

2021年2月第 二 版 印张:20 1/4

2021年2月第五次印刷 字数:483 000

定价:88.00 元

(如有印装质量问题,我社负责调换)

中国科学院教材建设专家委员会规划教材
高等院校教材

动物细胞工程

第2版

主 编 邓 宁

副主编 周 燕 张守全 唐 勇

编 委 (以姓名笔画为序)

卫恒习 (华南农业大学)

王敏强 (烟台大学)

朱 宏 (哈尔滨师范大学)

李佳楠 (江汉大学)

杨志杰 (甘肃农业大学)

张守全 (华南农业大学)

周 燕 (华东理工大学)

赵会敏 (广西大学)

唐 勇 (暨南大学)

黄金林 (扬州大学)

魏 强 (西北农林科技大学)

王 宏 (暨南大学)

邓 宁 (暨南大学)

李世杰 (东北农业大学)

李树峰 (东北农业大学)

宋其芳 (暨南大学)

陈建华 (福建师范大学)

周世力 (江汉大学)

赵建夫 (暨南大学)

唐业刚 (武汉生物工程学院)

谢 浩 (武汉理工大学)

科 学 出 版 社

北 京

目 录

第一章 动物细胞工程概论	1
第一节 动物细胞工程的研究内容	2
第二节 动物细胞工程的地位和作用	8
第三节 动物细胞工程的发展历程	9
第四节 动物细胞工程的应用与展望	16
第二章 动物细胞工程基础	20
第一节 动物细胞的结构与功能	20
第二节 生殖细胞的发生与受精	26
第三节 动物细胞工程基本研究方法	32
第三章 动物细胞培养	44
第一节 动物细胞体外培养及影响因素	45
第二节 动物细胞培养技术	65
第三节 动物细胞培养工程及生物反应器	80
第四节 动物细胞培养技术的应用	100
第四章 动物细胞融合	104
第一节 细胞融合的生物学基础与分子机制	104
第二节 动物细胞融合技术	107
第三节 动物细胞融合技术的应用	113
第五章 单克隆抗体	118
第一节 单克隆抗体制备基本原理	119
第二节 单克隆抗体制备的基本流程	120
第三节 人源单克隆抗体技术	129
第四节 单克隆抗体技术的应用	137
第六章 干细胞	147
第一节 胚胎干细胞	147
第二节 成体干细胞	160
第三节 诱导多能干细胞	171
第四节 组织工程	175
第七章 基因打靶与转基因动物	180
第一节 基因打靶	180
第二节 转基因动物的制备	193
第三节 基因打靶技术与转基因动物的应用	199

DONGWU FANZHIXUE
SHIYAN JIAOCHENG

动物繁殖学 实验教程

陆阳清 许惠艳◎主编



首批全国优秀出版社



中国农业出版社

图书在版编目 (CIP) 数据

动物繁殖学实验教程 / 陆阳清, 许惠艳主编. —北京: 中国农业出版社, 2024. 2
ISBN 978-7-109-31512-9

I. ①动… II. ①陆… ②许… III. ①动物—繁殖—实验—教材 IV. ①S814-33

中国国家版本馆 CIP 数据核字 (2023) 第 240003 号

中国农业出版社出版

地址: 北京市朝阳区麦子店街 18 号楼

邮编: 100125

责任编辑: 何 微 文字编辑: 耿韶磊

版式设计: 王 晨 责任校对: 吴丽婷

印刷: 北京通州皇家印刷厂

版次: 2024 年 2 月第 1 版

印次: 2024 年 2 月北京第 1 次印刷

发行: 新华书店北京发行所

开本: 787mm×1092mm 1/16

印张: 10.5

字数: 255 千字

定价: 28.00 元

版权所有·侵权必究

凡购买本社图书, 如有印装质量问题, 我社负责调换。

服务电话: 010-59195115 010-59194918

《动物繁殖学实验教程》

编 审 人 员

- 主 编 陆阳清（广西大学）
许惠艳（广西大学）
副主编 李俊杰（河北农业大学）
黄 贺（东北农业大学）
参 编 陈 祥（贵州大学）
卫恒习（华南农业大学）
杜 明（内蒙古农业大学）
刘 梅（湖南农业大学）
莫显红（赤峰学院）
郑 鹏（东北农业大学）
任子利（西藏农牧学院）
赵彦玲（西藏农牧学院）
审 稿 卢克焕（广西大学）

前言

第一篇 基础实验

1

实验一 雌、雄动物生殖器官解剖构造的观察	2
一、生殖器官的相关介绍	2
二、实验主体	3
三、作业	13
四、实验技术应用及研究案例	13
五、参考文献	13
实验二 睾丸、卵巢组织学切片观察	15
一、组织学技术的相关介绍	15
二、实验主体	16
三、作业	19
四、实验技术应用及研究案例	19
五、参考文献	19
实验三 生殖激素效价的生物测定	21
一、生殖激素生物学检测的相关介绍	21
二、实验主体	22
三、作业	24
四、实验技术应用及研究案例	25
五、参考文献	25
实验四 精液品质的感官检查及精子活力、密度与畸形率的测定	27
一、种畜精液研究的相关介绍	27
二、实验主体	28
三、作业	31
四、实验技术应用及研究案例	32
五、参考文献	32
实验五 猪精液的稀释及液态精液保存	33
一、精液稀释及保存的相关介绍	33
二、实验主体	34



项目批准号	31402072
申请代码	C170104
归口管理部门	
依托单位代码	51064208A0499-0932



3 1402072 1006716

国家自然科学基金委员会 资助项目计划书

资助类别：青年科学基金项目

亚类说明：

附注说明：

项目名称：猪精液蛋白OPN和CRISP1表达差异与种公猪繁殖力的相关性及其机制研究

资助经费：24万元 执行年限：2015.01-2017.12

负责人：卫恒习

通讯地址：广州市天河区五山路483号华南农业大学动物科学学院

邮政编码：510642 电 话：020-85284869

电子邮件：weihengxi@163.com

依托单位：华南农业大学

联系人：苏弟华 电 话：020-85280070

填表日期：2014年08月25日

国家自然科学基金委员会制

第 28 页，共 307 页

Version: 1.006.716



国家自然科学基金委员会资助项目计划书填报说明

- 一、项目负责人收到《关于国家自然科学基金资助项目批准及有关事项的通知》（以下简称《批准通知》）后，请认真阅读本填报说明和自然科学基金相关项目及财务管理办法（查阅<http://www.nsfc.gov.cn/>），按《批准通知》的要求认真填写《国家自然科学基金委员会资助项目计划书》（以下简称《计划书》）。
- 二、填写《计划书》时要求科学严谨、实事求是、表述清晰、准确。《计划书》经主管科学部审核批准后，将作为项目研究计划执行和检查、验收的依据。
- 三、《计划书》简表部分自动生成，其他部分按以下要求填写：
 - （一）各类获资助项目都必须填写中、英文摘要及主题词，按批准经费填报经费预算表。
 - （二）正文撰写：
 1. 对于面上项目、青年科学基金项目、地区科学基金项目，如果《批准通知》中没有修改要求的，只需选择“研究内容和研究目标按照申请书执行”即可；如果《批准通知》中明确要求调整研究内容的，须选择“根据研究方案修改意见更改”并填报相关修改内容。
 2. 对于重点项目、重大项目、科学仪器基础研究专款项目及国家重大科研仪器设备研制专项（自由申请）项目，须选择“根据研究方案修改意见更改”，根据《批准通知》的要求填报研究内容，不得自行降低、更改研究目标（或仪器研制指标）或缩减关键的研究内容。此外，还要突出以下几点：
 - 1) 研究的难点和在实施过程中可能碰到的问题（或仪器研制风险），拟采用的研究方案和技术路线；
 - 2) 项目主要参与者分工，并请说明课题及合作单位之间的关系与分工。
 3. 对于国家杰出青年科学基金、优秀青年科学基金和海外及港澳学者合作研究基金项目，须选择“根据研究方案修改意见更改”，按下列提纲撰写：
 - 1) 研究方向；
 - 2) 结合国内外研究现状，说明研究工作的学术思想和科学意义（限两个页面）；
 - 3) 研究内容、研究方案及预期目标（限两个页面）；
 - 4) 分年度进度安排；
 - 5) 研究队伍的组成情况。
 4. 对于其他类型项目，参照面上项目填报。



简表

申请者信息	姓 名	卫恒习	性 别	男	出生年月	1980年02月	民 族	汉族
	学 位	博士			职称	副研究员		
	电 话	020-85284869		电子邮件		weihengxi@163.com		
	传 真			个人网页				
	工 作 单 位	华南农业大学						
	所 在 院 系 所							
依托单位信息	名 称	华南农业大学					代码	51064208A0499
	联 系 人	苏弟华		电子邮件		kyc.jhk@scau.edu.cn		
	电 话	020-85280070		网站地址		http://web.scau.edu.cn/kjc/		
合作单位信息	单 位 名 称							代 码
项目基本信息	项 目 名 称	猪精液蛋白OPN和CRISP1表达差异与种公猪繁殖力的相关性及其机制研究						
	资 助 类 别	青年科学基金项目				亚 类 说 明		
	附 注 说 明							
	申 请 代 码	C170104: 畜禽繁殖学						
	基 地 类 别							
	执 行 年 限	2015.01-2017.12						
	资 助 经 费	24.0000万元						



项目摘要

中文摘要(500字以内):

提高种公猪繁殖性能是畜牧科学研究的焦点之一,精子受精能力是体现公畜繁殖性能的重要指标,并与精液蛋白的作用密切相关。猪精液蛋白与精子受精能力和公猪繁殖性能的关系与作用机制亟待阐释。本项目拟利用统计学方法从大群体公猪中筛选出常规精液指标合格、但繁殖性能存在差异的两个群体(高繁组和低繁组)为主要研究对象;通过双向电泳、免疫印记、ELISA等技术对两组公猪精液中的蛋白(如OPN、CRISP1等)进行分析和定量,再联合公猪繁殖成绩建立相关精液蛋白与繁殖性能的相关性模型;然后通过检测目标蛋白在公猪生殖器官、精清和精子的表达分布,并利用体外受精、人工授精等技术研究目标蛋白在受精过程中的作用,探索并阐释目标蛋白对精子受精能力的影响及作用机制。本项目研究可为准确评定精液受精能力提供蛋白标记、提高人工授精和种公猪繁殖效率;还可作为种公猪育种提供重要参考依据;同时也可为人类生殖不孕不育的研究和治疗提供参考。

关键词: 种公猪; 繁殖能力; 精液; 骨桥蛋白OPN; CRISP1

Abstract(limited to 500 words):

The improvement of boar reproductive performance is one of the scientific focuses in animal husbandry. The sperm fertilization ability, which closely related to the roles of semen proteins, is one of the important indicators reflecting male animal reproductive ability. The relationships and mechanism between boar semen proteins and sperm fertilization ability or boar breeding performance are eagerly need to be elucidated. This project intends to use statistical methods for selecting two animal groups (high breeding and low breeding group) as the main research objects from a large boar group based on a criterion of qualified conventional semen indexes but different breeding performance. Then with two-dimensional electrophoresis, immune signatures and ELISA technologies to analyze and quantify the semen proteins (e.g., OPN, CRISP1, etc.) of the two group animals mentioned above. And then joint with boar breeding achievements, a correlation model related sperm protein and reproductive performance will be set up. On the other hand, the expression and distribution of the objective proteins were detected in boar reproductive organs, seminal plasma and sperm. And the effect of objective proteins in the process of fertilization was studied by using artificial insemination, in vitro fertilization and related technologies, so as to explore and elucidate the effect and mechanism of objective protein actions with the sperm fertilization ability. This project can provide protein markers for accurate evaluation of semen fertilization capacity, improving the efficiency of artificial insemination and boar reproduction; also it can provide important reference basis for boar breeding; At the same time, it can also provide reference for the research and treatment of infertility in human reproduction.

Keywords: Boar; Reproductive ability; Semen; Osteopontin; CRISP1



项目组主要成员

编号	姓名	出生年月	性别	职称	学位	单位名称	电话	电子邮件	项目分工	每年工作 时间 (月)
1	卫恒习	1980.02	男	副研究员	博士	华南农业大学	020-85284869	weihengxi@163.com	项目负责人	8
2	张哲	1984.03	男	讲师	博士	华南农业大学	020-85282019	zhezhang@scau.edu.cn	精液蛋白与公猪繁殖力关联分析	8
3	刘满清	1977.09	女	实验师	硕士	华南农业大学	020-85280277	liumanqing@scau.edu.cn	猪精液蛋白检测、原位杂交	8
4	陈预明	1980.10	男	博士生	硕士	华南农业大学	020-85285897	35610623@qq.com	样品采集、目标蛋白和抗体的制备	10
5	白银山	1982.05	男	博士生	硕士	华南农业大学	020-85285897	xuefei200403@163.com	目标蛋白定位与理化性质分析	10
6	张涛	1987.02	男	硕士生	学士	华南农业大学	020-85285897	799548036@qq.com	目的蛋白及其抗体对精液品质和人工授精效果的影响	10
7	陈志林	1989.01	男	硕士生	学士	华南农业大学	020-85285897	1264786804@qq.com	目标蛋白及其抗体对精子受精能力的影响	10
8	袁梦	1989.06	女	硕士生	学士	华南农业大学	020-85285897	417754407@qq.com	目标蛋白及抗体对精子获能的影 响	10
总人数				高级	中级	初级	博士后	博士生	硕士生	硕士生
8				1	2	0	0	2		3



经费预算表

(金额单位:万元)

预算编制说明:

1. 在填报本表之前, 请根据项目资助类别认真阅读相关的资助经费管理办法; 经费预算的编制以申请书中的《经费申请表》为基础, 以《国家自然科学基金项目资助批准通知书》中的资助金额为依据;
2. 编制经费预算时, 不考虑不可预见因素和前期投入;
3. 购置与试制仪器设备在5万元以上(包括5万元)时, 须在报告正文中逐项说明用途和必要性。

科目	预算经费	备注(计算依据与说明)
一. 研究经费	19.2000	
1. 科研业务费	7.4000	
(1) 测试/计算/分析费	4.0000	项目研究所需的精液、蛋白及DNA测试分析
(2) 能源/动力费	0	
(3) 会议费/差旅费	2.4000	国内调研和学术会议等产生的会议费和差旅费
(4) 出版物/文献/信息传播事务费	1.0000	文章修改及版面费, 专利申请及文献打印费
(5) 其他	0	
2. 实验室材料费	10.3000	
(1) 原材料/试剂/药品购置费	10.3000	试验材料、试剂药品和试验耗材等的费用
(2) 其他	0	
3. 仪器设备费	1.5000	
(1) 购置	1.5000	Eppendorf移液器购置及仪器维修费
(2) 试制	0	
4. 实验室改装费	0	
5. 协作费	0	
二. 国际合作与交流费	0	
1. 出境国际旅费	0	
2. 境外合作人员来华生活费	0	
3. 来华举办学术会议费	0	
4. 其他	0	
三. 劳务费	3.6000	直接参加项目研究的研究生、博士后人员的劳务费。
四. 管理费	1.2000	项目管理费, 不得超过预算经费的5%
合 计	24.0000	
与本项目相关的其他经费来源	国家其他计划资助经费	0
	其他经费资助(含部门匹配)	0
	其他经费来源合计	0



报告正文

研究内容和研究目标按照申请书执行。



国家自然科学基金资助项目签批审核表

<p>我接受国家自然科学基金的资助，将按照申请书、项目批准意见和计划书负责实施本项目（批准号：31402072），严格遵守国家自然科学基金委员会关于资助项目管理、财务等各项规定，切实保证研究工作时间，认真开展研究工作，按时报送有关材料，及时报告重大情况变动，对资助项目发表的论著和取得的研究成果按规定进行标注。</p> <p>项目负责人（签章）： 年 月 日</p>		<p>我单位同意承担上述国家自然科学基金项目，将保证项目负责人及其研究队伍的稳定和研究项目实施所需的条件，严格遵守国家自然科学基金委员会有关资助项目管理、财务等各项规定，并督促实施。</p> <p>依托单位（公章） 年 月 日</p>					
本栏目由基金委填写	<p>科学处审查意见：</p>						
	<p>建议年度拨款计划（本栏目为自动生成，单位：万元）：</p>						
	年度	总额	第一年	第二年	第三年	第四年	第五年
	金额						
	<p>科学部审查意见：</p> <p>负责人（签章）： 年 月 日</p>						
本栏目主要用于重大项目等	<p>相关局室审核意见：</p> <p>负责人（签章）： 年 月 日</p>						
	<p>委领导审批意见：</p> <p>委领导（签章）： 年 月 日</p>						

国家自然科学基金 资助项目准予结题通知

卫恒习 同志：

您承担的国家自然科学基金项目：（猪精液蛋白OPN和CRISP1表达差异与种公猪繁殖力的相关性及其机制研究），批准号：（31402072）按有关规定已审核完毕，准予结题。

与本项目资助有关的后续成果，请您继续及时报送。

祝您在研究工作中取得更好的成绩！



子课题任务合同书

(2022 年度)

子课题名称:	快长长寿分子标记开发
所属课题编号:	NK2022110203
课题牵头单位:	四川德康农牧食品集团股份有限公司
子课题承担单位:	华南农业大学
子课题负责人:	卫恒习
执行期限:	2022 年 6 月 30 日 至 2022 年 12 月 31 日

2022 年 6 月

填写说明

- 一、子课题任务合同书甲方即课题牵头单位，乙方即子课题承担单位。
- 二、子课题任务合同书中的单位名称，请按规范全称填写，并与单位公章一致。
- 三、子课题任务合同书中文字体须用宋体小四号字填写，英文字体须用 Times New Roman 号字填写。
- 四、凡不填写内容的栏目，请用“无”表示。
- 五、乙方完成子课题任务合同书填写，提交甲方审核确认后，用 A4 纸打印、装订、签章。一式五份报项目牵头签章，项目牵头单位、课题牵头单位、课题负责人、子课题牵头单位和子课题负责人各一份。
- 六、子课题任务合同书按照内部资料要求进行填写、报送、保管，不得公开。
- 七、《项目申报书》是本任务合同书填报的重要依据，任务合同书填报不得降低考核指标，不得自行对主要研究内容作调整。《项目申报书》和本任务合同书将共同作为课题过程管理、综合绩效评价（验收）和监督评估的重要依据。

基本信息表

所属课题		快长长寿母本新品系培育					
所属课题编号		NK2022110203					
子课题名称		快长长寿分子标记开发					
子课题承担单位	单位名称	华南农业大学					
	法定代表人	刘雅红		单位性质		事业单位	
	单位主管部门	广东省教育厅		组织机构代码		124400004554165634	
	通信地址	广东省广州市天河区五山路 483 号		邮政编码		510642	
	单位开户名称	华南农业大学					
	银行账号	3602002609000310520		开户地点		广州市天河区五山路 448 号	
	开户银行(全称)	中国工商银行广州五山支行		银行机构代码		102581000546	
	子课题管理部门负责人	倪慧群		联系方式		020-85283435	
	财务管理部门负责人	刘烨		联系方式		020-85288032	
子课题负责人	姓 名	卫恒习	性 别	男	出生日期	1980 年 02 月	
	国 籍	中国	身份证号码	130531198002062019			
	工作单位	华南农业大学		职 务	副系主任		
	最高学位	<input checked="" type="checkbox"/> 博士 <input type="checkbox"/> 硕士 <input type="checkbox"/> 学士 <input type="checkbox"/> 其他					
	职 称	<input type="checkbox"/> 正高级 <input checked="" type="checkbox"/> 副高级 <input type="checkbox"/> 中级 <input type="checkbox"/> 其他					
	电子邮箱	weihengxi@163.com		联系方式		15902067686	
经费估算		总经费 15.00 万元。其中，中央财政经费 15.00 万元，地方配套资金 0.00 万元，自筹资金 0.00 万元。					
子课题周期节点		起始时间	2022 年 6 月 30 日		结束时间	2022 年 12 月 31 日	
		实施周期	6 个月				
课题参加人数	共 2 人	高级职称 1 人，中级职称 0 人，初级职称 0 人，其他 1 人					
		博士学位 1 人，硕士学位 1 人，学士学位 0 人，其他 0 人					

一、子课题总体目标及年度考核指标

（一）总体目标（2022 年—2026 年）

1. 研制配套系新品种创新技术

创新技术	数量
快长性能精准评定技术体系	1 套
快长长寿精准表型数据库	1 个
快长长寿基因组信息数据库	1 个
申请快长长寿母本新品系培育相关国家专利	1 件以上
申请快长长寿母本新品系培育相关软件著作权	1 项
研发高效育种或良繁技术体系	1 套
挖掘并验证快长、长寿性能功能基因	5 个以上
发表项目相关科研论文	4 篇以上

（二）子课题年度考核指标（2022 年度）

1. 初步构建快长长寿新品系表型数据库 1 个。
2. 初步构建快长长寿新品系基因组信息数据库 1 个。

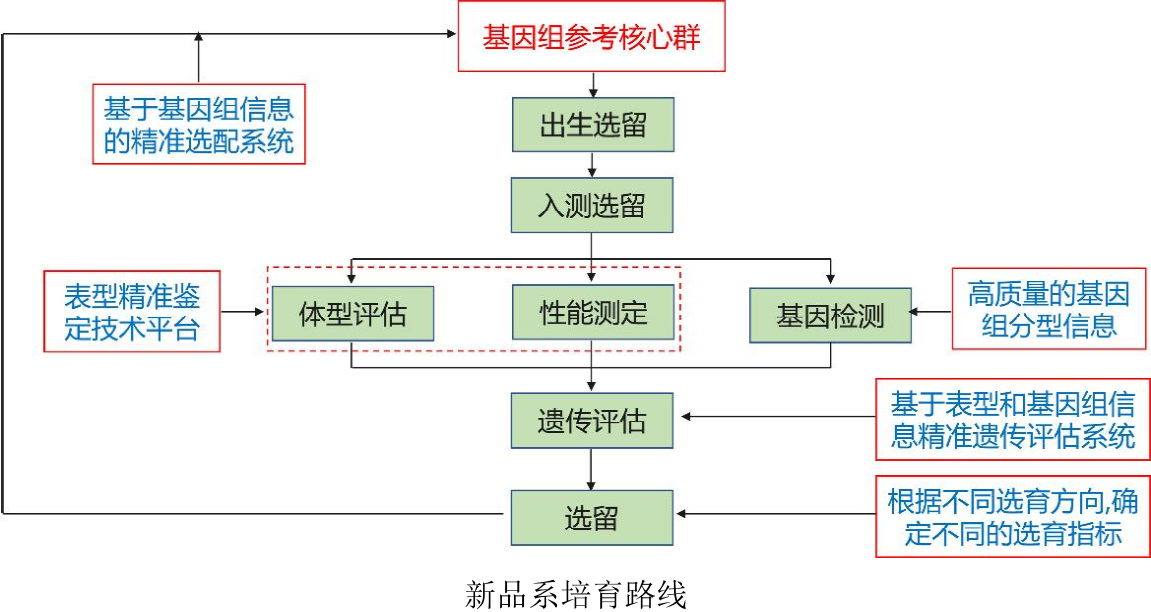
（三）子课题年度标志性成果（2022 年度）

快长长寿新品系表型数据库。

二、考核方式

考核指标	考核方式
快长长寿新品系表型数据库	科技报告

三、技术路线



四、子课题组织实施机制

（一）子课题负责人权责

1. 负责制定技术方案，并严格完成课题负责人制定的任务目标和考核指标；
2. 负责课题整体技术方案的制定及调整，做好实施进度和完成质量的全程管控，明确节点任务目标和考核指标，确保项目进度与计划匹配；
3. 负责对课题参与单位承担任务完成进度的把控与指导；
4. 负责组建课题执行专家小组，根据课题实施情况，有权对课题参与单位、经费预算等提出调整建议以及对参与人员或团队提出奖惩建议；
5. 有权查阅课题技术、财务等文档资料，查验配套经费落实情况、配套研发试验条件和生产条件支撑能力和质量；
6. 课题经费中应设置课题负责人工作经费；
7. 课题负责人所在单位应支持其开展相关工作。

（二）组织方式

1. 本子课题在主管部门的领导和指导下，由课题牵头单位统一组织实施。
2. 课题负责人负责子课题申报、实施、执行过程监督、阶段考核、项目验收等工作的组织管理，对各参与单位进行过程管理和绩效考核，确保各项研究任务顺利完成。

（三）奖惩措施

1. 经年度考核，子课题承担单位未按课题任务合同书要求完成考核指标，项目领导小组办公室有权终止项目的实施，追回已拨付资金。
2. 经年度考核、监督检查、审计认定，发现子课题承担单位存在提供虚假情况骗取项目资金、侵占或挪用项目资金、未及时实施等重大违规行为，项目领导小组办公室将终止课题实施，并追缴已拨付资金。同时，对子课题承担单位和相关责任人追究行政和法律责任。
3. 由于子课题承担单位或相关参与人员泄密而导致国家利益受到损失，相关单位和人员应承担行政或者法律责任。

五、子课题牵头单位保障措施

（一）全力以赴提供支持

严格按照课题任务指标和子课题任务合同书要求，兑现各项保障条件，按时保质保

量完成项目目标。按照《NK 管理办法（试行）》要求，优先落实兼职兼薪、权益分享、股权激励等政策，针对参与项目的人员，在绩效考核、职称评聘、岗位晋升、经费使用、研究生指标、荣誉奖励、后勤保障等方面制定专门的激励保障措施。

（二）严格项目过程管理

根据子课题任务需要，制定涵盖组织协调、技术研发、财务管理、人事管理、内部监管等全方位、全过程的项目管理制度，对项目过程实行精细化管理。子课题过程形成的技术底稿、原始凭证、审批文件等重要文档资料由专人管理、立档备查。

（三）自觉主动接受监督

子课题执行过程中，定期向课题领导小组办公室定期报送课题进展。按照年度考核通知要求，自觉主动接受 NK 领导小组办公室监督。

（四）全面落实保密制度

严格遵守国家保密法律法规和 NK 保密管理规定，制定项目保密管理制度，从严限定项目知悉范围。子课题参与人员对所获得的项目文件及项目相关信息，不复制、不传播、不扩散至无关的单位和个人。不在任何公开场合发表关于项目的言论，不在任何媒体、媒介上对项目情况进行宣传。

六、知识产权保障措施及权益分配机制

（一）知识产权保障措施

子课题推进过程中，强化知识产权的保护意识，提高知识产权保护力度。通过开展知识产权法律、法规培训，制定知识产权管理的各项规章制度，提高子课题参加单位人员产权意识，避免产生知识产权侵权行为，在课题研究过程中，全方位贯穿知识产权保护，及时组织、督促参与单位对具有自主知识产权的技术尽早申请专利。根据《中华人民共和国促进科技成果转化法》《国务院办公厅关于深化种业体制改革提高创新能力的意见》等文件精神，加快促进成果向现实生产力转变。

（二）权益分配机制

在子课题执行期间独立取得成果的产权归各自研究单位所有，在充分尊重和保护知识产权的前提下，对子课题产生的研究成果实现共享。

七、风险分析及对策

（一）芯片的知识产权和技术风险及对策

分子设计育种和基因组选种选配是新品系和配套系的高效选育的关键技术。利用育

种芯片检测个体的遗传信息是实现这些关键技术的高效必要流程，当前生猪育种领域所用芯片主要为外国制造，因此芯片的知识产权和技术对种猪集团存在较大风险，为避免将来在此处被“卡脖子”，专门设立相关研究内容，研发低成本高效率的液相芯片设计技术，自主解决育种芯片的问题。

（二）知识产权和技术标准风险及对策

子课题实施过程中，加强知识产权体系建设，建立完善的知识产权管理制度和管理流程，规范研发成果专利申请、技术秘密等，形成科学、合理、科学有效的管理制度。实施知识产权风险预警制度。在子课题实施过程中，及时将快长长寿母本新品系培育过程中形成的技术体系制定技术标准，将知识产权与技术标准有效融合，形成“技术专利化-专利标准化-标准许可化”的链条，增强快长长寿母本新品系的核心竞争力。通过制定技术标准，促进新品种培育过程中产生的技术得到大面积推广，从而提高培育新品系的市场占有率，并进一步推动国内生猪新品种培育的技术创新，提升核心竞争力。项目立足于市场，制定集技术创新、知识产权保护、技术标准制定于一体的联动机制，将“技术+知识产权+标准”的布局贯穿于项目实施过程中新技术的研究、开发、应用的全过程，形成“创新---知识产权---标准---创新”的有效循环、螺旋式上升机制。把课题实施过程中研发的新技术申请知识产权，再将知识产权融入技术标准，实现快长长寿母本新品系集成技术创新成果的知识产权保护并以标准的形式在市场上推广应用。

八、子课题参加人员基本情况表

填表说明：

1. 专业技术职称：A. 正高级 B. 副高级 C. 中级 D. 初级 E. 其他；

2. 投入本课题的全时工作时间（人月）是指在课题实施期间该人总共为课题工作的满月度工作量；累计是指课题组所有人员投入人月之和；

3. 人员分类代码：A. 课题负责人 B. 课题骨干（指子课题负责人） C. 其他人员(仅填固定工作人员)；

4. 工作单位：填写单位全称，其中高校要具体填写到所在院系。

姓名	性别	出生日期	国籍	证件类型	证件号码	专业技术职称	职务	最高学位	专业	投入本课题的全时工作时间（人月）	人员分类代码	工作单位	签名
卫恒习	男	1980-02-06	中国	身份证	130531198002062019	B	副主任	博士	动物遗传育种与繁殖	3	B	华南农业大学动物科学学院	
全洪燕	女	1989-04-10	中国	身份证	43042219890410212X	E	无	硕士	动物遗传育种与繁殖	3	C	华南农业大学动物科学学院	
累计										6	/	/	/

九、经费预算

表 1 子课题预算支出科目表

金额单位：万元

序号	预算科目名称	金额
	(1)	(2)
1	一、中央财政资金	15.00
2	(一) 直接费用	13.05
3	1. 设备费	/
4	其中：购置设备费	
5	2. 业务费	10.30
6	3. 劳务费	2.75
7	(二) 间接费用	1.95
8	二、其他来源资金	0.00
9	三、合计	15.00

表 2 子课题设备费——购置/试制设备预算明细表

金额单位：万元

填表说明：1. 设备分类：购置、试制； 2. 购置设备类型：通用、专用； 3. 试制设备不需填本列表（9）列、（10）列、（11）列、（12）列； 4. 设备单价的单位为万元/台套，设备数量的单位为台套； 5. 单价 50 万元以下的设备不用填写； 6. 本表只填写中央财政资金购置（试制）的设备。												
序号	设备名称	设备分类	功能和 技术指标	单价	数量	金额	购置或试 制单位	安置单位	购置设备 类型	主要生产厂 家及国别	规格型号	拟开放共享 范围
	(1)	(2)	(3)	(4)	(5)	(6)	(7)	(8)	(9)	(10)	(11)	(12)
/	/	/	/	/	/	/	/	/	/	/	/	/
单价 50 万元以上购置设备合计							/	/	/	/	/	/
单价 50 万元以上试制设备合计							/	/	/	/	/	/
累计							/	/	/	/	/	/

课题预算说明

（一）中央财政资金

预算的编制要坚持任务相关性、政策相符性和经济合理性，实事求是编制提出课题预算。填报时，直接费用应按设备费、业务费、劳务费三个类别填报，每个类别结合科研任务按支出用途进行说明。除 50 万元以上的设备外，其他费用只提供基本测算说明，不需要提供明细。

1. 设备费（是指课题实施过程中购置或试制专用仪器设备，对现有仪器设备进行升级改造，以及租赁外单位仪器设备而发生的费用等。计算类仪器设备和软件工具可在设备费科目编列。填报时，50 万元以上的设备详细说明，50 万元以下的设备费用分类说明。）

无。

2. 业务费（是指在课题实施过程中消耗的各种材料、低值易耗品等、发生的测试化验加工、燃料动力、出版文献、信息传播、知识产权事务、会议、差旅、国际合作与交流以及其他与课题实施直接相关的各项费用。编报时，对单笔大额支出、对外委托支出重点说明。）

（1）材料费：2.61 万元

用于购买课题实施过程中消耗的各种材料、低值易耗品等。

（2）测试化验加工费：6.00 万元

用于课题实施过程中发生的测试化验加工的费用。

（3）出版/文献/信息传播/知识产权事务费：0.69 万元

用于课题研究相关的信息传播、文献出版及专利申请等所需的费用。

（4）差旅/会议/国际交流合作费 1.00 万元

用于课题实施过程中所产生的差旅、会议及合作交流的费用。

3. 劳务费（是指在课题实施过程中支付给参与课题的研究生、博士后、访问学者以及课题聘用的研究人员、科研辅助人员、科研（财务）助理等的劳务性费用；支付给临时聘请的咨询专家的费用等。课题聘用人员由单位缴纳的社会保险补助、住房公积金等可纳入劳务费列支。）

（1）劳务性费用：2.25 万元

用于课题实施过程中支付给参与课题的研究生、博士后、访问学者以及课题聘用人员等的劳务性费用。

(2) 专家咨询费：0.50 万元

用于课题实施过程中支付给临时聘请的咨询专家的费用。

(二) 其他来源资金

对其他来源资金主要用途、支出预算做简要说明。

无。

十、其他需要补充的材料

无。

十一、双方责任

1. 甲乙双方根据《国务院办公厅关于改革完善中央财政科研经费管理的若干意见》（国办发〔2021〕32号）等有关文件规定，及有关法律、政策和管理要求，签署本任务合同书。

根据本任务合同书，甲方应向乙方拨付子课题年度经费 15.00 万元。项目年度经费拨付到乙方指定的下列账户：

收款单位：华南农业大学

开户银行：中国工商银行广州五山支行

账 号：3602002609000310520

2. 子课题承担单位和子课题负责人全力以赴开展研发，严格按照课题任务指标和本课题任务合同书要求，按时保质保量完成研发目标。不得以任何理由降低课题目标要求，拖延课题进展，推诿工作责任。

3. 子课题承担单位和子课题负责人定期向课题牵头单位报送课题进展，若经年度考核，子课题牵头单位未按课题任务合同书要求完成考核指标，课题牵头单位有权建议调整经费或终止子课题的实施单位、追回已拨付资金。对本课题所有成果产出（包括但不限于新产品、新技术、标准、专利等）的真实性、与课题的关联性负责，落实科研作风学风和科研诚信主体责任。

4. 子课题承担单位和子课题负责人严格遵守国家保密法律法规，从严限定课题知悉范围，并与核心涉密人员签订保密协议。

5. 课题经费实行专款专用、单独核算；全部用于与本课题研究工作相关的支出，不截留、挪用、侵占，不用于与科学研究无关的支出；接受并积极配合相关部门的监督检查。如有违反，课题牵头单位和课题负责人以及相关成果产出者愿接受项目主管单位和相关部门做出的各项处理决定，包括但不限于终止课题执行、追回课题（课题）经费，取消一定期限国家科技计划课题申报资格，记入科研诚信严重失信行为数据库以及主要负责人接受相应党纪政纪处理等。

十二、需要约定的其他内容

无

课题任务合同书签署

课题牵头单位（甲方）：四川德康农牧食品集团股份有限公司



法定代表人签字：

课题负责人签字：

朱研



子课题承担单位（乙方）：华南农业大学



法定代表人签字：

刘雅红

子课题负责人签字：卫恒习

(公章)

年 月 日

合同编号: 2019BT02N630

密级: 非密



004102840082


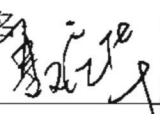
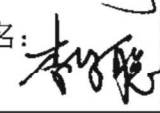

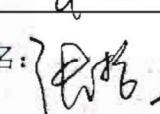
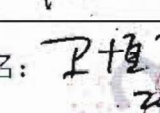

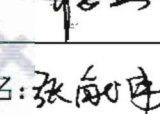
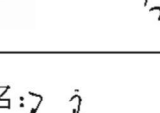
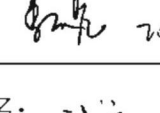
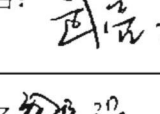
“广东特支计划”本土创新创业团队 合同书

团队名称	畜禽种业自主创新团队		
研究方向	动物遗传育种与繁殖		
研究技术领域	第一领域	N. 现代种业和精准农业-N03. 现代种业	
	第二领域	N. 现代种业和精准农业-N04. 精准农业	
开展项目名称	畜禽种业自主创新团队		
项目所属类型	基础与应用基础研究		
是否青年团队	是		
是否粤港澳联合团队	否		
管理单位(甲方)	广东省科学技术厅		
团队带头人(乙方)	聂庆华		
团队核心成员(乙方)	李崇聪 李刚 张哲 卫恒习 杨杰 张献伟 季从亮 武亮		
用人单位(丙方1)	华南农业大学		
协作单位(丙方2)	温氏食品集团股份有限公司		
归口管理部门(丁方)	省属单位		
团队联系人	徐海平		
联系人联系方式	手机	13580406668	邮箱 nqinghua@scau.edu.cn
实施年限	自合同生效之日起至之后五年		

广东省科学技术厅制

2020年3月

八、合同签署各方意见

甲方	单位名称	广东省科学技术厅	 (单位公章) 2020年9月14日
	法定代表人或法人代理	签名(签章)	
乙方	带头人签名	签名:  2020年8月1日	本人作为团队带头人/核心成员, 自愿接受“广东特支计划”本土创新创业团队项目资金的资助, 保证本合同书及其附件材料真实、合法、有效, 保障在粤工作时间, 坚持严肃的学术和科研态度, 遵守科研诚信、科研伦理规范, 遵守有关知识产权约定, 努力推进项目进展, 按要求对项目取得成果进行标注, 按期完成合同约定各项任务目标。
	核心成员签名	签名:  2020年8月1日	
	核心成员签名	签名:  2020年7月30日	
	核心成员签名	签名:  2020年7月30日	
	核心成员签名	签名:  2020年7月30日	
	核心成员签名	签名:  2020年8月1日	
	核心成员签名	签名:  2020年7月30日	
	核心成员签名	签名:  2020年7月30日	
	核心成员签名	签名:  2020年7月30日	
	核心成员签名	签名:  2020年7月30日	
	核心成员签名	签名: _____ 年 月 日	

丙方(1)	单位名称	 华南农业大学 (单位公章) 2020年 8月 1日	本单位同意承担“广东特支计划”本土创新创业团队项目，保证本合同书及其附件材料真实、合法、有效，支持、督促乙方在岗工作并确保落实自筹资金及有关保障条件，建立健全项目管理制度，合理合规使用省财政资金，及时报告重大变动情况，按期完成合同约定各项任务目标。
	法定代表人或法人代理	签名(签章) 	
丙方(2)	单位名称	 温氏食品集团股份有限公司 (单位公章) 2020年 2月 1日	本单位同意作为协作单位承担“广东特支计划”本土创新创业团队项目，保证本合同书及附件材料中涉及协作单位部分内容真实、合法、有效，确保落实有关保障条件，建立健全项目管理制度，合理合规使用省财政资金，及时报告重大变动情况，按期完成合同约定各项任务目标。
	法定代表人或法人代理	签名(签章) 	
丁方	单位名称		地级以上市科技部门 (单位公章) 年 月 日
	法定代表人或法人代理	签名(签章)	
	单位名称		地级以上市委组织部 (单位公章) 年 月 日
	法定代表人或法人代理	签名(签章)	

“广东特支计划”本土创新创业团队项目 任务书

项目名称：畜禽种业自主创新团队项目

项目计划类别：现代种业

项目编号：2019BT02N630

研究任务承担单位（甲方）：华南农业大学

项目主持人：聂庆华

研究分任务承担单位（乙方）：华南农业大学

课题负责人：卫恒习

起止年限：2020 年 7 月 30 日—2025 年 7 月 30 日

一、研究内容（500 字以内）		
<p>(1) 公猪精子发生、精液质量及受精能力的调控机制，建立公猪高繁殖力精液蛋白标记，建立提高公猪精液品质和繁殖性能的相关技术措施。</p> <p>(2) 母猪卵泡发育和发情排卵的调控机制，重点研究非编码 RNAs 等功能分子对卵泡发育的调控作用、母猪断奶-发情的生殖内分泌规律，建立发情-排卵-输精控制相结合的高效母猪定时输精和批次化生产技术。</p> <p>(3) 研究和建立种畜禽精液保存技术、家畜体外受精、胚胎移植、性别控制、生殖细胞体外培养和胚胎冷冻保存等动物繁殖技术。</p>		
二、考核指标		
<p>1、申请专利 2 项，中期考核前获得授权专利 1 项，结题前获得授权专利 2 项；</p> <p>2、获国家自然科学基金 1 项，省部级科研项目 1 项；</p> <p>3、发表 SCI 一区论文 1 篇；</p> <p>4、主编或参编专著 1 部；</p> <p>5、培养硕士 5 名；</p> <p>6、吸引科研骨干名，高级职称人才名；</p> <p>7、获广东省科技进步奖 1 项；</p> <p>8、年度研究报告、中期考核及结题验收相关材料和报告。</p>		
三、进度安排		
年度	年度工作内容	阶段目标
2020.8-2021.7	猪精液质量与受精能力研究	发表论文 1-2 篇，申请专利 1 项
2021.8-2022.7	母猪断奶发情生殖内分泌规律研究	发表论文 1 篇
2022.8-2023.7	母猪发情调控技术研究	发表论文 1 篇，申请专利 1 项
2023.8-2024.7	猪卵泡发育、发情排卵与	发表论文 1-2 篇

		定时输精相关机制研究			
2024.8-2025-7		猪性别控制、配子和胚胎冷冻等技术研究		发表文章 1-2 篇，申请专利 1 项	
四、团队研究人员					
课题负责人					
姓名	性别	年龄	职称	身份证号码	所在单位
卫恒习	男	40	副研究员	130531198002062019	华南农业大学
骨干成员					
张守全	男	56	教授	110108196407089334	华南农业大学
孟立	男	36	讲师	372922198405063631	华南农业大学
李莉	女	49	高级畜牧师	44010619710301186x	华南农业大学
五、经费预算					
经费支出科目		金额(单位:万元)		用途说明	
材料费		57.50		用于项目执行过程中实验动物、试剂、离心管等低值易耗品的采购及运输、装卸、整理等费用	
测试化验加工费		25.00		用于项目研究过程中支付给外单位(包括依托单位内部独立经济核算单位)的检验、测试、化验及加工等费用	
燃料动力费		0		项目实施过程中直接使用的相关仪器设备、科学装置等运行发生的水、电、气、燃料消耗费用等	
出版、文献、信息传播、知识产权事务费		3.00		用于支付出版费、资料费、专用软件购置费、文献检索和查新费用、专利申请及其他知识产权事务费用	
会议费/差旅费/国际合作与交流费		10.50		用于项目实施过程中采样、参加学术交流、科学考察、业务调研和业务培训等所发生的差旅费、市内交通费用;学术年会;研究人	

		员出国合作与外国专家来华学术交流等费用
劳务费	4.00	项目实施过程中支付给参与项目的研究生补助与博士后等的劳动性费用
专家咨询费	0	
其它	0	
合计	100.00	

六、合约条款

甲方（项目主持人）：聂庆华

乙方（研究任务负责人）：卫恒习

甲乙双方根据项目管理单位（广东省科学技术厅）与团队成员签订的“广东特支计划”本土创新创业团队项目（项目编号：2019BT02N630）合同书要求，经沟通和协商，乙方自愿承接“畜禽种业自主创新团队”项目研究任务，双方就课题实施达成如下协议：

- 1、甲方为乙方在“畜禽种业自主创新团队”项目研发经费中提供 100 万元的报账额度，乙方按照项目经费管理要求和财务管理制度报账，实行专款专用，不得弄虚作假、挪用、挤占课题经费或违反相关法律法规。
- 2、甲方按任务书规定进行工作协调，乙方按照双方约定的研究内容和考核指标开展研究工作，按甲方要求及时提供年度研究报告、中期考核总结材料及结题验收报告，交由甲方汇总后及时上报广东省科学技术厅。任务执行过程中，甲方有权不定期检查课题研究进度。
- 3、任务执行过程中，乙方如需调整任务，应向甲方提出变更内容及其理由的申请报告，经甲方审核后报广东省科学技术厅备案。
- 4、项目实施过程中发表的相关论文等签约各方必须注明“由广东省‘珠江人才计划’本土创新科研团队项目（项目编号：2019BT02N630）资助”（supported by Local Innovative and Research Teams Project of Guangdong Pearl River Talents Program (2019BT02N630)）。

- 5、任务执行过程中双方独立取得的技术成果，可自行开发、转让，并完全受益；双方合作完成的则由双方协商确定。
- 6、甲乙双方要求变更或解除合约，应提前 30 日书面通知另一方。
- 7、任务执行过程中若有争议时，甲乙双方应按广东省科技管理办法有关条款通过协商的方式解决，协商不成时，双方向广东省科学技术厅申请调解。
- 8、任务书正式文本一式三份（甲乙双方各 1 份，甲乙双方科技管理部门 1 份）。

七、签约各方签章

项目主持人（甲方）（签字）：

研究任务负责人（乙方）（签字）：

甲方所在单位（公章）：


年 月 日

乙方所在单位（公章）：


年 月 日

受理编号: c1530550100280

项目编号: 2015A020208015

文件编号: 粤科规财字[2015]150号



广东省省级科技计划项目 合同书

项目名称: 提高种公猪繁殖能力的相关技术研究集成与示范

计划类别: 农村科技领域

项目起止时间: 2016-01-01 至 2018-12-31

管理单位(甲方): 广东省科学技术厅

承担单位(乙方): 华南农业大学

乙方主管部门(丙方): 华南农业大学

通讯地址: 广东省广州市天河区五山路483号

邮政编码: 510642

单位电话: 020-38632819

项目负责人: 卫恒习

联系电话: 020-85284869

项目联系人: 卫恒习

联系电话: 020-85284869

广东省科学技术厅
二〇一四年制

一、项目实施内容

1. 主要研究内容

(1) 研究对象的获取与统计分析

收集大量种公猪的生产数据，利用统计学方法分析，建立数学模型将种公猪分为不同繁殖力（高、中、低）的群体。再利用体外实验（如体外受精）对高、低繁殖力种公猪的精液受精能力进行检测，结合数学模型结果，筛选出高繁殖力和低繁殖力种公猪各5头，作为主要研究对象。

(2) 不同繁殖力种公猪精液蛋白成分差异检测

分别采集高、低繁殖力种公猪的精液，利用高通量蛋白检测技术筛选出一批在高、低繁殖力种公猪精液中差异表达的蛋白。然后，利用生物信息学方法对这些差异蛋白进行功能分析，寻找并确定几个与精子受精能力密切相关的蛋白作为候选目标蛋白。

(3) 精子受精能力相关候选蛋白的功能研究

获得目标蛋白的重组蛋白和特异抗体，分别添加到相应精液中，再利用体外受精、人工授精等手段检测特定蛋白或抗体对精子受精能力或受胎率和产仔数的影响，从而确定能真实反映精子受精能力的新标记。

(4) 精液新蛋白标记的应用与示范

利用新发现的蛋白标记，对猪场种公猪的繁殖力进行预测，并通过人工授精等来验证该标记预测的准确性。然后将可靠的标记应用于种公猪的选育、精液受精能力评价等工作，可充分发挥优良种公猪的繁殖能力、提高人工授精效果。

2. 拟解决的关键问题和技术路线

(1) 拟解决关键问题

如何高效选择高繁殖力种公猪？建立能够反映精液受精能力和种公猪繁殖力的蛋白标记，完善和提高猪人工授精技术效果。

(2) 技术路线

利用统计学方法从大量已有的种公猪生产数据中选择出高繁殖性能的种公猪群体和低繁殖性能的种公猪群体；然后通过体外实验（如体外受精），真正从上述群体中筛选出高、低繁殖力种公猪作为研究对象；通过分析两组种公猪的精液蛋白成分差异，筛选出精液差异表达蛋白，并结合生物信息学分析，确定与种公猪精液受精能力相关的候选蛋白；再通过体内、外实验确定这些蛋白质对精液保存、精子获能和受精的影响，得到能真实反映公猪精液受精能力的蛋白标记；然后，利用该蛋白标记在生产中筛选出真正高繁殖力种公猪，进行人工授精效果验证，并推广。

3. 创新点

(1) 探索能反映精子受精能力的蛋白质标记，为种猪选育和繁殖力评定提供参考依据，同时为提高猪人工授精效果与繁殖效率提供改进的方向。

(2) 阐释精液中重要蛋白成分在受精过程中的作用机制，为生殖生物学理论研究提供重要支持。

二、项目考核指标

1. 项目完成后提供的研究开发成果及形式（须明确产品、专利、版权、标准等成果的类型及数量）					
成果形式		成果数量	成果形式		成果数量
发明专利	申请	1	引进人才(人)		0
	授权		培养人才(人)		3
实用新型专利	申请	0	科技人才奖励(人)		0
	授权		技术标准制定	牵头(个)	0
外观设计专利	申请			参与(个)	0
	授权		科技报告(篇)		
国外专利	PCT受理	0	软件著作权(项)		0
	授权		论文论著(篇)		4
获得国家级奖项(项)		0	其中：被收录论文数(篇)	SCI	1
获得省级奖项(项)		0		EI	0
新服务(项)		0		ISTP	0
新产品（或新材料、新装备、新品种（系））		0	新工艺（或新方法、新模式、新技术）		0
创新载体项目必填		技术服务数量（项）			
		服务企业数量（家）			
科技金融项目必填		开展培训宣讲活动场次(次)			
		服务企业数量(家)			
		帮助企业融资(万元)			
		引进专业机构(家)			
院士工作站项目必填		引进院士及其团队科技成果转化数量			
		院士开展的战略咨询和技术指导次数			
		院士年进站次数			
		院士及院士团队年进站时间			
软科学项目必填		决策咨询报告(篇)(至少1篇)			
		研究总报告(篇)(至少1篇)			
		研究中期报告(篇)			
		研究分报告(篇)			
		调研报告(篇)			
		专著(篇)[须注明“广东省软科学研究计划项目(项目编号：)资助”]			
		核心期刊论文(篇)[以第一作者发表，须注明“广东省软科学研究计划项目(项目编号：)资助”]			
		其他()			

第65页，共307页

三、项目进度和阶段目标

开始日期	结束日期	主要工作内容
2016-01-01	2016-12-31	分析种公猪生产成绩记录，筛选出高繁殖力和低繁殖力的两个研究群体；采集研究对象的精液，利用双向电泳、iTRAQ等技术分析其中精液蛋白的表达情况，筛选出两组研究对象之间的精液差异蛋白，并进行相关生物信息学分析。
2017-01-01	2017-12-31	种公猪精液差异蛋白与实际繁殖性能的相关性分析，结合生物信息学分析结果确定目标蛋白。购买或体外表达制备目的蛋白及其抗体，建立相关蛋白定量检测技术。利用原位杂交、ELISA等技术、研究目的蛋白在公猪生殖系统中的表达与分布情况，以及对精液保存的影响。
2018-01-01	2018-12-31	研究目标蛋白及其抗体对常规精液品质、精子获能、精子受精和胚胎发育能力的影响。研究目标蛋白及其抗体对人工授精效果的影响，探索提高种公猪繁殖能力的综合技术措施。撰写论文，进行结题。

四、承担、参与单位工作分工及经费分配情况

承担/参与单位名称 (盖章)	工作分工	总经费分摊 (万元)	省科技厅经费分配 (万元)
华南农业大学	种公猪繁殖性能的统计学分析、种公猪精液蛋白差异检测与精子受精能力新蛋白标记的筛选、以及课题组织协调工作	18.00	18.00
蕉岭县泰农黑猪发展有限公司	猪人工授精技术体系改良与推广应用示范。主要包括：目标精液蛋白及其抗体对精液常规品质、精子保存的影响，猪人工授精实验验证目标蛋白标记的有效性，新技术体系的推广应用示范。	12.00	12.00
	合计	30.00	30.00

五、项目总经费及省科技厅经费预算

1. 省科技厅经费下达总额：（大写）叁拾万圆整；（小写）30.00万元；						
2. 省科技厅经费年度下达计划：（第一期）30.00万元；（余额）0.00万元						
3. 总经费开支预算计划：						
经费筹集情况：						（单位：万元）
总投入经费：30.00						
	省科技厅经费	自筹资金				合计
		自有资金	贷款	地方政府投入	其它	
已投入经费：	0	0	0	0	0	0.00
新增经费：	30.00	0	0	0	0	30.00
政府部门、境外资金及其他资金投入情况说明：	无					

新增经费预算：					（单位：万元）
新增经费总额			省科技厅经费		
支出经费	经费额	用途说明	经费额	用途说明	
基建费：					
1、直接费用：	28.50		28.50		
(1) 设备费：	4.50	用于精子分析系统等设备的购置或维修	4.50	用于精子分析系统等设备的购置或维修	
(2) 材料费：	11.00	用于实验研究所需试剂盒、抗体、重组蛋白、细胞因子等药品、耗材的购置	11.00	用于实验研究所需试剂盒、抗体、重组蛋白、细胞因子等药品、耗材的购置	

(3)测试化验加工外协费:	3.00	精液蛋白定量分析检测,免疫组化与激光共聚焦检测等	3.00	精液蛋白定量分析检测,免疫组化与激光共聚焦检测等
(4)燃料动力费:	0	无	0	无
(5)差旅费:	4.00	用于国内课题调研、学术交流等的差旅费	4.00	用于国内课题调研、学术交流等的差旅费
(6)会议费:	0	无	0	无
(7)国际合作与交流费:	0	无	0	无
(8)出版/文献/信息传播/知识产权事务费:	2.00	用于出版文献版面费、专利申请费、论文打印等的费用	2.00	用于出版文献版面费、专利申请费、论文打印等的费用
(9)租赁费:	0	无	0	无
(10)人员费:	3.60	用于研究生或临时聘用人员的劳务费	3.60	用于研究生或临时聘用人员的劳务费
(11)专家咨询费:	0.40	聘请专家对课题指导的咨询费	0.40	聘请专家对课题指导的咨询费
(12)直接费用其他支出:	0	无	0	无
(13)科技金融服务体系其他费用:	0.00		0.00	
①信用评级补贴:				
②大赛场租:				
③特派员奖励与补贴:				
2、间接费用:	1.50		1.50	
管理费:	1.50	课题管理费	1.50	课题管理费
合计:	30.00		30.00	

六、人员信息

项目负责人情况								
姓名	年龄	性别	职称	职务	学历	在项目中承担的任务	所在单位	签名
卫恒习	35	男	副研究员	无	博士研究生	负责项目总体设计与实施	华南农业大学	

主要研究开发人员								
姓名	年龄	性别	职称	职务	学历	在项目中承担的任务	所在单位	签名
张守全	51	男	教授	无	博士	种公猪繁殖性能数据收集与整理	华南农业大学	
李莉	44	女	高级畜牧师	无	硕士	精液品质检测、体外受精	华南农业大学	
林佳炜	27	男	未取得	公司法人	本科	猪人工授精技术体系优化与推广示范	蕉岭县泰农黑猪发展有限公司	
陈志林	26	男	未取得	研究生	本科	精液蛋白成分检测与差异蛋白筛选	华南农业大学	
高凤磊	31	女	未取得	研究生	硕士	精子受精能力体外检测	华南农业大学	
叶超	25	男	未取得	研究生	本科	精液差异蛋白生物信息学分析	华南农业大学	
吴俊辉	25	男	未取得	研究生	本科	目标蛋白功能检测，对获能和受精能力的影响	华南农业大学	
林辉苑	49	男	未取得	总经理	本科	目标蛋白对猪精液常规品质的影响	蕉岭县泰农黑猪发展有限公司	
林婷芳	22	女	未取得	办公室副主任	大专	人工授精技术改进与示范	蕉岭县泰农黑猪发展有限公司	
黄娟	29	女	未取得	公司财务	本科	现场人工授精数据整理与分析	蕉岭县泰农黑猪发展有限公司	

七、承担、参与单位合作协议（须与申报书中合作协议或意向书相一致）

甲方：华南农业大学

乙方：蕉岭县泰农黑猪发展有限公司

甲乙双方本着相互协作的精神，合作完成2015年广东省科技计划（公益研究与能力建设）项目“提高种公猪繁殖能力的相关技术研究集成与示范”，经过协商达成如下协议，并由双方共同恪守。

一、双方负责人：

甲方：华南农业大学为项目申报单位，负责人为 卫恒习

乙方：蕉岭县泰农黑猪发展有限公司为项目参与单位，负责人为 林佳炜

二、研究分工：

甲方：项目研究总体设计与实施，主要负责种公猪繁殖性能的统计学分析，种公猪精液蛋白差异检测与精子受精能力新蛋白标记的筛选与功能研究。

乙方：主要负责猪人工授精技术体系改良与应用示范。包括目标蛋白及抗体对精液常规品质和精子保存的影响，猪人工授精新技术体系集成与应用示范。

三、研究成果归属：

各方独自完成的研究成果归各方所有，双方共同完成的研究成果双方共享。

四、经费分配：

该项目申报经费 30 万元，若项目按该经费立项，则甲方拨付乙方经费 12 万元；若立项经费有所削减，则甲乙双方在填报项目计划书时签订补充协议重新约定合作经费金额、具体科目预算、拨款时间及其他未尽事宜。

本协议一式两份。甲乙双方各持1份，若项目本年度未获得立项，则此协议自动失效。

八、合同条款

第一条 甲方与乙方根据《中华人民共和国合同法》及国家有关法规和规定，为顺利完成（2015）年**提高种公猪繁殖能力的相关技术研究集成与示范**专项项目（项目编号：2015A020208015）经协商一致，特订立本合同，作为甲乙双方在项目实施管理过程中共同遵守的依据。

第二条 甲方的权利义务：

1. 按合同书规定进行经费核拨的有关工作协调。
2. 根据甲方需要，在不影响乙方工作的前提下，定期或不定期对乙方项目的实施情况和经费使用情况进行检查或抽查。
3. 根据《广东省科技计划项目信用管理办法(试行)》对乙方进行科技计划信用管理。

第三条 乙方的权利义务：

1. 确保落实自筹经费及有关保障条件。
2. 按合同书规定，对甲方核拨的经费实行专款专用，单独列账，并随时配合甲方进行监督检查。
3. 使用财政资金采购设备、原材料等，按照《广东省实施〈中华人民共和国招标投标法〉办法》有关规定，符合招标条件的须进行招标。
4. 项目实施完成或实施到一定程度，须按照《广东省省级科技计划项目结题管理的实施细则（试行）》提出验收或终止结题的申请，并按甲方要求做好项目结题工作。
5. 在每年1月向甲方如实提交上年度工作情况报告，报告内容包含上年度项目进展情况、经费决算和取得的效果等。
6. 按照国家和省有关规定，每年须提交年度科技报告；项目验收时，须提交验收科技报告。

第四条 在履行本合同的过程中，如出现广东省相关政策法规重大改变等不可抗力情况，甲方有权对所核拨经费的数量和时间进行相应调整。

第五条 在履行本合同过程中，需要对项目起止时间、项目经费使用（包括自筹经费、经费分配及经费支出预算等）、项目内容（包括研发内容、技术指标、经济指标及成果指标等）、项目名称、项目承担单位（包括承担单位更名、承担单位替换）、参与单位、项目负责人和成员等进行变更的，甲乙双方按照《广东省省级科技计划项目合同书管理的实施细则（试行）》有关规定执行。

第六条 在履行本合同的过程中，当事人一方发现可能导致项目整体或部分失败的情形时，应及时通知另一方，并采取适当措施减少损失，没有及时通知并采取适当措施，致使损失扩大的，应当就扩大的损失承担责任。

第七条 本项目技术成果的归属、转让和实施技术成果所产生的经济利益的分享，除双方另有约定外，按国家和广东省有关法规执行。

第八条 属技术保密的项目，甲乙双方应另行订立技术保密条款，作为本合同正式内容的一部分，与本合同具有同等效力。

第九条 根据项目具体情况，经双方另行协商订立的附加条款，作为本合同正式内容的一部分，与本合同具有同等效力。

第十条 本合同的争议应由双方本着协商一致的原则解决，如双方协商不成的，则应向甲方所在地法院提起诉讼。

第十一条 保密条款：

1. 本合同保密内容范围为：

(/)

2. 本合同保密期限为：

(/)

3. 乙方应与可能知悉保密内容的人员签订技术秘密保护协议。

4. 各方应建立技术秘密保护制度。

5. 属技术保密的项目必须经省负责技术保密部门审查后，确定可否发表或用于国际合作和交流。

第十二条 甲方可根据具体情况决定乙方是否需要单位担保，若需要保证单位，应订立担保条款，作为本合同正式内容一部分。当乙方不履行或不完全履行本合同，以及没有或没有完全承担违约责任时，乙方的保证单位承担连带保证责任。

第十三条 本合同一式六份，各份具有同等效力。甲方存三份，乙方存二份，丙方存一份，本合同自签字之日起生效，有效期至项目结题后一年内。各方均应负合同的法律责任，不应受机构、人事变动的影响。

说明：本合同书中，凡是当事人约定无需填写的内容，应在空白处划（/）。

九、本合同签约各方

管理单位（甲方）：广东省科学技术厅（盖章）

单位地址：广州市连新路171号大院信息大楼

法定代表人（或授权代表）：黄宁生（签章）

联系人（经办人）姓名：林振亮（签章）

Email: linz1@gdstc.gov.cn

电话：020-83163905

年 月 日

承担单位（乙方）：华南农业大学（盖章）

二级部门：华南农业大学动物科学学院

单位地址：广东省广州市天河区五山路483号

法定代表人（或法人代理）：陈晓阳（签章）

联系人（项目主管）姓名：石睿（签章）

Email: 77909213@qq.com

电话：020-85283435

开户单位名称：华南农业大学

开户银行及帐号：广东广州工行五山支行 3602002609000310520

年 月 日

乙方主管部门（丙方）：华南农业大学（盖章）

单位地址：广东省广州市天河区五山路483号

法定代表人（或法人代理）：陈晓阳（签章）

联系人（项目主管）姓名：石睿（签章）

Email: 77909213@qq.com

电话：020-85283435

开户单位名称：华南农业大学

开户银行及帐号：广东广州工行五山支行 3602002609000310520

年 月 日

九、本合同签约各方

管理单位(甲方): 广东省科学技术厅 (盖章)

单位地址: 广州市连新路171号大院信息大楼

法定代表人(或授权代表): 黄宁生 (签章)

联系人(经办人)姓名: 林振亮 (签章)

Email: linzl@gdstc.gov.cn

电话: 020-83163905

年 月 日

承担单位(乙方): 华南农业大学 (盖章)

二级部门: 华南农业大学动物科学学院

单位地址: 广东省广州市天河区五山路483号

法定代表人(或法人代理): 陈晓阳 (签章)

联系人(项目主管)姓名: 石睿 (签章)

Email: 77909213@qq.com

电话: 020-85283435

开户单位名称: 华南农业大学

开户银行及帐号: 广东广州工行五山支行 3602002609000310520

年 月 日

乙方主管部门(丙方): 华南农业大学 (盖章)

单位地址: 广东省广州市天河区五山路483号

法定代表人(或法人代理): 陈晓阳 (签章)

联系人(项目主管)姓名: 石睿 (签章)

Email: 77909213@qq.com

电话: 020-85283435

开户单位名称: 华南农业大学

开户银行及帐号: 广东广州工行五山支行 3602002609000310520

年 月 日

受理编号: c1730550100113

项目编号: 2017A020208061

文件编号: 粤科规财字[2017]50号

广东省省级科技计划项目 合同书

项目名称: 经产母猪新型高效综合繁殖技术与示范

专项资金类别: 公益研究与能力建设

计划类别: 农村科技领域

项目起止时间: 2017-01-01 至 2019-12-31

管理单位(甲方): 广东省科学技术厅

承担单位(乙方): 华南农业大学

乙方主管部门(丙方): 华南农业大学

通讯地址: 广东省广州市天河区五山路483号

邮政编码: 510642

单位电话: 020-38632819

项目负责人: 卫恒习

联系电话: 020-85284869

项目联系人: 卫恒习

联系电话: 15902067686



(广东科技微信公众号)

广东省科学技术厅
二〇一七年制



(受理纸质材料二维码)

一、研发内容和关键技术

1. 主要研究内容

(1) 国产细胞工程来源生殖激素（rFSH和rhCG）对母猪诱导发情的研究

选取一批母猪，随机分成4组，第一组作为阴性对照组不进行任何处理，第二组为阳性对照组使用进口PG600处理，第三组和第四组分别使用一倍剂量和二倍剂量的国产激素的进行处理。通过比较发情率、发情集中度、发情持续时间、投入成本等指标来评价使用国产细胞工程来源激素代替昂贵生殖激素的可行性、以及筛选出适宜的应用剂量。

(2) 国产细胞工程来源生殖激素对经产母猪同期发情-排卵的技术研究

依据rFSH和rhCG注射间隔的不同，制定（短间隔、中间隔、长间隔）3种同期发情-排卵技术方案，在经产母猪上进行试验。以自然发情组作为对照，通过比较同期发情率、发情集中度、发情持续时间、发情-排卵时间间隔（B超观察卵巢状态）、是否便于生产管理等指标来筛选最佳的同期发情、排卵技术程序。

(3) 利用国产细胞工程来源生殖激素进行经产母猪程序化发情-排卵-授精综合技术与示范

利用最佳的国产激素同期发情、排卵技术方案进行经产母猪同期发情处理，在激素处理后的不同时间（如16h、24h、32h）进行人工授精，以常规人工授精技术作为对照，通过比较发情率、受胎率、分娩率、窝产仔数、断奶-发情间隔、非生产天数，繁殖效率等指标来确定效果最好的处理，制定经产母猪程序化的发情-排卵-输精控制综合技术，并在猪场进行应用示范。

2. 拟解决的关键问题及技术路线

(1) 当前生殖激素（如PG600等）价格较高，阻碍了动物繁殖新技术在养殖场的应用。细胞工程来源重组生殖激素具有活性高、成本低的优点，有望替代价格昂贵的生殖激素，有助于促进繁殖新技术的开发与推广应用。

(2) 建立高效的经产母猪高发情-排卵-输精综合技术，解决当前猪场广泛存在的母猪发情率低，受胎率低等问题，提高母猪利用率和繁殖性能。

本项目首先通过母猪诱导发情试验，确定国产重组激素的使用效果和适宜的使用剂量；然后分别建立和优化经产母猪发情、排卵及输精的控制技术，最后对各项最优化的技术方案进行集成，建立新型高效的经产母猪发情-排卵-授精综合繁殖技术，进行应用示范。

3. 创新点

(1) 优化集成，建立一套经产母猪发情排卵精确控制与适时输精综合技术程序。

(2) 以高活性、低成本的国产细胞工程重组激素代替进口或昂贵激素，降低技术成本，有助于新技术在生产中推广应用。

二、项目考核指标

1. 项目完成后提供的研究开发成果及形式（须明确产品、专利、版权、标准等成果的类型及数量）					
成果形式		成果数量	成果形式		成果数量
发明专利	申请	0	引进人才(人)		0
	授权	0	培养人才(人)		2
实用新型专利	申请	0	科技人才奖励(人)		0
	授权	0	技术标准制定	牵头(个)	0
外观设计专利	申请	0		参与(个)	1
	授权	0	科技报告(篇)		1
国外专利	PCT受理	0	软件著作权(项)		0
	授权	0	论文论著(篇)		3
获得国家级奖项(项)		0	其中：被收录论文数(篇)	SCI	0
获得省级奖项(项)		0		EI	0
新服务(项)		0		ISTP	0
新产品（或新材料、新装备、新品种（系））		0	新工艺（或新方法、新模式、新技术）		0
创新载体项目必填		技术服务数量（项）			
		服务企业数量（家）			
科技金融项目必填		开展培训宣讲活动场次(次)			
		服务企业数量(家)			
		帮助企业融资(万元)			
		引进专业机构(家)			
院士工作站项目必填		引进院士及其团队科技成果转化数量			
		院士开展的战略咨询和技术指导次数			
		院士年进站次数			
		院士及院士团队年进站时间			
软科学项目必填		决策咨询报告(篇)（至少1篇）			
		研究总报告(篇)			
		研究中期报告(篇)			
		研究分报告(篇)			
		调研报告(篇)			
		专著(篇)[须注明“广东省软科学研究计划项目(项目编号：)资助”]			
		核心期刊论文(篇)[以第一作者发表，须注明“广东省软科学研究计划项目(项目编号：)资助”]			
		其他()			

第80页，共307页

三、项目进度和阶段目标

开始日期	结束日期	主要工作内容
2017-01-01	2017-12-31	进行试验材料、试验猪群等的准备，进行国产激素rFSH和rhCG对猪诱导发情的效果检测，确定有效地激素使用剂量。
2018-01-01	2018-12-31	制定经产母猪同期发情、排卵的技术方案，并通过试验筛选最佳的技术方案，为后续新型综合繁殖技术的建立奠定基础
2019-01-01	2019-12-31	在前期基础上，制定经产母猪发情-排卵-授精控制综合技术方案，并通过试验筛选出最佳技术程序。新型综合繁殖技术的应用示范，数据整理，准备结题。

四、承担、参与单位工作分工及经费分配情况

承担/参与单位名称 (盖章)	工作分工	总经费分摊 (万元)	省科技厅经费分配 (万元)
华南农业大学	总体试验方案的制定，联系协调试验猪场，并完成相关试验研究。	10.50	10.50
广州威生医药科技有限公司	负责细胞工程来源相关生殖激素的生产与供给，协助完成相关现场试验。	4.50	4.50
	合计	15.00	15.00

五、项目总经费及省科技厅经费预算

1. 省科技厅经费下达总额：（大写）壹拾伍万圆整；（小写）15万元；						
2. 省科技厅经费拨付方式：一次性拨款						
3. 省科技厅经费年度下达计划：（大写）壹拾伍万圆整；（小写）15万元；						
分期				经费(万元)		
第1期				15		
4. 总经费开支预算计划：						
经费筹集情况：						(单位：万元)
总投入经费：15.00						
	省科技厅经费	其它资金				合计
		自有资金	贷款	地方政府投入	其它	
已投入经费：						
新增经费：	15.00	0	0	0	0.00	15.00
政府部门、境外资金及其他资金投入情况说明：	无					

新增经费预算:			(单位: 万元)	
	新增经费总额		省科技厅经费	
支出经费	经费额	用途说明	经费额	用途说明
基建费:				
1、直接费用:	14.25		14.25	
(1) 设备费:				
(2) 材料费:	7.60	用于购买饲料、生殖激素、精液输精耗材和其他试剂耗材的费用	7.60	用于购买猪饲料、生殖激素、精液输精耗材和其他试剂耗材的费用
(3) 测试化验加工外协费:				
(4) 燃料动力费:				
(5) 差旅费/会议费/国际合作与交流费:	1.50	用于试验实施, 调研, 参加学术会议等所产生的差旅费	1.50	用于试验实施, 调研等所产生的差旅费
(6) 出版/文献/信息传播/知识产权事务费:	1.20	用于信息查询, 文献出版等产生的费用	1.20	用于信息查询, 文献出版等产生的费用
(7) 劳务费:				
(8) 人员费:	3.60	用于研究生和临时聘用人员的劳务费	3.60	用于研究生和临时聘用人员的劳务费
(9) 专家咨询费:	0.35	聘请专家进行试验咨询或指导的费用	0.35	聘请专家进行试验咨询或指导的费用
(10) 直接费用其他支出:				
(11) 科技金融服务体系其他费用:				
①信用评级补贴:				
②大赛场租:				
③特派员奖励与补贴:				
2、间接费用:	0.75		0.75	
(1) 间接成本:	0.75	管理费	0.75	项目管理费
(2) 管理成本:				
(3) 绩效支出:				
合计:	15.00		15.00	

特别提醒: 2017年3月份, 广东省《关于进一步完善省级财政科研项目资金管理等政策的实施意见(试行)》(粤委办〔2017〕13号)出台, 对间接费用比例、劳务费开支范围、人员费用安排等进行了调整优化。为及时拨付2017年度科研经费, 平台直接提取申报书相关信息生成合同书并进行了预签订, 但各项目负责人、承担单位、主管部门须认真领会相关文件精神, 2017年立项的项目, 合同书签订完成后2个月内通过平台提请项目经费变更或确认, 对相关经费开支进行细化完善, 否则, 将影响其科研信用评级或申报新的省级科技项目。

六、人员信息

项目负责人情况								
姓名	年龄	性别	职称	职务	学历	在项目中承担的任务	所在单位	签名
卫恒习	38	男	副研究员	无	博士研究生	负责试验方案制定与实施安排	华南农业大学	

主要研究开发人员								
姓名	年龄	性别	职称	职务	学历	在项目中承担的任务	所在单位	签名
张守全	52	男	教授	无	博士研究生	试验猪场及现场试验的组织协调	华南农业大学	
李莉	45	女	高级畜牧师	无	硕士研究生	应用细胞工程来源生殖激素进行猪诱导发情的研究	华南农业大学	
吴俊辉	26	男	未取得	临床试验专员	硕士研究生	生殖激素使用剂量筛选与优化	广州威生医药科技有限公司	
邓衡露	31	女	未取得	质量研究工程师	本科	经产母猪发情、排卵试验研究	广州威生医药科技有限公司	
冯美莹	27	女	未取得	无	博士研究生	经产母猪发情-排卵控制技术研究	华南农业大学	
黄虎	29	男	未取得	研发工程师	硕士研究生	经产母猪输精技术优化	广州威生医药科技有限公司	
叶超	26	男	未取得	无	硕士生	母猪发情-排卵-授精综合控制技术研究	华南农业大学	

七、承担、参与单位合作

甲方：华南农业大学

乙方：广州威生医药科技有限公司

甲乙双方本着相互协作的精神，合作完成2017年度广东省科技发展专项资金项目（第二批），农村科技领域，专题二十一：现代农业新技术研究与成果转化示范项目“经产母猪新型高效综合繁殖技术研究与示范”，经过协商达成如下协议，并由双方共同恪守。

一、双方负责人：

甲方 华南农业大学 为项目申报单位，负责人为 卫恒习

乙方 广州威生医药科技有限公司 为项目参与单位，负责人为 吴俊辉

二、研究分工：

甲方：主要负责项目申报，制定研究方案，安排和完成相关试验。

乙方：主要负责提供本项目所需生殖激素，协助甲方完成现场试验。

三、研究成果归属：

各方独自完成的研究成果归各方所有，双方共同完成的研究成果双方共享。

四、经费分配：

本项目申报经费 15 万元，若项目获批立项，该项目获得的政府资助资金分配如下：甲方 70%，乙方 30%。具体支付方式根据项目经费管理制度另行约定。

五、其他未尽事宜由合作双方另行协商。

本协议一式三份。甲乙双方各持1份，若项目本年度未获得立项，则此协议自动失效。

八、合同条款

第一条	甲方与乙方根据《中华人民共和国合同法》及国家有关法规和规定，为顺利完成（2017）年经产母猪新型高效综合繁殖技术与示范 专项项目（项目编号： 2017A020208061 ）经协商一致，特订立本合同，作为甲乙双方在项目实施管理过程中共同遵守的依据。
第二条	甲方的权利义务： 1. 按合同书规定进行经费核拨的有关工作协调。 2. 根据甲方需要，在不影响乙方工作的前提下，定期或不定期对乙方项目的实施情况和经费使用情况进行检查或抽查。 3. 根据《广东省科技计划项目信用管理办法(试行)》对乙方进行科技计划信用管理。
第三条	乙方的权利义务： 1. 确保落实自筹经费及有关保障条件。 2. 按合同书规定，对甲方核拨的经费实行专款专用，单独列账，并随时配合甲方进行监督检查。 3. 使用财政资金采购设备、原材料等，按照《广东省实施〈中华人民共和国招标投标法〉办法》有关规定，符合招标条件的须进行招标。 4. 项目实施完成或实施到一定程度，须按照《广东省省级科技计划项目结题管理的实施细则（试行）》提出验收或终止结题的申请，并按甲方要求做好项目结题工作。 5. 在每年1月向甲方如实提交上年度工作情况报告，报告内容包含上年度项目进展情况、经费决算和取得的效果等。 6. 按照国家和省有关规定，每年须提交年度科技报告；项目验收时，须提交验收科技报告。
第四条	在履行本合同的过程中，如出现广东省相关政策法规重大改变等不可抗力情况，甲方有权对所核拨经费的数量和时间进行相应调整。
第五条	在履行本合同过程中，需要对项目起止时间、项目经费使用（包括自筹经费、经费分配及经费支出预算等）、项目内容（包括研发内容、技术指标、经济指标及成果指标等）、项目名称、项目承担单位（包括承担单位更名、承担单位替换）、参与单位、项目负责人和成员等进行变更的，甲乙双方按照《广东省省级科技计划项目合同书管理的实施细则（试行）》有关规定执行。
第六条	在履行本合同的过程中，当事人一方发现可能导致项目整体或部分失败的情形时，应及时通知另一方，并采取适当措施减少损失，没有及时通知并采取适当措施，致使损失扩大的，应当就扩大的损失承担责任。
第七条	本项目技术成果的归属、转让和实施技术成果所产生的经济利益的分享，除双方另有约定外，按国家和广东省有关法规执行。

第八条	属技术保密的项目，甲乙双方应另行订立技术保密条款，作为本合同正式内容的一部分，与本合同具有同等效力。
第九条	根据项目具体情况，经双方另行协商订立的附加条款，作为本合同正式内容的一部分，与本合同具有同等效力。
第十条	本合同的争议应由双方本着协商一致的原则解决，如双方协商不成的，则应向甲方所在地法院提起诉讼。
第十一条	保密条款： 1. 本合同保密内容范围为： (/) 2. 本合同保密期限为： (/) 3. 乙方应与可能知悉保密内容的人员签订技术秘密保护协议。 4. 各方应建立技术秘密保护制度。 5. 属技术保密的项目必须经省负责技术保密部门审查后，确定可否发表或用于国际合作和交流。
第十二条	甲方可根据具体情况决定乙方是否需要单位担保，若需要保证单位，应订立担保条款，作为本合同正式内容一部分。当乙方不履行或不完全履行本合同，以及没有或没有完全承担违约责任时，乙方的保证单位承担连带保证责任。
第十三条	本合同一式六份，各份具有同等效力。甲方存三份，乙方存二份，丙方存一份，本合同自签字之日起生效，有效期至项目结题后一年内。各方均应负合同的法律责任，不应受机构、人事变动的影响。
说明：本合同书中，凡是当事人约定无需填写的内容，应在空白处划（/）。	

九、本合同签约各方

管理单位（甲方）：广东省科学技术厅（盖章）		
单位地址：连新路171号		
法定代表人（或授权代表）：	黄宁生	（签章）
立项责任人：	刘世伟	（签章）
		年 月 日
承担单位（乙方）：华南农业大学（盖章）		
二级部门：华南农业大学动物科学学院		
单位地址：五山路483号		
法定代表人（或法人代理）：	陈晓阳	（签章）
联系人（项目主管）姓名：	郑鹏	（签章）
Email: kjcgxk@scau.edu.cn		
电话：020-85283435 / 13560344902		
开户单位名称：华南农业大学		
开户银行及帐号：	广东广州工行五山支行	3602002609000310520
		年 月 日
乙方主管部门（丙方）：华南农业大学（盖章）		
单位地址：五山路483号		
法定代表人（或法人代理）：	陈晓阳	（签章）
		年 月 日

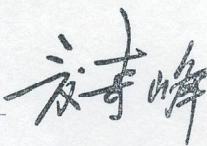
九、本合同签约各方

管理单位（甲方）：广东省科学技术厅（盖章）

单位地址：连新路171号

法定代表人（或授权代表）：

黄宇生



（签章）

立项责任人：刘世伟



（签章）

2017-07-26
年 月 日

承担单位（乙方）：华南农业大学

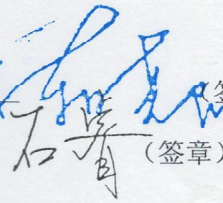
（盖章）

二级部门：华南农业大学动物科学学院

单位地址：五山路483号

法定代表人（或法人代理）：

陈晓阳



（签章）

联系人（项目主管）姓名：

石睿

（签章）

Email: kjcgxk@scau.edu.cn

电话：020-85285390 / 13430350923

开户单位名称：华南农业大学

开户银行及帐号：广东广州工行五山支行 3602002609000310520



2017年 7月 2日

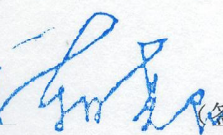
乙方主管部门（丙方）：华南农业大学

（盖章）

单位地址：五山路483号

法定代表人（或法人代理）：

陈晓阳



（签章）



2017年 7月 2日

626

受理编号: c20140500000288

项目编号: 2020A1515010976

文件编号: 粤基金字(2020)4号

广东省基础与应用基础研究基金项目

合同书

项目名称: 断奶母猪PRL/VI分泌规律及其对卵泡血管发生的调控作用

项目类别: 广东省自然科学基金-面上项目

项目起止时间: 2019-10-01 至 2022-09-30

管理单位(甲方): 广东省基础与应用基础研究基金委员会

依托单位(乙方): 华南农业大学

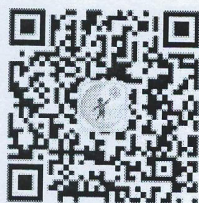
通讯地址: 广东省广州市天河区五山路483号

邮政编码: 510642

单位电话: 020-85283435

项目负责人: 卫恒习

联系电话: 020-85284869



(广东科技微信公众号)

广东省基础与应用基础研究
基金委员会
二〇一九年制



(受理纸质材料二维码)

一、主要研究内容和要达到的目标

主要研究内容:

(1) 母猪断奶后1周, 血清PRL/VI水平及相关生殖激素水平的检测

从母猪断奶当天开始, 每天上、下午定时采血1次, 制备血清。利用ELISA测定血清中PRL、FSH、LH、E2、P4等激素含量, 在利用western blot检测血清中PRL/VI的相对比例与含量。

跟踪记录母猪断奶发情情况, 探索PRL/VI水平与母猪断奶发情的关系。

(2) 断奶后不同时间, 母猪垂体、卵巢和卵泡液中PRL/VI水平及相关基因分子检测

采集断奶后不同时间母猪的垂体和卵巢, 记录卵巢上的卵泡数量和大小。用注射器采集每个卵巢上直径最大的10个卵泡的卵泡液(即该时期的优势卵泡), 利用ELISA和Western blot测定PRL/VI、E2等激素的含量和水平。

制备断奶后不同时间, 母猪垂体和卵巢组织的蛋白样品和RNA样品。利用qRT-PCR在RNA水平检测PRL等生殖激素、相关激素受体(PRLR、FSHR、LHR等)、相关组织蛋白酶(CTSD、MMP和BMP-1)以及血管发生相关基因(VEGF、FGF2等)的表达水平; 利用ELISA和Western blot在蛋白水平上测定PRL/VI等相关激素、组织蛋白酶和血管发生关键基因的表达情况。初步探索PRL/VI生成及其与卵泡血管发生的调控关系。

(3) 利用卵泡细胞体外培养研究PRL/VI对卵泡血管发生关键基因的表达调控作用

从屠宰场收集断奶经产母猪卵巢, 剥离直径3-5mm的健康卵泡, 采用机械和酶消化的方法制备卵泡颗粒细胞和卵泡膜细胞, 进行体外培养。

在培养液中, 添加含有不同PRL/VI水平的猪血清(前期已测定PRL/VI水平的自制血清), 或者添加不同水平PRL/VI重组蛋白。培养48 h后, 利用qRT-PCR和免疫荧光染色技术等检测PRL、PRLR、VEGF、FGF2等关键基因的表达情况, 阐释PRL/VI对卵泡血管发生的调控作用。

要达到的目标:

(1) 揭示母猪断奶后1周内, PRL/VI内分泌及卵巢旁分泌变化规律。

(2) 阐明PRL/VI对卵泡血管发生的调控作用。

(3) 发表论文2-3篇, 其中SCI论文1篇;

(4) 培养研究生1-2人。

二、研究成果及形式

论文及专著情况	国家统计局刊物以上刊物 发表论文（篇）		2		科技报告（篇）		1	
	专著（册）		0					
专利情况(项)	发明专利		实用新型专利		外观设计专利		国外专利	
	申请	授权	申请	授权	申请	授权	申请	授权
	0	0	0	0	0	0	0	0

三、项目进度和阶段目标

1. 项目起止时间： 2019-10-01 至 2022-09-30		
2. 项目实施进度及阶段主要目标：		
开始日期	结束日期	主要工作内容
2019-10-01	2020-09-30	进行断奶初产母猪采血、血清制备及断奶发情率统计，开展血清PRL/VI等激素水平检测及其内分泌变化规律研究。同时，收集断奶后不同时间母猪的垂体和卵巢组织，统计卵巢卵泡发育情况，并制备卵泡液。
2020-10-01	2021-09-30	开展断奶后不同时间，母猪垂体、卵巢和卵泡液中PRL/VI水平及其受体、相关组织蛋白酶以及卵泡血管发生关键基因等的表达检测，揭示PRL/VI的旁分泌规律，并初步探索PRL/VI对卵泡血管发生的调控作用。
2021-10-01	2022-09-30	开展猪卵泡颗粒细胞和卵泡膜细胞体外培养试验，通过在培养液中添加不同水平PRL/VI，研究PRL/VI对卵泡细胞血管发生关键基因表达的调控作用。对试验结果进行总结，发表论文，结题验收。

四、项目总经费及省基金委经费预算

1. 省基金委经费下达总额：（大写）壹拾万圆整；（小写）10万元；

2. 省基金委经费年度下达计划：

年度	2020 年	年	年	年	年
经费(万元)	10.00				

3. 总经费及省基金委经费开支预算计划：

经费筹集情况：

(单位：万元)

省基金委经费	自筹资金				合计
	自有资金	贷款	地方政府投入	其它	
10.00	0	0	0	0	10.00

政府部门、境外资金及其他资金投入情况说明：

无。

- (1) 依托单位是项目资金管理的责任主体，项目负责人是项目资金使用的直接责任人；
- (2) 面上项目经费试点实施“包干制”，不需填报经费开支具体科目预算；
- (3) 经费支出应实际用于项目研究支出，直接经费支出不设科目比例限制，间接经费支出比例按照省级财政科研项目资金管理有关规定执行；
- (4) 项目结题验收须提交经费决算表，不得列支基建费；
- (5) 港澳依托单位承担的面上项目，经费开支标准按照依托单位科研经费管理有关规定执行。

五、人员信息

项目负责人								
姓名	证件号码	年龄	性别	职称	学历	在项目中承担的任务	所在单位	签名
卫恒习	130531198002062019	40	男	副研究员	博士研究生	项目负责人	华南农业大学	卫恒习

项目组主要成员								
姓名	证件号码	年龄	性别	职称	学历	在项目中承担的任务	所在单位	签名
孟立	372922198405063931	36	男	讲师	博士研究生	猪卵泡细胞体外培养与基因表达检测	华南农业大学	孟立
张守全	110108196407089334	56	男	教授	博士研究生	断奶母猪血液和组织样采集	华南农业大学	张守全
李莉	44010619710301186X	49	女	高级畜牧师	硕士研究生	猪卵巢卵泡分离、卵泡细胞制备与培养	华南农业大学	李莉
范玉珊	441881199603040243	24	女	未取得	本科	血液及卵泡液PRL/VI等激素测定	华南农业大学	范玉珊
黄康法	44080419951027053X	25	男	未取得	本科	卵巢和垂体PRL/VI旁分泌及相关基因表达检测	华南农业大学	黄康法
郭聪慧	410727199205054949	28	女	未取得	本科	PRL/VI、PRLR与相关组织蛋白酶表达检测	华南农业大学	郭聪慧

六、依托

承担/参与
(盖章)

华南农业

六、依托单位与合作单位的合作协议

承担/参与单位名称 (盖章)	工作分工	总经费分摊 (万元)	省基金委经费分配 (万元)
华南农业大学	承担全部拟研究内容。	10.00	10.00
	合计	10.00	10.00



2020A1515010976

七、合同条款

第一条 甲方与乙方根据《中华人民共和国合同法》及国家有关法规和规定，为顺利完成（2020）年断奶母猪PRL/VI分泌规律及其对卵泡血管发生的调控作用 专项项目（文件编号：粤基金字（2020）4号）经协商一致，特订立本合同，作为甲乙双方在项目实施管理过程中共同遵守的依据。

第二条 甲方的权利义务：

1. 按合同书规定进行经费核拨的有关工作协调。
2. 根据甲方需要，在不影响乙方工作的前提下，定期或不定期对乙方项目的实施情况和经费使用情况进行检查或抽查。
3. 根据《广东省科技计划项目信用管理办法(试行)》对乙方进行科技计划信用管理。

第三条 乙方的权利义务：

1. 确保落实自筹经费及有关保障条件。
2. 乙方是项目资金管理的责任主体，应当建立健全科研项目资金管理制度，严格按照省科技经费使用范围和有关规定管好用好财政资金；应当按合同书规定，对甲方核拨的经费实行专款专用，单独列账，并随时配合甲方进行监督检查。
3. 实施“包干制”的面上项目及青年基金项目，依托单位应参照国家杰出青年科学基金试点项目经费使用“包干制”要求，制定经费使用“包干制”内部管理规定。项目经费支出应实际用于研发活动相关支出，使用范围限于设备费、材料费、测试化验加工费、燃料动力费、差旅/会议/国际合作与交流费、出版/文献/信息传播/知识产权事务费、劳务费、专家咨询费、依托单位管理费用、绩效支出以及其他合理支出。依托单位管理费用由依托单位根据实际管理支出情况与项目负责人协商确定。绩效支出由项目负责人根据实际科研需要和相关薪酬标准自主确定，依托单位按照现行工资制度进行管理。其余用途经费无额度限制，由项目负责人根据实际需要自主决定使用。项目验收时应提交经费决算表。
4. 项目负责人是项目资金使用的直接责任人，对资金使用的合规性、合理性、真实性和相关性承担法律责任。
5. 使用财政资金采购设备、原材料等，按照《广东省实施〈中华人民共和国招标投标法〉办法》有关规定，符合招标条件的须进行招标。
6. 项目合同任务完成后，或合同书规定的任务、指标及经费投入等提前完成的，乙方可按照《广东省省级科技计划项目结题管理实施细则（试行）》提出验收结题申请，并按甲方要求做好项目验收结题工作。
7. 若项目发生需要终止结题的情况，乙方须按照《广东省省级科技计划项目结题管理的实施细则（试行）》提出终止结题申请，并按甲方要求做好项目终止结题工作。
8. 在每年规定时间内向甲方如实提交上年度工作情况报告，报告内容包含上年度项目进展情况、经费决算和取得的成果等。
9. 按照国家和省有关规定，提交科技报告及其他材料。
10. 利用甲方的经费获得的研究成果，项目负责人和参与者应当注明获得“广东省基础与应用基础研究基金（英文：Guangdong Basic and Applied Basic Research Foundation）（项目编号）”资助或作有关说明。

第五条 在履行本合同的过程中，当事人一方发现可能导致项目整体或部分失败的情形时，应及时通知另一方，并采取适当措施减少损失，没有及时通知并采取适当措施，致使损失扩大的，应当就扩大的损失承担责任。

第六条 本项目技术成果的归属、转让和实施技术成果所产生的经济利益的分享，除双方另有约定外，按国家和广东省有关法规执行。

第七条 根据项目具体情况，经双方另行协商订立的附加条款，作为本合同正式内容的一部分，与本合同具有同等效力。

第八条 本合同一式三份，各份具有同等效力。甲、乙方及项目负责人各执一份，三方签字、盖章后即生效，有效期至项目结题后一年内。各方均应负合同的法律责任，不应受机构、人事变动的影响。

第九条 乙方必须接受甲方聘请的本项目合同监理单位的监督和管理。监理单位按照甲方赋予的权利对本项目合同的履行进行审核、进度调查，对项目合同变更、经费使用情况进行监督管理及组织项目验收。

说明：1. 本合同书中，凡是当事人约定无需填写的内容，应在空白处划（/）。

2. 委托代理人签订本合同书的，应出具合法、有效的委托书。

八、本合同签约各方

管理单位（甲方）：广东省基础与应用基础研究基金委员会（盖章）

法定代表人（或法人代理）：（签章）

年 月 日

依托单位（乙方）：华南农业大学（盖章）

法定代表人（或法人代理）：刘雅红（签章）

联系人（项目主管）姓名：郑鹏（签章）

Email: kjcgxk@scau.edu.cn

电话：020-85283435 / 13560344902

开户单位名称：华南农业大学

开户银行名称：广东广州工行五山支行

开户银行帐号：3602002609000310520

2020年3月6日

联系人（项目负责人）姓名：卫恒习（签名）

卫恒习

Email: weihengxi@163.com

电话：020-85284869

2020年3月17日

受理编号: c24140500002183

项目编号: 2024A1515012529

文件编号: 粤基金字(2024)7号

广东省基础与应用基础研究基金项目

任务书

项目名称: 催乳素通过circSTIP1靶向SGK3调控猪卵泡颗粒细胞增殖的机制研究

项目类别: 广东省自然科学基金-面上项目

项目起止时间: 2024-01-01 至 2026-12-31

管理单位(甲方): 广东省基础与应用基础研究基金委员会

依托单位(乙方): 华南农业大学

通讯地址: 广东省广州市天河区五山路483号

邮政编码: 510642

单位电话: 020-85283435

项目负责人: 卫恒习

联系电话: 020-85284869



(广东科技微信公众号)



(查看任务书信息)



(受理纸质材料二维码)

广东省基础与应用基础研究
基金委员会
二〇二〇年制

填写说明

一、项目任务书内容原则上要求与申报书相关内容保持一致，不得无故修改。

二、项目承担单位通过广东省科技业务管理阳光政务平台下载项目任务书，按要求完成签名盖章后扫描上传到广东省科技业务管理阳光政务平台。

三、签名盖章说明。请分别在单位工作分工及经费分配情况页、人员信息页、签约各方页等地方按要求签字或盖章，签章不合规或错漏将不予受理。其中，人员信息页要求所有参与人员本人亲笔签名，代签或印章无效，漏签将不予受理。

四、本任务书自签字并加盖公章之日起生效，各方均应负本任务书的法律责任，不应受机构、人事变动影响。

五、根据《广东省科学技术厅广东省财政厅关于深入推进省基础与应用基础研究基金项目经费使用“负面清单+包干制”改革试点工作的通知》（粤科规范字（2022）2号），2022年度及以后立项资助的全部省基金项目（包括省自然科学基金、省市联合基金、省企联合基金项目等）均适用“负面清单+包干制”，项目提交申请书和任务书时无需编制费用明细科目预算。

一、主要研究内容和要达到的目标

本项目在前期原创性工作基础上,开展:(1)不同剂量催乳素对猪卵泡颗粒细胞增殖与凋亡的影响及circRNA转录组分析;(2)circSTIP1、miR-182-5p和SGK3对猪颗粒细胞增殖与凋亡的影响以及三者之间靶向调节关系研究,具体包括:circSTIP1、miR-182-5p和SGK3三者之间靶标关系验证,过表达/干扰miR-182-5p对猪颗粒细胞增殖及SGK3等基因表达的影响,过表达/干扰circSTIP1对猪颗粒细胞增殖及SGK3等基因表达的影响,过表达/干扰SGK3对猪颗粒细胞增殖及相关基因表达的影响;(3)PRL和circSTIP1是否通过PI3K-AKT信号通路影响颗粒细胞的增殖与凋亡,包括:PI3K抑制剂联合circSTIP1过表达/干扰对颗粒细胞增殖凋亡的影响,PI3K抑制剂联合PRL处理对猪颗粒细胞增殖凋亡的影响。

通过本项目研究,将阐明PRL和circSTIP1调控猪卵泡颗粒细胞增殖与凋亡的作用机制,为促进猪卵泡发育和断奶后发情技术研究提供理论参考依据。发表论文3-5篇,其中SCI 2篇,培养研究生4人。

二、项目预期获得的研究成果及形式

论文及专著情况	国家统计局刊物以上刊物 发表论文（篇）		4		科技报告（篇）		1	
	其中被SCI/EI/ISTP收录 论文数（篇）		2		培养人才（人）		4	
	专著（册）		0		引进人才（人）		0	
专利情况(项)	发明专利		实用新型专利		外观设计专利		国外专利	
	申请	授权	申请	授权	申请	授权	申请	授权
	0	0	0	0	0	0	0	0

三、项目进度和阶段目标

(一) 项目起止时间： 2024-01-01 至 2026-12-31		
(二) 项目实施进度及阶段主要目标：		
开始日期	结束日期	主要工作内容
2024-01-01	2024-12-31	开展不同剂量催乳素对猪卵泡颗粒细胞增殖凋亡的影响及转录组表达谱分析，获得一批受催乳素调控的差异表达circRNA及mRNA，并利用生物信息学方法进行功能分析和关联分析。发表论文1篇。
2025-01-01	2025-12-31	探究circSTIP1、miR-182-5p和SGK3之间的是否存在靶向调控关系，及其对猪卵泡颗粒细胞增殖与凋亡的影响。发表论文1-2篇。
2026-01-01	2026-12-31	探究催乳素和circSTIP1是否通过PI3K-AKT信号通路调节颗粒细胞的增殖与凋亡，阐释其作用机制；发表论文1-2篇，撰写科技报告，结题验收。

四、项目总经费及省基金委经费预算

1. 省基金委经费下达总额： （大写）壹拾伍万圆整；（小写 ）15万元；					
2. 省基金委经费年度下达计划：					
年度	2024 年	年	年	年	年
经费(万元)	15.00				

五、人员信息

项目负责人								
姓名	证件号码	年龄	性别	职称	学历	在项目中承担的任务	所在单位	签名
卫恒习	130531198002062019	44	男	副研究员	博士研究生	项目负责人	华南农业大学	卫恒习

项目组主要成员								
姓名	证件号码	年龄	性别	职称	学历	在项目中承担的任务	所在单位	签名
孟立	372922198405063931	40	男	讲师	博士研究生	催乳素对circ-S TIP1的调节作用	华南农业大学	孟立
李莉	44010619710301186X	53	女	高级实验师	硕士研究生	细胞培养与基因 表达调控	华南农业大学	李莉
张守全	110108196407089334	60	男	教授	博士研究生	研究技术指导	华南农业大学	张守全
周滢滢	352201199907073225	25	女	未取得	本科	circ-STIP1与GS K3的靶向关系及 作用通路	华南农业大学	周滢滢
游玉彬	421221199911012911	25	男	未取得	本科	GSK3调节颗粒细 胞增殖的信号通 路	华南农业大学	游玉彬
王明明	411422199710045114	27	男	未取得	本科	GSK3过表达和干 扰试验	华南农业大学	王明明
张文浩	140109200011031014	24	男	未取得	本科	催乳素对颗粒细 胞增殖的转录组 分析	华南农业大学	张文浩

六、工作分工及财政经费分配

承担/参与单位名称 (盖章)	工作分工	省级财政科技资金分配 (万元)
华南农业大学	独立完成全部研究任务。	15.00
	合计	15.00

七、任务书条款

第一条 甲方与乙方根据《中华人民共和国民法典》及国家有关法规和规定，按照《广东省科学技术厅关于广东省基础与应用基础研究基金（省自然科学基金、联合基金等）项目管理的实施细则（试行）》《省级科技计划项目任务书管理细则》《广东省省级科技计划项目验收结题工作规程（试行）》等规定，为顺利完成（2024）年催乳素通过circSTIP1靶向SGK3调控猪卵泡颗粒细胞增殖的机制研究专项项目（项目编号：2024A1515012529）经协商一致，特订立本任务书，作为甲乙双方在项目实施管理过程中共同遵守的依据。

第二条 甲方的权利义务：

1. 按任务书规定进行经费核拨的有关工作协调。
2. 根据甲方需要，在不影响乙方工作的前提下，定期或不定期对乙方项目的实施情况和经费使用情况进行检查或抽查。
3. 根据《广东省科研诚信管理办法（试行）》等规定对乙方进行科技计划信用管理。

第三条 乙方的权利义务：

1. 确保落实自筹经费及有关保障条件。
2. 按任务书规定，对甲方核拨的经费实行专款专用，单独列账，并随时配合甲方进行监督检查。
3. 经费使用按照广东省级财政科研项目经费使用等有关规定进行管理。
4. 项目依托单位应制定经费使用“负面清单+包干制”内部管理制度并报甲方备案。
5. 使用财政资金采购设备、原材料等，按照《广东省实施〈中华人民共和国招标投标法〉办法》有关规定，符合招标条件的须进行招标。
6. 项目任务书任务完成后，或任务书规定的任务、指标及经费投入等提前完成的，乙方可提出验收结题申请，并按甲方要求做好项目验收结题工作。
7. 若项目发生需要终止结题的情况，乙方须提出终止结题申请，并按甲方要求做好项目终止结题工作。
8. 在每年规定时间内向甲方如实提交上年度工作情况报告，报告内容包含上年度项目进展情况、经费决算和取得的成果等。
9. 按照国家和省有关规定，提交科技报告及其他材料。
10. 利用甲方的经费获得的研究成果，项目负责人和参与者应当注明获得“广东省基础与应用基础研究基金（英文：Guangdong Basic and Applied Basic Research Foundation）（项目编号）”资助或作有关说明。
11. 乙方要恪守科学道德准则，遵守科研活动规范，践行科研诚信要求，不得抄袭、剽窃他人科研成果或者伪造、篡改研究数据、研究结论；不得购买、代写、代投论文，虚构同行评议专家及评议意见；不得违反论文署名规范，擅自标注或虚假标注获得科技计划（专项、基金等）等资助；不得弄虚作假，骗取科技计划（专项、基金等）项目、科研经费以及奖励、荣誉等；不得有其他违背科研诚信要求的行为。
12. 确保本项目开展的研究工作符合我国科技伦理管理相关规定。

第四条 在履行本任务书的过程中，如出现广东省相关政策法规重大改变等不可抗力情况，甲方有权对所核拨经费的数量和时间进行相应调整。

第五条 在履行本任务书的过程中，当事人一方发现可能导致项目整体或部分失败的情形时，应及时通知另一方，并采取适当措施减少损失，没有及时通知并采取适当措施，致使损失扩大的，应当就扩大的损失承担责任。

第六条 本项目技术成果的归属、转让和实施技术成果所产生的经济利益的分享，除双方另有约定外，按国家和广东省有关法规执行。

第七条 根据项目具体情况，经双方另行协商订立的附加条款，作为本任务书正式内容的一部分，与本任务书具有同等效力。

第八条 本任务书一式三份，各份具有同等效力。甲、乙方及项目负责人各执一份，三方签字、盖章后即生效，有效期至项目结题后一年内。各方均应负任务书的法律责任，不应受机构、人事变动的影响。

第九条 乙方必须接受甲方聘请的本项目任务书监理单位的监督和管理。监理单位按照甲方赋予的权利对本项目任务书的履行进行审核、进度调查，对项目任务书变更、经费使用情况进行监督管理及组织项目验收。

说明：1. 本任务书中，凡是当事人约定无需填写的内容，应在空白处划（/）。

2. 委托代理人签订本任务书的，应出具合法、有效的委托书。

八、本任务书签约各方

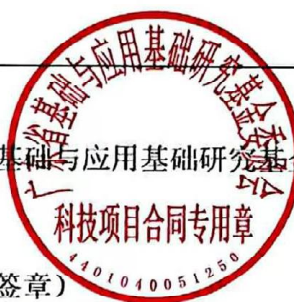
管理单位（甲方）：

广东省基础与应用基础研究基金委员会（盖章）

法定代表人（或法人代理）：

曾路

（签章）



2024 年 05 月 22 日

依托单位（乙方）： 华南农业大学

法定代表人（或法人代理）： 薛红卫

联系人（项目主管）姓名： 倪慧群

Email: kjcgxk@scau.edu.cn

电话： 020-85283435 / 15920301530

开户单位名称： 华南农业大学

开户银行名称： 广东广州工行五山支行

开户银行账号： 3602002609000310520

薛红卫
倪慧群

2024 年 5 月 31 日

联系人（项目负责人）姓名： 卫恒习

（签名）

卫恒习

Email: weihengxi@163.com

电话： 020-85284869

2024 年 5 月 23 日

广东省重点领域研发计划项目 合作任务书

项目名称： 畜禽种质资源高效安全保存与恢复技术体系创新
及应用

项目编号： 2022B0202110002

依托单位（甲方）： 广东省农业科学院动物科学研究所

项目负责人： 邹娴

合作研究单位（乙方）： 华南农业大学

合作研究任务负责人： 卫恒习

合作研究任务名称： 畜禽精液和胚胎冷冻保存与恢复技术研究

起止年限：2022 年 1 月 1 日至 2025 年 12 月 31 日

签订日期：2022 年 8 月 23 日

经协商一致，双方就畜禽种质资源高效安全保存与恢复技术体系创新及应用，项目编号：2022B0202110002 的研究等签订本任务书。

一、受托任务研究目标、研究内容和拟解决的关键问题

挖掘影响精子或胚胎冷冻保存效果的标记 1 个以上；开发胚胎活性相关的标记 1 个以上；建立高效的家畜精液冷冻保存技术体系 1 套；研发有效的鸡精液冷冻保存技术 1 套；提出高效的家畜胚胎冷冻保存技术体系 1-2 套；形成畜禽精液冷冻保存技术质量检测体系和家畜冷冻胚胎质量评价体系各 1 个；家畜精液冷冻-解冻后的复苏率、精子活力与受精能力较技术改良前提高 5%-10%，使冻精复苏率总体达到 50%-60%，精子活力总体达到 40%-50%，配种受胎率达到 50%-60%以上；鸡冷冻精子的复苏率达到 70%以上，受精率达到 5%-10%；家畜胚胎冷冻-解冻复苏率和发育率较技术改良前提高 5%-10%；人工授精、胚胎移植等方法恢复广东畜禽品种 1 个以上。

二、拟采取的研究方法、技术路线及实验方案

1.鸡精液冷冻保存技术研究。通过改良冷冻基础液配方、筛选冷冻保护剂、优化冷冻-解冻工艺等来建立有效的鸡精液冷冻保存技术；对冷冻保存后的精子进行超微结构电镜观察，分析冷冻保存对精子结构与功能的影响。

2.畜禽精液冷冻保存与高效利用技术研究。围绕如何降低畜禽精液冷冻-解冻过程中的物理损伤、化学损伤和氧化损伤，从冷冻保护剂剂量与组合、冷冻精液剂型、精液冷冻-解冻操作程序与工艺、新型抗氧化物质等多方面进行技术改进、优化与集成。重点开展精子冷冻损伤修复及提高精子受精能力的探索性研究，拟在精子解冻复苏过程中通过添加猪浓缩精清、高效抗氧化剂、细胞膜功能调节药物、体外重组精子结构蛋白等措施来降低或修复精子质膜损伤或氧化损伤，提高精子受精能力。

3.家畜胚胎（卵子）冷冻与恢复利用技术研究。对不同家畜胚胎开展系统性的冷冻保存技术研究，筛选适宜冷冻的胚胎发育阶段、优化冷冻液和解冻液成分、优化冷冻-解冻技术程序及工艺、改进胚胎体外培养体系等，对各技术环节进行优化集成，建立稳定高效的胚胎冷冻保存技术体系。

三、年度研究计划及进展

2022 年 1 月 1 日-2022 年 12 月 31 日：发掘猪 SSCs 特异表达、胚胎（卵子）活性、精子功能或胚胎冷冻保存效果相关的基因或标记。申请发明专利 1 件以上，发表高水平文章 1 篇以上，完成年度技术进展报告 1 份。

2023 年 1 月 1 日-2023 年 12 月 31 日：研究、优化畜禽精液和胚胎的冷冻技术。申请发明专利 1 件以上，发表高水平文章 1 篇以上，培养人才 1 名，完成年度技术进展报告 1 份。

2024 年 1 月 1 日-2024 年 12 月 31 日：提出有效的鸡精液冷冻保存技术，建立高效的家畜精液和胚胎冷冻保存技术体系，形成一定规模的广东地方畜种的体细胞、精子库和胚胎（卵子）库，人工授精、胚胎移植等方法恢复广东家畜品种 2 个。申请发明专利 1 件以上，发表高水平文章 1 篇以上，培养人才 1 名，完成年度技术进展报告 1 份。

2025 年 1 月 1 日-2025 年 12 月 31 日：形成畜禽精液冷冻保存技术质量检测体系和家畜冷冻胚胎质量评价体系，建立一套畜禽种质资源中长期保存与恢复技术体系。发表高水平文章 1 篇以上，完成科技报告和项目结题验收。

四、预期研究成果

技术工艺流程固定，技术体系处于成熟阶段，形成可推广应用的技术并示范应用，应用效果到达预期保种目标，提供应用证明。培养研究生 2-3 名，申请专利 3 个，发表文章 4 篇以上（第一标注）。

五、经费支付方式及使用：

财政总经费 36.00 万元；

（一）在科技厅拨款到达甲方后 60 天内将乙方所属经费拨付给乙方。

（二）经费预算

科目名称	乙方经费	用途说明
一、直接经费	29.5	
设备费	0	无
材料费	14.0	项目实施过程中需要消耗的各种原材料、辅助材料、低值易耗品、元器件、试剂、耗材、包装物等的费用
测试化验加工费	4.8	项目实施过程中必须支付给外单位的检验、测试、设计、化验及加工等费用
燃料动力费	0	无
差旅、会议、国际合作交流费	1.8	项目实施过程中开展科学实验、科学考察、业务调研、学术交流等所发生的外埠、差旅、市内交通等费用



出版/文献/信息 传播/知识产权 事物费	3.3	项目实施过程中需要支付的出版费、专用软件购买费、文献检索费、专利申请及其他知识产权事务等费用
劳务费	5.2	项目实施过程中支付给研究生、博士后、临时聘用人员的劳务支出及社会保险等
人员费	0	项目实施过程中项目执行人员工资性支出
专家咨询费	0.4	项目实施过程中支付给临时聘请的咨询专家的费用
二、间接费用	6.5	项目承担单位在组织实施项目过程中发生的无法在直接费用中列支的相关费用，包括房屋、水电费用和绩效支出等
管理费	2.16	管理费
参与人员绩效	4.34	参与人员绩效

六、知识产权归属和分享:

1 项目研究形成的论文，须注明广东省重点领域研发计划资助，项目编号 2022B0202110002 (英文标注: Key Realm R&D Program of GuangDong Province)。

2 在项目执行过程中由乙方自主研发取得的科技成果，乙方享有该成果的专利申请权、使用权、署名权、荣誉权和申请奖励权；甲方享有该成果的优先使用权，但没有转让权。

3 在项目执行过程中由甲乙双方共同获得的科技成果，该成果的专利申请权利为双方共有；当一方不同意申请专利的，另一方不得申请专利。

七、违约责任:

项目实施过程中，乙方每年须撰写项目年度进展报告。项目结束后，乙方须认真总结，撰写结题报告，编制经费决算。

1 甲方未能按任务书约定的经费数提供经费，导致乙方研究工作延误的，由甲方承担责任。

2 因乙方的原因导致研究工作未能按期完成，或者研究成果未能达到任务书约定考核指标的，乙方应当采取措施尽快完成研究工作或者使研究成果达到

任务书要求，并承担由此而增加的费用。

3 乙方无正当理由未履行任务书时，甲方有权停拨、追缴部分或者全部经费，由此造成的经济损失由乙方承担。

4 乙方违反经费使用规定或经甲方检查确认计划进度不符合任务书约定的，甲方有权减拨或停拨后续经费，由此产生的损失由乙方负担；情节严重的，甲方有权终止任务书，乙方应当返还甲方已拨付的经费。

5 任何一方因不可抗力不能履行任务书义务时，应及时通知另一方。在出现不可抗力的情况下，双方均采取适当措施减轻损失。任何一方因未采取措施或采取措施不当导致损失扩大的，应当对扩大的损失承担责任。

八、争议的解决办法：

在本任务书履行过程中发生争议，双方应当协商解决，也可以请求主管部门进行调解。

双方不愿协商、调解解决或者协商、调解不成的，双方商定申请广州仲裁委员会仲裁。

九、名词和术语的解释：无

十、其它：

本任务书自双方签字盖章后生效。对本任务书任何条款的修改、补充或更改，双方必须签订书面协议并签字盖章后方可生效。

本任务书正本一式贰份，具有同等法律效力。

本任务书自 2022 年 1 月 1 日至 2025 年 12 月 31 日有效。



甲 方	单位名称 (盖章)	广东省农业科学院动物科学研究所		
	项目负责人	邹娴 (签字)		
	联系人	邹娴		
	通信地址	广州市天河区大丰一街1号		
	电话	13632390581	Email	zouxian08@163.com
	开户银行	工行广州市五山支行		
	帐号	3602002609000229829-000000001	邮政编码	510642
乙 方	单位名称 (盖章)	华南农业大学		
	项目负责人	卫恒习 (签字)		
	联系人	卫恒习		
	通信地址	广州市天河区五山路483号		
	电话	15902067686	Email	Weihengxi@163.com
	开户银行	广州工商银行五山支行		
	帐号	3602002609000310520	邮政编码	510642



项目批准号	31572397
申请代码	C170104
归口管理部门	
依托单位代码	51064208A0499-0932



3 15723 971004680

国家自然科学基金委员会 资助项目计划书

资助类别：面上项目

亚类说明：

附注说明：常规面上项目

项目名称：种公猪精液蛋白组高通量iTRAQ检测及其繁殖性能调控机制研究

直接费用：63万元 间接费用：12.2万元

项目资金：75.2万元 执行年限：2016.01-2019.12

负责人：张守全

通讯地址：广州市天河区五山路483号

邮政编码：510642 电 话：020-85285087

电子邮件：sqzhang@scau.edu.cn

依托单位：华南农业大学

联系人：全锋 电 话：020-85280070

填表日期：2015年08月23日

国家自然科学基金委员会制

第 119 页，共 307 页

Version: 1.004.680



国家自然科学基金委员会资助项目计划书填报说明

- 一、项目负责人收到《关于国家自然科学基金资助项目批准及有关事项的通知》（以下简称《批准通知》）后，请认真阅读本填报说明，参照国家自然科学基金相关项目管理办法及《国家自然科学基金资助项目资金管理办法》（请查阅国家自然科学基金委员会官方网站首页“政策法规”-“管理办法”栏目），按《批准通知》的要求认真填写和提交《国家自然科学基金委员会资助项目计划书》（以下简称《计划书》）。
- 二、填写《计划书》时要求科学严谨、实事求是、表述清晰、准确。《计划书》经国家自然科学基金委员会相关项目管理部门审核批准后，将作为项目研究计划执行和检查、验收的依据。
- 三、《计划书》各部分填写要求如下：
 - （一）简表：由系统自动生成。
 - （二）摘要及关键词：各类获资助项目都必须填写中、英文摘要及关键词。
 - （三）项目组主要成员：计划书中列出姓名的项目组主要成员由系统自动生成，与申请书原成员保持一致，不可随意调整。如果批准通知中“项目评审意见及修改意见表”中“对研究方案的修改意见”栏目有调整项目组成员相关要求的，待项目开始执行后，按照项目成员变更程序另行办理。
 - （四）资金预算表：按批准资助的直接费用填报资金预算表和预算说明书，其中的劳务费、专家咨询费金额不应高于申请书中相应金额；间接费用及项目总经费由系统自动生成。国家重大科研仪器研制项目还应按照预算评审后批复的直接费用各科目金额填报资金预算表、预算说明书及相应的预算明细表。
 - （五）正文：
 1. 面上项目、青年科学基金项目、地区科学基金项目：如果《批准通知》中没有修改要求的，只需选择“研究内容和研究目标按照申请书执行”即可；如果《批准通知》中“项目评审意见及修改意见表”中“对研究方案的修改意见”栏目明确要求调整研究期限和研究内容等的，须选择“根据研究方案修改意见更改”并填报相关修改内容。
 2. 重点项目、重点国际（地区）合作研究项目、重大项目、国家重大科研仪器研制项目：须选择“根据研究方案修改意见更改”，根据《批准通知》的要求填写研究（研制）内容，不得自行降低、更改研究目标（或仪器研制的技术性能与主要技术指标以及验收技术指标）或缩减研究（研制）内容。此外，还要突出以下几点：
 - （1）研究的难点和在实施过程中可能遇到的问题（或仪器研制风险），拟采用的研究（研制）方案和技术路线；
 - （2）项目主要参与者分工，合作研究单位之间的关系与分工，重大项目还需说明课题之间的关联；
 - （3）详细的年度研究（研制）计划。



3. 国家杰出青年科学基金、优秀青年科学基金和海外及港澳学者合作研究基金项目：须选择“根据研究方案修改意见更改”，按下列提纲撰写：
 - (1) 研究方向；
 - (2) 结合国内外研究现状，说明研究工作的学术思想和科学意义（限两个页面）；
 - (3) 研究内容、研究方案及预期目标（限两个页面）；
 - (4) 年度研究计划；
 - (5) 研究队伍的组成情况。
4. 对于其他类型项目，参照面上项目的方式进行选择和填写。



简表

申请者信息	姓 名	张守全	性 别	男	出生年月	1964年07月	民 族	汉族
	学 位	博士			职称	教授		
	电 话	020-85285087		电子邮件	sqzhang@scau.edu.cn			
	传 真	02085280740		个人网页				
	工 作 单 位	华南农业大学						
	所 在 院 系 所	动物科学学院						
依托单位信息	名 称	华南农业大学					代码	51064208A0499
	联 系 人	全锋		电子邮件	kycjkh@scau.edu.cn			
	电 话	020-85280070		网站地址	http://web.scau.edu.cn/kjc/			
合作单位信息	单 位 名 称							代 码
项目基本信息	项 目 名 称	种公猪精液蛋白组高通量iTRAQ检测及其繁殖性能调控机制研究						
	资 助 类 别	面上项目			亚 类 说 明			
	附 注 说 明	常规面上项目						
	申 请 代 码	C170104: 畜禽繁殖学						
	基 地 类 别							
	执 行 年 限	2016.01-2019.12						
	直 接 费 用	63万元			间 接 费 用	12.2万元		
	项 目 资 金	75.2万元						



项目摘要

中文摘要(500字以内):

提高种公猪繁殖能力是畜牧业发展的核心问题之一,精子受精能力是公猪繁殖性能的重要指标,受到精液蛋白的影响和调控。精液蛋白组学是当前动物繁殖领域的研究热点,精液蛋白与精子受精能力和公猪繁殖性能的关系与作用机制亟待阐释。本项目拟将以科学方法获得的高繁殖力和低繁殖力的合格种公猪、以及全基因组选择的顶级公猪作为主要研究对象,采用高通量iTRAQ蛋白检测技术筛选精液差异表达蛋白,并用生物统计和生物信息学方法分析精液蛋白与公猪繁殖性能的相关性,得到一批新的繁殖性能相关目标蛋白;再通过检测目标蛋白(如GPxs等)在公猪生殖器官、精子和卵子的表达分布,利用体外受精、人工授精等技术研究目标蛋白在受精过程的作用,探索并阐释目标蛋白对精子受精能力的影响及作用机制。本项目研究可为准确评定精液受精能力提供蛋白标记、提高人工授精和种公猪繁殖效率;还可为公猪育种提供重要参考;同时也为人类生殖不孕不育的研究和治疗提供参考。

关键词: 公猪; 繁殖性能; 精液蛋白; 受精能力

Abstract(limited to 4000 words):

The improvement of boar reproductive performance is one of the core problem in animal husbandry. The sperm fertilization ability, which is regulated by semen proteins, is one of the important indicators reflecting boar reproductive ability. Semen proteomics is a hot spot in current research of animal reproduction, and the relationships and mechanism between boar semen proteins and sperm fertilization ability or boar breeding performance are eagerly need to be elucidated. This project intends to take the selected boars of high breeding and low breeding by a scientific method, and the top boars selected by whole genome selection, as the main research objects from a large boar group based on a criterion of qualified conventional semen indexes. Semen differentially expressed proteins were detected with a high flux screening iTRAQ technology, and then a series of new reproductive performance related proteins will be got by using biometric and bioinformatics methods to analyze the correlation between the proteins and boar breeding performance. Then the expression and distribution of the objective proteins (such as GPxs) were detected in boar reproductive organs, sperm and oocyte. And the effect of objective proteins in the process of fertilization was studied by using artificial insemination, in vitro fertilization and related technologies, so as to explore and elucidate the effect and mechanism of objective protein actions with the sperm fertilization ability. This project can provide protein markers for accurate evaluation of semen fertilization capacity, improving the efficiency of artificial insemination and boar reproduction; also it can provide important reference basis for boar breeding; At the same time, it can also provide reference for the research and treatment of infertility in human reproduction.

Keywords: boar; reproductive performance; semen protein; fertilization ability



项目组主要成员

编号	姓名	出生年月	性别	职称	学位	单位名称	电话	证件号码	项目分工	每年工作 时间 (月)
1	张守全	1964. 07	男	教授	博士	华南农业大学	020-85285087	110108196407089334	项目负责人	6
2	卫恒习	1980. 02	男	副研究员	博士	华南农业大学	020-85284869	130531198002062019	精液品质检测、体外受精、胚胎培养	6
3	李莉	1971. 03	女	高级畜牧师	硕士	华南农业大学	020-85280277	44010619710301186X	精液采集与ITRAQ蛋白分析	8
4	刘国乾	1987. 03	男	博士生	硕士	华南农业大学	020-85285897	341225198703140135	差异蛋白功能分析与繁殖相关蛋白质谱筛选	10
5	陈预明	1980. 10	男	博士生	硕士	华南农业大学	020-85285897	441282198010093410	候选差异蛋白与种公猪繁殖性能关联分析	10
6	陈志林	1989. 01	男	硕士生	学士	华南农业大学	020-85285897	445321198901202816	目标蛋白在公猪生殖系统中的分布与定位定量检测	10
7	冯美莹	1989. 05	女	硕士生	学士	华南农业大学	020-85285897	441827198905167925	目标蛋白对精子体外受精能力的影响	10
8	刘凯	1989. 03	男	硕士生	学士	华南农业大学	020-85285897	370883198903016551	目标蛋白对人工授精受孕率的影响	10
9	叶超	1990. 03	男	硕士生	学士	华南农业大学	020-85285897	412827199003104554	目标蛋白的理化特性分析与抗体制备	10
10	付超	1989. 04	男	硕士生	学士	华南农业大学	020-85285897	14010619890407	目标蛋白对精子获能和精卵识别的影响	10

第6页



国家自然科学基金项目资金预算表（定额补助）

项目名称：种公猪精液蛋白组高通量iTRAQ检测及其繁殖性能调控机制研究

项目负责人：张守全

金额单位：万元

序号	科目名称	金额	备注
	(1)	(2)	(3)
1	一、项目资金支出	75.2000	/
2	(一) 直接费用	63.0000	
3	1、设备费	2.0000	
4	(1) 设备购置费	2.0000	小型仪器、易损耗仪器配件的购置
5	(2) 设备试制费	0.0000	
6	(3) 设备改造与租赁费	0.0000	
7	2、材料费	26.0000	试验原材料、试剂耗材、低值易耗品等的采购
8	3、测试化验加工费	15.0000	本项目所需的检验、测试、化验及加工等费用
9	4、燃料动力费	0.0000	
10	5、差旅费	4.0000	开展试验、调研、学术交流等的差旅、交通费
11	6、会议费	0.0000	
12	7、国际合作与交流费	0.0000	
13	8、出版/文献/信息传播/知识产权事务费	3.0000	出版费、资料费、专利申请及其他相关费用
14	9、劳务费	13.0000	在校研究生、博士后和临时聘用人员的劳务费
15	10、专家咨询费	0.0000	
16	11、其他支出	0.0000	
17	(二) 间接费用	12.2000	项目管理费、科研用房、课题组绩效支出等费
18	其中：绩效支出	3.0500	
19	二、自筹资金	0.0000	



预算说明书

(请对各项支出的主要用途和测算理由及合作研究外拨资金等内容进行详细说明,可根据需要另加附页。)

本项目批准直接经费为 63.0 万元,具体金额预算如下:

1、设备费共计 2.0 万元

用于易损耗仪器配件的购置,如荧光显微镜的高压汞灯和生物显微镜的灯泡等四年预计 1.2 万元;为保障猪场现场试验研究顺利进行,计划购买一套移液枪,预计 0.8 万元;合计 2.0 万元。

2、材料费共计 26.0 万元

精液采集、精液蛋白提取与浓缩纯化所需试剂、耗材和试剂盒的费用,预计 4.0 万元;重组蛋白和抗体购置,预计 8.0 万元;新蛋白的体外表达、骨架载体以及相关分子生物学工具酶的购置、新蛋白抗体的制备等,预计 5.0 万元;精子获能和体外受精试验所需卵巢、培养液、细胞因子、激素等试验试剂和耗材的购置,预计 6.0 万元;人工授精试验所需试剂与耗材的费用,预计 2.0 万元;其他实验室常规试剂和材料费等,预计 1.0 万元;合计 26.0 万元。

3、测试化验加工费共计 15.0 万元

精液蛋白 iTRAQ 检测与分析费用预计 20 样本 \times 7000 元/样本=14.0 万元;精子和生殖器官组织切片免疫组化检测、激光共聚焦显微镜检测预计 0.5 万元;蛋白体外重组相关 DNA 引物合成、DNA 序列检测等费用预计 0.5 万元;合计 15.0 万元。

4、差旅费共计 4.0 万元

为加强学术交流,掌握最新研究动态,项目主要参加人员四年拟参加国内学术交流约 10 人次的会议注册、差旅费用预计约 3.5 万元;以及去试验猪场采样等活动所产生的差旅费约 0.5 万元;合计 4.0 万元。

5、出版/文献/信息传播/知识产权事务费共计 3.0 万元

用于资料查新与获取、论文修改与发表版面费等预计 2.4 万元;专利申请、论文打印、网络和信息传播等费用,预计 0.6 万元;合计 3.0 万元。

6、劳务费共计 13.0 万元

用于四年内支付参与本项目研究的研究生劳务费,预计每年平均有 6 位研究生参与本课题研究,平均每人每月 500 元,则 500 元/月 \times 6 人 \times 10 月 \times 4 年=12.0 万元;为了较好完成猪场的采精、人工授精等现场试验,需要临时聘请 1 位技术人员,预计聘期约 4 个月,每月 2500 元,预计 1.0 万元;合计 13.0 万元。

另外,按照国家自然科学基金项目资金管理办法规定,间接费用共计 12.2 万元,其中绩效支出费用为 3.05 万元。

项目负责人签字:

科研部门公章:

财务部门公章:



报告正文

研究内容和研究目标按照申请书执行。



国家自然科学基金资助项目签批审核表

<p>我接受国家自然科学基金的资助，将按照申请书、项目批准意见和计划书负责实施本项目（批准号：31572397），严格遵守国家自然科学基金委员会关于资助项目管理、财务等各项规定，切实保证研究工作时间，认真开展研究工作，按时报送有关材料，及时报告重大情况变动，对资助项目发表的论著和取得的研究成果按规定进行标注。</p> <p>项目负责人（签章）： 年 月 日</p>		<p>我单位同意承担上述国家自然科学基金项目，将保证项目负责人及其研究队伍的稳定和研究项目实施所需的条件，严格遵守国家自然科学基金委员会有关资助项目管理、财务等各项规定，并督促实施。</p> <p>依托单位（公章） 年 月 日</p>					
本栏目由基金委填写	<p>科学处审查意见：</p>						
	<p>建议年度拨款计划（本栏目为自动生成，单位：万元）：</p>						
	年度	总额	第一年	第二年	第三年	第四年	第五年
	金额						
	<p>科学部审查意见：</p> <p>负责人（签章）： 年 月 日</p>					<p>负责人（签章）： 年 月 日</p>	
本栏目主要用于重大项目等	<p>相关局室审核意见：</p> <p>负责人（签章）： 年 月 日</p>						
	<p>委领导审批意见：</p> <p>委领导（签章）： 年 月 日</p>						



项目批准号	32272873
申请代码	C1704
归口管理部门	
依托单位代码	51064208A0499-0932



国家自然科学基金 资助项目计划书 (预算制项目)

资助类别：面上项目

亚类说明：

附注说明：

项目名称：IZUM02蛋白提高公猪繁殖性能的机理研究

直接费用：54万元 执行年限：2023.01-2026.12

负责人：张守全

通讯地址：广州市天河区五山路483号

邮政编码：510642 电 话：020-85285087

电子邮件：sqzhang@scau.edu.cn

依托单位：华南农业大学

联系人：唐家林 电 话：020-85280070

填表日期：2022年09月16日

国家自然科学基金委员会制

第 130 页，共 307 页

Version: 1.003.317



国家自然科学基金资助项目计划书填报说明 （预算制项目）

- 一、项目负责人收到《国家自然科学基金资助项目批准通知》（以下简称《批准通知》）后，请认真阅读本填报说明，参照国家自然科学基金相关项目管理办​​法和新修订的《国家自然科学基金资助项目资金管理办法》（以下简称《资金管理办法》，请查阅国家自然科学基金委员会官方网站首页“政策法规”栏目），按《批准通知》的要求认真填写和提交《国家自然科学基金资助项目计划书》（以下简称《计划书》）。
- 二、填写《计划书》时要科学严谨、实事求是、表述清晰、准确。《计划书》经国家自然科学基金委员会相关项目管理部门审核批准后，将作为项目研究计划执行、检查和验收的依据。
- 三、《计划书》各部分填写要求如下：
 - （一）简表：由系统自动生成。
 - （二）摘要及关键词：各类获资助项目都应当填写中、英文摘要及关键词。
 - （三）项目组主要成员：计划书中列出姓名的项目组主要成员由系统自动生成，与申请书原成员保持一致，不可随意调整。如果《批准通知》所附“项目评审意见及修改意见表”中“修改意见”栏目有调整项目组成员相关要求的，待项目开始执行后，按照项目成员变更程序另行办理。
 - （四）资金预算表：根据批准的项目资助额度，按规定调整项目预算，并按照《国家自然科学基金项目计划书预算表编制说明》填报资金预算表和预算说明书。
 - （五）正文：
 1. 面上项目、地区科学基金项目：如果《批准通知》所附“项目评审意见及修改意见表”中“修改意见”栏目没有修改要求的，只需选择“研究内容和研究目标按照申请书执行”即可；如果《批准通知》中上述栏目明确要求调整研究期限或研究内容等的，须选择“根据研究方案修改意见更改”并填报相关修改内容。
 2. 重点项目、重点国际（地区）合作研究项目、重大项目、国家重大科研仪器研制项目、原创探索计划项目：须选择“根据研究方案修改意见更改”，根据《批准通知》的要求填写研究（研制）内容，不得自行降低、更改研究目标（或仪器研制的技术性能与主要技术指标、验收技术指标等）或缩减研究（研制）内容。此外，还要突出以下几点：
 - （1）研究的难点和在实施过程中可能遇到的问题（或仪器研制风险），拟采用的研究（研制）方案和技术路线；
 - （2）项目主要参与者分工，合作研究单位（如有）之间的关系与分工，重大项目还需说明课题之间的关联；
 - （3）详细的年度研究（研制）计划。
 3. 创新研究群体项目：须选择“根据研究方案修改意见更改”，按下列提纲撰写：
 - （1）研究方向；



- (2) 结合国内外研究现状，说明研究工作的学术思想和科学意义（限两个页面）；
 - (3) 研究内容、研究方案及预期目标（限两个页面）；
 - (4) 年度研究计划；
 - (5) 研究队伍的组成情况。
4. 基础科学中心项目：须选择“根据研究方案修改意见更改”，根据《批准通知》的要求和现场考察专家组的意见和建议，进一步完善并细化研究计划，按下列提纲撰写：
 - (1) 五年拟开展的研究工作（包括主要研究方向、关键科学问题与研究内容）；
 - (2) 研究方案（包括骨干成员之间的分工及合作方式、学科交叉融合研究计划等）；
 - (3) 年度研究计划；
 - (4) 五年预期目标和可能取得的重大突破等；
 - (5) 研究队伍的组成情况。
5. 对于其他类型项目，参照面上项目的方式进行选择和填写。



简表

项目负责人信息	姓 名	张守全	性 别	男	出生年月	1964年07月	民 族	汉族
	学 位	博士			职称	教授		
	是否在站博士后	否			电子邮件	sqzhang@scau.edu.cn		
	电 话	020-85285087			个人网页			
	工 作 单 位	华南农业大学						
	所 在 院 系 所	动物科学学院						
依托单位信息	名 称	华南农业大学					代码	51064208A0499
	联 系 人	唐家林			电子邮件	kycjkh@scau.edu.cn		
	电 话	020-85280070			网站地址	http://kjc.scau.edu.cn/		
合作单位信息	单 位 名 称							
项目基本信息	项 目 名 称	IZUM02蛋白提高公猪繁殖性能的机理研究						
	资 助 类 别	面上项目				亚 类 说 明		
	附 注 说 明							
	申 请 代 码	C1704: 畜禽繁殖学						
	基 地 类 别							
	执 行 年 限	2023.01-2026.12						
	直 接 费 用	54万元						



项目摘要

<p>中文摘要:</p> <p>受精蛋白在精卵融合中发挥重要作用，直接影响公猪的繁殖性能。我们前期发现IZUM02蛋白在公猪睾丸和精子中特异性表达，精子中该蛋白浓度与公猪繁殖性能呈显著正相关，且IZUM02抗体抑制体外受精的受精率和卵裂率。IZUM02蛋白能显著提高公猪繁殖性能，但相关机制尚不清楚。本项目将以长白公猪为研究对象，探究不同生长时期IZUM02在生殖组织中的定位和表达水平及其与繁殖性能的相关性；制备猪IZUM02蛋白及其单克隆抗体，比较高低IZUM02组中精子活力参数、IZUM02蛋白定位模式和表达水平，并分析猪精稀释液添加该蛋白对体外受精的影响；IP-MS鉴定IZUM02互作蛋白并进行生信分析，通过分析互作蛋白表达、与IZUM02的共定位及体外受精试验来探究其对IZUM02重定位以及精卵融合的影响。研究结果将阐明IZUM02提高公猪繁殖性能的机制，为IZUM02蛋白成为评定高繁公猪的分子标记提供理论基础。</p>
<p>Abstract:</p> <p>Fertilization proteins play an important role in sperm-egg fusion, which directly affects the reproductive performance of boars. We previously found that IZUM02 protein was specifically expressed in testis and sperm of boars. The concentration of IZUM02 protein in sperm was significantly positively correlated with the reproduction performance of boars, and IZUM02 antibody inhibited the fertilization rate and cleavage rate of in vitro fertilization. IZUM02 protein can significantly improve the reproductive performance of boars, but the related mechanism remains unclear. This study will use Landrace boars as our research object to explore the localization and expression level of IZUM02 in reproductive tissues at different growth stages and its correlation with reproductive performance. We will prepare porcine IZUM02 protein and its monoclonal antibody, compare sperm motility parameters, IZUM02 protein localization pattern and expression level in high and low IZUM02 groups, and analyze the effect of adding this protein in porcine semen diluent on in vitro fertilization. The interaction proteins of IZUM02 will be identified by IP-MS and analyzed by bioinformatics. We will explore the effect of interacting proteins on IZUM02 protein relocation and sperm-egg fusion by analyzing the expression level of interacting proteins, co-localization with IZUM02 and in vitro fertilization. These results will clarify the mechanism of IZUM02 protein to improve the reproductive performance of boars, and provide a theoretical basis for IZUM02 protein to become a molecular marker for evaluating high-breeding boars.</p>
<p>关键词(用分号分开): 猪; 繁殖性能; IZUM02蛋白; 精卵融合</p>
<p>Keywords(用分号分开): Pig; reproductive performance; IZUM02 protein; sperm-egg fusion</p>



项目组主要成员

编号	姓名	出生年月	性别	职称	学位	单位名称	电话	证件号码	项目分工	每年工作 时间 (月)
1	张守全	1964. 07	男	教授	博士	华南农业大学	020-85285087	110108196407089334	项目负责人	6
2	卫恒习	1980. 02	男	副研究员	博士	华南农业大学	020-85284869	130531198002062019	项目参与人	6
3	李莉	1971. 03	女	高级实验师	硕士	华南农业大学	020-85280277	44010619710301186X	项目参与人	6
4	孟立	1984. 05	男	讲师	博士	华南农业大学	020-85284869	372922198405063931	项目参与人	6
总人数		高级		中级		初级		博士后	博士生	硕士生
10		3		1					1	5



项目批准号: 32272873

项目负责人：张守全

金额单位：万元

序号	科目名称	金额
1	一、基金资助项目直接费用合计	54.0000
2	1、设备费	0.0000
3	其中：设备购置费	0.0000
4	2、业务费	40.3000
5	3、劳务费	13.7000
6	二、其他来源资金	0.0000
7	三、合计	54.0000

注：请按照项目研究实际需要合理填写各科目预算金额。



预算说明书

（请按照《国家自然科学基金项目计划书预算表编制说明》等的有关要求，按照政策相符性、目标相关性和经济合理性原则，实事求是编制项目预算。填报时，直接费用应按设备费、业务费、劳务费三个类别填报，每个类别结合科研任务按支出用途进行说明。填报时，对单价 ≥ 50 万元的设备详细说明，对单价 < 50 万元的设备费用分类说明，对合作研究单位资质及资金外拨情况、自筹资金进行必要说明。）

本项目直接经费为54.00万元，均为国家自然科学基金资助，项目所在单位基本配备了试验研究所需的仪器设备，不需要专门为本项目购买5万元以上大型仪器。具体金额预算如下：

1、业务费（40.30万元）

材料耗材费（24.41万元）

1) 3月龄、6月龄和15月龄公猪(试验动物)购买，每个时期各3头猪，平均每头猪5500元， $5500\text{元}/\text{头} \times 3\text{头} \times 3\text{时期} = 49500\text{元}$ ；计划购买30只成年C57BL雌性小鼠，平均每只30元， $30\text{元}/\text{只} \times 30\text{只} = 900\text{元}$ ，合计50400元。2) 各种试剂盒（蛋白质提取试剂盒， $50\text{T}/580\text{元}/\text{盒} \times 10\text{盒} = 5800\text{元}$ ；蛋白质浓度测定试剂盒， $500\text{T}/388\text{元}/\text{盒} \times 2\text{盒} = 776\text{元}$ ；总RNA提取试剂盒， $100\text{T}/320\text{元}/\text{盒} \times 5\text{盒} = 1600\text{元}$ ；逆转录试剂盒， $100\text{T}/755\text{元}/\text{盒} \times 5\text{盒} = 3775\text{元}$ ；qRT-PCR试剂盒， $200\text{T}/4126\text{元}/\text{盒} \times 3\text{盒} = 12378\text{元}$ ；IZUM02 ELISA试剂盒， $96\text{T}/2980\text{元}/\text{盒} \times 3\text{盒} = 8940\text{元}$ ；精子顶体形态检测试剂盒， $20\text{次}/1318\text{元}/\text{盒} \times 1\text{盒} = 1318\text{元}$ ），合计34587元。3) 免疫荧光试验及Western-blot所需试剂购置，预计20000元。4) 慢病毒转染试剂+单克隆抗体制备等试剂，预计52850元；5) 精子获能和体外受精试验所需卵巢、培养液、细胞因子、激素等试验试剂和耗材的购置，预计40000元。6) 耗材费用：（培养皿、培养瓶、离心管、冻存管、EP管、枪头、一次性滤器、注射器、超高速离心管和玻璃吸管等35000元）+常规试验试剂等，预计45000元。7) 小鼠饲养费 $250\text{元}/\text{包} \times 1\text{包}/\text{月} \times 5\text{月} = 1250\text{元}$ 。

测试试验加工费用（6.49万元）

1) 各生殖组织切片免疫组化和原位杂交检测（免疫组化， $30\text{元}/\text{片} \times 45\text{片} = 1350\text{元}$ ；原位杂交， $300\text{元}/\text{片} \times 45\text{片} = 13500\text{元}$ ），合计14850元。2) 免疫共沉淀样品的质谱鉴定，预计50000元；

差旅/会议/国际合作与交流费（5.40万元）

1) 为加强学术交流，掌握最新研究动态，项目主要参加人员四年拟参加国内学术交流约12人次的会议注册、差旅费用约42000元；2) 以及去试验猪场采样等活动所产生的差旅费约12000元；

出版/文献/信息传播/知识产权事务费（4.00万元）

1) 用于资料查新与获取、论文修改与发表版面费等预计30000元；2) 专利申请相关费用预计6000元；3) 论文打印、网络和信息传播等费用，预计4000元；

2、劳务费（13.70万元）

1) 用于四年内支付参与本项目研究的研究生劳务费。

博士研究生1人，劳务费800元/月，每年参与工作10个月，工作4年，共32000元

硕士研究生5人，劳务费500元/月，每年参与工作10个月，工作4年，共100000元

2) 临时用工费（5000元）：支付给临时用工的费用，如采样时固定公猪、采血等临时用工。



报告正文

研究内容和研究目标按照申请书执行。



国家自然科学基金项目负责人、依托单位承诺书

国家自然科学基金项目负责人承诺书

本人郑重承诺：我接受国家自然科学基金的资助，严格遵守中共中央办公厅、国务院办公厅《关于进一步加强科研诚信建设的若干意见》《关于进一步弘扬科学家精神加强作风和学风建设的意见》《关于加强科技伦理治理的意见》等规定，及国家自然科学基金委员会关于资助项目管理、项目资金管理等各项规章，在《计划书》填写及项目执行过程中：

（一）按照《批准通知》《国家自然科学基金资助项目计划书填报说明》的要求填写《计划书》，未自行降低、更改目标任务或约定要求，或缩减研究（研制）内容；

（二）树立“红线”意识，严格履行科研合同义务，按照《计划书》负责实施本项目（批准号：32272873），切实保证研究工作时间，按时报送有关材料，及时报告重大情况变动，不违规将科研任务转包、分包他人，不以项目实施周期外或不相关成果充抵交差；

（三）遵守科研诚信、科技伦理规范和学术道德，认真开展研究工作，对资助项目发表的论著和取得的科研成果按规定进行标注，不在非本项目资助的成果或其他无关成果上标注本项目批准号，反对无实质学术贡献者“挂名”，不在成果署名、知识产权归属等方面侵占他人合法权益，并如实报告本人及项目组成员发生的违背科研诚信要求的任何行为；

（四）尊重科研规律，弘扬科学家精神，严谨求实，追求卓越，反对浮夸浮躁、投机取巧，不人为夸大学术或技术价值，不传播未经科学验证的现象和观点；

（五）将项目资金全部用于与本项目研究工作相关的支出，并结合科研活动需要，科学合理安排项目资金支出进度；

（六）做好项目组成员的教育和管理，确保遵守以上相关要求。

如违背上述承诺，本人愿接受国家自然科学基金委员会和相关部门做出的各项处理决定。

项目负责人（签字）：

年 月 日

依托单位科研管理部门：

负责人（签章）：

年 月 日

依托单位财务管理部门：

负责人（签章）：

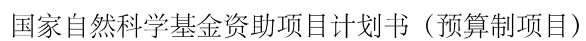
年 月 日

国家自然科学基金项目依托单位承诺书

我单位同意承担上述国家自然科学基金项目，将保证项目负责人及其研究队伍的稳定和研究项目实施所需的条件，严格遵守国家自然科学基金委员会有关资助项目管理、项目资金管理、科研诚信管理和科技伦理管理等各项规定，并督促实施。

依托单位（公章）

年 月 日



本栏目由自然科学基金委填写

负责人（签章）：
年 月 日

负责人（签章）：
年 月 日

国家重点研发计划
课题任务书

课题名称： 经产母猪定时输精及批次化繁殖技术研发与示范

所属项目： 畜禽繁殖调控新技术研发

所属专项： 畜禽重大疫病防控与高效安全养殖综合技术研发

项目牵头承担单位： 中国农业大学

课题承担单位： 北京市农林科学院

课题负责人： 刘彦

执行期限： 2017 年 07 月 至 2020 年 12 月

中华人民共和国科学技术部制

2017 年 07 月 08 日

0003YF 2017YFD0501902 2017-07-08 15:05:10



负责人	证件类型	身份证	证件号码	132521196511040037	
	所在单位	北京市农林科学院			
	最高学位	□博士■硕士□学士□其他			
	职 称	■正高级□副高级□中级□初级□其他		职务	副所长
	电子邮箱	liuyanxms@163.com		移动电话	13910419699
课题联系人	姓 名	白佳桦	电子邮箱	bai_jiahua@126.com	
	固定电话	010-51503110	移动电话	15801450572	
	证件类型	身份证	证件号码	230805198108110020	
课题财务负责人	姓 名	徐恋	电子邮箱	xmscaiwu@163.com	
	固定电话	010-51503495	移动电话	15201201901	
	证件类型	身份证	证件号码	420104198012272026	
其他参与单位	序号	单位名称		单位性质	组织机构代码
	1	北京市农林科学院		事业型研究单位	12110000400638193R
	2	华南农业大学		大专院校	124400004554165634
	3	重庆市畜牧科学院		事业型研究单位	12500000450402779M
	4	四川农业大学		大专院校	450718925
	5	扬州大学		大专院校	466007837
课题参加人数	43 人。其中：		高级职称 14 人，中级职称 5 人，初级职称 2 人，其他 22 人；		
			博士学位 11 人，硕士学位 13 人，学士学位 17 人，其他 2 人。		
课题简介 (限 500 字以内)	基于环境、营养、管理等因素导致国内规模化猪场母猪断奶后不能及时发情或不发情，使得繁殖障碍问题多发，断奶母猪群繁殖节律不整齐，母猪淘汰率加大，最终造成母猪繁殖效率显著低于国外养猪发达国家水平；与此同时，国内现有的每天查情配种繁殖模式，导致同一栋生长猪舍接纳不同繁殖批次的猪群，使得猪场断奶后的猪只生产无法实现整个栋舍的全进全出，不同批次猪群的混养直接引发多种病原累积和疫病顽疾的存留，严重制约了猪场的疫病防控和健康养殖。目前在欧美等养猪业发达的国家，已经初步建立了以定时输精技术为核心的批次化生产管理，真正意义上实现了猪场生产的全进全出，在保持高繁殖水平的同时，				

九、课题参加人员基本情况表

序号	姓名	性别	出生日期	身份证号码 (军官证、护照)	技术 职称	职务	学位	专业	投入本课题的 全时工作时间 (人月)	人员 分类	在课题中分 担的任务	工作单位
1	刘彦	男	1965-11-04	132521196511040037	正高级	副所长	硕士	动物繁殖	24	课题负责人	定时输精与批 次化生产技术 研究	北京市农林科学院
2	张守全	男	1964-07-08	110108196407089334	正高级	无	博士	动物繁殖	24	课题骨干	定时输精与批 次化生产技术 研究与基地示 范	华南农业大学动物科技学院
3	黄毓茂	男	1964-09-27	440106196409271977	副高级	无	博士	兽医	27	课题骨干	定时输精与批 次化生产技术 研究与基地示 范	华南农业大学兽医学院
4	郭宗义	男	1965-09-02	513101196509020015	正高级	所长	硕士	畜牧	24	课题骨干	同期分娩及示 范	重庆市畜牧科学院
5	林燕	女	1979-12-26	511025197912260885	副高级	无	博士	动物营养与 饲料科学	32	课题骨干	母猪繁殖营养 研究	四川农业大学动物营养研究所
6	孙晓梅	女	1986-01-13	232101198601133224	中级	无	博士	动物遗传育 种与繁殖	24	课题骨干	定时输精机理 研究	扬州大学动物科技学院
7	白佳桦	女	1981-08-11	230805198108110020	中级	无	博士	生物科学类	20	其他研究人 员	定时输精与批 次化生产技术 研究	北京市农林科学院



8	许晓玲	女	1980-07-18	511123198007183661	副高级	无	博士	动物生产与兽医类	20	其他研究人员	定时输精与批 次化生产技术 研究	北京市农林科学院
9	冯涛	男	1980-07-07	622801198007070452	副高级	无	博士	动物生产与兽医类	32	其他研究人员	定时输精与批 次化生产技术 研究	北京市农林科学院
10	潘红梅	女	1979-08-15	510524197908150165	副高级	无	硕士	畜牧兽医	18	其他研究人员	同期分娩及示 范	重庆市畜牧科学院
11	张亮	男	1982-02-01	510231198202011237	副高级	无	硕士	畜牧兽医	18	其他研究人员	同期分娩及示 范	重庆市畜牧科学院
12	苏丹萍	女	1965-04-10	45010319650410052X	其他	无	学士	兽医	12	其他研究人员	定时输精与批 次化生产技术 研究与基地示 范	华南农业大学兽医学院
13	卫恒习	男	1980-02-06	130531198002062019	副高级	无	博士	动物繁殖	24	其他研究人员	定时输精与批 次化生产技术 研究与基地示 范	华南农业大学动物科学学院
14	李莉	女	1971-03-01	44010619710301186X	正高级	无	硕士	动物繁殖	24	其他研究人员	定时输精与批 次化生产技术 研究与基地示 范	华南农业大学动物科学学院
15	徐盛玉	女	1983-01-30	510303198301302523	副高级	无	博士	动物营养与 饲料科学	28	其他研究人员	母猪繁殖营养 研究	四川农业大学动物营养研究所
16	吴彩梅	女	1978-02-21	230523197802211245	副高级	无	硕士	动物营养与	28	其他研究人员	母猪繁殖营养 研究	四川农业大学动物营养研究所



单位研究经费支出预算明细表

表B5 课题编号： 2017YFD0501902 课题名称： 经产母猪定时输精及批次化繁殖技术研发与示范 金额单位：万元

填表说明： 1.单位类型分课题承担单位、课题参与单位； 2.组织机构代码指企事业单位国家标准代码，单位若已三证合一请填写单位统一社会信用代码，无组织机构代码的单位填写“000000000000”。											
序号	单位名称	组织机构代码-统一社会信用代码		单位类型	任务分工	研究任务负责人	合计	中央财政资金		其他来源资金	
		(1)	(2)					小计	其中：间接费用		
1	北京市农林科学院		统一社会信用代码	12110000400638193R	课题承担单位	负责“经产母猪定时输精及批次化繁殖技术总体设计，重点开展经产母猪同期排卵程序优化与改进，集成适用于中小规模猪场的批次化高效繁殖生产工艺并示范。	刘彦	98.00	16.38		
2	华南农业大学		统一社会信用代码	124400004554165634	课题参与单位	优化改进经产母猪同期排卵程序，提高猪群的断奶同步性和发情同步性，建立批次化生产，疫病防控程序，集成示范大型猪场批次化高效繁殖生产工艺。协助开展添加NAC、NCG等提高经产母猪受胎率试验。	张守全/黄毓茂	120.00	19.00		

国家重点研发计划课题合作协议（2017 年度）

为了更好的完成国家重点研发计划中“畜禽重大疫病防控与高效安全养殖综合技术研发”中“畜禽繁殖调控新技术研发”项目下课题“经产母猪定时输精及批次化繁殖技术研发与示范”的研究目标，本着优势互补、协同配合、共同发展的原则，经平等协商，课题主持单位北京市农林科学院（甲方）和课题参加单位 华南农业大学（乙方）达成如下协议。

1. 甲乙双方承诺遵守国家重点研发计划项目和经费管理办法及其他相关法律文件。

2. 乙方的研究任务是：（1）开展经产母猪同期排卵定时输精技术应用程序优化与改进；（2）围绕提高断奶猪群的发情同步性，开展相关机理研究；（3）建立批次化生产疫病防控程序；（4）集成大型猪场批次化高效繁殖生产工艺并示范；（5）开展添加 N-乙酰半胱氨酸（NAC）、N-氨甲酰谷氨酸（NCG）等提高经产母猪受胎率试验；（6）接受课题统一安排的其他任务。

考核指标：（1）制定母猪定时输精技术处理程序 1-2 项；（2）建立批次化生产疫病防控程序 1-2 套；（3）建立批次化高效繁殖生产技术核心示范基地 1-2 家，初产母猪淘汰率降低 5-10%，批次妊娠率 85%以上；（4）发表本研究内容相关的 SCI 论文 3 篇（第一标注为本课题）；申请发明专利 2 项。

3. 乙方国拨经费 120.00 万元（具体支出科目预算由课题主持单位另行下达），自筹经费 0 万元。如最终获批经费有变化，项目牵头单位有权对各课题和各参加单位的经费进行调整。

4. 甲方应按照合同任务书规定及时将经费拨付给乙方。

5. 乙方应根据课题任务书要求及时开展相关研究，并定期报告课题进展和研究数据，按照研究计划及考核指标要求按时、保质、保量地完成任务。

6. 乙方积极配合项目组的安排，按要求完成项目任务。如乙方在课题执行过程中，出现研究进展严重滞后、研究方案的重大改动、经费不合理开支等方面的情形，应及时上报给项目及课题组织单位。

7. 各方合作研究产生的科研成果和知识产权归本项目共有，未经项目负责人同意，相关成果（文章、专利等）不得用于申报各类奖励。

8. 本协议一式十份。

甲方（公章）：北京市农林科学院

法人（签章）：

日期：

乙方（公章）：华南农业大学

法人（签章）：

日期：2017.6.20

刘彦

张子全
董毓成

检索证明

根据委托人提供的论文材料，委托人华南农业大学动物科学学院 卫恒习 2 篇论文收录情况如下表。

序号	论文名称	发表刊物及发表的年月卷期/页码等	作者排名	论文等级	作者工作单位	收录情况	影响因子	中科院大分区
1	Age-Specific Gene Expression Profiles of Rhesus Monkey Ovaries Detected by Microarray Analysis	BIOMED RESEARCH INTERNATIONAL 出版年: 2015 卷期: 2015 页码: - 文献号: 625192 文献类型: Article	第一作者	B 类	华南农业大学 动物科学学院	SCI	IF2-year=2.134 IF5-year=2.149 (2015)	生物 3 区 Top 期刊: 否 (2015)
2	Optimizing of Activation Protocols and Production of Transgenic Pigs Expressing Human Lysozyme by Somatic Cell Nuclear Transfer	PROGRESS IN BIOCHEMISTRY AND BIOPHYSICS 出版年: 2013 出版日期: JAN 卷期: 40 1 页码: 72-79 文献类型: Article	第一作者		华南农业大学 动物科学学院	SCI	IF2-year=0.29 IF5-year=0.221 (2013)	无

说明: 论文等级和中科院大分区按《华南农业大学学术论文评价方案(试行)》划分。

报告免责声明: 如未盖章, 报告无效



检索证明

根据委托人提供的论文材料，委托人华南农业大学动物科学学院 卫恒习 8 篇论文收录情况如下表。

序号	论文名称	发表刊物及发表的年月卷期/页码等	作者排名	论文等级	作者工作单位	收录情况	影响因子	中科院大类分区
1	Investigation Into the Relationship Between Sperm Cysteine-Rich Secretory Protein 2 (CRISP2) and Sperm Fertilizing Ability and Fertility of Boars	FRONTIERS IN VETERINARY SCIENCE 出版年: 2021 出版日期: APR 30 卷期: 8 页码: - 文献号: 653443 文献类型: Article	通讯作者	A 类	华南农业大学 动物科学学院	SCI	IF2-year=3.471 IF5-year=3.821 (2021)	农林科学 2 区 Top 期刊: 否 (2021)
2	PF-05231023 reduces lipid deposition in apolipoprotein E-deficient mice by inhibiting the expression of lipid synthesis genes	FRONTIERS IN VETERINARY SCIENCE 出版年: 2024 出版日期: JUL 31 卷期: 11 页码: - 文献号: 1429639 文献类型: Article	共同通讯作者 (倒数第一)	A 类	华南农业大学 动物科学学院	SCI	IF2-year=2.9 IF5-year=3.3 (2024)	农林科学 2 区 Top 期刊: 否 (2025)
3	Semen Protein CRISP3 Promotes Reproductive Performance of Boars through Immunomodulation	INTERNATIONAL JOURNAL OF MOLECULAR SCIENCES 出版年: 2024 出版日期: FEB	共同通讯作者 (倒数第一)	B 类	华南农业大学 动物科学学院	SCI	IF2-year=4.9 IF5-year=5.7 (2024)	生物学 3 区 Top 期刊: 否 (2025)

	卷期: 25 4 页码: - 文献号: 2264 文献类型: Article								
4	Identification of new protein biomarkers associated with the boar fertility using iTRAQ-based quantitative proteomic analysis	INTERNATIONAL JOURNAL OF BIOLOGICAL MACROMOLECULES 出版年: 2020 出版日期: NOV 1 卷期: 162 页码: 50-59 文献类型: Article	并列第一作者, 共同通讯作者	A类		华南农业大学 动物科学学院	SCI	IF2-year=6.953 IF5-year=6.737 (2020)	化学 2 区 Top 期刊: 是 (2020)
5	Cloprostenol sodium improves reproductive performance of multiparous sows during lactation	FRONTIERS IN VETERINARY SCIENCE 出版年: 2024 出版日期: JAN 31 卷期: 11 页码: - 文献号: 1342930 文献类型: Article	共同通讯作者	A类		华南农业大学 动物科学学院	SCI	IF2-year=2.9 IF5-year=3.3 (2024)	农林科学 2 区 Top 期刊: 否 (2025)
6	Epigallocatechin-3-Gallate Promotes the in vitro Maturation and Embryo Development Following IVF of Porcine Oocytes	DRUG DESIGN DEVELOPMENT AND THERAPY 出版年: 2021 卷期: 15 页码: 1013-1020 文献类型: Article	通讯作者	B类		华南农业大学 动物科学学院	SCI	IF2-year=4.319 IF5-year=4.556 (2021)	医学 3 区 Top 期刊: 否 (2021)

7	A novel identified circ-ANKRD1 targets the miR-27a-3p/SFRP1 signaling pathway and modulates the apoptosis of granulosa cells	ENVIRONMENTAL SCIENCE AND POLLUTION RESEARCH 出版年: 2021 出版日期: NOV 卷期: 28 41 页码: 57459-57469 文献类型: Article	通讯作者	B类	华南农业大学 动物科学学院	SCI	IF2-year=5.19 IF5-year=5.053 (2021)	环境科学与生态学 3区 Top 期刊: 否 (2021)
8	Perfluorooctanoic acid inhibits the maturation rate of mouse oocytes cultured in vitro by triggering mitochondrial and DNA damage	BIRTH DEFECTS RESEARCH 出版年: 2021 出版日期: AUG 15 卷期: 113 14 页码: 1074-1083 文献类型: Article	共同通讯作者	B类	华南农业大学 动物科学学院	SCI	IF2-year=2.661 IF5-year=2.871 (2021)	医学 4区 Top 期刊: 否 (2021)

说明: 论文等级和中科院大类分区按《华南农业大学学位论文评价方案(试行)》划分。

报告免责声明: 如未盖章, 报告无效



检索证明

根据委托人提供的论文材料，委托人华南农业大学动物科学学院 卫恒习 2 篇论文收录情况如下表。

序号	论文名称	发表刊物及发表的年月卷期/页码等	作者排名	论文等级	作者工作单位	收录情况	影响因子	中科院大类分区
1	猪催乳素的真核表达与生物活性验证	华南农业大学学报 出版年：2024 卷期： 页码： - 文献号： 文献类型：	通讯作者	B 类	华南农业大学 动物科学学院	北大核心	无	无
2	左旋肉碱对猪卵母细胞体外成熟、脂肪代谢和孤雌胚胎发育的影响	华南农业大学学报 出版年：2014 卷期： 页码： - 文献号： 文献类型：	通讯作者	B 类	华南农业大学 动物科学学院	北大核心	无	无

说明：论文等级和中科院大类分区按《华南农业大学学位论文评价方案（试行）》划分。

报告免责声明：如未盖章，报告无效



Research Article

Age-Specific Gene Expression Profiles of Rhesus Monkey Ovaries Detected by Microarray Analysis

Hengxi Wei,¹ Xiangjie Liu,¹ Jihong Yuan,² Li Li,¹ Dongdong Zhang,²
Xinzheng Guo,¹ Lin Liu,² and Shouquan Zhang¹

¹Guangdong Provincial Key Lab of Agro-Animal Genomics and Molecular Breeding, National Engineering Research Center for Breeding Swine Industry, College of Animal Science, South China Agricultural University, Guangzhou, Guangdong 510642, China

²State Key Laboratory of Medicinal Chemical Biology, Department of Cell Biology and Genetics, College of Life Sciences, Nankai University, Tianjin 300071, China

Correspondence should be addressed to Shouquan Zhang; sqzhang@scau.edu.cn

Received 7 June 2015; Accepted 29 July 2015

Academic Editor: Dominique Alfandari

Copyright © 2015 Hengxi Wei et al. This is an open access article distributed under the Creative Commons Attribution License, which permits unrestricted use, distribution, and reproduction in any medium, provided the original work is properly cited.

The biological function of human ovaries declines with age. To identify the potential molecular changes in ovarian aging, we performed genome-wide gene expression analysis by microarray of ovaries from young, middle-aged, and old rhesus monkeys. Microarray data was validated by quantitative real-time PCR. Results showed that a total of 503 (60 upregulated, 443 downregulated) and 84 (downregulated) genes were differentially expressed in old ovaries compared to young and middle-aged groups, respectively. No difference in gene expression was found between middle-aged and young groups. Differentially expressed genes were mainly enriched in cell and organelle, cellular and physiological process, binding, and catalytic activity. These genes were primarily associated with KEGG pathways of cell cycle, DNA replication and repair, oocyte meiosis and maturation, MAPK, TGF-beta, and p53 signaling pathway. Genes upregulated were involved in aging, defense response, oxidation reduction, and negative regulation of cellular process; genes downregulated have functions in reproduction, cell cycle, DNA and RNA process, macromolecular complex assembly, and positive regulation of macromolecule metabolic process. These findings show that monkey ovary undergoes substantial change in global transcription with age. Gene expression profiles are useful in understanding the mechanisms underlying ovarian aging and age-associated infertility in primates.

1. Introduction

In the past few decades, ovarian aging has been considered one of the most detrimental factors contributing to pregnancy failure, and the age-related decline in female fecundity has distinct implications in view of the current trend of postponing childbearing [1, 2]. Premature ovarian failure (POF), also known as premature menopause, affects 1%-2% of women younger than 40 years of age and 0.1% of women younger than 30 years of age [3] and is another common cause of female infertility [4].

Rhesus monkeys (*Macaca mulatta*) are the most frequently used nonhuman primate model, because they live in close association with each other and have many similarities

with humans in anatomy, physiology, and genetics [5]. Many parameters including circadian rhythm, seasonality, and hormonal effects on the brain in the rhesus macaque have been studied using species-specific gene microarrays [6]. Experimental analysis of the aging process (or senescence) has been challenging [7]. As the value of the aging model of the rhesus monkey increases with completion of the sequencing of the rhesus genome [8], it is necessary to make more efficient and extensive use of this model to understand the processes underlying aging and disease in humans [9]. Several theories of aging have been proposed, including free radical [10], glycation [11], and caloric restriction [12, 13] theories. Mechanisms of aging that involve mitochondria [14], DNA damage and repair [15], DNA methylation [16],

telomeres [17], and cellular senescence and apoptosis [18] have also been proposed. The primary reason for the decline with age in female fertility is the gradual loss of oocytes and follicles, which were formed during embryonic development [19]. Chromosomal abnormalities, mitochondrial DNA mutations, telomere shortening, and even aging itself have been suggested to be related to the decreased oocyte quality associated with aging, and it was concluded that ovarian aging may be only a specific reflection of general aging [20]. The new hypothesis of protein glycation and that of oxidative stress and mitochondrial dysfunction, which are closely related to calcium regulation, are considered to be the main cellular and molecular mechanisms underlying aging of the ovarian follicle [21].

Previous studies identified genes that are differentially expressed in an age-dependent manner using microarray analysis of mouse oocytes, ovary, and ovarian surface epithelial cells as well as human oocytes [22–27]. In rhesus monkey, microarray analysis has been performed to identify the mechanisms involved in the brain's white matter aging and corpus luteum regression [28, 29]. However, there is still a paucity of knowledge about primate ovarian failure, because the ovary is a functional unit, and most age-related changes in gene expression are species-specific [30, 31]. In order to investigate the molecular and biological mechanisms of ovarian aging and to identify genes that may play a role in oocyte/ovarian aging or POE, we performed genome-wide microarray analysis of ovaries from young, middle-aged, and old rhesus monkeys. The genes affected by aging may serve as important targets for delaying ovarian aging or for the clinical treatment of POE.

2. Materials and Methods

2.1. Animals. All animal procedures were performed according to guidelines developed by the China Council on Animal Care, and protocols were approved by the Animal Care and Use Committee of Guangdong Province, China. The approval ID is SCXK (Guangdong) 2004-0011 and the permit number is SYXK (Guangdong) 2007-0081. The monkeys were housed in ordinary animal facilities in a temperature-controlled (25°C) and light-regulated (12 h light/12 h dark) room and fed commercial nonhuman primate diets twice daily, supplemented with fresh fruits and water ad libitum. Female rhesus monkeys were all reproductive and healthy and randomly chosen from three different aged groups according to experimental design and supplied by Guangxi Grandforest Scientific Primate Company, Ltd.

The experimental design is briefly as follows: the old group (18 to 19 years) had lost their reproductive capacity; the middle-aged group (7 to 8 years) had good reproductive capacity; and the young group (3 to 4 years) had normal estrous cycles but had never bred. The ovary collection time of young and middle-aged monkeys was approximately at the proestrus stage according to their reproductive records. A minimal number of 3 monkeys of each group were used in this study to minimize ethical concerns. All individual ovaries from the three groups were examined histologically and by microarray analysis to investigate the ovary status

the gene expression profiles, and the differentially expressed genes between groups.

2.2. Ovary Collection. All monkeys were housed under the same conditions, and the ovary collection was conducted in October. Monkeys were deeply anaesthetized with 4 mL of 3% sodium pentobarbital per kilogram of body weight by intravenous injection and sacrificed by femoral artery exsanguination and, simultaneously, transcatheterially perfused with 4 L of Krebs-Henseleit buffer (prepared under RNase-free conditions and containing 6.41 mM Na_2HPO_4 , 1.67 mM NaH_2CO_3 , 137 mM NaCl, 2.68 mM KCl, 5.55 mM glucose, 0.34 mM CaCl_2 , and 2.14 mM MgCl_2 , pH 7.4) at 4°C [29]. Surgery was carried out according to standard operating procedures. Some organs were collected by other institutions, and only one ovary of each monkey was allocated to our laboratory. The ovaries were cut in half vertically at their widest point, and one half was immediately frozen in liquid nitrogen and sent to CapitalBio Corporation (Beijing, China) in dry ice for microarray analysis; the other half was transported to our laboratory in dry ice for histological and qRT-PCR analysis.

2.3. Histological Analysis and Follicle Counting. The half-ovaries from young, middle-aged, and old monkeys were again cut in half vertically at their widest points. One part of the tissue was randomly selected and stored in liquid nitrogen for further qRT-PCR validation of microarray results. The other part was immersed in 4% paraformaldehyde for 24 h and then dehydrated in increasing concentrations of ethanol and in xylene. The tissues were embedded in paraffin, and sections of 5 μm were cut and aligned on glass microscope slides. After deparaffinization in xylene, the sections were rehydrated through decreasing concentrations of ethanol in water and stained with hematoxylin and eosin Y. The tissue sections were dehydrated again, coverslips were applied with neutral gum, and sections were viewed and photographed with an Olympus BX53F microscope. To avoid counting a structure twice, one out of every 20 serial sections was analyzed for the number of follicles in different developmental stages using slightly modified standard methods [32, 33], and all the whole sections were analyzed. Primordial and primary follicles were identified by the presence of an oocyte surrounded by a single layer of flat or cuboidal cells. Secondary follicles were characterized as having more than one layer of granulosa cells with no visible antrum. Antral follicles possessed areas of follicular fluid (antrum) or a single large antral space. These follicles with normal morphology were scored as healthy follicles. And atretic follicles were characterized with shrank nuclei and degenerate oocytes and loosened layer of granulosa cells. And the relic atretic follicles were defined as atretic follicles without clear oocyte nuclei, which were not counted as atretic follicles in our statistics. A one-way ANOVA analysis was used to assess the statistical significance of follicles among different groups.

2.4. RNA Isolation and Microarray Analysis. RNA was isolated from each half-ovary sent to CapitalBio for microarray detection and validation of the microarray data by quantitative real-time polymerase chain reaction (qRT-PCR).

Total RNA was extracted using TRIzol reagent (Invitrogen, Carlsbad, CA, USA) and further purified using the Qiagen RNeasy Mini Kit (Germantown, MD, USA) according to the manufacturer's instructions. RNA quality was assessed by formaldehyde agarose gel electrophoresis, and the RNA was quantitated spectrophotometrically.

The *M. mulatta* Genome Array (Affymetrix) containing 47,000 transcripts was obtained from CapitalBio Corporation (Beijing, China). RNA derived from each of the nine monkeys was run on an individual microarray, and microarray experiments were performed as described previously [34]. After hybridization, the arrays were scanned with LuxScan 10 K-A scanner (CapitalBio) and the data from the obtained images were extracted using LuxScan 3.0 software (CapitalBio). A space and intensity-dependent normalization based on a LOWESS program was employed [35]. For each test and control sample, two hybridization processes were performed by using a reversal of the fluorescent dye strategy. Only genes with consistent differential expression (both above 1.5-fold change) in both microarray assays were selected as differentially expressed genes. The description of this microarray study follows the Minimum Information About a Microarray Experiment (MIAME) guidelines [36], and the data was submitted to Gene Expression Omnibus (GEO) with accession number of GSE44533.

2.5. Validation of Microarray Results by qRT-PCR. Twenty-five differentially expressed genes were randomly selected and validated with the same RNA preparations that were used to generate microarray data, and 8 out of the 25 genes were again validated with the new RNA samples from the same ovary tissues by qRT-PCR. Beta-actin was used as an internal standard. The gene-specific qRT-PCR primers were designed according to the coding sequences (Table 1). Briefly, total RNA from each of the nine monkeys was digested with DNase I (TaKaRa, Dalian, China). First-strand cDNAs were synthesized with oligo(dT) primers using a PrimeScript II 1st Strand cDNA Synthesis Kit (code D6210A, TaKaRa). Quantitative RT-PCR was performed using the SsoFast EvaGreen Supermix (Bio-Rad, Hercules, CA) and CFX96 Quantitative Real-Time PCR Detection System (Bio-Rad). Each 20 μ L qRT-PCR mixture included 10 μ L SsoFast EvaGreen Supermix, 1 μ L cDNA, 0.2 μ M primers, and 8.6 μ L double-distilled water. PCR was carried out under conditions of initial denaturation at 95°C for 30 sec, followed by 40 cycles of denaturation at 95°C for 5 sec, annealing at 60°C for 30 sec, and extension at 72°C for 30 sec. A melting curve was plotted from 65°C to 95°C to check the specificity of the amplified product. Each of the amplifications was carried out in duplicate, and the mean values were calculated using the $\Delta\Delta C_t$ method. The results (fold change) were determined and expressed as $2^{\Delta\Delta C_t}$ according to the following formula:

$$\Delta\Delta C_t = (C_{tij} - C_{t\beta\text{-actin}j}) - (C_{ti1} - C_{t\beta\text{-actin}1}), \quad (1)$$

where C_{tij} and $C_{t\beta\text{-actin}j}$ are the C_t values for gene i and β -actin, respectively, in sample j . C_{ti1} and $C_{t\beta\text{-actin}1}$ are the C_t values in sample 1, expressed as the standard [37]. Student's t -test or one-way ANOVA analysis was used to assess the

statistical significance of differential expression levels of each gene among the three groups of monkeys using GraphPad Prism 5.0 software.

2.6. GO Terms and KEGG Pathway Analysis. Gene Ontology (GO) terms and Kyoto Encyclopedia of Genes and Genomes (KEGG) pathway were analyzed using the free, web-based Molecular Annotation System 3.0 (MAS 3.0, <http://bioinfo.capitalbio.com/mas3/>). Gene products were analyzed according to the GO ontologies molecular function, biological process, and cellular component. The P values less than 0.01 were considered significance. All differentially expressed genes were input, and the results obtained with the categories of GO terms and the KEGG pathways were presented in the form of a Microsoft Excel 2007 spreadsheet.

Due to the lack of comprehensive gene annotation information for *M. mulatta*, we assumed that the orthologous genes conserved between human and *M. mulatta* were functionally conserved. The relationships between human and *M. mulatta* genes were based on Ensembl release 74 (<http://www.ensembl.org/>) and retrieved using Bio-Mart (<http://www.biomart.org/>). We used human-*M. mulatta* orthologs to identify the differently expressed genes. The functional annotation of these human genes in the functional category and KEGG pathway was performed using DAVID Bioinformatics Resources [38]. Probabilities were evaluated by Bonferroni correction, and values less than 0.001 were considered significant.

3. Results and Discussion

3.1. Aged Monkey Ovaries Show Morphological Changes and Differentially Expressed Genes. Our results showed great change in ovarian morphology of different aged monkeys. In young and middle-aged monkey ovaries, follicles at various developmental stages, including many primordial and primary, several secondary, and mature follicles, were observed. The numbers of primordial and primary and secondary follicles significantly decreased with age, and the number of antral follicles increased significantly from young to middle-aged ovary, as we previously reported in [39], whereas only a few primary or atretic follicles and no antral follicles were seen in the ovaries of old monkeys (Figure 1). Herein, we found that the total follicles and the number of healthy follicles significantly decreased with aging, and the number of atretic follicles increased significantly in middle-aged groups and then decreased in the old groups when compared to young animals (Table 2). The morphology of the ovarian surface epithelium also changed with age. In young ovaries, the germinal epithelium was smooth, thick, and clearly distinguishable from the cortex. In the middle-aged ovary, the germinal epithelium was thin, and, in the old ovary, epithelial fibrosis had taken place, making the epithelium indistinguishable from the cortex (Figure 1).

Nine microarrays representing ovaries collected from three monkeys in each of the age groups were analyzed. Approximately 47,000 probe sets detected 35,000 genes (see GSE44533, in GEO database). The log-log scatter plot analysis showed good quality of the microarray assays (Figure 2(a)).

TABLE 1: Primers used for qRT-PCR.

RefSeq transcript ID	Gene symbol	Sequence (5' to 3')	Amplicon size (bp)
XM_001096328	<i>MRAP</i>	S: GCTGCTCCTCTTCCTCATCC A: TCAGTTCTGCTCCCTGGCTC	204
XM_001104871	<i>MMP9</i>	S: AGTCCACCCTTGTGCTCTTC A: CTGCCACCCGAGTGTAAC	103
NM_001042638	<i>THY1</i>	S: CCTGACCCGTGAGACAAAG A: GGTGAAGGCGGATAAGTAGAG	127
XM_001109859	<i>LOC717872</i>	S: GTGAACGGTCGCCTGTATC A: AAAACTGGGGTCCTTGAGC	241
XM_001097914	<i>IGFBP4</i>	S: AATTCGAGACCGGAGCAC A: GGATGGGAATGATGTAGAGGT	170
XM_001103253	<i>NASP</i>	S: GGGCTTGGCTTATGGGT A: ATCTCGGGTAGCAGTTCCTT	177
XM_001085259	<i>PTTG1</i>	S: GCTTTGGGAACCGTCAAC A: TTCTGGATAGGCATCGTCTG	153
XR_011039	<i>AURKA</i>	S: TCTGTGGCACCCTGGACTA A: AGGAGGCTTCCCAACTAAAA	119
XM_001085850	<i>BCL2L10</i>	S: GTGACAGCCTGGTGGAAGA A: AAGCCTGGATCAGCAGTTT	220
XM_001084147	<i>BARD1</i>	S: GAAAGCCCAAGCCAGACA A: ACTTTGCCCTGCCGAAC	151
XM_001101192	<i>TACC3</i>	S: ATGTGCCACCCAAGAACG A: AGCCAAAGGAGCCTCAAGT	122
XM_001095416	<i>THBD</i>	S: TGTGAGCACTTCTGCGTTCC A: CCAGGTCGTAGCCAGGTTT	199
XM_001083479	<i>DNMT3A</i>	S: GGTTTACCCACCTGTCCCA A: CACCTGAATGCCCAAGTCC	109
XM_001114760	<i>ZP3</i>	S: GCACTCCAAGCCATTCCA A: GGCCCACTGCTCTACTTCATA	158
XR_010378	<i>LOC703074</i>	S: GAACTCTTCAAGCGTGTCTCA A: CCAGGTCGTTTCATGTTGCT	130
XM_001087511	<i>WASF1</i>	S: CTTTCTGCCTTGCCATTTAG A: AGGTGGGTATCGGTTTCG	133
XR_011694	<i>LOC707199</i>	S: GACCTGAAGGACCGTTTG A: CAGGAGGAAGTTGTGGGAGAT	132
XM_001106702	<i>MCM3</i>	S: AAGATGGGGATTTCATACGACC A: GCCTTCAACCTGGATTCACT	139
XM_001098017	<i>IGF2BP3</i>	S: ATCTGAACGCCTTGGGTC A: TTGCTCAAACCTGCGGGTA	101
XM_001105684	<i>XRCC6</i>	S: GCGAGCACTCAGCAGGTTA A: GTCTTGGTTTTCACTGGTTCAT	141
XM_001094077	<i>HELLS</i>	S: ACTTCCTAACTGGATGGCTGAG A: GCTGTAAACGCATTTCCGGTCT	188
XM_001095697	<i>CDK1</i>	S: CCTAGCATCCCACGTCAAA A: ATGATTCACTGCCATTTTGC	109
XM_001093457	<i>FGF14</i>	S: CCAAGATCCCCAGCTCAA A: TGGAACAACACGCAGTC	158
XM_001104061	<i>UBE2C</i>	S: TATGCCTGGACATCCTGAAG A: GGGACTATCAATGTTGGGTTC	104
XM_001093770	<i>THBS1</i>	S: GCCAGGGCGTCGAATAT A: TGCCATTGCCAGCGTAG	168
NM_001033084.1	<i>ACTB</i>	S: GCCCTGAGGCTCTCTTCCA A: CGGATGTCCACGTCACACTT	100

ACTB served as internal control. S: sense; A: antisense.

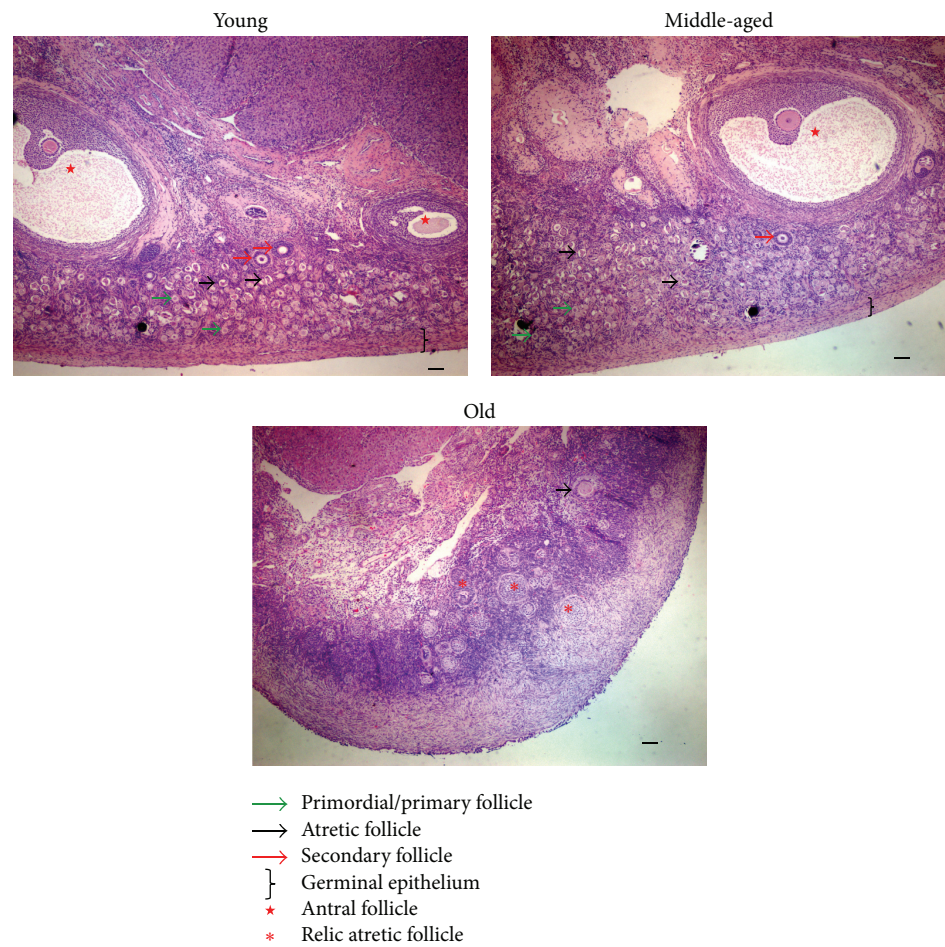


FIGURE 1: Morphology of monkey ovaries of different ages. Hematoxylin and eosin Y-stained sections of ovaries from monkeys of indicated ages. Key to structures indicated by symbols appears below images. Bar = 100 μ m.

TABLE 2: Comparison analysis of follicles numbers in different aged monkey ovaries.

Groups	Number of ovaries counted	Number of sections counted per ovary	Number of healthy follicles per ovary per animal (mean \pm SEM)	Number of atretic follicles per ovary per animal (mean \pm SEM)*	Total follicles per ovary per animal (mean \pm SEM)
Young	3	31	22097 \pm 1243.0 ^A	400.7 \pm 21.4 ^A	22498 \pm 1264.0 ^A
Middle-aged	3	33	12581 \pm 512.7 ^B	534.7 \pm 39.1 ^B	13115 \pm 499.4 ^B
Old	3	20	7.3 \pm 2.3 ^C	2.7 \pm 1.1 ^C	10.0 \pm 1.3 ^C

* Atretic follicles with no obvious oocytes were not counted. A, B, and C in each column indicate significant differences among groups ($P < 0.001$).

The remarkable influence of age was demonstrated by hierarchical cluster analysis (Figure 2(b)). After SAM analysis of the microarray data, 503 genes were differentially expressed (fold change, +1.5 or -1.5) between the old and the young groups; of these, 60 were upregulated in the ovaries of old monkeys (Figure 3(a)). Only 84 genes were differentially expressed between the old and middle-aged groups, all of which were downregulated in the ovaries of old monkeys. These two sets of 503 and 84 differentially expressed genes shared 75 common genes (Figure 3(a)). No difference in gene expression was found between the middle-aged and young

groups. Of the total of 512 differentially expressed genes, the functions of 264 genes, of which 35 were upregulated and 229 were downregulated, are still unknown (highlighted in Table S1 in Supplementary Material available online at <http://dx.doi.org/10.1155/2015/625192>).

The current work firstly presents the global gene expression profile of ovarian aging in rhesus monkey. Although previous research has focused on ovarian aging in mice [26, 40, 41], the aging process is quite different between mice and humans [30], emphasizing the need for human or nonhuman primate tissue to elucidate the mechanism of aging of human

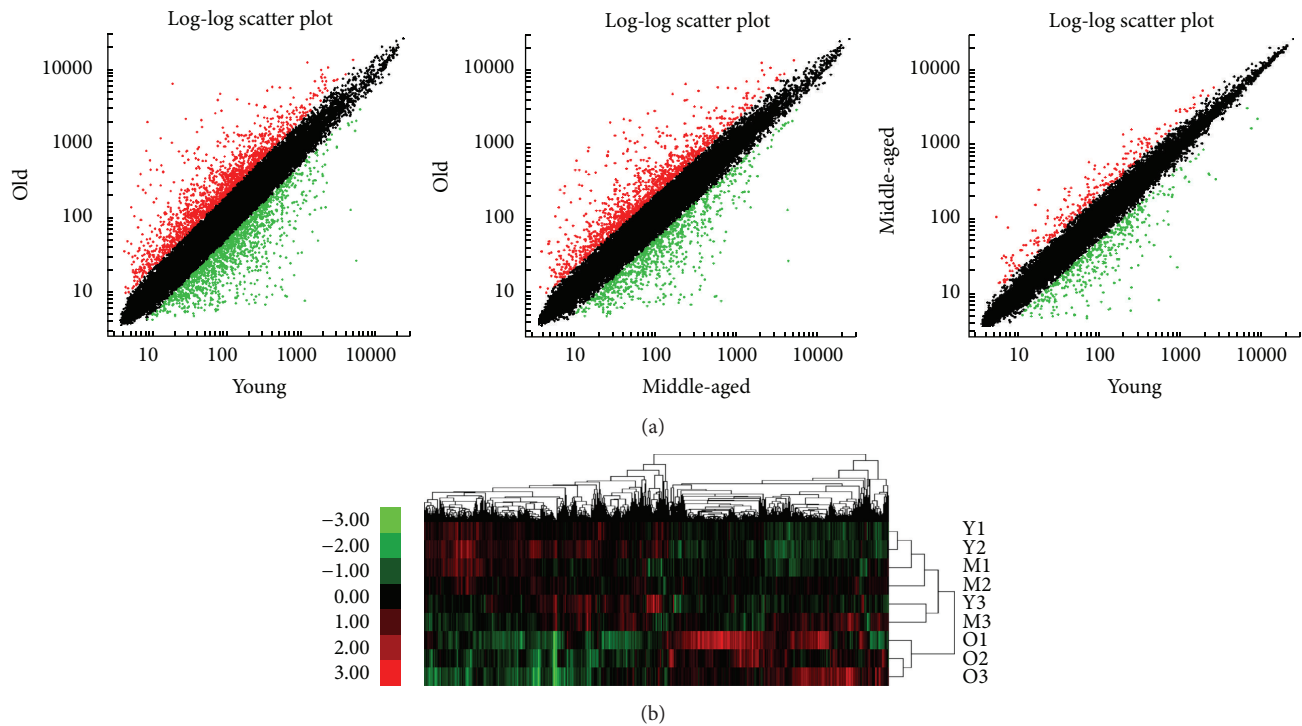


FIGURE 2: Gene expression profiles of monkey ovaries of different ages. (a) Log-log scatter plot analysis between groups of different ages. It shows good quality of microarray data; the red and green dots indicate upregulated and downregulated genes, respectively. (b) Hierarchical cluster of differentially expressed genes in old (O), middle-aged (M), and young (Y) groups. The expression level of each gene is standardized to a mean value of 0 and standard deviation (SD) of 1. The mean value is represented by black, gene expression above the mean level is represented by red, and expression below the mean is represented by green. The intensity of the pseudocolor reflects the number of SDs from the mean, as indicated in key at left. 1–3: animals 1–3 in each group.

ovaries. The gene expression profiles of metaphase II oocytes derived from women of different ages suggest that cell cycle, oxidative stress and DNA repair, meiosis and spindle function, and ubiquitination might be affected by age [22]; however, the processes underlying ovarian aging remain obscure. Although our study is limited, as whole ovaries were sampled which contain multiple cell types [27, 42], hundreds of differentially expressed genes were found related to age, and such global gene expression profiles of monkey ovaries of different ages constitute a useful resource. In the future, investigations of age-related differential gene expression in individual cell types are warranted. Although not focused on aging, a novel resource of nonhuman primate oocytes and preimplantation embryos has already been established which might facilitate gene expression pattern analysis in single cell types [31, 43].

3.2. Validation of Microarray Data by qRT-PCR. Quantitative RT-PCR was performed to validate 25 differentially expressed genes selected randomly (5 upregulated and 20 downregulated in old ovaries) using the same RNA preparations used to generate microarray data (Table 3). As expected, MRAP and MMP9 were expressed at significantly different levels ($P < 0.05$) in the old and young groups and were upregulated in the old group. THY1, Loc717872, and IGBBP4 showed

the same trend toward upregulation in old ovaries, although no significant differences were found using Student's *t*-test. Microarray and qRT-PCR data were in good agreement with most genes that were significantly downregulated, or trending in that direction, in old ovaries. However, some significant differential expression identified by microarray analysis (e.g., of *BARD1*, *LOC707199*, *IGF2BP3*, and *XRCC6*) was not validated by qRT-PCR analysis (Table 3). Surprisingly, microarray analysis found that *THBD* was downregulated in old ovaries; however, qRT-PCR analysis showed a trend toward upregulation (Table 3). Moreover, some genes were identified as significantly differentially expressed by qRT-PCR but not by microarray analysis, including *MRAP*, *HELLS*, *CDK1*, and *UBE2C* in old versus middle-aged ovaries (Table 3). This could result from an experimental artifact or the different significance levels calculated [37]. Furthermore, eight out of the 25 genes were randomly selected and validated by qRT-PCR analysis with new RNA samples, and the results were in agreement with those of the previous validation and microarray analysis (Figure 4), indicating the reliability of the microarray data.

3.3. GO Terms and KEGG Pathway Analysis. All differentially expressed genes were input into MAS 3.0 and assigned to individual GO terms for *M. mulatta*, with 53.15%, 30.58%, and

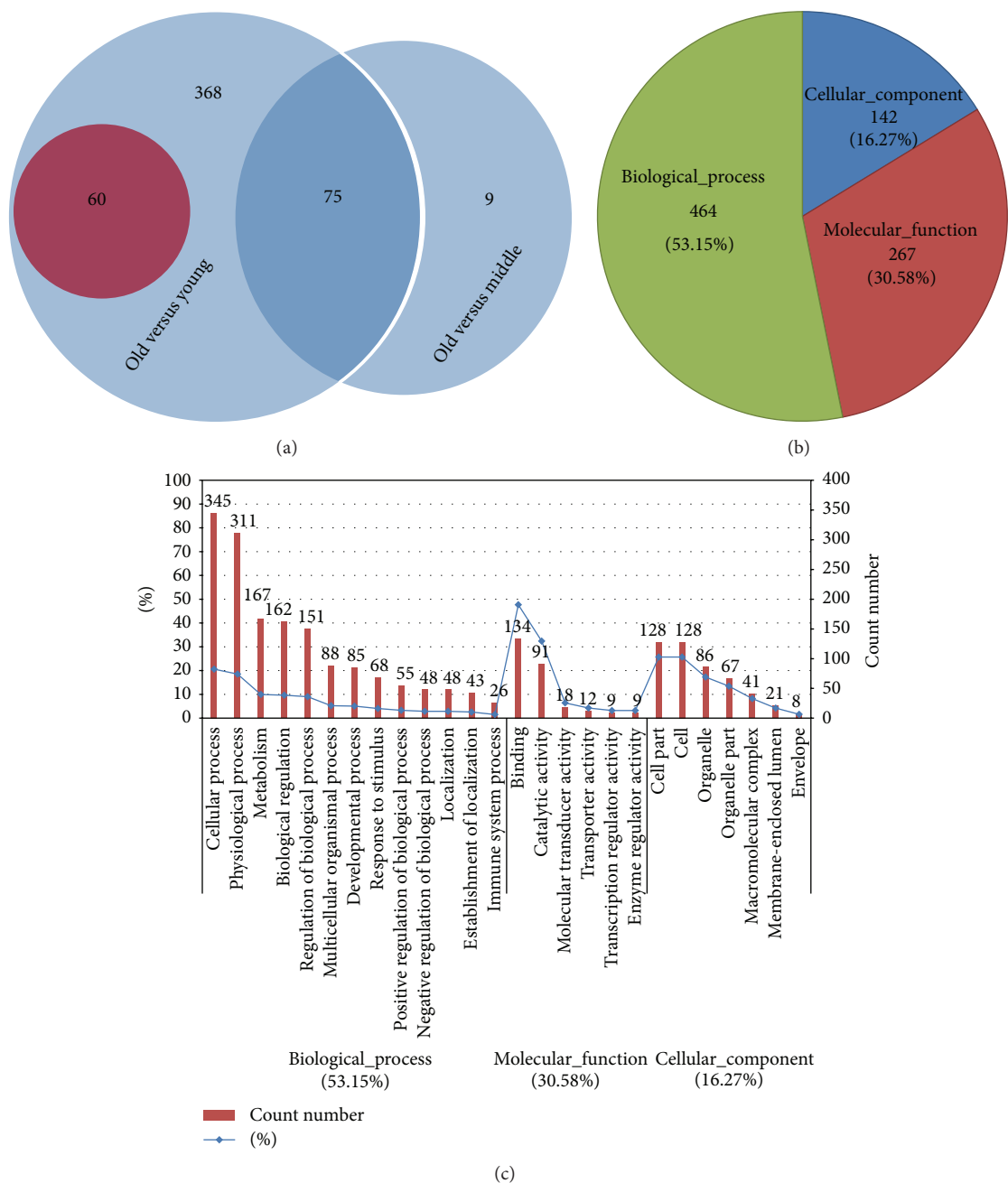


FIGURE 3: The age-related ovaries' differentially expressed genes and their GO term analysis. (a) Venn diagram of differentially expressed genes in different aged monkey ovaries. The circle with red and blue background indicates upregulated and downregulated genes, respectively. The number of differentially expressed genes was marked on the corresponding area. (b) Pie diagram of GO mapping of the total 512 differentially expressed genes found in the present study. The gene count numbers and their ratio were marked in the diagram. (c) The GO term analysis of the total 512 differentially expressed genes. The number over each column is the gene count number; the blue line shows the percent of each column item in the corresponding categories of biological process, molecular function, and cellular component.

16.27% representing the main functional categories of biological process, molecular function, and cellular component, respectively (Figure 3(b)). For the ontology "biological process," the main functional categories were "cellular process," "physiological process," "metabolism," and "biological regulation." For the ontology "molecular function," the differentially expressed genes were mainly enriched in "binding" and

"catalytic activity." For the ontology "cellular component," the "cell part," "cell," and "organelle" were the first three categories (Figure 3(c) and Table S2). The GO term analysis showed that great changes of nucleus and microtubules of ovary cells might take place mainly by abnormal transcription regulation, DNA repair, and ligand binding affected by age. Cell cycle, oxidative stress and DNA repair, meiosis and

TABLE 3: qRT-PCR validation of microarray data by using the data-generated RNA samples.

Gene symbol	Microarray ratio		qRT-PCR ratio				RefSeq transcript ID
	O versus M	O versus Y	O versus M	<i>t</i> -test (<i>P</i> value)	O versus Y	<i>t</i> -test (<i>P</i> value)	
Upregulated genes							
<i>MRAP</i>	—	22.8616	19.1597	0.030*	45.2548	0.027*	XM_001096328
<i>MMP9</i>	—	5.2734	14.4765	0.815	4.2191	0.002**	XM_001104871
<i>THY1</i>	—	2.8757	1.3062	0.273	1.6950	0.098	NM_001042638
<i>LOC717872</i>	—	7.0041	1.3145	0.054	3.3168	0.073	XM_001109859
<i>IGFBP4</i>	—	2.2457	0.8946	0.417	1.4958	0.403	XM_001097914
Downregulated genes							
<i>NASP</i>	0.4166	0.3654	0.2207	0.0001**	0.2588	0.0001**	XM_001103253
<i>PTTG1</i>	0.2017	0.1803	0.2505	0.045*	0.2811	0.002**	XM_001085022
<i>AURKA</i>	0.3774	0.2893	0.3221	0.043*	0.1231	0.002**	XR_011039
<i>BCL2L10</i>	0.0369	0.0279	0.0000	0.001**	0.0000	0.032*	XM_001085850
<i>BARD1</i>	0.3524	0.2966	0.5953	0.193	0.2293	0.015*	XM_001084147
<i>TACC3</i>	0.1866	0.1238	0.1756	0.004**	0.0884	0.004**	XM_001101192
<i>THBD</i>	0.4251	0.4500	3.5801	0.160	3.8106	0.845	XM_001095416
<i>DNMT3A</i>	0.3844	0.3167	0.1805	0.0004**	0.0634	0.0001**	XM_001083234
<i>ZP3</i>	0.0804	0.0347	0.0005	0.020*	0.0003	0.0002**	XM_001114760
<i>LOC703074</i>	0.0294	0.0265	0.0010	0.001**	0.0012	0.001**	XR_010378
<i>WASF1</i>	0.2458	0.2101	0.3482	0.0001**	0.1213	0.0001**	XM_001087511
<i>LOC707199</i>	0.4462	0.3053	0.7749	0.435	0.2752	0.041*	XR_011694
<i>MCM3</i>	0.2856	0.212	0.3024	0.0001**	0.0734	0.002**	XM_001106702
<i>IGF2BP3</i>	0.1042	0.0617	0.2369	0.092	0.0993	0.024*	XM_001098017
<i>FGF14</i>	0.1707	0.1074	0.2601	0.005**	0.0696	0.002**	XM_001093457
<i>XRCC6</i>	—	0.4987	0.8063	0.855	0.5597	0.146	XM_001105684
<i>HELLS</i>	—	0.2874	0.227	0.0001**	0.1330	0.0005**	XM_001094077
<i>CDK1</i>	—	0.0942	0.1716	0.0001**	0.1137	0.0005**	XM_001095697
<i>UBE2C</i>	—	0.1019	0.3849	0.016*	0.1806	0.001**	XM_001104061
<i>THBS1</i>	0.3518	—	0.3748	0.001**	0.1309	0.069	XM_001093770

O: old group; M: middle-aged group; Y: young group; —: no significant difference in gene expression; **P* < 0.05; ***P* < 0.01.

spindle function, and ubiquitination have been considered to be affected by age [22], which is consistent with our results. Our findings for rhesus monkey ovary showed that many differentially expressed genes were involved in transcription regulation, cell cycle, DNA replication and repair, and some other important, aging-related biological processes (Table S2). We found that most of the genes (such as *THY1*, *HELL*, and *ZP3*) related to aging are similar to those previously identified in aging mouse ovaries [26], but some of the differentially expressed genes in pathways are quite different. For example, the important genes *Nfkb1*, *Trp53*, and *Tert* were differentially expressed in mouse, as reported by other groups [17, 25, 26, 44], but no age-related differences in these genes were found in monkeys. However, the genes *NLRP4*, *NLRP11*, *BCL2L10*, *CYP11A*, *FADS1*, and *XRCC6*, which are related to regulation of NFkB, apoptosis, and TERT function [45–48], were differentially expressed in monkey ovaries. This discrepancy might be due to species-specific differences and/or different ovarian physiological status.

The results also indicated that 11 KEGG pathways were associated with the genes differentially expressed between the old and the young and middle-aged groups (Table

S3). A few pathways that have been widely reported to be associated with the aging process, such as “cell cycle” and “TGF-β,” appeared in our results. It was reported that the TGF-β signaling pathway is constitutively active in aging of myogenic progenitors [49] and brain [50, 51]. We found that these KEGG pathways contained only a limited number of genes due to the lack of comprehensive annotation of the *M. mulatta* genome (Table S3).

3.4. KEGG Pathway Analysis with Human-*M. mulatta* Orthologs. Human-*M. mulatta* orthologs were used to select the differentially expressed genes, and 476 annotated genes, 51 upregulated and 425 downregulated, were identified (Table S4). Analysis with DAVID Bioinformatics Resources 6.7 [38] showed that the differentially expressed genes were mainly enriched in the following seven KEGG pathways: “cell cycle,” “oocyte meiosis,” “progesterone-mediated oocyte maturation,” “p53 signaling pathway,” “DNA replication,” “mismatch repair,” and “nucleotide excision repair,” and all genes involved were downregulated in the old ovaries (Table 4). It is well known that aging is associated with both a decrease in the efficiency of repair and an accumulation of DNA damage

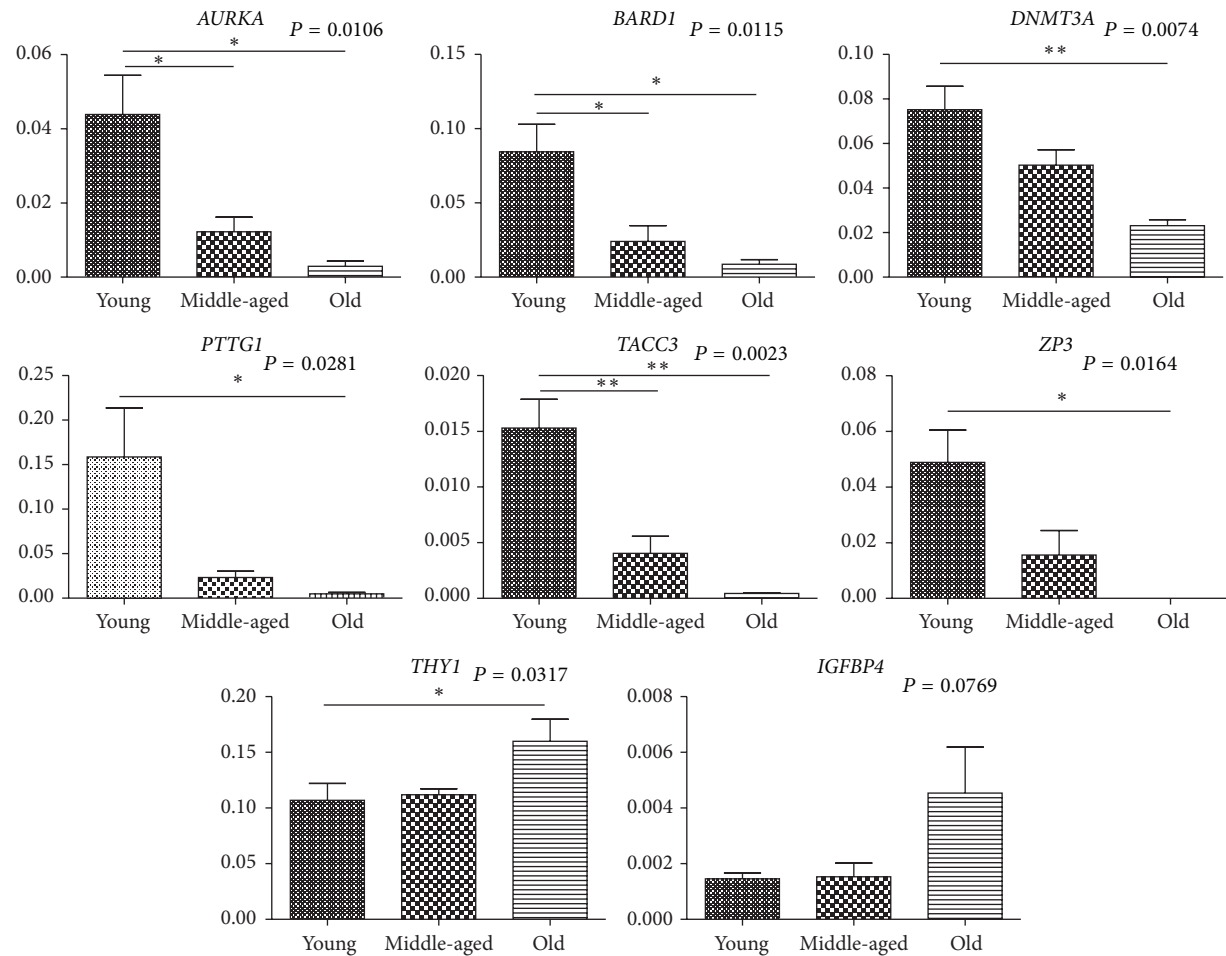


FIGURE 4: Validation of microarray results by qRT-PCR analysis of new RNA samples. * $P < 0.05$; ** $P < 0.01$; P values are indicated for each gene.

TABLE 4: KEGG pathway analysis with the orthologs genes conserved between human and *M. mulatta*.

KEGG pathway	Genes
Cell cycle	<i>CCNE1, CHEK1, BUB1, HDAC2, TTK, CCNB1, PTTG1, CDC20, CDK1, BUB1B, MCM5, ORC6L, MCM3, MCM7, MAD2L1, PLK1, and CCNB2</i>
Oocyte meiosis	<i>CDK1, CCNE1, PPP3CB, BUB1, CCNB1, PTTG1, MAD2L1, PLK1, STAG3, CDC20, CCNB2, and AURKA</i>
Progesterone-mediated oocyte maturation	<i>CDK1, HSPCA, BUB1, CCNB1, MAD2L1, PLK1, and CCNB2</i>
p53 signaling pathway	<i>CDK1, CCNE1, CHEK1, CCNB1, CCNB2, and BID</i>
DNA replication	<i>RFC3, MCM5, RFC4, POLD1, POLD3, FEN1, MCM3, and MCM7</i>
Mismatch repair	<i>RFC3, RFC4, POLD1, POLD3, and MSH2</i>
Nucleotide excision repair	<i>RFC3, RFC4, POLD1, and POLD3</i>

[52, 53]. In our results, the genes involved in DNA replication and repair pathways were all downregulated in old monkey ovaries (Figure 5, Tables 4 and 5), which might indicate cellular senescence, caused by accumulation of damage to nuclear and mitochondrial DNA, decline in the function of stress resistance, which might lead to apoptosis and immune response [30, 44, 54]. In cell cycle and oocyte meiosis pathways, the differentially expressed genes involved were

all downregulated in old ovaries except for the *Cpebs* gene (Figure 6), which reflected the lower control ability of cell proliferation and oocyte maturation. It has been reported that *Cpebs* have the function of balancing between senescence and proliferation depending on translational repression and/or activation, which can be regulated by progesterone. With the lack of progesterone in old animals, the function of *Cpebs* trends toward translational repression [55]. The

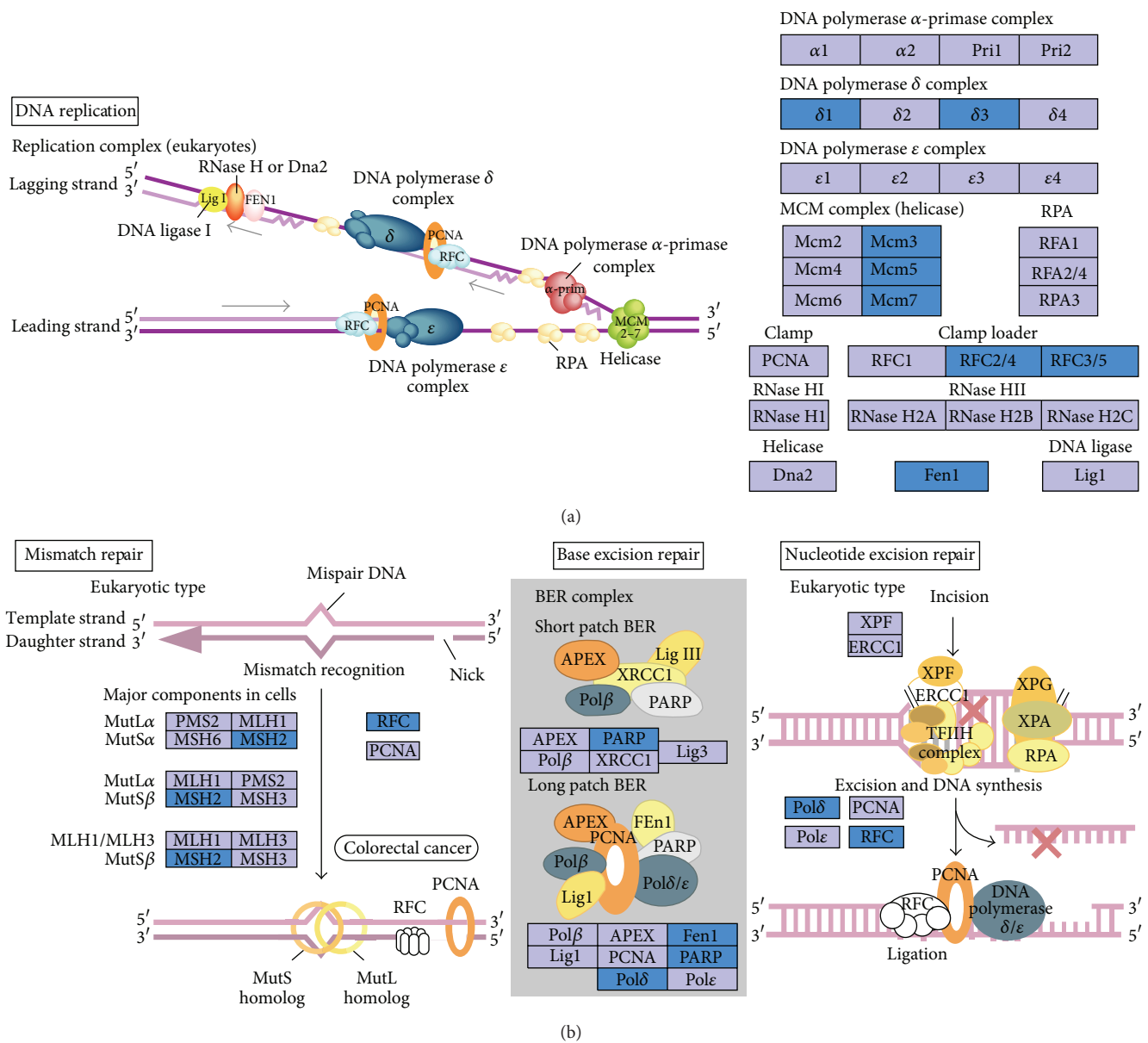


FIGURE 5: Differentially expressed genes involved in DNA replication pathway (a) and DNA repair pathway (b). Blue boxes backgrounds indicate genes differentially downregulated in old *M. mulatta* ovaries.

p53 signaling pathway is intimately involved in aging and apoptosis according to a previous report [56]. A few popular mechanisms related to aging are listed in Table 5 by analyzing our microarray data, which shares some similarities to the previous reports in mice [25, 26].

In order to identify pronounced, age-related changes in gene expression in the ovary, we conducted further functional annotation focused on *GOTERM_BP_FAT* and *KEGG_PATHWAY* of 51 orthologs genes upregulated in old versus young ovary and 58 orthologs genes downregulated in old versus young and middle-aged ovary in old ovary (Table S4). We found that the functions of upregulated genes were enriched mainly in negative regulation of cellular biological processes, aging, defense responses,

oxidation/reduction, cell growth, and KEGG pathways of “leukocyte transendothelial migration” and “biosynthesis of unsaturated fatty acids” (Table 6). The functions of downregulated genes were enriched primarily in cell cycle, reproduction, chromatin organization and regulation of transcription, DNA and RNA process, methylation, and KEGG pathways of “cell cycle,” “oocyte meiosis,” “progesterone-mediated oocyte maturation,” and “spliceosome” (Table 7). These data indicate that ovarian aging is accompanied with the increases in defense and immune responses and oxidation reduction, the decreases in capacity for reproduction, cell division, DNA replication and repair, and some changes of epigenetic regulation. These findings will be helpful for tracking biomarkers and understanding mechanisms of ovary aging in primates.

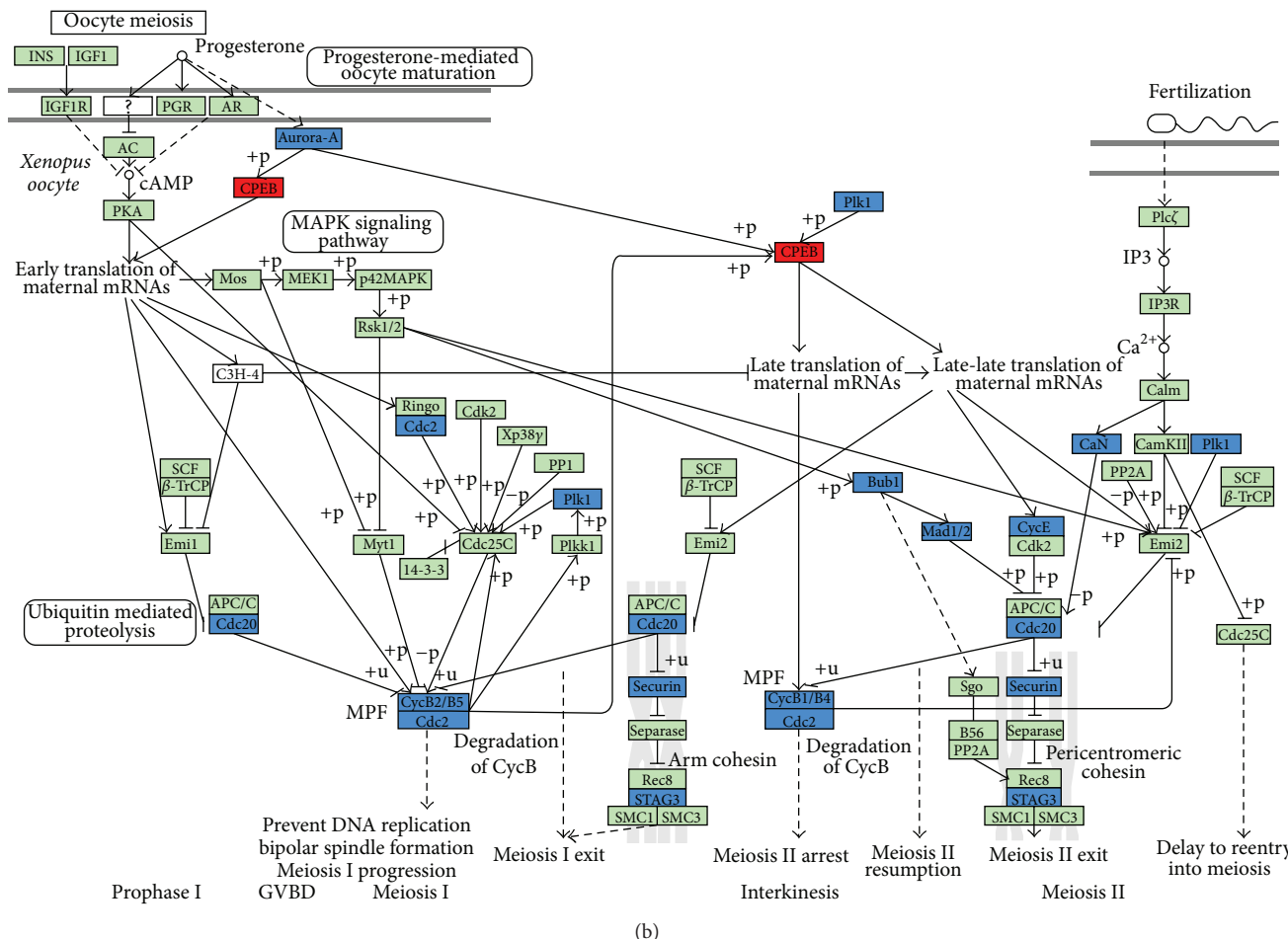


FIGURE 6: Differentially expressed genes involved in cell cycle (a) and oocyte meiosis (b) pathways. Blue backgrounds indicate genes differentially downregulated and red indicate genes differentially upregulated in old *M. musculus* ovaries.

TABLE 5: Analysis of differentially expressed orthologs genes with popular mechanisms of aging.

Mechanisms	Genes involved
Mitochondrion	<i>ALDH18A1, ALDOC* , ARG2, BCL2L10, BID, CAPRN2, CYP11A1* DSP, FAM136A, FEN1, GATM, ILF3, LACTB2* MTIF3, NADKDI* , P4HA1, PPP3CB, RARS2, SHMT1, TOMM34, TPPI* , and USP30</i>
Oxidation reduction and electron transport	<i>ALDH18A1, AOX1* , CYP11A1* , FADSI* , HSD17B1, KDM1A, LDHAL6A, NARE, NELLI, P4HA1, and RETSAT*</i>
Apoptosis	<i>ALDOC* , ARHGEF7, AVEN, BARD1, BCL2L10, BCLAF1, BID, BRCA1, BUB1B, CASP2, CDK1, CSEIL, DEDD, F2, GAL, HELLS, KRT8, MAEL, MMP9* , MSH2, NELLI, NPM1, SOX4, TIA1, TUBB, and TUBB2C</i>
Immune system	<i>AOX1* , BCL11A, CCNB2, CHD7, CHIT1* , CLEC1A* , F2, GAL, GLMN, IGFBP4* , IGHE, IL1R1* , ILF2, JARID2, MASPI* , MMP9* , MSH2, OPRK1, PPP3CB, SOX4, TACC3, TCF3, THY1* , TUBB, TUBB2C, and XRCC6</i>
DNA replication and repair	<i>ASF1A, BARD1, BRCA1, CCNO, CHAF1A, CHEK1, DKC1, DTL, FANCE, FANCI, FEN1, GINS2, HMGAI, MCM10, MCM3, MCM5, MCM7, MORF4L1, MSH2, NASP, NEIL3, ORC6L, PAPD7, PARP1, POLD1, POLD3, PTTG1, RAD50, RAD51, RAD51C, RBM4, RFC3, RFC4, RMI2, RUVBL2, SFPQ, SSRP1, TDPI, TRIP13, TYMS, and XRCC6</i>
Methylation	<i>DHX9, DNMT3A, DNMT3B, FBL, FUS, HELLS, HMGAI, HNRNPD, HNRNPK, HNRNPU, HNRPDL, ILF3, MAEL, PABPC4, PRMT5, PRMT7, RAPIA* , RASL10A, RHOQ* , RRAS2, SFPQ, SRSF1, SUV39H2, TDRD1, TGS1, THOC4, TUBA1B, and TUBB</i>
Reproduction	<i>AMH, BCL2L10, CCNB1, CCNE1, CELSR2, CEP57, CHD7, CHEK1, DAZAP1, DEDD, DNMT3A, FIGLA, HIST1H1A, HSF2BP, LHX8, MAEL, MBD2, MSH2, NLRP14, NPM2, OOEP, PPAP2B* , PRMT7, PTTG1, RAD51C, RPL39L, STRBP, TDRD1, TRIP13, ZP2, ZP3, and ZP4</i>
Aging	<i>NPM1, ENG* , MSH2, FADSI* , and ALDOC*</i>
Telomere	<i>DKC1, PARP1, XRCC6, and RAD50</i>

*Orthologs genes upregulated in old monkey ovaries.

TABLE 6: Results of functional annotation of orthologs genes upregulated in old monkey ovary compared to young monkey ovary.

Category	Term	Genes
Regulation of cellular process	Negative regulation of catalytic activity/negative regulation of molecular function	<i>PKIG, CAST, ENG, APOC1, and THY1</i>
	Negative regulation of cellular component organization	<i>RHOQ, APOC1, and THY1</i>
	Negative regulation of nitrogen compound metabolic process/negative regulation of cellular biosynthetic process/negative regulation of biosynthetic process	<i>PKIG, ENG, PBXIP1, APOC1, and CCDC85B</i>
Aging	Aging	<i>ENG, FADSI, and ALDOC</i>
Defense response	Response to wounding	<i>IGFBP4, AOX1, ENG, TFPI, and MASPI</i>
	Defense response	<i>CLEC1A, IGFBP4, AOX1, IL1R1, and MASPI</i>
	Response to endogenous stimulus	<i>CYP11A1, RHOQ, FADSI, and ALDOC</i>
Oxidation reduction	Oxidation reduction/fat-soluble vitamin metabolic process/unsaturated fatty acid biosynthetic process	<i>CYP11A1, AOX1, RETSAT, FADSI, and FADS2</i>
Cell growth	Regulation of cell growth	<i>IGFBP4, WISP2, and CCDC85B</i>
KEGG_PATHWAY	Leukocyte transendothelial migration	<i>MMP9, RAPIA, MYL9, and THY1</i>
	Biosynthesis of unsaturated fatty acids	<i>FADSI, FADS2</i>

Functional categories of genes were assembled from annotation and PubMed.

4. Conclusion

Our results demonstrate substantial differences in ovarian gene expression between old and middle-aged or young rhesus monkeys. These differences exist at the level of trans-

cription of genes involved in critical biological functions and pathways in the ovary/oocytes, which probably affect aging process through DNA damage, mitochondrial dysfunction, oxidative stress and immune response, and epigenetics. Thus, age-specific gene expression profiling can provide information on processes that may be related to ovarian/oocyte aging

TABLE 7: Results of functional annotation of orthologs genes downregulated in old monkey ovary compared to young and middle-aged monkey ovary.

Category	Term	Genes
Cell cycle	Cell cycle/mitosis/mitotic cell cycle/nuclear division/cell division/organelle fission	<i>BARD1, RAD51, CDCA2, BUB1, TTK, CCNB1, PTTG1, KIF15, SUV39H2, NCAPH, NCAPG, MCM3, TACC3, OIP5, CCNB2, and AURKA</i>
Cellular macromolecules	Macromolecular complex assembly/macromolecular complex subunit organization/protein complex biogenesis/assembly	<i>TGSI, RAD51, TUBB2C, DNAAF2, ASF1A, OOEP, HIST1H1D, and ENSG00000112290</i>
Reproduction	Sexual reproduction/reproductive cellular process/gamete generation/oocyte development/fertilization	<i>FIGLA, ZP3, BCL2L10, CCNB1, OOEP, DNMT3A, PTTG1, ZP2, and AMH</i>
Chromatin	Chromosome organization/chromatin assembly or disassembly/chromatin organization	<i>SUV39H2, NCAPH, WHSC1, NCAPG, ASF1A, DNMT3A, PTTG1, HIST1H1D, and DNMT3B</i>
Regulation of cellular process	Positive regulation of macromolecule metabolic process/positive regulation of nitrogen compound metabolic process	<i>BARD1, RAD51, TESC, ASF1A, TTK, and CCNB1</i>
	Regulation of transcription	<i>FUBP1, OTX2, FIGLA, TGSI, MLFIIP, TESC, ASF1A, ZNF77, SUV39H2, HNRNPD, ELAVL2, DNMT3A, and MCM3</i>
	Regulation of apoptosis or cell death	<i>BARD1, TUBB2C, and BCL2L10</i>
DNA	DNA metabolic process	<i>RMI2, BARD1, RAD51, GINS2, ASF1A, DNMT3A, MCM3, and PTTG1</i>
	DNA repair/response to DNA damage stimulus	<i>BARD1, RAD51, ASF1A, and PTTG1</i>
RNA	RNA splicing/mRNA processing/mRNA metabolic process	<i>SRSF2, TGSI, HNRNPD, HNRNPAIL2, and ENSG00000135486</i>
Methylation	Biopolymer methylation/methylation	<i>SUV39H2, TGSI, DNMT3A, and DNMT3B</i>
KEGG.PATHWAY	Cell cycle	<i>BUB1, TTK, CCNB1, MCM3, PTTG1, and CCNB2</i>
	Oocyte meiosis	<i>BUB1, CCNB1, PTTG1, CCNB2, and AURKA</i>
	Progesterone-mediated oocyte maturation	<i>BUB1, CCNB1, and CCNB2</i>
	Spliceosome	<i>SRSF2, HNRNPAIL2, and ENSG00000135486</i>

Functional categories of genes were assembled from annotation and PubMed.

and possibly reveal a contribution of altered gene expression to decreased fertility.

Conflict of Interests

The authors declare that there is no conflict of interests regarding the publication of this paper.

Authors’ Contribution

Hengxi Wei and Xiangjie Liu contributed equally to the work. Hengxi Wei and Xiangjie Liu contributed to data collection and paper drafting. Jihong Yuan and Dongdong Zhang were involved in ovary histological analysis. Li Li and Xinzheng Guo contributed to data analysis and statistics. Lin Liu contributed to revising the paper. Shouquan Zhang contributed to study concept and design.

Acknowledgments

This work was supported by the National Basic Research Program of China [973 Program, 2010CB945001, 2011CB944202, and 2011CBA01004]. And the authors also thank Dr. Yayan Xiong of Sun Yat-Sen University for aid in data analysis.

References

[1] F. J. Broekmans, M. R. Soules, and B. C. Fauser, “Ovarian aging: mechanisms and clinical consequences,” *Endocrine Reviews*, vol. 30, no. 5, pp. 465–493, 2009.

[2] J. S. Younis, “Ovarian aging: latest thoughts on assessment and management,” *Current Opinion in Obstetrics and Gynecology*, vol. 23, no. 6, pp. 427–434, 2011.

[3] C. B. Coulam, S. C. Adamson, and J. F. Annegers, “Incidence of premature ovarian failure,” *Obstetrics & Gynecology*, vol. 67, no. 4, pp. 604–606, 1986.

[4] A. N. Shelling, “Premature ovarian failure,” *Reproduction*, vol. 140, no. 5, pp. 633–641, 2010.

[5] R. A. Gibbs, J. Rogers, M. G. Katze et al., “Evolutionary and biomedical insights from the rhesus macaque genome,” *Science*, vol. 316, no. 5822, pp. 222–234, 2007.

[6] H. F. Urbanski, N. C. Noriega, D. R. Lemos, and S. G. Kohama, “Gene expression profiling in the rhesus macaque: experimental design considerations,” *Methods*, vol. 49, no. 1, pp. 26–31, 2009.

[7] Y. Takahashi, M. Kuro-o, and F. Ishikawa, “Aging mechanisms,” *Proceedings of the National Academy of Sciences of the United States of America*, vol. 97, no. 23, pp. 12407–12408, 2000.

- [8] G. Yan, G. Zhang, X. Fang et al., "Genome sequencing and comparison of two nonhuman primate animal models, the cynomolgus and Chinese rhesus macaques," *Nature Biotechnology*, vol. 29, no. 11, pp. 1019–1023, 2011.
- [9] G. S. Roth, J. A. Mattison, M. A. Ottinger, M. E. Chachich, M. A. Lane, and D. K. Ingram, "Aging in rhesus monkeys: relevance to human health interventions," *Science*, vol. 305, no. 5689, pp. 1423–1426, 2004.
- [10] D. Harman, "Aging: a theory based on free radical and radiation chemistry," *Journal of gerontology*, vol. 11, no. 3, pp. 298–300, 1956.
- [11] V. M. Monnier, "Toward a Maillard reaction theory of aging," *Progress in Clinical and Biological Research*, vol. 304, pp. 1–22, 1989.
- [12] E. J. Masoro, "Caloric restriction and aging: an update," *Experimental Gerontology*, vol. 35, no. 3, pp. 299–305, 2000.
- [13] K. Shinmura, "Effects of caloric restriction on cardiac oxidative stress and mitochondrial bioenergetics: potential role of cardiac sirtuins," *Oxidative Medicine and Cellular Longevity*, vol. 2013, Article ID 528935, 11 pages, 2013.
- [14] C. Leeuwenburgh, R. Pamplona, and A. Sanz, "Mitochondria and ageing," *Journal of Aging Research*, vol. 2011, Article ID 782946, 3 pages, 2011.
- [15] V. A. Bohr and R. M. Anson, "DNA damage, mutation and fine structure DNA repair in aging," *Mutation Research DNAging*, vol. 338, no. 1–6, pp. 25–34, 1995.
- [16] B. C. Richardson, "Role of DNA methylation in the regulation of cell function: autoimmunity, aging and cancer," *Journal of Nutrition*, vol. 132, no. 8, pp. 2401s–2405s, 2002.
- [17] M. A. Blasco, "Telomere length, stem cells and aging," *Nature Chemical Biology*, vol. 3, no. 10, pp. 640–649, 2007.
- [18] J. Campisi, "Cellular senescence and apoptosis: how cellular responses might influence aging phenotypes," *Experimental Gerontology*, vol. 38, no. 1–2, pp. 5–11, 2003.
- [19] M. J. Faddy, R. G. Gosden, A. Gougeon, S. J. Richardson, and J. F. Nelson, "Accelerated disappearance of ovarian follicles in mid-life: implications for forecasting menopause," *Human Reproduction*, vol. 7, no. 10, pp. 1342–1346, 1992.
- [20] M. Dorland, R. J. van Kooij, and E. R. Te Velde, "General ageing and ovarian ageing," *Maturitas*, vol. 30, no. 2, pp. 113–118, 1998.
- [21] C. Tatone, F. Amicarelli, M. C. Carbone et al., "Cellular and molecular aspects of ovarian follicle ageing," *Human Reproduction Update*, vol. 14, no. 2, pp. 131–142, 2008.
- [22] M. L. Grøndahl, C. Yding Andersen, J. Bogstad, F. C. Nielsen, H. Meinertz, and R. Borup, "Gene expression profiles of single human mature oocytes in relation to age," *Human Reproduction*, vol. 25, no. 4, pp. 957–968, 2010.
- [23] T. Hamatani, G. Falco, M. G. Carter et al., "Age-associated alteration of gene expression patterns in mouse oocytes," *Human Molecular Genetics*, vol. 13, no. 19, pp. 2263–2278, 2004.
- [24] N. M. Steuerwald, M. G. Bermúdez, D. Wells, S. Munné, and J. Cohen, "Maternal age-related differential global expression profiles observed in human oocytes," *Reproductive BioMedicine Online*, vol. 14, no. 6, pp. 700–708, 2007.
- [25] A. Zimon, A. Erat, T. Von Wald et al., "Genes invoked in the ovarian transition to menopause," *Nucleic Acids Research*, vol. 34, no. 11, pp. 3279–3287, 2006.
- [26] A. A. Sharov, G. Falco, Y. Piao et al., "Effects of aging and calorie restriction on the global gene expression profiles of mouse testis and ovary," *BMC Biology*, vol. 6, article 24, 2008.
- [27] N. Gava, C. L. Clarke, C. Bye, K. Byth, and A. de Fazio, "Global gene expression profiles of ovarian surface epithelial cells in vivo," *Journal of Molecular Endocrinology*, vol. 40, no. 5–6, pp. 281–296, 2008.
- [28] R. L. Bogan, M. J. Murphy, and J. D. Hennebold, "Dynamic changes in gene expression that occur during the period of spontaneous functional regression in the rhesus macaque corpus luteum," *Endocrinology*, vol. 150, no. 3, pp. 1521–1529, 2009.
- [29] J. A. Duce, S. Podvin, W. Hollander, D. Kipling, D. L. Rosene, and C. R. Abraham, "Gene profile analysis implicates Klotho as an important contributor to aging changes in brain white matter of the rhesus monkey," *Glia*, vol. 56, no. 1, pp. 106–117, 2008.
- [30] S. K. Kim, "Common aging pathways in worms, flies, mice and humans," *Journal of Experimental Biology*, vol. 210, part 9, pp. 1607–1612, 2007.
- [31] P. Zheng, B. Patel, M. McMenamin et al., "The primate embryo gene expression resource: a novel resource to facilitate rapid analysis of gene expression patterns in non-human primate oocytes and preimplantation stage embryos," *Biology of Reproduction*, vol. 70, no. 5, pp. 1411–1418, 2004.
- [32] S. M. Nichols, B. D. Bavister, C. A. Brenner, P. J. Didier, R. M. Harrison, and H. M. Kubisch, "Ovarian senescence in the rhesus monkey (*Macaca mulatta*)," *Human Reproduction*, vol. 20, no. 1, pp. 79–83, 2005.
- [33] B. Bolon, T. J. Bucci, A. R. Warbritton, J. J. Chen, D. R. Mattison, and J. J. Heindel, "Differential follicle counts as a screen for chemically induced ovarian toxicity in mice: results from continuous breeding bioassays," *Fundamental and Applied Toxicology*, vol. 39, no. 1, pp. 1–10, 1997.
- [34] J. Yu, L. Zhang, A. Chen et al., "Identification of the gene transcription and apoptosis mediated by TGF-beta-Smad2/3-Smad4 signaling," *Journal of Cellular Physiology*, vol. 215, no. 2, pp. 422–433, 2008.
- [35] Y. H. Yang, S. Dudoit, P. Luu et al., "Normalization for cDNA microarray data: a robust composite method addressing single and multiple slide systematic variation," *Nucleic Acids Research*, vol. 30, no. 4, article e15, 2002.
- [36] A. Brazma, P. Hingamp, J. Quackenbush et al., "Minimum information about a microarray experiment (MIAME)—toward standards for microarray data," *Nature Genetics*, vol. 29, no. 4, pp. 365–371, 2001.
- [37] E. Bourneuf, F. Héroult, C. Chicault et al., "Microarray analysis of differential gene expression in the liver of lean and fat chickens," *Gene*, vol. 372, no. 1–2, pp. 162–170, 2006.
- [38] W. da Huang, B. T. Sherman, and R. A. Lempicki, "Systematic and integrative analysis of large gene lists using DAVID bioinformatics resources," *Nature Protocols*, vol. 4, no. 1, pp. 44–57, 2009.
- [39] J. Yuan, D. Zhang, L. Wang et al., "No evidence for neo-oogenesis may link to ovarian senescence in adult monkey," *Stem Cells*, vol. 31, no. 11, pp. 2538–2550, 2013.
- [40] J. Lim and U. Luderer, "Oxidative damage increases and antioxidant gene expression decreases with aging in the mouse ovary," *Biology of Reproduction*, vol. 84, no. 4, pp. 775–782, 2011.
- [41] L. A. Lovasco, K. A. Seymour, K. Zafra, C. W. O'Brien, C. Schorl, and R. N. Freiman, "Accelerated ovarian aging in the absence of the transcription regulator TAF4B in mice," *Biology of Reproduction*, vol. 82, no. 1, pp. 23–34, 2010.

- [42] A. Uyar, S. Torrealday, and E. Seli, "Cumulus and granulosa cell markers of oocyte and embryo quality," *Fertility and Sterility*, vol. 99, no. 4, pp. 979–997, 2013.
- [43] K. E. Latham, "The primate embryo gene expression resource in embryology and stem cell biology," *Reproduction, Fertility and Development*, vol. 18, no. 8, pp. 807–810, 2006.
- [44] C. R. Balistreri, G. Candore, G. Accardi, G. Colonna-Romano, and D. Lio, "NF- κ B pathway activators as potential ageing biomarkers: targets for new therapeutic strategies," *Immunity and Ageing*, vol. 10, no. 1, article 24, 2013.
- [45] S. Kim, X. Bi, M. Czarny-Ratajczak et al., "Telomere maintenance genes SIRT1 and XRCC6 impact age-related decline in telomere length but only SIRT1 is associated with human longevity," *Biogerontology*, vol. 13, no. 2, pp. 119–131, 2012.
- [46] J. D. Xu, X. X. Cao, Z. W. Long et al., "BCL2L10 protein regulates apoptosis/proliferation through differential pathways in gastric cancer cells," *The Journal of Pathology*, vol. 223, no. 3, pp. 400–409, 2011.
- [47] R. Li, Y. Yang, Y. An et al., "Genetic polymorphisms in DNA double-strand break repair genes XRCC5, XRCC6 and susceptibility to hepatocellular carcinoma," *Carcinogenesis*, vol. 32, no. 4, pp. 530–536, 2011.
- [48] X. Tian, G. Pascal, and P. Monget, "Evolution and functional divergence of NLRP genes in mammalian reproductive systems," *BMC Evolutionary Biology*, vol. 9, article 202, 2009.
- [49] M. L. Beggs, R. Nagarajan, J. M. Taylor-Jones, G. Nolen, M. MacNicol, and C. A. Peterson, "Alterations in the TGF β signaling pathway in myogenic progenitors with age," *Aging Cell*, vol. 3, no. 6, pp. 353–361, 2004.
- [50] K. P. Doyle, E. Cekanaviciute, L. E. Mamer, and M. S. Buckwalter, "TGF β signaling in the brain increases with aging and signals to astrocytes and innate immune cells in the weeks after stroke," *Journal of Neuroinflammation*, vol. 7, article 62, 2010.
- [51] L. Yin, A. Morita, and T. Tsuji, "The crucial role of TGF- β in the age-related alterations induced by ultraviolet A irradiation," *Journal of Investigative Dermatology*, vol. 120, no. 4, pp. 703–705, 2003.
- [52] I. Velezghaninov, V. Mezenceva, O. Shostal, A. Baranova, and A. Mbskalev, "Age dynamics of DNA damage and CpG methylation in the peripheral blood leukocytes of mice," *Mutation Research—Fundamental and Molecular Mechanisms*, vol. 775, pp. 38–42, 2015.
- [53] A. A. Moskalev, M. V. Shaposhnikov, E. N. Plyusnina et al., "The role of DNA damage and repair in aging through the prism of Koch-like criteria," *Ageing Research Reviews*, vol. 12, no. 2, pp. 661–684, 2013.
- [54] N. Kourtis and N. Tavernarakis, "Cellular stress response pathways and ageing: intricate molecular relationships," *The EMBO Journal*, vol. 30, no. 13, pp. 2520–2531, 2011.
- [55] G. Fernández-Miranda and R. Méndez, "The CPEB-family of proteins, translational control in senescence and cancer," *Ageing Research Reviews*, vol. 11, no. 4, pp. 460–472, 2012.
- [56] M. V. Poyurovsky and C. Prives, "P53 and aging: a fresh look at an old paradigm," *Aging*, vol. 2, no. 7, pp. 380–382, 2010.

猪克隆胚胎激活方法优化与转人溶菌酶基因克隆猪的生产*

卫恒习^{1, 2)} 李俊^{2, 3)} 董佳²⁾ 马育芳²⁾ 高凤磊¹⁾
 李秋艳²⁾ 张守全¹⁾ 李 宁^{2)**}

⁽¹⁾ 广东省农业动物基因组学与分子育种重点实验室, 华南农业大学动物科学学院, 广州 510642;

⁽²⁾ 农业生物技术国家重点实验室, 中国农业大学生物学院, 北京 100193;

⁽³⁾ 河北医科大学第一医院生殖医学中心, 石家庄 050031)

摘要 为了提高转基因克隆效率和获得转人溶菌酶基因克隆猪, 研究了不同电激活参数和化学辅助激活方法对猪克隆胚胎和孤雌胚胎体外发育的影响。结果发现: 电场强度会显著影响克隆胚胎的融合率和体外发育能力($P < 0.05$), 电脉冲次数对克隆胚胎体外发育促进作用不显著($P > 0.05$), 而相同电激活条件下克隆胚胎和孤雌胚胎的体外发育能力变化趋势不同; 电激活后再利用放线菌酮+细胞松弛素 B(CHX+CB)处理 4 h 能显著提高克隆胚胎的囊胚率($P < 0.05$), 而用二甲基氨基嘌呤(6-DMAP)处理没有提高克隆胚胎囊胚率($P > 0.05$), 但 6-DMAP 或 CHX+CB 处理均可显著提高孤雌胚胎的囊胚率($P < 0.05$)。上述结果表明, 最佳的孤雌激活条件并不一定是克隆胚胎的最佳激活条件。本研究中猪克隆胚胎的最佳激活方法为 1.6 kV/cm、100 μ s、2 次直流电脉冲间隔 100 μ s, 再辅以 CHX+CB 处理 4 h。利用优化的激活条件成功获得了乳腺特异表达人溶菌酶的转基因猪, 为猪转基因育种奠定了基础。

关键词 体细胞克隆, 胚胎激活, 转基因, 人溶菌酶, 猪
学科分类号 Q819, S828.9

DOI: 10.3724/SP.J.1206.2012.00082

在当前养猪业, 致病菌的感染会严重影响到仔猪的生长和成活, 且容易产生抗药性, 是全世界范围内亟待解决的重要问题之一。溶菌酶是一种天然的广谱抗菌素, 对细菌、真菌和病毒都具有很好的抑制作用, 已经广泛应用于食品和医药等领域^[1]。有研究报道, 给仔猪饲喂表达人溶菌酶(human lysozyme, hLY)的转基因羊奶, 可改善断奶仔猪的胃肠道功能, 抵抗致病性大肠埃希菌(EPEC)的感染, 且不会引起炎症反应^[2-3]。人乳中溶菌酶的含量和杀菌活性远远高于牛和猪^[1, 4]。因此, 如果在猪乳中高水平表达人溶菌酶, 将有助于提高仔猪的抗病性和成活率。为了验证这一想法, 需要制备在乳腺中特异表达人溶菌酶基因的转基因猪。

目前, 转基因克隆技术是制备转基因家畜最为有效的方法^[5]。自世界首例体细胞克隆猪诞生以来, 已经获得了多种转基因的克隆猪^[6-11], 但转 hLY 基因猪尚未见报道。当前体细胞克隆猪的效率仍然较低(1%~2%)^[12-13], 严重制约了转基因克隆猪

在畜牧业和科学研究中的应用。猪体细胞克隆技术是一项复杂的技术体系, 受到供体细胞、受体胞质、融合与激活、胚胎培养、胚胎移植和显微操作等多个技术环节的影响^[12], 其中融合与激活是克隆胚胎制备和启动发育的关键因素, 在很大程度上决定着克隆胚胎的发育能力。当卵母细胞的核被体细胞核置换以后, 必须进行激活才能够使胚胎启动发育。关于猪克隆胚胎激活的报道较多, 最常用的方法是电激活^[14]。为了提高激活效果, 一些化学药物如二甲基氨基嘌呤(6-DMAP)、放线菌酮(CHX)、细胞松弛素 B(CB)、二硫苏糖醇(DTT)、蛋白酶体

* 国家转基因育种重大专项(2008ZX08006-001), 国家重点基础研究发展计划(973)(2011CB944202)和广东省自然科学基金(S2011040001123)资助项目。

** 通讯联系人。

Tel: 010-62733323, E-mail: ninglcau@cau.edu.cn

收稿日期: 2012-02-17, 接受日期: 2012-07-24

第 167 页, 共 307 页

抑制剂 MG132 等分别被用于电激活后的联合辅助激活^[12, 14-19]。但是, 大多数优化激活条件的研究是利用猪卵母细胞孤雌激活进行的, 最佳孤雌激活条件是否就是最佳克隆胚胎激活条件呢? 该问题尚无明确答案。因此, 本研究比较了不同电激活和化学辅助激活条件下, 猪孤雌激活胚胎和克隆胚胎的体外发育效果, 并利用优化的激活条件生产乳腺特异表达人溶菌酶的转基因猪, 以期探索提高仔猪成活率的转基因猪新品种培育提供依据。

1 材料与方法

1.1 试验材料

除特别注释外, 所有化学试剂购自 Sigma 公司 (St. Louis, MO, USA)。基础成熟液 TCM199 购自 Gibco 公司, 成熟培养时添加 10% 猪卵泡液 (porcine follicular fluid, pFF), 10 μ g/L 表皮生长因子 (epidermal growth factor, EGF), 10 U/ml 人绒毛膜促性腺激素 (human chorionic gonadotrophin, hCG), 10 U/ml 孕马血清促性腺激素 (pregnant mare serum gonadotropin, PMSG) 和 0.57 mol/L 的 L-半胱氨酸。pFF 为自制^[20]。采卵液为 DPBS, 添加 0.1% 聚乙烯醇 (polyvinyl alcohol, PVA)。电融合激活液为 (0.25 mol/L 甘露醇, 0.1 mmol/L CaCl_2 , 0.1 mmol/L MgCl_2 , 0.5 mmol/L HEPES 和 0.01% PVA)。胚胎培养液为添加 0.3% 无脂肪酸 BSA 的 PZM3 (Porcine zygote medium 3) 液。转基因载体 pBC1-hLY-GFP-NEO 由农业生物技术国家重点实验室构建^[21]。由上海生工合成公司 PCR 检测引物: 人溶菌酶基因 PCR 上游引物 5' CAAGTAATACGCTGTTTCCTC 3', 下游引物 5' TGGTACACACCTGTAGTCAC 3'; 绿色荧光蛋白基因 PCR 上游引物 5' TGCAGTGCTTCAGCCGCTAC 3', 下游引物 5' CTCAGGTAGTGGTTGTCGGG 3'。

1.2 试验方法

1.2.1 猪卵母细胞的采集与体外成熟培养。从屠宰场获取初情期前母猪卵巢放入 37℃ 含青、链霉素的生理盐水中, 3 h 内运回实验室。用连接 18 号针头的 10 ml 注射器抽吸直径 3~6 mm 的卵泡, 将抽取液倒入培养皿中, 在体视显微镜下捡取胞质均匀、卵丘细胞 3 层以上且包裹紧密的卵丘-卵母细胞复合体 (cumulus oocyte complex, COCs)。用成熟培养液洗涤 3 次后, 转移到每孔含 500 μ l 成熟培养液的 4 孔板中, 每孔培养 60~100 枚 COCs, 并覆盖 400 μ l 石蜡油。培养条件为 39℃、5% CO_2 、95% 空气和饱和湿度。经过 42~44 h 成熟培养后,

用 1 g/L 的透明质酸酶 (Gibco 公司) 脱去卵丘细胞, 在体视镜下 (SMZ1000, Nikon) 挑选形态正常并且排出第一极体的卵母细胞, 放入 Hepes 缓冲的 NCSU-23 液^[19]中置于培养箱中备用。

1.2.2 转人溶菌酶基因猪胎儿成纤维细胞的准备。取妊娠 25 天的中国实验用小型猪胎儿, 建立猪胎儿成纤维细胞系, 方法见参考文献[22], 利用建立的雌性 Sw8 细胞系进行转基因操作, 待细胞生长至 70%~80% 汇合时, 利用脂质体 Lipofectamine 2000 (Invitrogen 公司) 介导的方法将线性化的 pBC1-hLY-GFP-NEO 乳腺特异表达载体转染至细胞, 筛选得到转基因细胞阳性率 95% 以上的细胞系, 并进行冻存, 方法见参考文献[21, 23]。在核移植前 5 天左右解冻转基因细胞, 使细胞密度达到 100% 汇合, 再继续培养 1~2 天后便可用于核移植。用 0.1% 胰蛋白酶消化并收集细胞, 放置 4℃ 备用。利用荧光显微镜和 PCR 方法对转基因细胞进行鉴定与检测。

1.2.3 猪克隆胚胎制备、融合激活与孤雌激活。

猪卵母细胞成熟培养后, 在装有显微操作仪的倒置显微镜下去核, 然后与一个成纤维细胞进行重构, 制备重构胚胎, 操作方法见参考文献[22]。将恢复 1 h 左右的重构胚分批转移到融合液中洗涤平衡 2~3 min, 再转移到充满融合液的融合槽内, 调整重构胚的位置使供体细胞和受体卵细胞接触面与电场方向垂直, 随后用电融合仪 CUY-21 (BEX, Nepa, Japan) 进行融合并同时激活。猪孤雌激活条件与克隆胚融合激活条件一致。

试验 1: 比较了不同电场强度 (0.8, 1.2, 1.6, 2.0 kV/cm)、相同脉冲时间 (100 μ s) 下, 猪孤雌胚胎和克隆胚胎的体外发育效果。试验 2: 比较了不同化学辅助激活处理对猪孤雌胚胎和克隆胚胎体外发育的影响, 胚胎激活后随机分为 3 组, 第 1 组不作处理作为对照, 第 2 组用 2 mmol/L 6-DMAP 处理 4 h, 第 3 组用 10 mg/L CB 和 10 mg/L CHX 处理 4 h, 之后转移到胚胎培养液中进行培养。实验 3: 比较了 1.6 kV/cm、100 μ s 条件下, 1 次电脉冲和 2 次电脉冲对克隆胚胎体外发育的影响, 2 次电脉冲间隔时间为 100 μ s。

1.2.4 胚胎体外培养与囊胚细胞计数。将激活后的胚胎转入预先平衡 2 h 以上的胚胎培养液滴 PZM3 中继续培养, 培养条件为 39℃、5% O_2 、5% CO_2 、95% N_2 和饱和湿度。在培养第 2 天和第 7 天分别

观察记录卵裂和囊胚发育情况. 将第 7 天的囊胚用 4% 多聚甲醛固定 10 min, 再用 DPBS 洗涤 3 次后, 转移到 10 mg/L Hoechst33342 中染色 10 min, 压片后在荧光显微镜下观察记录囊胚细胞数.

1.2.5 胚胎移植与妊娠诊断. 制备的猪克隆胚胎在融合激活 12~48 h 后, 经手术法将胚胎移植到自然发情 1~3 天的受体母猪输卵管内(以出现压背反应为发情第 0 天), 每头受体猪移植克隆胚胎 100~200 枚. 胚胎移植后第 30 天, 对未返情的受体母猪进行首次超声波妊娠检测, 之后定期跟踪胎儿发育情况, 调整饲养管理, 直至受体母猪分娩.

1.2.6 转基因克隆猪的鉴定. 克隆猪出生后第 2 天, 剪取耳组织带回实验室进行克隆猪耳成纤维细胞建系, 方法见参考文献[22], 在荧光显微镜下观察克隆猪耳组织细胞 GFP 表达情况. 提取克隆猪耳成纤维细胞 DNA, 用 PCR 方法检测 *hLY* 和 *GFP*

基因整合情况, 并利用 Southern 杂交和 Western blot 技术检测 *hLY* 基因整合和表达情况, 参见文献[24]. 同时, 对转 *hLY* 基因的克隆猪进行微卫星标记检测, 方法参见文献[25].

1.2.7 统计分析. 所有实验重复 3 次以上, 利用 SAS9.0 软件进行 *t* 检验和单因素方差分析, 利用 *Q* 法进行多重比较. $P < 0.05$ 表示差异显著.

2 结 果

2.1 转入溶菌酶基因(pBC1-hLY-GFP-NEO)细胞系的筛选与鉴定

通过筛选得到了表达绿色荧光蛋白的转 *hLY* 基因的细胞系 Sw8-*hLY* (图 1a), 在荧光显微镜下检测 GFP 阳性率达到 95.3%(286/300). 并对 2 个 GFP 阳性细胞克隆进行了 *hLY* 基因 PCR 检测, 结果均为阳性(图 1b).

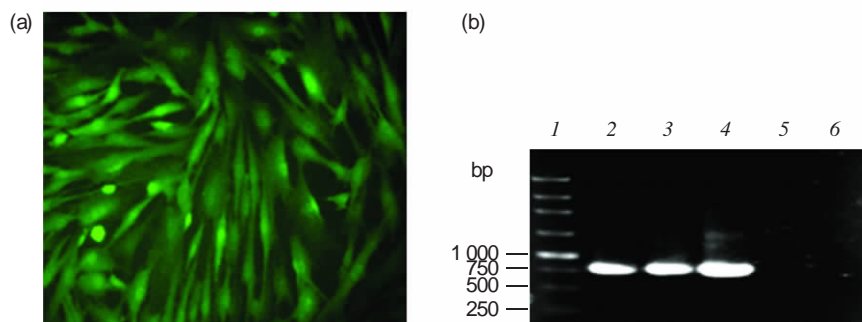


Fig. 1 Identification of Sw8-*hLY* transgenic cell lines

(a) Representative image of GFP expression of Sw8-*hLY* cells under fluorescent microscope. (b) The integration of *hLY* gene was identified in two clones of Sw8-*hLY* cells by PCR analysis, bands of product length is 780 bp. DNA of pBC1-hLY-GFP-NEO plasmid served as positive control, DNA of non-transfection Sw8 cells as negative control and distilled water as blank (non-template control). The same as below. 1: Marker; 2: Sw8-*hLY*-clone 1; 3: Sw8-*hLY*-clone 2; 4: Positive control; 5: Negative control; 6: Blank.

2.2 不同电场强度和脉冲次数对猪孤雌胚胎和克隆胚胎体外发育的影响

由图 2 可见, 不同电场强度激活的猪克隆胚胎和孤雌激活胚胎体外发育的变化趋势并不完全一致(图 2a, 图 2b). 孤雌激活胚胎在 0.8 kV/cm 电场强度下的卵裂率显著低于 1.2 kV/cm、1.6 kV/cm 和 2.0 kV/cm 组($P < 0.05$, 图 2a), 而克隆胚胎的卵裂率在 4 组之间差异不显著(图 2b). 从囊胚率来看, 孤雌激活胚胎在 1.6 kV/cm 和 2.0 kV/cm 之间没有显著差异($P > 0.05$), 但它们均显著高于 0.8 kV/cm 和 1.2 kV/cm 组($P < 0.05$, 图 2a), 而克隆胚胎囊胚

率在 0.8 kV/cm、1.2 kV/cm 和 2.0 kV/cm 之间差异不显著, 1.6 kV/cm 组的囊胚率显著高于 0.8 kV/cm 和 1.2 kV/cm 组($P < 0.05$, 图 2b). 不同电场强度对克隆胚胎的融合率具有显著影响, 1.6 kV/cm 和 2.0 kV/cm 组的融合率显著高于 0.8 kV/cm 和 1.2 kV/cm 组($P < 0.05$, 图 2c). 2 次电脉冲具有提高克隆胚胎体外发育能力的趋势, 但统计分析差异不显著($P > 0.05$, 图 2d). 通过综合比较, 可以得出 1.6 kV/cm、100 μ s、2 次电脉冲间隔 100 μ s 是最佳的克隆胚胎融合激活参数.

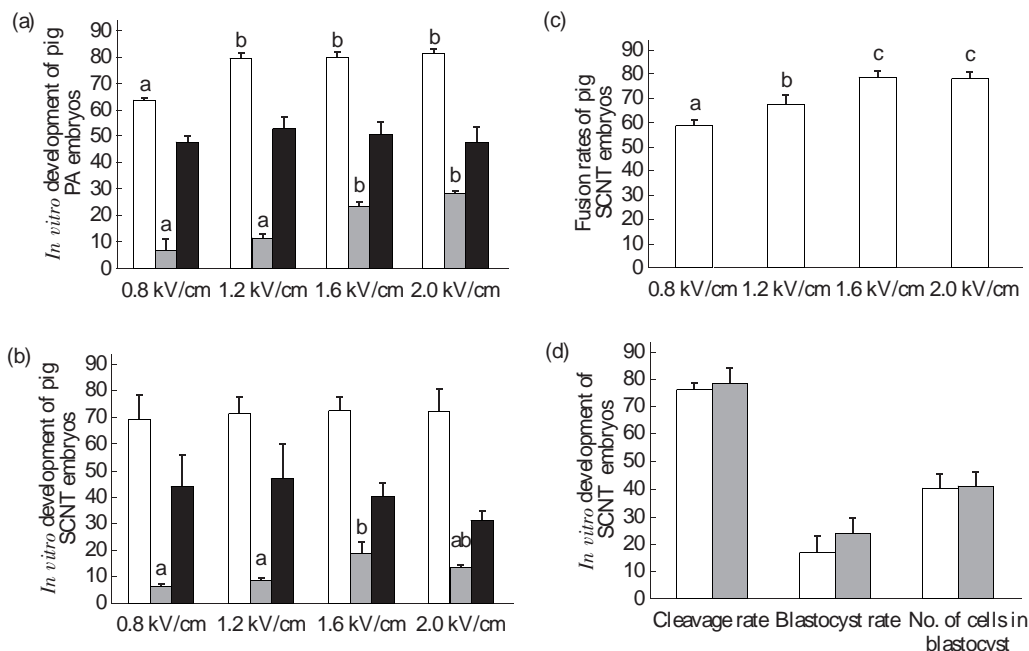


Fig. 2 *In vitro* development of embryos derived from PA and SCNT at different electric activation parameters

Columns without common letters were significantly different ($P < 0.05$). The same as below. (a, b) □: Cleavage rate; ■: Blastocyst rate; ▨: No. of cells in blastocyst. (c) □: Fusion rate. (d) □: One electric pulse; ■: Two electric pulse.

2.3 不同化学辅助激活对猪孤雌胚胎和克隆胚胎体外发育的影响

由图 3 可见, 电激活后联合 6-DMAP 或 CHX+CB 化学辅助激活能够显著提高猪孤雌胚胎的卵裂率和囊胚率, 而且 CHX+CB 处理的囊胚率

显著高于 6-DMAP 组 ($P < 0.05$, 图 3a). CHX+CB 辅助激活处理能够显著提高猪克隆胚胎囊胚率 ($P < 0.05$), 并且其卵裂率和囊胚细胞数也有增加的趋势(图 3b). 因此, 电激活后用 CHX+CB 处理 4 h 是最佳的辅助激活方法.

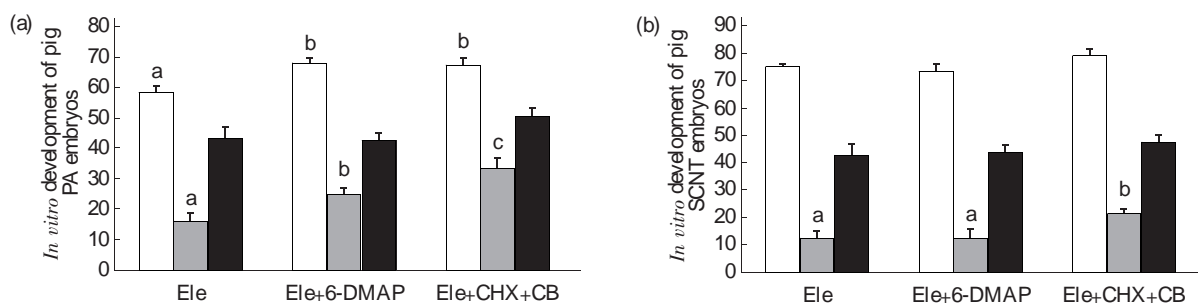


Fig. 3 Development of PA(a) and SCNT(b) embryos activated by electroporation(Ele)

Electroporation followed by incubation in the presence of 6-DMAP (Ele+6-DMAP) and electroporation followed by CHX (Ele+CHX) treatment. □: Cleavage rate; ■: Blastocyst rate; ▨: No. of cells in blastocyst.

2.4 转基因克隆猪的生产与鉴定

将 680 枚克隆胚胎移植到 5 头受体母猪的输卵管中, 在移植后第 30 天用 B 超检查, 共有 4 头妊娠, 移植妊娠率 80%, 其中 3 头怀孕到期, 移植分娩

率 60%, 出生了 5 头克隆猪(其中 1 头为死胎).

5 头克隆猪的耳组织, 在荧光显微镜下均可

观察到 GFP 蛋白表达, 且大部分 GFP 阳性细胞分布于毛囊(图 4b). 通过 PCR 检测发现, 5 头克隆猪 *GFP* 基因检测结果均为阳性(图 4c), 但是只有 3 头克隆猪为 *hLY* 基因阳性, 表明另外 2 头克隆猪的 *hLY* 基因丢失(图 4d). 微卫星检测结果表明, 3 头

hLY 转基因阳性克隆猪的遗传组成与供体细胞完全一致, 而与代孕母猪没有亲缘关系(表 1). 而 Southern 印迹和 Western blot 的检测结果表明, 我们得到了转 *hLY* 基因的克隆猪, 并且能够在乳腺中表达, 参见文献[24].

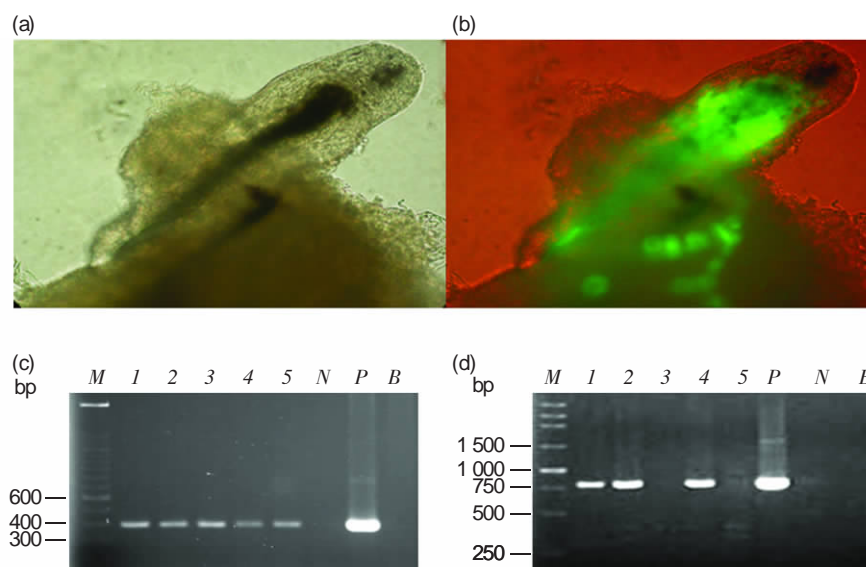


Fig. 4 Identification of transgenic cloned piglets

(a, b) Representative images of tissues from ear skin of cloned piglets under fluorescent microscope in white light (a) and white light plus blue light (b). (c, d) PCR analysis of *GFP* gene (c) and *hLY* (d) gene integration in cloned piglets. 1~5: The bands amplified from DNA of different cloned piglets, the PCR product length is 403 bp (c) and 780 bp (d) respectively. P: Positive control; N: Negative control; B: Blank control; M: Marker.

Table 1 Microsatellite analysis of *hLY* transgenic cloned piglets

Microsatellites	One surrogate mother	Donor cell	Piglet Sw8-1	Piglet Sw8-2	Piglet Sw8-4
SW940	150/154	146/156	146/156	146/156	146/156
S0089	142/146	143/154	143/154	143/154	143/154
SW742	205/205	199/213	199/213	199/213	199/213
SW2540	95/106	106/106	106/106	106/106	106/106
SW2049	94/96	90/94	90/94	90/94	90/94
SW1856	195/197	179/191	179/191	179/191	179/191
SW1473	168/170	168/170	168/170	168/170	168/170
SW1987	164/164	158/164	158/164	158/164	158/164

3 讨 论

人乳中溶菌酶的含量和活性均远远高于猪、牛、羊等动物^[1,4]. 为了探索在猪乳中表达人溶菌酶是否有助于提高仔猪成活率, 本研究利用 *pBCI-hLY-GFP-NEO* 表达载体和体细胞克隆技术, 成功生产了能在乳腺中表达 *hLY* 基因的克隆猪, 共 307 页

国实验用小型猪, 为提高仔猪成活率的转基因猪品种培育打下良好基础. 同时, 对猪克隆胚胎的激活方法进行了优化, 并比较了不同激活条件下猪孤雌胚胎和克隆胚胎的体外发育能力. 结果发现, 电场强度会显著影响克隆胚胎融合率和孤雌胚胎与克隆胚胎的囊胚率, 而电脉冲次数对克隆胚胎发育影响不显著(图 2). 电激活后再利用 CHX+CB 处理 4 h

能够显著提高猪孤雌胚胎和克隆胚胎的囊胚发育率(图 3), 但是猪孤雌胚胎和克隆胚胎发育能力在不同激活条件下的变化趋势并不完全一致, 为克隆胚胎激活条件的进一步优化提供了参考依据。通过综合比较, 得出 1.6 kV/cm、100 μ s、2 次电脉冲间隔 100 μ s, 再辅助以 CHX+CB 处理 4 h 是最佳的猪克隆胚胎激活方法。

提高转基因猪的生产效率对人类疾病模型、异种器官移植研究和提高养猪业生产效益等方面具有重要的意义。影响体细胞克隆效率的因素很多, 其中融合与激活是关键因素之一。克隆胚胎的激活是一个受精模拟过程。在受精胚胎, 精卵结合会引起细胞内钙库释放 Ca^{2+} , 产生钙波或钙振荡, 引发一系列磷酸化和去磷酸化事件, 其中有丝分裂酶原激活蛋白激酶(MAPK)的去磷酸化可使 MPF 活性迅速降低, 从而使卵子活化^[12, 19]。而电激活是在高压直流脉冲作用下, 使激活液中的 Ca^{2+} 进入细胞, 引起细胞内 Ca^{2+} 升高, 从而激活胚胎发育^[14]。电场强度、电脉冲时间和电脉冲次数均可影响胚胎激活效果^[26-27]。1 次电激只能引起卵子中 Ca^{2+} 升高 1 次, 多次电激可诱导卵子 Ca^{2+} 浓度多次升高^[28]。本研究发现, 1.6 kV/cm 电场强度组的克隆胚胎融合率和囊胚率显著高于 0.8 kV/cm 和 1.2 kV/cm 组(图 2), 虽然 2 次电脉冲的克隆胚胎发育能力有所提高, 但与对照组差异不显著, 与 Lee 等^[27]的报道相似, 说明电场强度是重要的电激活参数, 而电脉冲次数对猪克隆胚胎的激活促进作用不明显。另外, 本研究还发现, 猪孤雌胚胎囊胚率随着电场强度的升高而增加, 而猪克隆胚胎囊胚率随着电场强度的升高先升后降(图 2), 表明最佳的孤雌激活参数不一定就是最佳的克隆胚胎激活参数, 应该利用克隆胚胎, 而不是孤雌激活胚胎, 进行克隆胚胎最佳激活条件的筛选, 为进一步完善克隆胚胎激活条件指明了方向。虽然一次电刺激足以引起猪卵母细胞的活化^[27], 但是卵子的活化程度可能与胚胎的发育能力密切相关。大量的研究表明, 电激活后再联合化学辅助激活有助于提高克隆胚胎或孤雌激活胚胎的发育能力^[14-19]。6-DMAP 是一种蛋白激酶抑制剂, 它能够降低 MAPK 的活性而使 MPF 失活。CHX 是一种蛋白质合成抑制剂, 能够有效抑制 MPF 的合成。本研究结果表明, 利用 6-DMAP 或 CHX+CB 进行辅助激活处理均能显著提高猪孤雌胚胎囊胚率, 其中 CHX+CB 处理效果更加显著, 而且能够显著提高克隆胚胎囊胚率(图 3), 与前人的报道结果相

一致^[19, 27]。

溶菌酶是一类天然非特异性免疫蛋白, 具有抗菌、抗病毒和增强免疫力的功能。在乳腺中特异表达人溶菌酶的研究已经在小鼠、牛、羊上获得成功^[3, 21, 29], 但在猪上尚未见报道。本研究利用改良的乳腺特异表达载体 *pBCI-hLY-GFP-NEO* 成功获得了 5 头雌性转基因猪, 其中有 3 头检测到有 *hLY* 和 *GFP* 基因同时整合, 另外 2 头则只检测到 *GFP* 基因整合(图 4)。其原因可能是在基因转染前转基因载体发生降解或者在基因整合时 *hLY* 基因片段被破坏所致。据报道, 随着转基因猪生长和传代, 也会产生外源基因拷贝数减少或丢失的现象^[30], 但其具体机制仍然未知。另外, 获得高纯度的转基因阳性细胞是生产转基因克隆猪的重要前提条件, 虽然本研究使用的转基因细胞系 GFP 阳性率达到 95%以上, 但它是多个细胞克隆的混合体, 这也可能造成所获得的克隆猪外源基因整合情况不完全一致。本研究获得的 *hLY* 转基因猪有 2 头存活到成年并配种产仔, 通过 DNA 印迹和蛋白质印迹检测结果进一步表明我们成功获得了能够在乳腺中表达 *hLY* 的转基因猪^[24]。但是, 猪乳中表达 *hLY* 能否提高仔猪免疫力和成活率, 还有待于进一步研究。

总之, 本研究对融合激活条件进行了优化, 提高了猪克隆胚胎的体外发育能力, 同时指出了孤雌胚胎最佳激活条件并不一定是克隆胚胎的最佳激活条件。利用优化的猪克隆胚胎激活条件首次成功获得了在乳腺中特异表达 *hLY* 基因的转基因中国实验用小型猪, 为提高仔猪成活率的转基因猪品种培育奠定了坚实的基础。

参 考 文 献

- [1] Benkerroum N. Antimicrobial activity of lysozyme with special relevance to milk. *African J Biotechnology*, 2008, 7 (25): 4856-4867
- [2] Cooper C A, Brundige D R, Reh W A, *et al.* Lysozyme transgenic goats' milk positively impacts intestinal cytokine expression and morphology. *Transgenic Res*, 2011, 20 (6): 1235-1243
- [3] Brundige D R, Maga E A, Klasing K C, *et al.* Lysozyme transgenic goats' milk influences gastrointestinal morphology in young pigs. *J Nutr*, 2008, 138 (5): 921-926
- [4] Shahani K M, Kwan A J, Friend B A. Role and significance of enzymes in human milk. *Am J Clin Nutr*, 1980, 33 (8): 1861-1868
- [5] Piedrahita J A, Olby N. Perspectives on transgenic livestock in agriculture and biomedicine: An update. *Reproduction Fertility and Development*, 2011, 23 (1): 56-63
- [6] Dai Y F, Vaught T D, Boone J, *et al.* Targeted disruption of the alpha-1,3-galactosyltransferase gene in cloned pigs. *Nat Biotechnol*,

- 2002, **20** (3): 251-255
- [7] Lai L, Park K W, Cheong H T, *et al.* Transgenic pig expressing the enhanced green fluorescent protein produced by nuclear transfer using colchicine-treated fibroblasts as donor cells. *Molecular Reproduction and Development*, 2002, **62** (3): 300-306
- [8] Lai L, Kang J X, Li R, *et al.* Generation of cloned transgenic pigs rich in omega-3 fatty acids. *Nat Biotechnol*, 2006, **24** (4): 435-436
- [9] Ahn K S, Won J Y, Park J K, *et al.* Production of human cd59-transgenic pigs by embryonic germ cell nuclear transfer. *Biochem Biophys Res Commun*, 2010, **400** (4): 667-672
- [10] Sommer J R, Estrada J L, Collins E B, *et al.* Production of elovl4 transgenic pigs: A large animal model for stargardt-like macular degeneration. *British J Ophthalmology*, 2011, **95** (12): 1749-1754
- [11] Kim Y J, Ahn K S, Kim M J, *et al.* Targeted disruption of ataxia-telangiectasia mutated gene in miniature pigs by somatic cell nuclear transfer. *Reproduction Fertility and Development*, 2012, **24** (1): 124-124
- [12] Vajta G, Zhang Y H, Machaty Z. Somatic cell nuclear transfer in pigs: Recent achievements and future possibilities. *Reproduction Fertility and Development*, 2007, **19** (2): 403-423
- [13] Lai L X, Prather R S. Production of cloned pigs by using somatic cells as donors. *Cloning Stem Cells*, 2003, **5** (4): 233-241
- [14] Whitworth K M, Li R, Spate L D, *et al.* Method of oocyte activation affects cloning efficiency in pigs. *Molecular Reproduction and Development*, 2009, **76** (5): 490-500
- [15] Song K, Hyun S H, Shin T, *et al.* Post-activation treatment with demecolcine improves development of somatic cell nuclear transfer embryos in pigs by modifying the remodeling of donor nuclei. *Molecular Reproduction and Development*, 2009, **76** (7): 611-619
- [16] Sugimura S, Kawahara M, Wakai T, *et al.* Effect of cytochalasins b and d on the developmental competence of somatic cell nuclear transfer embryos in miniature pigs. *Zygote*, 2008, **16** (2): 153-159
- [17] Nanassy L, Lee K, Javor A, *et al.* Effects of activation methods and culture conditions on development of parthenogenetic porcine embryos. *Anim Reprod Sci*, 2008, **104** (2-4): 264-274
- [18] De Sousa P A, Dobrinsky J R, Zhu J, *et al.* Somatic cell nuclear transfer in the pig: Control of pronuclear formation and integration with improved methods for activation and maintenance of pregnancy. *Biol Reprod*, 2002, **66** (3): 642-650
- [19] 马育芳, 卫恒习, 李 燕, 等. 化学激活和季节对克隆猪出生率的影响. *中国科学 C 辑: 生命科学*, 2009, **39** (4): 384-391
Ma Y F, Wei H X, Li Y, *et al.* *Science in China Series C: Life Sciences*, 2009, **39** (4): 384-391
- [20] 卫恒习, 李 俊, 李秋艳, 等. 瘦素对猪卵母细胞体外成熟及克隆猪妊娠率的影响. *自然科学进展*, 2008, **18** (11): 1320-1324
Wei H X, Li Jun, Li Q Y, *et al.* *Progress in Natural Science*, 2008, **18** (11): 1320-1324
- [21] 于政权, 樊宝良, 戴蕴平, 等. 转基因小鼠乳腺表达重组人溶菌酶. *科学通报*, 2003, **48** (20): 2149-2153
Yu Z Q, Fan B L, Dai Y P, *et al.* *Chin Sci Bull*, 2003, **48** (20): 2149-2153
- [22] 张运海, 潘登科, 孙秀柱, 等. 利用体细胞核移植技术生产表达绿色荧光蛋白的猪转基因克隆胚胎. *中国科学 C 辑: 生命科学*, 2005, **35** (5): 439-445
Zhang Y H, Pan D K, Sun X Z, *et al.* *Science in China Series C: Life Science*, 2005, **35**(5): 439-445
- [23] 李秋艳, 卫恒习, 郭 英, 等. 利用体细胞核移植技术生产表达增强绿色荧光蛋白(egfp)的转人溶菌酶基因(hly)的猪克隆胚胎. *自然科学进展*, 2008, **18** (10): 1157-1162
Li Q Y, Wei H X, Guo Y, *et al.* *Prog Natural Science*, 2008, **18** (10): 1157-1162
- [24] Tong J, Wei H, Liu X, *et al.* Production of recombinant human lysozyme in the milk of transgenic pigs. *Transgenic Res*, 2011, **20** (2): 417-419
- [25] 潘登科, 张运海, 孙秀柱, 等. 低氧培养早期胚胎克隆小型猪(sus scrofa). *科学通报*, 2006, **51** (4): 415-419
Pan D K, Zhang Y H, Sun X Z, *et al.* *Chin Sci Bull*, 2006, **51**(4): 415-419
- [26] Zimmermann U. Electric field-mediated fusion and related electrical phenomena. *Biochim Biophys Acta*, 1982, **694** (3): 227-277
- [27] Lee J W, Tian X C, Yang X. Optimization of parthenogenetic activation protocol in porcine. *Molecular Reproduction and Development*, 2004, **68** (1): 51-57
- [28] Collas P, Fissore R, Robl J M, *et al.* Electrically induced calcium elevation, activation, and parthenogenetic development of bovine oocytes. *Molecular Reproduction and Development*, 1993, **34** (2): 212-223
- [29] Yang B, Wang J, Tang B, *et al.* Characterization of bioactive recombinant human lysozyme expressed in milk of cloned transgenic cattle. *PLoS One*, 2011, **6** (3): e17593
- [30] Kong Q, Wu M, Huan Y, *et al.* Transgene expression is associated with copy number and cytomegalovirus promoter methylation in transgenic pigs. *PLoS One*, 2009, **4** (8): e6679

Optimizing of Activation Protocols and Production of Transgenic Pigs Expressing Human Lysozyme by Somatic Cell Nuclear Transfer*

WEI Heng-Xi^{1,2}, LI Jun^{2,3}, TONG Jia², MA Yu-Fang², GAO Feng-Lei¹,
LI Qiu-Yan², ZHANG Shou-Quan¹, LI Ning^{2**}

⁽¹⁾ Guangdong Provincial Key Laboratory of Agro-Animal Genomics and Molecular Breeding, College of Animal Science,
South China Agricultural University, Guangzhou 510642, China;

⁽²⁾ State Key Laboratory for Agrobiotechnology and Department of Animal Physiology, China Agricultural University, Beijing 100193, China;

⁽³⁾ Reproductive medical center, 1st hospital of Hebei medical university, Shijiazhuang 050031, China)

Abstract In order to improve the cloning efficiency and obtain human lysozyme (*hLY*) gene transgenic pigs, the present study was carried out to investigate the effects of different electric activation parameters and chemicals on *in vitro* development of embryos derived from parthenogenesis (PA) and somatic cell nuclear transfer (SCNT). The results showed that the electric strength could influence the fusion rate and developmental ability of SCNT embryos ($P < 0.05$), and number of electric pulses had no significant effect on SCNT embryos development ($P > 0.05$), yet different variation tendency was found in developmental ability between PA and SCNT embryos under same activation parameters. The blastocyst rate of SCNT embryos was improved when treated with CHX+CB for 4 h after electric activation ($P < 0.05$), whereas 6-DMAP did not ($P > 0.05$). On the contrary, either CHX+CB or 6-DMAP treatment after electric pulses could improve the blastocyst rate of PA embryos, indicating that the best activation method for PA was not necessarily the best for SCNT. The best activation protocol of SCNT embryos in our study is two pulses of 100 μ s, direct current of 1.6 kV/cm electric strength with 100 μ s interval, and followed by CHX+CB treatment for 4 h. With the activation protocol, the mammary gland expressed *hLY* transgenic pigs were generated. It could help for improving piglets survival rate in transgenic breeding.

Key words somatic cell nuclear transfer, embryo activation, transgene, human lysozyme, pig

DOI: 10.3724/SP.J.1206.2012.00082

* This work was supported by grants from The National Transgenic Breeding Program of China (2008ZX08006-001), National Basic Research Program of China (2011CB944202) and Guangdong Natural Science Foundation (S2011040001123).

** Corresponding author.

Tel: 86-10-62733323, E-mail: ninglcau@cau.edu.cn

Received: February 17, 2012 Accepted: July 24, 2012



Investigation Into the Relationship Between Sperm Cysteine-Rich Secretory Protein 2 (CRISP2) and Sperm Fertilizing Ability and Fertility of Boars

Fenglei Gao^{1,2†}, Ping Wang^{1†}, Kai Wang¹, Yushan Fan¹, Yuming Chen¹, Yun Chen¹, Chao Ye³, Meiying Feng^{1,4}, Li Li¹, Shouquan Zhang¹ and Hengxi Wei^{1*}

OPEN ACCESS

Edited by:

Arumugam Kumaresan,
National Dairy Research Institute
(ICAR), India

Reviewed by:

Pablo Daniel Cetica,
Universidad de Buenos
Aires, Argentina
Ivan Cunha Bustamante-Filho,
Universidade do Vale do Taquari -
Univates, Brazil

*Correspondence:

Hengxi Wei
weihengxi@scau.edu.cn

[†]These authors have contributed
equally to this work

Specialty section:

This article was submitted to
Animal Reproduction -
Theriology,
a section of the journal
Frontiers in Veterinary Science

Received: 14 January 2021

Accepted: 08 April 2021

Published: 30 April 2021

Citation:

Gao F, Wang P, Wang K, Fan Y,
Chen Y, Chen Y, Ye C, Feng M, Li L,
Zhang S and Wei H (2021)
Investigation Into the Relationship
Between Sperm Cysteine-Rich
Secretory Protein 2 (CRISP2) and
Sperm Fertilizing Ability and Fertility of
Boars. *Front. Vet. Sci.* 8:653413.
doi: 10.3389/fvets.2021.653413

¹ Guangdong Provincial Key Lab of Agro-animal Genomics and Molecular Breeding, National Engineering Research Center for Breeding Swine Industry, College of Animal Science, South China Agricultural University, Guangzhou, China, ² Department of Tropical Agriculture and Forestry, College of Guangdong Agriculture Industry Business Polytechnic, Guangzhou, China, ³ Technology Department, Guangdong Wen's Foodstuffs Group Co., Ltd., Yunfu, China, ⁴ College of Life Sciences, Zhaoqing University, Zhaoqing, China

The proteins in the seminal plasma and on the sperm surface play important roles in sperm function and numerous reproductive processes. The cysteine-rich secretory proteins (CRISPs) are enriched biasedly in the male reproductive tract of mammals, and CRISP2 is the sole member of CRISPs produced during spermatogenesis; whereas the role of CRISP2 in fertilization and its association with fertility of boars are still unclear. This study aimed to investigate the relationship between the sperm CRISP2 and boar fertility, and explore its impact sperm fertilizing ability. The levels of CRISP2 protein in sperm were quantified by ELISA; correlation analysis was performed to evaluate the association between CRISP2 protein levels and boar reproductive parameters. Meanwhile, the expression of CRISP2 in boar reproductive organs and sperm, and the effects of CRISP2 on *in vitro* fertilization (IVF) were examined. The results showed that boars with high sperm levels of CRISP2 had high fertility. The protein levels of CRISP2 in sperm were positively correlated with the litter size ($r = 0.412$, $p = 0.026$), the number of live-born piglets ($r = 0.421$, $p = 0.023$) and the qualified piglets per litter ($r = 0.381$, $p = 0.042$). CRISP2 is specifically expressed in the testis and sperm of adult boars, and its location on sperm changed mainly from the post-acrosomal region to the apical segment of acrosome during capacitation. The cleavage rate was significantly decreased by adding the anti-CRISP2 antibody to the IVF medium, which indicates CRISP2 plays a critical role in fertilization. In conclusion, CRISP2 protein is specifically expressed in the adult testis and sperm and is associated with sperm fertilizing ability and boar fertility. Further mechanistic studies are warranted, in order to fully decipher the role of CRISP2 in the boar reproduction.

Keywords: CRISP2, sperm, fertilization, fertility, boar

INTRODUCTION

Boar fertility and sperm fertilizing ability are key factors for improving pig production levels and economic benefits, especially in the modern intensive pig industry where artificial insemination (AI) is widely used (1, 2). Proteins, in both the seminal plasma and on the sperm surface, play important regulatory roles in maintaining sperm motility, fertilizing ability, and sperm-egg interaction and are closely related to the fertility of male animals (3, 4). Recently, proteomics approaches identified candidate protein markers in semen for evaluating male fertility, which can help select superior males and improve the production level in animal husbandry (3, 5).

Cysteine-rich secretory proteins (CRISPs) are members of the CRISP, antigen 5 and pathogenesis-related protein 1 (CAP) superfamily and are enriched biasedly in the male reproductive tract of mammals (6, 7). CRISPs are two domain proteins with an N-terminal CAP domain and a cysteine-rich domain (CRD) at the C-terminus called the CRISP domain. The CRISP domain consists of a hinge region and an ion channel region, and eight disulfide bonds in the hall molecule can stabilize structure of CRISPs (7–9). So far, four CRISPs, CRISP1–4, have been found in mice, and three CRISPs, CRISP1–3, have been found in humans, horses and pigs (6, 9, 10).

CRISP2, known as testis-specific protein 1 (Tpx-1), is the sole CRISP produced during spermatogenesis. CRISP2 is localized in the acrosome and tail of sperm, and is released from the acrosome and reassociated at the equatorial segment during the acrosome reaction (11). The reduced expression of CRISP2 in ejaculated spermatozoa has been reported to decrease pregnancy rates in Holstein bulls (12). CRISP2 is necessary for sperm function and male fertility in mice and humans (7, 11), and CRISP2-knockout mice exhibit subfertility phenotypes with an abnormal sperm function (7, 13). Recently, it has been shown that there is a strong relationship between CRISP2 and human spermatogenesis and infertility (14, 15). The expression of CRISP2 was down-regulated in patients with teratoasthenozoospermia, asthenozoospermia or teratozoospermia (16). Contrary to the knowledge gained from mice and humans, the function of CRISP2 in pig reproduction is poorly characterized except for the mRNA expression in reproductive organs (8, 17).

In this study, the relationship between sperm CRISP2 and boar fertility was investigated, and its function on sperm fertilizing ability and the expression profile in sperm and reproductive tissues were analyzed. The present study may reveal the association between the expression level of CRISP2 sperm and the boar fertility, and provide novel insights about CRISP2 expression and function relative to pig reproduction, which could help to enrich the knowledge of sperm CRISP2 and develop new biomarker of male fertility.

Abbreviations: AI, artificial insemination; BUG, bulbourethral gland; CAP, CRISP, antigen 5 and pathogenesis-related protein 1; CRD, cysteine-rich domain; CRISP2, cysteine-rich secretory protein 2; SVG, seminal vesicle gland; Tpx-1, testis-specific protein 1.

MATERIALS AND METHODS

Ethics Statement

This work was approved by the Ethics Committee on Animal Experimentation of South China Agricultural University. The license number is SYXK (Guangdong) 2019-0136.

Samples

Thirty-three Yorkshire semen samples and the fertility data for each boar were supplied by Shuitai Pig Farm (Guangdong, China). The protein samples of sperm were extracted immediately after semen collection. The sperm proteins were extracted with a whole protein extraction kit (KeyGEN, Jiangsu, China) according to the manufacturer's instructions. Briefly, the sperm samples were centrifuged at 10,000 rpm for 5 min. Supernatant was discarded and sperm pellet was washed thrice with ice-cold DPBS. The sperm pellet was incubated with ice-cold lysis buffer with 1 mM phenylmethylsulfonyl fluoride (PMSF), and the tubes were incubated on ice for 4 min and vortexed for 30 s for 5 times. After incubation, the tubes were centrifuged at 14,000 rpm at 4°C for 4 min. After centrifugation, supernatant was retained as the sperm protein samples.

The reproductive tissues (at least 3 samples) of immature (3 months old) and adult (24 months old) male and female pigs from Shuitai Farm were collected immediately after slaughter and stored in liquid nitrogen or fixed in 4% paraformaldehyde. Testis, epididymis (distal caput), bulbourethral gland (BUG), prostate, and seminal vesicle gland (SVG) were collected from the males. Ovaries, oviduct, uterine horn, uterine body, and cervix were collected from females. The oocytes and granulosa cells were collected from the ovaries in a local slaughterhouse, and the isolation of granulosa cells was performed according to previous study (18). The total RNA and protein of each sample were extracted by using an RNeasy Mini Kit (Qiagen, Hilden, Germany) and a whole protein extraction kit (KeyGEN), respectively, according to the manufacturer's instructions. Purity and concentration of RNA were measured using a NanoDrop ND-1000 instrument (Thermo Fisher Scientific, Waltham, USA). RNA integrity was evaluated using an Agilent 2100 Bioanalyzer (Agilent, San Jose, USA). For protein extraction from tissue samples, the tissues were homologized in lysis buffer containing 1 mM PMSF and were then subjected to centrifugation (14,000 rpm) for 5 min at 4°C. The supernatant was collected as the protein samples.

The protein levels of samples were measured and diluted to an appropriate concentration with a BCA protein assay kit (KeyGEN) according to the manufacturer's instructions. Briefly, a standard curve (range 0–2,000 µg/mL) was derived with nine points of serial dilution with bovine serum albumin (BSA) and a working reagent. All samples and standard points were replicated three times. The samples (100 µL each) were mixed with 2.0 mL of working reagent and incubated at 37°C for 30 min. After cooling to room temperature, each absorbance difference, which was subtracted by averaged absorbance of blank standard replicates at 562 nm, was measured by a spectrometer, and the absorbance differences were converted to µg/mL via the standard curve. If a protein concentration exceeded the upper limit of

the standard curve of 2,000 $\mu\text{g/mL}$, the sample was diluted until it could be measured within the standard range, and the final concentrate was calibrated considering the dilution factor.

Enzyme-Linked Immunosorbent Assay (ELISA) Detection and Fertility Correlation Analysis of Sperm CRISP2

The protein levels of CRISP2 of each sample were quantified with a porcine CRISP2 ELISA kit (PG1898, TSZ, USA). The assay range was 18–1,450 pg/mL according to the kit instructions. The relative expression level of CRISP2 protein was obtained by dividing the protein levels of CRISP2 by the total protein content. The correlation between the relative content of CRISP2 and the fertility data was conducted using Pearson correlation analysis.

In vitro Fertilization (IVF)

The IVF experiment was conducted as previously reported (19). Briefly, porcine ovaries were obtained from a slaughterhouse and transported to the laboratory in sterile 0.9% NaCl at 38.5°C within 2 h of slaughter. Oocytes were aspirated from follicles (3–6 mm in diameter) with an 18-gauge needle attached to a disposable syringe. Oocytes covered with multilayers of cumulus cells were selected. Oocytes collected were cultured for 44–6 h and denuded in 1 mg/ml hyaluronidase in DPBS by mechanically pipetting; then, 10–15 oocytes were grouped and transferred to the 50 μl mTBM fertilization medium containing 2.5 mM caffeine and 2 mg/ml bovine serum albumin (BSA; fraction V) covered with mineral oil. The fresh semen provided by the Shuitai Farm was washed three times by centrifugation with DPBS supplemented with 0.1% BSA at 1,500 rpm for 4 min. The spermatozoa pellets were resuspended and diluted to 1×10^6 sperm/ml with mTBM for capacitation in the CO_2 incubator for 30 min. Then, the capacitated sperm were added to the drop containing oocytes with a final sperm concentration of 1×10^5 sperm/ml and co-incubated for 6 h at 39°C in an atmosphere of 5% CO_2 in air. After fertilization, the oocytes were washed 3 times and cultured with PZM3 medium at 39°C, 5% O_2 , 5% CO_2 , 90% N_2 , and 100% humidity. The cleavage rate was determined after culturing for 48 h.

The effect of CRISP2 on fertilization was tested by adding the anti-CRISP2 antibody (SAB2501635, Sigma, USA) to the fertilization medium mTBM. Briefly, 2 μl of the antibody was added to 500 μl fertilization medium to a final concentration of 2 $\mu\text{g/ml}$ of anti-CRISP2 antibody. The same volume of dilution medium (20 mM Tris (pH 7.3) + 150 mM NaCl + 0.02% sodium azide + 0.5% BSA) or the IgG were added as controls.

Reverse Transcriptase PCR and Quantitative Real-Time PCR (qRT-PCR)

The gene expression of CRISP2 in different reproductive organs of different aged male and female pigs was examined by reverse transcriptase PCR. The primers used in the analysis are presented in Table 1. The PCR conditions were as follows: initial denaturation at 94°C for 5 min, followed by 35 cycles of

denaturation at 94°C for 30 s, annealing at 60°C for 30 s and extension at 72°C for 40 s, and a final extension at 72°C for 7 min.

The relative expression levels of CRISP2 in the reproductive organs of male and female pigs at different ages were further verified by qRT-PCR using a SYBR-Green RT-PCR Kit (Thermo Fisher Scientific) in an Applied Biosystems 7900HT Real-time PCR Thermal Cycler (Applied Biosystems, Foster City, USA). GAPDH was employed as an internal control, and each sample was analyzed three times. The mean values were calculated using the $\Delta\Delta\text{Ct}$ method as previously reported (20). The PCR conditions were as follows: initial denaturation at 95°C for 3 min, followed by 40 cycles of denaturation at 95°C for 10 s, annealing at 60°C for 10 s and extension at 72°C for 30 s. The qRT-PCR primers are listed in Table 1.

Western Blot

The proteins (20 μg) of adult boar reproductive tissues and sperm were separated by SDS-PAGE using 12% (v/v) gels and transferred onto PVDF membranes (Millipore, Billerica, MA, USA). After blocking with 5% non-fat milk for 1 h at room temperature, the membranes were incubated with primary antibodies against CRISP2 (1:1,000; SAB2501635, Sigma, USA) or β -actin (1:1,000; HC201, TransGen Biotech, China) overnight at 4°C. The membranes were washed 3 times for 10 min each with TBST (0.1% Tween 20, 20 mM Tris/HCl, 150 mM NaCl; pH 8.0) and incubated for 1 h with horseradish peroxidase (HRP)-conjugated rabbit anti-goat (1:3,000; E030130-02; Earthox, San Francisco, USA) or goat-anti-mouse (1:3,000; HS201, TransGen Biotech, China) secondary antibodies at room temperature for 1 h. The membranes were incubated for 5 min with the enhanced chemiluminescence (ECL) detection reagent in the dark and then exposed with a Tanon-5200 Imaging System (Tanon, Shanghai, China). β -actin was used as the internal control, and the relative protein expression levels of CRISP2 were analyzed by using ImageJ software (<https://imagej.nih.gov/ij/index.html>).

Immunohistochemistry Assay

Immunohistochemical detection of CRISP2 in the adult tissues of testis was carried out on 5 μm tissue sections mounted onto siliconized slides. Briefly, paraffin sections were dewaxed with xylene, rehydrated in a graded series of ethanol, and antigen retrieval was performed by heating at 95°C in 10 mM sodium citrate (pH 6.0). Endogenous peroxidase was quenched with 0.3% H_2O_2 in methanol for 15 min at room temperature. After 3 washes in PBS (pH 7.4), the slides were incubated in a blocking solution containing 3% BSA for 30 min at room temperature. Sections were incubated overnight at 4°C with antibodies against CRISP2 (1:150; SAB2501635; Sigma, USA), and the primary antibody replaced with normal IgG diluted was served as a negative control. After washing 3 times in PBS, sections were incubated with HRP-conjugated secondary antibodies for 50 min at room temperature. Then, the sections developed with a DAB chromogenic solution and counterstained with a hematoxylin solution. Sections were dehydrated, cleared, covered with Permunt solution (Fisher, NH, USA) and viewed under an Olympus BX53F microscope (Olympus, Japan).

TABLE 1 | RT-PCR and qRT-PCR primers.

	Genes	Forward (5'-3')	Reverse (5'-3')	Product size (bp)
RT-PCR	<i>GAPDH</i>	CCACCGTCCAGCGAGAAC	CAGCCGAGGAGGTGAGCC	432
	<i>CRISP2</i>	ACTCCCAATGGTGCTGTTTC	ATCCAACGCGGTAAGATGAG	418
qRT-PCR	<i>GAPDH</i>	GAGATCCCGCCAACATCAAAT	GTTACGCCCATCACAACAT	170
	<i>CRISP2</i>	TGTACAGAGCAAACAGGGCA	GTTGATTGGCACGGTAGGC	194

Immunofluorescence Staining

To evaluate the distribution of CRISP2 in the sperm before and after capacitation, immunofluorescence detection was performed as previously described (21). The sperm before and after *in vitro* capacitation were fixed with 4% paraformaldehyde for 20 min, washed three times with PBS, permeabilized with 0.5% Triton-100 for 10 min, and blocked in 1% BSA (Sigma) for 30 min. The sperm were incubated with a goat anti-CRISP2 antibody (1:200; SAB2501635, Sigma, USA) at 4°C overnight and washed three times in PBS. After that, the sperm were incubated with Alexa Fluor 568-donkey anti-goat IgG (1:100; A-11057, Thermo Fisher) 1 h at 37°C in the dark. The samples were coated onto slides and observed under a fluorescence microscope (BX53F, Olympus).

Statistical Analysis

All the data analysis was performed using the SPSS 18.0 software (IBM, USA). All the data were expressed as mean \pm standard deviation. The correlation between the relative content of CRISP2 and the fertility data was conducted using Pearson correlation analysis. The unpaired Student's *t*-test was performed to assess the significant differences between treatment groups. $P < 0.05$ was considered statistically significant.

RESULTS

Correlation Between the Sperm CRISP2 Protein Levels and Boar Reproductive Parameters

The relative content of CRISP2 in sperm of 33 boars was detected by ELISA, and effective data was obtained for 29 boars, because a few ELISA wells showed null data. The sperm CRISP2 protein levels and boar reproductive parameters of 29 boars were shown in **Supplementary Table 1**. The 29 boars were divided into low CRISP2 and high CRISP2 group based on the median values of the sperm CRISP2 protein levels. The correlation analysis listed in **Table 2** showed that the protein levels of sperm CRISP2 were significant positive correlation with the boar breeding parameters of litter size ($r = 0.412$, $p = 0.026$), live-born piglets per litter ($r = 0.421$, $p = 0.023$) or qualified piglets per litter ($r = 0.381$, $p = 0.042$), but not with parturition rate ($r = 0.029$, $p = 0.880$) or boar fecundity ($r = 0.315$, $p = 0.096$).

To further analyze the correlation between sperm CRISP2 protein levels and the reproductive capacity of boars and to even explore their feasibility as biomarkers for screening boars with high fertility, we ranked the boars corresponding to their protein levels of sperm CRISP2 and divided them into 2 groups: the high CRISP2 group ($n = 14$) and the low CRISP2 group ($n = 15$).

TABLE 2 | Correlation analysis between the content of CRISP2 in sperm and the boar reproductive parameters.

Protein	Reproductive parameters	Pearson correlation coefficient (<i>r</i>)	<i>P</i> -value
Sperm CRISP2	Litter size	0.412	0.026
	No. live-born piglets/litter	0.421	0.023
	No. qualified piglets/litter	0.381	0.042
	Parturition rate	0.029	0.880
	Boar fecundity [#]	0.315	0.096

[#]Fecundity equals litter size multiplied by the parturition rate. The number of boars is $n = 29$, bred 1,842 sows in total.

TABLE 3 | Effect of sperm CRISP2 on boar reproductive performance.

Items	Low CRISP2	High CRISP2
No. of boars	14	15
No. of sows bred	977	865
CRISP2 relative content (10^{-7})	3.26 ± 0.34	$14.85 \pm 1.48^{**}$
Litter size	12.18 ± 0.26	$13.08 \pm 0.17^{**}$
Live-born piglets/litter	11.57 ± 0.27	$12.61 \pm 0.20^{**}$
Qualified piglets/litter	10.39 ± 0.26	$11.18 \pm 0.17^{*}$
Parturition rate (%)	92.95 ± 1.51	93.26 ± 1.22
Boar fecundity	11.32 ± 0.33	$12.21 \pm 0.28^{*}$

* $p < 0.05$; ** $p < 0.01$.

TABLE 4 | Effect of anti-CRISP2 antibodies on the cleavage rate of *in vitro* fertilization.

Groups	No. of oocytes	No of cleaved	Cleavage rate/%
Control	324	192	59.53 ± 2.54^a
IgG	248	143	57.81 ± 2.19^a
Anti-CRISP2	261	131	50.37 ± 1.94^b

The experiment included 6 replicates. Different letters in the same column indicate significant differences, $P < 0.05$.

The reproductive parameters of the boars are shown in **Table 3**. There is no significant difference in the number of sows bred (low CRISP2 group: 977 vs. high CRISP2 group: 865) and parturition rate (low CRISP2 group: $92.95 \pm 1.51\%$ vs. high CRISP2 group: $93.26 \pm 1.22\%$) between low CRISP2 group and high CRISP2 group. The litter size (low CRISP2 group: 12.18 ± 0.26 vs. high CRISP2 group: 13.08 ± 0.17), live-born piglets per litter (low

CRISP2 group: 11.57 ± 0.27 vs. high CRISP2 group: 12.61 ± 0.20), qualified piglets per litter (low CRISP2 group: 10.39 ± 0.26 vs. high CRISP2 group: 11.18 ± 0.17) and boar fecundity (low CRISP2 group: 11.32 ± 0.33 vs. high CRISP2 group: 12.21 ± 0.28) in the CRISP2 group were significantly higher than that in the low CRISP2 group. These results indicated that CRISP2 might play critical roles in the sperm fertilizing ability or boar fertility, and might have the potential to serve as a biomarker for selecting high fertility boars.

Effect of CRISP2 on *in vitro* Fertilization

The effect of the CRISP2 protein on the cleavage rate of *in vitro* fertilization was indirectly investigated by adding the anti-CRISP2 antibody to the fertilization medium during *in vitro* fertilization. As shown in Table 4, the cleavage rate in anti-CRISP2 group ($50.37 \pm 1.94\%$) was significantly lower than that of the control group ($59.53 \pm 2.54\%$) and the IgG group ($57.81 \pm 2.19\%$), which suggests that CRISP2 plays a critical role in the process of fertilization.

CRISP2 Expression in the Reproductive Organs of Pigs

To elucidate the potential role of CRISP2 in the sperm fertilizing ability and boar fertility, the mRNA expression of *CRISP2* in the reproductive organs of male and female pigs with different ages was detected by reverse transcriptase PCR. As shown in Figure 1, *CRISP2* was expressed specifically in the testis and epididymis of adult boars, and no expression was detected in the reproductive tissues examined from the female pigs (Figure 1A).

To verify the *CRISP2* expression patterns detected by reverse transcriptase PCR, qRT-PCR was conducted on the expression levels of *CRISP2* in the testis, epididymis, SVG, prostate,

bulbourethral gland, sperm, ovary and oviduct of adult, and 3-month-old pigs. The results showed that *CRISP2* mRNA was highly expressed in adult testis and sperm (Figure 1B).

The protein level expression of CRISP2 in the boar reproductive organs and semen were further detected by Western blot. The results showed that CRISP2 was mainly expressed in the testis and sperm (Figure 1C).

Immunohistochemical Analysis of CRISP2 in the Testis of Adult Boars

The distribution of CRISP2 in the testis tissues was detected by immunohistochemical analysis. The results showed that the CRISP2 protein was expressed in the cytoplasm of spermatogonia, spermatocytes, and sperm cells in the seminiferous tubules (Figure 2).

Immunofluorescence Detection of CRISP2 in Sperm Before and After Capacitation

To gain further insight into the function of CRISP2 in fertilization, immunofluorescence detection of CRISP2 before and after sperm capacitation was carried out. As shown in Figure 3, CRISP2 is mainly distributed in the post-acrosomal region, neck, and tail of sperm before capacitation and relocated to the apical segment and posterior of the acrosome and to the middle piece of the tail after sperm capacitation. The number of CRISP2-staining sperm in the apical segment and posterior of the acrosome and middle piece of the tail after capacitation was significantly higher than that before capacitation (before capacitation: $20.63 \pm 2.22\%$ vs. after capacitation: $70.23 \pm 2.15\%$, $P < 0.001$).

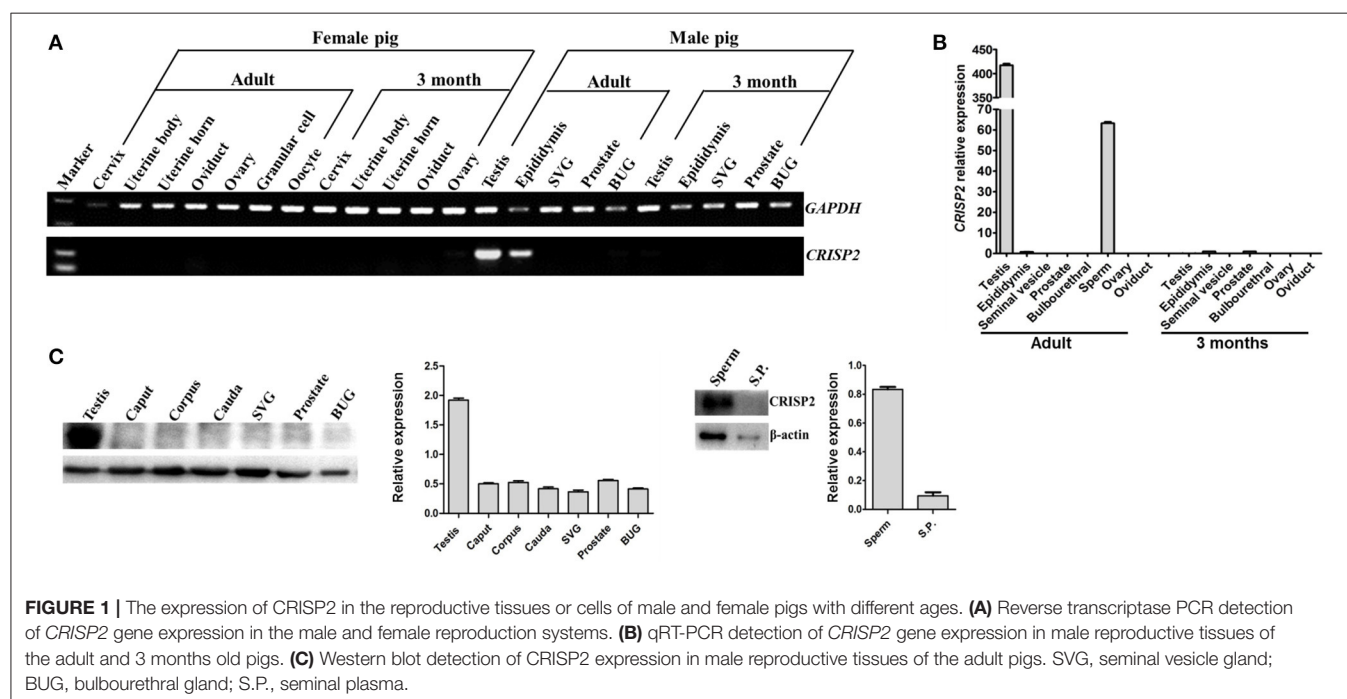


FIGURE 1 | The expression of CRISP2 in the reproductive tissues or cells of male and female pigs with different ages. **(A)** Reverse transcriptase PCR detection of *CRISP2* gene expression in the male and female reproduction systems. **(B)** qRT-PCR detection of *CRISP2* gene expression in male reproductive tissues of the adult and 3 months old pigs. **(C)** Western blot detection of CRISP2 expression in male reproductive tissues of the adult pigs. SVG, seminal vesicle gland; BUG, bulbourethral gland; S.P., seminal plasma.

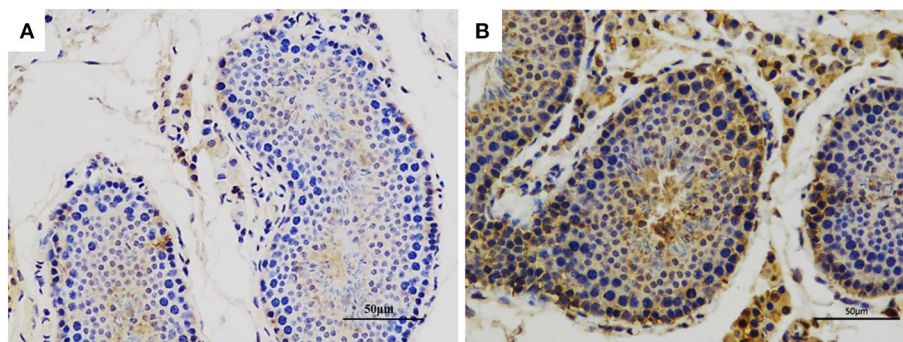


FIGURE 2 | Immunohistochemical analysis of CRISP2 in the testis of adult boars. **(A)** The negative control (IgG control). **(B)** The CRISP2 immunohistochemistry of adult testis. The brown region represents the distribution of target proteins.

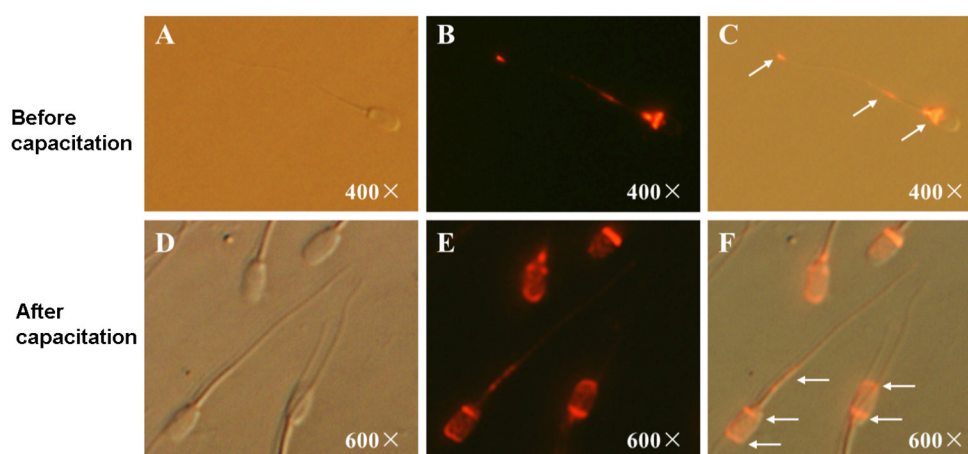


FIGURE 3 | Immunofluorescent staining of CRISP2 in sperm before and after capacitation. **(A–C)** Representative images of the immunofluorescent staining of CRISP2 in sperm before capacitation; **(A)** images taken under light microscope, **(B)** images taken under fluorescent scope; **(C)** merged images. **(D–F)** Representative images of the immunofluorescent staining of CRISP2 in sperm after capacitation; **(D)** images taken under light microscope, **(E)** images taken under fluorescent scope; **(F)** merged images. The white arrow indicates the distribution of the target proteins.

DISCUSSION

The present study for the first time showed that the protein level of sperm CRISP2 were positively correlated with the reproductive parameters of litter size, the number of live-born piglets and qualified piglets per litter. Furthermore, the expression profile and the localization of CRISP2 in the reproductive tissues and sperm provide evidence that CRISP2 may play critical roles in sperm fertilizing ability and boar fertility.

CRISPs are members of the CAP superfamily and are expressed specifically in the male reproductive tract in mammals (6, 9). CRISP2 is the sole CRISP produced in the testis during spermatogenesis, and it is specifically localized in the acrosome and tail of sperm. Consistently, our results showed that CRISP2 was expressed specifically in the testis and epididymis of adult boars. CRISP2 is essential for sperm function and male fertility in mice and humans (7, 11). Decreased CRISP2 protein level in sperm was associated with human male infertility (14–16). Studies from Lim et al., indicated that CRISP2 was a quantitative

determinant of the ability of sperm to undergo the acrosome reaction, and optimal CRISP2 production was necessary for maximal fecundity in mice (7). Consistently, our results revealed that boars with high levels of sperm CRISP2 protein in boars were associated high reproductive performance.

Although the possible roles of sperm CRISP2 in sperm-oocyte interactions have been investigated in mice and humans (7, 11, 22, 23), the role of CRISP2 and its molecular function in male fertility are still poorly understood, especially in boars. CRISP2-deficient mouse lines show that appropriate CRISP2 expression is necessary for optimal sperm and male fertility (7). Recent studies have shown that sperm CRISP2 is mainly distributed at the acrosome and the tail of wild-type sperm (7, 24, 25). Sperm CRISP2 is associated with the anterior and posterior of the acrosome in capacitated sperm, and CRISP can be released from the acrosome and relocated to the equatorial segment during the acrosome reaction, thereby participating in sperm-egg interaction (11). Our results showed that CRISP2 is mainly distributed in the post-acrosomal region, neck and tail of

sperm before capacitation and relocated to the apical segment and posterior of the acrosome and to the middle piece of the tail after sperm capacitation, which suggest that this process may be associated with sperm-oocyte interaction in the pigs. It has been reported that CRISP2 is involved in the calcium flow through ryanodine receptors and the effect may be associated with CatSper, the main calcium channel in sperm, which is vital for sperm motility and male fertility (26, 27).

Busso et al. (23) reported that the anti-CRISP2 antibody significantly decreased the percentage of penetrated eggs of *in vitro* fertilization through a specific participation at the sperm-egg fusion (23). Consistently, our experiments showed that the anti-CRISP2 antibody, significantly decreased the cleavage rate of *in vitro* fertilization in pigs (Table 4). Our study further found that CRISP2 is mainly distributed in the posterior of the acrosome, neck and tail of boar intact sperm and relocated to the anterior and posterior of the acrosome and the tail middle piece of capacitated sperm (Figure 3), which is similar but not entirely consistent with the reports in humans and mice mentioned above. The mRNA of *CRISP2* has been reported to be expressed specifically in boar testis (8). Our results by qRT-PCR and western blot showed that CRISP2 was highly expressed in the sperm and testis of adult boars but not in the ovaries and oviducts of female pigs.

There are several limitations in the present study. Firstly, the present study used the polyclonal CRISP2 antibody to perform the CRISP2 immunohistochemistry of adult testis, which may lead to the non-specific bindings in the testis outside the seminiferous tubes. Future studies may use more specific monoclonal CRISP2 antibodies to confirm its distribution in the testis. Secondly, the sample size in the present study was small, and further studies with large sample size should be considered. Thirdly, the present study only determined effects of CRISP2 antibody on the cleavage rate, and future studies may consider evaluate the effects of CRISP2 antibody on different stages of fertilization.

CONCLUSION

In summary, our experiments revealed that the testis and sperm-specific CRISP2 is associated with sperm fertilizing ability and boar fertility and that sperm CRISP2 has the potential to serve as a fertility biomarker. Further mechanistic studies are

warranted, in order to fully decipher the role of CRISP2 in the boar reproduction.

DATA AVAILABILITY STATEMENT

The original contributions presented in the study are included in the article/Supplementary Material, further inquiries can be directed to the corresponding author/s.

ETHICS STATEMENT

This work was approved by the Ethics Committee on Animal Experimentation of South China Agricultural University. The license number is SYXK (Guangdong) 2019-0136.

AUTHOR CONTRIBUTIONS

HW conceived the study and drafted the manuscript. FG, PW, KW, YF, and YunC performed the experiments. YumC, CY, and MF analyzed the data. LL and SZ prepared the figures and tables. All authors approved the manuscript for submission.

FUNDING

This study was supported by grants from the Science and Technology Innovation Strategy Projects of Guangdong Province (2018B020203002), the Local Innovative and Research Teams Project of Guangdong Province (2019BT02N630), the Natural Science Foundation of Guangdong Province (2020A1515010976), and the National Natural Science Foundation of China (31402072).

ACKNOWLEDGMENTS

The authors acknowledge the Guangdong Wens Foodstuff Co., Ltd. for providing the experimental materials of semen, pigs and the boar reproductive data.

SUPPLEMENTARY MATERIAL

The Supplementary Material for this article can be found online at: <https://www.frontiersin.org/articles/10.3389/fvets.2021.653413/full#supplementary-material>

REFERENCES

- Jung M, Rudiger K, Schulze M. *In vitro* measures for assessing boar semen fertility. *Reprod Domest Anim.* (2015) 50(Suppl. 2):20–4. doi: 10.1111/rda.12533
- Roca J, Broekhuijsen ML, Parrilla I, Rodriguez-Martinez H, Martinez EA, Bolarin A. Boar differences in artificial insemination outcomes: can they be minimized? *Reprod Domest Anim.* (2015) 50(Suppl. 2):48–55. doi: 10.1111/rda.12530
- Rahman MS, Kwon WS, Pang MG. Prediction of male fertility using capacitation-associated proteins in spermatozoa. *Mol Reprod Dev.* (2017) 84:749–59. doi: 10.1002/mrd.22810
- Druart X, De Graaf S. Seminal plasma proteomes and sperm fertility. *Anim Reprod Sci.* (2018) 194:33–40. doi: 10.1016/j.anireprosci.2018.04.061
- Kwon WS, Rahman MS, Ryu DY, Park YJ, Pang MG. Increased male fertility using fertility-related biomarkers. *Sci Rep.* (2015) 5:15654. doi: 10.1038/srep15654
- Gibbs GM, Roelants K, O'bryan MK. The CAP superfamily: cysteine-rich secretory proteins, antigen 5, and pathogenesis-related 1 proteins—roles in reproduction, cancer, immune defense. *Endocr Rev.* (2008) 29:865–97. doi: 10.1210/er.2008-0032
- Lim S, Kierzek M, O'connor AE, Brenker C, Merriner DJ, Okuda H, et al. CRISP2 is a regulator of multiple aspects of sperm function and male fertility. *Endocrinology.* (2019) 160:915–24. doi: 10.1210/en.2018-01076

8. Vadnais ML, Foster DN, Roberts KP. Molecular cloning and expression of the CRISP family of proteins in the boar. *Biol Reprod.* (2008) 79:1129–34. doi: 10.1095/biolreprod.108.070177
9. Hu J, Merriner DJ, O'connor AE, Houston BJ, Furic L, Hedger MP, et al. Epididymal cysteine-rich secretory proteins are required for epididymal sperm maturation and optimal sperm function. *Mol Hum Reprod.* (2018) 24:111–22. doi: 10.1093/molehr/gay001
10. Weigel Muñoz M, Carvajal G, Curci L, Gonzalez SN, Cuasnicu PS. Relevance of CRISP proteins for epididymal physiology, fertilization, and fertility. *Andrology.* (2019) 7:610–7. doi: 10.1111/andr.12638
11. Nimlamool W, Bean BS, Lowe-Krentz LJ. Human sperm CRISP2 is released from the acrosome during the acrosome reaction and re-associates at the equatorial segment. *Mol Reproduct Dev.* (2013) 80:488–502. doi: 10.1002/mrd.22189
12. Arangasamy A, Kasimanickam VR, Dejarnette JM, Kasimanickam RK. Association of CRISP2, CCT8, PEBP1 mRNA abundance in sperm and sire conception rate in Holstein bulls. *Theriogenology.* (2011) 76:570–7. doi: 10.1016/j.theriogenology.2011.03.009
13. Brukman NG, Miyata H, Torres P, Lombardo D, Caramelo JJ, Ikawa M, et al. Fertilization defects in sperm from Cysteine-rich secretory protein 2 (Crisp2) knockout mice: implications for fertility disorders. *Mol Hum Reprod.* (2016) 22:240–51. doi: 10.1093/molehr/gaw005
14. Zhou JH, Zhou QZ, Lyu XM, Zhu T, Chen ZJ, Chen MK, et al. The expression of cysteine-rich secretory protein 2 (CRISP2) and its specific regulator miR-27b in the spermatozoa of patients with asthenozoospermia. *Biol Reprod.* (2015) 92:28. doi: 10.1095/biolreprod.114.124487
15. Zhou JH, Zhou QZ, Yang JK, Lyu XM, Bian J, Guo WB, et al. MicroRNA-27a-mediated repression of cysteine-rich secretory protein 2 translation in asthenoteratozoospermic patients. *Asian J Androl.* (2017) 19:591–5. doi: 10.4103/1008-682X.185001
16. Gholami D, Yazdi RS, Jami MS, Ghasemi S, Gilani MAS, Sadeghinia S, et al. The expression of Cysteine-Rich Secretory Protein 2 (CRISP2) and miR-582-5p in seminal plasma fluid and spermatozoa of infertile men. *Gene.* (2020) 730:144261. doi: 10.1016/j.gene.2019.144261
17. Song CY, Gao B, Wu H, Wang XY, Zhou HY, Wang SZ, et al. Spatial and temporal gene expression of Fn-Type II and cysteine-rich secretory proteins in the reproductive tracts and ejaculated sperm of chinese meishan pigs. *Reproduct Domestic Anim.* (2011) 46:848–53. doi: 10.1111/j.1439-0531.2011.01753.x
18. Shan X, Yu T, Yan X, Wu J, Fan Y, Guan X, et al. Proteomic analysis of healthy and atretic porcine follicular granulosa cells. *J Proteomics.* (2021) 232:104027. doi: 10.1016/j.jprot.2020.104027
19. Jun L, Hengxi W, Yan L, Qiuyan L, Ning L. Identification of a suitable endogenous control gene in porcine blastocysts for use in quantitative PCR analysis of microRNAs. *Sci China Life Sci.* (2012) 55:126–31. doi: 10.1007/s11427-012-4289-8
20. Wei H, Liu X, Yuan J, Li L, Zhang D, Guo X, et al. Age-specific gene expression profiles of rhesus monkey ovaries detected by microarray analysis. *Biomed Res Int.* (2015) 2015:625192. doi: 10.1155/2015/625192
21. Bai YS, Zhu C, Feng MY, Wei HX, Li L, Tian XC, et al. Previously claimed male germline stem cells from porcine testis are actually progenitor Leydig cells. *Stem Cell Res Ther.* (2018) 9:200. doi: 10.1186/s13287-018-0931-0
22. Ellerman DA, Cohen DJ, Da Ros VG, Morgenfeld MM, Busso D, Cuasnicu PS. Sperm protein “DE” mediates gamete fusion through an evolutionarily conserved site of the CRISP family. *Dev Biol.* (2006) 297:228–37. doi: 10.1016/j.ydbio.2006.05.013
23. Busso D, Goldweic NM, Hayashi M, Kasahara M, Cuasnicu PS. Evidence for the involvement of testicular protein CRISP2 in mouse sperm-egg fusion. *Biol Reproduct.* (2007) 76:701–8. doi: 10.1095/biolreprod.106.05.6770
24. O'bryan MK, Sebire K, Meinhardt A, Edgar K, Keah HH, Hearn MT, et al. Tpx-1 is a component of the outer dense fibers and acrosome of rat spermatozoa. *Mol Reprod Dev.* (2001) 58:116–25. doi: 10.1002/1098-2795(200101)58:1<;116::AID-MRD14>;3.0.CO;2-8
25. Busso D, Cohen DJ, Hayashi M, Kasahara M, Cuasnicu PS. Human testicular protein TPX1/CRISP-2: localization in spermatozoa, fate after capacitation and relevance for gamete interaction. *Mol Hum Reprod.* (2005) 11:299–305. doi: 10.1093/molehr/gah156
26. Ren D, Navarro B, Perez G, Jackson AC, Hsu S, Shi Q, et al. A sperm ion channel required for sperm motility and male fertility. *Nature.* (2001) 413:603–9. doi: 10.1038/35098027
27. Qi H, Moran MM, Navarro B, Chong JA, Krapivinsky G, Krapivinsky L, et al. All four CatSper ion channel proteins are required for male fertility and sperm cell hyperactivated motility. *Proc Natl Acad Sci USA.* (2007) 104:1219–23. doi: 10.1073/pnas.0610286104

Conflict of Interest: CY was employed by the Guangdong Wen's Foodstuffs Group Co., Ltd., company.

The remaining authors declare that the research was conducted in the absence of any commercial or financial relationships that could be construed as a potential conflict of interest.

Copyright © 2021 Gao, Wang, Wang, Fan, Chen, Chen, Ye, Feng, Li, Zhang and Wei. This is an open-access article distributed under the terms of the Creative Commons Attribution License (CC BY). The use, distribution or reproduction in other forums is permitted, provided the original author(s) and the copyright owner(s) are credited and that the original publication in this journal is cited, in accordance with accepted academic practice. No use, distribution or reproduction is permitted which does not comply with these terms.



OPEN ACCESS

EDITED BY

Ahmed Abdeen,
Benha University, Egypt

REVIEWED BY

Mustafa Shukry,
Kafrelsheikh University, Egypt
Afaf Abdelkader,
Benha University, Egypt

*CORRESPONDENCE

Li Li

✉ lili007@scau.edu.cn

Hengxi Wei

✉ weihengxi@scau.edu.cn

RECEIVED 10 May 2024

ACCEPTED 10 July 2024

PUBLISHED 31 July 2024

CITATION

Zhao J, Liu X, Yue J, Zhang S, Li L and Wei H (2024) PF-05231023 reduces lipid deposition in apolipoprotein E-deficient mice by inhibiting the expression of lipid synthesis genes. *Front. Vet. Sci.* 11:1429639. doi: 10.3389/fvets.2024.1429639

COPYRIGHT

© 2024 Zhao, Liu, Yue, Zhang, Li and Wei. This is an open-access article distributed under the terms of the [Creative Commons Attribution License \(CC BY\)](#). The use, distribution or reproduction in other forums is permitted, provided the original author(s) and the copyright owner(s) are credited and that the original publication in this journal is cited, in accordance with accepted academic practice. No use, distribution or reproduction is permitted which does not comply with these terms.

PF-05231023 reduces lipid deposition in apolipoprotein E-deficient mice by inhibiting the expression of lipid synthesis genes

Juan Zhao, Xuelong Liu, Jingyu Yue, Shouquan Zhang, Li Li* and Hengxi Wei*

State Key Laboratory of Swine and Poultry Breeding Industry, National Engineering Research Center for Breeding Swine Industry, Guangdong Provincial Key Lab of Agro-animal Genomics and Molecular Breeding, College of Animal Science, South China Agricultural University, Guangdong, China

Fibroblast growth factor 21 (FGF21) is a peptide hormone that is primarily expressed and secreted by the liver. The hormone is crucial for regulation of glucose homeostasis, lipid metabolism, and energy balance. Compared with natural FGF21, FGF21 analogs have become drug candidates for the treatment of cardiovascular and metabolic diseases owing to their long half-life and greater stability *in vitro*. Apolipoprotein E (*ApoE*)-knockout (*ApoE*^{−/−}) mice exhibit progressive disruptions in lipid metabolism *in vivo* and develop further atherosclerosis pathological features owing to *ApoE* deletion. Therefore, this study used an *ApoE*^{−/−} mouse model to investigate the effects of a long-acting FGF21 analog (PF-05231023) on lipid metabolism and related parameters. Eighteen *ApoE*^{−/−} female mice were fed a Western diet equivalent for 12 weeks, and then randomly assigned to intraperitoneally receive either physiological saline (the control group) or 10 mg/kg PF-05231023 (the treatment group) three times a week for seven consecutive weeks. Body composition, glucose tolerance, blood and liver cholesterol, triglyceride levels, liver vacuolization levels, peri-ovarian white adipocyte hypertrophy, aortic atherosclerotic plaque formation, and the expression of genes related to lipid metabolism in adipose tissue were subsequently assessed before and after treatment. The aortic atherosclerotic plaque area was reduced in mice in the PF-05231023 treatment group compared with that in the saline group. Although the effect of PF-05231023 on the plasma biochemical indexes of mice was small, it significantly reduced lipid levels and lipid droplet accumulation in the liver, and reduced adipocyte hypertrophy in white adipose tissue. Transcriptome analysis of adipose tissue showed that PF-05231023 treatment downregulated the expression of lipid synthesis-related genes and inhibited the sterol regulatory element binding transcription factor 1 gene, thereby improving lipid deposition. PF-05231023 effectively improved the lipid metabolism of *ApoE*^{−/−} mice, demonstrating an anti-atherosclerotic effect and providing a scientific basis and experimental foundation for the clinical treatment of cardiovascular diseases by using long-acting FGF21 analogs.

KEYWORDS

PF-05231023, long-acting FGF21 analogs, lipid metabolism, apolipoprotein E (ApoE), mice

1 Introduction

Excessive consumption of calorie-rich foods leading to obesity-related diseases is now recognized as a major cause of disability around the world (1). Mechanistically, caloric intake that exceeds adipose tissue storage capacity is associated with the accumulation of ectopic lipids in non-adipose organs and the induction of low-grade tissue inflammation, endoplasmic reticulum stress, and insulin resistance (2, 3). These metabolic defects increase the risk of serious diseases, including type 2 diabetes, non-alcoholic steatohepatitis, cardiovascular disease and various forms of cancer. However, to date, specific drugs for these diseases remain limited.

Fibroblast growth factor 21 (FGF21) is a peptide hormone that is primarily expressed and secreted by the liver and adipose tissue (4, 5). The hormone acts in an endocrine manner and targets liver and adipose tissue (6). Increasing evidence suggests an important role for FGF 21 in the regulation of glucose and lipid homeostasis through multifaceted and inter-organ crosstalk. Moreover, FGF 21 has been recognized as a potential target for metabolic abnormalities (7). Although the role of FGF21 in obesity, diabetes, and non-alcoholic fatty liver disease (NAFLD) in humans and animals has been extensively studied (8–10), the hormone's short circulating half-life (30–120 min) and its tendency to aggregate *in vitro* limit its clinical application (11). To overcome these limitations, the long-acting FGF21 analog, PF-05231023, was developed. The analog possesses better anti-aggregation and *in vivo* degradation effects than that of natural FGF21 (12–14). PF-05231023 contains two modified human FGF21 molecules that are linked to the humanized immunoglobulin 1 antibody backbone, which was designed to prolong the analog's half-life and bioavailability (15). Compared with that of natural FGF21, PF-05231023 exhibits a 70-fold increase in half-life, demonstrating promising clinical potential *in vitro*. Similarly, administration of LY2405319, an FGF21 analog, reduced atherosclerotic plaques and blood lipid levels in *Apoe*^{−/−} mice (16). Clinical trials have demonstrated the potential of recombinant FGF21 for the treatment of type 2 diabetes, obesity, and other comorbidities, but its physiological role in atherosclerosis (AS) has only gained attention in recent years (16, 17).

In studies involving apolipoprotein E-knockout (*Apoe*^{−/−}) mice, treatment with recombinant human

FGF21 prevented the formation of atherosclerotic plaques (18).

However, the specific mechanism by which PF-05231023 modulates lipid metabolism and protects against AS in *Apoe*^{−/−} mice remains unclear, and its impact on lipid metabolism-related pathways has yet to be elucidated. Therefore, we hypothesized that PF-05231023 would improve lipid metabolism and atherogenesis in *Apoe*^{−/−} mice. Hence, in this study, we used an *Apoe*^{−/−} mouse model of lipid metabolism disorder, using mice fed a Western diet equivalent (WD), to investigate the specific mechanism by which PF-05231023 alleviates lipid metabolism disorders. We investigated this from a novel perspective of adipose tissue, with the expectation of providing insights for the development of more effective and safer drugs for the treatment of metabolic diseases.

2 Materials and methods

2.1 Experimental reagents

PF-05231023 (AbMole Company; M10048, Shanghai, China), a total cholesterol (TC) test kit and triglyceride (TG) test kit (Nanjing Jiancheng Biotechnology Research Institute; A111-1-1, A110-1-1, Nanjing, China), D-anhydrous glucose (Solarbio; G8150, Beijing, China), hematoxylin and eosin (HE) staining solutions (Reagan Biotech; DH001, DH0044, Beijing, China), Oil Red O dye solution (Wuhan Seville Biotechnology Co., Ltd.; G1015, Wuhan, China), and TRIzol reagent (Takara; T9108, Beijing, China) were used in this study. The reverse transcription kit and quantitative polymerase chain reaction (PCR) detection kit were both procured from Vazyme (R323-01, Q711-02, Nanjing, China).

2.2 Animal experiments

Eighteen 4-week-old female *Apoe*^{−/−} C57BL/6 mice, weighing 17–20 g, were purchased from the Shanghai Model Organisms Center, Inc. (Shanghai, China). The animal quality was certified as SYXK (Shanghai, China) 2019-0002. Six 4-week-old C57BL/6 female mice with the same genetic background, weighing 16–17 g, were procured from the Guangdong Medical Experimental Animal Center with an animal quality license of SYXK (Guangdong, China) 2022-0002. All animal experiments strictly complied with the regulations of the Animal Ethics Committee of South China Agricultural University. The mice were housed and fed at room temperature (22 ± 2°C), with a 12-h light/12-h dark cycle and had free access to food and drinking water.

2.3 Experimental design

After acclimating to the environment for 1 week, the mice were randomly divided into two groups: *Apoe*^{−/−} + WD + PF-05231023 (*n* = 6) and *Apoe*^{−/−} + WD + saline group (*n* = 6). These groups were fed a WD for 12 weeks to build the AS model, followed by a 7-week treatment period of either 10 mg/kg of PF-05231023 (15) or an equivalent volume of saline intraperitoneally injected on Monday, Wednesday, and Friday every week. Additionally,

Abbreviations: *Apoe*, apolipoprotein E; *Apoe*^{−/−}, *Apoe* knockout; WD, western diet; *Srebf1*, Sterol-regulatory element binding protein 1; TG, triglyceride; TC, total cholesterol; IPGTT, intraperitoneal glucose tolerance test; HE, hematoxylin and eosin; GO, gene ontology; KEGG, Kyoto Encyclopedia of Genes and Genomes; DEG, differentially expressed gene; *Fasn*, fatty acid synthesis; *Acaca*, acetyl CoA carboxylase alpha; *Acacb*, acetyl CoA carboxylase beta; *Scd1*, steroyl CoA depletion 1; DIO, diet-induced obese mice; FGF21, fibroblast growth factor 21; NAFLD, non-alcoholic fatty liver disease; AS, atherosclerosis; PCR, polymerase chain reaction; qPCR, quantitative PCR; qRT-PCR, quantitative reverse transcription PCR; ANOVA, analysis of variance; CC, cellular component; MF, molecular function; BP, biological processes; RNA-Seq, RNA sequencing; *Elovl1*, very long chain fatty acid elongase 1; *Elovl6*, very long chain fatty acid elongase 6; *Abcg5*, adenosine triphosphate-binding cassette transporter G5; *Abcg8*, adenosine triphosphate-binding cassette transporter G8.

C57BL/6 female mice + control diet (WT + Control) served as the healthy control group ($n = 6$), and *Apoe*^{-/-} mice + control diet (*Apoe*^{-/-} + Control) served as the transgenic control group ($n = 6$). The composition of the WD and control diet is shown in Table 1.

Throughout the feeding period, the weights of the mice were recorded weekly. Their food and water were also replaced weekly. Body composition analysis of the mice was conducted at weeks 12 and 19 of feeding, and an intraperitoneal glucose tolerance test (IPGTT) was performed during the 7th week of treatment. Blood samples were collected from the eyeballs and perfused with physiological saline to dissect the aorta. Subsequently, the mouse liver, subcutaneous fat, brown fat, and white fat around the ovaries were stored at -80°C for subsequent analysis. Experimental design is shown in Figure 1.

2.4 Body composition analysis

Body composition analysis was performed on mice at weeks 12 and 19. Before testing, place the mice between two paper cups, gently squeeze them, and perform stress induced bowel movements to minimize experimental errors. Subsequently, they were placed in a live animal body composition analyzer to record their body weight, body fat weight, lean meat weight, and their percentage.

2.5 IPGTT

Mice were transferred to a clean cage, where they were fasted for 5 h, during which they had access to water. After the fasting period, their weight was measured, and the appropriate amount of glucose injection was calculated based on their weight. Fasting blood glucose levels were measured, and a glucose solution was injected into the abdominal cavity at a standard concentration of 2 mg/g (19). Blood glucose levels were monitored at 15, 30, 60, 90, and 120 min post-injection using a blood glucose meter.

2.6 Organize sample collection

Blood collection from the eyeballs: After anesthetizing the mice with ether (20), the mice were fixed with one hand, and the eyeballs were removed with sterilized forceps; the blood was collected into 1.5 ml tubes, and left to stand for 4 h. The blood was centrifuged at 3,000 rpm for 15 min at 4°C in a centrifuge (Eppendorf, Hamburg, Germany), and the supernatant was pipetted into 200 μl tubes and store it in a -80°C freezer for further research.

After completion of blood sampling, the mice were executed by dislocation method, and the lower limbs and head were fixed on a foam plate to take white adipose tissue around the ovaries (sexual fat), subcutaneous fat, and brown fat of mice. One side was fixed in paraformaldehyde for subsequent embedding; the other side was placed in liquid, the other side was placed in liquid nitrogen and stored in the refrigerator at -80°C .

Then, the thoracic cavity of the mice was cut open from the diaphragm upward to expose the heart, and a small opening was cut out of the right apical heart, and pre-cooled saline was injected from the left apical heart with a 1 ml syringe until the outflow from

the opening of the right apical heart was clear and the color of the liver was gradually changed to lighter; the aorta of the mice was dissected under the body microscope, and the peri-arterial blood vessels and fat were stripped off, and the aortic arch was fixed in paraformaldehyde for subsequent staining analysis (21).

2.7 Biochemical analysis of serum and liver

The collected blood samples were centrifuged at 3,000 rpm for 15 min at 4°C to separate the serum. Liver tissue (30 mg) was homogenized with phosphate-buffered saline, and the supernatant was collected for further analysis. Serum and liver TC, and TG levels were measured according to the manufacturer's instructions provided with the reagent kit.

2.8 Histological analysis of liver, aorta, and adipose tissue

White fat surrounding the left hepatic lobule, aorta, and left ovary was fixed in 4% paraformaldehyde for 24 h. Subsequently, the liver and fat were embedded in paraffin sections (thickness = 5 μm) and subjected to HE staining. Lipid accumulation in the liver and adipocyte hypertrophy in the fat were observed and photographed under a 20 \times biological microscope (SOPTOP, EX20, Suzhou, China). The aorta was longitudinally placed on a black gel, and blood vessels were cut longitudinally under a stereomicroscope (Olympus Corporation, SZ2-ILST, Tokyo, Japan). Oil Red O staining was performed, and lipid deposition in the aorta was observed using a 4 \times microscope (SOPTOP, EX20). Image View software was used for image stitching, and analysis was performed using ImageJ1 software.

2.9 Extraction of RNA from mouse adipose tissue

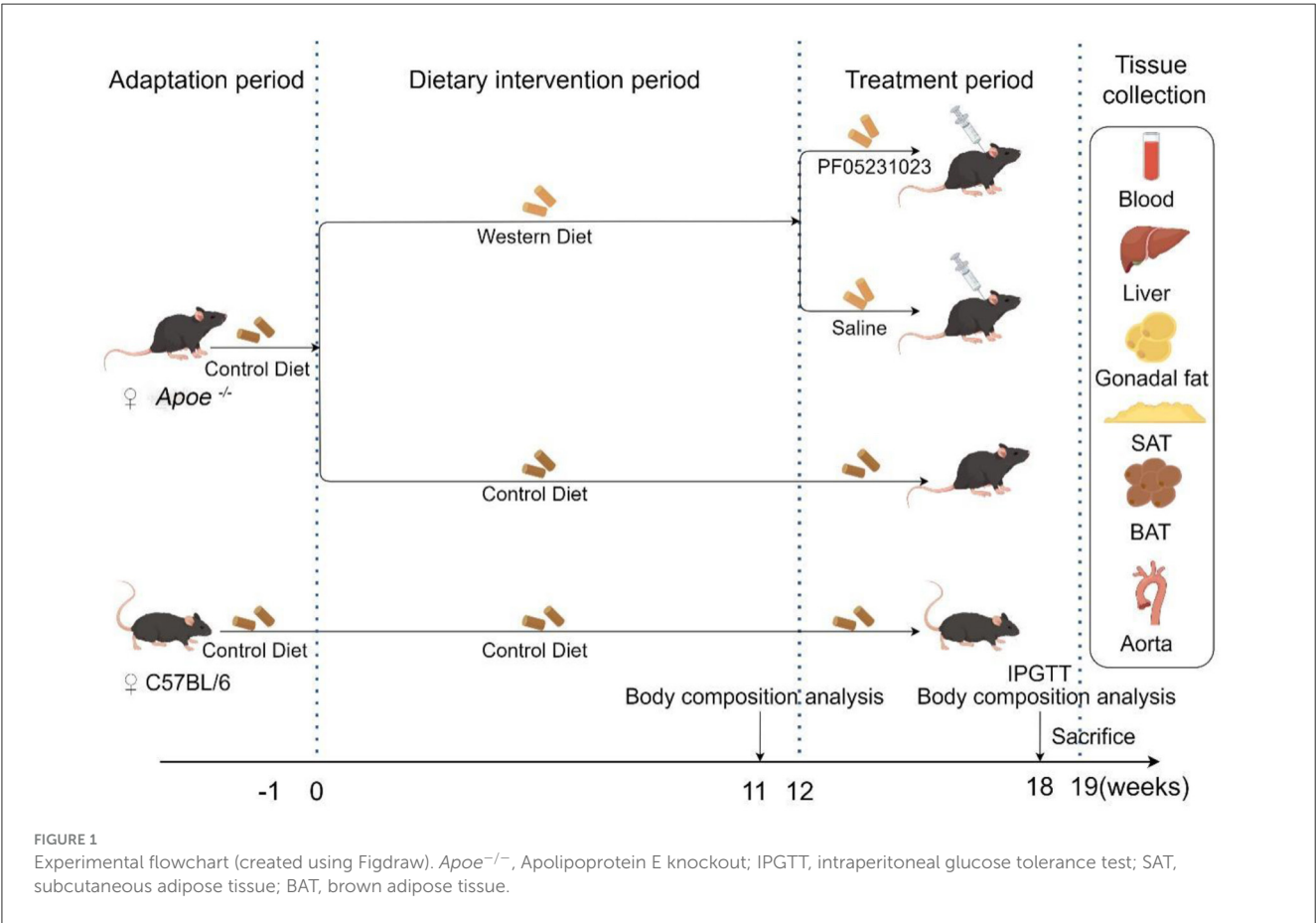
Three mice were randomly selected from the *Apoe*^{-/-} + WD + PF-05231023 and *Apoe*^{-/-} + WD + saline group ($n = 6$). The white fat tissue surrounding the ovaries was collected, and total RNA was extracted from this adipose tissue using TRIzol reagent. The purity of samples was assessed using a NanoPhotometer[®] Thermo Fisher spectrophotometer (Massachusetts, USA), whereas the integrity and concentration of the RNA samples were determined using the Agilent Technologies (CA, USA) 2100 RNA Nano 6000 Assay Kit.

2.10 Library construction and sequencing

Following total RNA extraction, eukaryotic mRNA was enriched using oligo (dT) magnetic beads. A buffer was then added for mRNA fragmentation, and mRNA was used as a template to synthesize the complementary DNA (cDNA) first and second strands. The cDNA was purified, and the resulting purified double-stranded cDNA was subjected to end repair, addition of base A, and addition of sequencing adapters. Fragments were screened to

TABLE 1 Western diet equivalent (WD) and control diet compositions.

Nutrient	WD (purified) feed		WD (control) feed	
	Mass ratio %	Energy ratio %	Mass ratio %	Energy ratio %
Protein	17.5	15.5	17	17
Carbohydrate	48.5	42.5	71	73
Fat	21	42	4.3	10
Total	87	100	92.3	100
Energy	4.7 kcal/g		3.9 kcal/g	
Product	Mass ratio g/kg	kcal	Mass ratio g/kg	kcal
Casein	195	780	195	780
DL-Methionine	3	12	3	12
Sucrose	341	1,364	341	1,364
Com starch	150	600	504.4	2,017.6
Cellulose	50	0	50	0
Natural cream	210	1,890	52.5	472.5
Ethoxyquin	0.04	0	0.04	0
Mineral mix AIN76A	35	16.5	35	16.5
Calcium carbonate	4	0	4	0
Vitamin Mix AIN-76A	10	39	10	39
Choline bitartrate	2	0	2	0
Cholesterol	1.5	0		
TOTAL	1,001.54	4,701.5	1,196.94	4,701.6



recover ~350 bp of cDNA, and PCR enrichment was performed to obtain a cDNA library. After passing the quality inspection using Qubit 3.0 and Agilent 2100, the constructed library was sequenced using a high-throughput sequencing platform (Agilent Technologies Inc, California, USA) with a PE150 sequencing strategy. The sequencing was conducted by Annoroad Gene Technology (Beijing, China).

2.11 Differential gene analysis and functional enrichment

Gene differential expression analysis was performed using DESeq2, with screening criteria for differential genes set at FoldChange ≥ 1.5 , p -value ≤ 0.05 , and $padj \leq 1$. For Gene Ontology (GO) and Kyoto Encyclopedia of Genes and Genomes (KEGG) enrichment analysis of differentially expressed mRNA, we used the Database for Annotation, Visualization, and Integrated Discovery (<https://david.ncifcrf.gov/tools.jsp>). We used the microbiome websites (<http://www.bioinformatics.com.cn> and <https://www.omicshare.com/tools/>) for analysis and visualization.

2.12 Real-time fluorescence quantitative reverse transcription PCR

To validate RNA sequencing (RNA-Seq) data, eight differentially expressed genes (DEG) related to metabolism were randomly selected for quantitative reverse transcription PCR (qRT-PCR) validation, with β -actin serving as an internal reference gene. Primer sequences and related information are provided in Table 2. The RNA sample used for qRT-PCR amplification was the same as the RNA sample used for constructing the RNA-Seq library mentioned above when using the Vazyme reverse transcription kit.

2.13 Statistical analysis

Unless otherwise specified, statistical analysis was conducted using one-way analysis of variance (ANOVA). We performed

multiple comparisons after one-way ANOVA, compared each column, and rated the average of each column. Data is expressed as mean \pm standard error mean, and $p < 0.05$ is considered statistically significant. All statistical analyses were performed using GraphPad Prism 8.0.

3 Results

3.1 The effects of PF-05231023 administration on body weight and fat in $Apoe^{-/-}$ mice

During the first week of feeding, there was no significant difference in body weights among all mice, although the $Apoe^{-/-}$ mice exhibited a slightly higher body weight than that of the WT + Control group. After 12 weeks of the feeding regimen, there was no significant difference in weights between the $Apoe^{-/-}$ + WD + PF-05231023 group and the $Apoe^{-/-}$ + WD + saline group. However, a significant difference in weights was noted between the WT + Control group and the $Apoe^{-/-}$ + Control group ($p < 0.05$). PF-05231023 treatment was initiated after the 12th week. During the 7-week treatment period, the weight of mice in the $Apoe^{-/-}$ + WD + PF-05231023 group increased in the first week, gradually decreased, and then remained stable thereafter. The weight of the $Apoe^{-/-}$ + WD + saline group showed a slight upward trend; however, the difference was not significant between the two groups. Furthermore, a significant difference in body weight was noted between the $Apoe^{-/-}$ + Control group and the $Apoe^{-/-}$ + WD + saline group ($p < 0.01$). A significant difference in body weight was also observed between the WT + Control group and the $Apoe^{-/-}$ + Control group ($p < 0.05$, Figure 2A), as well as between the $Apoe^{-/-}$ + WD + PF-05231023 group and the $Apoe^{-/-}$ + WD + saline group before mouse sampling ($p < 0.05$, Figure 2B). These results indicate that PF-05231023 treatment affected the body weight of $Apoe^{-/-}$ mice.

Body composition analysis conducted before and after treatment revealed no significant fluctuation in fat content between the WT + Control and $Apoe^{-/-}$ + Control groups (Figure 2C). Both the $Apoe^{-/-}$ + WD + PF-05231023 and $Apoe^{-/-}$ + WD + saline groups showed a decrease in fat content before and

TABLE 2 Study primer sequences.

Gene	Accession number	(5'-3')	(3'-5')
β -actin	NM_007393	GTGACGTTGACATCCGTAAAGA	GCCGGACTCATCGTACTCC
<i>Agpat2</i>	NM_026212.2	CAGCCAGGTTCTACGCCAAG	TGATGCTCATGTTATCCACGGT
<i>Angptl8</i>	NM_001080940.1	CCCTCAATGGCGTGACAGA	CCACCTGAATCTCCGACAGG
<i>Mrap</i>	NM_029844.4	CCTGGCTACCTTCGTGGTG	GGGAGGTTGAAGCTGTGAGTC
<i>Pla2g2e</i>	NM_012044.2	CCAGTGGACGAGACGGATTG	AGCAGCTCTCTGTACACTC
<i>Dbi</i>	NM_007830.4	CAAGCTACTGTGGGCGATGTA	CACATAGGTCTTCATGGCACTTT
<i>B3gnt5</i>	NM_001159407.1	TGGCTTTGTAAACAATTCCTGT	GAACGTCGCCCATAGTTTTCA
<i>Cr2</i>	NM_001368765.1	TGTCATCCCGACATGCAAAGA	ACACTGACTAGAGGGTTGTCC
<i>Ltf</i>	NM_008522.3	TGATGACACCCGAAACCTG	TCCCAAACCTGAACCTGTTGGT
<i>Ucp2</i>	NM_001417452.1	GTGGTGGTCGGAGATACCAGA	GGGCAACATTGGGAGAAGTCC

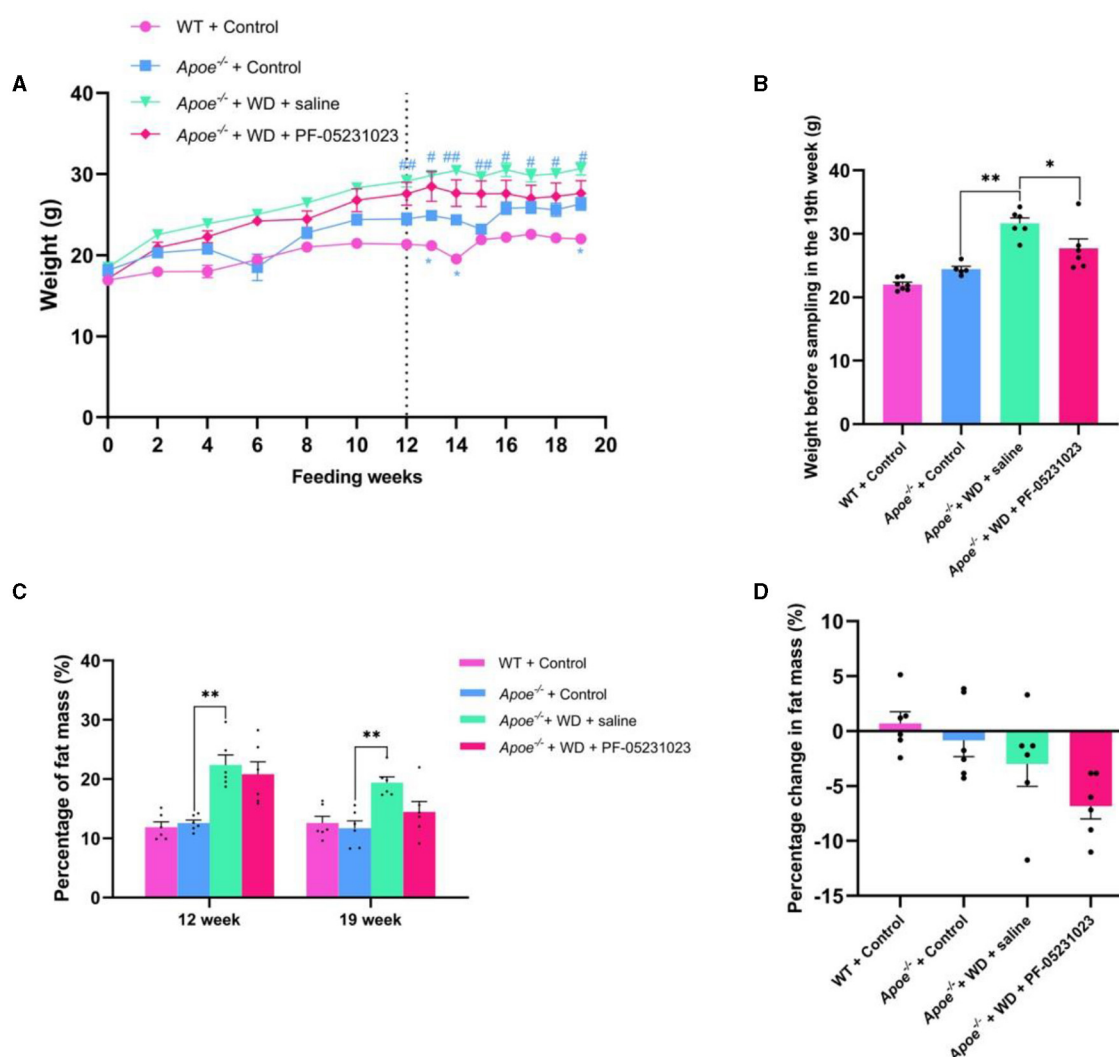


FIGURE 2

(A) Changes in body weight of *Apoe*^{-/-} mice during feeding and treatment. *indicates a significant difference between the WT + Control group and the *Apoe*^{-/-} + Control group (* $p < 0.05$, ** $p < 0.01$), whereas # indicates a significant difference between the *Apoe*^{-/-} + Control group and the *Apoe*^{-/-} + WD + saline group (# $p < 0.05$, ## $p < 0.01$). Control represents the Western-style diet control group, and WD indicates the Western-style diet purification group. (B) Body weight of mice before sampling. (C) Fat content before and after treatment. (D) Fat mass change after treatment.

after treatment (Figure 2C). Specifically, the saline group showed a decrease of 2.99%, whereas the PF-05231023 group exhibited a decrease of 6.82%. The proportion of decrease in the PF-05231023 group was more than twice that in the control group. Overall, the proportion of fat that decreased in the PF-05231023 group was higher than that in the saline group (Figure 2D). These results indicate that PF-05231023 causes a slight decrease in fat content in *Apoe*^{-/-} mice.

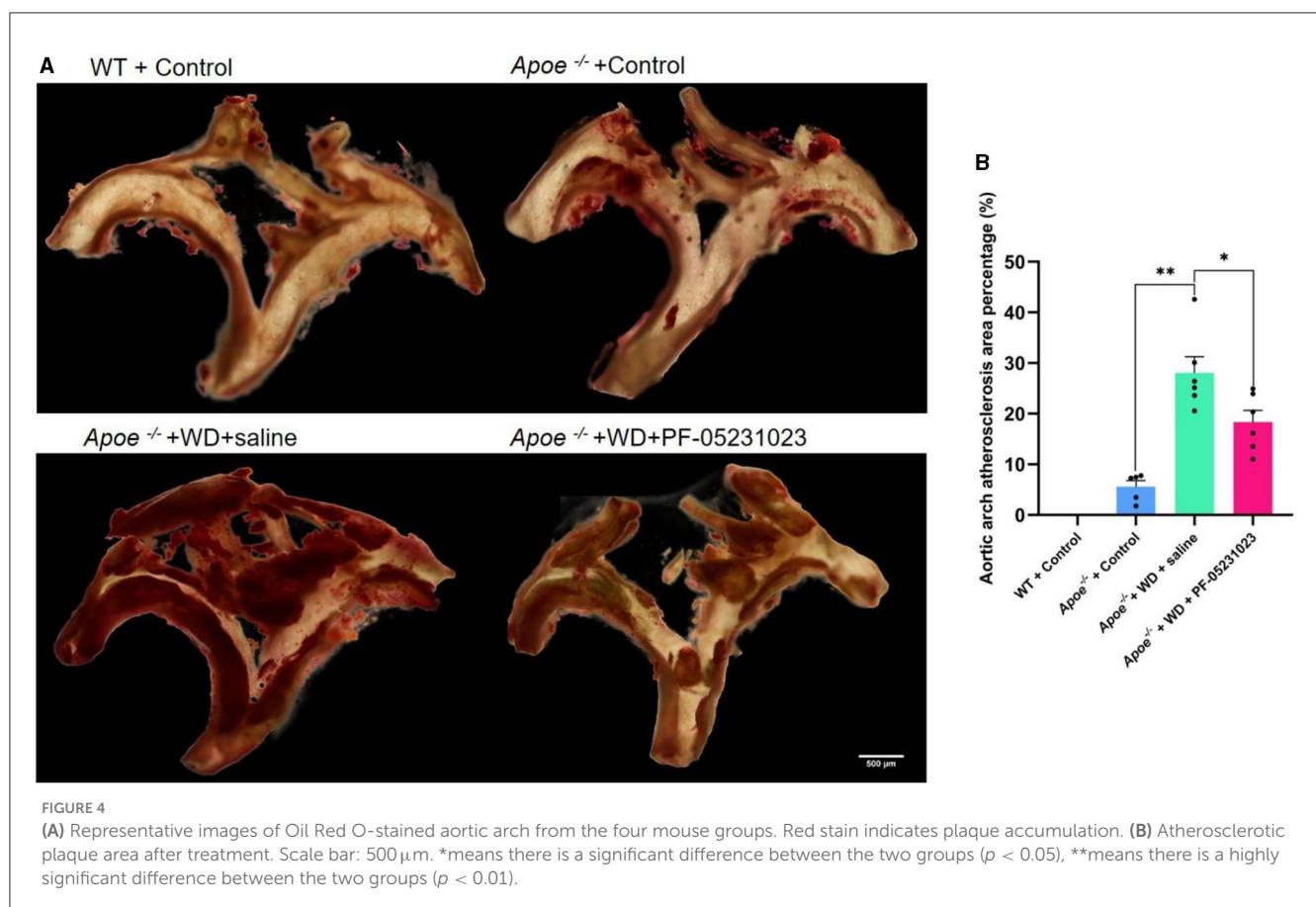
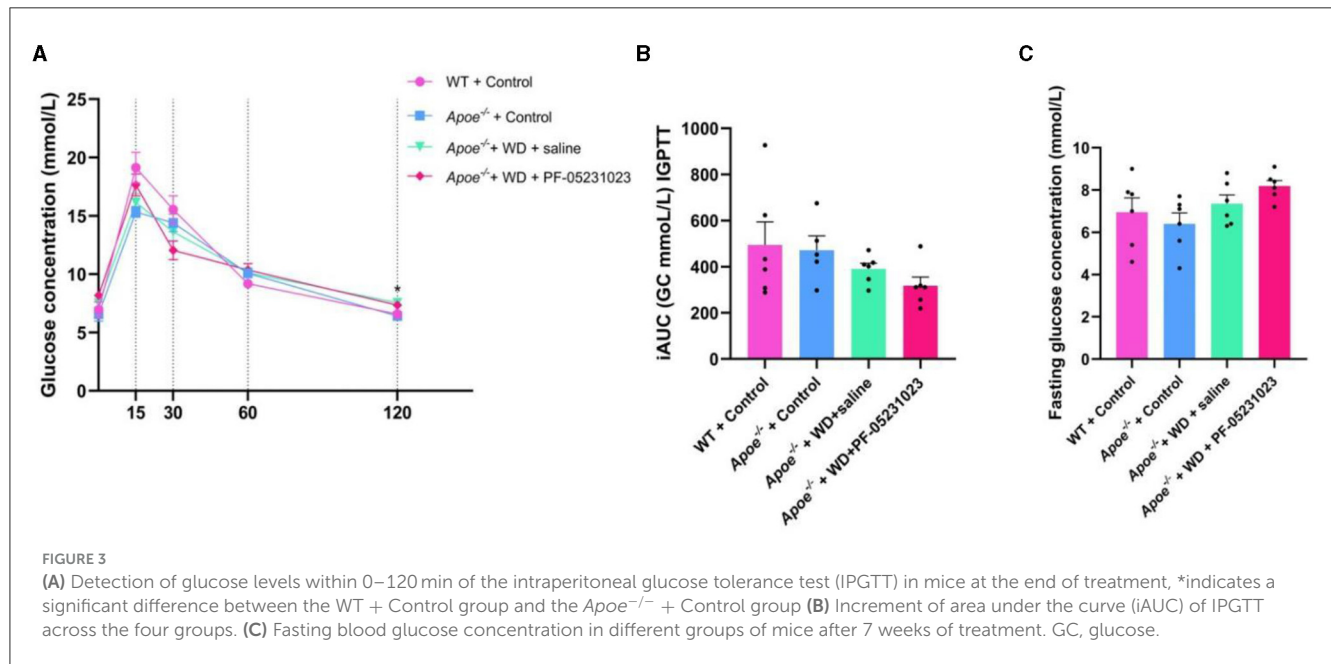
3.2 The effects of PF-05231023 on blood glucose levels in *Apoe*^{-/-} mice

At the end of 7 weeks of treatment, mice were subjected to an IPGTT. Within 120 min of the IPGTT, mice treated with PF-05231023 showed the fastest decrease in blood glucose levels at 30 min compared with that in the group injected with physiological

saline (Figure 3A). The area under the glucose curve was also lower than that for the control group (Figure 3B). Although blood glucose levels were slightly higher in the fasting state (Figure 3C), no statistical difference was observed. These results indicate that the effect of PF-05231023 treatment on blood glucose levels in *Apoe*^{-/-} mice was modest. Plasma lipid level analysis revealed no significant decrease in TC and TG levels in the plasma of mice treated with PF-05231023 compared with that of mice treated with physiological saline (data not shown).

3.3 The effects of PF-05231023 on the aorta of *Apoe*^{-/-} mice

Oil Red O staining analysis was performed on the aortic arch. The WT + Control group exhibited a normal aortic wall with no lipid deposition. However, partial lipid deposition was observed in



the aortic wall of the *Apoe*^{-/-} + Control group. The intima of the aorta in the *Apoe*^{-/-} + WD + saline group appeared relatively fragile, with a substantial amount of lipid deposition noted on the vessel wall. Compared with that in the saline injection group,

the *Apoe*^{-/-} + WD + PF-05231023 group showed reduced lipid deposition on the vessel wall and milder plaque lesions (Figure 4A). Furthermore, the plaque area was significantly smaller compared with that in the saline injection group (Figure 4B; $p < 0.05$). These

results indicate that PF-05231023 reduced plaque accumulation in the aortic arch of *Apoe*^{-/-} mice.

3.4 The effects of PF-05231023 on lipid deposition and biochemical levels in the liver of *Apoe*^{-/-} mice

Liver sections stained with HE were examined under a microscope at 200× magnification. Compared with that in the group injected with saline, mice treated with PF-05231023 exhibited a smaller area of hepatic fat vacuolization (Figure 5A) and a significant decrease in lipid deposition (Figure 5B, $p < 0.01$). This decrease approached the level observed in the *Apoe*^{-/-} + Control group, indicating that PF-05231023 improved hepatic steatosis in *Apoe*^{-/-} mice. In addition, the TC levels in the livers of mice from the *Apoe*^{-/-} + WD + PF-05231023 group were lower than those in the saline group (Figure 5D). Although TG levels did not

show statistical differences, there was a slight trend of decrease (Figure 5E). PF-05231023 also improved liver weight (Figure 5C).

3.5 The effects of PF-05231023 on *Apoe*^{-/-} mouse adipose tissue

Sections of white adipose tissue around the ovaries were subjected to HE staining and examined using a microscope at 200× magnification. The adipocytes in the WT + Control group mice were tightly arranged, had small cell diameters, and possessed small volumes (Figure 6A). Compared with those in the WT + Control group, the *Apoe*^{-/-} + Control group exhibited slightly larger cell diameters and volumes (Figure 6A). The volume and diameter of adipocytes in the *Apoe*^{-/-} + WD + saline group were increased, exhibiting characteristics of uneven cell size and irregular shape (Figure 6A). However, in the *Apoe*^{-/-} + WD + PF-05231023 group, adipocytes were smaller than those in the *Apoe*^{-/-}

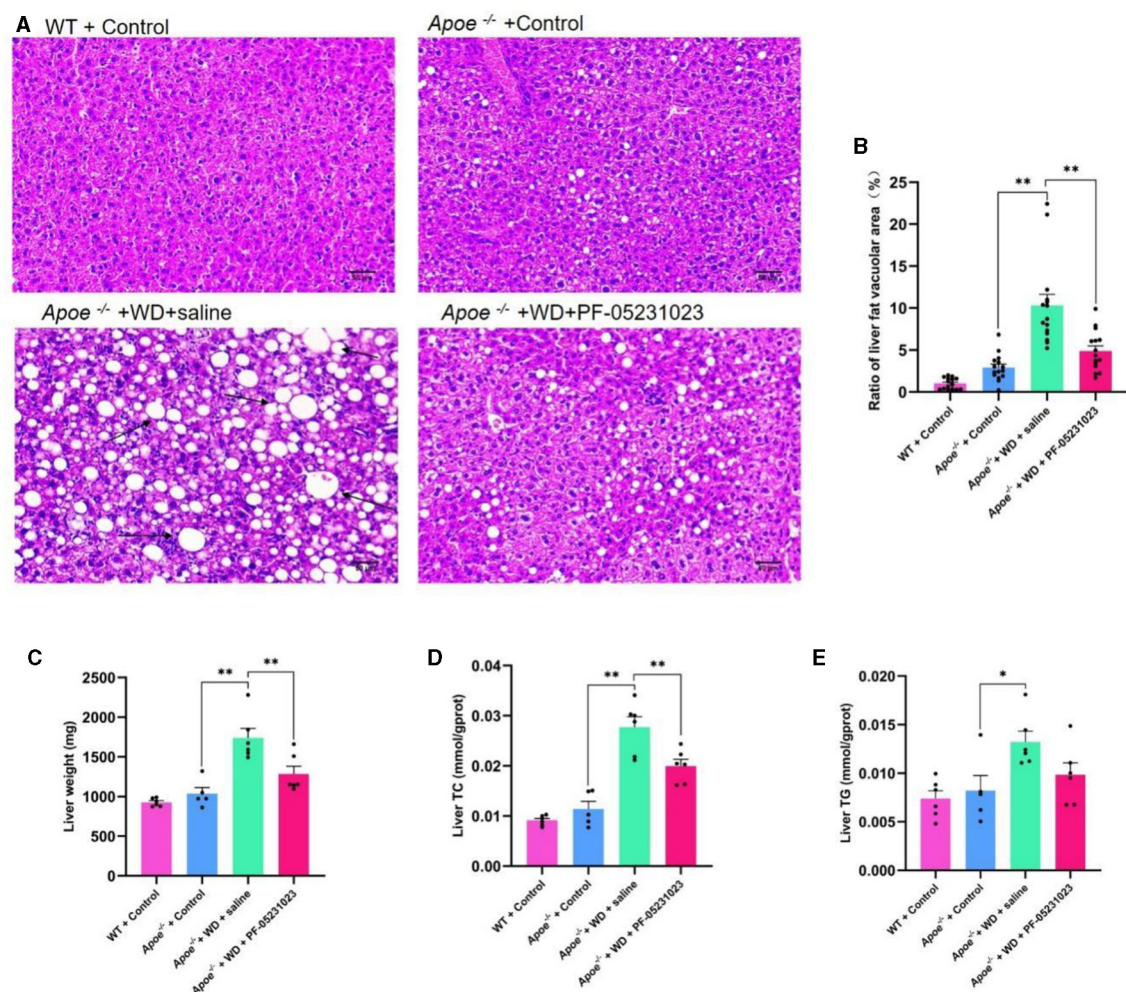


FIGURE 5

(A) Representative images of hematoxylin and eosin (HE)-stained livers from the four mouse groups. The black arrows indicates the main lesions. (B) Percentage of liver vacuolization. (C) Liver weight after sampling. (D) Total cholesterol (TC) content in the liver. (E) Liver triglyceride (TG) levels. Scale bar: 50 μ m. *means there is a significant difference between the two groups ($p < 0.05$), **means there is a highly significant difference between the two groups ($p < 0.01$).

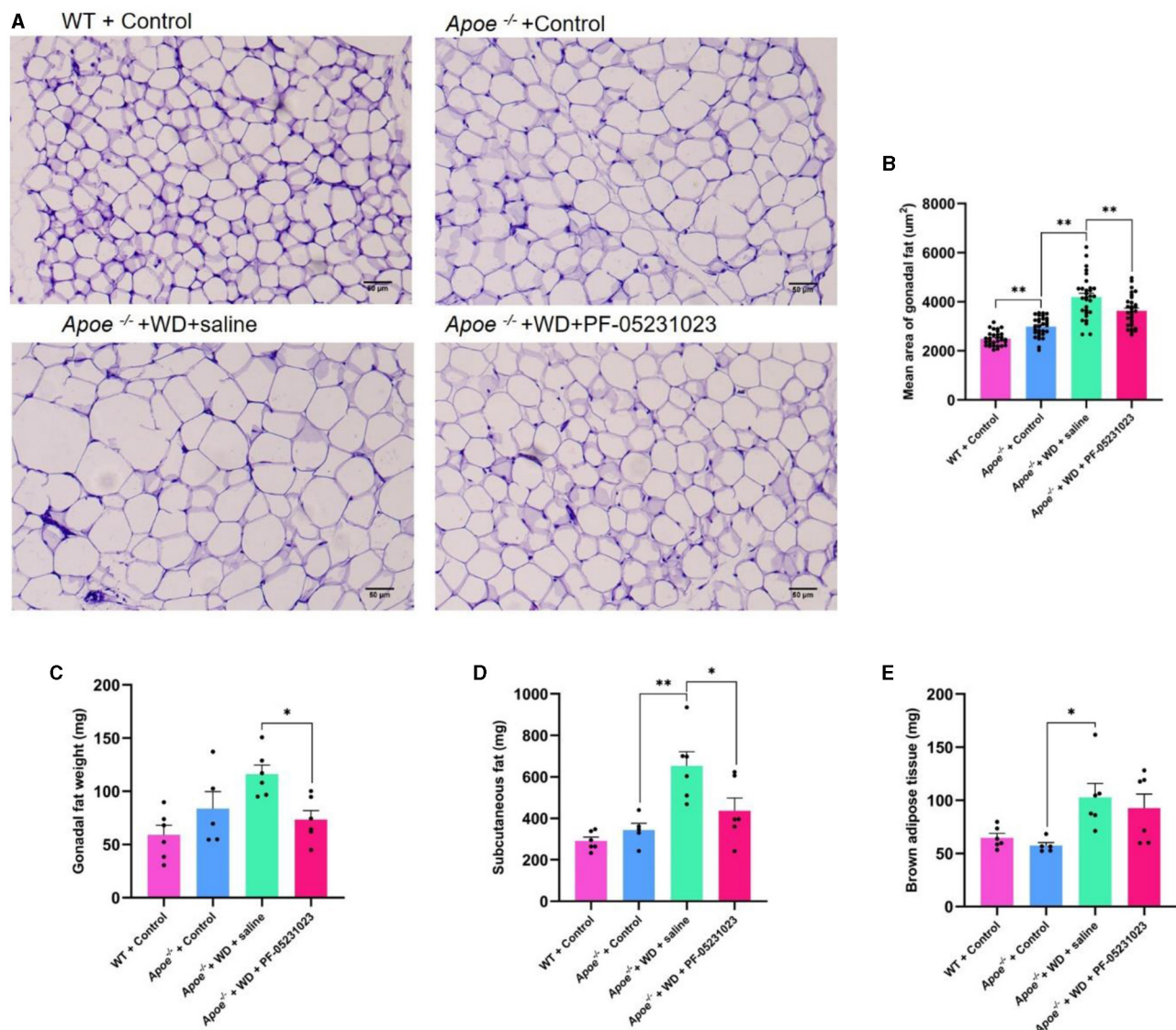


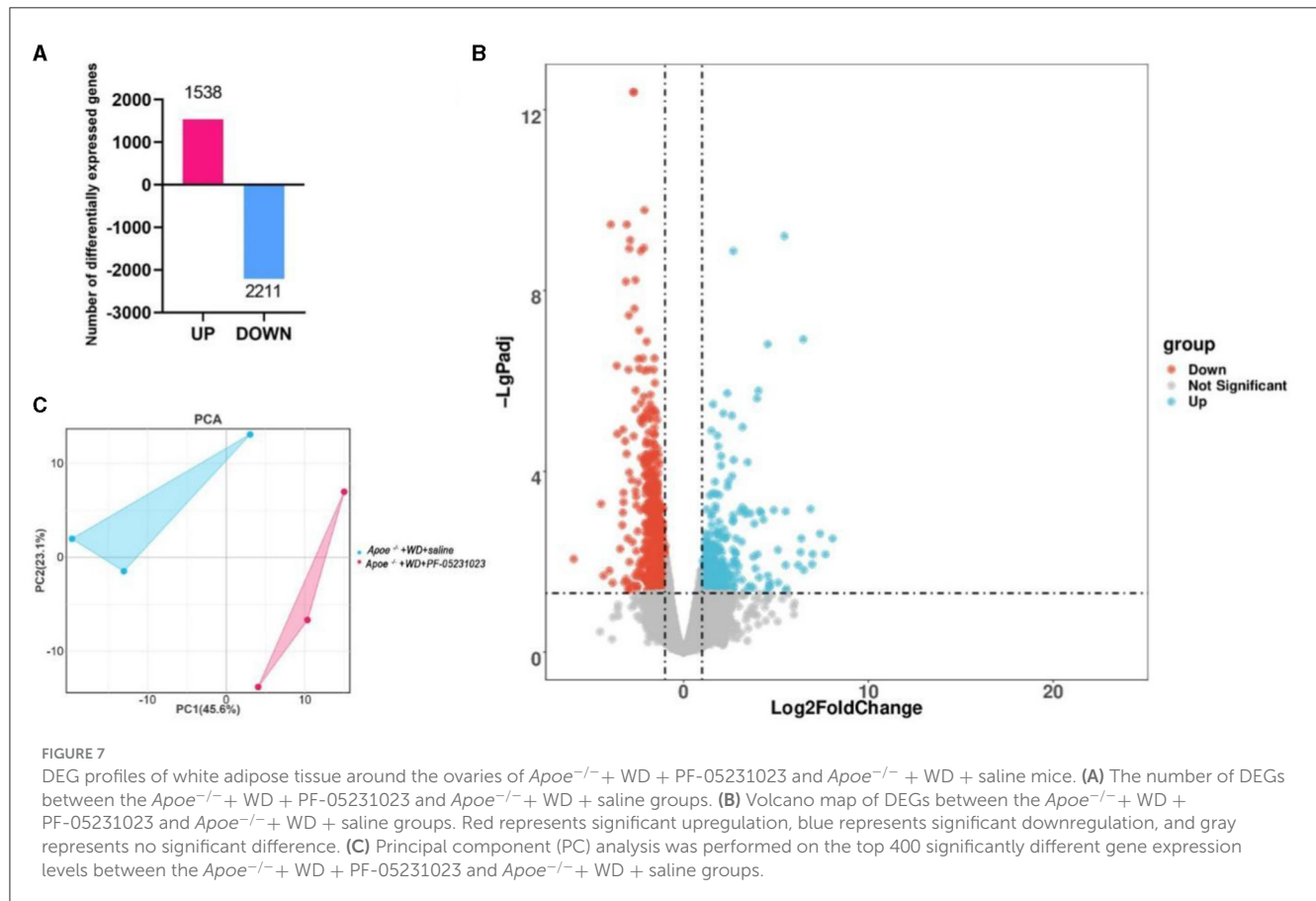
FIGURE 6

(A) Representative images of Hematoxylin and eosin (HE)-stained white adipose tissue around the ovaries of mice in the four study groups. (B) Average area of white adipocytes around the ovaries. (C) Weight of white fat around the ovaries after sampling. (D) Subcutaneous fat weight after sampling. (E) Weight of brown fat after sampling. Scale bar: 50 μm. *means there is a significant difference between the two groups ($p < 0.05$), **means there is a highly significant difference between the two groups ($p < 0.01$).

+ WD + saline group, with reduced volume and diameter and more regular arrangement (Figure 6A). The average area of white adipocytes around the ovaries significantly decreased in the average area of adipose tissue cells in the *Apoe*^{-/-} + WD + PF-05231023 group compared with that in the *Apoe*^{-/-} + WD + saline group (Figure 6B, $p < 0.05$). Weight statistics were obtained for white, subcutaneous, and brown fat around the ovaries after sampling. Compared with that in the *Apoe*^{-/-} + WD + saline group, the *Apoe*^{-/-} + WD + PF-05231023 group showed a significant decrease in the weight of white fat around the ovaries (Figure 6C) and subcutaneous fat (Figure 6D, $p < 0.05$), whereas no statistically significant difference was noted in terms of brown fat (Figure 6E, $p > 0.05$).

3.6 DEGs and functional annotation analysis

We conducted sequencing analysis of the white adipose tissue around the ovaries in the *Apoe*^{-/-} + WD + PF-05231023 group and the *Apoe*^{-/-} + WD + saline group. Three biological replicates were used for each group. Our sequencing results revealed a total of 3,749 DEGs between *Apoe*^{-/-} + WD + PF-05231023 and *Apoe*^{-/-} + WD + saline mice, including 1,538 upregulated genes and 2,211 downregulated genes (Figure 7A; screening parameter | log₂ Fold change | ≥ 1 and $q < 0.05$). The volcano plot analysis a more intuitive up-and-down regulation of DEGs (Figure 7B). Principal component analysis



of these DEGs demonstrated high similarity within the groups (Figure 7C).

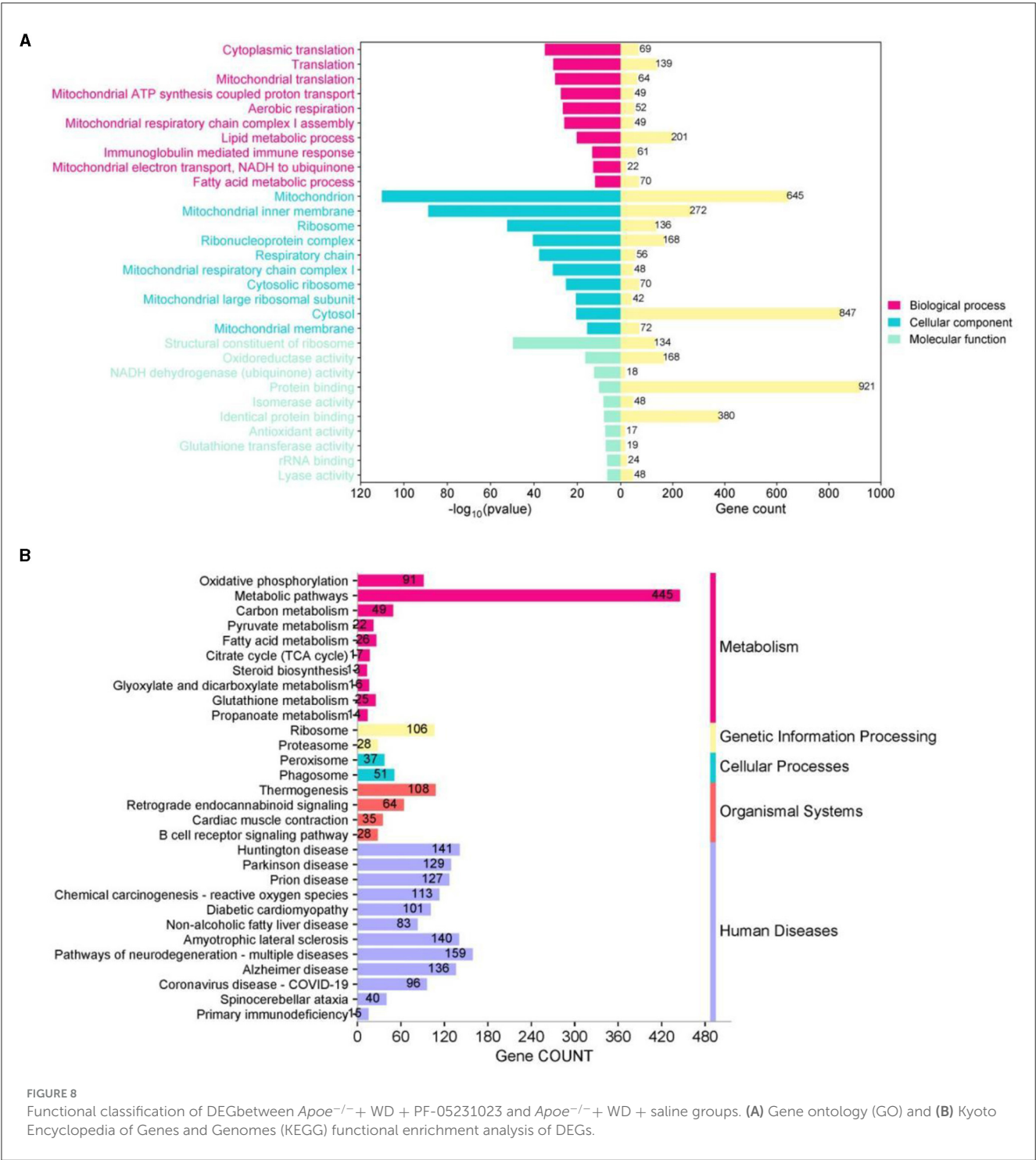
We used the GO and KEGG databases to classify DEG functions (Figure 8). In the top 10 biological processes (BP), cellular component (CC), and molecular function (MF), GO enrichment analysis showed that BP was primarily associated with translation, aerobic respiration, lipid metabolism, and immune response processes, whereas CC was mainly concentrated in mitochondria, ribosomes, respiratory chains, and other cellular parts. In MF, enrichment was observed in ribosomal structural components, oxidoreductase activity, and homologous protein binding, and other functional aspects (Figure 8A). We also annotated DEGs based on the KEGG database and noted that 3,749 DEGs were concentrated in 81 KEGG pathways within six categories: metabolism, genetic information processing, environmental information processing, cellular processes, biological systems, and human diseases. Among these pathways, apart from human diseases, the most DEGs were in metabolic processes, including oxidative phosphorylation, metabolic pathways, fatty acid metabolism, steroid biosynthesis, glutathione metabolism, and propionic acid metabolism (Figure 8B).

Six pathways were closely related to lipid metabolism in the KEGG analysis, including fatty acid metabolism, steroid biosynthesis, fatty acid elongation, fatty acid biosynthesis, fatty acid degradation, and cholesterol metabolism, as shown in Figure 9. In the fatty acid metabolism pathway, key genes involved in fatty acid synthesis, such as fatty acid synthase (*Fasn*), acetyl CoA carboxylase

alpha (*Acaca*), and acetyl CoA carboxylase beta (*Acacb*), were significantly downregulated, whereas key genes involved in fatty acid oxidation, such as *Cpt1ab*, were upregulated. In the fatty acid elongation pathway, *Mecr*, very long chain fatty acid elongase 1 (*Elovl1*), and very long chain fatty acid elongase 6 (*Elovl6*) were significantly downregulated. In the steroid biosynthesis pathway, genes related to cholesterol synthesis, such as farnesyl-diphosphate farnesyltransferase 1 and squalene epoxidase, were significantly downregulated. In addition, steroyl CoA depletion 1 (*Scd1*) and adipogenin, which are involved in fat production, were significantly downregulated, whereas adenosine triphosphate-binding cassette transporter G8 (*Abcg8*), which promotes cholesterol efflux, was significantly upregulated. The levels of sterol regulatory element binding transcription factor 1 (*Srebf1*) also significantly decreased. Table 3 provides a detailed description of the genes involved in these pathways.

3.7 Real-time fluorescence quantitative PCR validation results

To verify the reliability of the transcriptional data, we randomly selected nine DEGs with high expression levels for quantitative PCR (qPCR) analysis. The qPCR results were consistent with the trends observed in the transcriptome analysis, confirming the accuracy and reliability of the transcriptome sequencing results.

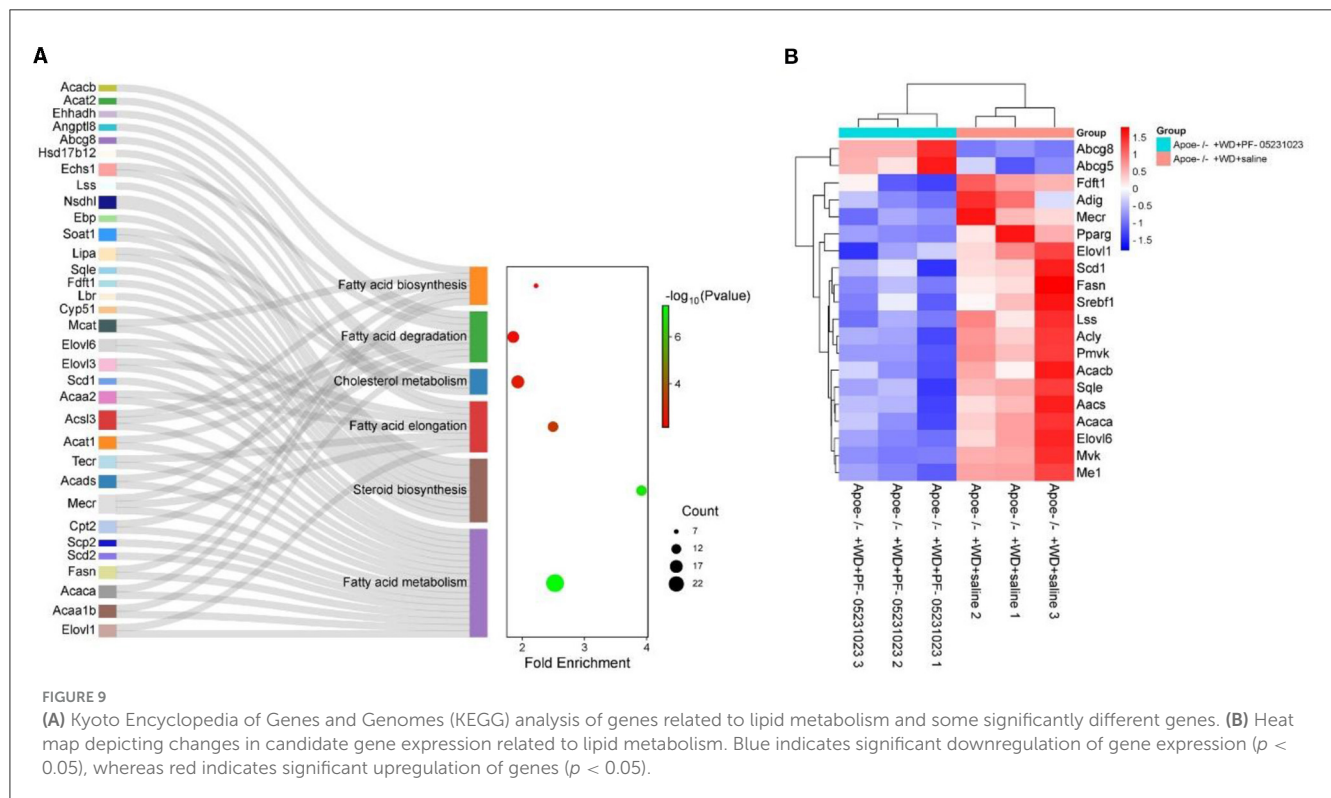


(Figure 10A). Moreover, a high correlation was observed between the qPCR and RNA-Seq data, with $R^2 = 0.943$ (Figure 10B).

4 Discussion

FGF21 analogs have been studied in clinical trials for type 2 diabetes and NAFLD and have demonstrated generally good tolerability. This study confirms that the long-acting FGF21 analog PF-05231023 reduces the accumulation of atherosclerotic

plaques and improves lipid metabolism in the liver and adipose tissue of *Apoe*^{-/-} mice, thereby indicating the clinical potential of the FGF21 analog in treating AS. In this study, the body weights of *Apoe*^{-/-} mice treated with PF-05231023 gradually decreased until changes were observed prior to sampling. This result aligns with those of previous studies that reported weight loss in response to administration of FGF21 analogs in diet-induced obese mice (DIO) (22), and in Gubra Amylin NASH DIO mice (10). Although some clinical trials have suggested weight reduction after FGF21 analog treatment in



subjects with obesity, type 2 diabetes, and fatty liver disease, the evidence for weight loss in subjects with obesity remains inconclusive (23). For example, in a clinical trial evaluating the safety and tolerability of PF-05231023 in patients with obesity with hypertriglyceridemia, PF-05231023 reduced TG and low-density lipoprotein cholesterol levels without causing body weight reduction (24).

After 7 weeks of treatment, the WT + Control and *Apoe*^{-/-} + Control groups showed minimal changes in body fat percentage. Conversely, both the PF-05231023 treatment and the physiological saline control groups showed a declining trend in body fat percentage, with the PF-05231023 treatment group demonstrating a more significant decrease. We hypothesize that this reduction in body fat percentage is likely attributed to the weekly intraperitoneal injections administered to both mouse groups, causing a certain degree of stress. This is supported by the observation that the two control groups, which did not receive intraperitoneal injections, did not show significant changes in body fat. FGF21 reduces blood sugar levels in diabetic rodents, obese mice, and monkey models (10). However, this study found that although there was no statistically significant difference in fasting blood glucose levels between *Apoe*^{-/-} mice injected with PF-05231023 and those injected with physiological saline, the former group showed an improvement in glucose tolerance. PF-05231023 does not significantly affect blood glucose control (11, 15). These minor differences in glucose improvement may be attributed to the slight differences in the pharmacology of FGF21 analogs (15). Additionally, injection of PF-05231023 had no significant effect on the reduction of plasma lipids in *Apoe*^{-/-} mice. Similarly, no significant reduction in plasma TG levels was detected in

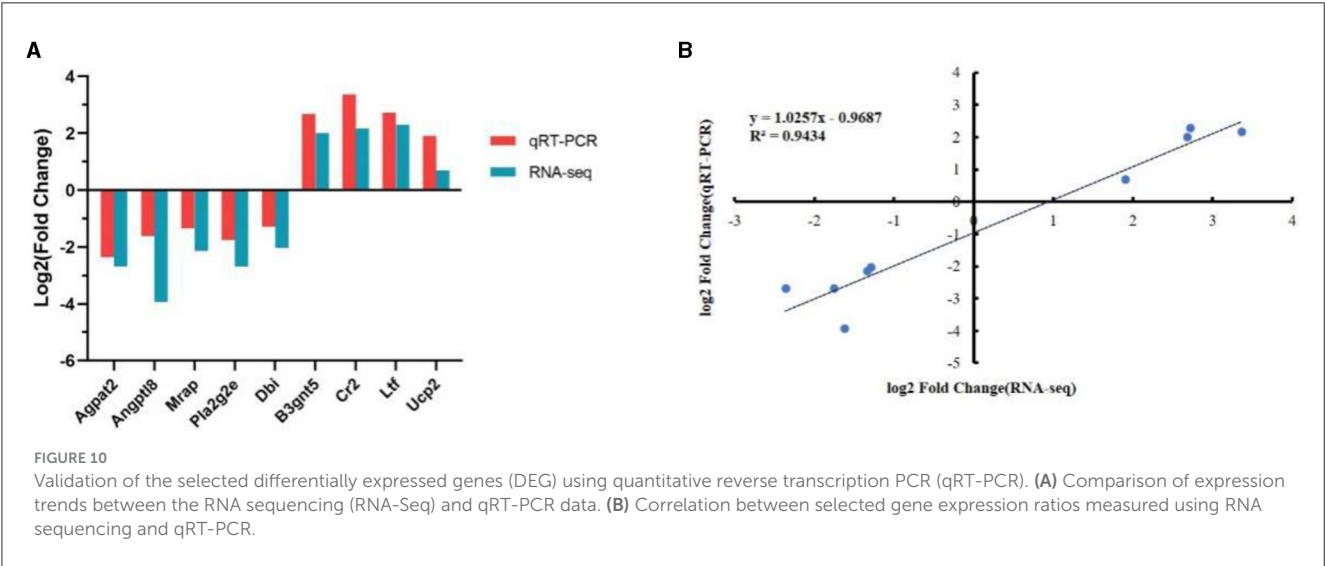
DIO mice treated with FGF21 (25). A study conducted on obese Göttingen mini pigs also found that FGF21 had no effect on pig plasma lipids, partly because of the very low circulating lipid levels in the mini pigs, which rendered FGF21 ineffective in reducing pig plasma lipids (26). The reason plasma lipid levels exhibited no significant effect in the current study remains unclear and could be a topic for further research. Numerous studies have investigated the role of FGF21 in AS. For example, a study using *Apoe*^{-/-} mice demonstrated that FGF21 alleviated AS by enhancing Fas-mediated apoptosis (27). Another study reported that FGF21 upregulates autophagy-mediated cholesterol efflux via receptor for activated C kinase 1 to inhibit AS (17). Furthermore, FGF21 alleviates AS by inhibiting focal pyroptosis in vascular endothelial cells, mediated by the NLR family pyrin domain containing three inflammasome (28). Thus, several mechanisms have been proposed for the inhibition of AS. In our study, PF-05231023 administration reduced fat accumulation in the liver and significantly reduced TC and TG content in the liver. This result aligns with the conclusion that PF-05231023 treatment reduces liver TC and TG in NAFLD, and reduces plasma liver injury markers alanine aminotransferase and aspartate aminotransferase (10). Additionally, our results are also consistent with research indicating that FGF21 improved lipid droplet size in the liver (16), as did the FGF21 analog LY2405319 (12). In various diet-induced, genetically modified, or chemically induced models, PF-05231023 treatment reduces the weight of brown fat, subcutaneous fat, and white adipose tissue, and it reduces adipocyte size in the white adipose tissue around the ovaries. FGF21-specific-knockout mice exhibit weight gain, decreased lipolysis, and reduced energy expenditure in the adipose tissue, leading to adipose tissue

hypertrophy (11). However, FGF21 treatment reduces weight gain, improves lipid levels in adipocytes, and reduces inflammatory cell infiltration (29).

TABLE 3 DEGs involved in *de novo* adipogenesis, cholesterol biosynthesis, and fatty acid elongation pathways.

Gene	Description	Log ₂ FC	q-Value
<i>Aacs</i>	Acetoacetyl-CoA synthetase	−1.17186	0.000651
<i>Abcg8</i>	Adenosine triphosphate-binding cassette transporter G8	4.083074	0.011935
<i>Acaca</i>	Acetyl-CoA carboxylase alpha	−1.45815	9.53E−05
<i>Acacb</i>	Acetyl-CoA carboxylase beta	−1.09862	0.018698
<i>Acly</i>	Adenosine triphosphate citrate lyase	−1.83961	0.000663
<i>Adig</i>	Adipogenin	−2.0744	7.65E−06
<i>Elovl1</i>	Very long chain fatty acid elongase 1	−0.73961	0.004791
<i>Elovl6</i>	Very long chain fatty acids elongase 6	−2.31099	2.56E−07
<i>Fasn</i>	Fatty acid synthase	−1.8984	2.83E−05
<i>Fdft1</i>	Farnesyl-diphosphate farnesyltransferase 1	−1.11442	0.002743
<i>Lss</i>	Lanosterol synthase	−1.12141	0.01039
<i>Me1</i>	Malic enzyme 1	−1.93987	3.80E−07
<i>mecr</i>	Mitochondrial trans-2-enoyl-CoA reductase	−1.37633	1.43E−05
<i>Mvk</i>	Mevalonate kinase	−1.35399	2.01E−07
<i>Pmvk</i>	Phosphomevalonate kinase	−1.76177	2.03E−08
<i>Pparg</i>	Peroxisome proliferative activated receptor gamma	−1.23941	0.000471
<i>Scd1</i>	Stearoyl-CoA desaturase 1	−0.87024	0.004249
<i>Sqle</i>	Squalene epoxidase	−1.0713	0.002529
<i>Srebf1</i>	STEROL regulatory element binding transcription factor 1	−1.01262	0.010143

To better understand the molecular pathways associated with PF-05231023 and its effect on lipid metabolism in adipose tissue, we analyzed gene expression in the white adipose tissue around the ovaries. First, we annotated DEGs using the KEGG database and noted that most of the DEGs were concentrated in the categories related to metabolism and human diseases. By combining KEGG and GO functional analyses, we observed that pathways related to metabolism and human disease were downregulated in the differential gene set. Enrichment results for human disease show that PF-05231023 has a significant positive impact on the pathways associated with neurodegenerative diseases, including Alzheimer’s disease (30), Parkinson’s disease (31, 32), Huntington’s disease, and amyotrophic lateral sclerosis. This finding suggests a potential role for long-acting FGF21 analogs in neuroprotection. FGF21 can modulates anti-inflammatory and antioxidant stress responses through nuclear factor kappa-B and adenosine 5′-monophosphate-activated protein kinase/protein kinase B signaling pathways, thereby protecting nerves from damage and mitigating neurodegenerative changes (33). Furthermore, our analysis revealed that PF-05231023 significantly downregulated the expression of genes related to NAFLD. This downregulation would lead to an improvement in the symptoms of this disease (34). This beneficial effect of PF-05231023 may be attributed to the direct regulation of lipid metabolism through insulin, resulting in reduced lipid accumulation in the liver. In the metabolic category, we identified several DEGs involved in metabolic pathways and lipid metabolism. We found that PF-05231023 significantly downregulated *Srebf1*, further leading to a decrease in the expression of *Fasn*, *Acaca*, *Acacb*, and *Scd1*. *Srebf1* is an important transcription factor that regulates lipid metabolism related enzymes primarily expressed in the liver and adipocytes. The transcription factor induces *de novo* adipogenesis by regulating the expression of adipogenic genes, such as *Acaca* and *Acacb*, *Fasn* (35), and *Scd1* (36, 37). *Acaca* and *Acacb* catalyze rate-limiting reactions in the biogenesis of long-chain fatty acids (38). *Fasn* is a key synthase in the process of fatty acid biosynthesis (38), which catalyzes *de novo* fatty acid synthesis by converting acetyl CoA and malonyl CoA to palmitic acid esters (39), and *Scd1* regulates the expression of



unsaturated fatty acid biosynthesis genes and mitochondrial fatty acid oxidation (38). Moreover PF-05231023 also reduced the expression of adenosine triphosphate citrate lyase, which is an important enzyme in the cholesterol and fatty acid biosynthesis pathway upstream of *Fasn* (38), thereby promoting the biosynthesis of cholesterol and fatty acids by producing acetyl CoA from citrate (40). *Elovl1* and *Elovl6* are downregulated by *Srebf1*, which also leads to a decrease in fatty acid synthesis. Moreover, we observed a significant upregulation of *Abcg8* and an upregulation trend of adenosine triphosphate-binding cassette transporter G5 (*Abcg5*). The ABCG5/ABCG8 complex transports cholesterol and phytosterols from intestinal cells to the intestinal cavity for fecal treatment, thereby promoting cholesterol efflux and reducing cholesterol accumulation (41).

5 Conclusion

In summary, we confirmed that PF-05231023 reduces liver cholesterol and TG levels as well as lipid deposition in WD-fed *Apoe*^{−/−} mice and has the potential to counteract the development of AS. Further analysis of adipose tissue indicated that PF-05231023 reduces the expression of genes involved in adipogenesis, cholesterol synthesis, and fatty acid derivative pathways. Moreover, we found that the specific mechanism by which PF-05231023 inflicts these effects is to inhibit the expression of *Srebf1* and further inhibit the expression of genes related to lipid generation, thereby reducing lipid synthesis. However, the specific role of this pathway requires further investigation.

5.1 Study limitations

In the current study, we revealed the ameliorative effects of PF-05231023 on lipid metabolism as well as inhibitory effects on the expression of lipogenesis-related genes. However, the specific pathways regulated by PF-05231023 remain to be fully elucidated. Hence, the following aspects need to be further investigated: the mechanism by which PF-05231023 down-regulates *Srebf1* expression, whether *Srebf1* is linked to the expression of other lipogenesis-related genes, and the regulatory pathways between *Srebf1* and other lipogenesis-related genes.

Data availability statement

The datasets presented in this study can be found in online repositories. The names of the repository/repositories and accession number(s) can be found below: NCBI SRA (accession: PRJNA1113307).

Ethics statement

The procedures for animal handling for experiments were approved by the Committee of Experimental Animal Management at South China Agricultural University, China (protocol number: CEAM-SCAU-2023-0002). Moreover, all applicable rules and

regulation of the organization and government were followed regarding the ethical use of experimental animals. The studies were conducted in accordance with the local legislation and institutional requirements. Written informed consent was obtained from the owners for the participation of their animals in this study.

Author contributions

JZ: Conceptualization, Data curation, Formal analysis, Investigation, Methodology, Software, Supervision, Validation, Visualization, Writing – original draft, Writing – review & editing. XL: Investigation, Methodology, Validation, Visualization, Writing – review & editing. JY: Investigation, Methodology, Validation, Visualization, Writing – review & editing. SZ: Investigation, Methodology, Validation, Visualization, Writing – review & editing. LL: Formal analysis, Investigation, Methodology, Visualization, Writing – review & editing. HW: Conceptualization, Funding acquisition, Methodology, Project administration, Resources, Supervision, Writing – review & editing.

Funding

The author(s) declare financial support was received for the research, authorship, and/or publication of this article. This study was supported by the Guangdong Basic and Applied Basic Research Foundation (Grant Nos. 2022A1515012208, 2024A1515012529, and 2024A1515013145), the Local Innovative and Research Teams Project of Guangdong Province (Grant No. 2019BT02N630), and the State Key Laboratory of Swine and Poultry Breeding Industry research project (Grant No. ZQQZ-10).

Acknowledgments

The authors greatly appreciate the contributions made to this article, especially the valuable suggestions provided by Prof. Li Meng for this experiment. The authors would like to thank Editage (www.editage.cn) for English language editing. The authors would also like to thank Ms. Xing Yushu from the University of Bristol for her help in data analysis.

Conflict of interest

The authors declare that the research was conducted in the absence of any commercial or financial relationships that could be construed as a potential conflict of interest.

Publisher's note

All claims expressed in this article are solely those of the authors and do not necessarily represent those of their affiliated organizations, or those of the publisher, the editors and the reviewers. Any product that may be evaluated in this article, or claim that may be made by its manufacturer, is not guaranteed or endorsed by the publisher.

References

- Ng M, Fleming T, Robinson M, Thomson B, Graetz N, Margono C, et al. Global, regional, and national prevalence of overweight and obesity in children and adults during 1980–2013: a systematic analysis for the Global Burden of Disease Study 2013 [published correction appears in *Lancet*. 2014 Aug 30;384(9945):746]. *Lancet*. 2014; 766–81. doi: 10.1016/S0140-6736(14)60460-8
- Samuel VT, Shulman GI. The pathogenesis of insulin resistance: integrating signaling pathways and substrate flux. *J Clin Invest*. (2016) 126:12–22. doi: 10.1172/JCI77812
- Shulman GI. Ectopic fat in insulin resistance, dyslipidemia, and cardiometabolic disease [published correction appears in *N Engl J Med*. 2014 Dec 4;371:2241]. *N Engl J Med*. (2014) 371:1131–41. doi: 10.1056/NEJMr1011035
- Dolegowska K, Marchelek-Mysliwiec M, Nowosiad-Magda M, Slawinski M, Dolegowska B. FGF19 subfamily members: FGF19 and FGF21. *J Physiol Biochem*. (2019) 75:229–40. doi: 10.1007/s13105-019-00675-7
- Fisher FM, Maratos-Flier E. Understanding the physiology of fgf21. *Annu Rev Physiol*. (2016) 78:223–41. doi: 10.1146/annurev-physiol-021115-105339
- Tan H, Yue T, Chen Z, Wu W, Xu S, Weng J, et al. Targeting FGF21 in cardiovascular and metabolic diseases: from mechanism to medicine. *Int J Biol Sci*. (2023) 19:66–88. doi: 10.7150/ijbs.73936
- Chen Z, Yang L, Liu Y, Huang P, Song H, Zheng P, et al. The potential function and clinical application of FGF21 in metabolic diseases. *Front Pharmacol*. (2022) 13:1089214. doi: 10.3389/fphar.2022.1089214
- Fisher FM, Kleiner S, Douris N, Fox EC, Mepani RJ, Verdeguez F, et al. FGF21 regulates PGC-1 α and browning of white adipose tissues in adaptive thermogenesis. *Genes Dev*. (2012) 26:271–81. doi: 10.1101/gad.177857.111
- Gimeno RE, Moller DE. FGF21-based pharmacotherapy – potential utility for metabolic disorders. *TEM*. (2014) 25:303–11. doi: 10.1016/j.tem.2014.03.001
- Nielsen MH, Gillum MP, Vrang N, Jelsing J, Hansen HH, Feigh M, et al. Hepatoprotective effects of the long-acting fibroblast growth factor 21 analog pf-05231023 in the gan diet-induced obese and biopsy-confirmed mouse model of nonalcoholic steatohepatitis. *Am J Physiol-Gastroint Liver Physiol*. (2023) 324:G378–88. doi: 10.1152/ajpgi.00157.2022
- Geng L, Lam K, Xu A. The therapeutic potential of FGF21 in metabolic diseases: from bench to clinic. *Nat Rev Endocrinol*. (2020) 16:654–67. doi: 10.1038/s41574-020-0386-0
- Gaich G, Chien JY, Fu H, Glass LC, Deeg MA, Holland WL, et al. The effects of LY2405319, an FGF21 analog, in obese human subjects with type 2 diabetes. *Cell Metab*. (2013) 18:333–40. doi: 10.1016/j.cmet.2013.08.005
- Huang J, Ishino T, Chen G, Rolzin P, Osothprarop TE, Retting K, et al. Development of a novel long-acting antidiabetic FGF21 mimetic by targeted conjugation to a scaffold antibody. *J Pharmacol Exp Ther*. (2013) 346:270–80. doi: 10.1124/jpet.113.204420
- Veniant MM, Komorowski R, Chen P, Stanislaus S, Winters K, Hager T, et al. Long-acting FGF21 has enhanced efficacy in diet-induced obese mice and in obese rhesus monkeys. *Endocrinology*. (2012) 153:4192–203. doi: 10.1210/en.2012-1211
- Talukdar S, Zhou Y, Li D, Rossulek M, Dong J, Somayaji V, et al. long-acting FGF21 molecule, PF-05231023, decreases body weight and improves lipid profile in non-human primates and type 2 diabetic subjects. *Cell Metab*. (2016) 23:427–40. doi: 10.1016/j.cmet.2016.02.001
- Maeng HJ, Lee GY, Bae JH, Lim S. Effect of fibroblast growth factor 21 on the development of atheromatous plaque and lipid metabolic profiles in an atherosclerosis-prone mouse model. *Int J Mol Sci*. (2020) 21:6836. doi: 10.3390/ijms21186836
- Xiaolong L, Dongmin G, Liu M, Zuo W, Huijun H, Qiufen T, et al. FGF21 induces autophagy-mediated cholesterol efflux to inhibit atherogenesis via rack1 up-regulation. *J Cell Mol Med*. (2020) 24:4992–5006. doi: 10.1111/jcmm.15118
- Lin Z, Pan X, Wu F, Ye D, Zhang Y, Wang Y, et al. Fibroblast growth factor 21 prevents atherosclerosis by suppression of hepatic sterol regulatory element-binding protein-2 and induction of adiponectin in mice. *Circulation*. (2015) 131:1861–71. doi: 10.1161/CIRCULATIONAHA.115.015308
- McGuinness OP, Ayala JE, Laughlin MR, Wasserman DH. NIH experiment in centralized mouse phenotyping: the Vanderbilt experience and recommendations for evaluating glucose homeostasis in the mouse. *Am J Physiol Endocrinol Metab*. (2009) 297:E849–55. doi: 10.1152/ajpendo.90996.2008
- Pan L. *Atlas of Experimental Pathology Techniques*. Beijing: Science Press (2012).
- Centa M, Ketelhuth DFJ, Malin S, Gisterå A. Quantification of atherosclerosis in mice. *J Vis Exp*. (2019) 148:e59828. doi: 10.3791/59828
- Weng Y, Chabot JR, Bernardo B, Yan Q, Zhu Y, Brenner MB, et al. Pharmacokinetics (PK), pharmacodynamics (PD) and integrated PK/PD modeling of a novel long acting FGF21 clinical candidate PF-05231023 in diet-induced obese and leptin-deficient obese mice. *PLoS ONE*. (2015) 10:e0119104. doi: 10.1371/journal.pone.0119104
- Shao W, Jin T. Hepatic hormone FGF21 and its analogues in clinical trials. *Chronic Dis Transl Med*. (2022) 8:19–25. doi: 10.1016/j.cdtm.2021.08.005
- Kim AM, Somayaji VR, Dong JQ, Rolph TP, Weng Y, Chabot JR, et al. Once-weekly administration of a long-acting fibroblast growth factor 21 analogue modulates lipids, bone turnover markers, blood pressure and body weight differently in obese people with hypertriglyceridaemia and in non-human primates. *Diabetes Obes Metab*. (2017) 19:1762–72. doi: 10.1111/dom.13023
- Coskun T, Bina HA, Schneider MA, Dunbar JD, Hu CC, Chen Y, et al. Fibroblast growth factor 21 corrects obesity in mice. *Endocrinology*. (2008) 149:6018–27. doi: 10.1210/en.2008-0816
- Christoffersen B, Straarup EM, Lykkegaard K, Fels JJ, Sass-Orum K, Zhang X, et al. FGF21 decreases food intake and body weight in obese gottingen minipigs. *Diabetes Obes Metab*. (2019) 21:592–600. doi: 10.1111/dom.13560
- Yan X, Gou Z, Li Y, Wang Y, Zhu J, Xu G, et al. Fibroblast growth factor 21 inhibits atherosclerosis in apoe^{-/-} mice by ameliorating fas-mediated apoptosis. *Lipids Health Dis*. (2018) 17:203. doi: 10.1186/s12944-018-0846-x
- Zeng Z, Zheng Q, Chen J, Tan X, Li Q, Ding L, et al. FGF21 mitigates atherosclerosis via inhibition of nlrp3 inflammasome-mediated vascular endothelial cells pyroptosis. *Exp Cell Res*. (2020) 393:112108. doi: 10.1016/j.yexcr.2020.112108
- Xu J, Lloyd DJ, Hale C, Stanislaus S, Chen M, Sivits G, et al. Fibroblast growth factor 21 reverses hepatic steatosis, increases energy expenditure, and improves insulin sensitivity in diet-induced obese mice. *Diabetes*. (2009) 58:250–9. doi: 10.2337/db08-0392
- Chen S, Chen ST, Sun Y, Xu Z, Wang Y, Yao SY, et al. Fibroblast growth factor 21 ameliorates neurodegeneration in rat and cellular models of Alzheimer's disease. *Redox Biol*. (2019) 22:101133. doi: 10.1016/j.redox.2019.101133
- Desai BN, Singhal G, Watanabe M, Stevanovic D, Lundasen T, Fisher FM, et al. Fibroblast growth factor 21 (fgf21) is robustly induced by ethanol and has a protective role in ethanol associated liver injury. *Mol Metab*. (2017) 6:1395–406. doi: 10.1016/j.molmet.2017.08.004
- Yang C, Wang W, Deng P, Li C, Zhao L, Gao H, et al. Fibroblast growth factor 21 modulates microglial polarization that attenuates neurodegeneration in mice and cellular models of parkinson's disease. *Front Aging Neurosci*. (2021) 13:778527. doi: 10.3389/fnagi.2021.778527
- Kang K, Xu P, Wang M, Chunyu J, Sun X, Ren G, et al. Fgf21 attenuates neurodegeneration through modulating neuroinflammation and oxidant-stress. *Biomed Pharmacother*. (2020) 129:110439. doi: 10.1016/j.biopha.2020.110439
- Raptis DD, Mantzoros CS, Polyzos SA. Fibroblast growth factor-21 as a potential therapeutic target of nonalcoholic fatty liver disease. *Therap Clin Risk Manag*. (2023) 19:77–96. doi: 10.2147/TCRM.S352008
- Palmer DG, Rutter GA, Tavare JM. Insulin-stimulated fatty acid synthase gene expression does not require increased sterol response element binding protein 1 transcription in primary adipocytes. *Biochem Biophys Res Commun*. (2002) 291:439–43. doi: 10.1006/bbrc.2002.6467
- Foretz M, Guichard C, Ferré P, Foufelle F. Sterol regulatory element binding protein-1c is a major mediator of insulin action on the hepatic expression of glucokinase and lipogenesis-related genes. *PNAS*. (1999) 96:12737–42. doi: 10.1073/pnas.96.22.12737
- Yu S, Song JH, Kim HS, Hong S, Park SK, Park SH, et al. Patulin alleviates hepatic lipid accumulation by regulating lipogenesis and mitochondrial respiration. *Life Sci*. (2023) 326:121816. doi: 10.1016/j.lfs.2023.121816
- Song T, Wang P, Li C, Jia L, Liang Q, Cao Y, et al. Salidroside simultaneously reduces de novo lipogenesis and cholesterol biosynthesis to attenuate atherosclerosis in mice. *Biomed Pharmacother*. (2021) 134:111137. doi: 10.1016/j.biopha.2020.111137
- Su M, Cao D, Wang Z, Duan Y, Huang Y. Fatty acid synthase inhibitor platensimycin intervenes the development of nonalcoholic fatty liver disease in a mouse model. *Biomedicines*. (2022) 10:5. doi: 10.3390/biomedicines10010005
- Burke AC, Huff MW. Atp-citrate lyase: genetics, molecular biology and therapeutic target for dyslipidemia. *Curr Opin Lipidol*. (2017) 28:193–200. doi: 10.1097/MOL.0000000000000390
- Yu XH, Qian K, Jiang N, Zheng XL, Cayabyab FS, Tang CK, et al. ABCG5/ABCG8 in cholesterol excretion and atherosclerosis. *Clin Chim Acta*. (2014) 428:82–8. doi: 10.1016/j.cca.2013.11.010



Article

Semen Protein CRISP3 Promotes Reproductive Performance of Boars through Immunomodulation

Yonghui Bu, Ping Wang, Siqi Li, Li Li, Shouquan Zhang * and Hengxi Wei *

State Key Laboratory of Swine and Poultry Breeding Industry, National Engineering Research Center for Breeding Swine Industry, Guangdong Provincial Key Laboratory of Agro-Animal Genomics and Molecular Breeding, College of Animal Science, South China Agricultural University, Guangdong 510642, China; buyonghui813@163.com (Y.B.)

* Correspondence: sqzhang@scau.edu.cn (S.Z.); weihengxi@scau.edu.cn (H.W.);
Tel.: +86-20-85284869 (S.Z. & H.W.)

Abstract: Semen proteins play an important role in male reproductive performance and sperm fertilization ability and can be used as potential biomarkers to evaluate male fertility. The role of cysteine-rich secretory protein 3 (CRISP3) in male reproduction remains unknown. This study aimed to investigate the role of CRISP3 in the reproductive performance of boars. Our results showed that the CRISP3 protein content was significantly and positively correlated with boar fertility, sow delivery rate, and litter size. CRISP3 is highly expressed in the bulbourethral gland of adult boars and is enriched in the seminal plasma. It is localized in the post-acrosomal region of the sperm head and migrates to the anterior end of the tail after capacitation. The CRISP3 recombinant protein did not affect sperm motility and cleavage rate, but it significantly downregulated the mRNA expression of inflammatory factors IL- α , IL-1 β , and IL-6 and the protein expression of IL- α and IL-6 in lipopolysaccharide (LPS)-induced RAW264.7 cells, indicating that CRISP3 has an immunomodulatory function. In conclusion, our study suggests that semen CRISP3 protein levels positively correlate with reproductive performance, which may be achieved by regulating immune responses in the female reproductive tract.



Citation: Bu, Y.; Wang, P.; Li, S.; Li, L.; Zhang, S.; Wei, H. Semen Protein CRISP3 Promotes Reproductive Performance of Boars through Immunomodulation. *Int. J. Mol. Sci.* **2024**, *25*, 2264. <https://doi.org/10.3390/ijms25042264>

Academic Editor: Elisabetta Baldi

Received: 24 January 2024

Revised: 9 February 2024

Accepted: 9 February 2024

Published: 14 February 2024



Copyright: © 2024 by the authors. Licensee MDPI, Basel, Switzerland. This article is an open access article distributed under the terms and conditions of the Creative Commons Attribution (CC BY) license (<https://creativecommons.org/licenses/by/4.0/>).

Keywords: CRISP3; boar; fertility; sperm; reproductive tract immunity

1. Introduction

Semen proteins in sperm or seminal plasma clearly play an important role in regulating sperm functions, such as maintaining sperm motility, assisting sperm capacitation, and sperm–egg binding. These functions are closely related to the reproductive ability of male animals [1,2] and are potential fertility markers for sperm function and fertility [3]. With the rapid development of proteomics, using biomarkers to screen boars for high reproductive performance [4] is of great significance for improving the production level of animal husbandry.

Cysteine-rich secreted proteins (CRISPs) are an important family of proteins found in the semen of mammals [5–8]. CRISPs are a branch of the CRISP, Antigen5, and Pathogenesis-related Protein1 superfamily of proteins [9]. Four CRISP proteins have been identified in mice and three in humans, horses, and pigs, and they are highly enriched in the male reproductive tract [10]. Recent studies have shown that the CRISP1 protein can regulate Ca²⁺ channels, and that it plays an important role in preventing sperm hyperactivation [11,12]. An abnormal expression of CRISP2 is associated with fertility problems in humans, and its expression is significantly lower in patients with azoospermia or asthenospermia than in normal fertile men [13,14]. Moreover, recent studies have shown that the expression level of CRISP3 is related to male infertility [13]. Sperms lacking the CRISP4 protein severely affected the fertilization ability of cumulus–oocyte complexes,

oocytes with intact zona pellucida, and oocytes without zona pellucida in vitro [15]. The deletion of all four CRISP genes in mice resulted in severe subfertility [16].

The CRISP3 protein was first identified in mouse salivary glands [17] and human neutrophils [18] and is the least-studied member of the CRISP family. Unlike other members, CRISP3 is widely expressed in exocrine organs [19], immune organs, and, to a lesser extent, reproductive organs [20,21]. Studies have shown that human CRISP3 is not involved in gamete fusion [22]. The CRISP3 gene knockout mice showed that, compared to normal mice, there was no significant difference in the fertilization rate of the knockout mice, but the blastocyst rate and the number of pups were significantly reduced [17]. CRISP3 protein is involved in the immune response and has a defensive role [23], which can inhibit the binding of sperm to polymorphonuclear neutrophils and prevent sperm from being cleared in the female reproductive tract [24]. We analyzed the differentially expressed proteins in the sperm of boars with high and low fertility using iTRAQ technology [25] and found that CRISP3 was highly expressed in the semen of boars with high fertility. Consistent with previous reports, CRISP3 protein may be related to the reproductive performance of boars.

This study revealed a relationship between the expression level of CRISP3 protein in semen and the reproductive performance of boars. The expression of CRISP3 protein and CRISP3 antibody in sperm and reproductive tissues and the possible mechanism of its function in sperm fertilization was analyzed. This study enriches the expression profile of the CRISP3 protein, provides new ideas for its function in the process of pig reproduction and provides new evidence for CRISP3 as a potential biomarker of male fertility.

2. Results

2.1. Correlation between Sperm CRISP3 Protein Levels and Reproductive Parameters in Boars

The total protein concentration in the semen or seminal plasma of 33 boars was determined using the BCA method, while the CRISP3 protein concentration was measured through ELISA, and its relative concentration was calculated. After excluding outliers, the relative CRISP3 protein content of the sperm of 25 boars and the seminal plasma of 30 boars was finally obtained. Scatter plots of CRISP3 protein relative content data are represented in Figure S1. The results showed that the sperm CRISP3 protein level was significantly positively correlated with the sow's farrowing rate and reproductive efficiency ($p < 0.05$). The CRISP3 protein level in seminal plasma was significantly positively correlated with litter size and reproductive efficiency ($p < 0.05$) (Figure 1).

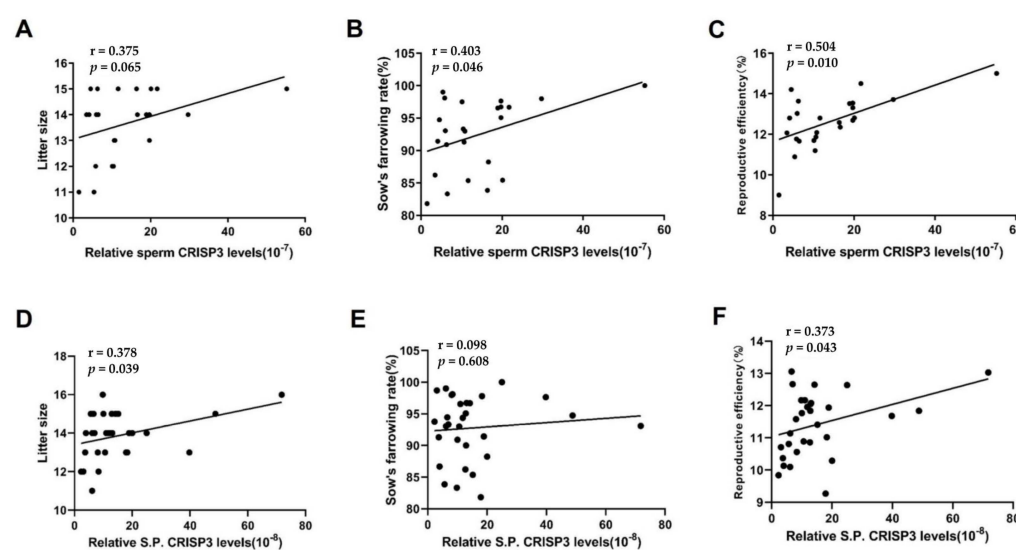


Figure 1. Correlation analysis between the content of CRISP3 and the boar reproductive parameters. Reproductive efficiency equals litter size multiplied by the sow's farrowing rate. For sperm CRISP3, 25 boars inseminated 1324 sows (A–C); for seminal plasma CRISP3, 30 boars inseminated 1779 sows (D–F).

2.2. Expression, Purification, and Identification of Recombinant CRISP3 Protein and Antibody

Obtaining an active CRISP3 protein is a key step in investigating the specific mechanisms by which CRISP3 proteins regulate reproductive performance. CRISP3 protein was expressed in CHO-K1 cells, and the supernatant and CHO-K1 cells were collected for identification (Figure S2) and purified using HisTrap HP column tag affinity chromatography. The purified recombinant CRISP3 protein exhibits a molecular weight of 28 kDa with the predicted value, indicating successful expression. To conduct a more comprehensive analysis of the recombinant CRISP3 protein, the purified peptide underwent LC-MS/MS analysis. The amino acid sequence of CRISP3 was determined using LC-MS/MS analysis and subsequently compared with the NCBI database (Accession No. XP_003128480.1). The resulting peptide coverage exceeded 70% (Figure S3).

BALB/C mice were immunized with the recombinant protein CRISP3. Through cell fusion, hybridoma cell screening, subcloning, and ascites preparation and purification, CRISP3 monoclonal antibodies were finally obtained. The heavy and light chains of CRISP3 were 55 and 25 kDa, respectively, on SDS-PAGE, which were consistent with the characteristics of the antibody (Figure S4). The purified antibody concentration was 2.0 mg/mL.

The specificity of the CRISP3 antibody was identified by using the testis and the bulbourethral gland tissues of boars. The amino acid homology of porcine CRISP1, CRISP2, and CRISP3 was also compared. The results showed that the amino acid identity of porcine CRISP1 with CRISP2 and CRISP3 was 42%, and the amino acid identity of CRISP2 and CRISP3 was 63%. The results of the Western blot showed that the CRISP3 antibody could recognize the CRISP3 protein in boar testis and bulbourethral gland tissue, while the CRISP2 antibody could only recognize the target protein in boar testis tissue but not in the bulbourethral gland tissue. Since the anti-CRISP3 antibody also recognizes a band of the same molecular weight as the band recognized by the anti-CRISP2 antibody in the testis, a cross-reaction between them cannot be completely excluded (Figure S5).

To verify whether CRISP3 recombinant proteins have glycosylation modifications, CRISP3 recombinant proteins were treated with glycosidase F for 20 h at 37 °C and subjected to Western blot analysis. The results showed that, compared with the CRISP3 recombinant protein without glycosidase F treatment, the gray value of the CRISP3 recombinant protein treated with glycosidase F increased at 21 kDa and decreased at 29 kDa, the total gray value was similar (Figure S6). These results indicate that CRISP3 recombinant proteins have glycosylation modifications.

2.3. Expression and Localization of CRISP3 in Porcine Reproductive Organs and Semen

To investigate the potential involvement of the CRISP3 protein in boar fertilization capacity and reproductive capability, we conducted an analysis of CRISP3 gene expression in the reproductive organs of boars using the RT-PCR technique. According to Figure 2A, CRISP3 expression was observed in the testis, epididymis, seminal vesicle, prostate gland, bulbourethral glands, and vas deferens of adult and 3-month-old boars.

Following that, the expression level of CRISP3 was subsequently validated. qRT-PCR was employed to determine the relative expression levels of CRISP3 in various reproductive organs of adult and 3-month-old pigs, including the testis, epididymis, seminal vesicle, prostate gland, bulbourethral glands, and vas deferens. The findings of this study indicate that CRISP3 was highly expressed in the testis, prostate gland, bulbourethral gland, and vas deferens of adult boars, and in the testis, seminal vesicle, prostate gland, bulbourethral glands, and vas deferens of 3-month-old boars. Notably, Figure 2B demonstrates its highest expression in the bulbourethral glands of adult boars.

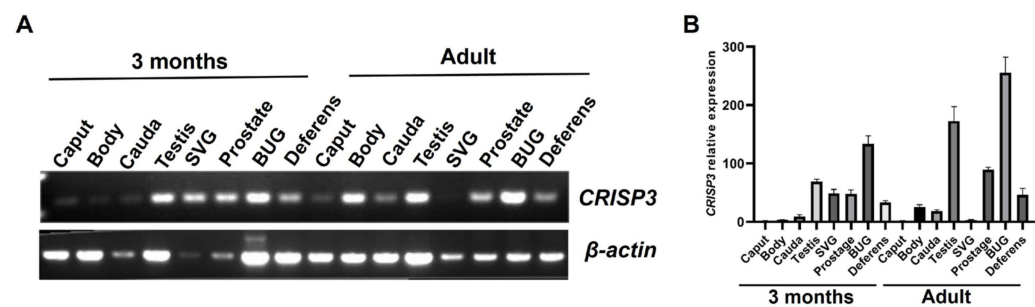


Figure 2. The expression of the CRISP3 gene in the reproductive tissues or cells of boars of different ages. (A) Reverse transcriptase PCR detection of CRISP3 gene expression in the boar reproduction systems. (B) qRT-PCR detection of CRISP3 gene expression in male reproductive tissues of adult and 3-month-old pigs.

The Western blotting technique was utilized to determine the relative abundance of CRISP3 protein in the reproductive organs and semen of boars across different age groups. The study findings revealed that CRISP3 protein exhibited expression in various adult and 3-month-old male pig reproductive organs, including the testis, epididymis, seminal vesicle gland, prostate, and bulbourethral glands. Notably, a particularly elevated expression level of CRISP3 was observed in the bulbourethral glands. In addition, we found that, in the 3 months of boar epididymis, seminal vesicle and prostate gland, and seminal vesicle gland and prostate of adult boar, CRISP3 protein has two kinds of forms, namely, glycosylated and non-glycosylated forms. CRISP3 was found in a non-glycosylated form in 3-month-old boar testis and adult boar testis, epididymis, and sperm, while it was found in a glycosylated form in the bulbourethral glands and seminal plasma, as illustrated in Figure 3. The obtained results exhibited congruity with our prior research outcomes.

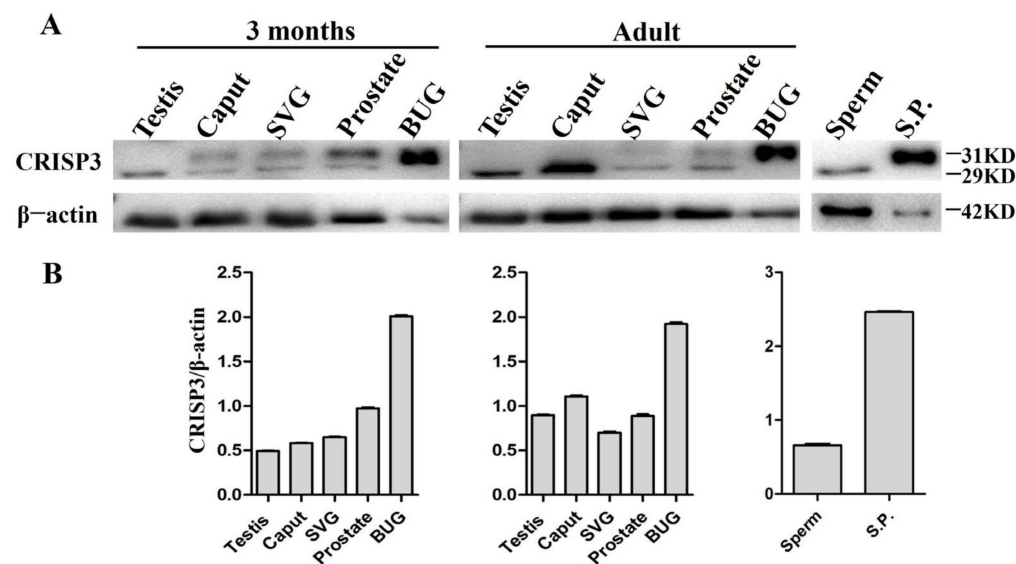


Figure 3. The expression of CRISP3 protein in the reproductive tissues or cells of male pigs with different ages. (A) Western blot analysis of CRISP3 protein expression in adult and 3-month-old male reproductive tissues. SVG, seminal vesicle gland; BUG, bulbourethral gland; S.P., seminal plasma; (B) Western blot analysis of CRISP3 protein expression in adult and 3-month-old boars' reproductive tissues using Image J software.

Immunohistochemistry was used to detect the distribution of the CRISP3 in the epididymis, prostate, seminal vesicle gland, and bulbourethral glands of adult boars. The findings indicated that the expression of CRISP3 was observed in the cytoplasm of luminal gland epithelial cells in the head, body, and tail of the epididymis and accessory gonads, as compared to the negative control group (Figure 4).

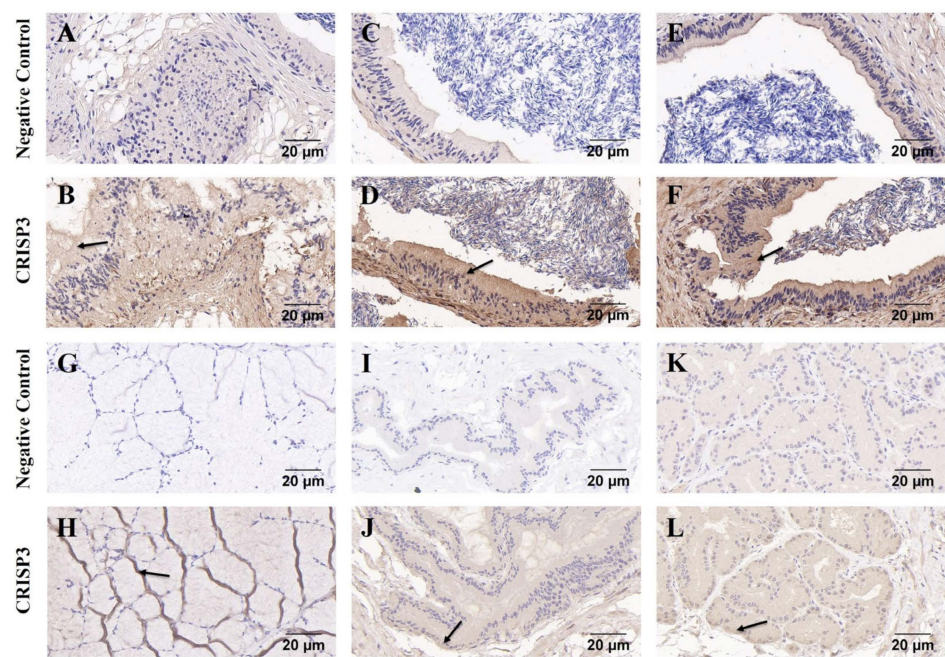


Figure 4. Immunohistochemical analysis of CRISP3 in epididymis and accessory gonads of adult boars. (A–F) Immunohistochemical analysis of the head, body, and tail of the epididymis of adult boars. (G–L) Immunohistochemical analysis of bulbourethral gland, seminal vesicle gland, and prostate gland in adult boars, respectively.

The localization of the CRISP3 in sperm was examined using immunofluorescence techniques both before and following sperm capacitation. The results revealed that CRISP3 was mostly present in the post-acrosomal region of the sperm head prior to capacitation. However, after capacitation, CRISP3 was shown to relocate to the mid-upper portion of the sperm tail (Figure 5). The complete picture is shown in Figure S7.

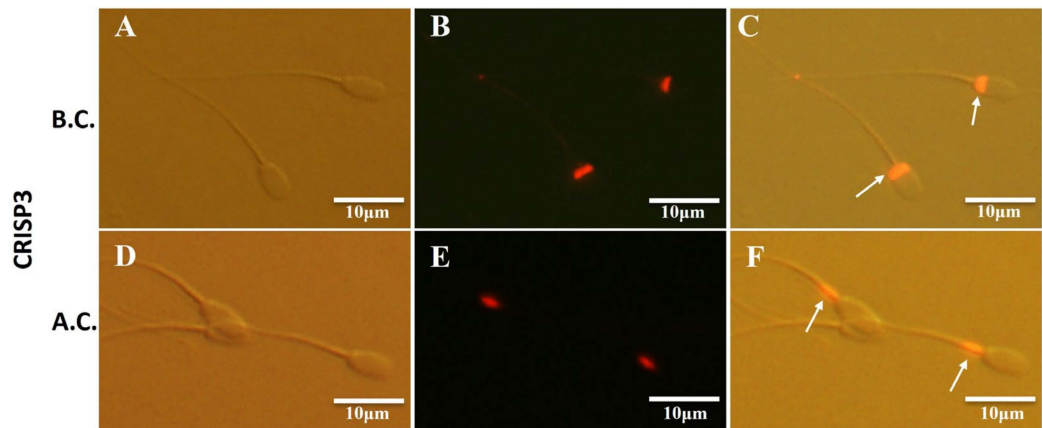


Figure 5. Immunofluorescent staining of CRISP3 in sperm before and after capacitation. (A–C) Representative images of the immunofluorescent staining of CRISP3 in sperm before capacitation; (A) images taken under light microscope, (B) images taken under fluorescent scope; (C) merged images. (D–F) Representative images of the immunofluorescent staining of CRISP3 in sperm after capacitation; (D) images taken under light microscope, (E) images taken under fluorescent scope; (F) merged images. B.C., before capacitation; A.C., after capacitation. The arrow indicates the distribution of the target proteins.

2.4. The Effect of CRISP3 Protein on Sperm Function and Fertilization Ability

The present study aimed to evaluate the impact of the CRISP3 protein on sperm function and its ability to fertilize. There were no statistically significant variations seen

in sperm motility and other motility parameters between the group that received CRISP3 antibody treatment for a duration of 30 min and the negative control group ($p > 0.05$) (Table 1).

Table 1. Relevance analysis of parameters associated with sperm motility between the negative control group and the group treated with anti-CRISP3 antibodies.

Motility Parameters	Negative Control	Anti-CRISP3 Antibody	<i>p</i> Value
TM (%)	76.75 ± 2.80	76.06 ± 1.32	0.836
VSL (µm/s)	28.57 ± 0.81	28.96 ± 0.64	0.722
VCL (µm/s)	48.79 ± 1.70	49.60 ± 1.31	0.725
VAP (µm/s)	34.97 ± 0.98	35.07 ± 0.92	0.944
ALH (µm)	14.48 ± 0.41	14.53 ± 0.38	0.942
WOB (%)	68.00 ± 2.00	64.00 ± 1.00	0.137
BCF (Hz)	0.74 ± 0.01	0.73 ± 0.01	0.624
LIN (%)	58.00 ± 1.00	58.00 ± 0.00	0.519
MAD (°)	114.45 ± 2.71	103.81 ± 4.26	0.103
STR (%)	82.00 ± 1.00	83.00 ± 1.00	0.482

TM, total motility; PM, progressive motility; VCL, curvilinear velocity; VSL, straight line velocity; VAP, average path velocity; ALH, mean amplitude of head lateral displacement; WOB, wobble; BCF, beat cross frequency; LIN, linearity; MAD, mean angular displacement; STR, straightness; Negative control meant that sperm were exposed to IgG; Values are expressed as mean ± standard error of the mean; The experiment consisted of three replicates.

To investigate the effect of the CRISP3 recombinant protein on sperm mitochondrial function-related genes, the relative mRNA expression levels of COX5B, ATP5F1, UQCRC1, CYC1, and NDUFS8 genes in sperm were detected after incubation with 3, 5, 10, and 20 µg/mL CRISP3 recombinant proteins in semen for 4 h. The results showed that there was no significant difference in the mRNA expression of COX5B, ATP5F1, UQCRC1, CYC1, and NDUFS8 genes between the sperm treated with 3, 5, 10, and 20 µg/mL CRISP3 recombinant proteins and the blank control group (Figure S8).

The addition of the CRISP3 antibody to sperm during in vitro capacitation showed no significant difference in the acrosomal integrity rate of sperm before and after capacitation compared with the negative control IgG ($p > 0.05$) (Figure 6).

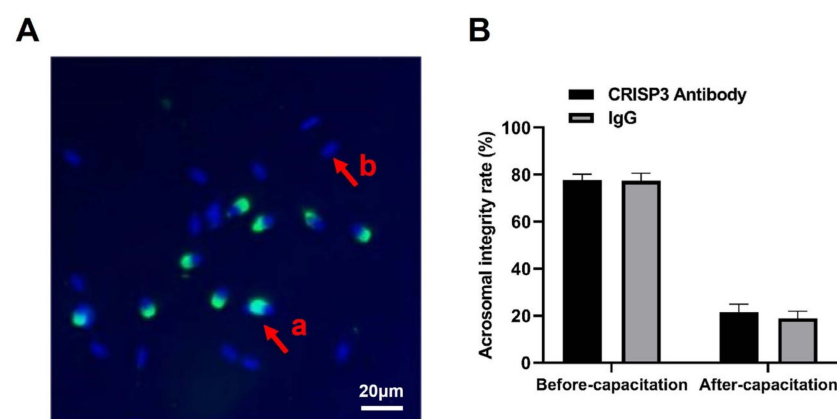


Figure 6. Effects of the CRISP3 antibody on the rate of acrosomal integrity after sperm capacitation in vitro. (A) Sperm in different statuses. Sperm samples were fixed with FITC-PNA and Hoechst33342 and scored according to the state of the acrosome. a: sperm has not experienced an acrosome reaction, and b: indicates that an acrosome reaction has occurred. (B) Analysis of sperm acrosome reaction rate before and after capacitation with CRISP3 antibody. The data are presented as the mean ± SEM, $n = 3$.

During the process of IVF, the inclusion of the CRISP3 antibody in the fertilization medium allowed for the subsequent assessment of the embryo cleavage rate after 48 h.

The findings indicated that there were no statistically significant disparities in the rate of cleavage among the anti-CRISP3 group ($55.04 \pm 0.89\%$), control group ($59.53 \pm 2.54\%$), and IgG group ($57.50 \pm 2.03\%$) ($p > 0.05$) (Table 2).

Table 2. Effect of anti-CRISP3 antibodies on the cleavage rate of in vitro fertilization.

Groups	No. of Oocytes	No. of Cleaved	Cleavage Rate %
Control	324	192	59.53 ± 2.54^A
IgG	273	157	57.50 ± 2.03^A
Anti-CRISP3	279	153	55.04 ± 0.89^A

Values are expressed as mean \pm standard error of the mean; the experiment included six replicates. Different letters in the same column indicate significant differences ($p < 0.05$).

2.5. CRISP3 Protein Inhibited LPS-Induced Production of Inflammatory Factors in RAW264.7 Cells

To verify the immunoactivity of the CRISP3 protein and explore the effect of the CRISP3 protein on the expression of intracellular inflammatory factors, we used LPS to induce RAW264.7 cells to establish an inflammation model, and different concentrations of CRISP3 protein were incubated with RAW264.7 cells in the presence or absence of LPS for 6 h. The results demonstrated that different concentrations of CRISP3 protein did not affect inflammatory factor mRNA levels without LPS ($p > 0.05$). Nevertheless, when exposed to LPS, there was a notable augmentation in the relative mRNA expression levels of IL-6, IL-1 α , and IL-1 β . Pre-incubation with 3, 5, 10, and 20 $\mu\text{g/mL}$ CRISP3 proteins for 30 min significantly decreased the relative mRNA expression levels of IL-6, IL-1 α , and IL-1 β . In comparison to the control group that did not receive any treatment, there was a notable reduction in the mRNA expression levels of IL-6, IL-1 α , and IL-1 β ($p < 0.01$) (Figure 7).

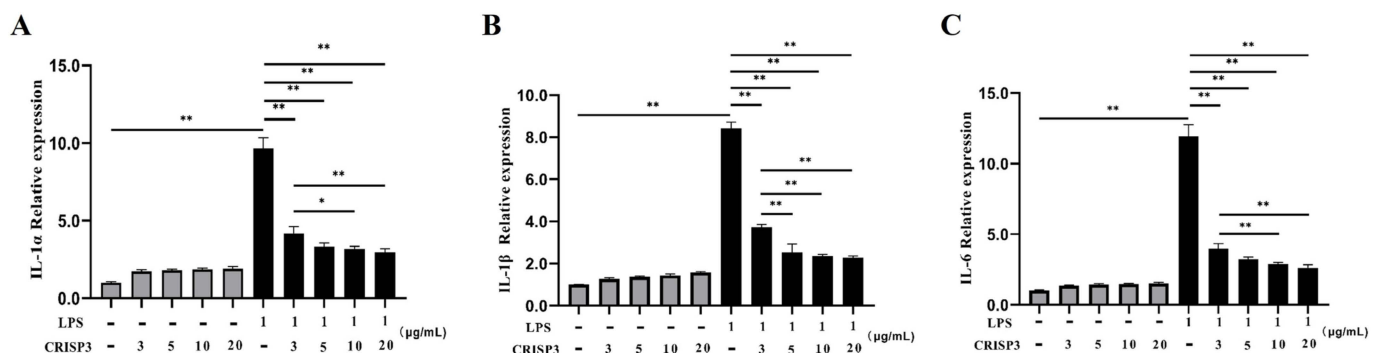


Figure 7. Effect of CRISP3 protein on the mRNA expression levels of inflammatory cytokines IL-1 α , IL-1 β , and IL-6 in RAW264.7 cells induced by LPS. (A) IL-1 α mRNA expression level; (B) IL-1 β mRNA expression level; (C) IL-6 mRNA expression level. GAPDH was included in the standardization of all samples as an internal reference gene, and the data were expressed as the mean \pm SEM of three independent experiments, * $p < 0.05$, ** $p < 0.01$.

The western blot analysis revealed that the application of recombinant CRISP3 at concentrations of 3 and 5 $\mu\text{g/mL}$ resulted in a significant decrease in the expression levels of the inflammatory components IL-6 and IL-1 α protein, which were triggered by LPS (Figure 8).

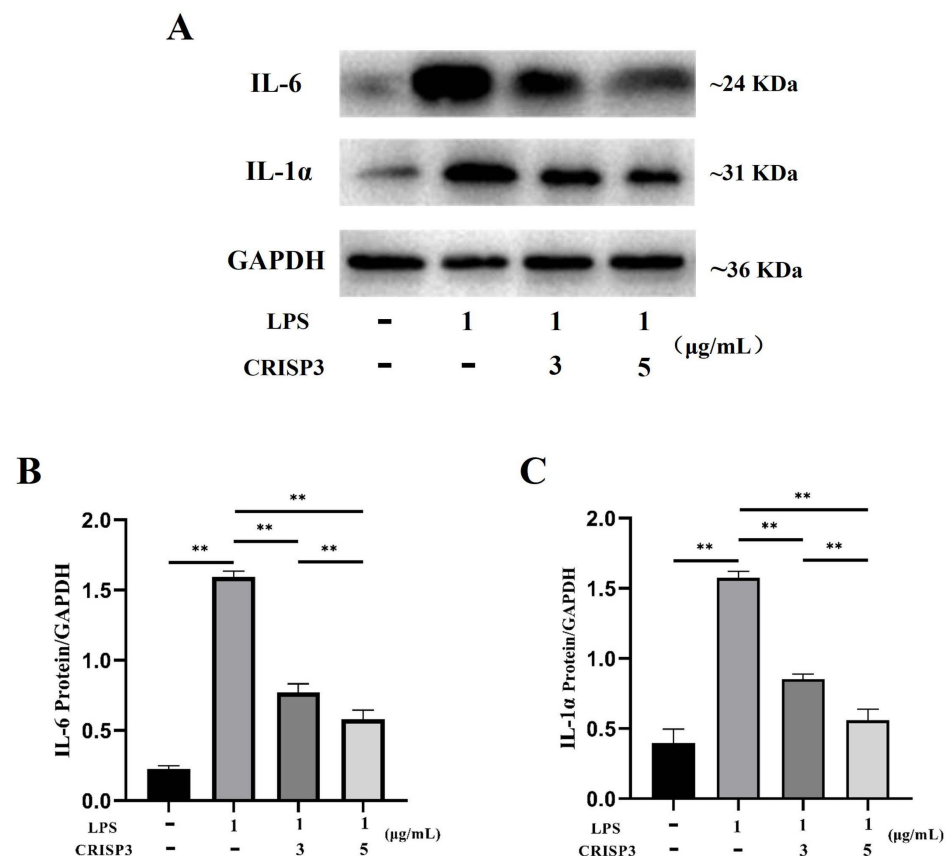


Figure 8. Effect of CRISP3 on the expression levels of IL-1α and IL-6 proteins in RAW264.7 cells induced by LPS. (A) Western blot analysis of IL-1α and IL-6 protein expression levels in RAW264.7 cells. (B) Western blot analysis of IL-6 protein expression level by Image J. (C) Western blot analysis of IL-1α protein expression level by Western blot. Normalized by GAPDH, the data were represented by the mean of three independent experiments \pm SEM, ** $p < 0.01$.

3. Discussion

In this study, we analyzed, for the first time, the correlation between the relative content of the sperm protein CRISP3 and the reproductive parameters of boars. We found that the semen CRISP3 protein level was significantly positively correlated with the fertility of boars, sow delivery rate, and litter size. Monoclonal antibodies against CRISP3 were prepared to reveal the expression and localization of CRISP3 in reproductive organs and sperm at the gene and protein levels, which did not affect the fertilization ability of the sperm. The immunoregulatory function of CRISP3 was confirmed in an inflammatory model using LPS-induced RAW264.7 cells.

Usuga et al. found high concentrations of CRISP3 in horse semen, and the concentration in the semen was positively correlated with the pregnancy rate in the first cycle after artificial insemination [26,27]. Similar findings have been reported by Doty et al. CRISP3 appears to attach to the sperm surface and is positively correlated with fertility [9,28], which is consistent with the observed patterns. Sperm proteins are synthesized and secreted by the testes, epididymis, and accessory gonads. Proteins in semen are assembled or bound to the surface of the sperm during sperm formation, maturation, or fertilization and play a role in the fertilization process. It has been reported that CRISP3 is expressed in the testis and epididymis of humans and through the accessory gonads of mice, but not in the epididymis of rats [7,23]. In this study, the reproductive organs of male and female sows of different ages were selected to explore the distribution of CRISP3 in the reproductive systems of male and female sows at both the gene and protein levels. CRISP3 was expressed in the testis, prostate, and bulbourethral glands of adult and 3-month-old male pigs and was enriched in sperm and semen, consistent with the results of

Song et al. [29]. We found that the expression of CRISP3 in the bulbourethral glands of adult and 3-month-old male pigs was higher than that in the other tissues. It was previously found that CRISP3 has two isoforms in human and horse semen [23,28,30], 29 kDa and 31 kDa, respectively, depending on its glycosylation status [7]. The present study revealed two forms of CRISP3 in the epididymis, seminal vesicles, and prostate glands. In the testes and sperm, CRISP3 is non-glycosylated, whereas in the bulbourethral glands and semen, CRISP3 is glycosylated. Indirect immunofluorescence localized CRISP3 to the acrosome and tail of human-capacitated sperm [23,31]. Our results showed that CRISP3 was mainly present in the post-acrosome region of the sperm head before capacitation, and CRISP3 was shown to relocate to the mid-upper part of the sperm tail after capacitation. The specific mechanism of this phenomenon may be that the CRISP3 protein is localized on the surface of the head and migrates to the tail with capacitation, or it is lost from the head and exposed to the tail with capacitation.

Our results showed that sperm CRISP3 was positively correlated with boar fertility, sow delivery rate, and litter size. However, the addition of the CRISP3 antibody to sperm had no significant effect on sperm motility or other parameters. In addition, CRISP3 antibodies do not affect cleavage rates, which has also been demonstrated in the description of human CRISP3 proteins [23]. Double knockout of CRISP1 and CRISP3 in male mice showed a significant reduction in litter size after mating compared to the control group. However, there was no difference in the number of fertilized eggs recovered from the fallopian tube compared to the control group [16]. The positive effects of CRISP3 on the boars' reproductive ability may be achieved by regulating other reproductive processes. CRISP3 is expressed in reproductive and immune organs, such as the thymus and spleen, which have innate immune functions [32]. Lipopolysaccharide, as a component of gram-negative bacteria, can induce a series of harmful inflammatory responses [33]. RAW264.7 cells are an immortalized mouse macrophage cell line that has been widely used in vitro, and LPS can induce macrophages to release IL-1, IL-6, and other potent inflammatory factors [34]. Therefore, we use a macrophage model to assess the impact of pig CRISP3 recombinant protein on the inflammation induced by LPS. The results showed that the CRISP3 recombinant protein could significantly reduce the LPS-induced expression of IL-1 and IL-6, which proved its immunosuppressive activity. Examination of the sperm in the uterus of female mice after mating with the male CRISP1 and CRISP3 double knockout models showed that the sperm in the uterus of female mice mated with the control group moved freely in the uterine fluid, whereas most of the sperm in the double knockout model group did not move and showed a clustering phenomenon [17] due to the lack of CRISP3 in the seminal plasma. Defects in uterine sperm motility may eventually lead to delayed fertilization and defects in embryonic development [32]. CRISP3 is present in equine seminal plasma and protects sperm from smooth passage through the female reproductive tract by inhibiting neutrophil-mediated phagocytosis of sperm in utero [9,28]. Therefore, CRISP3 may positively affect the reproductive ability of boars by regulating the immune function of the female reproductive tract.

This study examined the effect of CRISP3 recombinant protein on a mouse macrophage cell line in vitro. In the future, systemic studies using CRISP3 should be considered to further verify the effect of CRISP3 on female reproductive tract immunity.

4. Materials and Methods

4.1. Animals and Samples

Boar tissue samples and semen were collected from the Guangdong Wenshi Shuitai Breeding Farm, and production data for each boar were obtained. The breed of boars and mating sows is Large White. AI was conducted on a single farm with a single dose of 4-billion sperm, and the insemination method was cervical intraoral insemination. Only semen that conforms to the appearance and smell of normal sperm, motility of more than 70%, abnormal rate of less than 20%, and 80 mL of semen containing at least 4-billion sperm are used for AI and other analysis. Sperm and seminal plasma were extracted immediately

after semen collection, and tissue samples were taken immediately after slaughter and kept in liquid nitrogen. The male BALB/C mice, aged 6–8 weeks, were procured from the Guangdong Medical Laboratory Animal Center, and ovaries from female pigs were obtained from a nearby abattoir.

4.2. Extraction of Protein and Nucleic Acid

As per the guidelines provided by the manufacturer, the Whole Protein Extraction Kit (KeyGen Biotech, Nanjing, China) was used to extract total protein from sperm and tissue samples, and part of the tissue was cut and ground, or the semen was centrifuged at 10,000 rpm for 5 min. After collecting the supernatant, the precipitate was washed 2–3 times with precooled Dulbecco's Phosphate-Buffered Saline (DPBS). The precipitate was resuspended in lysis buffer containing phosphatase inhibitors, PMSF, and protease inhibitors. After 30 s of swirling and 4 min on ice, the supernatant was centrifuged at 12,000 rpm (4 °C) for 5 min. The supernatant was added to precooled acetone in the ratio 1:2, placed at −20 °C for 4 h, 20 min of centrifugation at 12,000 rpm followed by the discarding of the supernatant and a brief period on ice to collect the precipitate.

RNA was isolated from all samples with an RNeasy Mini Kit (Qiagen, Hilden, Germany). The measurement of RNA purity and concentration was conducted using a NanoDrop ND-1000 instrument (Thermo Fisher Scientific, Waltham, MA, USA). The assessment of RNA integrity was conducted utilizing an Agilent 2100 Bioanalyzer. (Agilent, San Jose, CA, USA).

The quantification of protein levels was conducted utilizing a Bicinchoninic Acid (BCA) Protein Assay Kit (KeyGen Biotech, Nanjing, China). In brief, the BCA working solution was configured according to proportion. Eight concentrations of protein standard solutions were serially diluted with deionized water to establish the standard curve (protein concentration range 0–2000 µg/mL). The total volume of tested samples was 20 µL. All samples and standards were repeated three times, and 200 µL BCA working solution was added. The measurement of absorbance was conducted using colorimetry at a specific wavelength of 562 nm, and, subsequently, a standard curve was constructed. The corresponding protein content (µg/µL) was determined using a standard curve.

4.3. Detection of Semen CRISP3 by Enzyme-Linked Immunosorbent Assay (ELISA) and Analysis of Its Correlation with Reproduction

The content of CRISP3 in the sperm and seminal plasma of boars was detected using a CRISP3 ELISA Kit (PG1898, TSZ, USA), following the instructions provided by the manufacturer. All samples, standards, and blank controls were analyzed thrice, and the detection range was 12–1200 pg/mL. The relative concentration of CRISP3 was assessed by calculating the ratio of CRISP3 protein concentration in sperm and seminal plasma to their respective total protein concentrations. Employ Pearson's correlation analysis to examine the relationship between the relative concentrations of CRISP3 protein in sperm and seminal plasma, and the production data of sows involved in mating.

4.4. Preparation of CRISP3 Protein and Antibody

The cDNA of porcine CRISP3 was acquired from the bulbourethral gland tissue of pigs. Based on the genomic DNA sequence of CRISP3 (GenBank accession No. NC_010449.5), the amplified fragment of CRISP3 containing the restriction site was obtained by utilizing forward and reverse primers (5'-GGTGAATTCGCCACCATGGAGACCGACACCCTG-3' and 5'-ATCGGATCCTCAATGATGATGATGATGATGGTAG-3', respectively), which was subsequently inserted into the EcoR I and BamH I sites of pLVX. The recombinant plasmid was introduced into competent *Escherichia coli* (*E. coli*) JM109 cells via transfection. Single colonies were established in bacteriolytic broth (LB) containing 100 µg/mL ampicillin at 37 °C and incubated with shaking at 200 rpm/min. The positive clones identified by enzymatic digestion were verified by sequencing. After comparing the sequencing results, the plasmids were extracted.

The HEK293T and CHO-K1 cell lines were inoculated into a 10 cm cell culture dish with a cell density of 1×10^5 cells/mL. The cells were then grown in Dulbecco's Modified Eagle Medium (DMEM) supplemented with 10% fetal bovine serum (FBS) and maintained in an environment with 5% CO₂ at a temperature of 37 °C until the cell confluence reached 60%. The HEK293T cells were transfected with recombinant pLVX-CRISP3 and pLVX vector plasmids using LentiFit (HanBio, Shanghai, China), whereas the negative control consisted of the empty vector. After 48 h, the virus solution was collected, concentrated, and used to infect CHO-K1 cells. After selection with puromycin (Thermo Fisher Scientific, USA), the supernatant of CHO-K1 cells was collected and loaded onto a HisTrap HP column (Cytiva, Marlborough, MA, USA). The CRISP3 protein was purified in accordance with the guidelines (HisTrap HP GEexpress Kit manual) provided by the manufacturer and subsequently subjected to dialysis using a phosphate buffer solution (PBS). The purity of the sample was assessed using sodium dodecyl sulfate-polyacrylamide gel electrophoresis (SDS-PAGE), while the sample identification was achieved through liquid chromatography-tandem mass spectrometry (LC-MS/MS). The recombinant CRISP3 protein was stored at −80 °C until its utilization.

Mouse monoclonal antibodies against recombinant CRISP3 protein were prepared according to a previous method [28]. In brief, a total of three administrations were performed every 2 weeks in five BALB/C mice, with each administration consisting of inoculation with 100 µg recombinant CRISP3 protein. Serum was collected from anesthetized mice according to animal welfare standards, and serum titers were determined using ELISA. Based on the serum antibody titer test results, spleen cells from suitable mice were selected for cell fusion with sp2/0 cells, followed by screening and subcloning of hybridoma cells, and, finally, preparation of ascites. Affinity-purified monoclonal antibodies (immunoglobulin G [IgG] fraction) were used as described previously [35]. Purified antibodies were stored in a buffer (50% glycerol, 0.1% sodium azide, 0.1% gelatin) at −80 °C until its utilization.

4.5. Reverse Transcriptase PCR and Quantitative Real-Time PCR (qRT-PCR)

RT-PCR was used to find CRISP3 expression in the various reproductive organs of male and female pigs of various ages. The target gene sequence was queried in the National Center for Biotechnology Information (NCBI) (GenBank accession No. NC_010449.5) database, and, subsequently, the primers were generated. The sequences are presented in Table S1. The protocol for the PCR was conducted as follows: an initial pre-denaturation step at a temperature of 95 °C for a duration of 3 min, followed by 35 cycles of denaturation at 95 °C for 15 s, annealing at 58 °C for 15 s, and extension at 72 °C for 60 s, followed by a complete extension at 72 °C for 5 min. The expression of the CRISP3 gene in male and female pig reproductive organs at different ages, as well as IL-1β, IL-1α, and IL-6 in RAW264.7 cells, was confirmed using qRT-PCR. The SYBR qPCR Kit (Vazyme, Nanjing, China) was employed, with GAPDH utilized as the internal reference control. Each sample underwent three replicates. The reaction protocol involved pre-denaturation at 95 °C for 3 min, 40 cycles of denaturation at 95 °C for 10 s, annealing at 60 °C for 30 s, and melting curve acquisition at 95 °C, 60 °C, and 95 °C for 15 s. It was done on an Applied Biosystems 7900HT Real-Time PCR Thermal Cycler. (Applied Biosystems, Foster City, CA, USA).

4.6. Western Blotting

The reproductive organ tissues of boars from various age groups, the proteins present in adult boar semen, and the proteins from RAW264.7 cells were isolated using a 12% SDS-PAGE and subsequently transferred onto polyvinylidene difluoride (PVDF) membranes (Millipore, Burlington, MA, USA). After 1 h of blocking with 5% skim milk powder at room temperature, PVDF membranes were washed with TBST (137 mM NaCl, 20 mM Tris, 0.1% Tween-20, pH 7.6) and incubated with primary antibodies overnight at 4 °C. Anti-CRISP3, Anti-CRISP2 antibody (1:2000, SAB2501636, Sigma, Marlborough, MA, USA), IL-1α, and IL-6 (1:1000, Abcam, Waltham, MA, USA) and control antibodies β-actin and GAPDH (1:2000, TransGen, Beijing, China) were employed. After washing the membranes,

Goat Anti-Rabbit IgG (H + L) Horseradish Peroxidase (HRP) or Goat Anti-Mouse IgG (H + L) HRP (1:2000, Thermo Fisher Scientific, Waltham, MA, USA) were incubated for 1 h. Automatic imaging equipment (Tanon5200, Shanghai, China) was used to image the membranes after washing and incubating them with chemiluminescence solution in a dark room for 2 min. The experiment was repeated at least three times. The Image J software (<https://imagej.nih.gov/ij/index.html>, accessed on 23 January 2024) was utilized for the comparative analysis of protein expression levels.

4.7. Immunohistochemistry

Freshly collected urethral bulbar glands from adult boars were fixed in paraformaldehyde for 48 h and embedded in paraffin. The samples were subjected to immunohistochemistry using paraffin sections. In short, 5 μ m tissue sections were mounted on silicated slides for analysis; the paraffin sections underwent deparaffinization using xylene and subsequent rehydration through a series of graded ethanol solutions. The sections were boiled in 10 mM citric acid (pH 6.0) and incubated in 3% H₂O₂ at 26 °C for 25 min in the dark. Three percent bovine serum albumin (BSA) was equally applied to the tissues and blocked at room temperature for one hour. Next, an anti-CRISP3 antibody (1:1000) was incubated overnight at 4 °C. After three PBS washes, the slides were incubated with Goat Anti-Mouse IgG (H + L) HRP (1:2000, Thermo Fisher Scientific, USA) at 37 °C for 1 h. Fresh DAB chromophore solution was then added. Slides were counterstained with hematoxylin and examined with an Olympus BX53F microscope (Olympus, Tokyo, Japan).

4.8. Immunofluorescence Staining

Before and after capacitation *in vitro*, the sperm density was adjusted and evenly coated on the slide, air-dried for 50 min, fixed in 4% paraformaldehyde for 1 h, rinsed with PBS, blocked with 10% goat serum at 37 °C for 1 h, and then treated overnight at 4 °C with anti-CRISP3 antibody (1:1000). Goat anti-Mouse IgG (H + L) antibody (1:1000, Thermo Fisher, USA) was incubated for 1 h at 37 °C, followed by thorough washing with PBS. The specimens were analyzed under a fluorescence microscope (BX53F, Olympus, Tokyo, Japan).

4.9. In Vitro Fertilization Assay

In vitro culture and fertilization of oocytes were performed as previously described [36]. Pig ovaries were procured from a nearby abattoir and expeditiously conveyed to the laboratory within a time frame of 4 h while maintaining a temperature of 37 °C. A sterile syringe retrieved follicular fluid from 3–6 mm follicles and washed it three times with 37 °C DPBS-PVA. Under a microscope, cumulus–oocyte complexes (COCs) were picked out. COCs were washed and placed in 500 μ L of mineral oil-covered *in vitro* maturation media in a four-well plate. (Medium TCM199 supplemented with 10 IU/mL pregnant horse serum gonadotropin, 10 IU/mL human chorionic gonadotropin, 0.1 mg/mL L-cysteine, 10% porcine follicular fluid, 10% fetal bovine serum, and 10 ng/mL epidermal growth factor), the oocytes were cultivated at 38.5 °C in an incubator with 5% CO₂ for 44–48 h. Cumulus cells were digested with 0.1% hyaluronidase, washed three times in fertilization fluid, and transferred to mineral oil-covered fertilization fluid. Fresh semen was washed thrice, and the sperm concentration reached 1×10^6 sperm/mL with mTBM containing BSA. Fertilization drop with oocytes was incubated for 6 h at 38.5 °C in 5% CO₂ with capacitated sperms, then transferred to pre-balanced PZM-3 embryo culture medium. The recipient semen was treated with an antibody solution at a final concentration of 2 μ g/mL. As a negative control, an equal volume of IgG was also added. After 48 h, fertilization rates were assessed using a 200 \times microscope (Leica Microsystems, Wetzlar, Germany).

4.10. Sperm Motility Assay

Semen samples from the breeding farm were held at 17 °C and quickly transported to the lab for sperm analyses, including motility and morphology. Sperm were resuspended

at 5×10^6 sperm/mL after three washings in DPBS with 1 mg/mL BSA. Sperm motility was assessed using a computer-assisted sperm analysis system (CASA; Integrated Sperm Analysis System, ISAS, V1.0; Proiser, Valencia, Spain) with a 37 °C constant temperature table. Following that, droplets measuring 5 µL from each sample were carefully deposited into a disposable counting chamber (Leja, Nieuw-Vennep, The Netherlands) with a depth of 20 µm. These samples were then subjected to analysis utilizing the Computer-Assisted Sperm Analysis (CASA) system. The assessed sperm kinematic parameters encompassed the mean values of total motility (%), curvilinear velocity ($\mu\text{m}\cdot\text{s}^{-1}$), straight-line velocity ($\mu\text{m}\cdot\text{s}^{-1}$), average path velocity ($\mu\text{m}\cdot\text{s}^{-1}$), amplitude of lateral head displacement (µm), whiplash frequency (Hz), wobble (%), linearity (%), mean angular displacement (degree), and straightness (%).

4.11. Sperm Capacitation and AR Evaluation

Collected semen samples were washed twice with DPBS to remove sperm and resuspended in modified Tris-buffered medium (mTBM; 11.3 mM NaCl, 0.3 mM KCl, 1 mM CaCl_2 , 0.5 mM pyruvate, 1.1 mM glucose, and 2 mM TRIS) containing 1 mg/mL BSA. CRISP3 antibody or control IgG was also added at 20 µg/mL. Sperm were placed at 37 °C in a 5% CO_2 incubator for 180 min for capacitation. Capacitated sperm were incubated with 10 µg/mL FITC-conjugated peanut agglutinin (FITC-PNA, Sigma, Marlborough, MA, USA) at 25 °C for 30 min and washed twice with PBS. Sample smears were air-dried on slides and incubated with Hoechst33342 (10 µg/mL, Sigma, Marlborough, MA, USA) for 5 min at room temperature in the dark. Analysis was performed using a fluorescence microscope (BX53F, Olympus, Tokyo, Japan). For each sample, approximately 400 spermatozoa were scored to classify the different patterns as reactive (fluorescence in the acrosome region) or nonreactive (no fluorescence in the acrosome region).

4.12. Immunocompetence Assay

Mouse monocytic macrophage leukemia cells (RAW264.7) were cultivated on 6-well plates at a concentration of 5×10^5 cells/mL. The cells were then incubated overnight in a 37 °C incubator with 5% CO_2 and 100% humidity in DMEM supplemented with 10% FBS to ensure cell adherence. After 3, 5, 10, and 20 µg/mL of CRISP3 protein processing for 30 min, 1 µg/mL lipopolysaccharide (LPS) (Solarbio, Beijing, China) was added to induce inflammation. To avoid the effect of the protein itself on the cells, only 3, 5, 10, and 20 µg/mL CRISP3 protein groups were added. CRISP3 protein and LPS were dissolved in PBS, and the cells were harvested 6 h later for qRT-PCR and Western blot analysis. All experiments were repeated thrice.

4.13. Statistical Analysis

All statistical analyses used SPSS (version 18.0; IBM Corp., Armonk, NY, USA) and GraphPad Prism 8 (version 8.0.2; La Jolla, CA, USA). All data are shown as mean \pm standard error. The relationship between CRISP3 protein content and reproductive factors was examined using Pearson's correlation analysis. Statistical differences among groups were determined using the student's *t*-test and ANOVA. Statistical significance was attributed to those *p* values < 0.05.

5. Conclusions

In our study, we found that the sperm CRISP3 protein content was significantly positively correlated with the reproductive performance of boars. The CRISP3 protein was abundant in the bulbourethral glands of adult boars, distributed in the post-acrosomal region and tail of the sperm head, and it was relocalized to the upper middle part of the tail after capacitation. We also found that the CRISP3 plays an anti-inflammatory role by inhibiting LPS-induced production of inflammatory factors in RAW264.7 cells. This study revealed that CRISP3 protein regulates the immune function of the female reproductive tract and provides new clues for CRISP3 protein as a marker of male fertility.

Supplementary Materials: The following supporting information can be downloaded at: <https://www.mdpi.com/article/10.3390/ijms25042264/s1>.

Author Contributions: Conceptualization, H.W. and S.Z.; methodology, Y.B. and P.W.; validation, Y.B., S.L. and P.W.; formal analysis, Y.B. and P.W.; investigation and data curation, Y.B. and S.L.; writing—original draft, Y.B. and L.L.; writing—review and editing, S.Z. and H.W.; project administration, H.W.; funding acquisition, H.W. and S.Z. All authors have read and agreed to the published version of the manuscript.

Funding: This study was supported by the Key Realm R&D Program of Guangdong Province (Grant No. 2022B0202110002) and the Local Innovative and Research Teams Project of Guangdong Province (Grant No. 2019BT02N630); The National Natural Science Foundation of China (Grant No. 32272873 and 31402072).

Institutional Review Board Statement: All experiments were approved by the guidelines of Guangdong Province regarding the review of the welfare and ethics of laboratory animals. The license number is SYXK (Guangdong) 2022-0136.

Informed Consent Statement: Not applicable.

Data Availability Statement: The data presented in this study are available on request from the corresponding author.

Acknowledgments: The authors acknowledge the Guangdong Wens Foodstuff Co., Ltd. (Yunfu, China) for providing the experimental materials of semen and the boar reproductive data, and thank Fenglei Gao for the data curation support.

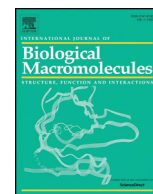
Conflicts of Interest: The authors declare no conflict of interest.

References

1. Druart, X.; de Graaf, S. Seminal plasma proteomes and sperm fertility. *Anim. Reprod. Sci.* **2018**, *194*, 33–40. [\[CrossRef\]](#)
2. Shang, X.; Shen, C.; Liu, J.; Tang, L.; Zhang, H.; Wang, Y.; Wu, W.; Chi, J.; Zhuang, H.; Fei, J.; et al. Serine protease PRSS55 is crucial for male mouse fertility via affecting sperm migration and sperm-egg binding. *Cell Mol. Life Sci.* **2018**, *75*, 4371–4384. [\[CrossRef\]](#)
3. Roca, J.; Perez-Patino, C.; Barranco, I.; Padilla, L.C.; Martinez, E.A.; Rodriguez-Martinez, H.; Parrilla, I. Proteomics in fresh and preserved pig semen: Recent achievements and future challenges. *Theriogenology* **2020**, *150*, 41–47. [\[CrossRef\]](#)
4. Taylor, J.F.; Schnabel, R.D.; Sutovsky, P. Identification of genomic variants causing sperm abnormalities and reduced male fertility. *Anim. Reprod. Sci.* **2018**, *194*, 57–62. [\[CrossRef\]](#) [\[PubMed\]](#)
5. Jalkanen, J.; Huhtaniemi, I.; Poutanen, M. Mouse cysteine-rich secretory protein 4 (CRISP4): A member of the Crisp family exclusively expressed in the epididymis in an androgen-dependent manner. *Biol. Reprod.* **2005**, *72*, 1268–1274. [\[CrossRef\]](#) [\[PubMed\]](#)
6. Magdaleno, L.; Gasset, M.; Varea, J.; Schambony, A.M.; Urbanke, C.; Raida, M.; Topfer-Petersen, E.; Calvete, J.J. Biochemical and conformational characterisation of HSP-3, a stallion seminal plasma protein of the cysteine-rich secretory protein (CRISP) family. *FEBS Lett.* **1997**, *420*, 179–185. [\[CrossRef\]](#) [\[PubMed\]](#)
7. Udby, L.; Lundwall, A.; Johnsen, A.H.; Fernlund, P.; Valtonen-Andre, C.; Blom, A.M.; Lilja, H.; Borregaard, N.; Kjeldsen, L.; Bjartell, A. beta-Microseminoprotein binds CRISP-3 in human seminal plasma. *Biochem. Biophys. Res. Commun.* **2005**, *333*, 555–561. [\[CrossRef\]](#) [\[PubMed\]](#)
8. Vadnais, M.L.; Foster, D.N.; Roberts, K.P. Molecular cloning and expression of the CRISP family of proteins in the boar. *Biol. Reprod.* **2008**, *79*, 1129–1134. [\[CrossRef\]](#) [\[PubMed\]](#)
9. Hu, J.; Merriner, D.J.; O'Connor, A.E.; Houston, B.J.; Furic, L.; Hedger, M.P.; O'Bryan, M.K. Epididymal cysteine-rich secretory proteins are required for epididymal sperm maturation and optimal sperm function. *Mol. Hum. Reprod.* **2018**, *24*, 111–122. [\[CrossRef\]](#) [\[PubMed\]](#)
10. Lim, S.; Kierzek, M.; O'Connor, A.E.; Brenker, C.; Merriner, D.J.; Okuda, H.; Volpert, M.; Gaikwad, A.; Bianco, D.; Potter, D.; et al. CRISP2 Is a Regulator of Multiple Aspects of Sperm Function and Male Fertility. *Endocrinology* **2019**, *160*, 915–924. [\[CrossRef\]](#)
11. Ernesto, J.I.; Weigel, M.M.; Battistone, M.A.; Vasen, G.; Martinez-Lopez, P.; Orta, G.; Figueiras-Fierro, D.; De la Vega-Beltran, J.L.; Moreno, I.A.; Guidobaldi, H.A.; et al. CRISP1 as a novel CatSper regulator that modulates sperm motility and orientation during fertilization. *J. Cell Biol.* **2015**, *210*, 1213–1224. [\[CrossRef\]](#)
12. Sun, X.H.; Zhu, Y.Y.; Wang, L.; Liu, H.L.; Ling, Y.; Li, Z.L.; Sun, L.B. The Catsper channel and its roles in male fertility: A systematic review. *Reprod. Biol. Endocrinol.* **2017**, *15*, 65. [\[CrossRef\]](#) [\[PubMed\]](#)
13. Gholami, D.; Amirmahani, F.; Yazdi, R.S.; Hasheminia, T.; Teimori, H. MiR-182-5p, MiR-192-5p, and MiR-493-5p Constitute a Regulatory Network with CRISP3 in Seminal Plasma Fluid of Teratozoospermia Patients. *Reprod. Sci.* **2021**, *28*, 2060–2069. [\[CrossRef\]](#)

14. Heidary, Z.; Zaki-Dizaji, M.; Saliminejad, K.; Khorramkhorshid, H.R. Expression Analysis of the CRISP2, CATSPER1, PATE1 and SEMG1 in the Sperm of Men with Idiopathic Asthenozoospermia. *J. Reprod. Infertil.* **2019**, *20*, 70–75.
15. Carvajal, G.; Brukman, N.G.; Weigel, M.M.; Battistone, M.A.; Guazzzone, V.A.; Ikawa, M.; Haruhiko, M.; Lustig, L.; Breton, S.; Cuasnicu, P.S. Impaired male fertility and abnormal epididymal epithelium differentiation in mice lacking CRISP1 and CRISP4. *Sci. Rep.* **2018**, *8*, 17531. [[CrossRef](#)] [[PubMed](#)]
16. Curci, L.; Brukman, N.G.; Weigel, M.M.; Rojo, D.; Carvajal, G.; Sulzyk, V.; Gonzalez, S.N.; Rubinstein, M.; Da, R.V.; Cuasnicu, P.S. Functional redundancy and compensation: Deletion of multiple murine Crisp genes reveals their essential role for male fertility. *FASEB J.* **2020**, *34*, 15718–15733. [[CrossRef](#)] [[PubMed](#)]
17. Haendler, B.; Kratzschmar, J.; Theuring, F.; Schleuning, W.D. Transcripts for cysteine-rich secretory protein-1 (CRISP-1; DE/AEG) and the novel related CRISP-3 are expressed under androgen control in the mouse salivary gland. *Endocrinology* **1993**, *133*, 192–198. [[CrossRef](#)]
18. Kjeldsen, L.; Cowland, J.B.; Johnsen, A.H.; Borregaard, N. SGP28, a novel matrix glycoprotein in specific granules of human neutrophils with similarity to a human testis-specific gene product and a rodent sperm-coating glycoprotein. *FEBS Lett.* **1996**, *380*, 246–250. [[CrossRef](#)]
19. Kratzschmar, J.; Haendler, B.; Eberspaecher, U.; Roosterman, D.; Donner, P.; Schleuning, W.D. The human cysteine-rich secretory protein (CRISP) family. Primary structure and tissue distribution of CRISP-1, CRISP-2 and CRISP-3. *Eur. J. Biochem.* **1996**, *236*, 827–836. [[CrossRef](#)]
20. Evans, J.; D'Sylva, R.; Volpert, M.; Jamsai, D.; Merriner, D.J.; Nie, G.; Salamonsen, L.A.; O'Bryan, M.K. Endometrial CRISP3 is regulated throughout the mouse estrous and human menstrual cycle and facilitates adhesion and proliferation of endometrial epithelial cells. *Biol. Reprod.* **2015**, *92*, 99. [[CrossRef](#)]
21. Schambony, A.; Gentzel, M.; Wolfes, H.; Raida, M.; Neumann, U.; Topfer-Petersen, E. Equine CRISP-3: Primary structure and expression in the male genital tract. *Biochim. Biophys. Acta* **1998**, *1387*, 206–216. [[CrossRef](#)] [[PubMed](#)]
22. Da, R.V.; Munoz, M.W.; Battistone, M.A.; Brukman, N.G.; Carvajal, G.; Curci, L.; Gomez-Ellas, M.D.; Cohen, D.B.; Cuasnicu, P.S. From the epididymis to the egg: Participation of CRISP proteins in mammalian fertilization. *Asian J. Androl.* **2015**, *17*, 711–715. [[CrossRef](#)]
23. Lee, U.; Nam, Y.R.; Ye, J.S.; Lee, K.J.; Kim, N.; Joo, C.H. Cysteine-rich secretory protein 3 inhibits hepatitis C virus at the initial phase of infection. *Biochem. Biophys. Res. Commun.* **2014**, *450*, 1076–1082. [[CrossRef](#)]
24. Doty, A.; Buhi, W.C.; Benson, S.; Scoggin, K.E.; Pozor, M.; Macpherson, M.; Mutz, M.; Troedsson, M.H. Equine CRISP3 modulates interaction between spermatozoa and polymorphonuclear neutrophils. *Biol. Reprod.* **2011**, *85*, 157–164. [[CrossRef](#)]
25. Chen, Y.; Wei, H.; Liu, Y.; Gao, F.; Chen, Z.; Wang, P.; Li, L.; Zhang, S. Identification of new protein biomarkers associated with the boar fertility using iTRAQ-based quantitative proteomic analysis. *Int. J. Biol. Macromol.* **2020**, *162*, 50–59. [[CrossRef](#)] [[PubMed](#)]
26. Usuga, A.; Rojano, B.A.; Restrepo, G. Association of the cysteine-rich secretory protein-3 (CRISP-3) and some of its polymorphisms with the quality of cryopreserved stallion semen. *Reprod. Fertil. Dev.* **2018**, *30*, 563–569. [[CrossRef](#)] [[PubMed](#)]
27. Restrepo, G.; Rojano, B.; Usuga, A. Relationship of cysteine-rich secretory protein-3 gene and protein with semen quality in stallions. *Reprod. Domest. Anim.* **2019**, *54*, 39–45. [[CrossRef](#)]
28. Mistretta, V.I.; Cavalier, E.; Collette, J.; Chapelle, J.P. Production of monoclonal antibodies. *Rev. Med. Liege* **2009**, *64*, 248–252.
29. Song, C.Y.; Gao, B.; Wu, H.; Wang, X.Y.; Zhou, H.Y.; Wang, S.Z.; Li, B.C.; Chen, G.H.; Mao, J.D. Spatial and temporal gene expression of Fn-type II and cysteine-rich secretory proteins in the reproductive tracts and ejaculated sperm of Chinese Meishan pigs. *Reprod. Domest. Anim.* **2011**, *46*, 848–853. [[CrossRef](#)]
30. Anklesaria, J.H.; Pandya, R.R.; Pathak, B.R.; Mahale, S.D. Purification and characterization of CRISP-3 from human seminal plasma and its real-time binding kinetics with PSP94. *J. Chromatogr. B* **2016**, *1039*, 59–65. [[CrossRef](#)]
31. Weigel, M.M.; Carvajal, G.; Curci, L.; Gonzalez, S.N.; Cuasnicu, P.S. Relevance of CRISP proteins for epididymal physiology, fertilization, and fertility. *Andrology* **2019**, *7*, 610–617. [[CrossRef](#)] [[PubMed](#)]
32. Gonzalez, S.N.; Sulzyk, V.; Weigel, M.M.; Cuasnicu, P.S. Cysteine-Rich Secretory Proteins (CRISP) are Key Players in Mammalian Fertilization and Fertility. *Front. Cell Dev. Biol.* **2021**, *9*, 800351. [[CrossRef](#)]
33. Liu, H.; Yu, H.; Gu, Y.; Xin, A.; Zhang, Y.; Diao, H.; Lin, D. Human beta-defensin DEFB126 is capable of inhibiting LPS-mediated inflammation. *Appl. Microbiol. Biotechnol.* **2013**, *97*, 3395–3408. [[CrossRef](#)]
34. Rhule, A.; Navarro, S.; Smith, J.R.; Shepherd, D.M. Panax notoginseng attenuates LPS-induced pro-inflammatory mediators in RAW264.7 cells. *J. Ethnopharmacol.* **2006**, *106*, 121–128. [[CrossRef](#)]
35. Hnasko, R.M.; McGarvey, J.A. Affinity Purification of Antibodies. *Methods Mol. Biol.* **2015**, *1318*, 29–41. [[CrossRef](#)] [[PubMed](#)]
36. Li, J.; Wei, H.; Li, Y.; Li, Q.; Li, N. Identification of a suitable endogenous control gene in porcine blastocysts for use in quantitative PCR analysis of microRNAs. *Sci. China Life Sci.* **2012**, *55*, 126–131. [[CrossRef](#)] [[PubMed](#)]

Disclaimer/Publisher's Note: The statements, opinions and data contained in all publications are solely those of the individual author(s) and contributor(s) and not of MDPI and/or the editor(s). MDPI and/or the editor(s) disclaim responsibility for any injury to people or property resulting from any ideas, methods, instructions or products referred to in the content.



Identification of new protein biomarkers associated with the boar fertility using iTRAQ-based quantitative proteomic analysis

Yuming Chen^{a,1}, Hengxi Wei^{a,1,*}, Yanting Liu^a, Fenglei Gao^b, Zhilin Chen^c, Ping Wang^a, Li Li^a, Shouquan Zhang^{a,*}

^a National Engineering Research Center for Breeding Swine Industry, Guangdong Provincial Key Lab of Agro-animal Genomics and Molecular Breeding, College of Animal Science, South China Agricultural University, Guangzhou 510642, China

^b Department of Tropical Agriculture and Forestry, College of Guangdong Agriculture Industry Business Polytechnic, Guangzhou, Guangdong 510507, China

^c Technology Department, Guangdong Wen's Foodstuffs Group Co., Ltd., Yunfu, Guangdong 527400, China

ARTICLE INFO

Article history:

Received 17 February 2020

Received in revised form 10 June 2020

Accepted 11 June 2020

Available online 15 June 2020

Keywords:

iTRAQ

Fertility

Spermatozoa

SPACA4

IZUMO2

Reproductive performance

ABSTRACT

In this study, we performed the isobaric tags for relative and absolute quantitation (iTRAQ) proteomic analysis in the spermatozoa of Landrace boars with different fertility potentials and investigated the ability of sperm acrosome associated 4 (SPACA4) and IZUMO family member 2 (IZUMO2) to predict the reproductive perform of boars. The iTRAQ results revealed that 202 proteins were up-regulated and 43 proteins were down-regulated in the spermatozoa from high fertility boars. SPACA4 and IZUMO2 protein levels were significantly up-regulated in the spermatozoa from high fertility boars. SPACA4 and IZUMO2 expression were specifically detected in the adult boar testis. SPACA4 levels were positively correlated with Sow's farrowing rate and reproductive efficiency, but not litter size. IZUMO2 were positively correlated with litter size, Sow's farrowing rate and reproductive efficiency. Treating the boar semen with SPACA4 or IZUMO2 antibodies for 30 min and 60 min failed to affect the sperm motility; while treating the semen with SPACA4 antibody significantly reduced the fertilization and cleavage rates. Similar results for fertilization and cleavage rates were found in IZUMO2 antibody-treated semen. Collectively, our results indicated that protein levels of SPACA4 and IZUMO2 in the spermatozoa were positively related to the reproductive performance of Landrace boars.

© 2018 Elsevier B.V. All rights reserved.

1. Introduction

Male infertility is the cause of about 50% of all infertility cases in the animal breeding industry [1,2]. Thus, the diagnosis and prognosis of male fertility are extremely important for the theranostic purpose of infertility management. Artificial insemination (AI) has been used for breeding in about 90% of swine livestock, and selection of breeding males is very important for the genetic improvement swine [2–4]. The analysis of the semen quality has been commonly used for predicting the male fertility. Nevertheless, the conventional analysis of semen including sperm morphology, motility and kinematics has limited predictive values on the male fertility [5]. In this regard, development of novel methods for predicting male fertility of swine is of great scientific and economic significance.

Recently, high-throughput screening technologies such as proteomic analysis have been employed to identify potential proteins that

are associated with male fertility of swine [6,7]. Labas et al., performed the analysis of epididymal sperm maturation using matrix-assisted laser desorption/ionization profiling and top-down mass spectrometry and characterized the peptidome of epididymal spermatozoa from boar [8]. Kwon et al., employed proteomic approaches to analyse the negative fertility markers in inferior boar spermatozoa and identified 20 differentially expressed proteins that can be potentially used as biomarkers for predicting inferior male fertility [9]. Further studies revealed that Ras-related protein Rab-2A and ubiquinol-cytochrome c reductase core protein 1 expression in spermatozoa after capacitation can help differentiate superior male fertility from below-average fertility [6]. A recent study by Feugang et al., performed in-depth proteomic analysis of boar spermatozoa via shotgun and gel-based methods, which allowed the identification of over 2000 proteins for a comprehensive bioinformatics analysis of their biological functions [10]. Recently, a new in-depth analytical approach of the porcine seminal plasma proteome revealed some proteins as potential biomarkers of fertility in AI boars [11]. With the development of proteomic techniques, the isobaric tags for relative and absolute quantitation (iTRAQ) technology have been widely used in quantitative proteomics research due to its unique advantages [12,13]. However, the application of this technology in

* Corresponding authors at: College of Animal Science, South China Agricultural University, 483 Wushan Road, Tianhe District, Guangzhou, Guangdong 510642, China.

E-mail addresses: weihengxi@scau.edu.cn (H. Wei), sqzhang@scau.edu.cn (S. Zhang).

¹ Both authors contributed equally to this work.

proteomic analysis of boar semen samples to identify potential biomarkers for predicting boar fertility has been not reported yet.

In this study, we employed the iTRAQ technology to analyse the differentially expressed proteins in the spermatozoa from high and low fertility boars. The bioinformatics analysis of the biological functions of the differentially expressed proteins was also performed. In the validation studies, we verified that two proteins including sperm acrosome associated 4 (SPACA4) and IZUMO family member 2 (IZUMO2) were associated the productive performance of the boars. This study may provide some new evidence for these identified proteins as potential biomarkers for the fertility of boars.

2. Materials and methods

2.1. Animal ethics statement

All the animal experiments were performed in accordance with the guidelines of the ethical treatment of animals and were approved by the Animal Ethics Committee of South China Agricultural University.

2.2. Collection and preparation of boar spermatozoa of different fertility

In the first set of experiments, semen samples were collected from 3 high fertility boars and 3 low fertility boars (see Table 1). The definition of high fertility and low fertility boars was based on investigation by Zhang et al., from our institute [14]. Each sample was washed by centrifugation at 500g for 20 min using discontinuous Percoll gradients to remove dead spermatozoa and seminal plasma. Resulting spermatozoa were incubated for 30 min at 37 °C in 5% CO₂ in air with 1 mL modified tissue culture medium 199 (mTCM 199; containing 0.91 mM sodium pyruvate, 3.05 mM D-glucose, 2.92 mM calcium lactate, and 2.2 g/L sodium bicarbonate; Sigma-Aldrich). The spermatozoa from both groups were then processed for iTRAQ analysis and validation studies.

In the second set of experiments, spermatozoa samples were collected from 22 adult boars, and the spermatozoa was collected for the enzyme-linked immunosorbent assay (ELISA) analysis for SPACA4 and IZUMO2 protein levels. The reproductive performance (litter size, Sow's farrowing rate and reproductive efficiency) of the 22 adult boars were collected from the record Guangdong Guangsanbao farm Ltd. (Guangzhou, China).

2.3. Preparation of protein samples

The protein samples were prepared by using the Whole Cell Lysis Assay kit (KeyGen BioTECH., Nanjing China) according to the manufacturer's protocol. The spermatozoa samples were extracted with lysis buffer 3 (7 M urea, 2 M thiourea, 4% CHAPS, 40 mM Tris-HCl, pH 8.5) containing 1 mM PMSF and 2 mM ethylenediaminetetraacetic acid (EDTA) by sonicating in ice for 5 min. Total proteins were isolated from the supernatant by centrifugation at 4 °C, 25,000g for 20 min. The proteins were reduced with 10 mM dithiothreitol at 56 °C for 1 h and then alkylated by 55 mM iodoacetamide in the darkroom for 45 min. After centrifuging at 4 °C, 25,000g, an aliquot of the supernatant was taken for determination of protein concentration by the Bradford protein assay kit (Thermo Fisher Scientific, Waltham, USA).

Table 1
Characteristics of animals used for iTRAQ analysis.

	High reproductive performance (n = 3)	Low reproductive performance (n = 3)
Litter size	10.80 ± 0.38	9.55 ± 0.39*
Sow's farrowing rate (%)	79.23 ± 6.07	72.41 ± 6.47
Reproductive efficiency (n)	8.58 ± 0.88	6.93 ± 0.80*

* P < 0.05

2.4. iTRAQ Labelling and strong cation-exchange chromatography (SCX) fractionation

Total protein (100 µg) was taken out of each sample solution and then the protein was digested with Trypsin Gold (Promega, Madison, USA) with the ratio of protein: trypsin = 30: 1 at 37 °C for 16 h. After trypsin digestion, peptides were dried by vacuum centrifugation. Peptides were reconstituted in 0.5 M TEAB and processed according to the manufacturer's protocol for 8-plex iTRAQ reagent (Applied Biosystems, Foster City, USA). Briefly, one unit of iTRAQ reagent was thawed and reconstituted in 24 L isopropanol. Samples were labelled with the iTRAQ tags (3 samples from high reproductive group were labelled with 113, 114 and 115; 3 samples from low reproductive group were labelled with 117, 118 and 119) [15], and were incubated at room temperature for 2 h. The labelled peptide mixtures were then pooled and dried by vacuum centrifugation. SCX chromatography was performed with a LC-20AB HPLC Pump system (Shimadzu, Kyoto, Japan). The iTRAQ-labelled peptide mixtures were reconstituted with 4 mL buffer A (25 mM NaH₂PO₄ in 25% acetonitrile, pH 2.7) and loaded onto a 4.6 × 250 mm Ultremex SCX column containing 5 µm particles (Phenomenex, Torrance, USA). The peptides were eluted at a flow rate of 1 mL/min with a gradient of buffer A for 10 min, 5–60% buffer B (25 mM NaH₂PO₄, 1 M KCl in 25% acetonitrile, pH 2.7) for 27 min, 60–100% buffer B for 1 min. The system was then maintained at 100% buffer B for 1 min before equilibrating with buffer A for 10 min prior to the next injection. Elution was monitored by measuring the absorbance at 214 nm, and fractions were collected every 1 min. The eluted peptides were pooled into 20 fractions, desalted with a Strata X C18 column (Phenomenex) and vacuum-dried.

2.5. LC-ESI-MS/MS analysis based on Triple TOF 5600

Each fraction was resuspended in buffer A (5% acetonitrile, 0.1% formic acid) and centrifuged at 20,000 g for 10 min, the final concentration of peptide was about 0.5 µg/µl on average. 10 µL supernatant was loaded on a LC-20AD nanoHPLC (Shimadzu, Kyoto, Japan) by the autosampler onto a 2 cm C18 trap column. Then, the peptides were eluted onto a 10 cm analytical C18 column (inner diameter 75 µm) packed in-house. The samples were loaded at 8 L/min for 4 min, then the 35 min gradient was run at 300 nL/min starting from 2 to 35% buffer B (95% acetonitrile, 0.1% formic acid), followed by 5 min linear gradient to 60%, then, followed by 2 min linear gradient to 80%, and maintenance at 80% buffer B for 4 min, and finally return to 5% in 1 min.

Data acquisition was performed with a TripleTOF 5600 System (AB SCIEX, Concord, USA) fitted with a Nanospray III source (AB SCIEX) and a pulled quartz tip as the emitter (New Objectives, Woburn, USA). Data was acquired using an ion spray voltage of 2.5 kV, curtain gas of 30 psi, nebulizer gas of 15 psi, and an interface heater temperature of 150 °C. The MS was operated with a RP of greater than or equal to 30,000 FWHM for TOF MS scans. For IDA, survey scans were acquired in 250 ms and as many as 30 product ion scans were collected if exceeding a threshold of 120 counts per second (counts/s) and with a 2+ to 5+ charge-state. Total cycle time was fixed to 3.3 s. Q2 transmission window was 100 Da for 100%. Four time bins were summed for each scan at a pulser frequency value of 11 kHz through monitoring of the 40 GHz multichannel TDC detector with four-anode channel detect ion. A sweeping collision energy setting of 35 ± 5 eV coupled with iTRAQ adjust rolling collision energy was applied to all precursor ions for collision-induced dissociation. Dynamic exclusion was set for 1/2 of peak width (15 s), and then the precursor was refreshed to the exclusion list.

2.6. Data analysis

Raw data files acquired from the AB SCIEX TripleTOF 5600 were converted into .mgf files using AB SCIEX MS Data Converter 1.3 beta and the

.mgf files were used for protein identification. Proteins identification was performed by using Mascot search engine (Matrix Science, London, UK; version 2.3.02). For protein identification, Gln- > \$pyro-Glu (N-term Q), Oxidation (M), Deamidated (NQ) as the potential variable modifications, and Carbamidomethyl (C), iTRAQ8plex (N-term), iTRAQ8plex (K) as fixed modifications. The charge states of peptides were set to +2 and +3. Specifically, an automatic decoy database search was performed in Mascot by choosing the decoy checkbox in which a random sequence of database is generated and tested for raw spectra as well as the real database. To reduce the probability of false peptide identification, only peptides with significance scores (≥ 20) at the 99% confidence interval by a Mascot probability analysis greater than /identity0 were counted as identified. Each confident protein identification involves at least one unique peptide [16]. For protein quantitation, it was required that a protein contains at least two unique peptides. The quantitative protein ratios were weighted and normalized by the median ratio in Mascot. We only used ratios with p -values < 0.05 , and only fold changes of > 1.2 were considered as significant [16].

2.7. Function analysis of differentially expressed proteins

Functional annotations of the proteins were conducted using Blast2GO program against the non-redundant protein database (NCBI). Cluster of Orthologous Groups (KOG) database (<http://www.ncbi.nlm.nih.gov/KOG/>), Gene Ontology (GO) and the Kyoto encyclopedia of genes and genomes (KEGG) database (<http://www.genome.jp/kegg/>) were used to classify and group these identified proteins [17–19]. KOG is the database for protein orthologous classification. Every protein in KOG is supposed to derive from a same protein ancestor. Gene Ontology (GO) is an international standardization of gene function classification system and provides a set of dynamic updating controlled vocabulary to describe genes and gene products attributes in the organism. GO has 3 Ontologies which can describe molecular function, cellular component and biological process, respectively. KEGG pathway is a collection of manually drawn pathway maps representing our knowledge on the molecular interaction and reaction networks.

2.8. Reverse Transcriptase PCR (RT-PCR)

Total RNA from different tissues were extracted using TRIzol reagent (Invitrogen, Carlsbad, USA) according to the manufacturer's protocol. The genomic DNA in the preparation was eliminated by using RNase-Free DNase I (Qiagen). Total RNA was reversely transcribed into cDNA in a reaction primed by oligo deoxynucleotide T (dT) 12–15 primer using Superscript II reverse transcriptase (Invitrogen) according to the manufacturer's instructions. The primer sequences for the respective genes are shown in Supplemental Table S1. Amplification of the products of expected size was verified by electrophoresis on 3% agarose gel.

2.9. Immunohistochemistry (IHC) analysis of SPACA4 in the testes and epididymis

The testis and epididymis were fixed in 4% paraformaldehyde (PFA) and were embedded in paraffin. The embedded tissues were section into 5 μ m slices on a microtome. For the IHC staining, the sectioned slices were subjected to antigen retrieval and were then incubated with 3% normal goat serum (Abcam, Cambridge, UK) for 1 h at room temperature. After that, the sections were incubated with primary antibodies against SPACA4 (Biorbyt, Cambridge, UK) or unrelated rabbit IgG (Abcam) at 4 °C overnight. After 4×5 min wash in Tris-buffered saline with 0.1% Tween 20, sections were incubated with a biotinylated anti-rabbit immunoglobulin G (Abcam) at room temperature for 1 h. The slices were then incubated with avidin-biotin-peroxidase complexes (Abcam). The antigens were visualized after incubation with a 3,3'-diaminobenzidine solution (Abcam).

2.10. Immunofluorescent staining of SPACA4 in the sperm

The localization of SPACA4 in the boar sperm was detected using immunofluorescent staining. Briefly, the collected semen was centrifuged at 2000g for 10 min, and the sperm was collected by re-suspending the pellet with DPBS. The sperm was fixed by 4% PFA for 20 min followed by incubating with 0.5% Triton X-100 for 15 min. After blocking with 1% bovine serum albumin for at room temperature for 1 h, the sperm was incubated with SPACA4 primary antibodies (Biorbyt) at 4 °C overnight. After that, the sperm was incubated with the Alexa Fluor® 568-conjugated secondary antibodies (Abcam) at 37 °C for 1 h. The localization of the stained SPACA4 was examined under a fluorescent microscope.

2.11. Western blot analysis

Protein samples from the boar tissues were extracted using the radioimmunoprecipitation assay buffer containing the protease inhibitors (Roche, Basel, Switzerland). The concentrations of the extracted proteins were determined by the Bradford protein assay kit (Thermo Fisher Scientific). Equal amount of proteins (30 μ g) were resolved by electrophoresis on a 10% sodium dodecyl sulphate-polyacrylamide gel electrophoresis gel. The separated proteins were then transferred to the polyvinylidene difluoride (PVDF) membrane. The PVDF membrane was then blocked by 1.5% skimmed milk at room temperature for 1 h and were then incubated with IZUMO2 antibody (Sant Cruz Biotechnology, Dallas, USA) at 4 °C overnight. After overnight incubation, the membrane was then probed against the horseradish peroxidase-conjugated secondary antibodies (Abcam) at room temperature for 2 h. The western blot band on the membrane was visualized by using the enhanced chemiluminescence kit (Thermo Fisher Scientific).

2.12. ELISA determination of SPACA4 and IZUMO2 protein levels

The protein expression levels of SPACA4 and IZUMO2 were determined by respective porcine SPACA4 and IZUMO2 ELISA kits (TSZ Biosciences, Shanghai, China) according to the manufacturer's protocol.

2.13. Measurement of sperm motility

Sperm motility was evaluated by using a computer-assisted sperm analysis system (CASA, TOX IVOS, Hamilton Thorne Research, Inc., Beverly, MA, USA) using the procedures previously described [20]. Aliquots (8 μ L) of a semen sample were pipetted into a pre-warmed sperm-counting chamber (depth, 20 μ m; Leja slides, Spectrum Technologies, Healdsburg, USA). The CASA was subsequently conducted to evaluate the sperm motility variables. Each semen sample was measured three times, and the average value was the final motility value reported.

2.14. In vitro fertilization (IVF) and culture

The *in vitro* fertilization and culture were performed as described by Abeydeera et al., [21]. For the antibodies treatment, the boar semen was incubated with SPACA4 or IZUMO2 antibodies for different durations (0, 30 and 60 mins) and the rabbit IgG was served as negative controls. The fertilization rate and cleavage rate were evaluated under a stereomicroscope (Nikon, Japan) at 15 h and 24 h after IVF.

2.15. Statistical analysis

All the experimental results were expressed as mean \pm standard deviation. The correlation between protein levels and reproductive performance was analysed using Pearson correlation test. Significant differences between/among different treatment groups were analysed using unpaired Student's t -test or one-way ANOVA followed by

Bonferroni's post-hoc test. $P < 0.05$ was considered to be statistically significant.

3. Results

3.1. Identification and analysis of the proteins from boar semen

The spermatozoa from high fertility and low fertility boars were collected for the iTRAQ analysis. The reproductive performance of the boars was shown in Table 1. The boars with high reproductive performance had significantly higher litter size and reproductive

efficiency (Table 1). For the protein analysis, the error distribution of peptides was firstly checked to confirm the quality control, and there was a small mass error and all the data tend to be normal (Fig. 1A). A total of 2089 proteins from the boar spermatozoa portion were detected, and >90% of the proteins were with a mass of 10–70 kDa and >100 kDa (Fig. 1B). The peptide length was mainly detected at 7–14 amino acids (Fig. 1C). The number of proteins with sequence coverage were demonstrated in Fig. 1D. Proteins with a single peptide, 2–5 peptides, 6–10 peptides and ≥ 11 peptides consisted of 684, 882, 362 and 321 proteins, respectively (Fig. 1E).

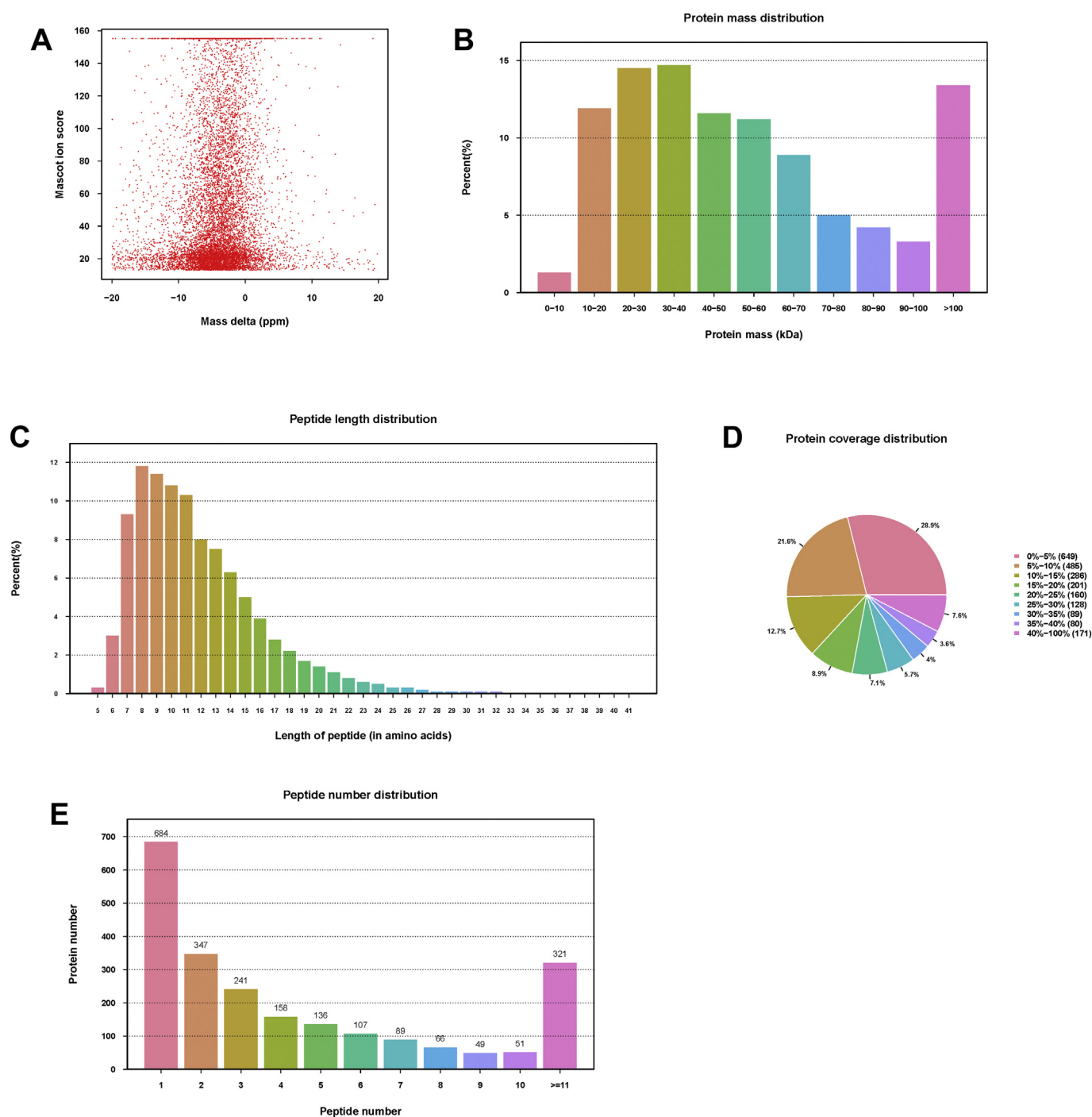


Fig. 1. Identification and analysis of the proteomics from boar semen. (A) Mass error distribution of the proteins (B) Identified proteins were grouped based on the protein mass. (C) Identified proteins were grouped based on the peptide length. (D) The identified proteins were classified into pie charts based on the protein sequence coverage. (E) The number of peptides that match to proteins as shown by Protein Pilot.

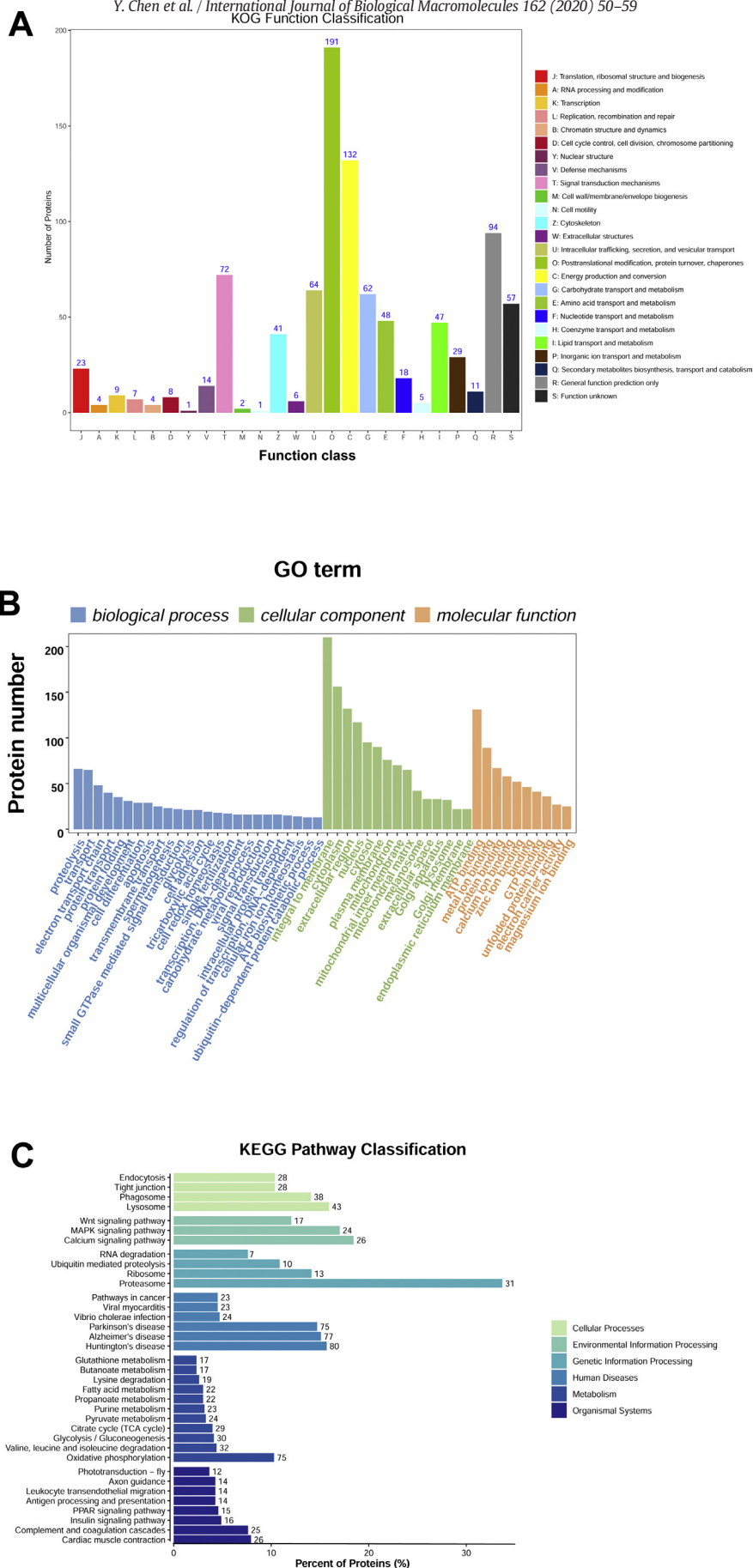


Fig. 2. KOG, GO and KEGG analysis of the proteomics from boar spermatozoa. (A) KOG analysis of differentially expressed proteins in boar spermatozoa. (B) GO analysis of differentially expressed proteins in boar spermatozoa. (C) KEGG pathway analysis of differentially expressed proteins in boar spermatozoa.

3.2. KOG, GO and KEGG analysis of the proteomics from boar spermatozoa

The identified proteins from boar spermatozoa were further subjected to the KOG function classification, and the results showed that large proportion of proteins involve in the “posttranslational modification”, “energy production and conversion” and “carbohydrate transport and metabolism” (Fig. 2A). In terms of the GO analysis, a large proportion of proteins in the biological process involves in “proteolysis” and “transport” (Fig. 2B). In the cellular component, the proteins are related to “integral to membrane”, “cytoplasm”, “extracellular region”, “nucleus” and so on (Fig. 2B). In the molecular function, the proteins were mainly related to “ATP”, “metal ion binding”, “protein binding” (Fig. 2B). KEGG pathway classification results showed that the number of proteins involved in “proteasome”, “oxidative phosphorylation”, “lysosome” and “calcium signalling pathway” is 31, 75, 43 and 26, respectively (Fig. 2C).

As shown in Fig. 3A, the differentially expressed proteins in boar spermatozoa were shown; 202 proteins are up-regulated and 43 proteins are down-regulated (Fig. 3A; see Supplemental Table S2 for the differentially expressed proteins). The GO enrichment analysis showed that “mitochondrion”, “mitochondrial inner membrane”, “keratin filament”, “ATP synthesis coupled proton transport” and so on were significantly enriched (Fig. 3B). The KEGG enrichment analysis revealed that “oxidative phosphorylation”, “Parkinson's disease” and so on were significantly enriched (Fig. 3C).

3.3. Identification of SPACA4 and IZUMO2 proteins in the boar reproductive systems

Among the differentially expressed proteins, we measured the levels of proteins including SPACA4 and IZUMO2 in the boar spermatozoa by using ELISA. The protein levels of SPACA4 and IZUMO2 in the spermatozoa from high fertility boars were 6.1 ± 2.7 and 5.8 ± 4.3 times higher than that from low fertility boars. The RT-PCR results showed that the SPACA4 gene (~257 bp fragment) and IZUMO2 gene (~505 bp fragment) were detected in the testis of adult boars, but not in epididymis of adult boars or the reproductive systems of 3-month-old boars (Fig. 4A). The IHC analysis confirmed that SPACA4 protein was detected in the testis but not in the epididymis of the adult boars (Fig. 4B). The immunofluorescent staining found that SPACA4 was located in the front acrosome and back section of the sperm head (Fig. 4C). The western blot analysis showed that IZUMO2 was mainly detected in the testis of adult boars, but not in the epididymis or ductus deferens of adult boars, or in the reproductive systems of the 3-month-old boars (Fig. 4B).

3.4. Correlation between SPACA4/IZUMO2 proteins and reproductive performance of the boars

To validate the correlation between SPACA4/IZUMO2 protein levels and reproductive performance of the boars, we analysed the protein levels of SPACA4 and IZUMO2 as determined by ELISA in the spermatozoa from 22 adult boars. The relative protein levels of SPACA4 and IZUMO2 were $8.27 \pm 3.08 (x10^{-8})$ and $11.02 \pm 4.33 (10^{-8})$, respectively. The protein level of SPACA4 was positively correlated with Sow's farrowing rate (Fig. 5B) and reproductive efficiency (Fig. 5C), but not litter size (Fig. 5A). In addition, the protein level of IZUMO2 was positively correlated with litter size (Fig. 5D), Sow's farrowing rate (Fig. 5E) and reproductive efficiency (Fig. 5F).

Furthermore, we ranked the reproductive efficiency of 22 boars from high to low, and selected the first 8 boars as the high fertility group, and the last 8 as the low fertility group. The litter size, Sow's farrowing and reproductive efficiency in the high fertility group were significantly higher than that in the low fertility group (Fig. 6A–C). Consistently, the protein levels of SPACA4 and IZUMO2 in the high fertility group were significantly higher than that in the low fertility group (Fig. 6D and E).

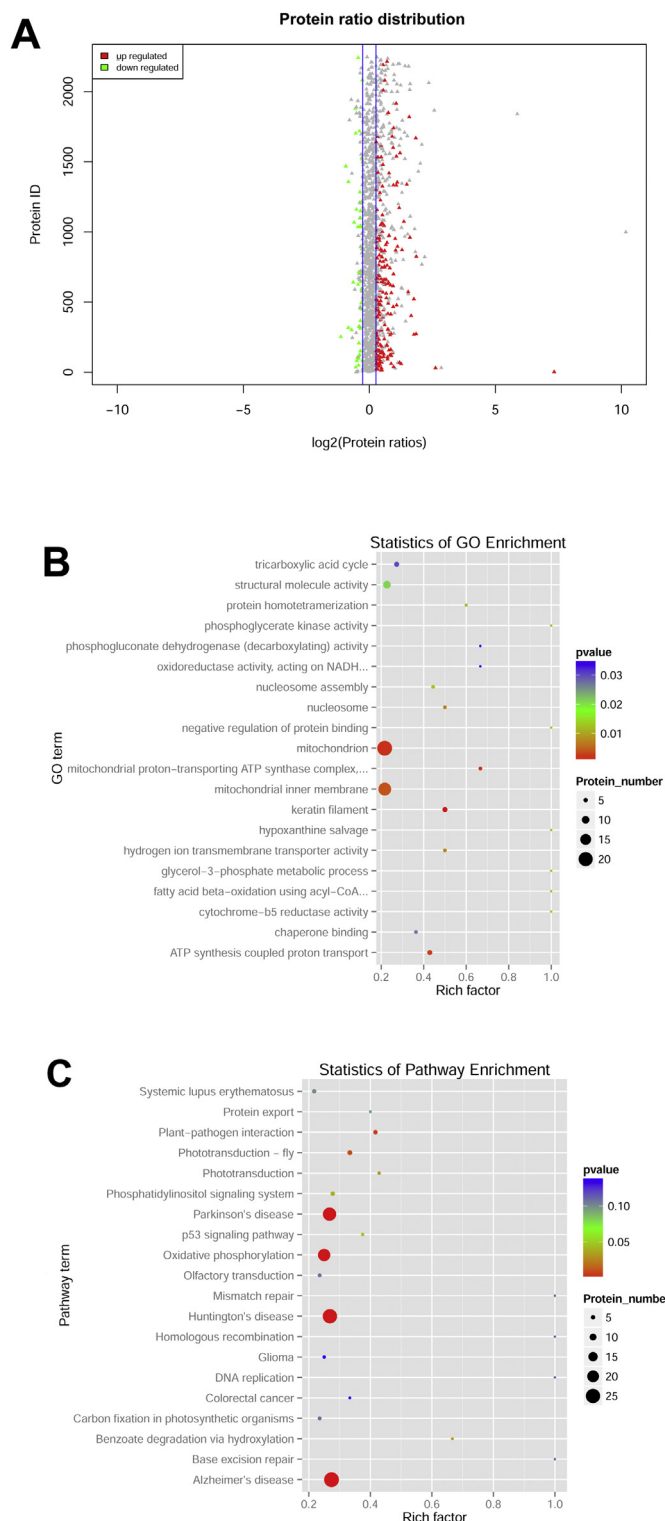


Fig. 3. GO enrichment and KEGG enrichment of differentially expressed proteins in boar spermatozoa. (A) Protein ratio distribution of the differentially expressed proteins in boar spermatozoa. (B) GO enrichment analysis of differentially expressed proteins in boar spermatozoa. (C) KEGG enrichment of differentially expressed proteins in boar spermatozoa.

3.5. Effects of SPACA4 and IZUMO2 antibodies on the sperm motility, fertilization rate and cleavage rate

In order to confirm the role of SPACA4 and IZUMO2 on the reproductive performance of boars, we treated the semen with respective SPACA4 and IZUMO2 antibodies. Treating the semen with SPACA4 or

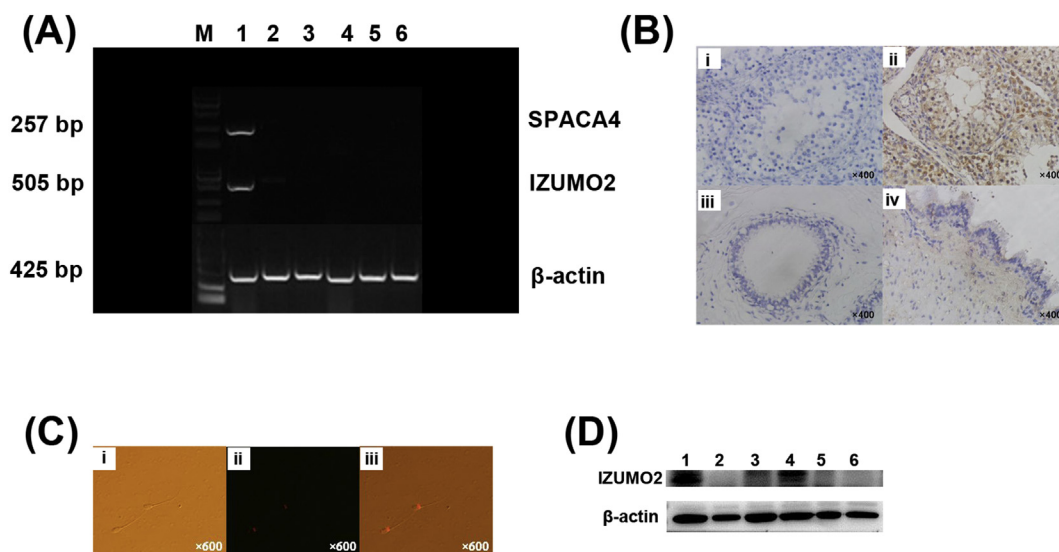


Fig. 4. Identification of SPACA4 and IZUMO2 proteins in the boar reproductive systems. (A) RT-PCR of SPACA4 and IZUMO2 in the testis, epididymis and ductus deferens. M. Marker; 1. Testis of adult boars; 2. Epididymis of adult boars; 3. Ductus deferens of adult boars; 4. Testis of 3-month-old boars; 5. Epididymis of 3-month-old boars; 6. Ductus deferens of 3-month-old boars. (B) Immunohistochemistry analysis of SPACA4 protein expression in the testis and epididymis from adult boars. (C) Immunofluorescent staining of SPACA4 proteins in the sperms. (D) Western blot analysis of IZUMO2 proteins in testis, epididymis and ductus deferens. 1. Testis of adult boars; 2. Epididymis of adult boars; 3. Ductus deferens of adult boars; 4. Testis of 3-month-old boars; 5. Epididymis of 3-month-old boars; 6. Ductus deferens of 3-month-old boars.

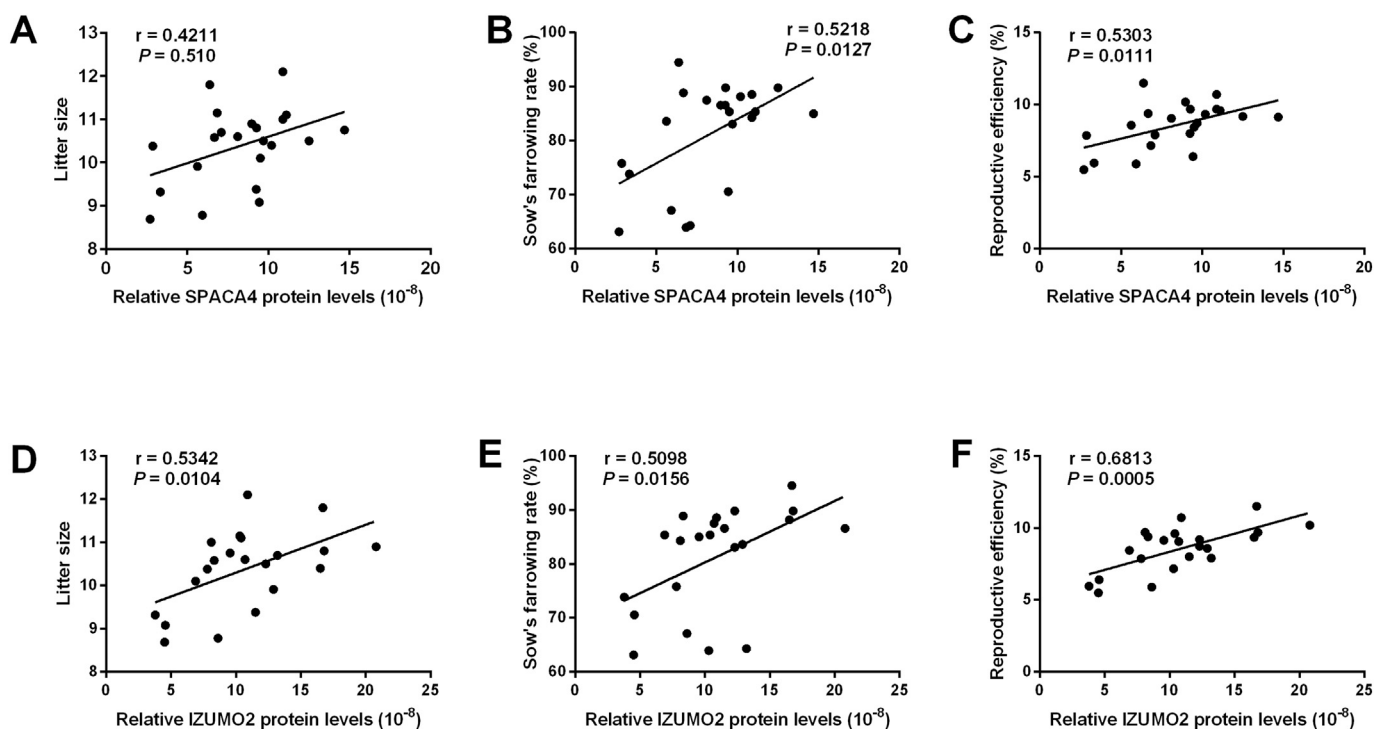


Fig. 5. Correlation between SPACA4/IZUMO2 proteins and reproductive performance of the boars. The correlation between SPACA4 protein levels and (A) Sow's litter size, (B) Sow's farrowing rate and (C) reproductive efficiency was analysed by Pearson correlation test. The correlation between IZUMO2 protein levels and (D) Sow's litter size, (E) Sow's farrowing rate and (F) reproductive efficiency was analysed by Pearson correlation test.

IZUMO2 antibodies for 30 min and 60 min failed to affect the sperm motility (Table 2). Treatment with SPACA4 antibody significantly reduced the fertilization rate to $37.91\% \pm 7.64\%$ when compared to the control group (fertilization rate: $46.16\% \pm 4.97\%$; Table 3). Consistently, IZUMO2 antibody treatment also reduced the fertilization rate when compared to the control group (Table 3). In addition, SPACA4 and IZUMO2 antibodies treatments both reduced the cleavage rate when compared to the control group (Table 4 and Table 5).

4. Discussion

The prediction of male fertility is essential for the successful breeding and profitable farm management in the animal industry [2]. Due to the limitations of using conventional semen analysis for male fertility prediction, more efforts have been made to improve the prediction using the high-through technologies. Among these technologies, proteomics have been widely applied to identify the novel biomarkers for

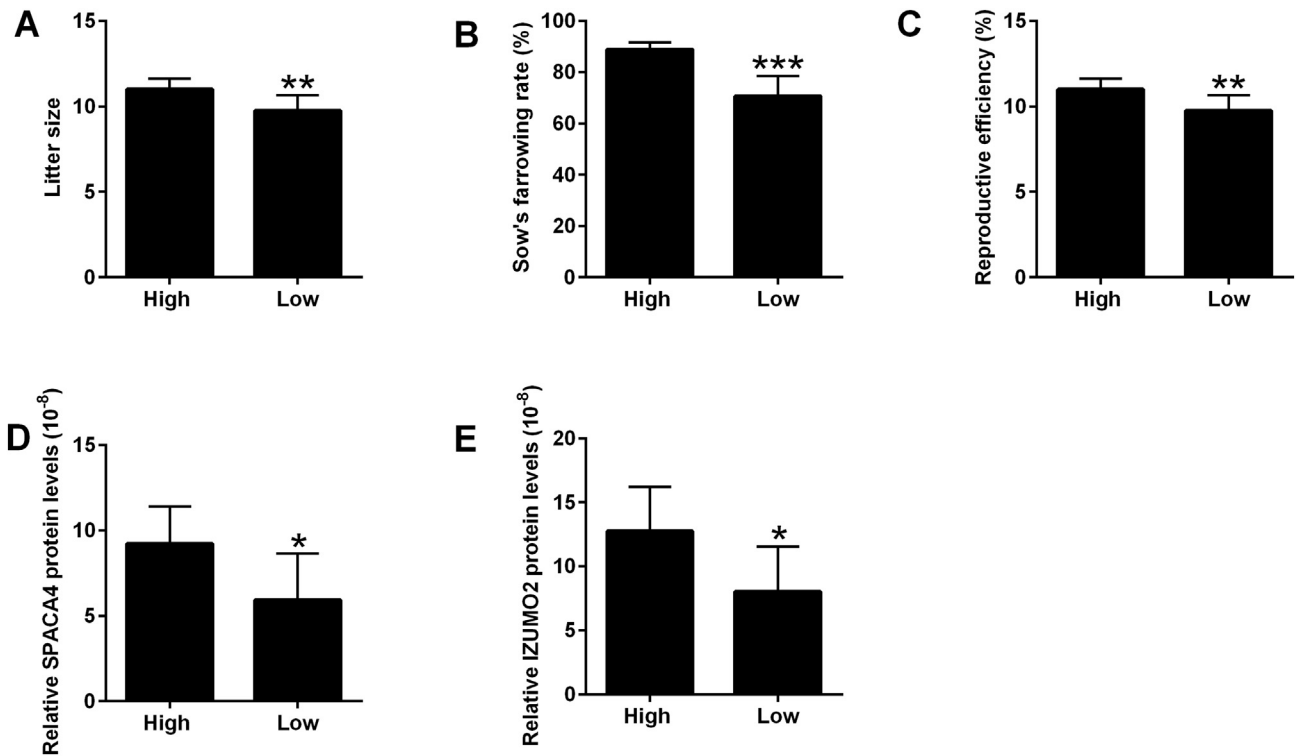


Fig. 6. Expression levels of SPACA4 and IZUMO2 protein levels in the spermatozoa from boars. (A) Litter size, (B) Sow's farrowing rate and (C) Reproductive efficiency were determined in the high reproductive and low reproductive boars. Protein levels of (D) SPACA4 and (E) IZUMO2 in spermatozoa from high productive and low productive boars. $N = 8$. * $P < 0.05$, ** $P < 0.01$ and *** $P < 0.001$.

Table 2
Effects of SPACA4 and IZUMO2 antibodies treatment on the sperm motility.

Group	Sperm motility (%)		
	0 min	30 min	60 min
Control	97.34 \pm 1.11	91.87 \pm 3.94	86.99 \pm 5.55
SPACA4 antibody	97.23 \pm 0.94	92.69 \pm 2.20	90.21 \pm 2.64
IZUMO2 antibody	95.65 \pm 1.03	90.51 \pm 2.17	86.99 \pm 1.58

Table 3
Effects of SPACA4 and IZUMO2 antibodies treatment on the fertilization rate.

Group	Oocytes (n)	Fertilized eggs (n)	Fertilization rate (%)
Control	280	130	46.16 \pm 4.97
SPACA4 antibody	268	104	37.91 \pm 5.64*
IZUMO2 antibody	284	98	35.51 \pm 2.33*

* $P < 0.05$

Table 4
Effects of SPACA4 antibody treatment on the cleavage rate.

Group	Oocytes (n)	Cleavage (n)	Cleavage rate (%)
Control	429	221	51.45 \pm 13.05
SPACA4 antibody	373	162	45.29 \pm 13.20*

* $P < 0.05$

Table 5
Effects of IZUMO2 antibody treatment on the cleavage rate.

Group	Oocytes (n)	Cleavage (n)	Cleavage rate (%)
Control	313	184	58.29 \pm 12.84
IZUMO2 antibody	304	122	39.88 \pm 5.67*

* $P < 0.05$

male fertility [7]. In the present study, we employed the iTRAQ technology to screen over the boar spermatozoa and to subsequently identify the potential biomarkers for predicting the boar fertility. Our results revealed that around 2000 proteins from iTRAQ analysis were annotated, and the bioinformatics analysis of these differentially expressed proteins indicated several biological functions and pathways that may be associated with male fertility. In the further validation experiments, we identified two protein biomarkers including SPACA4 and IZUMO2, and these two proteins were positively correlated with the reproductive performance of the boars. The present study may provide new evidence of SPACA4 and IZUMO2 as potential biomarkers predicting the boar fertility.

The application of iTRAQ for proteomic analysis has been used in identifying novel biomarkers for male fertility across different species. Xie et al., used the iTRAQ to successfully identify new epididymal luminal fluid proteins involved in sperm maturation in male rats [22]. Li et al., used the iTRAQ approach to analyse the sturgeon spermatozoa proteome and identified creatine kinase, mitochondrial 1, ubiquitous and lactate dehydrogenase B as the potential biomarkers for the prediction of sperm quality [23]. D'Amours et al., identified diazepam-binding inhibitor-like 5, tetraspanin-8 and triosephosphate isomerase 1 as putative markers of the fully functional sperm subpopulation in the bulls by using iTRAQ proteomic analysis [24]. In the present study, we used the iTRAQ approach to analyse the proteomics of the spermatozoa from low and high fertility boars. In the analysis, a total of 2089 proteins were identified. The bioinformatics analysis revealed the potential biological functions and pathways of the differentially expressed proteins. In the KOG function, proteins were found to involve "energy production and conversion"; while in the GO analysis, a large proportion of proteins involved in "ATP binding"; and consistently, KEGG analysis also indicated the involvement of these differentially expressed protein in "energy metabolism". In fact, the energy metabolism has been found to be associated with the male fertility from previous studies

[25–27]. These results may imply that proteins related to energy metabolism may be important in predicting male fertility in boars.

Among the differentially expressed proteins, SPACA4 and IZUMO2 attracted our attention, as the SPACA and IZUMO families have been reported to involve in the fertilization of the sperms [28,29]. Thus, we further validated the protein expression levels of SPACA4 and IZUMO2 in the spermatozoa from low and high fertility boars. Our results showed that both SPACA4 and IZUMO2 protein levels were up-regulated in the spermatozoa from high fertility boars. SPACA4 is highly conserved in mammals and belongs to a type of glycosylphosphatidylinositol anchoring protein. SPACA4 is a transmembrane protein with a transmembrane region close to the carboxy terminus and a putative transamidase cleavage site on the original protein and shares a similar function to the Ly-6 and urokinase plasminogen activator receptor superfamily. SPACA4 is specifically expressed in the testes, and SPACA4 is located on the outer, inner and stroma of the sperm acrosome [29]. In addition, SPACA4 is also specifically expressed in human and mouse testes [30]. Shetty et al., found that SPARC4 antibody inhibited the fusion between sperm and oocytes, suggesting that SPACA4 may have certain effects on sperm-egg interaction [29]. The microarray gene expression analysis identified SPACA4 as a potential biomarker for non-obstructive azoospermia in men [31]. In our study, the expression of SPACA4 was specifically detected in the adult boar testes and SPACA4 protein was located in the front acrosome and back section of the sperm head, which was consistent with previous findings in mice and human [30]. The present study also showed that SPACA4 protein level in the boar spermatozoa was positively correlated with the boar reproductive performance, which was in consistent with the findings by Malcher et al., [31]. Furthermore, our results also showed that treatment boar spermatozoa with SPACA antibody reduced the fertilization rate and cleavage rate. In fact, Shetty et al., found that SPACA4 antibody treatment impaired the fusion between sperm and oocytes in the mice [29]. A later study by Marvin et al., showed that plasminogen improved mouse fertilization by interactions with inner acrosomal membrane-bound MMP2 and SPACA4 [32]. Collectively, these results implied that SPACA4 protein may play an important role in the interactions between sperm and oocytes. IZUMO2 belongs to the superfamily of IZUMO proteins, and IZUMO1, one of the IZUMO family members, has been well-documented for its role in male fertility [33–35]. However, the role of IZUMO2 was less understood, due to the lack of specific antibodies for IZUMO2. Clark et al. found that IZUMO2 antibodies were detected in the infertile female reproductive tract fluid, suggesting that IZUMO2 on normal male sperm could be bound by IZUMO2 antibodies in the female reproductive tract with infertility to cause infertility [28]. In the present study, IZUMO2 was detected specifically in the adult boar testes. IZUMO2 protein levels in the spermatozoa were positively correlated with the boar reproductive performance. In addition, treatment with IZUMO2 antibodies significantly reduced the fertilization and cleavage rates. Collectively, IZUMO2 may exhibit similar effects of IZUMO1 to affect the interaction between the sperm and oocytes. Though SPACA4 and IZUMO2 were correlated with reproductive performance of the adult boars, the correlation coefficient is not high, suggesting the moderate correlation. The moderate correlation may be due to some variations in a small sample size, and future studies should include more samples to consolidate the current findings.

5. Conclusion

In summary, the present study for the first time performed the proteomic analysis of the spermatozoa from high and low reproductive performance boars by using iTRAQ technology. The bioinformatics analysis revealed the significantly enriched biological functions and pathways of the differentially expressed proteins. Further validation experiments revealed that SPACA4 and IZUMO2 were distributed in the testis and sperm of adult boar and involved in the fertilization process. The spermatozoa protein levels of SPACA4 and IZUMO2 were

significantly positively related to the reproductive performance of Landrace boars. This study provides a theoretical basis for breeding boars with high reproductive performance by using protein markers.

Supplementary data to this article can be found online at <https://doi.org/10.1016/j.ijbiomac.2020.06.102>.

Authors' contributions

Yuming Chen, Hengxi Wei and Shouquan Zhang: Conceptualization, Methodology. Yuming Chen and Yanting Liu: Investigation. Fenglei Gao and Ping Wang: Statistical analysis. Yuming Chen and Hengxi Wei: Original draft preparation. Hengxi Wei and Zhilin Chen: Reviewing and Editing.

Funding

This study was supported by grants of the National Natural Science Foundation of China (31402072 and 31572397), the National Key R&D Program of China (2017YFD0501902), the Science and Technology Innovation Strategy projects of Guangdong Province (2018B020203002).

Declaration of competing interest

None.

Acknowledgements

None.

References

- [1] O.A. Peltoniemi, A. Tast, R.J. Love, Factors effecting reproduction in the pig: seasonal effects and restricted feeding of the pregnant gilt and sow, *Anim. Reprod. Sci.* 60–61 (2000) 173–184.
- [2] J. Roca, M.L. Broekhuijse, I. Parrilla, H. Rodriguez-Martinez, E.A. Martinez, A. Bolarin, Boar differences in artificial insemination outcomes: can they be minimized? *Reproduction in Domestic Animals = Zuchthygiene* 50 (Suppl. 2) (2015) 48–55.
- [3] M.S. Rahman, W.S. Kwon, M.G. Pang, Prediction of male fertility using capacitation-associated proteins in spermatozoa, *Mol. Reprod. Dev.* 84 (9) (2017) 749–759.
- [4] L.J. Zak, A.H. Gaustad, A. Bolarin, M. Broekhuijse, G.A. Walling, E.F. Knol, Genetic control of complex traits, with a focus on reproduction in pigs, *Mol. Reprod. Dev.* 84 (9) (2017) 1004–1011.
- [5] A. Kunavongkrit, A. Suriyasomboon, N. Lundeheim, T.W. Heard, S. Einarsson, Management and sperm production of boars under differing environmental conditions, *Theriogenology* 63 (2) (2005) 657–667.
- [6] W.S. Kwon, M.S. Rahman, D.Y. Ryu, Y.J. Park, M.G. Pang, Increased male fertility using fertility-related biomarkers, *Sci. Rep.* 5 (2015), 15654.
- [7] P. Sutovsky, Proteomic analysis of mammalian gametes and sperm-oocyte interactions, *Society of Reproduction and Fertility Supplement* 66 (2009) 103–116.
- [8] V. Labas, L. Spina, C. Belleanne, A.P. Teixeira-Gomes, A. Gargaro, F. Dacheux, J.L. Dacheux, Analysis of epididymal sperm maturation by MALDI profiling and top-down mass spectrometry, *J. Proteome* 113 (2015) 226–243.
- [9] W.S. Kwon, S.A. Oh, Y.J. Kim, M.S. Rahman, Y.J. Park, M.G. Pang, Proteomic approaches for profiling negative fertility markers in inferior boar spermatozoa, *Sci. Rep.* 5 (2015), 13821.
- [10] J.M. Feugang, S.F. Liao, S.T. Willard, P.L. Ryan, In-depth proteomic analysis of boar spermatozoa through shotgun and gel-based methods, *BMC Genomics* 19 (1) (2018) 62.
- [11] C. Perez-Patino, I. Parrilla, I. Barranco, M. Vergara-Barberan, E.F. Simo-Alfonso, J.M. Herrero-Martinez, H. Rodriguez-Martinez, E.A. Martinez, J. Roca, New in-depth analytical approach of the porcine seminal plasma proteome reveals potential fertility biomarkers, *J. Proteome Res.* 17 (3) (2018) 1065–1076.
- [12] O. Chahrouh, D. Cobice, J. Malone, Stable isotope labelling methods in mass spectrometry-based quantitative proteomics, *J. Pharm. Biomed. Anal.* 113 (2015) 2–20.
- [13] R. Moulder, S.D. Bhosale, D.R. Goodlett, R. Lahesmaa, Analysis of the plasma proteome using iTRAQ and TMT-based isobaric labeling, *Mass Spectrom. Rev.* 37 (5) (2018) 583–606.
- [14] Z.C. S. Zhang, Y. Chen, J. Wu, H. Wei, L. Li, Mathematical model for evaluating fertilization abilities of landrace boars and establishing method for mathematical model China Patents CN105046082A issued April 10, 2018.
- [15] C. Pérez-Patino, I. Parrilla, J. Li, I. Barranco, E.A. Martínez, H. Rodríguez-Martínez, J. Roca, The proteome of pig spermatozoa is remodeled during ejaculation, *Molecular Cell Proteomics* MCP 18 (1) (2019) 41–50.

- [16] X.M. Pang, X. Zhou, S.Y. Su, C.Y. Chen, Z.X. Wei, Y.F. Tao, J.L. Liu, Identification of serum biomarkers for ischemic penumbra by iTRAQ-based quantitative proteomics analysis, *Proteomics Clin. Appl.* 13 (5) (2019), e1900009. .
- [17] R.L. Tatusov, N.D. Fedorova, J.D. Jackson, A.R. Jacobs, B. Kiryutin, E.V. Koonin, D.M. Krylov, R. Mazumder, S.L. Mekhedov, A.N. Nikolskaya, B.S. Rao, S. Smirnov, A.V. Sverdlov, S. Vasudevan, Y.I. Wolf, J.J. Yin, D.A. Natale, The COG database: an updated version includes eukaryotes, *BMC bioinformatics* 4 (2003) 41.
- [18] M. Ashburner, C.A. Ball, J.A. Blake, D. Botstein, H. Butler, J.M. Cherry, A.P. Davis, K. Dolinski, S.S. Dwight, J.T. Eppig, M.A. Harris, D.P. Hill, L. Issel-Tarver, A. Kasarskis, S. Lewis, J.C. Matese, J.E. Richardson, M. Ringwald, G.M. Rubin, G. Sherlock, Gene ontology: tool for the unification of biology, The Gene Ontology Consortium, *Nature Genetics* 25 (1) (2000) 25–29.
- [19] X. Mao, T. Cai, J.G. Olyarchuk, L. Wei, Automated genome annotation and pathway identification using the KEGG Orthology (KO) as a controlled vocabulary, *Bioinformatics (Oxford, England)* 21 (19) (2005) 3787–3793.
- [20] M.T. Gallagher, D.J. Smith, J.C. Kirkman-Brown, CASA: tracking the past and plotting the future, *Reprod. Fertil. Dev.* 30 (6) (2018) 867–874.
- [21] L.R. Abeydeera, B.N. Day, Fertilization and subsequent development in vitro of pig oocytes inseminated in a modified tris-buffered medium with frozen-thawed ejaculated spermatozoa, *Biol. Reprod.* 57 (4) (1997) 729–734.
- [22] S.W. Xie, G.T. Li, L.J. Qu, Y. Cao, Q. Wang, J.Y. Zhou, R.H. Zhong, X.J. Guo, Y. Zhu, Identification of new epididymal luminal fluid proteins involved in sperm maturation in infertile rats treated by Dutasteride using iTRAQ, *Molecules (Basel, Switzerland)* 21 (5) (2016).
- [23] P. Li, W. Guo, H. Yue, C. Li, H. Du, X. Qiao, Z. Liu, Q. Zhou, Q. Wei, Variability in the protein profiles in spermatozoa of two sturgeon species, *PLoS One* 12 (10) (2017), e0186003. .
- [24] O. D'Amours, E. Calvo, S. Bourassa, P. Vincent, P. Blondin, R. Sullivan, Proteomic markers of low and high fertility bovine spermatozoa separated by Percoll gradient, *Mol. Reprod. Dev.* 86 (8) (2019) 999–1012.
- [25] K.M. M, A. Kumaresan, S. Yadav, T.K. Mohanty, T.K. Datta, Comparative proteomic analysis of high- and low-fertile buffalo bull spermatozoa for identification of fertility-associated proteins, *Reproduction in domestic animals = Zuchthygiene* 54 (5) (2019) 786–794.
- [26] P. Thuwanut, P. Comizzoli, K. Pruksananonda, K. Chatdarong, N. Songsasen, Activation of adenosine monophosphate-activated protein kinase (AMPK) enhances energy metabolism, motility, and fertilizing ability of cryopreserved spermatozoa in domestic cat model, *J. Assist. Reprod. Genet.* 36 (7) (2019) 1401–1412.
- [27] M.S. Mousavi, A. Shahverdi, J. Drevet, V. Akbarinejad, V. Esmaeili, F.A. Sayahpour, T.R. Topraggaleh, P. Rahimizadeh, A. Alizadeh, Peroxisome Proliferator-Activated Receptors (PPARs) levels in spermatozoa of normozoospermic and asthenozoospermic men, *Syst Biol Reprod Med* 65 (6) (2019) 409–419.
- [28] S. Clark, R.K. Naz, Presence and incidence of izumo antibodies in sera of immunoinfertile women and men, *American Journal of Reproductive Immunology (New York, N.Y.: 1989)* 69 (3) (2013) 256–263.
- [29] J. Shetty, M.J. Wolkowicz, L.C. Digilio, K.L. Klotz, F.L. Jayes, A.B. Diekmann, V.A. Westbrook, E.M. Farris, Z. Hao, S.A. Coonrod, C.J. Flickinger, J.C. Herr, SAMP14, a novel, acrosomal membrane-associated, glycosylphosphatidylinositol-anchored member of the Ly-6/urokinase-type plasminogen activator receptor superfamily with a role in sperm-egg interaction, *J. Biol. Chem.* 278 (33) (2003) 30506–30515.
- [30] A.-f. Tang, Z.-d. Yu, Y.-t. Gui, X. Guo, X.-x. Li, W.-x. Liu, H. Zhu, Z.-m. Cai, Expression and bioinformatics analysis of SPACA4 in human and mice, *J. Reprod. Contracept.* 19 (1) (2008) 9–15.
- [31] A. Malcher, N. Rozwadowska, T. Stokowy, T. Kolanowski, P. Jedrzejczak, W. Zietkowiak, M. Kurpisz, Potential biomarkers of nonobstructive azoospermia identified in microarray gene expression analysis, *Fertil. Steril.* 100 (6) (2013) 1686–94. e1–7).
- [32] M.J. Ferrer, W. Xu, J. Shetty, J. Herr, R. Oko, Plasminogen improves mouse IVF by interactions with inner acrosomal membrane-bound MMP2 and SAMP14, *Biol. Reprod.* 94 (4) (2016) 88.
- [33] H. Aydin, A. Sultana, S. Li, A. Thavalingam, J.E. Lee, Molecular architecture of the human sperm IZUMO1 and egg JUNO fertilization complex, *Nature* 534 (7608) (2016) 562–565.
- [34] K. Kato, Y. Satouh, H. Nishimasu, A. Kurabayashi, J. Morita, Y. Fujihara, A. Oji, R. Ishitani, M. Ikawa, O. Nureki, Structural and functional insights into IZUMO1 recognition by JUNO in mammalian fertilization, *Nat. Commun.* 7 (2016), 12198. .
- [35] S.A. Young, H. Miyata, Y. Satouh, M. Muto, M.R. Larsen, R.J. Aitken, M.A. Baker, M. Ikawa, CRISPR/Cas9-mediated mutation revealed cytoplasmic tail is dispensable for IZUMO1 function and male fertility, *Reproduction (Cambridge, England)* 152 (6) (2016) 665–672.



OPEN ACCESS

EDITED BY

Jose Antonio Tapia,
University of Extremadura, Spain

REVIEWED BY

Alexander Grahofer,
University of Bern, Switzerland
Kampon Kaeoket,
Mahidol University, Thailand

*CORRESPONDENCE

Hengxi Wei

✉ weihengxi@scau.edu.cn

Shouquan Zhang

✉ sqzhang@scau.edu.cn

RECEIVED 22 November 2023

ACCEPTED 11 January 2024

PUBLISHED 31 January 2024

CITATION

Zhu X, Zhang X, Zhang Y, Li J, Li S, Zhang S,
Li L, Meng L, Wei H and Zhang S (2024)

Cloprostenol sodium improves reproductive
performance of multiparous sows during
lactation.

Front. Vet. Sci. 11:1342930.

doi: 10.3389/fvets.2024.1342930

COPYRIGHT

© 2024 Zhu, Zhang, Zhang, Li, Li, Zhang, Li,
Meng, Wei and Zhang. This is an open-access
article distributed under the terms of the
Creative Commons Attribution License
(CC BY). The use, distribution or reproduction
in other forums is permitted, provided the
original author(s) and the copyright owner(s)
are credited and that the original publication
in this journal is cited, in accordance with
accepted academic practice. No use,
distribution or reproduction is permitted
which does not comply with these terms.

Cloprostenol sodium improves reproductive performance of multiparous sows during lactation

Xuedan Zhu, Xinke Zhang, Yuqing Zhang, Jiahao Li, Siqi Li,
Siqi Zhang, Li Li, Li Meng, Hengxi Wei* and Shouquan Zhang*

State Key Laboratory of Swine and Poultry Breeding Industry, National Engineering Research Center for Breeding Swine Industry, Guangdong Provincial Key Lab of Agro-animal Genomics and Molecular Breeding, College of Animal Science of South China Agricultural University, Guangzhou, China

This study aimed to determine the effect of prostaglandin $F_{2\alpha}$ ($PGF_{2\alpha}$) analog (*D*-cloprostenol sodium and *DL*-cloprostenol sodium) administration on the milk yield of multiparous sows (MS) and piglet growth performance. In total, 320 Landrace×Yorkshire parturient MS were randomly divided into three groups on day 115 of pregnancy: without treatment ($N = 50$), with $75\mu g$ *D*-cloprostenol sodium ($N = 137$), and with $200\mu g$ *DL*-cloprostenol sodium ($N = 133$). After delivery, the sows treated with *D*-cloprostenol sodium and *DL*-cloprostenol sodium were randomly allocated into three subgroups, respectively: (i) no additional treatment after farrowing; (ii) administration of cloprostenol sodium at 3 h and 5 days after farrowing; and (iii) administration of cloprostenol sodium at 3 h, 5 days, and 10 days after farrowing. Cloprostenol sodium effectively induced sows to synchronize parturition approximately 23 h after administration and increased the daytime delivery rates ($p < 0.05$). Compared with *DL*-cloprostenol sodium, *D*-cloprostenol sodium shortened the farrowing duration and birth interval of sows for inducing farrowing ($p < 0.05$). Moreover, we observed that a single administration of both *D*-cloprostenol sodium and *DL*-cloprostenol sodium a day before delivery significantly reduced the rates of stillborn piglets type II in MS ($p < 0.05$). Compared to no treatment and single treatment with cloprostenol sodium, quartic treatments with cloprostenol sodium significantly increased the daily feed intake of MS, litter weight after weaning, and average daily gain of piglets ($p < 0.05$). Cloprostenol sodium improved the 21-day milk yield, with *D*-cloprostenol sodium showing the best effect, which increased lactation ability by 30.30% (176.72 kg vs. 135.63 kg) ($p < 0.05$). *DL*-cloprostenol sodium followed closely, increasing lactation ability by approximately 25.00% (169.71 kg vs. 135.63 kg) ($p < 0.05$). During lactation, sows administered with *D*-cloprostenol sodium observed increased serum prolactin levels. Compared to untreated sows, the sows administered with *D*-cloprostenol sodium and multiple *DL*-cloprostenol sodium visibly shortened the weaning-to-estrus interval (WEI) and weaning-to-service interval (WSI) ($p < 0.05$). Furthermore, quartic injections of *D*-cloprostenol sodium resulted in an 18 percentage point increase in the pregnancy rate of breeding sows compared to controls (82.61% vs. 64.58%) ($p > 0.05$). In summary, cloprostenol sodium could enhance the reproductive performance of MS, particularly in terms of lactation performance. Additionally, the effect of quartic injections of *D*-cloprostenol sodium was the most pronounced.

KEYWORDS

D-cloprostenol sodium, *DL*-cloprostenol sodium, reproductive performance, milk performance, farrowing induction, multiparous sow

1 Introduction

The lactation ability of sows is the most crucial factor affecting piglet growth rate and the number of piglets weaned per sow per year (PSY). The analysis of the milk yield from a pig farm in Denmark revealed that approximately 23.5% of colostrum (the milk within 24 h postpartum) yield were less than 5 kg, while only 30% of the sow's colostrum yield exceeded 7 kg (1). The colostrum yield dose was not equal to the colostrum intake of sucking piglets, and failure to obtain sufficient colostrum prior to weaning is one of the most important causes of piglet mortality. Hassan et al. found that 23.5% of piglets had a colostrum intake below 200 g, while 36% had a colostrum intake below 250 g (2). When the colostrum intake of piglets is less than 200 g, the pre-weaning mortality rates can reach as high as 43.3%; however, pre-weaning mortality can be reduced to 7.1% when the colostrum intake of piglets was more than 200 g (3). Induced parturition may affect colostrum yield in sows. The administration of oxytocin significantly reduces both the colostrum yield in sows and the colostrum intake by piglets, while PGF_{2α} analogs compensate for the deficiency of oxytocins (4). The timing of induced parturition also affects the composition of colostrum. Early initiation of delivery using cloprostenol sodium reduces the levels of IgG and total protein in colostrum (5).

The milk yield of the sows fails to satisfy the energy and protein requirements of piglets (9–10 pigs/litter) beyond day 8 of lactation, resulting in a gradual widening of this gap throughout lactation; as a result, milk production only meets approximately 50% of the needs of 21-day-old piglets for maximum growth (6). Stimulating mammary gland development represents the most practical approach to enhance milk yield in sows. Rapid breast development consists of three stages. The initial stage of rapid development occurs from 90 days of age until puberty and has received limited research attention to date. The second stage occurs during the one-third period after gestation and is the mature stage. The third stage occurs within the first 2 weeks of lactation, with limited studies available on this phase (7). Lactation deficiency is caused by both hereditary and acquired endocrine disorders (8). It has been reported that continuous injection of recombinant pig prolactin (PRL) for 28 days in prepubertal gilts weighing 75 kg can increase the content of parenchymal tissue, dry matter, total protein, and total DNA by upregulating the mRNA levels of PRL receptor (PRLR), STAT5A, and STAT5B in mammary tissues; thus, this treatment effectively promotes mammary gland development in gilts (9). An increasing number of studies aim to regulate the lactation performance of sows by exogenous hormones. The gilts were injected with 5 mg/day of porcine growth hormone on day 89 of pregnancy, and their mammary glands were collected for analysis on day 110 of pregnancy. The results showed that the treatment group exhibited a significant increase in the mass of mammary gland parenchyma (1,922.2 g vs. 1,576.1 g), and the mammary gland parenchyma of the treatment group contained more protein, glucose, DNA, and RNA (10). Furthermore, exogenous hormones such as estradiol and PGF_{2α} have been demonstrated to induce lactation in 81.3% of non-pregnant sows within 38–59 days after mating (11).

Maternal factors potentially affecting lactation include parity, preterm birth, dystocia, and residual placental fragments (8). PGF_{2α} serves as the main luteolytic factor (12), which can dissolve the corpus luteum and contract uterine smooth muscle. Consequently, PGF_{2α} is frequently used for estrus and farrowing synchronization in livestock.

Cloprostenol sodium is one of the most important synthetic analogs of PGF_{2α}, which is mainly eliminated by the lungs and kidneys with a half-life of up to 3 h (13, 14). Cloprostenol sodium (*DL*-cloprostenol sodium) exists as two optical isomers, which can be divided into *D*-isomer and *L*-isomer according to the relative configuration of the chiral carbon atoms. They are named *D*-cloprostenol sodium and *L*-cloprostenol sodium, respectively. The proportions of the two enantiomers in cloprostenol sodium are equal (15). *DL*-cloprostenol sodium has been widely used in livestock production for many years, while *D*-cloprostenol sodium has not been extensively used. Experimental evidence showed that *D*-cloprostenol sodium exhibited approximately three to four times greater efficacy in initiating luteal dissolution compared to *DL*-cloprostenol sodium, indicating that *L*-cloprostenol sodium may have no effect on luteal lysis or even demonstrate a reverse effect (15).

In light of the above findings, PGF_{2α} analogs, as uterine contractile agents, have been shown to accelerate placental discharge, reduce the incidence of uterine inflammation, and also enhance delivery performance and colostrum composition in sows. Although *DL*-cloprostenol sodium and *D*-cloprostenol sodium belong to PGF_{2α} analogs, their effects on lactating performance in sows have not been reported. The first 2 weeks of lactation are a crucial stage for promoting breast development and lactation. Meanwhile, as piglets grow, sows' milk in the middle and late stages of lactation may not adequately meet their growth and development needs. Consequently, we designed this experiment to investigate the effects of induced parturition before farrowing and injection with either 75 μg/time *D*-cloprostenol sodium (at the full-recommended dosage) or 200 μg/time *DL*-cloprostenol sodium (at the full-recommended dosage) at 3 h, 5 days, and 10 days postpartum on reproductive performance, milk quality, estrous cycle, serum lactation-related hormones in multiparous sows (MS), and the lactation growth performance of offspring piglets during lactation. These results may provide valuable technical guidance for the utilization of PGF_{2α} analogs, especially *D*-cloprostenol sodium, in sow lactation management.

2 Materials and methods

2.1 Experimental design

This study was conducted in a swine breeding herd consisting of 2,000 sows located in northern Guangdong between June and September 2022. The average daily minimum and maximum temperatures during the experimental period ranged from 28.0°C to 35.0°C. The 320 Yorkshire × Landrace MS randomly selected for this study had the same genetic background, a parity of 2–3, and similar body weights (approximately 185–250 kg), back fat thickness (approximately 14–23 mm), litter size (6–18 alive piglets), and other reproductive performance. The experimental MS were obtained from Guangdong Guanghui Huifeng Farm (Shaoguan City, Guangdong Province, China). They were reared in a conventional semi-open housing system. The experimental sows were transferred to the farrowing house 5–7 days prior to the estimated farrowing date. They were individually housed in crates until the weaning period, which occurred 21 ± 1 days after farrowing.

The experimental sows were classified into three groups based on the dose of *D*-cloprostenol sodium or *DL*-cloprostenol sodium

administered via an intramuscular injection in the neck between 11:30 a.m. and 12:00 a.m. 1 day prior to the expected delivery date of MS: Some sows underwent natural farrowing ($N=50$), whereas the remaining received a single administration of 75 μg (1 mL) *D*-cloprostenol sodium (75 $\mu\text{g}/\text{mL}$, 1 mL/sow, Ningbo Second Hormone Factory, Zhejiang Province, China; $N=137$) and 200 μg (2 mL) *DL*-cloprostenol sodium (100 $\mu\text{g}/\text{mL}$, 2 mL/sow, Ningbo Second Hormone Factory, Zhejiang Province, China; $N=133$) (Figure 1). Sows that had begun to deliver before 11:30 a.m. on day 115 of pregnancy were excluded from the experiment. The original litter weight and litter sizes of the piglets were assessed immediately after parturition. The sow injected with *D*-cloprostenol sodium ($n=1$) and *DL*-cloprostenol sodium ($n=1$) died due to dystocia during parturition. The occurrence of postpartum paralysis was observed in one sow after the injection of *DL*-cloprostenol sodium, while no clinical signs were reported in the others.

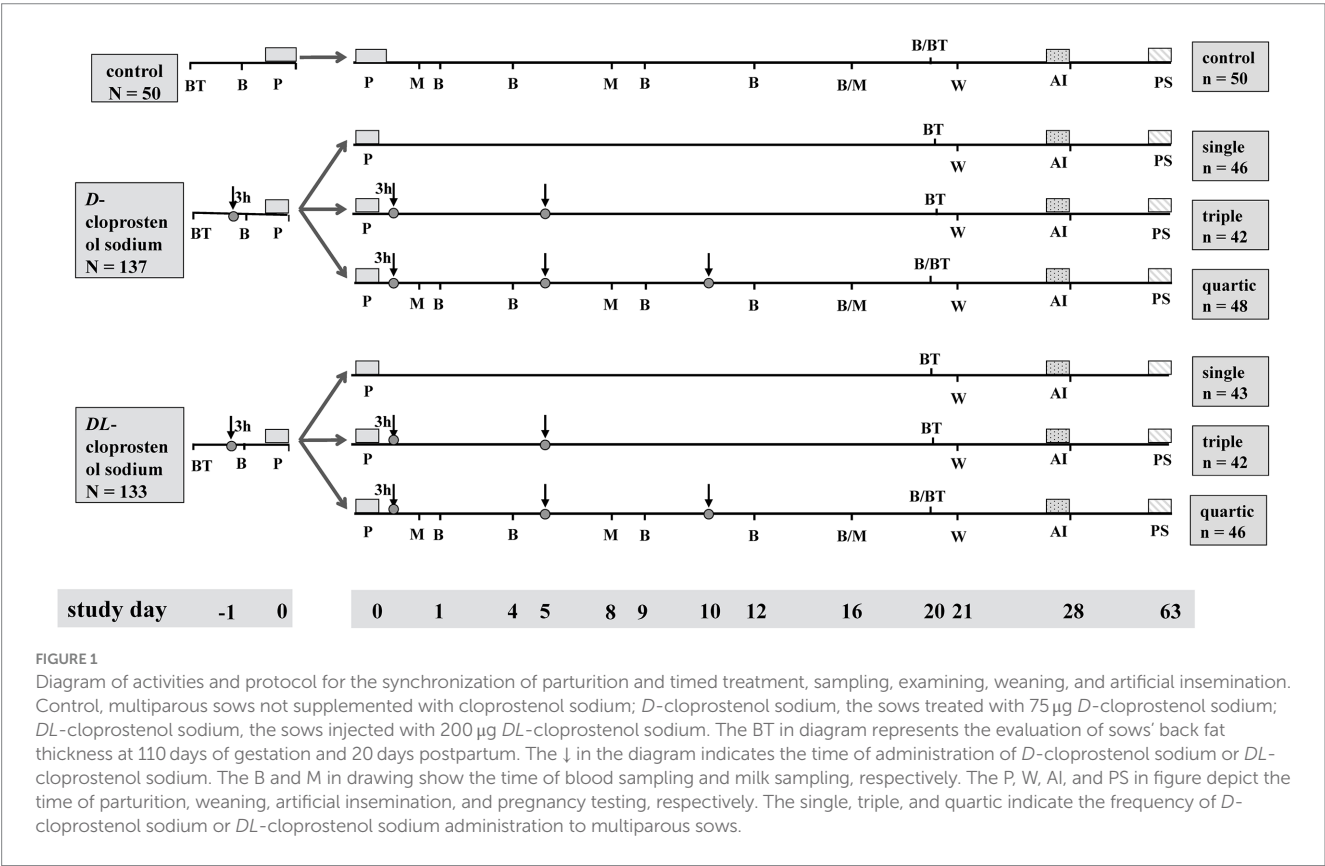
To evaluate the impact of cloprostenol sodium on lactation in MS, piglets were appropriately cross-fostered within the group within 3 h after delivery. However, piglets that were too small (<0.8 kg) and/or too weak (unable to stand or crawl) were swapped with non-trial piglets (0.8–1.2 kg), which ultimately ensured that the number of piglets per litter averaged approximately 10, with a balanced gender ratio that was essentially identical. For the milk performance study, the remaining sows that did not receive any oxytocin during farrowing with *D*-cloprostenol sodium ($N=136$) were randomly allocated into three subgroups: (i) the sows were not additionally treated postpartum ($n=46$); (ii) the sows were administered double doses of 75 $\mu\text{g}/\text{time}$ *D*-cloprostenol sodium at 3 h and 5 days after the end of farrowing, respectively ($n=42$); and

(iii) the sows were administered triple doses of 75 $\mu\text{g}/\text{time}$ *D*-cloprostenol sodium at 3 h, 5 days, and 10 days after the end of farrowing, respectively ($n=48$) (Figure 1). In all subgroups, the number of live piglets per litter and the weight of each litter were uniformly consistent.

The sows injected with *DL*-cloprostenol sodium received the same treatment. The remaining sows ($N=131$) were randomly allocated into three subgroups: (i) the sows were not additionally treated after farrowing ($n=43$); (ii) the sows were administered 200 $\mu\text{g}/\text{time}$ *DL*-cloprostenol sodium at 3 h and 5 days after the end of farrowing, respectively ($n=42$), and (iii) the sows were administered 200 $\mu\text{g}/\text{time}$ *DL*-cloprostenol sodium at 3 h, 5 days, and 10 days after the end of farrowing, respectively ($n=46$) (Figure 1). In all subgroups, the number of live piglets per litter and the litter weight were also consistent, respectively. During the pre-weaning growth period, piglets were unable to undergo cross-fostering among different subgroups.

2.2 Parturition process monitoring and postpartum management

Sows gave birth in calm environments. Two research teams, consisting of a total of six individuals, carefully supervised the parturition process for 24 h and ensured that there was at least one recording personnel in each farrowing house to record the timing of each piglet's birth and the expulsion of each placenta in the sow. Parturition duration was defined as the period from the first to the last piglet delivery, and placental expulsion duration was defined as the



period from the first to the last placental expulsion. Birth assistance was provided at an interval of >60 min after the parturition of the previous piglet or when the sows did not give birth to the first piglet for >4 h after breaking the amniotic fluid. Birth assistance included applying pressure to the sows' belly and manually extracting the fetus or placenta. The method of pressing the belly was as follows: First, the sow's udders were gently massaged using sterilized bare feet, inducing a constricted appearance of the sow's body and resulting in an arched belly. Subsequently, pressure was slowly applied from the front of the arch (close to heart) to the back (close to tail), which stimulated sustained power in the sow and promoted rapid piglet production. The administration of oxytocin should be avoided during the process of inducing farrowing. The total number of piglets born, the number of piglets born alive, the number of piglets born weak, and the number of stillborn piglets were also recorded at farrowing. Stillbirths can be classified into two types based on the time of death (16). Stillborn piglet type I includes deaths that occurs before the sow delivers and is most commonly attributed to infectious causes. The fetal death exhibits dull, pale skin without luster or a rotten body. Stillborn piglet type II is often associated with dystocia and intrauterine and birth canal asphyxia during parturition. The fetal death is characterized by a fresh, ruddy skin and an extended tongue in a state of asphyxia, with the mouth and nose obstructed by mucus.

Daytime was defined as the period of 0800–2,200 h based on the day-shift working time of the midwifery technical personnel, and the nighttime was defined as the period of 2,200–0800 h. If the sow delivered exactly at 0800 or 2,200 h, it would be divided according to the period when most piglets in the litter were born. At the end of the farrowing process, all MS were injected with a non-steroidal anti-inflammatory drug (tolfenamic acid, 2 mg/kg, Sivea (Qingdao) Bio pharmaceutical Co., Ltd., Shandong Province, China), an antibiotics (ceftiofur, 10 mg/kg, Zoetis Suzhou Biopharmaceutical Co., Ltd., Jiangsu Province, China), and a multivitamin (vitamin A, D and E; 10 mL/sow; Hebei Yuanzheng Pharmaceutical Co., Ltd., Hebei Province, China) through the neck muscles on days 1–3 postpartum. Piglets received the same care and supervision according to pig farm regulations, which included tail docking, tooth clipping on the first day of life, and intramuscular administration of iron supplement (iron dextran, 1 mL/piglet, Sivea (Qingdao) Bio pharmaceutical Co., Ltd., Shandong Province, China) on the third day of life. The sows were provided with the same feed and drinking water according to the management of the pig farms.

2.3 Collection and determination of serum hormones and milk components

In the quartic group, which includes the quartic *D*-cloprostenol sodium and *DL*-cloprostenol sodium groups, as well as the control group, three sows were randomly selected from each group for blood sample collection via the anterior jugular vein. Blood was collected from adult sows using the standing fixed method. The breeder lifted the upper jaw of the sow with a fixed rope to expose both sides of the prethoracic fossa. Another breeder put a needle in the direction of the low and vertical concave bottom of the right prethoracic fossa, took the required amount of blood, pressed the needle site with a cotton ball to stop bleeding, and relieved the sow. During the course of the study, a total of seven blood collections were performed on the selected sows, with 3 mL of blood samples being obtained in each instance. The day of delivery

was designated as day 0. The initial blood samples were conducted at 1,500 h on day 115 of the sows' gestation (day −1), 3 h post-administration of the first dose. Other blood samples were collected at 0900 h on days 1, 4, 9, 12, 16, and 20 after farrowing (Figure 1). After collection, all blood samples were incubated at room temperature ($30 \pm 2^\circ\text{C}$) for 10 min, followed by centrifugation at 4,000 r/min for 20 min. The serum was immediately sub-packed and transferred to -20°C for preservation. Serum samples were sent on dry ice to Beijing North Institute of Biotechnology Co., Ltd. to detect the concentrations of estradiol-17 β (E_2), PRL, and cortisol (COR) by radioimmunoassay and progesterone (P_4) using enzyme-linked immunosorbent assay.

Three sows, excluding the sows selected for blood collection, were randomly selected for milk collection from the quartic *D*-cloprostenol sodium group, quartic *DL*-cloprostenol sodium group, and control groups (Figure 1). The milk samples were collected three times, with each collection consisting of 2 mL. The colostrum was collected within a period of 12 h after farrowing, and mature milk was obtained by administering an injection of 10 IU (1 mL) oxytocin (10 IU/1 mL, 1 mL/sow, Ningbo Second Hormone Factory, Zhejiang Province, China) in the neck on 8 and 16 days post-farrowing. Milk samples were dispatched to Shanghai Enzyme Union Biotechnology Co., Ltd. under dry ice conditions for the purpose of quantifying fat, protein, and lactose concentrations through infrared spectroscopy.

2.4 Back fat and daily feed intake determination in MS

The back fat thickness of all MS was evaluated upon entering the farrowing house and on 20 days postpartum, utilizing an Abdominal Convex Probe and a Veterinary B-mode ultrasonic diagnostic instrument (WED-3000 V, Shenzhen Well. D Medical Electronics Co., Ltd., Guangdong Province, China). Each pig is measured three times simultaneously, and the average value was recorded. An ultrasound probe was placed approximately 6.5 cm from the dorsal midline on the last rib curve to measure the back fat thickness. The lactational back fat loss was calculated as the difference between back fat thickness when entering the farrowing house and on day 20 of lactation (Figure 1).

The daily feed intake of the MS was recorded from delivery until day 21 of lactation. The farrowing house is equipped with automatic feeders for each crate, ensuring precise quantification of the amount of feed for each individual feeding. Postpartum sows were fed twice a day at 0800 h and 1,700 h. On the day of parturition (day 0), an initial feeding amount of 0.5 kg was provided, followed by a daily increment of 1 kg until day 5. Subsequently, the feeder scale was adjusted based on each sow's previous intake to optimize and maximize *ad libitum* feeding until weaning. It is worth noting that the remaining feed in the tank needs to be weighed and recorded before each feeding. These feed refusals should be summarized at weaning. Subsequently, a statistical analysis was conducted to determine the daily feed intake of each sow from parturition until weaning.

2.5 Statistics of litter weaned weight and estimation of milk power

We collected the weights of newborn litter and weaning litter on day 21 of lactation. The average daily weaning gain (ADWG, g/d) of

TABLE 1 Effect of different cloprostenol sodium on the process of synchronized delivery in parturient sows (Means ± SD & Percentage).

Groups ¹	Control	D-cloprostenol sodium	DL-cloprostenol sodium	p-value
Number of sows	50	137	133	/
Gestation length, d	117.02 ± 1.02 ^a	115.91 ± 0.38 ^b	115.95 ± 0.46 ^b	< 0.001
Administration-to-delivery intervals, h ²	48.94 ± 26.68 ^a	22.93 ± 7.58 ^b	23.48 ± 8.52 ^b	< 0.001
Farrowing duration, min ³	305.70 ± 171.88 ^a	182.95 ± 73.16 ^c	217.33 ± 87.94 ^b	< 0.001
Birth interval, min	31.08 ± 19.61 ^a	17.89 ± 6.49 ^c	21.61 ± 7.91 ^b	< 0.001
Placenta expulsion duration, min ⁴	254.56 ± 87.47 ^a	180.72 ± 62.08 ^b	194.51 ± 78.02 ^b	< 0.001
Piglets with birth interval > 30 min, %	42.00 ^a	8.00 ^b	14.29 ^b	< 0.001
Farrowing assistance, %	10.00	8.03	15.03	0.342
Sow mortality at dystocia, %	0.00	0.73	0.75	0.454
Daytime delivery, % ⁵	42.00 ^b	92.70 ^a	87.22 ^a	< 0.001

¹Multiparous sows underwent natural farrowing (control group), and sows treated with a single dose of 75 µg *D*-cloprostenol sodium or 200 µg *DL*-cloprostenol sodium were induced to undergo parturition. ²No additional medication was given in control group, and the time from 1,200 h on day 115 of pregnancy to delivery was defined as the administration-to-delivery intervals. Other groups record according to the actual situation. ³The period from the first to the last piglet delivery. ⁴The period from the first to the last placental expulsion. ⁵Daytime was defined as 0800–2,200 h based on the day-shift working time of the midwifery technical personnel, and the nighttime was defined as 2,200–0800 h. If the sow was delivered at exactly 0800 or 2,200 h, it was divided according to the period when most piglets in the litter were born. ^{a,b,c}Different superscripts within rows differ significantly (*p* < 0.05).

the piglets from birth to weaning was calculated, as shown in Equation (1). The lactation ability refers to the algorithm of Lawlor et al. (17) as shown in Equation (2).

$$\text{ADWG (g/d)} = \left[\frac{\text{average body weight at weaning (g)}}{\text{—average body weight at birth (g)}} \right] / 21 \text{ days} \quad (1)$$

$$\begin{aligned} 21 - \text{day milk yield (kg)} &= \text{piglets of ADWG (g/d)} \times 21 \text{ days} \\ &\times \text{number of weaned piglets} \\ &\times 4 / 1000 \end{aligned} \quad (2)$$

2.6 Statistics of estrus after 7 days of weaning

The transfer of all MS from the parturition housing to the mating housing was completed on day 21 of lactation. According to regulations for the pig farm, boars were migrated twice daily to the mating housing for stimulation after weaning to induce sows' estrus. Data regarding the timing of estrus and artificial insemination (AI), the number of estrus and mating events within 7 days of weaning, and the number of pregnancies from 28 to 35 days after mating in weaned MS were recorded (Figure 1).

2.7 Statistical analyses

Huifeng Farm procedure data were organized using Excel 2013 software (Microsoft, Redmond, Washington, USA). Statistical analyses were performed using the GLM procedure of IBM SPSS Statistics 20 software (IBM, Armonk, NY, USA) and a two-way ANOVA of GraphPad Prism software (Santiago, CA, USA). For the experimental investigation of synchronized delivery, the GLM procedure included the different treatments (blank drug, *D*-cloprostenol sodium, and *DL*-cloprostenol sodium) were taken as fixed effects, and back fat

thickness at 110 days of gestation served as a covariate. Farrowing duration, birth interval, placenta expulsion duration, gestation length, administration-to-delivery intervals, litter size, and other indicators were treated as response variables;

Similarly, for the purpose of the lactation experiment, GLM included different treatments, the number of treatments [zero, single, triple and quartic injection(s)], and the interaction effects between them, all of which were taken as fixed effects. The pre-delivery back fat thickness was utilized as a covariable to examine the response variables, including daily feed intake, number of weaned piglets, total litter weight at weaning, average piglet weight at weaning, piglets of ADWG, 21-day milk yield, weaning back fat thickness, back fat loss, weaning-to-estrus interval (WEI), and weaning-to-service interval (WSI).

In addition, employing back fat thickness at 110 days of gestation as a covariate, we analyzed binary dependent variables such as estrus rates, conception rates, daytime delivery rates, rates of piglets with birth interval > 30 min, farrowing assistance rates, Stillborn Type I and Type II rates, and weak piglets rates using logistic regression model. GraphPad Prism software was employed to generate all line charts and bar charts, and the discrepancies were examined through a two-way ANOVA. The results were expressed as mean ± SD or percentage. Statistical significance was set at a *p* of <0.05.

3 Results

3.1 Delivery process

Delivery data were collected from 320 sows during the experiment (Table 1). In our experiment, oxytocin was not used to assist with the delivery. The administration of cloprostenol sodium synchronized the farrowing duration of the sows (Table 1). Compared with the control sows (from 1,200 h on day 115 of gestation until delivery), the sows induced by *D*-cloprostenol sodium and *DL*-cloprostenol sodium exhibited more concentrated delivery approximately 23 h after administration, resulting in significantly reduced

TABLE 2 Effect of synchronized delivery induced by different cloprostenol sodium on litter performance of multiparous sows (Means \pm SD & percentage).

Groups ¹	Control	D-cloprostenol sodium	DL-cloprostenol sodium	p-value
Number of sows	50	136	132	/
Number of piglets ²	573	1,550	1,500	/
Total number of born piglets	11.46 \pm 1.78	11.40 \pm 2.20	11.36 \pm 2.29	0.978
Number of born alive piglets	10.28 \pm 1.28	10.44 \pm 1.26	10.29 \pm 1.18	0.510
Number of born strong piglets ³	10.00 \pm 1.26	10.13 \pm 1.32	9.77 \pm 1.53	0.150
Born weak piglets, % ⁴	3.32	2.52	2.87	0.594
Stillborn piglet type I, % ⁵	2.97	2.52	3.07	0.638
Stillborn piglet type II, % ⁶	5.76 ^a	1.74 ^c	3.13 ^b	< 0.001
Total litter weight at birth, kg	14.93 \pm 2.63	15.35 \pm 2.65	15.05 \pm 2.64	0.492
Average piglet weight at birth, kg	1.46 \pm 0.23	1.48 \pm 0.23	1.47 \pm 0.23	0.875

¹Multiparous sows underwent natural farrowing (control group), and sows treated with a single dose of 75 μ g D-cloprostenol sodium or 200 μ g DL-cloprostenol sodium were induced to undergo parturition. ²Total number of piglets delivered by sows in each group. ³Piglets that are alive, weigh equal to or greater than 800 g, and suckle colostrum normally. ⁴Piglets that weigh less than 800 g or do not suckle colostrum. ⁵Fetal death occurs before the sow delivers and includes mummified piglets. ⁶Fetal death, occurring during a sow's parturition, is attributed to asphyxia within the birth canal and intrauterine. ^{a,b,c}Different superscripts within rows differ significantly ($p < 0.05$).

administration-to-delivery intervals of sows ($p < 0.05$). Administration started on day 115 of gestation at 1,130–1,200 h, followed by concentrated delivery from 1,000 to 1,100 h the next day. Additionally, in comparison with the control sows (42.00%), the sows induced D-cloprostenol sodium (92.70%) and DL-cloprostenol sodium (87.22%) exhibited significantly higher daytime delivery rates ($p < 0.05$). The treatment sows exhibited significantly shortened farrowing duration, birth interval, and placenta expulsion duration in comparison with the control sows ($p < 0.05$). The farrowing duration (182.95 min vs. 217.33 min, $p < 0.05$) and birth interval (17.89 min vs. 21.61 min, $p < 0.05$) were shorter when using D-cloprostenol sodium in comparison with DL-cloprostenol sodium. However, placenta expulsion duration induced by D-cloprostenol sodium did not show any significant differences compared to DL-cloprostenol sodium ($p < 0.05$).

The incidence of piglets with birth intervals >30 min in sows treated with D-cloprostenol sodium (8.00%) and DL-cloprostenol sodium (14.29%) was significantly lower than that in the control sows (42.00%) ($p < 0.05$). Birth assistance was observed for each group ($p = 0.342$): control group (10.00%), D-cloprostenol sodium group (8.03%), and DL-cloprostenol sodium group (15.03%). In contrast, the incidence of birth assistance in sows appeared to be reduced with D-cloprostenol sodium; however, no statistically significant difference was observed compared to the treatment of DL-cloprostenol sodium ($p > 0.05$). One dystocia that resulted in non-survival occurred in each sow's induced parturition, one with D-cloprostenol sodium, and one with DL-cloprostenol sodium. No deaths occurred in the control sows. However, no significant differences were observed among the groups ($p = 0.454$).

3.2 Newborn piglets' characteristics

The litter sizes of sows naturally farrowing compared with those treated with cloprostenol sodium approximately 23 h before farrowing (referred to as 24 h before farrowing for convenience) are shown in Table 2. Compared to the control group (5.76%), the incidence of

Stillborn Type II was lower in sows treated with D-cloprostenol sodium (1.74%) and DL-cloprostenol sodium (3.13%) ($p < 0.05$). Additionally, the rate of Stillborn Type I in the D-cloprostenol sodium group was less than that in the DL-cloprostenol sodium group ($p < 0.05$). There were no significant differences observed among all groups regarding rates of born weak piglets, Stillborn Type I ($p > 0.05$).

After farrowing, the MS treated with D-cloprostenol sodium and DL-cloprostenol sodium were randomly allocated into three subgroups (Figure 1). Remarkably, one sow exhibited postpartum paralysis symptoms in the DL-cloprostenol sodium group; thus, this sow would be excluded from subsequent trials. On average, there were no differences observed in back fat thickness on day 110 of gestation, adjusted litter size, and litter weight (Tables 3, 4).

3.3 Back fat change and daily feed intake of SOWS

The experiment excluded a total of eight sows due to agalactia, paralysis, or other diseases during lactation. One in each of the triple D-cloprostenol sodium, single DL-cloprostenol sodium, triple DL-cloprostenol sodium, and quartic D-cloprostenol sodium groups were excluded from the test of lactation ability. Additionally, two in each of the control and quartic D-cloprostenol sodium groups were excluded from the test data statistics. Daily feed intake and back fat loss of the sows in each group during lactation are shown in Table 3.

There were no significant differences in back fat thickness between sows on day 110 of gestation and day 20 of lactation ($p > 0.05$), and the observed back fat loss during lactation was not significant ($p > 0.05$). Moreover, the feed intake of sows exhibited an increase in proportion to the number of postpartum administration of cloprostenol sodium (Table 3). The mean daily feed intake of sows in the experimental group receiving triple and quartic doses of cloprostenol sodium was significantly higher compared to that of the sows not treated and administered with a single drug ($p < 0.05$). Under an identical number of treatments, no significant correlation was observed between daily food intake and drug type or dosage ($p > 0.05$).

TABLE 3 Effects of different injections of cloprostenol sodium on back fat and daily feed intake in sows during lactation (Means ± SD).

Variables	Control ¹	D-cloprostenol sodium ²			DL-cloprostenol sodium ³			p-values ⁴		
		Single	Triple	Quartic	Single	Triple	Quartic	Drug	Time	Int
Number of sows ⁵	50	46	42	48	43	42	46	/	/	/
Back fat thickness on day 110 of gestation, mm ⁶	17.07 ± 4.53	16.70 ± 4.86	17.48 ± 6.97	17.31 ± 6.11	16.77 ± 5.30	18.10 ± 6.56	17.01 ± 4.81	/	/	/
Number of weaned sows	48	46	41	46	42	41	45	/	/	/
Back fat thickness on day 20 of lactation, mm	15.19 ± 4.34	14.68 ± 4.22	15.79 ± 5.10	15.42 ± 4.91	14.42 ± 3.99	16.07 ± 5.41	14.94 ± 4.48	0.594	0.768	0.986
Back fat loss, mm	2.03 ± 4.13	2.01 ± 2.36	1.85 ± 3.27	1.88 ± 2.70	2.07 ± 3.34	2.12 ± 2.83	2.18 ± 1.74	0.594	0.768	0.986
The daily feed intake, kg	5.07 ± 0.69 ^b	5.25 ± 0.65 ^b	5.71 ± 0.57 ^a	5.83 ± 0.74 ^a	5.16 ± 0.66 ^b	5.61 ± 0.56 ^a	5.64 ± 0.76 ^a	0.121	< 0.001	0.630

^{1,2,3}Multiparous sows without any additional treatment (control). Sows were administered a single dose of 75 µg/time D-cloprostenol sodium or 200 µg/time DL-cloprostenol sodium, which was induced 24 h before delivery (Single); sows were administered a triple dose of cloprostenol sodium, 24 h before delivery, and again 3 h and 5 days after delivery (Triple); sows were administered four doses of cloprostenol sodium, 24 h before delivery, and again 3 h, 5 days, and 10 days after delivery (Quartic). ⁴p-values include main effects of drugs (control or cloprostenol sodium) and times of treatments (Time) and the interaction between drug and times (Int). ^{5,6}After parturition, sows treated with D-cloprostenol sodium and DL-cloprostenol sodium were randomly divided into three groups based on different postpartum treatment methods. The back fat thickness of sows in each subgroup was recorded before parturition. ^{ab}Different superscripts within rows differ significantly ($p < 0.05$).

TABLE 4 Effects of different injections of cloprostenol sodium on litter weight of weaned piglets and milk yield of sows during lactation (Means ± SD).

Variables	Control ¹	D-cloprostenol sodium ²			DL-cloprostenol sodium ³			p-values ⁴		
		Single	Triple	Quartic	Single	Triple	Quartic	Drug	Time	Int
Number of sows ⁵	50	46	42	48	43	42	46	/	/	/
Litter size ⁶	10.34 ± 1.19	10.43 ± 1.36	10.44 ± 1.27	10.48 ± 1.89	10.40 ± 1.43	10.34 ± 1.01	10.21 ± 1.04	/	/	/
Litter weight, kg ⁷	15.04 ± 2.51	15.31 ± 2.72	15.42 ± 2.74	15.38 ± 2.56	15.08 ± 2.46	15.45 ± 3.07	14.68 ± 2.37	/	/	/
Average piglet weight, kg ⁸	1.46 ± 0.22	1.47 ± 0.23	1.48 ± 0.22	1.47 ± 0.23	1.47 ± 0.25	1.51 ± 0.28	1.45 ± 0.24	/	/	/
Number of weaned sows	48	46	41	46	42	41	45	/	/	/
Number of weaned piglets	9.00 ± 1.22 ^b	9.35 ± 1.04 ^{ab}	9.59 ± 1.00 ^a	9.80 ± 0.86 ^a	9.36 ± 1.19 ^{ab}	9.37 ± 0.86 ^{ab}	9.49 ± 0.97 ^a	0.227	< 0.001	0.643
Total litter weight at weaning, kg	47.07 ± 8.47 ^d	51.55 ± 7.66 ^{bc}	55.23 ± 11.04 ^{ab}	58.83 ± 7.46 ^a	50.18 ± 8.03 ^{cd}	55.00 ± 8.40 ^{ab}	55.83 ± 9.10 ^a	0.192	< 0.001	0.663
Average piglet weight at weaning, kg	5.26 ± 0.87 ^c	5.53 ± 0.67 ^{bc}	5.75 ± 0.90 ^{ab}	6.00 ± 0.57 ^a	5.37 ± 0.56 ^c	5.88 ± 0.76 ^a	5.90 ± 0.89 ^a	0.678	< 0.001	0.668
ADWG of piglets, g ⁹	180.43 ± 35.72 ^c	194.80 ± 31.03 ^{bc}	203.24 ± 41.16 ^{ab}	214.50 ± 26.23 ^a	186.46 ± 25.32 ^c	207.29 ± 31.91 ^{ab}	213.88 ± 40.84 ^a	0.767	< 0.001	0.665
21-day milk yield, kg ¹⁰	135.63 ± 28.58 ^d	152.67 ± 28.54 ^{bc}	164.02 ± 39.84 ^{ab}	176.72 ± 26.69 ^a	146.24 ± 25.78 ^{cd}	163.02 ± 29.01 ^{ab}	169.71 ± 32.89 ^a	0.264	< 0.001	0.818

^{1,2,3}Multiparous sows without any additional treatment (control); sows were administered a single dose of 75 µg/time D-cloprostenol sodium or 200 µg/time DL-cloprostenol sodium, which was induced 24 h before delivery (Single); sows were administered a triple dose of cloprostenol sodium, 24 h before delivery and again 3 h and 5 days after delivery (Triple); sows were administered four doses of cloprostenol sodium 24 h before delivery and again 3 h, 5 days, and 10 days after delivery (Quartic). ⁴p-values include main effects of drugs (control or cloprostenol sodium) and times of treatments (Time) and the interaction between drug and times (Int). ^{5,6,7,8}After parturition, to evaluate the impact of cloprostenol sodium on lactation in MS, piglets underwent appropriately cross-fostered within the group within 3 h after delivery. However, piglets that were too small (< 0.8 kg) and/or too weak (unable to stand or crawl) could be swapped with non-trial piglets (0.8–1.2 kg). The number and weight of piglets suckled by sows in each subgroup were recorded. ⁹Per piglets from birth to weaning daily weight. ADWG, Average Daily Weaning Gain. ¹⁰The 21-day milk yield refers to the algorithm of Lawlor et al. (17). ^{ab,cd}Different superscripts within rows differ significantly ($p < 0.05$).

3.4 Weaned piglets’ performances

The lactation capacity of MS was assessed based on body weight at weaning, and the corresponding results are shown in Table 4. The number of weaned piglets in the sows treated with quartic doses of cloprostenol sodium and triple doses of D-cloprostenol sodium was significantly higher than that in the control group ($p < 0.05$). Similarly, the total litter weight at weaning in the quartic treatments of D-cloprostenol sodium groups (58.53 kg) and DL-cloprostenol sodium groups (55.83 kg) was significantly higher than that in the single injection group, which was approximately 51 kg ($p < 0.05$). Additionally, triple doses of cloprostenol sodium resulted in heavier weights compared to the control group’s weight of 47.07 kg ($p < 0.05$). The administration of a single dose of D-cloprostenol sodium also resulted in a higher litter weight of piglets ($p < 0.05$).

The average piglet weight at weaning, piglets’s ADWG, and litter weight at weaning showed consistent outcomes of change with the increase of the number of cloprostenol sodium treatments. The average piglet weight at weaning and ADWG in the quartic cloprostenol sodium treatments were higher than those in the single drug treatment and not administration ($p < 0.05$). Utilization of triple cloprostenol sodium also resulted in a significant

improvement in both average piglet weight and ADWG compared to the control group ($p < 0.05$). The same trend was observed for milk yield, which was calculated using Equation (2). All indices pertaining to weaned piglets are displayed in Table 4. Throughout the entire lactation period, the repeated quartic treatments exhibited the most favorable effect on the indicators of piglet weight and weight gain, followed by triple treatments and single treatment, respectively, and, finally, the control group without any additional treatment. In other words, the amount of weight gain in piglets during lactation was found to be solely associated with the frequency of administration of cloprostenol sodium ($p < 0.05$) but showed no significant correlation with its type ($p > 0.05$). Parturition induced with D-cloprostenol sodium, but not DL-cloprostenol sodium, had a positive effect on litter weight at weaning and 21-day milk yield ($p < 0.05$).

Conformably, compared to naturally lactating MS, the milk yield of sows that received repeated quartic doses of D-cloprostenol sodium was the highest, which showed a significant increase of 30.30% (176.72 kg vs. 135.63, $p < 0.05$). However, DL-cloprostenol sodium increased milk yield by 25.13% (169.71 kg vs. 135.63 kg, $p < 0.05$). Furthermore, triple treatments of cloprostenol sodium increased the milk yield by approximately 20% ($p < 0.05$). In addition, induced

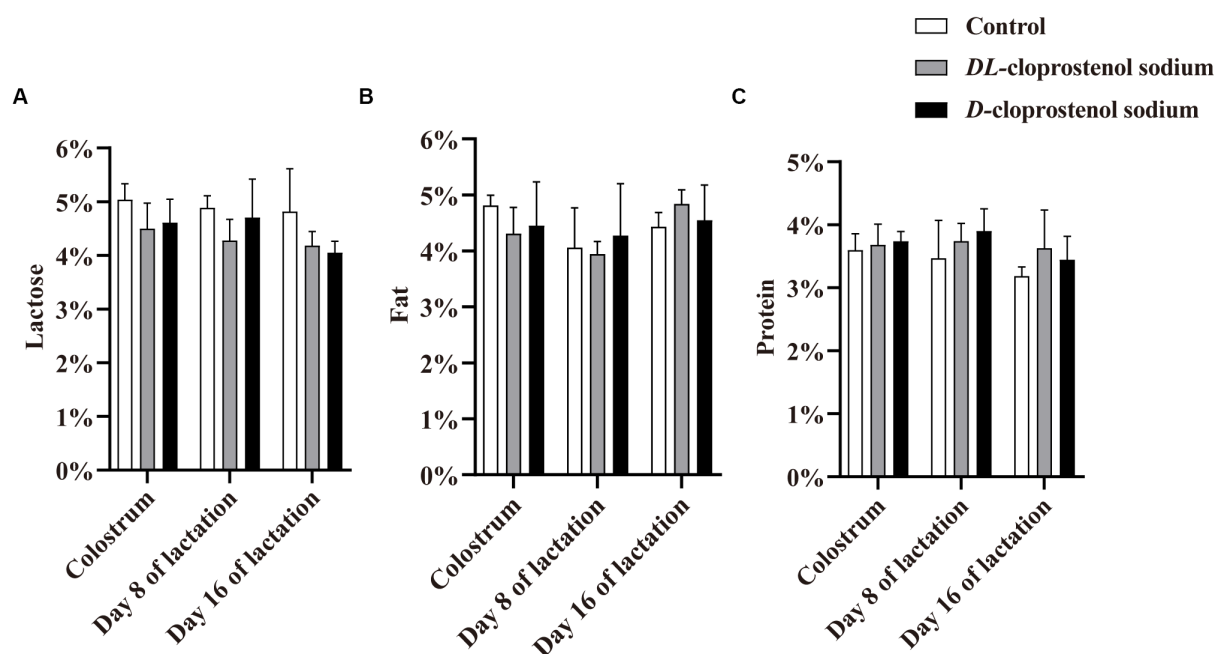


FIGURE 2

Concentration (%) of lactose (A), fat (B), and protein (C) in colostrum from multiparous sows within 12 h after parturition, as well as mature milk on the days 8 and 16 of lactation in both the control and treatment groups. Multiparous sows did not receive any additional treatment (Control, $n = 3$) and received 75 $\mu\text{g}/\text{time}$ *D*-cloprostenol sodium ($n = 3$) and 200 $\mu\text{g}/\text{time}$ *DL*-cloprostenol sodium ($n = 3$) quartic treatments, which were administered 24 h before delivery, 3 h and 5 days after delivery, and 3 h, 5 days, and 10 days after delivery, respectively.

parturition with a single dosage of *D*-cloprostenol sodium also was found to significantly increase the yield milk by 12.56% ($p < 0.05$).

3.5 Content of milk components

The administration of cloprostenol sodium appeared to decrease the tendency of lactose content during the whole lactation period in sows ($p > 0.05$) (Figure 2). Similarly, the sows administered with double doses of cloprostenol sodium 24 h before farrowing and 3 h after farrowing resulted in a reduction in colostrum milk fat content; however, this difference did not reach statistical significance ($p > 0.05$). Nonetheless, the cumulative administration of treatment quartic injections resulted in an increase in mature milk fat content on day 16 of lactation in sows ($p > 0.05$) (Figure 2B). As shown in Figure 2C, triple and quartic injections of cloprostenol sodium exhibited a non-significant increase in milk protein content during lactation ($p > 0.05$). In summary, the cumulative treatment of cloprostenol sodium affected milk components in the colostrum and mature milk of sows in the early, middle, and late stages of lactation ($p > 0.05$).

3.6 Serum levels of lactation-related hormones

Figure 3A shows that the injection of *D*-cloprostenol sodium ($p < 0.05$) or *DL*-cloprostenol sodium ($p > 0.05$) on day 115 of gestation results in an increase in PRL levels in sows 3 h after the first administration. Additionally, the injection of *D*-cloprostenol sodium

also led to a significant increase in PRL levels among lactating sows on day 4 ($p < 0.05$). Notably, both a single prenatal treatment and multiple postpartum treatments were found to elevate PRL levels during the lactation stage (Figure 3A). Receiving cloprostenol sodium treatment did not exert any significant impact on the serum estrogen levels in lactating sows (Figure 3B). Although a single dose cloprostenol sodium before parturition could reduce the levels of P_4 in sows 3 h after treatment ($p > 0.05$), multiple doses of the drugs had no perceptible effect during lactations (Figure 3C). The sows treated with double cloprostenol sodium, especially *DL*-cloprostenol sodium, observed the lower COR levels on the first day of lactation. In addition, utilization of multiple doses of *D*-cloprostenol sodium exhibited a propensity to increase serum COR levels throughout lactation; however, the difference was not statistically significant ($p > 0.05$) (Figure 3D).

3.7 Reproductive performance of weaned sows

The effects of cloprostenol sodium treatment on the reproductive performance of next-parity sows are shown in Table 5. Although statistical significances were not observed among treatments ($p > 0.05$), the tendencies toward improvements of estrus rates and AI rate within 7 days post-weaning were noted with cloprostenol sodium intervention. It appeared that the weaning-to-estrus interval (WEI) was not only related to the optical activity ($p < 0.05$) but also to the number of treatments ($p < 0.05$). Compared to control sows, the sows treated with *D*-cloprostenol sodium exhibited the reduction

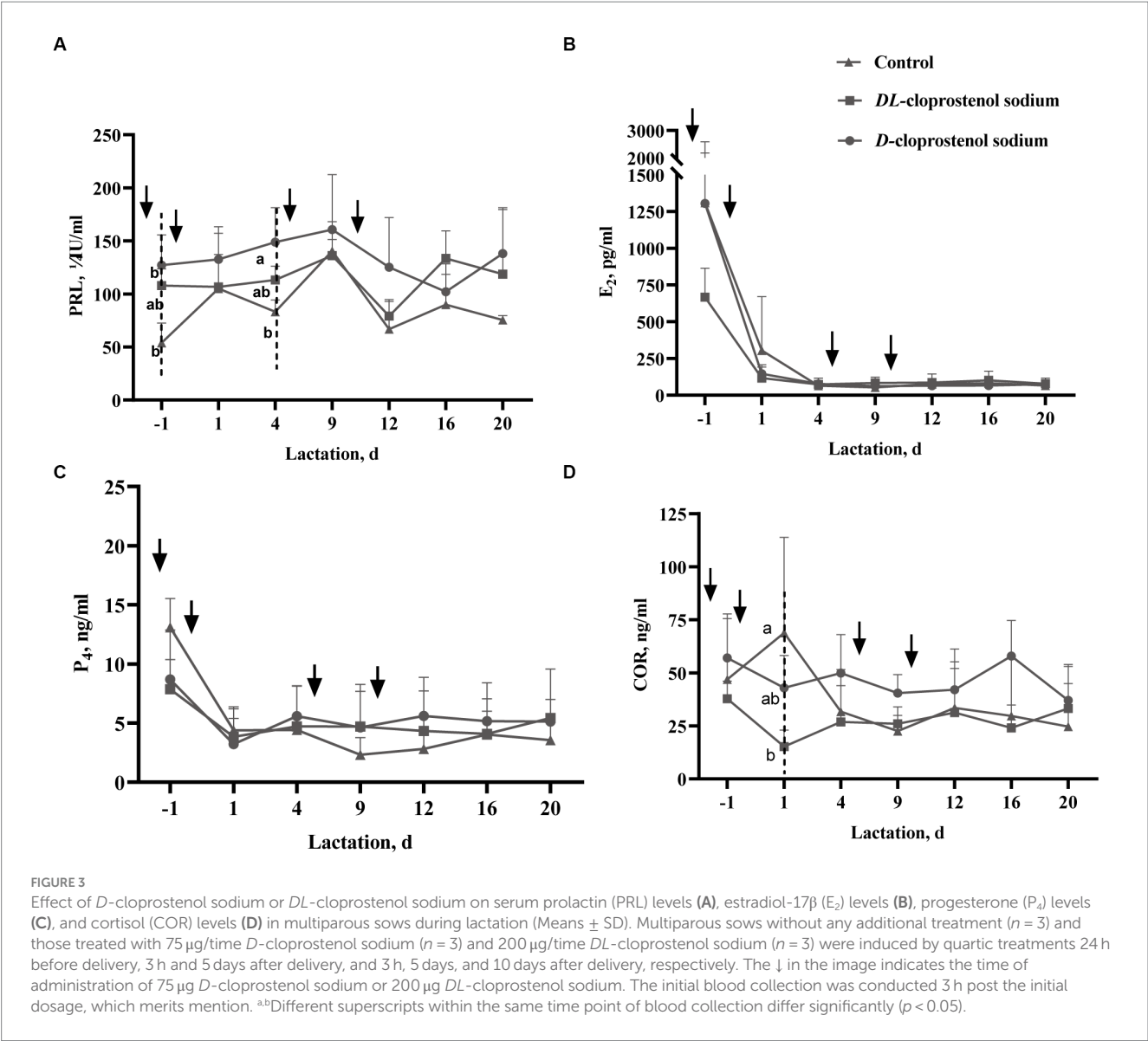


TABLE 5 Effects of different injection times of cloprostenol sodium on reproductive performance of weaned sows (Means \pm SD & percentage).

Variables	Control ¹	D-cloprostenol sodium ²			DL-cloprostenol sodium ³			p-values ⁴		
		Single	Triple	Quartic	Single	Triple	Quartic	Drug	Time	Int
Number of weaned sows	48	46	41	46	42	41	45	/	/	/
Estrus rate within 7 days after weaning, %	79.17	82.61	85.36	89.13	78.57	90.24	86.67	0.654	0.467	0.836
WEI, d ⁵	4.16 \pm 1.05 ^a	3.55 \pm 0.69 ^c	3.63 \pm 0.65 ^{bc}	3.61 \pm 0.67 ^{bc}	3.97 \pm 0.64 ^{ab}	3.76 \pm 0.68 ^{bc}	3.85 \pm 0.67 ^{ab}	0.037	0.001	0.494
AI rate within 7 days after weaning, % ⁶	68.75	73.91	78.05	84.78	71.43	78.05	82.22	0.487	0.304	0.949
WSI, d ⁷	5.21 \pm 0.89 ^a	4.62 \pm 0.70 ^b	4.69 \pm 0.64 ^b	4.67 \pm 0.58 ^b	4.93 \pm 0.74 ^{bc}	4.72 \pm 0.5 ^b	4.78 \pm 0.75 ^b	0.189	< 0.001	0.636
Conception rate sows, % ⁸	64.58	71.74	78.05	82.61	69.05	78.05	75.56	0.650	0.467	0.836

^{1,2,3}Multiparous sows without any additional treatment (control); sows were administered a single dose of 75 μ g/time *D*-cloprostenol sodium or 200 μ g/time *DL*-cloprostenol sodium, which was induced 24 h before delivery (single); sows were administered a triple dose of cloprostenol sodium 24 h before delivery and again 3 h and 5 days after delivery (triple); sows were administered four doses of cloprostenol sodium 24 h before delivery and again 3 h, 5 days, and 10 days after delivery (quartic). ⁴p-values include main effects of drugs (control or cloprostenol sodium) and times of treatments (Time) and the interaction between drug and times (Int). ^{5,6,7}WEI, weaning-to-estrus interval; AI, artificial insemination; WSI, weaning-to-service interval. ⁸The conception rate refers to the proportion of pregnant sows among weaned sows, rather than the proportion of mated sows. ^{a,b,c}Different superscripts within rows differ significantly ($p < 0.05$).

in WEI ($p < 0.05$). Moreover, the sows administered *D*-cloprostenol sodium or *DL*-cloprostenol sodium showed the shorter WSI compared to the control group ($p < 0.05$). The conception rates of the next parity of weaned sows in quartic *D*-cloprostenol sodium (82.61%) were higher than those of the control group (64.58%) ($p > 0.05$). Similarly, other treatments also improved conception rates in sows, but there were no significant difference either ($p < 0.05$).

4 Discussion

There is a divergence of opinions regarding the effects of PGF_{2α} and its analogs on the milk yield and milk composition in sows. Monteiro et al. (18) conducted a systematic analysis of eight articles to explain the effects of PGF_{2α} and its analogs on lactation in sows. Three of these articles reported the negative effects of PGF_{2α} drugs on lactation (5, 19, 20), three found that PGF_{2α} drugs had no significant effect on colostrum yield or piglet intake (4, 21, 22), one demonstrated that PGF_{2α} drugs could increase or decrease the content of certain cytokines to affect activity of colostrum (23), and one observed an increase in serum IgG concentration and weight gain in 3-day-old piglets (24). Previously, researchers have attempted to enhance the feed intake and milk yield of sows as well as the growth rate of piglets by employing various feed additives during the lactation period (25–27). This experiment aims to explore a novel pathway utilizing sex hormones to regulate the endocrine system and improve lactation performance during lactation. The effects of different injection times of PGF_{2α} analogs (75 µg *D*-cloprostenol sodium and 200 µg *DL*-cloprostenol sodium) on sows' lactation ability are also discussed.

4.1 Sows of synchronous delivery

This study commenced with inducing parturition. The sows were administered with *D*-cloprostenol sodium or *DL*-cloprostenol sodium in the neck muscle to initiate synchronized delivery at 1,130–1,200 h on the day before the actual expected delivery of sows with a parity of 2–3. The findings showed that it could accelerate the delivery process, significantly shortening the time from administration to delivery, farrowing duration, birth interval, and placenta excretion time and also significantly increasing daytime delivery rates in sows. Kaeoket et al. (28) used *D*-cloprostenol sodium to induce parturition in sows at 0700 h on days 113 and 114 of gestation, resulting in the simultaneous delivery of offspring approximately 25 h after administration (at 0800 h on the following day). In our experiment, the sows treated with *D*-cloprostenol sodium or *DL*-cloprostenol sodium showed synchronized parturition approximately 23 h after initiation of administration (at 1,000 h on the next day). This finding challenges the previously held perception that starting treatment with PGF_{2α} drugs at 0700 h on the day prior to expected delivery may be inappropriate.

Farrowing duration is negatively correlated with colostrum yield; each additional minute of farrowing duration reduces colostrum yield by 2.2 g (2). The delivery interval is defined as the farrowing duration divided by the total number of piglets born minus one, and the cumulative birth interval is a significant risk factor affecting piglet colostrum consumption (29). Although oxytocin can improve the progress of parturition (30), prevent postpartum vaginal bleeding (31), and promote rapid milk discharge in lactating sows (32), in the long run, it may lead to lactation disorders and reduce the birth vitality of piglets (18, 30). Even when oxytocin analogs and *DL*-cloprostenol sodium are employed to induce parturition, both the colostrum yield of sows and the colostrum intake of piglets are notably lower than those with *DL*-cloprostenol sodium alone or natural delivery (4), which suggests that PGF_{2α} analogs may appear to improve colostrum yield.

Our results demonstrate that *D*-cloprostenol sodium and *DL*-cloprostenol sodium can significantly reduce the rates of Stillborn Type II in MS from 5.76% to 1.74–3.13%, which indicates that inducing parturients with cloprostenol sodium is able to reduce fetal mortality within the sow birth canal during deliver and also suggests that it can effectively shorten farrowing duration. Previous studies have shown that the induction of parturition using PGF_{2α} and its analogs can reduce stillbirth rates by 28% (18). Additionally, our results align with previous studies that have reported stillbirth rates of 3–8% for piglets born naturally (33). Our calculated rate is 8.73%, slightly exceeding the range, which is the sum of 5.76% (Stillborn Type II) and 2.97% (Stillborn Type I). The stillbirth rates of piglets account for 27% of deaths pre-weaning (34). In another investigation, parturition was induced in 77 sows through the injection of 175 µg *DL*-cloprostenol sodium at 0700 h on day 114 of pregnancy, resulting in a total stillbirth rate of 5.3% (53/1004), with Stillborn Type II accounting for 79.2% (42/53) (35). Although Nguyen et al.'s study lacked a blank control group, we observed that the Stillborn Type II in the group with natural farrowing was significantly higher than those in the group treated with *DL*-cloprostenol sodium in our experiment. This finding infers that the proportion of Stillborn Type II during natural farrowing was much higher than 79.2%. Therefore, inducing parturients can effectively decrease the incidence of stillbirth, thereby enhancing animal welfare.

4.2 Characteristics of sows of lactation and weaning characteristics of piglets

Lower back fat thickness at the end of pregnancy may potentially hinder breast development, while thickness in the week before delivery is positively correlated with colostrum yield and lactation duration (1, 36). In our experiment, to minimize the effect of back fat thickness in late pregnancy, the average back fat thickness of each subgroup was controlled at approximately 17 mm. Additionally, in the GLM procedure analysis of weaning litter weight and other parameters, we incorporated pre-delivery back fat as a covariate. Data show that the difference among groups was less than 2 mm. The back fat thickness of each group was approximately 15 mm on day 20 of lactation, with a decrease of approximately 2 mm compared to late pregnancy. In our experiment, multiple doses of *D*-cloprostenol sodium or *DL*-cloprostenol sodium did not affect the loss of back fat thickness in lactating sows. The research showed that the loss of 2.5–4 mm in thickness during lactation does not impair the reproductive capacity of sows in the following parity as these sows can regain the lost thickness prior to the next AI (37).

Insufficient feed intake by lactating sows is associated with increased mortality rates of pre-weaning piglets and prolonged WEI of sows in hot areas (26). In our experiment, the daily feed intake of sows exhibited a growth trend with an increased frequency, and as the injection frequency increased, both the number and weight of weaned piglets gradually increased. Increasing feed intake enhances the nutritional level of lactating sows, leading to an increase in the milk yield of sows and higher weaning litter weight of piglets (26). Additionally, the absorbed nutrients are primarily utilized by the mammary glands in sows during lactation (38), and approximately 70% of the total energy requirement and 90% of the absorbed amino acids are used for milk production and mammary gland development

(39, 40). Therefore, it is speculated that cloprostenol sodium may improve lactation performance and mammary gland function by regulating the central nervous system in lactating sows.

In our experiment, sows injected with quartic doses of *D*-cloprostenol sodium observed a significant increase in the weaning litter weight by 24.98% and an 18.88% increase in the ADWG of the piglets. Despite an approximate 18% increase in the ADWG observed with *DL*-cloprostenol sodium, its impact on weaning litter weight was only 18.53%, which may be due to a slightly lower number of weaned piglets, as evidenced by the data. Approximately 4 g of milk are required for each gram of live piglet weight gain, which has not changed significantly over the last 30 years (41, 42). The algorithm for milk yield, as described by Lawlor et al. (17), indicates that the milk yield can be increased by 30.30% with quartic injections of *D*-cloprostenol sodium and by approximately 25% with repeated quartic injections of *DL*-cloprostenol sodium. Nonetheless, without considering optical isomers, repeating three injections of cloprostenol sodium only increased milk production by approximately 20%, which is lower than the enhancement achieved with four injections. Multivariable analyses conducted by Quesnel et al. (43) confirmed that colostrum intake was the predominant factor influencing piglet survival within 3 days after parturition, as well as pre-weaning survival, growth, and development. Administering dinoprost multiple times postpartum can increase the milk yield of sows and the colostrum intake of piglets, leading to increased litter weight of weaned piglets and improved growth performance of piglets before weaning (44). The milk yield of artificially lactating non-pregnant sows can be significantly increased 48 h and 108 h after the administration of PGF_{2α} (45). Notably, the chemical structure and half-life of cloprostenol sodium and dinoprost differ; cloprostenol sodium is more stable and has a longer half-life than dinoprost. Another study showed that *DL*-cloprostenol sodium-induced parturition tended to increase the colostrum yield of primiparous sows (4). Colostrum yield was not detected in this experiment. Nonetheless, our findings also demonstrated that the administration of *D*-cloprostenol sodium 24 h before delivery led to a significant increase in weaning weight and milk production within 21 days of lactation, while *DL*-cloprostenol sodium did not. These findings indicate that *D*-cloprostenol sodium may be more effective at increasing colostrum production.

Overall, the combination of inducing parturition before delivery and injecting multiple doses of cloprostenol sodium during the first 2 weeks of lactation can significantly enhance the growth of piglets and milk yield of sows. Among them, the administering of quartic injections (24 h prenatal; 3 h, 5 d, and 10 d postpartum) significantly improved the growth rate of piglets, with *D*-cloprostenol sodium proving to be the most effective.

4.3 Milk composition and lactation-related hormones levels in sows

Although there was no significant difference in lactose, milk fat, and milk protein between the sows treated with cloprostenol sodium and untreated sows, it was evident that four injections of two different types of cloprostenol sodium could lead to an increasing trend in milk protein and milk fat content during the middle and later stage of lactation. Other studies have shown that the content of lactose, fat, and

protein in sows' milk hardly varies greatly throughout lactation (46). These findings may also be related to the potential of multiple cloprostenol sodium in enhancing piglets' weaning litter weight and ADWG.

Hormones such as PRL, E₂, and P₄ are involved in regulating animal estrus and are closely related to mammary gland development as well as the initiation and maintenance of lactation (40, 47). In this study, it was observed that multiple injections of cloprostenol sodium improved the growth performance of piglets, which may also be attributed to lactation-related hormones. PRL is the most important hormone involved in lactation in sows. Induced parturition with *D*-cloprostenol sodium can significantly increase the PRL levels in prenatal sows. PRL promotes the synthesis of lactose, milk fat, and milk protein by activating the JAK2-STAT5 and PI3K-AKT1-mTOR pathways through the PRL receptor. P₄ is also essential for mammary gland development during puberty and pregnancy (48). Sow milk originates from blood circulation, but elevated serum P₄ levels can affect the milk quality of sows and increase piglets' diarrhea rates within 7 days (2). A sow that has just finished giving birth with high P₄ levels would result in less weight gain or even weight loss on their first day. For some sows, P₄ levels remained high even at 48 h after delivery, resulting in the average daily gain (ADG) of these piglets being below the normal level within 3 days of birth (49). The synthesis and secretion estrogen are influenced by the hypothalamic-pituitary axis. E₂ stimulates the extension of mammary ducts, proliferation of breast epithelial cells, and lactation (50, 51). High levels of P₄ before delivery inhibit the stimulatory effect of E₂ on PRL (52). In the experiment, multiple postpartum injections had no effect on E₂ and P₄ levels.

Sows undergo significant metabolic and physiological changes during childbirth within a short period, and they face heat stress throughout the entire lactation period. High temperatures and intense sucking stimulation in piglets both increase COR levels in sows, resulting in immunosuppression (53). In our experiment, the sows treated with double cloprostenol sodium showed reduced COR levels in the first postpartum period. Previous studies have shown that COR can serve as a marker of stress during lactation and has a positive effect on sow lactation (54). Martinez-Miro et al. (54) revealed that high concentrations of COR in sow saliva were associated with increased piglet mortality within 3 days. When the concentration of COR in sow saliva is low, the growth rate of piglets increases during lactation (55). In our experiment, the administration of *D*-chloroprostol sodium did not effectively reduce the levels of COR in the late and middle stages of lactation. However, there was no negative impact on the ADWG of piglets.

4.4 Reproductive performance of weaned sows

Injecting 75 μg *D*-cloprostenol sodium before or after farrowing shortened the WEI and WSI in weaned sows by approximately 0.5 days, which can be attributed to the effective dissolution of corpus luteum of pregnancy by *D*-cloprostenol sodium. Recently, findings indicate that *DL*-cloprostenol sodium can dissolve the corpus luteum more effectively and reduce P₄ levels more than dinoprostaglandin F_{2α} (56, 57). *D*-cloprostenol sodium is the dextral enantiomer of *DL*-cloprostenol sodium, which serves as the active component. In our

experiments, the progesterone level-lowering effects were found to be equivalent when administering 75 µg of *D*-cloprostenol sodium and 200 µg of *DL*-cloprostenol sodium. Administration of PGF_{2α} analogs can induce the expression of endometrial growth factors, promoting endometrial repair and accelerating the elimination of postpartum placenta and other foreign bodies, thereby reducing the occurrence of uterine inflammation (58). Notably, the utilization of quartic dose of *D*-cloprostenol sodium showed an increase in conception rates by approximately 18 percentage points for the weaned sows. Thus, the multiple administration of cloprostenol sodium during lactation effectively improves the utilization rate of weaned sows.

This study represents the first demonstration that administration of cloprostenol sodium during lactation can improve the lactation performance of sows, which is very important for the health and welfare of both the sow and the piglets. We acknowledge the small sample size of blood and colostrum samples and recognize that the results could have been more robust with a larger number of samples. We also acknowledge the administration of postpartum antimicrobials to all sows; however, this practice lacks prudence. Antimicrobials should only be used in animals that are diseased, and prophylactic usage should be avoided. The proper use of antimicrobials should be considered in future studies. Moreover, we did not assess colostrum yield or immunological parameters of milk or investigate the effect of cloprostenol sodium on udder development in MS during lactation.

5 Conclusion

In conclusion, the administration of a single dose of *D*-cloprostenol sodium and *DL*-cloprostenol sodium in the prenatal 24 h can significantly shorten delivery process and reduce the rates of stillborn piglets type II in MS. The milk yield of sows can be significantly increased by inducing delivery with cloprostenol sodium, especially 75 µg *D*-cloprostenol sodium. Multiple postpartum administrations of cloprostenol sodium can significantly improve weaning litter weight, milk yield, average daily feed intake, and speed of weight gain in piglets. Furthermore, the sows treated with *D*-cloprostenol sodium exhibited enhanced PRL levels. In total, quartic doses of *D*-cloprostenol sodium are administered for 24 h prior to delivery and at 3 h, 5 d, and 10 d postpartum, yielding the optimal reproductive performance in sows. However, further investigations are needed to confirm the underlying molecular mechanisms for these observed effects.

Data availability statement

The original contributions presented in the study are included in the article/supplementary material, further inquiries can be directed to the corresponding authors.

Ethics statement

All procedures followed the guidelines for the ethical treatment of animals and were approved by the Animal Ethics Committee of the South China Agricultural University (Approval number SCAU#0025). The studies were conducted in accordance with the local legislation

and institutional requirements. Written informed consent was obtained from the owners for the participation of their animals in this study.

Author contributions

XuZ: Conceptualization, Data curation, Investigation, Writing – original draft. XiZ: Data curation, Writing – original draft, Formal analysis. YZ: Investigation, Resources, Validation, Writing – original draft. JL: Investigation, Resources, Validation, Writing – original draft. SL: Data curation, Writing – original draft. SiZ: Data curation, Writing – original draft. LL: Supervision, Writing – original draft. LM: Validation, Writing – original draft. HW: Funding acquisition, Writing – review & editing. ShZ: Funding acquisition, Methodology, Project administration, Writing – review & editing.

Funding

The author(s) declare financial support was received for the research, authorship, and/or publication of this article. This study was supported by the National Natural Science Foundation of China (Project fund no: 32272873), the Project of Pig Innovation Team in Guangdong Modern Agricultural Research System (Project fund no: 2023KJ126), and the Local Innovative and Research Teams Project of Guangdong Province (Project fund no: 2019BT02N630) from the animal breeding laboratory of the College of Animal Science of South China Agricultural University.

Acknowledgments

The authors would like to thank the pharmaceutical companies who kindly supplied the *DL*-cloprostenol sodium, *D*-cloprostenol sodium, and oxytocin (Ningbo Second Hormone Factory) used in the experiment. The authors greatly appreciate Beijing North Institute of Biotechnology Co., Ltd. and Shanghai Enzyme Union Biotechnology Co., Ltd. for providing sample testing support. The authors also appreciate Guangdong Guanghui Huifeng Farm for providing the facilities and animals used in the experiment.

Conflict of interest

The authors declare that the research was conducted in the absence of any commercial or financial relationships that could be construed as a potential conflict of interest.

Publisher's note

All claims expressed in this article are solely those of the authors and do not necessarily represent those of their affiliated organizations, or those of the publisher, the editors and the reviewers. Any product that may be evaluated in this article, or claim that may be made by its manufacturer, is not guaranteed or endorsed by the publisher.

References

- Decaluwe R, Maes D, Cools A, Wuyts B, De Smet S, Marescau B, et al. Effect of Peripartal feeding strategy on colostrum yield and composition in sows. *J Anim Sci.* (2014) 92:3557–67. doi: 10.2527/jas.2014-7612
- Hasan S, Orro T, Valros A, Junnikkala S, Peltoniemi O, Oliviero C. Factors affecting sow colostrum yield and composition, and their impact on piglet growth and health. *Livest Sci.* (2019) 227:60–7. doi: 10.1016/j.livsci.2019.07.004
- Devillers N, Le Dividich J, Prunier A. Influence of colostrum intake on piglet survival and immunity. *Animal.* (2011) 5:1605–12. doi: 10.1017/S175173111100067X
- Boonraungrod N, Sutthiya N, Kumwan P, Tossakui P, Nuntapaitoon M, Muns R, et al. Control of parturition in swine using Pgf2 α in combination with Carbetocin. *Livest Sci.* (2018) 214:1–8. doi: 10.1016/j.livsci.2018.05.012
- Vallet JL, Miles JR. The effect of farrowing induction on colostrum and piglet serum Immunocrits is dependent on parity. *J Anim Sci.* (2017) 95:688–96. doi: 10.2527/jas.2016.0993
- Boyd DR, Kensinger RS, Harrell RJ, Bauman DE. Nutrient uptake and endocrine regulation of Milk synthesis by mammary tissue of lactating sows. *J Anim Sci.* (1995) 73:36–56. doi: 10.2527/1995.73suppl_236x
- Sørensen MT, Sejrsen K, Purup S. Mammary gland development in gilts. *Livest Prod Sci.* (2002) 75:143–8. doi: 10.1016/S0301-6226(01)00310-4
- Hannan FM, Elajnaf T, Vandenberg LN, Kennedy SH, Thakker RV. Hormonal regulation of mammary gland development and lactation. *Nat Rev Endocrinol.* (2023) 19:46–61. doi: 10.1038/s41574-022-00742-y
- Farmer C, Palin MF. Exogenous prolactin stimulates mammary development and alters expression of prolactin-related genes in Prepubertal gilts. *J Anim Sci.* (2005) 83:825–32. doi: 10.2527/2005.834825x
- Farmer C. Nutritional impact on mammary development in pigs: a review. *J Anim Sci.* (2018) 96:3748–56. doi: 10.1093/jas/sky243
- Kasazaki T, Tachino H, Sakatsume Y, Suzuki T, Noguchi M. Effect of Pseudopregnancy duration in nonpregnant sows on induced lactation. *Anim Sci J.* (2023) 94:e13815. doi: 10.1111/asj.13815
- Jonczyk AW, Piotrowska-Tomala KK, Skarzynski DJ. Effects of prostaglandin F(2 α) (Pgf(2 α)) on cell-death pathways in the bovine Corpus luteum (cl). *BMC Vet Res.* (2019) 15:416. doi: 10.1186/s12917-019-2167-3
- Piper PJ, Vane JR, Wyllie JH. Inactivation of prostaglandins by the lungs. *Nature.* (1970) 225:600–4. doi: 10.1038/225600a0
- Shrestha HK, Beg MA, Burnette RR, Ginther OJ. Plasma clearance and half-life of prostaglandin F2 α : a comparison between mares and heifers. *Biol Reprod.* (2012) 87:1–6. doi: 10.1095/biolreprod.112.100776
- Re G, Badino P, Novelli A, Vallisneri A, Girardi C. Specific binding of dl-Cloprostenol and D-Cloprostenol to Pgf2 α receptors in bovine Corpus luteum and myometrial cell membranes. *J Vet Pharmacol Ther.* (1994) 17:455–8. doi: 10.1111/j.1365-2885.1994.tb00277.x
- Jahn L, Schuepbach-Regula G, Nathues H, Grahofner A. Effect of 1,25-Dihydroxyvitamin D3-glycosides on the farrowing process and piglet vitality in a free farrowing system. *Animals (Basel).* (2022) 12:611. doi: 10.3390/ani12050611
- Lawlor PG, Lynch PB, Gardiner GE, Caffrey PJ, O'Doherty JV. Effect of liquid feeding weaned pigs on growth performance to harvest. *J Anim Sci.* (2002) 80:1725–35. doi: 10.2527/2002.8071725x
- Monteiro MS, Muro BBD, Poor AP, Leal DF, Carnevale RF, Shiroma MP, et al. Effects of farrowing induction with prostaglandins on farrowing traits and piglet performance: a systematic review and Meta-analysis. *Theriogenology.* (2022) 180:1–16. doi: 10.1016/j.theriogenology.2021.12.010
- Foisnet A, Farmer C, David C, Quesnel H. Farrowing induction induces transient alterations in prolactin concentrations and colostrum composition in Primiparous sows. *J Anim Sci.* (2011) 89:3048–59. doi: 10.2527/jas.2010-3507
- Jackson JR, Hurley WL, Easter RA, Jensen AH, Odle J. Effects of induced or delayed parturition and supplemental dietary fat on colostrum and Milk composition in sows. *J Anim Sci.* (1995) 73:1906–13. doi: 10.2527/1995.7371906x
- Otto MA, Machado AP, Moreira LP, Bernardi ML, Coutinho ML, Vaz IS Jr, et al. Colostrum yield and litter performance in multiparous sows subjected to farrowing induction. *Reprod Domest Anim.* (2017) 52:749–55. doi: 10.1111/rda.12975
- Tospitakkul P, Kraomkaew K, Thammasin K, Uttarak P, Nuntapaitoon M, Rensis FD, et al. Induction of parturition by double administration of prostaglandin F2 α in sows reduces the variation of gestation length without affecting the colostrum yield and piglet performance. *J Vet Med Sci.* (2019) 81:1334–40. doi: 10.1292/jvms.18-0725
- Hlavova K, Kudlackova H, Faldyna M. The impact of parturition induction with Cloprostenol on immunological parameters in the sow colostrum. *Porcine Health Manag.* (2020) 6:35. doi: 10.1186/s40813-020-00174-y
- Nguyen K, Cassar G, Friendship RM, Dewey C, Kirkwood RN. Stillbirth and Prewaning mortality in litters of sows induced to farrow with supervision compared to litters of naturally farrowing sows with minimal supervision. *J Swine Health Product.* (2011) 13:536–217. doi: 10.1016/j.jfms.2011.05.005
- Farmer C, Mathews AT, Hovey RC. Using Domperidone to induce and sustain hyperprolactinemia in late-pregnant gilts. *Domest Anim Endocrinol.* (2019) 66:14–20. doi: 10.1016/j.domaniend.2018.05.004
- Khamtawee I, Singdamrong K, Tatanan P, Chongpaisarn P, Tummaruk P. Cinnamon oil supplementation of the lactation diet improves feed intake of multiparous sows and reduces pre-weaning piglet mortality in a tropical environment. *Livest Sci.* (2021) 251:104657. doi: 10.1016/j.livsci.2021.104657
- Wang K, Chen Y, Zhang D, Wang R, Zhao Z, Feng M, et al. Effects of 25-hydroxycholecalciferol supplementation in maternal diets on reproductive performance and the expression of genes that regulate lactation in sows. *Anim Sci J.* (2020) 91:e13391. doi: 10.1111/asj.13391
- Kaeoket K. The effect of dose and route of administration of R-Cloprostenol on the parturient response of sows. *Reprod Domest Anim.* (2006) 41:472–6. doi: 10.1111/j.1439-0531.2006.00674.x
- Paththawan J, Padet T. Factors associated with colostrum consumption in neonatal piglets. *Livest Sci.* (2021) 251:104630. doi: 10.1016/j.livsci.2021.104630
- Jiarpinitnun P, Loyawatananan S, Sangratkanjanasin P, Kompong K, Nuntapaitoon M, Muns R, et al. Administration of Carbetocin after the First piglet was born reduced farrowing duration but compromised colostrum intake in newborn piglets. *Theriogenology.* (2019) 128:23–30. doi: 10.1016/j.theriogenology.2019.01.021
- Huang X, Xue W, Zhou J, Zhou C, Yang F. Effect of Carbetocin on postpartum hemorrhage after vaginal delivery: a meta-analysis. *Comput Math Methods Med.* (2022) 2022:6420738–6. doi: 10.1155/2022/6420738
- Garbers DL, First NL. The effects of ICI 33828 and oxytocin on Milk ejection and Milk production in the lactating sow. *J Reprod Fertil.* (1968) 17:551–3. doi: 10.1530/jrf.0.0170551
- Wülbers-Mindermann M, Algers B, Berg C, Lundeheim N, Sigvardsson J. Primiparous and multiparous maternal ability in sows in relation to indoor and outdoor farrowing systems. *Livest Prod Sci.* (2002) 73:285–97. doi: 10.1016/S0301-6226(01)00257-3
- Rangstrup-Christensen L, Krogh MA, Pedersen LJ, Sørensen JT. Sow-level risk factors for stillbirth of piglets in organic sow herds. *Animal.* (2017) 11:1078–83. doi: 10.1017/S1751731116002408
- Nguyen HN, Peerapol S. Risk factors for intrapartum stillbirth in piglets born from Cloprostenol-induced farrowing sows. *J Appl Anim Res.* (2022) 50:420–5. doi: 10.1080/09712119.2022.2089152
- Papatsiropoulos V, Argyris G, Papakonstantinou G, Meletis E, Tsekouras N, Kantas D, et al. Evaluation of an on-farm method to assess colostrum igg content in Hyperprolific sows. *Anim Reprod Sci.* (2022) 239:106958. doi: 10.1016/j.anireprosci.2022.106958
- Dourmad J-Y, Étienne M, Valancogne A, Dubois S, van Milgen J, Noblet J. Inraporc: a model and decision support tool for the nutrition of sows. *Anim Feed Sci Tech.* (2008) 143:372–86. doi: 10.1016/j.anifeedsci.2007.05.019
- Piantoni P, VandeHaar MJ. Symposium review: the impact of absorbed nutrients on energy partitioning throughout lactation. *J Dairy Sci.* (2023) 106:2167–80. doi: 10.3168/jds.2022-22500
- Boyd RD, Kensinger RS. *Metabolic precursors for Milk synthesis.* (1998).
- Rezaei R, Wu Z, Hou Y, Bazer FW, Wu G. Amino acids and mammary gland development: nutritional implications for Milk production and neonatal growth. *J Anim Sci Biotechnol.* (2016) 7:20. doi: 10.1186/s40104-016-0078-8
- Højgaard CK, Bruun TS, Theil PK. Impact of Milk and nutrient intake of piglets and sow Milk composition on piglet growth and body composition at weaning. *J Anim Sci.* (2020) 98:skaa060. doi: 10.1093/jas/skaa060
- Whittemore CT, Morgan CA. Model components for the determination of energy and protein requirements for breeding sows: a review. *Livest Prod Sci.* (1990) 26:1–37. doi: 10.1016/0301-6226(90)90053-9
- Quesnel H, Resmond R, Merlot E, Pere MC, Gondret F, Louveau I. Physiological traits of newborn piglets associated with colostrum intake, neonatal survival and Prewaning growth. *Animal.* (2023) 17:100843. doi: 10.1016/j.animal.2023.100843
- Maneetong P, Srisang C, Sunanta N, Muchalintamolee P, Pearodwong P, Suwimonteerabutr J, et al. Postpartum prostaglandin F2 α administration affects colostrum yield, immunoglobulin G, and piglet performance. *Anim Biosci.* (2021) 34:833–43. doi: 10.5713/ajas.20.0187
- Noguchi M, Suzuki T, Sato R, Sasaki Y, Kaneko K. Artificial lactation by exogenous hormone treatment in non-pregnant sows. *J Reprod Dev.* (2020) 66:453–8. doi: 10.1262/jrd.2020-034
- Craig JR, Dunshea FR, Cottrell JJ, Wijesiriwardana UA, Pluske JR. Primiparous and multiparous sows have largely similar colostrum and Milk composition profiles throughout lactation. *Animals (Basel).* (2019) 9:35. doi: 10.3390/ani9020035
- Lawrence RA. 3 – physiology of lactation In: Lawrence RA, Lawrence RM (editors) *Breastfeeding.* 9th ed. Amsterdam: Elsevier (2022). 58–92.
- Kim G, Lee JG, Cheong SA, Yon JM, Lee MS, Hong EJ, et al. Progesterone receptor membrane component 1 is required for mammary gland Developmentdagger. *Biol Reprod.* (2020) 103:1249–59. doi: 10.1093/biolre/iaaa164

49. de Passille AM, Rushen J, Foxcroft GR, Aherne FX, Schaefer A. Performance of young pigs: relationships with Periparturient progesterone, prolactin, and insulin of sows. *J Anim Sci.* (1993) 71:179–84. doi: 10.2527/1993.711179x
50. Neville MC, McFadden TB, Forsyth I. Hormonal regulation of mammary differentiation and milk secretion. *J Mammary Gland Biol Neoplasia.* (2002) 7:49–66. doi: 10.1023/a:1015770423167
51. Ni Y, Chen Q, Cai J, Xiao L, Zhang J. Three lactation-related hormones: regulation of hypothalamus-pituitary axis and function on lactation. *Mol Cell Endocrinol.* (2021) 520:111084. doi: 10.1016/j.mce.2020.111084
52. Blasiak M, Molik E. Role of hormones and growth factors in initiating and maintaining the lactation of seasonal animals. *Med Weter.* (2015) 71:467–71.
53. Morgan L, Meyer J, Novak S, Younis A, Ahmad WA, Raz T. Shortening sow restraint period during lactation improves production and decreases hair cortisol concentrations in sows and their piglets. *Animal.* (2021) 15:100082. doi: 10.1016/j.animal.2020.100082
54. Martinez-Miro S, Tecles F, Ramon M, Escibano D, Hernandez F, Madrid J, et al. Causes, consequences and biomarkers of stress in swine: an update. *BMC Vet Res.* (2016) 12:171. doi: 10.1186/s12917-016-0791-8
55. Baxter EM, Hall SA, Farish M, Donbavand J, Brims M, Jack M, et al. Piglets' behaviour and performance in relation to sow characteristics. *Animal.* (2023) 17:100699. doi: 10.1016/j.animal.2022.100699
56. Umaña Sedó SG, Figueiredo CC, Gonzalez TD, Duarte GA, Ugarte Marin MB, Crawford CA, et al. Evaluation of Luteolysis, follicle size, and time to ovulation in Holstein heifers treated with two different analogs and doses of prostaglandin-F2 α . *J Dairy Sci.* (2022) 105:5506–18. doi: 10.3168/jds.2021-21487
57. Veronese A, Marques O, Moreira R, Belli AL, Bilby TR, Chebel RC. Estrous characteristics and reproductive outcomes of Holstein heifers treated with 2 prostaglandin formulations and detected in estrus by an automated estrous detection or mounting device. *J Dairy Sci.* (2019) 102:6649–59. doi: 10.3168/jds.2018-15957
58. Fu C, Mao W, Gao R, Deng Y, Gao L, Wu J, et al. Prostaglandin F(2 α)-Ptgr signaling promotes proliferation of endometrial epithelial cells of cattle through cell cycle regulation. *Anim Reprod Sci.* (2020) 213:106276. doi: 10.1016/j.anireprosci.2020.106276

Epigallocatechin-3-Gallate Promotes the in vitro Maturation and Embryo Development Following IVF of Porcine Oocytes

This article was published in the following Dove Press journal:
Drug Design, Development and Therapy

Kangfa Huang¹
Chengde Li¹
Fenglei Gao²
Yushan Fan¹
Fanwen Zeng¹
Li Meng¹
Li Li¹
Shouquan Zhang¹
Hengxi Wei¹

¹National Engineering Research Center for Breeding Swine Industry, Guangdong Provincial Key Laboratory of Agro-Animal Genomics and Molecular Breeding, College of Animal Science, South China Agricultural University, Guangzhou, 510642, People's Republic of China; ²Department of Tropical Agriculture and Forestry, College of Guangdong Agriculture Industry Business Polytechnic, Guangzhou, Guangdong, 510507, People's Republic of China

Purpose: Epigallocatechin-3-gallate (EGCG) is a major ingredient of catechin polyphenols and exerts protective effects because of its strong antioxidant properties. As far as we know, there is still a lack of systematic research on the effects of EGCG on the in vitro maturation (IVM) and in vitro fertilization (IVF) of porcine oocytes. The present study aimed to determine the effects of EGCG on the IVM and IVF of porcine oocytes.

Methods: Porcine oocytes were treated with different concentrations of EGCG (5, 10 and 20 μ M), and the cumulus cell expansion, oocyte maturation rate, reactive oxygen species (ROS), glutathione (GSH) and malondialdehyde (MDA) levels, total antioxidant capacity were determined. The mRNA expression levels of oxidative stress- and apoptosis-associated genes were determined by quantitative real-time PCR. The cleavage rate and blastocyst rate of oocytes after 10 μ M EGCG treatment during IVM and IVF were also evaluated.

Results: EGCG at 5, 10 and 20 μ M significantly promoted cumulus cell expansion, and EGCG at 10 μ M increased the oocyte maturation rate. EGCG (10 μ M) treatment reduced the ROS and MDA levels, while increased the antioxidant capacity and GSH concentrations in the mature oocytes. The qRT-PCR results showed that EGCG treatment up-regulated the mRNA expression of catalase, glutathione peroxidase and superoxide dismutase in the mature oocytes. In addition, EGCG treatment also decreased the mRNA expression levels of Bax and caspase-3 and increased the Bcl-2 mRNA expression level in the mature oocytes. In addition, the cleavage rate and blastocyst rate of oocytes treated with 10 μ M EGCG during IVM and IVF were significantly higher than those of the control group.

Conclusion: Our results suggest that EGCG promotes the in vitro maturation and embryo development following IVF of porcine oocytes. The protective effects of EGCG on the oocytes may be associated with its antioxidant and anti-apoptosis properties.

Keywords: EGCG, porcine oocytes, IVM, antioxidant, anti-apoptosis, IVF

Introduction

The in vitro maturation (IVM) of the oocytes is a key step in the in vitro production of embryos for the livestock.^{1,2} Oocytes from IVM have the capacity in fertilization and developing into embryos, while the successful rate for embryo development from IVM oocytes is lower than that from in vivo-matured oocytes.³ The maturation of the oocytes requires both cytoplasmic and nuclear maturation, and incorrect cytoplasmic maturation has been suggested to contribute the poor developmental potential of IVM oocytes.³ Based on the previous studies, proper medium composition and culture conditions are essential for successful oocyte IVM.⁴

Correspondence: Hengxi Wei
National Engineering Research Center for Breeding Swine Industry, Guangdong Provincial Key Laboratory of Agro-Animal Genomics and Molecular Breeding, College of Animal Science, South China Agricultural University, Guangzhou, 510642, People's Republic of China
Tel +86-20-85284869
Email weihengxi@scau.edu.cn

Epigallocatechin-3-gallate (EGCG) is one of the major bioactive compounds in green tea and belongs to the catechin polyphenols.⁵ EGCG has been well-known for its role in chelating the transition metals and thus to decrease the oxidative stress level.⁵ In vitro and in vivo experimental studies have shown that EGCG possess various biological functions including prevention of chromosomal damage by reactive oxygen species (ROS), antibacterial activities, anti-tumor activities and inhibition of lipogenesis.⁵ In the IVM oocytes, Huang et al showed that EGCG in the IVM medium could reduce ROS level and apoptosis in bovine oocytes and increase the cumulus cell expansion.⁶ Roth et al showed that intraperitoneal injection of the antioxidant EGCG improves developmental competence and the quality of the embryos that develop from hyperthermia-treated oocytes in mice.⁷ Gadani et al showed that supplementation of EGCG to thawed boar sperm improved the in vitro fertilization (IVF).^{8,9} However, a recent study by Bucci et al demonstrated that EGCG supplementation to thawing medium failed to improve dog sperm quality or zona binding capacity.¹⁰

As far as we know, there is still a lack of systematic research on the effects of EGCG on the IVM and IVF of porcine oocytes. Whether EGCG can be used as an effective antioxidant for porcine oocytes cultured in vitro remains to be explored. The effects of EGCG on the IVM and IVF of porcine oocytes were systematically investigated. In addition, ROS level, antioxidant capacity, antioxidant- and apoptosis-associated gene mRNA expression levels in oocytes were determined by the in vitro assays.

Materials and Methods

Ethics Statement

This work was approved by the Ethics Committee on Animal Experimentation of South China Agricultural University.

EGCG Treatment

The EGCG compound was purchased from Sigma-Aldrich (St. Louis, USA) and was prepared as 1 mM stock concentration using M-199 medium (Sigma-Aldrich). To determine the effect of EGCG on the cumulus expansion index and in vitro maturation rate of the oocytes, and the ROS production of oocytes, different concentrations of EGCG (0, 5, 10 and 20 μ M) were supplemented to IVM medium (M-199 medium supplemented with 10% fetal bovine serum, 10% porcine follicular fluid, 0.57 mM cysteine, 10 ng/mL epidermal growth factor, 10 IU/mL pregnant mare serum gonadotrophin and 10

IU/mL human chorionic gonadotrophin). To determine the effects of EGCG on the total antioxidant capacity, glutathione (GSH) content, malondialdehyde (MDA) level and mRNA expression levels, EGCG (0 and 10 μ M) was supplemented to the IVM medium. To determine the effects of EGCG on the developmental potential of the oocytes, EGCG (0 and 10 μ M) were supplemented during IVM and/or IVF, or during IVM and/or IVC.

Oocyte Collection and in vitro Maturation

Ovaries were obtained from juvenile pigs slaughtered at a local slaughterhouse (Guangzhou Kongwangji Slaughterhouse, Guangzhou, China) and transferred to the laboratory in 0.9% saline at 37 °C within 2 h. Follicular fluid from 3–8 mm antral follicles was aspirated by a syringe with an 18-gauge needle attached. As previously described,¹¹ approximately 50 cumulus oocyte complexes (COCs) were cultured in 500 μ L of (IVM) medium, covered with mineral oil and cultured for 44 h at 38.5 °C in a 5% CO₂ incubator with humidified air.

Assessment of Cumulus Expansion and IVM of Oocytes

Cumulus expansion was recorded at 44 h of IVM. The assessment was blinded to eliminate bias. The degree of cumulus expansion for each COC was assessed according to a subjective scoring system on a scale of 0–4, where 0 indicates no expansion, 1 indicates the minimal expansion observable, 2 indicates expansion of the outer cumulus cell layers, 3 indicates expansion of all cumulus cell layers except the corona radiata and 4 indicates complete expansion of all cumulus cell layers.¹² The average score (0.0–4.0) for each group, in each replicate (4–6 replicates), was then calculated to obtain a value referred to as the cumulus expansion index. The extrusion of the first polar body in the oocytes were determined under a light microscope. Oocytes were classified as follows: immature (did not reach metaphase), mature (presented a metaphase II plate and the polar body), and abnormal (any chromosomal aberrations such as diploid, abnormal metaphase II, multidirectional spindle, and chromosomal dispersion). The oocyte maturation rate was calculated as follows: number of matured oocytes/total oocytes examined \times 100%.

Determination of ROS Levels

To determine the intracellular ROS content, 30 mature oocytes were incubated for 20 min at 38.5 °C in phosphate

buffered saline (PBS) containing 10 μM 2',7'-dichlorofluorescein diacetate fluorescent probe (Beyotime Biotechnology, Shanghai, China) in the dark. The oocytes were then washed with PBS supplemented with 1% bovine serum albumin. Images were captured by a confocal microscopy system (IX71, Olympus, Japan) with the same scanning settings among groups. Fluorescence intensity was calculated with ImageJ software.

Total Antioxidant Capacity Assay

The total antioxidant capacity in the oocytes were analyzed using Total Antioxidant Capacity Assay Kit with ABTS method (Beyotime, Beijing, China) according to the manufacturer's protocol. The ABTS test measures the total antioxidant capacity of a sample and it is based on the ABTS \cdot + radical discoloration. The cationic radical ABTS \cdot + is a chromophore that absorbs at a wavelength of 734 nm and is generated by an oxidation reaction of ABTS (2,2'-azino-bis- (3-ethylbenzthiazolin-6-ammonium sulfonate) with potassium persulfate.¹³

Quantification of GSH Content

GSH content was measured using the Total Glutathione Assay Kit (S0053, Beyotime, Beijing, China) according to the manufacturer's instructions. This kit employs a kinetic enzymatic recycling assay, based on the oxidation of GSH by 5,5'-dithiobis-(2-nitrobenzoic acid), [DTNB] to measure the total glutathione (tGSH) content of biological samples. Glutathione standards or treated samples are added to the microtiter plate wells, followed by DTNB and glutathione reductase. Addition of NADPH₂ to the wells initiates the progressive reduction of DTNB by GSH, causing a color increase that is monitored at 405 nm. Briefly, the samples were seeded into 96-well plates, and then 150 μL of detection solution was added to each well. After the samples were equilibrated at room temperature for 5 min, 50 μL of a -0.16 mg/mL NADPH solution was added. GSH content was determined by dividing the measured value of 5-thio-2-nitrobenzoic acid by the number of oocytes in each sample.

Quantification of Malondialdehyde (MDA) Level

The MDA level in the oocytes were analysed using MDA assay kit (Beyotime) according to the manufacturer's protocol. MDA reacts with thiobarbituric acid (TBA) to give a red compound which has a maximum absorbance at 532 nm. TBA reagent was prepared by mixing 0.2 mL SDS (8.1%), 1.5 mL acetic acid (20%, pH=3.5) and 1.5 mL TBA (0.8%)

together, then 100 μL of each homogenized oocyte samples was mixed with this 200 μL TBA reagent. The mixture was incubated in a boiling water bath for 15 min and then cooled on ice. After cooling, the mixture centrifuged at 4000 rpm for 10 mins. The absorbance of supernatant was determined at 532 nm against a blank.

In vitro Fertilization and Embryo Culture

The IVF experiment was conducted as previously reported.¹⁴ Briefly, oocytes collected from the local slaughterhouse were cultured for 44 h and denuded in 1 mg/mL hyaluronidase in DPBS by mechanically pipetting; then, 10–15 oocytes were grouped and transferred to the 50 μL mTBM fertilization medium (113.1 mM NaCl, 3.0 mM KCl, 7.5 mM CaCl₂·2H₂O, 20.0 mM Tris, 11.0 mM glucose, 5.0 mM sodium pyruvate) containing 2.5 mM caffeine and 2 mg/mL BSA (fraction V) covered with mineral oil. The fresh semen (from the Duroc pig with ~12 months old and a history of multiple breeding) provided by the Guangxi Yangxiang Company Co. Ltd (Guangxi, China) was washed three times by centrifugation with DPBS supplemented with 0.1% BSA at 1500 rpm for 4 min. The spermatozoa pellets were resuspended and diluted to 1×10^6 sperm/mL with mTBM for capacitation in the CO₂ incubator for 30 min. Then, the capacitated sperm were added to the drop containing oocytes with a final sperm concentration of 1×10^5 sperm/mL and co-incubated for 6 h at 39 °C in an atmosphere of 5% CO₂ in air. After fertilization, the oocytes were washed 3 times with PZM3 medium and cultured with PZM3 medium at 39 °C; 5% O₂, 5% CO₂, and 90% N₂; and 100% humidity. Embryonic cleavage and blastocyst formation were assessed at 48 h and 6 days after insemination, respectively. The formulas for assessing the cleavage and blastocyst rates were as follow: cleavage rate = number of cleavage/number of matured oocytes; blastocyst rate = number of blastocyst/number of matured oocytes.

Quantitative Real-Time PCR (qRT-PCR)

Total RNA was extracted from the matured oocytes using Trizol reagent (Invitrogen, USA), and quantified by measuring the absorbance at 260 nm. The RNA was reversely transcribed into cDNA using the HiScript[®] III RT SuperMix kit (Vazyme, Nanjing, China). The real-time PCR was performed on an qTOWER³ thermal cycler (Analytik Jena, Germany) using ChamQ[™] Universal SYBR[®] qPCR Master Mix kit (Vazyme). The mRNA expression levels of the detected genes were normalized by GAPDH, and were calculated using the 2^{- $\Delta\Delta\text{Ct}$} method. The sequences of the primers were shown in [Supplemental Table S1](#).

Statistical Analysis

All the data analysis was performed using the R Statistical Software (Version 3.6.3). All the data were presented as mean ± standard deviation. Significant differences between different treatment groups were evaluated using Permutation tests. $P < 0.05$ was considered statistically significant.

Results

Effects of EGCG on the Cumulus Expansion Index

The morphology of the mature oocytes and oocytes with the first polar body extrusion was shown in [Supplemental Figure S1A and S1B](#), respectively. Firstly, we examined the cumulus expansion index in the oocytes after being treated with different concentrations of EGCG, and as shown in [Table 1](#), EGCG at 5 and 10 μM significantly increased the cumulus expansion index when compared to the control group (5 μM group versus 0 μM group: 2.989 ± 0.068 versus 2.438 ± 0.081 ; 10 μM group versus 0 μM group: 3.079 ± 0.110 versus 2.438 ± 0.081). However, EGCG at 20 μM had no effect on the cumulus expansion index when compared to the control group (20 μM group versus 0 μM group: 2.879 ± 0.076 versus 2.438 ± 0.081).

Effects of EGCG on IVM Rate of the Oocytes

The effects of EGCG on the in vitro maturation rate of the oocytes were further determined. As shown in [Table 2](#), the oocyte maturation rate was higher in the 5 and 20 μM group when compared to the 0 μM EGCG control group; while the difference was not statistically significant ([Table 2](#)). On the other hand, 10 μM EGCG treatment significantly increased the oocyte maturation rate when compared to the 0 μM EGCG control group (10 μM group versus 0 μM group: $58.63 \pm 2.79\%$ versus $46.27 \pm 3.25\%$; $P < 0.05$).

Table 1 Effects of EGCG on the Cumulus Expansion Index

EGCG (μM)	Number of Oocytes	Cumulus Expansion Index
0	221	2.438 ± 0.081^b
5	220	2.989 ± 0.068^a
10	231	3.079 ± 0.110^a
20	226	$2.879 \pm 0.076^{a,b}$

Notes: The experiments were repeated for four times, and each group had ~50 oocytes for each replicate. Different superscript letters in the same column indicates statistically significant difference ($P < 0.05$).

Table 2 Effects of EGCG on the in vitro Maturation Rate of the Oocytes

EGCG (μM)	Number of Oocytes	Extrusion of the First Polar Body	Oocyte Maturation Rate
0	568	262	46.27 ± 3.25^b
5	604	328	54.43 ± 1.85^b
10	621	364	58.63 ± 2.79^a
20	579	300	51.85 ± 2.64^b

Notes: The experiment was repeated for 6 times, and each group had 50–150 oocytes for each replicate. Different superscript letters in the same column indicates statistically significant difference ($P < 0.05$).

Effects of EGCG on Oxidative Stress of the Oocytes

The ROS production of the EGCG-treated oocytes was determined by the ROS production assay. The representative images of the ROS fluorescent signals in oocytes after treatment with different concentrations of EGCG were shown in [Figure 1A](#). The quantification of the immunofluorescent staining showed that EGCG at 5 μM failed to affect the ROS production in the oocytes when compared to 0 μM control group ([Figure 1B](#)). EGCG at 10 and 20 μM significantly reduced ROS levels of the oocytes when compared to the 0 μM EGCG control group ([Figure 1B](#)).

As EGCG at 10 μM could increase the cumulus expansion index and oocyte maturation rate, and also reduce the ROS level in the oocytes, EGCG at 10 μM was chosen for the subsequent studies. As shown in [Figure 1C](#), EGCG at 10 μM significantly increased the antioxidant capacity of the oocytes when compared to the 0 μM control group ([Figure 1C](#)). In addition, the level of glutathione was increased while the level of MDA was decreased in the oocytes treated with 10 μM EGCG ([Figure 1D and E](#)).

Furthermore, the qRT-PCR was performed to the determine the mRNA expression levels of the oxidative stress-related genes including catalase (CAT), glutathione peroxidase (GPx) and superoxide dismutase (SOD). EGCG at 10 μM significantly up-regulated the mRNA expression levels of CAT, GPx and SOD when compared to the 0 μM control group ([Figure 2A–C](#)).

Effects of EGCG on the mRNA Expression Levels of Apoptosis-Related Genes in the Oocytes

The qRT-PCR was performed to the determine the mRNA expression levels of apoptosis-related genes including

Drug Design, Development and Therapy downloaded from https://www.dovepress.com/ by 222.201.226.51 on 02-Jan-2022
For personal use only.

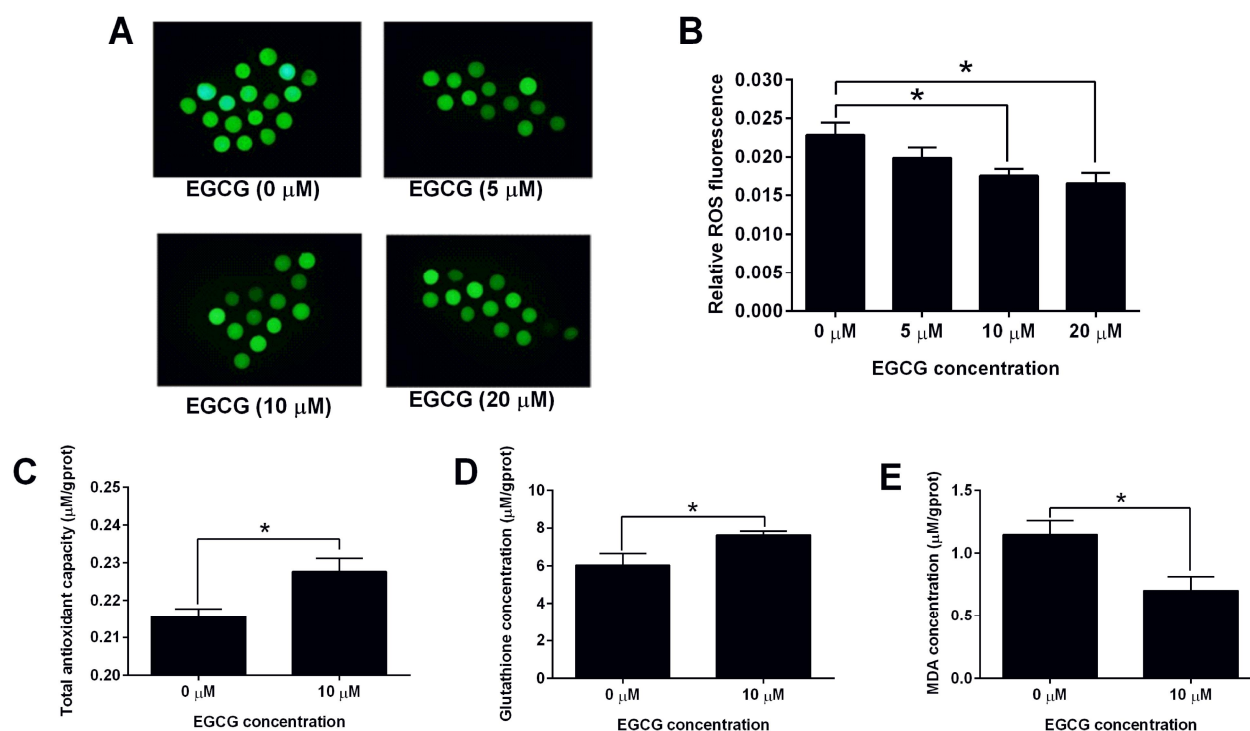


Figure 1 Effects of EGCG on the oxidative stress in the matured porcine oocytes. **(A)** The representative images of the ROS fluorescent signals in oocytes after treatment with different concentrations of EGCG. **(B)** The effects of EGCG on the ROS production of oocytes. The effects of EGCG on the antioxidant capacity **(C)**, glutathione concentration **(D)** and MDA concentration **(E)** in the matured oocytes were determined by respective in vitro assays. N = 3; significant differences were indicated as *P<0.05.

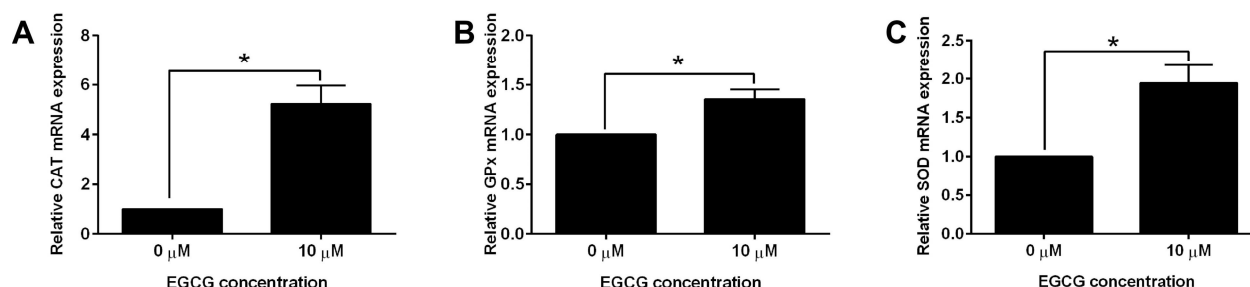


Figure 2 The effects of EGCG on the oxidative stress-related genes. **(A)** CAT, **(B)** GPx and **(C)** SOD mRNA expression levels of the matured oocytes after EGCG treatment were determined by qRT-PCR. N = 3; significant differences were indicated as *P<0.05.

Bax, Bcl-2 and caspase-3. EGCG at 10 μM significantly decreased the mRNA expression levels of Bax and caspase-3, and increased the mRNA expression level of Bcl-2 when compared to the 0 μM control group (Figure 3A–C).

Effects of EGCG Used During IVM and IVF on the Developmental Potential of the Oocytes

The representative images for the embryos and blastocysts were shown in [Supplemental Figure S1C–S1E](#). EGCG

treatment during IVF significantly increased the cleavage rate and blastocyst rate when compared to the control group (Table 3). EGCG treatment during IVM significantly increased the blastocyst rate, but not the cleavage rate when compared to the control group (Table 3). Moreover, EGCG treatment during both IVM and IVF significantly increased the cleavage rate and blastocyst rate when compared to the other three groups (Table 3). These results indicated that EGCG during IVM and IVF could promote the developmental potential of oocytes.

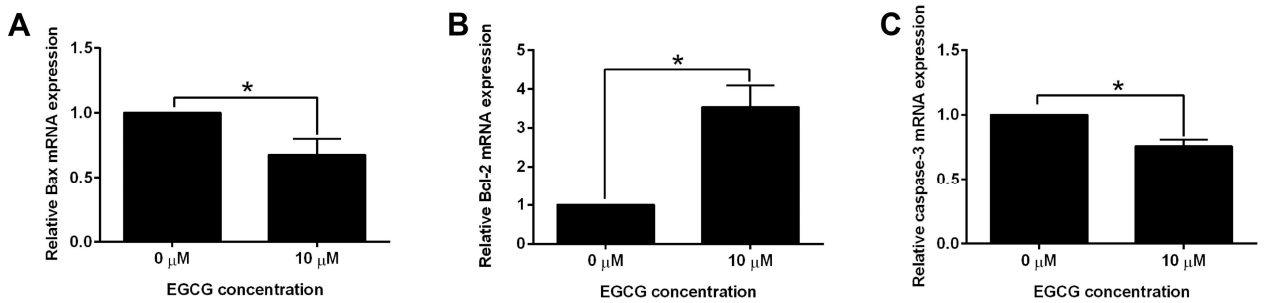


Figure 3 The effects of EGCG on the apoptosis-related genes. **(A)** Bax, **(B)** Bcl-2 and **(C)** caspase-3 mRNA expression levels of the matured oocytes after EGCG treatment were determined by qRT-PCR. N = 3; significant differences were indicated as *P<0.05.

Effects of EGCG Used During IVM and IVC on the Developmental Potential of the Oocytes

EGCG treatment during IVC significantly reduced the cleaved rate and blastocyst rate of the oocytes when compared to the group without EGCG treatment (Table 4). On the other hand, EGCG treatment during IVM significantly increased the cleavage rate and blastocyst rate of the oocytes when compared to the group without EGCG treatment (Table 4). EGCG treatment during IVM and IVC significantly decreased the cleavage rate and blastocyst rate of the oocytes when compared to the group without EGCG treatment and group with EGCG treatment during IVM (Table 4). Collectively, these results indicated that EGCG treatment during IVM increased the oocyte developmental potential while EGCG treatment during IVC attenuated the oocyte developmental potential.

Discussion

The IVM technique for the COC has been developed and applied to produce offspring in mammals including pigs, however, the rate of blastocytes formation following IVF is still low using IVM oocytes compared with that of in vivo-matured oocytes such as pigs.¹⁵ In pigs, the COCs are usually collected from medium size antral follicles (>3 mm diameter) where the oocyte has the ability to induce oocyte maturation, whereas follicular somatic cells do not acquire the ability to respond to ovulation stimuli. In addition, in vitro environments usually increase cell production of ROS, which has been implicated as a main cause of cell damage.¹⁶ Therefore, optimizing the culture conditions to mimic the in vivo environments is essential for the normal growth and maturation of oocytes. In the present study, different concentrations of EGCG were added to the culture medium of IVM, IVF and IVC to

Table 3 Effects of EGCG Used During IVM and IVF on the Developmental Potential of the Oocytes

EGCG (μM) During IVM	EGCG (μM) During IVF	Number of Mature Oocytes	Number of Cleaved Oocytes	Cleavage Rate (%)	Number of Blastocysts	Blastocyst Rate (%)
0	0	214	90	42.34 ± 1.76 ^c	48	22.01 ± 2.66 ^c
0	10	241	108	56.58 ± 4.19 ^b	61	30.91 ± 1.24 ^b
10	0	122	55	45.37 ± 3.40 ^c	33	26.81 ± 2.28 ^b
10	10	144	86	59.76 ± 3.96 ^a	51	35.29 ± 1.72 ^a

Note: Different superscript letters in the same column indicates statistically significant difference (P < 0.05).

Table 4 Effects of EGCG Used During IVM and IVC on the Developmental Potential of the Oocytes

EGCG (μM) During IVM	EGCG (μM) During IVC	Number of Mature Oocytes	Number of Cleaved Oocytes	Cleavage Rate (%)	Number of Blastocysts	Blastocyst Rate (%)
0	0	199	84	40.98 ± 2.71 ^b	52	25.37 ± 3.58 ^b
0	10	223	72	31.46 ± 5.72 ^c	44	19.63 ± 2.23 ^c
10	0	165	82	48.28 ± 2.13 ^a	52	30.23 ± 3.05 ^a
10	10	172	52	28.02 ± 4.60 ^c	33	17.96 ± 2.46 ^c

Note: Different superscript letters in the same column indicates statistically significant difference (P < 0.05).

observe the maturation quality of oocytes. EGCG at 10 μ M significantly improve the IVM of porcine oocytes. In this study, the supplementation of EGCG during IVF and IVC produces two different effects. Supplementation of 10 μ M EGCG during IVF can promote the cleavage rate of oocytes, which was consistent with findings from Spinaci et al, showing that supplementation of 10 μ M EGCG during IVF but not IVM significantly increased the fertilization rate.¹⁷ The effect of the addition of EGCG during IVF could be due to its action on the sperm not on the oocyte.

In the process of in vitro culture, oocytes and embryos are inevitably exposed to light and higher oxygen concentration than in vivo, which may lead to enhanced production of ROS (superoxide anion, hydrogen peroxide and highly reactive hydroxyl). A large number of studies have shown that the supplementation of antioxidants to the IVM medium can improve the developmental ability of the embryo. EGCG acts as antioxidant has been found to moderate the deleterious effects of maternal hyperthermia on follicle-enclosed oocytes in mice.⁷ Barberino et al demonstrated that EGCG attenuated apoptosis of preantral follicles through the phosphatidylinositol-3-kinase/protein kinase B signaling pathway after in vitro culture of sheep ovarian tissue.¹⁸ Huang et al suggested that 50 μ M EGCG can improve the bovine oocyte maturation, and the protective role of EGCG may be correlated with its antioxidative property.⁶ In combination with previous studies, our results indicated that the effects of EGCG on the IVM of porcine oocytes may be related to the antioxidant and anti-apoptosis effect, which was further explored in the present study.

Excessive accumulation of ROS can lead to oxidative stress, and our results showed that EGCG can increase the total antioxidant capacity and reduce the level of ROS and MDA in the porcine oocytes. This may be due to that EGCG can directly eliminate ROS and/or EGCG can act synergistically with the antioxidant system.⁵ Non-enzymatic systems rely on molecules to directly quench ROS, while enzymatic systems are composed of specific enzymes that detoxify ROS. In the latter, the SOD family is important in the regulation of oxidative stress. SOD is the only known enzyme that directly scavenges free radicals by catalyzing the dismutation of superoxide anion to hydrogen peroxide. SOD enzyme regulates the levels of superoxide and hydrogen peroxide produced by cells, and then regulates cell signal transduction.¹⁹ Catalase is an important antioxidant

and a marker enzyme of peroxisomes. It accounts for 40% of the total peroxisome enzymes. It is an antioxidant oligomerase with four identical subunits arranged in tetrahedrons, and is an important enzyme that protects cells from ROS oxidative damage.²⁰ Glutathione is a tripeptide composed of glutamic acid, cysteine and glycine containing γ -amide bonds and sulfhydryl groups. It can maintain the normal immune system function and has an antioxidant effect. Glutathione peroxidase (GPXs) combines GSH oxidation with H_2O_2 detoxification.²¹ Studies demonstrated that heat stress could produce oxidative stress in bubaline oocytes, which triggers the elimination of ROS by the antioxidant enzyme defense system.²² Our studies consistently showed that EGCG reduced the ROS level and MDA content of the oocytes, while increased the intracellular GSH content and total antioxidant capacity.

The apoptosis process can affect the quality and survival rate of the oocytes and thus to influence the embryonic development.²³ Bcl-2 family proteins play a key role in regulating cell death through the balanced interaction between pro-apoptotic and anti-apoptotic protein members.²⁴ The pro-apoptotic protein Bax is the core of mammalian mitochondrial-dependent apoptosis. Caspase-3 also plays an irreplaceable role in cell apoptosis. Caspase-3 is the most important terminal splicing enzyme in the process of cell apoptosis, and activated caspase-3 is the key executor of cell apoptosis. Our results showing that EGCG up-regulated the Bcl-2 mRNA expression level, but decreased Bax and caspase-3 mRNA expression levels. Collectively, these results implied that the antioxidant and anti-apoptotic effects of EGCG in porcine oocytes are largely related to the regulation of SOD1, CAT and GPX as well as the apoptosis-related genes.

In summary, our results suggest that EGCG promotes the in vitro maturation and embryo development following IVF of porcine oocytes. The protective effects of EGCG on the oocytes may be associated with its antioxidant and anti-apoptosis properties.

Funding

This study was supported by grants from the Natural Science Foundation of Guangdong Province (2020A1515010976), the Local Innovative and Research Teams Project of Guangdong Pearl River Talents Program (2019BT02N630), the Science and Technology Innovation Strategy Projects of Guangdong Province (2018B020203002).

Disclosure

The authors report no conflicts of interest in this work.

References

1. Abdelnour SA, Abd El-Hack ME, Swelum AA, et al. The usefulness of retinoic acid supplementation during in vitro oocyte maturation for the in vitro embryo production of livestock: a review. *Animals*. 2019;9(8). doi:10.3390/ani9080561
2. Paramio MT, Izquierdo D. Current status of in vitro embryo production in sheep and goats. *Reprod Domest Anim*. 2014;49(Suppl 4):37–48. doi:10.1111/rda.12334
3. Lu C, Zhang Y, Zheng X, et al. Current perspectives on in vitro maturation and its effects on oocyte genetic and epigenetic profiles. *Sci China Life Sci*. 2018;61(6):633–643. doi:10.1007/s11427-017-9280-4
4. Lonergan P, Fair T. Maturation of oocytes in vitro. *Annu Rev Anim Biosci*. 2016;4(1):255–268. doi:10.1146/annurev-animal-022114-110822
5. Steinmann J, Buer J, Pietschmann T, Steinmann E. Anti-infective properties of epigallocatechin-3-gallate (EGCG), a component of green tea. *Br J Pharmacol*. 2013;168(5):1059–1073. doi:10.1111/bph.12009
6. Huang Z, Pang Y, Hao H, Du W, Zhao X, Zhu H. Effects of epigallocatechin-3-gallate on bovine oocytes matured in vitro. *Asian-Australas J Anim Sci*. 2018;31(9):1420–1430. doi:10.5713/ajas.17.0880
7. Roth Z, Aroyo A, Yavin S, Arav A. The antioxidant epigallocatechin gallate (EGCG) moderates the deleterious effects of maternal hyperthermia on follicle-enclosed oocytes in mice. *Theriogenology*. 2008;70(6):887–897. doi:10.1016/j.theriogenology.2008.05.053
8. Gadani B, Bucci D, Spinaci M, Tamanini C, Galeati G. Resveratrol and epigallocatechin-3-gallate addition to thawed boar sperm improves in vitro fertilization. *Theriogenology*. 2017;90:88–93. doi:10.1016/j.theriogenology.2016.11.020
9. Bucci D, Spinaci M, Yeste M, et al. Combined effects of resveratrol and epigallocatechin-3-gallate on post thaw boar sperm and IVF parameters. *Theriogenology*. 2018;117:16–25. doi:10.1016/j.theriogenology.2018.05.016
10. Bucci D, Cunto M, Gadani B, Spinaci M, Zambelli D, Galeati G. Epigallocatechin-3-gallate added after thawing to frozen dog semen: effect on sperm parameters and ability to bind to oocytes' zona pellucida. *Reprod Biol*. 2019;19(1):83–88. doi:10.1016/j.repbio.2018.12.001
11. Nie JY, Zhu XX, Xie BK, et al. Successful cloning of an adult breeding boar from the novel Chinese Guike no. 1 swine specialized strain. *J Biotech*. 2016;6(2):218. doi:10.1007/s13205-016-0525-4
12. Vanderhyden BC, Caron PJ, Buccione R, Eppig JJ. Developmental pattern of the secretion of cumulus expansion-enabling factor by mouse oocytes and the role of oocytes in promoting granulosa cell differentiation. *Dev Biol*. 1990;140(2):307–317. doi:10.1016/0012-1606(90)90081-S
13. Pella R, Suárez-Cunza S, Orihuela P, et al. Oxidative balance in follicular fluid of ART patients of advanced maternal age and blastocyst formation. *JBRA Assist Reprod*. 2020;24(3):296–301. doi:10.5935/1518-0557.20200012
14. Li J, Wei H, Li Y, Li Q, Li N. Identification of a suitable endogenous control gene in porcine blastocysts for use in quantitative PCR analysis of microRNAs. *Sci China Life Sci*. 2012;55(2):126–131. doi:10.1007/s11427-012-4289-8
15. Okamoto A, Ikeda M, Kaneko A, Kishida C, Shimada M, Yamashita Y. The novel pig in vitro maturation system to improve developmental competence of oocytes derived from atretic non-vascularized follicle. *Biol Reprod*. 2016;95(4):7. doi:10.1095/biolreprod.116.138982
16. Cetica PD, Pintos LN, Dalvit GC, Beconi MT. Antioxidant enzyme activity and oxidative stress in bovine oocyte in vitro maturation. *IUBMB Life*. 2001;51(1):57–64. doi:10.1080/15216540152035073
17. Spinaci M, Volpe S, De Ambrogi M, Tamanini C, Galeati G. Effects of epigallocatechin-3-gallate (EGCG) on in vitro maturation and fertilization of porcine oocytes. *Theriogenology*. 2008;69(7):877–885. doi:10.1016/j.theriogenology.2008.01.005
18. Barberino RS, Santos JMS, Lins T, et al. Epigallocatechin-3-gallate (EGCG) reduces apoptosis of preantral follicles through the phosphatidylinositol-3-kinase/protein kinase B (PI3K/AKT) signaling pathway after in vitro culture of sheep ovarian tissue. *Theriogenology*. 2020;155:25–32. doi:10.1016/j.theriogenology.2020.05.037
19. Bresciani G, da Cruz IB, González-Gallego J. Manganese superoxide dismutase and oxidative stress modulation. *Adv Clin Chem*. 2015;68:87–130.
20. Pal S, Dey SK, Saha C, Tajmir-Riahi H-A. Inhibition of catalase by tea catechins in free and cellular state: a biophysical approach. *PLoS One*. 2014;9(7):e102460. doi:10.1371/journal.pone.0102460
21. Espinosa-Diez C, Miguel V, Mennerich D, et al. Antioxidant responses and cellular adjustments to oxidative stress. *Redox Biol*. 2015;6:183–197.
22. Waiz SA, Raies-UI-Haq M, Dhanda S, et al. Heat stress and antioxidant enzyme activity in bubaline (*Bubalus bubalis*) oocytes during in vitro maturation. *Int J Biometeorol*. 2016;60(9):1357–1366. doi:10.1007/s00484-015-1129-0
23. Boumela I, Assou S, Aouacheria A, et al. Involvement of BCL2 family members in the regulation of human oocyte and early embryo survival and death: gene expression and beyond. *Reproduction*. 2011;141(5):549–561. doi:10.1530/REP-10-0504
24. Soto P, Smith LC. BH4 peptide derived from Bcl-xL and Bax-inhibitor peptide suppresses apoptotic mitochondrial changes in heat stressed bovine oocytes. *Mol Reprod Dev*. 2009;76(7):637–646. doi:10.1002/mrd.20986

Drug Design, Development and Therapy

Dovepress

Publish your work in this journal

Drug Design, Development and Therapy is an international, peer-reviewed open-access journal that spans the spectrum of drug design and development through to clinical applications. Clinical outcomes, patient safety, and programs for the development and effective, safe, and sustained use of medicines are a feature of the journal, which has also

been accepted for indexing on PubMed Central. The manuscript management system is completely online and includes a very quick and fair peer-review system, which is all easy to use. Visit <http://www.dovepress.com/testimonials.php> to read real quotes from published authors.

Submit your manuscript here: <https://www.dovepress.com/drug-design-development-and-therapy-journal>



A novel identified circ-ANKHD1 targets the miR-27a-3p/SFRP1 signaling pathway and modulates the apoptosis of granulosa cells

Xiaoyan Li¹ · Fenglei Gao² · Yushan Fan¹ · Shefeng Xie¹ · Chengde Li¹ · Li Meng¹ · Li Li¹ · Shouquan Zhang¹ · Hengxi Wei¹

Received: 1 March 2021 / Accepted: 31 May 2021 / Published online: 5 June 2021

© The Author(s), under exclusive licence to Springer-Verlag GmbH Germany, part of Springer Nature 2021

Abstract

The specific expression profile and function of circular RNAs (circRNAs) in mammalian ovarian follicles, especially during the atresia process, are unclear. In this study, we verified and explored the expression and function of circ-ANKHD1 in granulosa cells. Our results showed that abundance of circ-ANKHD1 was significantly lower in the granulosa cells than that of ANKHD1. The expression of ANKHD1 was highest in the granulosa cells from follicles with a diameter of 5–6 mm and lowest in that with a diameter of 3–4 mm. Furthermore, the expression level of circ-ANKHD1 in the ovarian tissue of 1-day-old piglets was significantly higher than that of 17-month-old multiparous sows. The luciferase reporter assay showed the potential interaction between circ-ANKHD1 and miR-27a-3p/miR-142-5p. Furthermore, circ-ANKHD1 overexpression up-regulated SFRP1 expression, while miR-27a-3p overexpression suppressed SFRP1 expression in granulosa cells. Circ-ANKHD1 overexpression significantly decreased the cell apoptotic rates of the granulosa cells and repressed the cell population at G0/G1 and S phases but increased cell population at G2/M phase. Finally, circ-ANKHD1 overexpression increased the mRNA expression levels of Bcl-2 and cyclin D1 in the granulosa cells, while there are no effects on the mRNA expression levels of caspase-3, p53, Bax, and proliferating cell nuclear antigen. In conclusion, our study for the first time identified a novel circRNA, circ-ANKHD1 that may be associated with the biological functions of granulosa cells. Circ-ANKHD1 may promote the granulosa cell proliferation, but attenuate apoptosis, and these effects may be associated with modulation of miR-27a-3p/SFRP1.

Keywords Atresia · Granulosa cells · circ-ANKHD1 · miR-27a-3p · SFRP1 · Cell apoptosis

Xiaoyan Li and Fenglei Gao contributed equally to this work.

Responsible Editor: Lotfi Aleya

✉ Hengxi Wei
weihengxi@scau.edu.cn

Xiaoyan Li
915063371@qq.com

Fenglei Gao
1124157314@qq.com

Yushan Fan
648242687@qq.com

Shefeng Xie
2251078308@qq.com

Chengde Li
1097235578@qq.com

Li Meng
limeng@scau.edu.cn

Li Li
Lili007@scau.edu.cn

Shouquan Zhang
sqzhang@scau.edu.cn

¹ National Engineering Research Center for Breeding Swine Industry, Guangdong Provincial Key Lab of Agro-animal Genomics and Molecular Breeding, College of Animal Science, South China Agricultural University, Guangzhou 510642, China

² Department of Tropical Agriculture and Forestry, College of Guangdong Agriculture Industry Business Polytechnic, Guangzhou 510507, Guangdong, China

Introduction

With the rapid development of pig industry in China, improving the reproductive performance of sows has been the focus of animal husbandry workers (Xie et al. 2020; Yang et al. 2020). The reproductive performance of sows is affected by many factors including low rate of estrus, non-estrus, and delayed ovulation (Moreira et al. 2020; Roszkos et al. 2020). The estrus of sows depends on the development of follicles. In mammals, follicular atresia occurs at any stage and is a widespread physiological phenomenon (Cox 1997). Understanding underlying mechanisms of follicular atresia can improve the quantity and quality of ovulation, which is of great significance to the field of reproduction. Atresia and degeneration of follicles are triggered by granulosa cells, which play an important role in the development and atresia of follicles (Guthrie et al. 1995; Inoue et al. 2011). However, granulosa cell apoptosis is a complicated process, and its underlying mechanism is still unclear.

Unlike traditional RNA, circular RNA (circRNA) is a type of covalently closed circular structure RNA (noncoding RNA, ncRNA) without 5' and 3' structures and is processed by alternative splicing of precursor RNA (pre-mRNA) (Prats et al. 2020). CircRNA is widely and conservatively expressed in various species. CircRNA is relatively stable, as it is resistant to the degradation by RNA exonuclease (Prats et al. 2020). CircRNA has an important regulatory effect on genes via distinct mechanisms. Recent studies showed that circRNA plays a very important role in neurodevelopment, immunity, cancer, and economic traits of livestock and poultry (Huang et al. 2020, Li and Chen 2020, Rajappa et al. 2020). It has been reported that circRNAs mainly function as the miRNA sponges, thereby reducing the inhibitory effect of miRNAs on the targeted genes. For example, the overexpression of circ-EGFR promoted the production of estradiol and the growth of granulosa cells, and the down-regulation of circ-EGFR promoted the production of progesterone and inhibited the E2 secretion of granulosa cells. Circ-EGFR can regulate the Fyn gene expression by competitively binding with miR-125a-3p (Jia et al. 2018). Circ-PRMT5 has been identified as an oncogene in bladder cancer. Studies also showed that circ-PRMT5 was an oncogenic circRNA in non-small cell lung cancer (NSCLC) and regulated the progression of NSCLC by targeting the miR-377/382/498-EZH2 signaling axis (Wang et al. 2019). CircINHA could act as a sponge for miR-10a-5p to inhibit granulosa cell apoptosis in pig ovarian follicles (Guo et al. 2019). Wu et al. showed that circular RNA aplacirc_13267 up-regulated duck granulosa cell apoptosis by the apla-miR-1-13/THBS1 signaling pathway (Wu et al. 2020). However, the studies regarding the role of circRNA in reproductive sciences are still limited, which may need further exploration.

In our previous studies, the differentially expressed circRNAs were screened from healthy follicles and atretic follicles in the early stage (Meng et al. 2020). Among these circRNAs, we identified a novel circ-ANKHD1 in the granulosa cells. In this study, we validated the expression of circ-ANKHD1 in the granulosa cells and further explored the regulatory mechanisms of this novel circRNA in the proliferation and apoptosis of granulosa cells.

Materials and methods

Ethics statement

This work was approved by the Ethics Committee on Animal Experimentation of South China Agricultural University.

Cell culture

The isolation of granulosa cells from the pig ovaries was performed according to our previous methods (Meng et al. 2020). The 293FT cells were purchased from Thermo Fisher Scientific (Waltham, USA). For the cell culture, isolated granulosa cells or 293FT cells were seeded into 6-well or 12-well plates and cultured in Dulbecco's Modified Eagle Medium/Nutrient Mixture F-12 supplied with 10% FBS and 1% penicillin-streptomycin (Gibco, Thermo Fisher Scientific, Waltham, USA). All the cells were kept in a humidified incubator with 95% CO₂ at 37 °C.

Immunofluorescence staining

The cells were seeded on the glass slides and were then fixed with 4% paraformaldehyde for 30 min followed by washing with phosphate buffered saline (PBS) for 3 times. The cells were permeabilized with 0.2% Triton X-100 in PBS for 15 min and then blocked using 1% bovine serum albumin (BSA) in TBS (10 mM Tris-HCl, 150 mM NaCl, and 0.1% Tween 20; pH 7.5) for 1 h at room temperature. The cells were incubated with anti-follicle-stimulating hormone receptor (FSHR) polyclonal antibody (1:100; #Absin-abs120271, Absin Biotechnology Co. Ltd., Shanghai, China) in 1% BSA in TBS overnight at 4°C. The slides with the cells were washed twice for 5 min each time, followed by incubation with goat anti-rabbit IgG Alexa Fluor 568-Conjugated (Invitrogen, Carlsbad, USA) for 60 min. Phosphate buffered saline was used as the negative control for primary control to exclude non-specific staining. The nucleus was stained with Hoechst33342 (Hoechst AG, Frankfurt, USA). The slides were imaged using a Nikon E800 fluorescent microscope (Nikon, Tokyo, Japan).

MiRNAs, plasmids, and transfection

The miRNAs including the miRNA mimics (see Table 1 for the miRNA sequences) and the negative control miRNAs (mimics NC) were purchased from RiboBio company (Guangzhou, China). The circ-ANKHD1-overexpressing vector was generated using the pcDNA3.1 plasmid (GenePharma, Shanghai, China), and empty pcDNA3.1 vector was used as the negative control. For the cell transfections, the granulosa cells were seeded to the 6-well plates. When the confluence reached ~80% confluence, the cells were transfected with different miRNAs or plasmids by using Lipofectamine 3000 reagent (Invitrogen, Carlsbad, USA) according to the manufacturer's protocol.

RNA extraction

Total RNA samples from granulosa cells and tissues were extracted separately using TRIzol reagent (Invitrogen, Carlsbad, USA) according to the manufacturer's protocol. RNA integrity and quantity were assessed using standard denatured agarose gel electrophoresis and a NanoDrop ND-1000 spectrophotometer (Thermo Fisher Scientific, Waltham, USA), respectively.

RNase R treatment

The RNase R digestion was performed following previous protocols. Total RNA was incubated for 20 min at 37°C with RNase R treatment at 3 U/mg (Sigma-Aldrich, St. Louis, USA) to remove linear RNA. Reverse transcription was then performed on RNase R-treated RNA following the normal procedure.

Quantitative real-time PCR (qRT-PCR)

Reverse transcription for circRNAs and mRNA was implemented using Super-Script II (Takara, Dalian China) following the manufacturer's instructions. PCR was performed with a 1:5 dilution of cDNAs, and PCR products were used for electrophoresis in a 2% agarose gel. Direct PCR product

Sanger sequencing was performed by LGC Genomics (Berlin, Germany) Ready2 Run services. Quantitative RT-PCR was performed with a ChamQTM Universal SYBR® qPCR Master Mix (Vazyme, Nanjing, China) and a qTOWER3 touch detection system (Analytik Jena AG, Jena, Germany). The primer sequences for PCR were summarized in Table 2. The relative gene expression level was calculated using the comparative Ct method, and β -actin was used as the internal control.

Western blot assay

The proteins (20 μ g) of cells were separated by SDS-PAGE using 12% (v/v) gels and transferred onto PVDF membranes (Millipore, Billerica, MA, USA). After blocking with 5% non-fat milk for 1 h at room temperature, the membranes were incubated with primary antibodies against SFRP1 (1:1000; D260294, Sangon Biotech, Shanghai, China) or β -actin (1:1000; AF0003, Beyotime, China) overnight at 4 °C. The membranes were washed 3 times for 10 min each with TBST (0.1% Tween 20, 20 mM Tris/HCl, 150 mM NaCl; pH 8.0) and incubated for 1 h with horseradish peroxidase (HRP)-conjugated goat anti-rabbit (1:5000; D110058; Sangon Biotech) or goat-anti-mouse (1:1000; Beyotime) secondary antibodies at room temperature for 1 h. The membranes were incubated for 5 min with the enhanced chemiluminescence (ECL) detection reagent in the dark. β -actin was used as the internal control, and the relative protein expression levels of SFRP1 were analyzed by using ImageJ software (<https://imagej.nih.gov/ij/index.html>).

Prediction for circRNA/miRNA/mRNA pathways and dual-luciferase reporter assay

The relationship between circRNAs and miRNAs was predicted by using RegRNA2.0 (<http://regrna2.mbc.nctu.edu.tw/>), and predicted miRNAs were summarized in Table 3. The relationship between miR-27a-3p and its targeted genes were predicted by using TargetScan tool.

The full sequence of the circ-ANKHD1 was amplified from the genomic DNA and was subcloned into psiCHECK2 vector (Promega, Madison, USA). For the luciferase reporter assay, 293FT cells were seeded onto the 12-well plates. After culturing for 12 h, cells were co-transfected with luciferase reporter vector and the different miRNAs by using Lipofectamine 3000 reagent (Invitrogen, Carlsbad, USA) according to the manufacturer's protocol. At 48 h after co-transfection, the luciferase activities in the 293FT cells were determined by Dual-luciferase reporter assay kit (Promega, Madison, USA) according to the manufacturer's protocol.

Table 1 Sequences of miRNA mimics

MiRNAs	Sequences (5'-3')
miR-34a-5p	UGGCAGUGUCUUAGCUGGUUGU
miR-424-5p	CAGCAGCAAUUAUGUUUUGAA
miR-486-5p	UCCUGUACUGAGCUGCCCCGAG
miR-27a-3p	UUCACAGUGGCUAAGUUCGCG
miR-142-5p	CAUAAAGUAGAAAGCACUACU
miR-143-5p	GGUGCAGUGCUGCAUCUCUGGU

Table 2 Primer sequences for PCR

Primers	Forward (5'-3')	Reverse (5'-3')
AhR	AGAGAGTGGCATGATAGTGTTT	GCCTAGGTGTTTCATAATGTTG
Er α	AGGGAGAGGAGTTTGTGTG	TCTCCAGCAGCAGGTCATCG
Er β	GCTTCGTGGAGCTCAGCCTG	AGGATCATGGCCTTGACACAGA
circ-ANKHD1	GGAGGCTCGCATGGTTGAAT	GCTTCTAGTCGTGCCTGTGT
ANKHD1	CGAGGTGTCCGAGGTTGAAT	ACCTCAGGATCTGCAAAGGC
caspase-3	GGATTGAGACGGACAGTGCG	CCGTCCTTTGAATTCGCCA
Bcl-2	GGATAACGGAGGCTGGGATG	TTATGGCCCAGATAGGCACC
Bax	GCCCTTTTGCTTCAGGGTTTC	CAATGCGCTTGAGACACTCG
PCNA	GCAGAGCATGGACTCGTCTC	TTGGACATGCTGGTGAGGTT
cyclin D1	CTGGTGCCAACTGGTGTGTTG	CGTACTGGCCTTACGAGCAT
cyclin D2	AAGAGACCATTCCGCTGACG	TTCTCATTGGGCTGAGGCAG
p53	AAGGGAATTACGGGCCGAG	CACGCACCTCAAAGCTGTTC
β -actin	CCGTGAGAAGATGACCCAGATCATG	CGTGATCTCCTTCTGCATCCTGTC

Flow cytometry to detect cell apoptosis and cell cycle

The apoptosis of granulosa cells was assessed by flow cytometry using an Annexin V-fluorescein isothiocyanate (FITC)/

Table 3 Predicted miRNAs targeted by circ-ANKHD1

Motif name	Position	Score	Sequence
ssc-miR-135	395-418	133	acacggaggaaggagaaagcctgc
ssc-miR-27a	535-560	149	gtggaggctatttagatattgtgaa
ssc-miR-107	336-357	144	agatggggatgtgaatgctgtt
ssc-miR-34a	894-919	166	caaacagatgagatgcacatgcct
ssc-miR-221	727-750	130	gcagccagtgccaggtcatgtggaa
ssc-miR-503	236-259	137	gtgcactggatgaagctgctgctg
ssc-miR-30e-5p	528-551	130	agcatccagtgaggctatttaga
ssc-miR-499-3p	321-348	134	ggcagaggctgttcagatggggatgg
ssc-miR-143-5p	241-263	143	ctggatgaagctgctgctgcact
ssc-miR-143-5p	901-920	137	gatgagatgcacatgcctt
ssc-miR-486	721-741	151	atggaagcagccagtcaggt
ssc-miR-27b	637-659	149	ggaggattgttgacattgtgaa
ssc-miR-664-3p	431-452	137	gttcggctgggtattatgaatt
ssc-miR-34c	894-919	159	caaacagatgagatgcacatgcct
ssc-miR-142-5p	852-874	149	tatggttcgcttctacttgatg
ssc-miR-424	237-259	156	tgcactggatgaagctgctgctg
ssc-miR-196b-5p	597-625	136	gtctgcaacaggaaactgcactaactt
ssc-miR-324	324-348	134	agaggcttgttcagatggggatgtg
ssc-miR-769-5p	191-211	133	ttgcagatcctgaggtactcc
ssc-miR-194-3p	517-539	134	cccctaattggcagcatccagtgg
ssc-miR-1271	763-784	140	cttctagatcacgggagcaggca
ssc-miR-187	106-129	144	gtggatccagagacacagcacga
ssc-miR-187	250-270	138	gctgctgctgactgacacgg
ssc-miR-218b	872-896	148	atgctgtgcatgacagagcaca
ssc-miR-2476	759-779	153	agttcttctagatcacggggc

propidium iodide (PI) kit (Keygen, Nanjing, China). Briefly, cells with different treatments were harvested and suspended in Annexin V binding buffer. Then, cells were double-stained using FITC and PI for 15 min in the dark at room temperature, and cell apoptosis was assessed by a BD FACS Calibur (Beckman Coulter, USA).

For the cell cycle analysis, cells with different treatments were washed twice with cold PBS followed by incubating with 200 μ g/mL RNase A for 30 min at 37°C. After that, cells were stained with 100 μ g/mL PI for 30 min at room temperature. Cell cycle was assessed by a BD FACS Calibur (Beckman Coulter, USA).

Statistical analysis

The statistical analysis was performed using the GraphPad Prism version 7.00 (Graphpad, Software, San Diego, USA). Data were expressed as mean \pm standard deviation. The unpaired Student's t-test or one-way ANOVA followed by Bonferroni's multiple comparison tests was used to assess the significant differences between/among experimental groups. P-values < 0.05 were considered statistically significant.

Results

Characterization of the granulosa cells

The freshly isolated granulosa cells were in round or oval shape (Fig. 1A), and after culturing for 4 days, the morphology of the granulosa cells was mainly in spindle or irregular polygon shape (Fig. 1B). The reverse transcriptase PCR analysis showed that the expression of estrogen receptor alpha (ER α), aryl hydrocarbon receptor (AhR), and estrogen

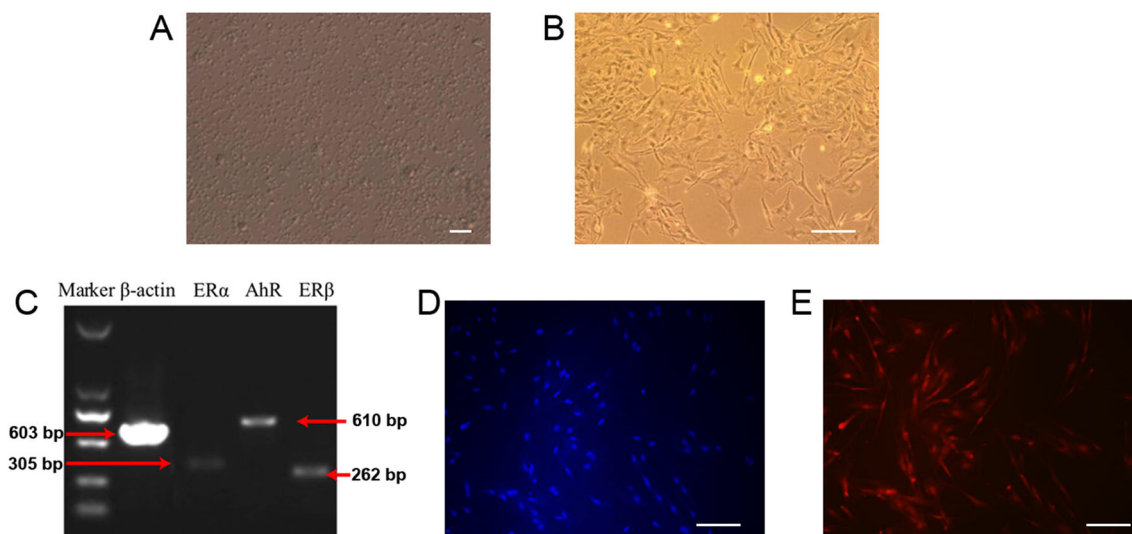


Fig. 1 Characterization of the granulosa cells. **A** Freshly isolated granulosa cells. Scale bar = 100 μ m; magnification: $\times 100$. **B** Isolated granulosa cells after culturing for 4 days. Scale bar = 100 μ m; magnification: $\times 200$. **C** Gel electrophoresis of β -actin, ER α , AhR, and

ER β genes as determined by RT-PCR in the isolated granulosa cells. **D** Hoechst33342 staining of the granulosa cells. Scale bar = 100 μ m; magnification: $\times 200$. **E** The immunofluorescent staining of FSHR in the granulosa cells. Scale bar = 100 μ m; magnification: $\times 200$

receptor beta (ER β) was detected in the granulosa cells (Fig. 1C). Further immunofluorescent staining detected the expression of FSHR in the granulosa cells (Fig. 1D).

Validation and characterization of circ-ANKHD1 in the granulosa cells

Firstly, we designed the divergent primers and convergent primers for circ-ANKHD1 and linear transcript. The cDNA and genomic DNA from granulosa cells were amplified and analyzed using agarose gel electrophoresis (Fig. 2A). Circ-ANKHD1 was further amplified by PCR, and the agarose gel electrophoresis identified a 936 bp product (Fig. 2B). Sanger sequencing of the PCR product indicated that the 2, 7 exon of ANKHD1 gene was back-spliced (G-G) to form the closed loop construction (Fig. 2C).

The homology of circ-ANKHD1 among different species was further analyzed. The percent identity and divergence matrix and phylogenetic tree among different species were constructed using the MegAlign software (Fig. 2D). The sequence of circ-ANKHD1 showed high sequence homologies with other species (100%, 95.3%, 95.3%, 91.3%, and 84.2% with *Sus scrofa*, *Homo Sapiens*, *Bos*, *Mus*, and *Gallus*, respectively; Fig. 2D).

Expression of circ-ANKHD1 in the granulosa cells and ovarian tissues

Firstly, qRT-PCR was performed to detect the expression of circ-ANKHD1 and ANKHD1 in the granulosa cells, and the results showed that abundance of circ-ANKHD1 was

significantly lower in the granulosa cells than that of ANKHD1 (Fig. 3A). The expression of circ-ANKHD1 in the granulosa cells with different size was further detected by qRT-PCR. As shown in Fig. 3B, the expression of ANKHD1 was highest in the granulosa cells with a diameter of 5–6 mm and lowest in the ones with a diameter of 3–4 mm. Furthermore, the expression level of circ-ANKHD1 in the ovarian tissue of 1-day-old piglets was significantly higher than that of 17-month-old multiparous sows (Fig. 3C).

Validation of the interaction between circ-ANKHD1 and its targeting miRNAs

The potential miRNAs targeted by circ-ANKHD1 was predicted by using RegRNA2.0 (<http://regrna2.mbc.nctu.edu.tw/>). The parameters are set as follows: species for RNA-RNA interaction region, *Sus scrofa*; score > 130 and free energy < -20 J. A total of 25 miRNAs were predicted to be targeted by circ-ANKHD1 (Table 3). Among these miRNAs, 6 miRNAs with highest scores and reported to be associated with cell proliferation and apoptosis were chosen for further validation studies. The luciferase report assay showed only miR-27a-3p mimics, and miR-142-5p mimics transfection significantly reduced the luciferase activities of psi-CHECK2-circ-ANKHD1 in 293FT cells when compared to their respective mimics NCs (Fig. 4), while the other miRNA mimics had no effects on the luciferase activities of psi-CHECK2-circ-ANKHD1 (Fig. 4). These results implied that circ-ANKHD1 could potentially interact with miR-27a-3p and miR-142-5p.

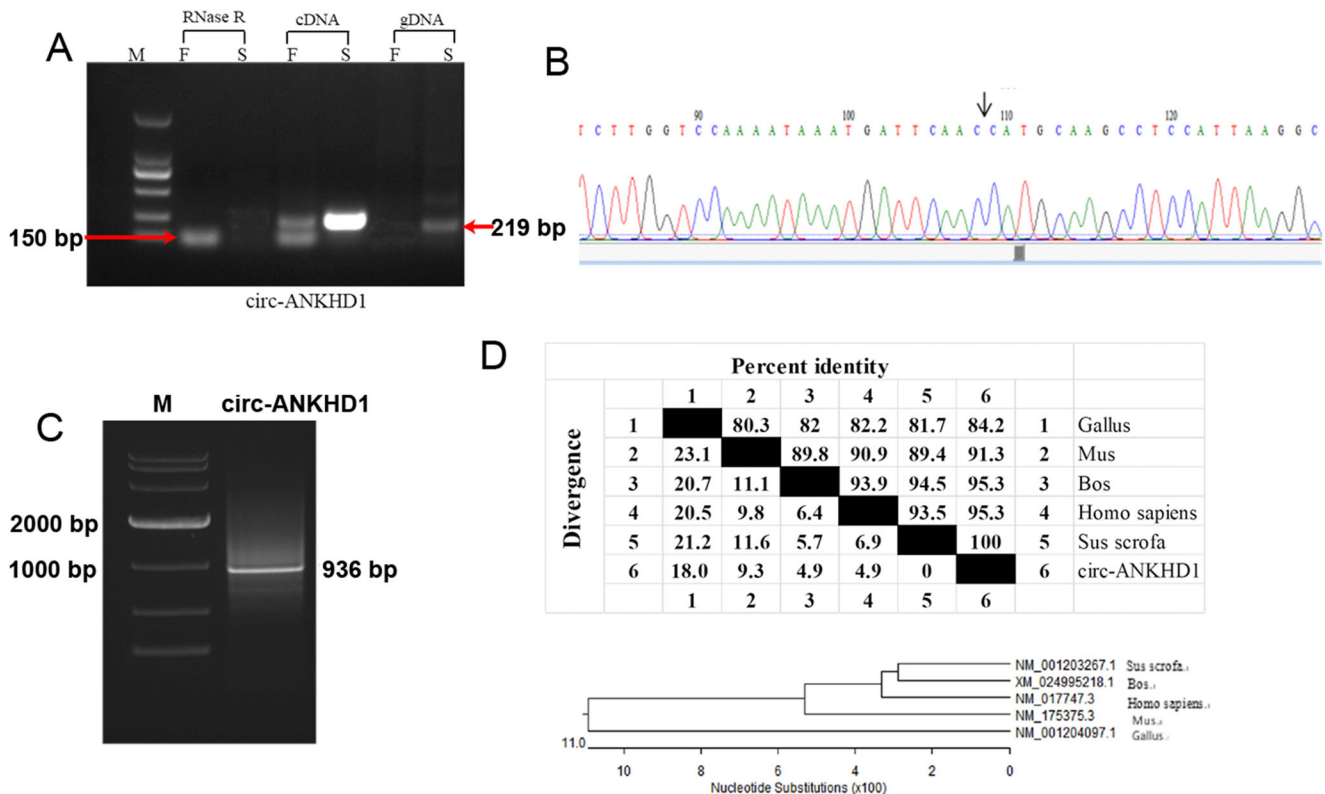


Fig. 2 Validation and characterization of circ-ANKHD1 in the granulosa cells. **A** The agarose gel electrophoresis was performed using the divergent primers and convergent primers to verify the existence of circ-ANKHD1 in granulosa cells. M = marker. **B** Representative examples of PCR products purified and sequenced to confirm circRNA junction

sites by Sanger sequencing. **C** The amplified PCR product of circ-ANKHD1 was shown by the agarose gel electrophoresis. M, marker. **D** Percent identity and divergence matrix and phylogenetic tree and of the circ-ANKHD1 sequence

Effects of circ-ANKHD1 and miR-27a-3p overexpression on the expression of SFRP1 in the granulosa cells

Furthermore, we constructed the circ-ANKHD1 overexpressing vector to transiently overexpress circ-ANKHD1 in granulosa cells, and pcDNA3.1-circ-ANKHD1 transfection significantly up-regulated the circ-ANKHD1 expression in the granulosa cells when compared to that transfected with pcDNA3.1 (Fig. 5). As the potential interaction between circ-ANKHD1 and miR-27a-3p has been detected by luciferase reporter assay, we further

predicted the binding sites between miR-27a-3p and its targets. As shown in Fig. 6A, the bioinformatics predicting results showed that both secreted frizzled-related protein 1 (SFRP1) 3' untranslated region and circ-ANKHD1 harbored the binding sites for miR-27a-3p. Further qRT-PCR and western blot results showed that circ-ANKHD1 overexpression significantly up-regulated SFRP1 mRNA and protein expression in the granulosa cells (Fig. 6B and C), while miR-27a-3p overexpression down-regulated SFRP1 mRNA and protein expression in the granulosa cells (Fig. 6D and E).

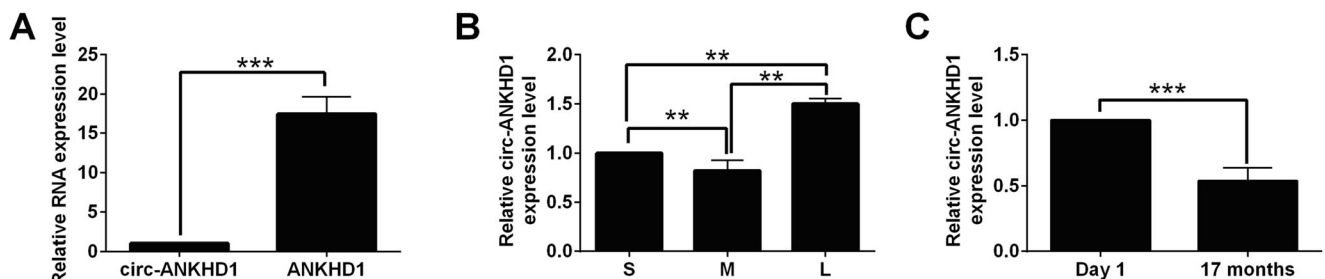
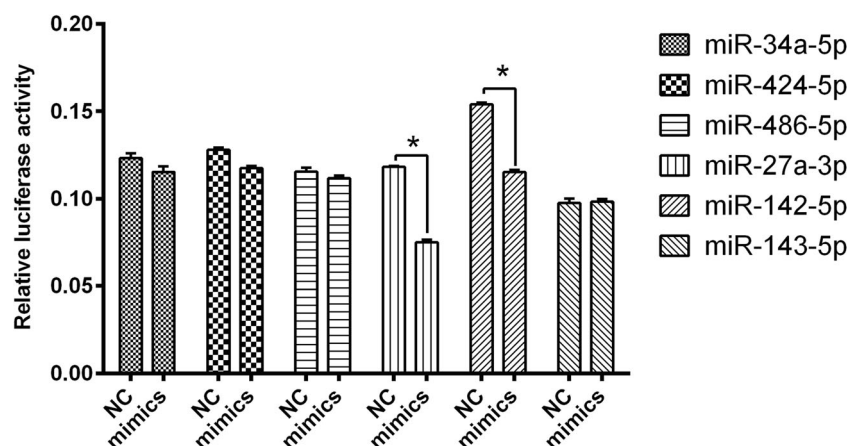


Fig. 3 Expression of circ-ANKHD1 in the granulosa cells. **A** The expression of ANKHD1 and circ-ANKHD1 in the granulosa cells was determined by qRT-PCR. **B** The expression of circ-ANKHD1 in granulosa

cells with different sizes was determined by qRT-PCR. **C** The expression of circ-ANKHD1 in the ovarian tissues from 1-day piglets and 17-month-old pigs. N = 3. **P < 0.01 and ***P < 0.001

Fig. 4 Validation of the interaction between circ-ANKHD1 and its targeting miRNAs. Luciferase activities of the pGL3-circ-ANKHD1 were determined in 293FT cells after being transfected with different miRNAs determined by the Dual-luciferase activity



Effects of circ-ANKHD1 on the cell apoptosis, cell cycle, and the mRNA expression levels of apoptosis-related mediators

Furthermore, granulosa cell apoptosis and cycle were determined by flow cytometry. As shown in Fig. 7A, circ-ANKHD1 overexpression significantly reduced the cell apoptotic rates of granulosa cells when compared to that transfected with pcDNA3.1. Consistently, circ-ANKHD1 overexpression repressed the cell population at G0/G1 and S phases but increased the cell population at G2/M phase (Fig. 7B). In order to further determine the effects of circ-ANKHD1 on the granulosa cell proliferation and apoptosis, we determined the mRNA expression levels of key mediators associated with cell proliferation and apoptosis. The qRT-PCR results further showed that circ-ANKHD1 overexpression increased the mRNA expression levels of Bcl-2 and cyclin D1 in the granulosa cells, while there were no effects on the mRNA expression levels of caspase-3, p53, Bax, and proliferating cell nuclear antigen (Fig. 7C).

Discussion

The reproductive activities of sows are associated with the changes of hormones. Reproductive hormones are regulated by hypothalamus-pituitary-ovarian axis in the body. Although hypothalamus plays a dominant role, the main factors affecting reproduction are the reproductive hormones secreted by the ovary and the pituitary gland. The follicles in the ovary secrete estrogen that can regulate the estrus of the sows and play an important role in animal reproduction. In each estrus cycle, follicles mature through three stages: recruitment, selection, and domination. Animals have many primordial follicles before birth, but most of them are atresia and degenerated (Inoue et al. 2011). The disappearance of follicles before birth is mainly caused by the apoptosis of oocytes, and the atresia of follicles after birth is mainly due to the apoptosis of granulosa cells (Guthrie et al. 1995). In our previous studies, the differentially expressed circRNAs were screened from healthy follicles and atretic follicles in the early stage

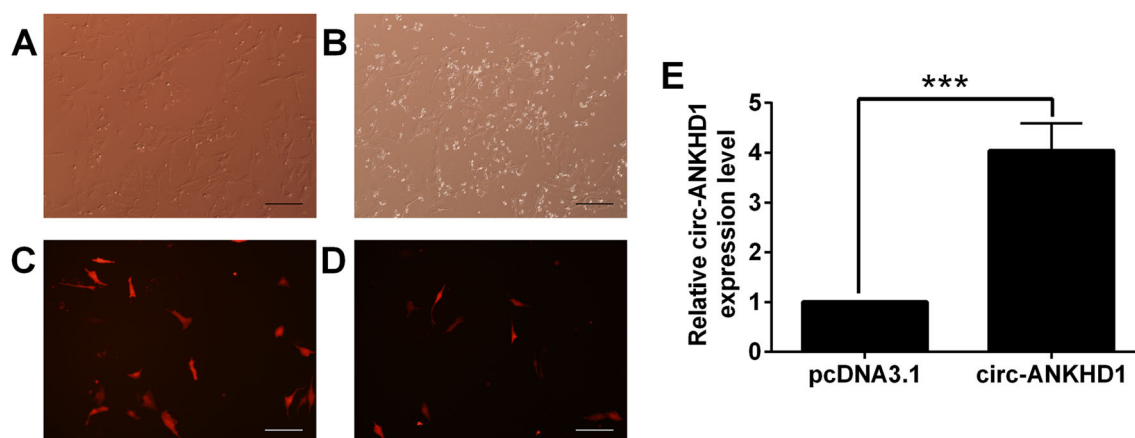


Fig. 5 The expression of circ-ANKHD1 in granulosa cells after being transfected with pcDNA3.1 or pcDNA3.1-circ-ANKHD1. **A** and **B** The cell morphology of the granulosa cells transfected with pcDNA3.1 (**A**) or pcDNA3.1-ANKHD1 (**B**). Scale bar = 100 μ m; magnification: $\times 200$. **C** and **D** The fluorescent imaging of the granulosa cells transfected with

pcDNA3.1 (**C**) or pcDNA3.1-ANKHD1 (**D**). Scale bar = 100 μ m; magnification: $\times 200$. **E** The expression of circ-ANKHD1 in granulosa cells transfected with pcDNA3.1 or pcDNA3.1-ANKHD1 was determined by qRT-PCR. N = 3. **P < 0.01

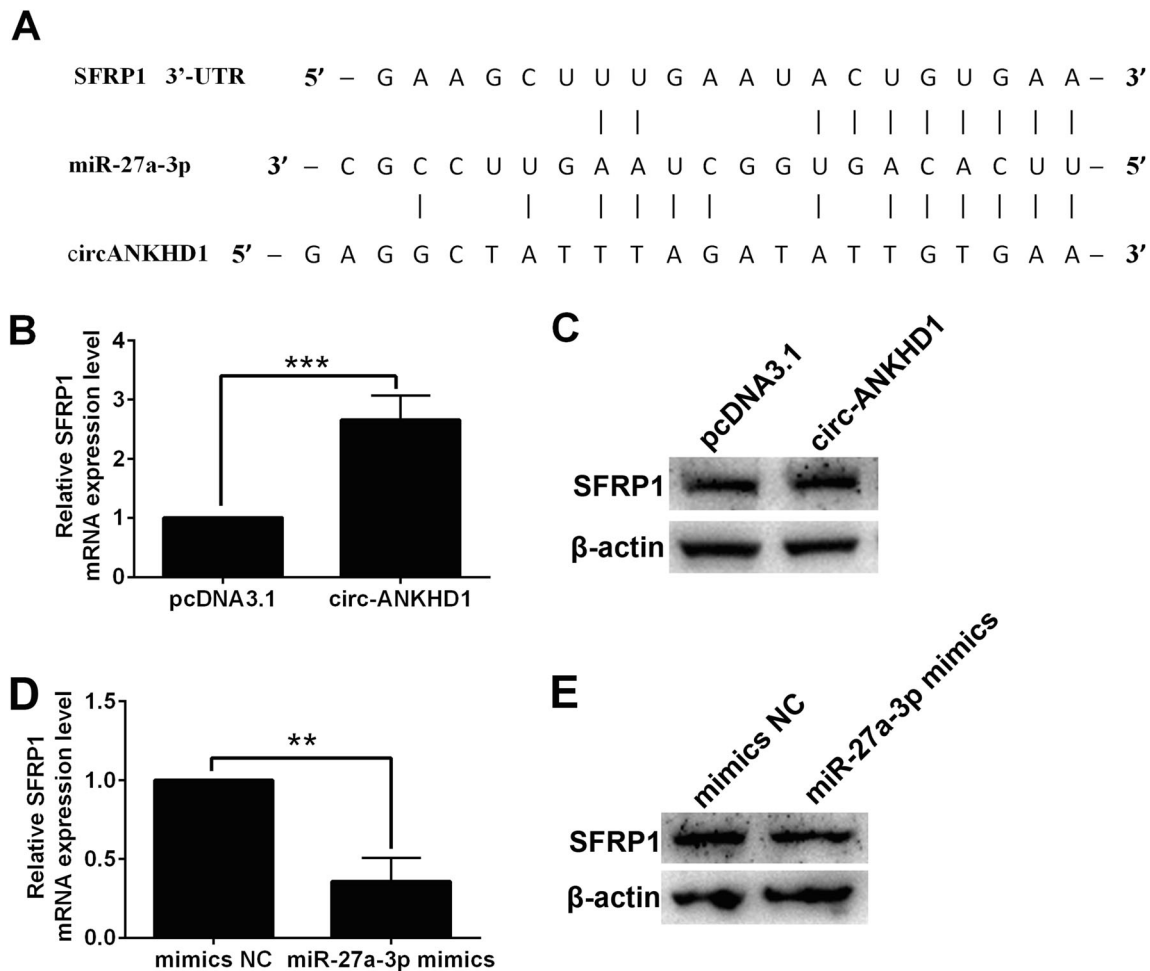


Fig. 6 SFRP1 was a target of miR-27a-3p. **A** The predicted binding sites between miR-27a-3p and SFRP1 3'-UTR/circ-ANKHD1. **B** and **C** The mRNA and protein expression of SFRP1 in granulosa cells after being transfected with pcDNA3.1 or circ-ANKHD1 was determined by qRT-

PCR and western blot assay, respectively. **D** and **E** The mRNA and protein expression of SFRP1 in granulosa cells after being transfected with mimics NC or miR-27a-3p mimics was determined by qRT-PCR and western blot assay, respectively. N = 3. **P < 0.01 and ***P < 0.001

(Meng et al. 2020). In this study, we verified and explored the expression and function of circ-ANKHD1 in granulosa cells.

Studies have shown that circRNAs play an important role in the occurrence of diseases (Prats et al. 2020). CircRNA is an important regulatory factor in the gene expression network and participates in a variety of biological processes (Prats et al. 2020), while little is known about the role of circRNAs in the process of follicular development and atresia. Studies have shown that circ-INHA was down-regulated in the process of follicular atresia and exerted anti-apoptotic effects on granulosa cells through targeting miR-10a-5p (Guo et al. 2019). Through high-throughput sequencing, differentially expressed circRNAs have been detected between healthy porcine follicular granulosa cells and atretic follicular granulosa cells (Meng et al. 2020). Among them, the expression level of circ-ANKHD1 in atretic follicles was ten times lower than that in healthy follicles. According to the results of sequencing, we first designed two sets of primers (convergent primers and

divergent primers). RT-PCR forward primers can amplify the products in both gDNA and cDNA templates, and reverse primers can amplify the products in cDNA but not in gDNA and are resistant to RNase R, which verified that the gene ANKHD1 can be spliced into a circle. It has been verified that circ-ANKHD1 is widely expressed in pig tissues. The expression abundance of circ-ANKHD1 in ovarian granulosa cells is lower than that of linear ANKHD1. The expression level of circ-ANKHD1 in 1-day-old ovaries is extremely significantly higher than that of adult sows. The homology analysis of circ-ANKHD1 showed that ANKHD1 genes of several different species were highly conserved. However, the ring formation of circ-ANKHD1 in different species needs further verification.

It has been reported that circRNAs mainly function as the miRNA sponges, thereby reducing the inhibitory effect of miRNAs on the targeted genes (Zucko and Boris-Lawrie 2020). By using the RegRNA2.0 (<http://www.targetscan.org>) tool, we found that circ-ANKHD1 could potentially

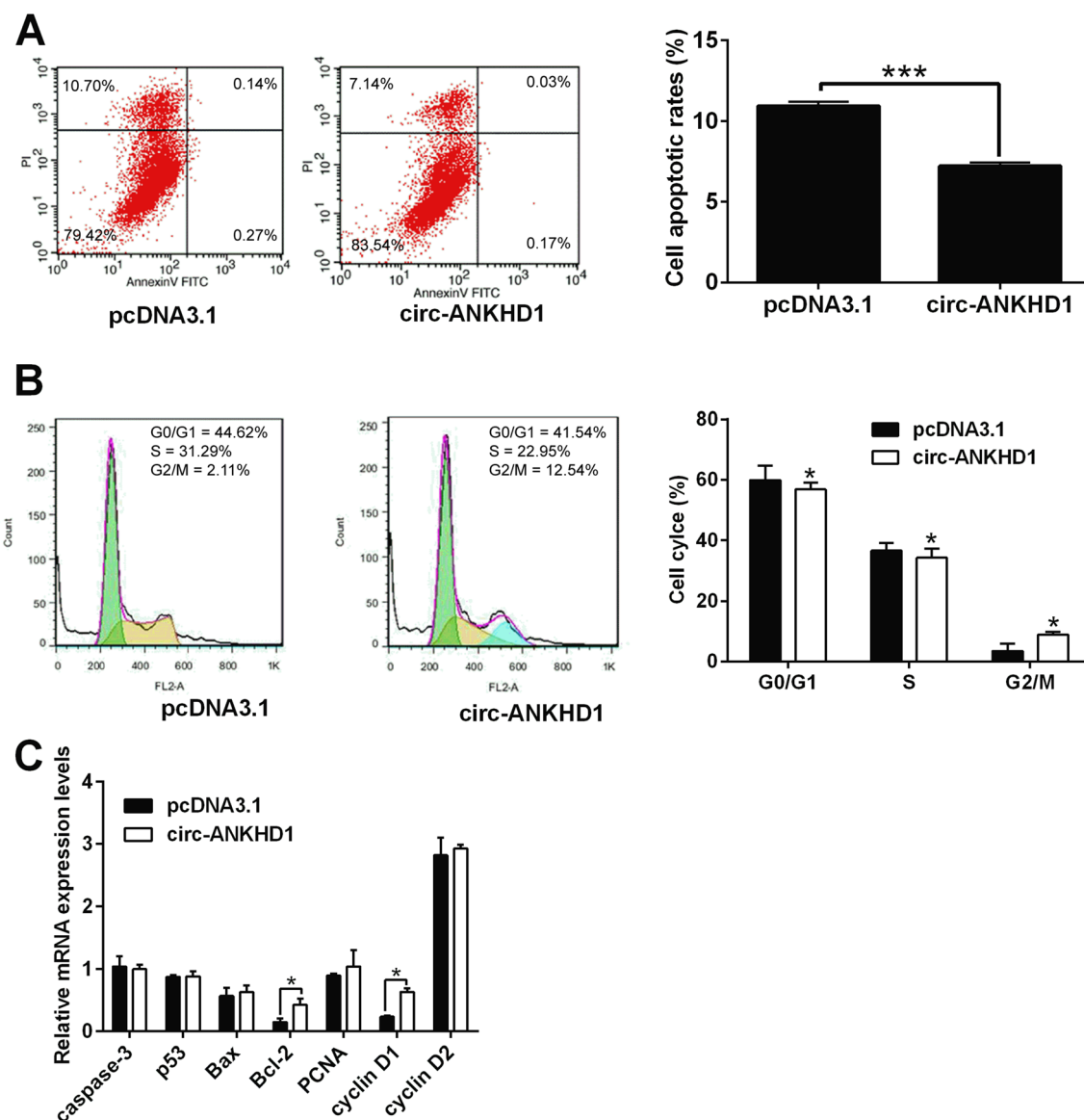


Fig. 7 Effects of circ-ANKHD1 overexpression on the cell apoptosis and cell cycle of granulosa cells. **A** The cell apoptotic rates and **B** cell cycle of the granulosa cells after being transfected with pcDNA3.1 or circ-ANKHD1 were determined by flow cytometry. The mRNA expression

levels of caspase-3, p53, Bax, Bcl-2, PCNA, cyclin D1, and cyclin D2 in the granulosa cells after being transfected with pcDNA3.1 or circ-ANKHD1 were determined by qRT-PCR. N = 3. *P < 0.05

interact with 25 miRNAs, and 6 miRNAs with highest scores and reported to be associated with cell proliferation and apoptosis were chosen for further validation studies. Among the 6 miRNAs, miR-27a-3p has been found to play an important role in the development of ovarian follicles (Zhang et al. 2018). In addition, miR-142-3p could inhibit the expression of protein tyrosine phosphatase non-receptor type 23, which subsequently affected the formation of testicular germ cell tumor (Tanaka et al. 2013). In the present study, miR-27a-3p mimics and miR-142-5p mimics transfection repressed the luciferase activity of psiCHECK2-circANKHD1, suggesting the potential interaction between circ-ANKHD1 and miR-27a-3p/miR-142-5p. Studies have shown that miR-27a-3p

exerted tumor-suppressive effects on liver cancer by targeting dual specificity phosphatase 16 (Li et al. 2018). In the study of colon cancer, SFRP1 was a downstream target gene of miR-27a-3p and exerted inhibitory effects on cell proliferation (Ba et al. 2017). The expression of SFRP1 mRNA and protein in human breast cancer cells and tissues was significantly lower than that of normal breast tissues and MCF10A cells. Inhibition of SFRP1 enhanced the proliferation, migration, and invasion of human breast cancer cells (Kong et al. 2017), and inhibition of miR-27a-3p increased SFRP1 mRNA and protein expression. In addition, miR-27a could regulate the proliferation, migration, and invasion of glioma cells via targeting Wnt/ β -actin signaling (Kong et al. 2017). To verify

whether circ-ANKHD1 can regulate miR-27a-3p by acting as a sponge and regulate its downstream targeting genes, circ-ANKHD1 and miR-27a-3p were overexpressed in granulosa cells. We found that circ-ANKHD1 overexpression up-regulated SFRP1 expression, while miR-27a-3p overexpression down-regulated SFRP1 expression in granulosa cells. SFRP1 is a gene that suppresses the Wnt signaling pathway. Studies have shown that the Wnt pathway plays a key role in the development of follicles, ovulation, and luteinization. Wnt4 was up-regulated and Wnt3 down-regulated in luteinizing granular cells in vitro. β -catenin is a core component in the Wnt pathway and is a multifunctional protein that plays a vital role in proliferation, growth, differentiation, and survival (Wu et al. 2017). Survivin and bone morphogenetic protein 4 (BMP4), as the downstream effector of β -catenin, are the survival factors of ovarian follicles and inhibit the apoptosis of granulosa cells (Johnson et al. 2002). BMP4 and bone morphogenetic protein 7 were found to inhibit the apoptosis of granulosa cells (Shimizu et al. 2012). However, there are also reports showing that miR-27a-3p mimics reduced the expression levels of Wnt3a and β -catenin in MRC-5 cells, suggesting that miR-27a-3p may repress Wnt3a/ β -catenin signaling pathway (Lv et al. 2019). Our results showed that circ-ANKHD1 overexpression up-regulated cyclin D1 expression in the granulosa cells, suggesting that the circ-ANKHD1 positively regulates cyclin D1 via sponging miR-27a-3p.

In the present study, we evaluated the effects of circ-ANKHD1 on the cell apoptosis and cell cycle of granulosa cells. In terms of cell cycle, circ-ANKHD1 overexpression reduced cell population at the G1/G0 and S phases and increased cell population at the G2/M phase. This may be explained by that the overexpression of circ-ANKHD1 induced an increase in the up-regulation of cyclin D1, a G1/S-specific cyclin, promoting the transition of cell cycle from G1 phase to S phase, thus promoting cell division. In addition, circ-ANKHD1 overexpression attenuated the cell apoptosis, which was in agreement with our previous findings showing that circ-ANKHD1 was up-regulated in the healthy follicles when compared to that in atresia follicles.

There are limitations existing in the present study. The present study only focused on the effects of circ-ANKHD1 on the cell proliferation and apoptosis of granulosa cells, while the effects of miR-27a-3p and SFRP1 on the cell proliferation and apoptosis have not been examined, which should be considered in our future study. Though miR-27a-3p could repress the expression of SFRP1, how miR-27a-3p regulates SFRP1 expression should be further examined. Though circ-ANKHD1 overexpression may promote the cell proliferation and attenuate apoptosis of granulosa cells, further studies may examine if circ-ANKHD1 silence could exert the opposite effects in granulosa cells. The mechanistic investigations of circ-ANKHD1 on the miR-27a-3p/SFRP1 were at the

preliminary stages, and more detailed mechanistic studies should be considered in the future plan. Moreover, our data has been limited to in vitro studies, and the functional role of circ-ANKHD1 should be explored in vivo studies in further experiments.

Conclusions

In conclusion, our study for the first time identified a novel circRNA, circ-ANKHD1 that may be associated with the biological functions of granulosa cells. Circ-ANKHD1 may promote the granulosa cell proliferation, but attenuate apoptosis, and these effects may be associated with modulation of miR-27a-3p/SFRP1. Further studies are warranted, in order to fully decipher the mechanistic role of circ-ANKHD1 in regulating granulosa cell proliferation and apoptosis.

Author contribution HW, XL, and FG conceived the study; XL, FG, YF, and SX performed the experiments; CL, LM, and LL performed statistical analysis; SZ prepared the figures; HW wrote the manuscript; all the authors approved for the manuscript submission.

Funding This study was supported by grants from the Local Innovative and Research Teams Project of Guangdong Pearl River Talents Program (2019BT02N630), the Natural Science Foundation of Guangdong Province (2020A1515010976), and the Science and Technology Innovation Strategy Projects of Guangdong Province (2018B020203002).

Availability of data and materials

All the data are available upon the request from the corresponding author.

Declarations

Ethics approval and consent to participate All the animal experimental procedures were approved by the Ethics Committee on Animal Experimentation of South China Agricultural University.

Consent for publication Not applicable.

Conflict of interest The authors declare no competing interests.

References

- Ba S, Xuan Y, Long ZW, Chen HY, Zheng SS (2017) MicroRNA-27a promotes the proliferation and invasiveness of colon cancer cells by targeting SFRP1 through the Wnt/ β -catenin signaling pathway. *Cellular physiology and biochemistry : international journal of experimental cellular physiology, biochemistry, and pharmacology* 42: 1920–1933
- Cox NM (1997) Control of follicular development and ovulation rate in pigs. *J Reprod Fertil Suppl* 52:31–46
- Guo T, Zhang J, Yao W, Du X, Li Q, Huang L, Ma M, Li Q, Liu H, Pan Z (2019): CircINHA resists granulosa cell apoptosis by upregulating CTGF as a ceRNA of miR-10a-5p in pig ovarian follicles.

- Biochimica et biophysica acta. Gene regulatory mechanisms 1862, 194420
- Guthrie HD, Grimes RW, Cooper BS, Hammond JM (1995) Follicular atresia in pigs: measurement and physiology. *J Anim Sci* 73:2834–2844
- Huang Y, Wang Y, Zhang C, Sun X (2020) Biological functions of circRNAs and their progress in livestock and poultry. *Reproduction in domestic animals = Zuchthygiene*
- Inoue N, Matsuda F, Goto Y, Manabe N (2011) Role of cell-death ligand-receptor system of granulosa cells in selective follicular atresia in porcine ovary. *The Journal of reproduction and development* 57: 169–175
- Jia W, Xu B, Wu J (2018) Circular RNA expression profiles of mouse ovaries during postnatal development and the function of circular RNA epidermal growth factor receptor in granulosa cells. *Metab Clin Exp* 85:192–204
- Johnson AL, Langer JS, Bridgham JT (2002) Survivin as a cell cycle-related and antiapoptotic protein in granulosa cells. *Endocrinology* 143:3405–3413
- Kong LY, Xue M, Zhang QC, Su CF (2017) In vivo and in vitro effects of microRNA-27a on proliferation, migration and invasion of breast cancer cells through targeting of SFRP1 gene via Wnt/ β -catenin signaling pathway. *Oncotarget* 8:15507–15519
- Li I, Chen YG (2020) Emerging roles of circular RNAs in innate immunity. *Curr Opin Immunol* 68:107–115
- Li JM, Zhou J, Xu Z, Huang HJ, Chen MJ, Ji JS (2018) MicroRNA-27a-3p inhibits cell viability and migration through down-regulating DUSP16 in hepatocellular carcinoma. *J Cell Biochem* 119:5143–5152
- Lv X, Li J, Hu Y, Wang S, Yang C, Li C, Zhong G (2019) Overexpression of miR-27b-3p targeting Wnt3a regulates the signaling pathway of Wnt/ β -catenin and attenuates atrial fibrosis in rats with atrial fibrillation. *Oxidative Med Cell Longev* 2019: 5703764
- Meng L, Teerds K, Tao J, Wei H, Jaklofsky M, Zhao Z, Liang Y, Li L, Wang CC, Zhang S (2020) Characteristics of circular RNA expression profiles of porcine granulosa cells in healthy and atretic antral follicles. *International journal of molecular sciences* 21
- Moreira RHR, Pérez Palencia JY, Moita VHC, Caputo LSS, Saraiva A, Andretta I, Ferreira RA, de Abreu MLT (2020) Variability of piglet birth weights: a systematic review and meta-analysis. *J Anim Physiol Anim Nutr* 104:657–666
- Prats AC, David F, Diallo LH, Roussel E, Tatin F, Garmy-Susini B, Lacazette E (2020) Circular RNA, the key for translation. *International journal of molecular sciences* 21
- Rajappa A, Banerjee S, Sharma V, Khandelia P (2020) Circular RNAs: emerging role in cancer diagnostics and therapeutics. *Front Mol Biosci* 7:577938
- Roszkos R, Tóth T, Mézes M (2020) Review: practical use of n-3 fatty acids to improve reproduction parameters in the context of modern sow nutrition. *Animals: an open access journal from MDPI* 10
- Shimizu T, Kayamori T, Murayama C, Miyamoto A (2012) Bone morphogenetic protein (BMP)-4 and BMP-7 suppress granulosa cell apoptosis via different pathways: BMP-4 via PI3K/PDK-1/Akt and BMP-7 via PI3K/PDK-1/PKC. *Biochem Biophys Res Commun* 417:869–873
- Tanaka K, Kondo K, Kitajima K, Muraoka M, Nozawa A, Hara T (2013) Tumor-suppressive function of protein-tyrosine phosphatase non-receptor type 23 in testicular germ cell tumors is lost upon overexpression of miR142-3p microRNA. *J Biol Chem* 288:23990–23999
- Wang Y, Li Y, He H, Wang F (2019) Circular RNA circ-PRMT5 facilitates non-small cell lung cancer proliferation through upregulating EZH2 via sponging miR-377/382/498. *Gene* 720:144099
- Wu XQ, Wang YQ, Xu SM, Liu JF, Bi XY, Wang ZQ, Zhang JP (2017) The WNT/ β -catenin signaling pathway may be involved in granulosa cell apoptosis from patients with PCOS in North China. *Journal of gynecology obstetrics and human reproduction* 46:93–99
- Wu Y, Xiao H, Pi J, Zhang H, Pan A, Pu Y, Liang Z, Shen J, Du J (2020) The circular RNA aplacirc_13267 upregulates duck granulosa cell apoptosis by the apla-miR-1-13/THBS1 signaling pathway. *J Cell Physiol* 235:5750–5763
- Xie Y, Xu Z, Wu Z, Hong L (2020) Sex manipulation technologies progress in livestock: a review. *Frontiers in veterinary science* 7:481
- Yang AQ, Chen B, Ran ML, Yang GM, Zeng C (2020) The application of genomic selection in pig cross breeding. *Yi chuan = Hereditas* 42:145–152
- Zhang S, Chen X, Huang Z, Chen D, Yu B, He J, Zheng P, Yu J, Luo J, Luo Y, Chen H (2018) Effects of MicroRNA-27a on myogenin expression and Akt/FoxO1 signal pathway during porcine myoblast differentiation. *Anim Biotechnol* 29:183–189
- Zucko D, Boris-Lawrie K (2020) Circular RNAs are regulators of diverse animal transcriptomes: one health perspective. *Front Genet* 11:999

Publisher's note Springer Nature remains neutral with regard to jurisdictional claims in published maps and institutional affiliations.

RESEARCH ARTICLE



WILEY

Perfluorooctanoic acid inhibits the maturation rate of mouse oocytes cultured in vitro by triggering mitochondrial and DNA damage

Conghui Guo^{1,2} | Zhihong Zhao^{1,2} | Kun Zhao^{1,2} | Jianhao Huang^{1,2} | Linshu Ding^{1,2} | Xiaogang Huang^{1,2} | Li Meng^{1,2} | Li Li^{1,2} | Hengxi Wei^{1,2} | Shouquan Zhang^{1,2}

¹National Engineering Research Center for Breeding Swine Industry, College of Animal Science, South China Agricultural University, Guangzhou, China

²Guangdong Province Key Laboratory of Molecular Breeding, College of Animal Science, South China Agricultural University, Guangzhou, China

Correspondence

Hengxi Wei and Shouquan Zhang, College of Animal Science, South China Agricultural University, Wushan Avenue, Tianhe District, Guangzhou 510642, China.

Email: weihengxi@scau.edu.cn (H. W.) and sqzhang@scau.edu.cn (S. Z.)

Funding information

The Guangdong provincial promotion project on preservation and utilization of local breed of livestock and poultry, Grant/Award Number: 2018; The Local Innovative and Research Teams Project of Guangdong Pearl River Talents Program, Grant/Award Number: 2019BT02N630; The Natural Science Foundation of Guangdong Province, Grant/Award Number: 2020A1515010976

Abstract

Background: Perfluorooctanoic acid (PFOA) is widely used in the manufacture of household and industrial products. It has certain toxicity and leaves many residues in the environment. Numerous studies have shown that PFOA exhibits endocrine disrupting properties and immunotoxicity and induces developmental defects. However, there is very little information regarding its toxicity on oocytes.

Methods: We cultured denuded oocytes in maturation medium supplemented with 0, 300, or 500 PFOA during IVM and evaluated the maturation of oocytes from the aspects of ROS(DCFH-DA), mitochondria(MitoOrange and JC-1), DNA damage(P-H2AX), and cytoskeleton(β -tubulin).

Results: Compared with the control group, the PFOA treatment group exhibited significantly reduced proportion of oocytes maturation. Furthermore, the DCFH-DA test showed that PFOA significantly increased reactive oxygen species (ROS) levels. PFOA disrupted mitochondrial distribution and decreased mitochondrial function as assessed using MitoOrange and JC-1. In addition, PFOA-treated oocytes exhibited a significantly higher percentage of P-H2AX, defective β -tubulin, abnormal chromosome alignment, lower expression of the anti-apoptotic gene Bcl-2, and higher expression of the apoptotic genes caspase3 and Bax.

Conclusion: In summary, PFOA could negatively and directly affect oocyte maturation in vitro and cause oxidative stress, mitochondrial function disruption, DNA damage, cytoskeleton damage, and apoptosis.

KEYWORDS

cytoskeleton, mitochondria, oocytes, PFOA, ROS

1 | INTRODUCTION

Perfluorooctanoic acid (PFOA) is a perfluorinated compound (PFC) that is resistant to hydrolysis, photolysis,

and biodegradation. Because of its stability, PFOA is widely used in consumer goods and in the manufacture of antifouling agents—for carpets and furniture—paints for paper and cloth—cosmetics and household

detergent auxiliaries, polytetrafluoroethylene products, and fire extinguishing foams (Bach et al., 2016; Giesy, Kannan, & Jones, 2001; Koskela et al., 2016). PFCs usually contain 4–14 carbon atoms arranged in long carbon chains. They have a long half-life and exert significant toxicity (Pevny, Bitter, Krueger, & Thorsten, 2015). PFOA contains eight fluorocarbon bonds and has been widely studied due to its toxic effects. It has been shown that PFOA can enter and exert toxicity in different tissues of the human and other animals body through diet, drinking water, and inhalation (Lam et al., 2014; Lunardi et al., 2016; Rashid, Ramakrishnan, Fields, & Irudayaraj, 2020).

It has been reported that PFOA can enter the follicular fluid through the blood-egg barrier, causing reproductive toxicity (Kang et al., 2020). Newborn rats injected with PFOA or perfluorooctane sulfonate (PFOS) showed reduced number of growing follicles and secondary follicles, thus reducing the number of oocytes and resulting in long-term inhibition of oocyte growth (Guizhen et al., 2018). PFOA can inhibit ovarian hormone secretion, damage follicular development, and lead to the loss of ovarian function (Suyun et al., 2018). Furthermore, PFOA can act on steroid-producing ovarian cells and affect sex hormone-dependent functions (Chaparro-Ortega et al., 2018).

Animal studies have shown that exposure to PFOA generates oxidative stress and apoptosis in vitro and in vivo; it can significantly inhibit the luteal function in pregnant mice through oxidative stress and apoptosis (Chen et al., 2017). Meanwhile, PFOA exposure has also been shown to increase the expression of apoptotic proteins p53 and Bax, and significantly decrease the expression of anti-apoptotic protein Bcl-2 in pregnant mice, resulting in the apoptosis of ovarian cells (Huang et al., 2013). In addition, exposure of in vitro cultured ovarian tissue to PFOA has been shown to result in excessive ROS generation in the ovaries (López-Arellano et al., 2019).

Although the effects of PFOA on the reproductive system have been reported, and PFOA and other PFCs can affect the gap junction intercellular communication (GJIC) between oocytes and granulosa cells, both in pig and mouse (Dominguez et al., 2016; Dominguez, Salazar, & Bonilla, 2019; López-Arellano et al., 2019). While, it remains unclear whether the PFOA directly affects oocytes or indirectly affects oocytes through granulosa cells. Therefore, the denuded oocytes were used to investigate the direct effect of PFOA on the maturation of mouse oocytes in vitro and to reveal the underlying mechanism. Cellular changes in oocytes exposed to PFOA were evaluated by measuring the ROS levels, mitochondrial function, spindle assembly, chromosome

arrangement, and apoptosis. This study will further help uncover the mechanism by which PFOA exerts toxic effects on oocyte maturation and would draw attention to the safety of PFOA substitutes.

2 | MATERIALS AND METHODS

2.1 | Animals

The 6-week-old female Kunming strain mice were obtained from Guangdong Medical Laboratory Animal Center and were bred at the experimental animal center of South China Agricultural University under a 12 hr light/dark cycle with water and food ad libitum. The animals were maintained in accordance with the regulations of the Animal Ethics Committee of South China Agricultural University.

2.2 | Oocyte collection and in vitro maturation

The mice were euthanized 48 hr after the intraperitoneal injection of 10 IU pregnant mare serum gonadotropin (PMSG); their bodies were dissected and the ovaries were collected. The germinal vesicle (GV) oocytes were collected in M199 medium (LIFE, 11150–059) after the ovaries were punctured with a 1 ml disposable syringe and the granulosa cells were blown out. For in vitro maturation (IVM), each aliquot of 50 naked oocytes was placed inside a droplet of 50 μ l maturation medium (M199 with 10% fetal bovine serum (FBS), 1 IU/ml follicle stimulating hormone (FSH), 1 IU/ml human chorionic gonadotropin (HCG), 1 μ g/ml estradiol (E_2), and 0.04 mg/ml sodium pyruvate) and incubated for 16 hr at 37°C in a humidified atmosphere of 5% CO_2 . Oocyte excretion of the first polar body is regarded as oocyte maturation.

2.3 | PFOA treatment

To evaluate the effect of PFOA (Sigma, 171,468) on IVM, a 100 mM stock solution was prepared by dissolving PFOA powder in 10% dimethyl sulfoxide (DMSO, Sigma). At the beginning of the 16-hr maturation period, aliquots from the PFOA stock solution or DMSO were added to the maturation medium to obtain 0 (DMSO, control), 300, and 500 μ M concentrations in each droplet containing the denuded oocytes. The selection of micromolar concentration was based on the in vitro toxicity of PFOA toward mouse ovaries and that of other PFCs to oocytes (López-Arellano et al., 2019; Martínez-Quezada et al., 2021).

2.4 | Intracellular ROS level measurement

The oocytes cultured for 16 hr after maturation were collected and incubated in a maturation medium containing 1 μ M DCFH-DA (Beyotime, S0033) for 30 min. After incubation, the oocytes were washed three times with DPBS-PVA, and fluorescence was observed under a fluorescence microscope (Olympus HT4-200) using the same exposure parameter. Fluorescence intensity was analyzed using ImageJ after normalization by subtracting the background intensity from each oocyte size (Wendan et al., 2018).

2.5 | Mitochondrial distribution and membrane potential assessment

The oocytes were stained to determine the distribution of active mitochondria after IVM for 16 hr. Oocytes were incubated in a maturation medium containing 1 μ M MitoOrange (Abbkine, KTC4004) for 30 min or JC-1 (Meilunbio, MA0038) for 20 min at 37°C in a humidified atmosphere containing 5% CO₂ (Jeong, Lee, Park, Kim, & Kim, 2020). Then, the labeled oocytes were washed with DPBS-PVA three times (1 min each). To quantify the fluorescence intensity, oocytes treated with PFOA or vehicle (DMSO) and stained using the same immunostaining procedure were photographed by employing the same fluorescence microscope parameters. Fluorescence intensity was analyzed using ImageJ software.

2.6 | Immunofluorescence staining

After culture for 16 hr, the denuded oocytes were fixed with 4% paraformaldehyde for 30 min and then washed with washing buffer (PBS containing 0.01% Triton X-100, 0.01% Tween, and 2% BSA). After that, the oocytes were sealed in washing buffer at 37°C for 2 hr and incubated overnight at 4°C with mouse anti- β -Tubulin antibody (1:1,000 Sigma, T5293) or phospho-histone H2A.X antibody (1:200, Santa Cruz, sc-51748). The next day, oocytes were washed with washing buffer (three times, 10 min each), and then incubated with goat anti-mouse secondary antibody (1:100, LIFE, A11029) at 37°C for 1 hr. After that, the cells were washed with washing buffer three times in the dark (10 min each). DNA staining was performed using Hoechst 33342 (LIFE, H3570) at room temperature for 5 min. Finally, oocytes were mounted on glass slides and observed under a fluorescence microscope (Olympus, HT4-200).

2.7 | RNA extraction and quantitative real-time PCR

Oocytes ($n = 50$) were collected after 16 hr of culture and total RNA was extracted using RNeasy Micro Kit (QIAGEN, 74004) according to the manufacturer's manual. The first strand cDNA was generated using the HiScript III first Strand cDNA Synthesis Kit (+gDNA wiper, Vazyme, R212-01). The apparatus (qTOWER³, Germany) was used in combination with a real-time PCR detection system. The relative gene expression (normalized to β -actin) was calculated using the $2^{-\Delta\Delta ct}$ method. The following primer sequences were used: β -actin F: 5'-CCACCATGTACCCAGGCATT-3'; β -actin R: 5'-CGGAC TCATCGTACTCCTGC-3'; Prdx2 F: 5'-TGTCCAGAATT ACGGCGTGTTG-3'; Prdx2R: 5'-CGTCTACAGAGCGTC CCACAG-3'; SOD2 F: 5'-GGGGGCCGCGGAGAGCAG CGGTCGTGTA-3'; SOD2 R: 5'-GGGGGCCGCGCCATGTG GCCGTGAGTGAG-3'; Bcl-2 F: 5'-CTGTGCCACCATGT GTCCATCTG-3'; Bcl-2 R: 5'-TCTCTGCGAAGTCACGAC GGTAG-3'; Bax F: 5'-CGTGAGCGGCTGCTTGTCTG-3'; Bax R: 5'-ATGCTGCAAAGGGACTGGATGGC-3'; Caspase3 F: 5'-AGTGGGACTGATGAGGAGGAGATGGC-3'; Caspase3 R: 5'-ATGCTGCAAAGGGACTGGATGAAC-3'; Beclin-1 F: 5'-AGGCAGTGCGGCTCCTATTC-3'; Beclin-1 R: 5'-T GAGGACACCCAGGCAAGACC-3'; LC3B F: 5'-TGTGTC CACTCCCATCTCCGAAG-3'; LC3B R: 5'-CCATTGCTGT CCCGAATGTCTCC-3'; ATG5 F: 5'-TGCGGTTGAGGCT CACTTTATGTC-3'; ATG5 R: 5'-GCTCCGTCGTGGTCAT TCTGC-3'.

2.8 | Statistical analysis

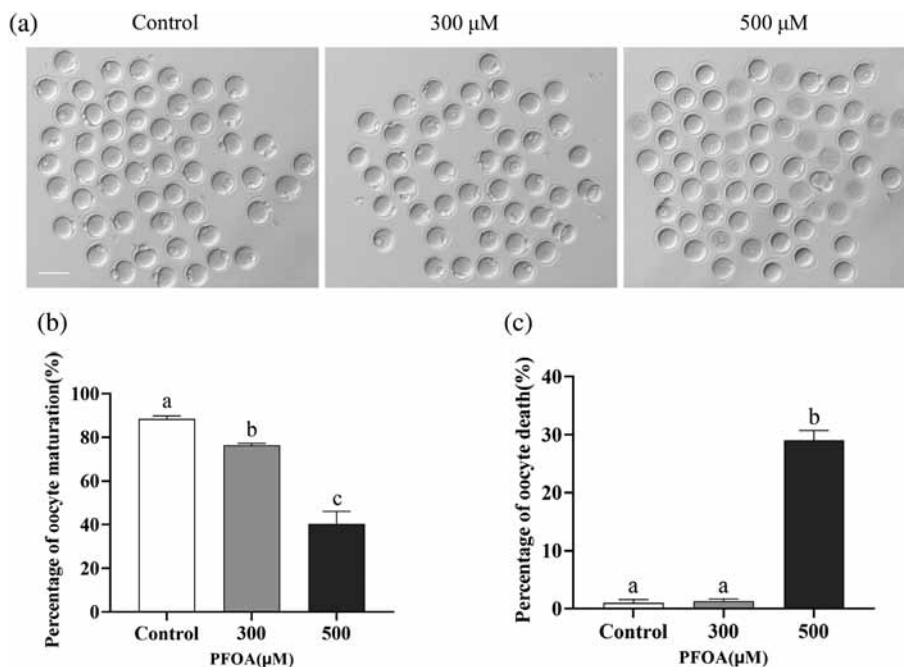
Independent experiments were repeated at least three times and the data are presented as mean \pm standard error of the mean (SEM). Differences among groups were tested statistically using one-way ANOVA with GraphPad Prism analysis software, and $p < .05$ was considered significant.

3 | RESULTS

3.1 | PFOA treatment reduced the extrusion rate of the first polar body from mouse oocytes

To evaluate the effect of PFOA on meiotic progression, we cultured denuded oocytes in maturation medium supplemented with 0, 300, or 500 μ M PFOA during IVM and investigated oocyte maturation. As shown in Figure 1a, treatment with 300 μ M PFOA significantly decreased the proportion of oocytes maturation ($p < .05$), and 500 μ M

FIGURE 1 Effects of PFOA exposure on the maturation of mouse oocytes. (a) Representative photographs from the control and PFOA-treated groups after 16 hr of IVM. Bar = 100 μ m. (b) The percentage of oocyte maturation in the control and PFOA-treated groups after 16 hr of IVM. ($n = 200$ per group). (c) The mortality of oocytes in the control and PFOA-treated groups after 16 hr of IVM. Data were obtained from three independent experiments, and the values are presented as the mean \pm SEM. The values marked by the different superscripts differ significantly ($p < .05$)



PFOA extremely significantly reduced the rate of oocyte maturation ($p < .01$; Figure 1b). The mortality of 500 μ M PFOA-treated oocytes was significantly higher than that of oocytes treated with other concentrations ($p < .01$), while the mortality of 300 μ M PFOA-treated oocytes was almost the same as that of the control oocytes ($p > .05$; Figure 1c).

3.2 | PFOA causes oxidative stress

Environmental pollutants and toxins tend to increase ROS production in cells, eventually inducing intracellular oxidative stress. To investigate how PFOA affected the developmental competence of oocytes, we firstly examined the levels of intracellular ROS. The 300 μ M PFOA was slightly higher than that in the control group ($p > .05$), and treatment with 500 μ M PFOA in a significant increase compared to the control ($p < .05$; Figure 2a,b). Then, we examined the expression of ROS-related genes. Treatment of oocytes with 500 μ M PFOA resulted in a significant increase in the levels of Prdx2 ($p < .05$) SOD2 ($p < .01$). Treatment of oocytes with 300 μ M PFOA resulted in a significant increase in the expression of SOD2 ($p < .05$), but not in the expression of Prdx2 ($p > .05$; Figure 2c).

3.3 | PFOA treatment interferes with mitochondrial organization and function

Mitochondria are important organelles that produce cellular energy through oxidative metabolism during oocyte

maturation, fertilization, and embryonic development. Therefore, the organization and function of mitochondria are key indicators of oocyte cytoplasmic maturation. Therefore, we evaluated mitochondrial distribution and activity in oocytes. The rate of aberrant mitochondrial distribution, such as the semi-peripheral and clustered distribution, was significantly higher in the 300 and 500 μ M PFOA-treated groups ($p < .01$), while in the control group, most oocytes exhibited a homogeneous mitochondrial distribution (Figure 3a,b). Furthermore, there was no significant difference between oocytes treated with 300 and 500 μ M PFOA ($p > .05$). In addition, a significantly reduced J-aggregate (high membrane potential)/J-monomer (low membrane potential) ratio was observed following treatment with 300 μ M ($p < .05$) and 500 μ M PFOA ($p < .01$). There was no significant difference between the groups treated with different concentrations of PFOA (Figure 3c,d). Thus, PFOA negatively affected mitochondrial organization and function during oocyte maturation.

3.4 | PFOA treatment triggers DNA damage and apoptosis

As ROS is associated with the occurrence of DNA damage, we next investigated whether PFOA exposure induces DNA damage in mouse oocytes. P-H2A.X staining marks DNA double-strand break sites, so it can be used as a marker of DNA damage (Ding et al., 2017). Bright P-H2A.X foci were commonly observed in PFOA-treated oocytes (Figure 4a). The frequency of P-

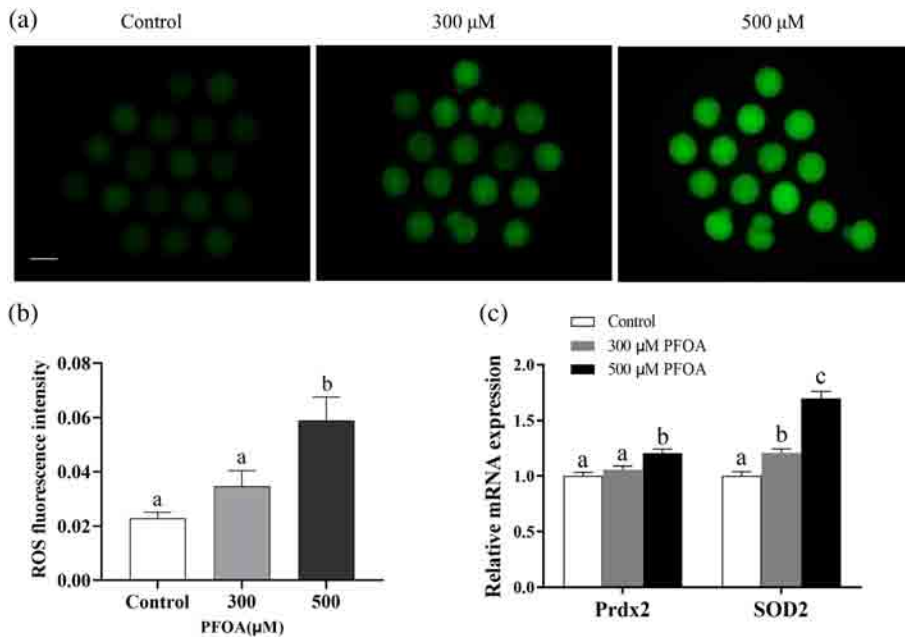


FIGURE 2 Effects of PFOA exposure during IVM on intracellular ROS levels. (a) Fluorescence images of oocytes treated with DCFH-DA for the measurement of intracellular ROS levels in the PFOA-treated and control groups. Bar = 50 μm. (b) Quantification of the fluorescence intensity in the PFOA-treated and control groups. ($n = 50$ per group). (c) The expression of ROS-related genes in the PFOA-treated and control groups. (Con; $n = 50$, PFOA; $n = 50$). Data were obtained from three independent experiments, and the values are presented as the mean \pm SEM. The values marked by the different superscripts differ significantly ($p < .05$)

H2AX-positive oocytes was significantly higher in oocytes treated with 300 μM ($p < .05$) and with 500 μM PFOA ($p < .01$) (Figure 4b). This evidence indicates that PFOA induces DNA damage. In addition, we investigated the expression of apoptosis-related genes and autophagy-related genes. The results revealed that the 500 μM PFOA-treated oocytes showed a significantly lower expression of Bcl-2 and higher expression of Bax and Caspase3 compared to the control ($p < .05$). There was no significant difference between the 300 μM PFOA-treated and the control groups ($p > .05$; Figure 4c). The expression of autophagy-related genes Beclin-1 and ATG5 was not significantly different between the PFOA-treated and control groups ($p > .05$). The expression of LC3B was significantly lower in the 500 μM PFOA-treated group compared to that in the control group ($p < .05$; Figure 4d). This evidence supports the hypothesis that PFOA exposure may induce apoptosis but not autophagy.

3.5 | PFOA treatment resulted in defective spindle morphogenesis and abnormal chromosome alignment in mouse oocytes

As the meiotic spindle plays an important role in the process of first polar body excretion, we hypothesized that the decrease in the first polar body expulsion rate of oocytes caused by PFOA treatment is related to abnormal spindle assembly. Therefore, we examined spindle morphology at metaphase II (MII) (6 hr) by

immunofluorescence. It was found that in the control oocytes, the spindle was typical barrel-shaped, and the chromosomes on the equatorial plate were arranged neatly, whereas the spindle of PFOA-treated oocytes showed abnormal shapes with misaligned chromosomes. The spindle structure following treatment with 300 μM PFOA was scattered and following treatment with 500 μM PFOA depolymerized, and the chromosomes were messy or condensed. (Figure 5a). The proportion of abnormal spindles in PFOA-treated oocytes was significantly higher than that in the control group. (Figure 5b). Therefore, we revealed that PFOA induced the loss of spindle in a dose-dependent manner, which can lead to the failure of chromosome segregation and cytokinesis during oocyte maturation.

4 | DISCUSSION

Although PFOA can abundant in humans and the environment and exert harmful effects in humans or animals, it is still widely used in industrial products of daily life in developing countries. (Nouredine, Branislav, Maria, Martine, & Vassilios, 2000) (Bartell, 2017). (Tsuda & Tsuda, 2016). Studies have shown that PFOA negatively affects female reproductivity by inducing loss of ovarian function, damaging follicular development, and causing primary ovarian insufficiency (Li, Bao, et al., 2018). In the present study, we demonstrated that PFOA negatively and directly affected the viability and maturation of mouse oocytes and identified mechanisms that may be involved in oocyte injury, including ROS,

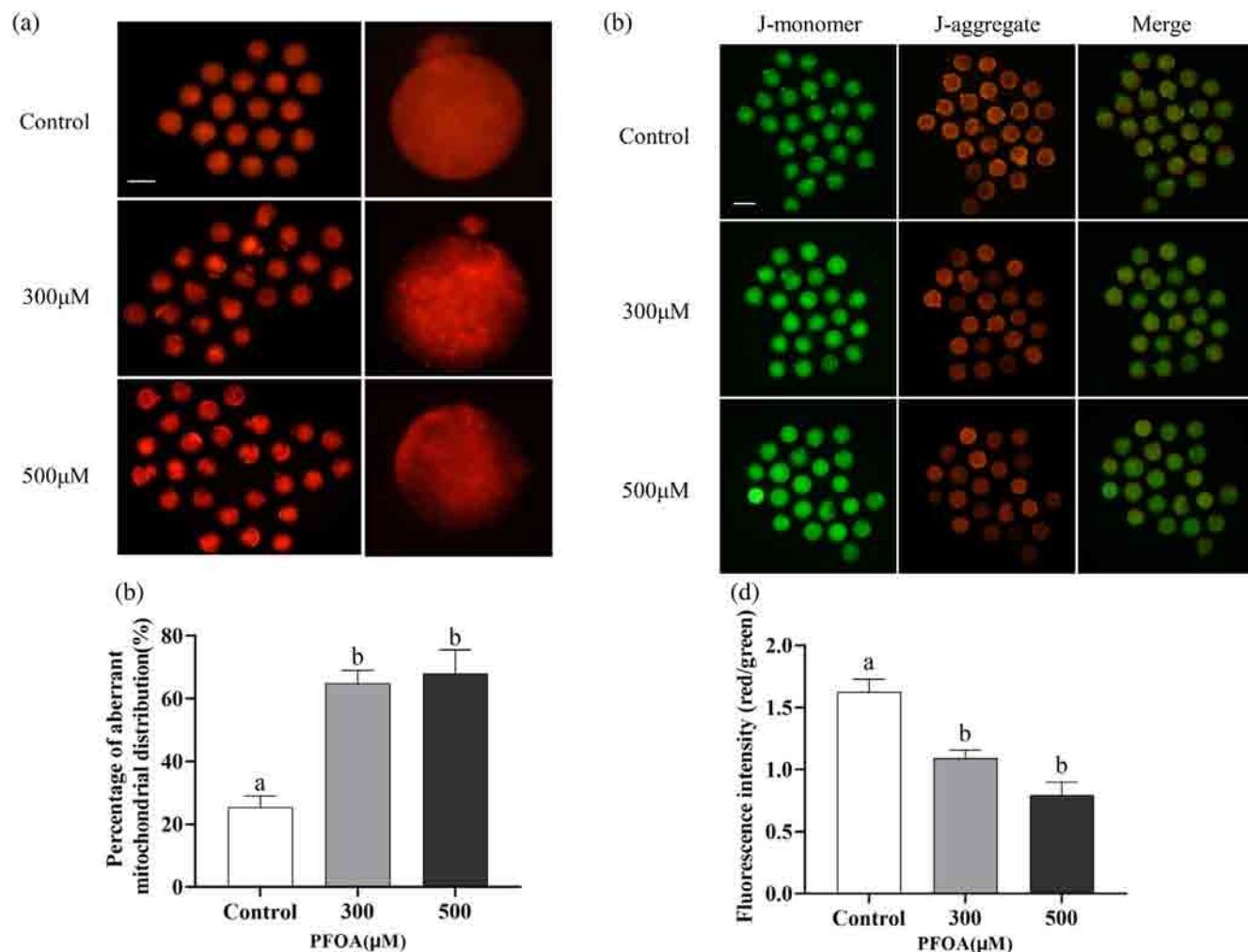


FIGURE 3 Effects of PFOA exposure during IVF on mitochondrial distribution and activity. (a) Fluorescence images of oocytes stained with MitoOrange from the PFOA-treated and control groups. Bar = 100 μm. (b) Percentage of oocytes with aberrant mitochondrial distribution in the PFOA-treated and control groups. ($n = 100$ per group). (c) Fluorescence images of oocytes stained with JC-1 in the PFOA-treated and control groups. Bar = 100 μm. (d) Quantification of the fluorescence intensity (red/green) in the indicated groups (Con; $n = 25$, PFOA; $n = 25$). Data were obtained from three independent experiments, and the values are presented as the mean \pm SEM. The values marked by the different superscripts differ significantly ($p < .05$)

mitochondrial defects, DNA damage, cytoskeletal changes, and apoptosis.

ROS is a natural by-product of cell metabolism and plays an important role in cell signal transduction and homeostasis. One of the known disruptors of oocyte developmental competence in vitro is oxidative stress, owing to the imbalance between the production and neutralization of ROS (Soto-Heras & Paramio, 2020). Excessive accumulation of ROS can induce lipid peroxidation, protein degradation, and DNA damage, which may lead to meiotic arrest. Previous studies have shown that the levels of ROS in mouse ovaries cultured in vivo or in vitro are positively correlated with PFOA concentration (López-Arellano et al., 2019). In this study, the expression of the antioxidant genes SOD2

and *Prdx2* increased significantly in the PFOA-treated oocytes, which may be caused by increased ROS levels. However, these antioxidant enzymes can only neutralize a small portion of free radicals, so the overall ROS content in cells remains increased. This suggests that PFOA induces oxidative stress during oocyte maturation. Furthermore, oxidative stress can disrupt mitochondrial function (Yang, Lim, Bazer, & Gwonhwa, 2018). In our study, PFOA-treated oocytes exhibited significantly higher aberrant mitochondrial distribution and membrane potential disruption, which indicated that PFOA compromised mitochondrial function and activity. Well-organized, evenly distributed mitochondria in the cytoplasm, and high mitochondrial membrane potential are considered to be important factors

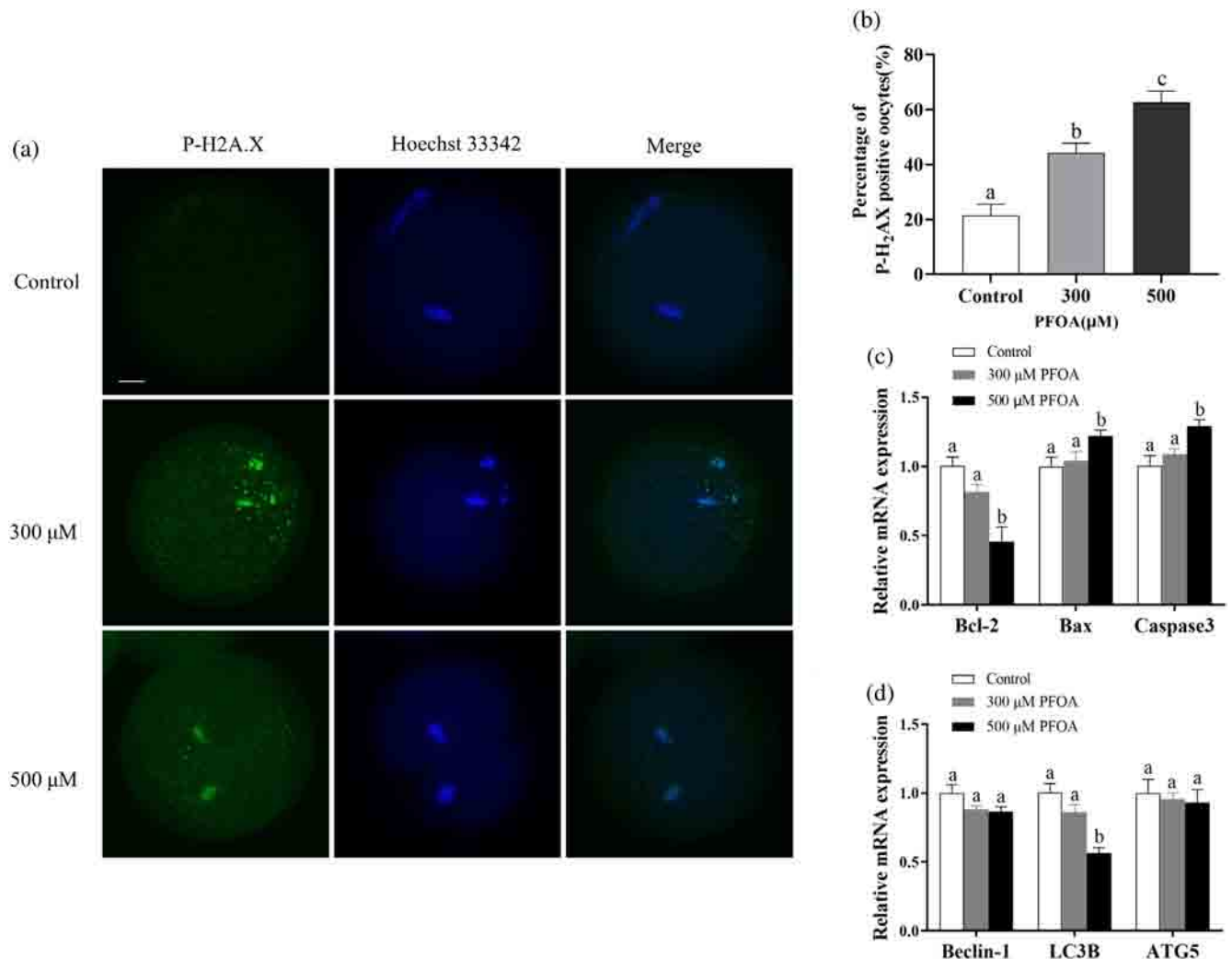


FIGURE 4 Effects of PFOA exposure during IVM on DNA damage, apoptosis and autophagy. (a) Fluorescence images of oocytes stained with an antibody against P-H2A.X from the PFOA-treated and control groups. Bar = 20 μ m. (b) Percentage of P-H2A.X-positive oocytes in the PFOA-treated and control groups (Con; $n = 50$, BP; $n = 50$). (c) The expression of apoptotic-related genes in the PFOA-treated and control groups. (Con; $n = 50$, PFOA; $n = 50$). (d) The expression of autophagy-related genes in the PFOA-treated and control groups (Con; $n = 50$, PFOA; $n = 50$). Data were obtained from three independent experiments, and the values are presented as the mean \pm SEM. The values marked by the different superscripts differ significantly ($p < .05$)

in oocyte cytoplasmic maturation (Brevini, Vassena, Francisci, & Gandolfi, 2005). Taken together, PFOA can cause oxidative stress and mitochondrial dysfunction during oocyte maturation in vitro.

ROS-related oxidative stress can also reduce the quality of oocytes by inducing DNA damage (Yu, Cui, Niedernhofer, & Wang, 2016). P-H2A.X has been used as a biomarker of DNA damage because the occurrence of P-H2A.X is closely related to DNA double-strand breaks (Ding et al., 2019). Previous studies have reported that cytotoxic chemicals such as bisphenol AF and butylparaben can induce DNA damage (Ding et al., 2017; Jeong et al., 2020). So, we examined oocytes treated with PFOA and found that the proportion of P-H2A.X-positive oocytes in the PFOA-treated group was significantly

higher than that in the control group, indicating that PFOA may attenuate oocyte maturation by inducing DNA double-strand breaks. In addition, it was also found that a large proportion of PFOA-treated oocytes showed abnormal spindles and dislocated chromosomes. In eukaryotes, microtubules are one of the main components of the cytoskeleton that consist of α - and β -tubulin. Microtubules, actin filaments, and chromatin not only interact to regulate chromosome segregation, but also cooperate to establish cell asymmetry (Azoury, Verlhac, & Dumont, 2009; Bennabi, Terret, & Verlhac, 2016). The abnormal localization of β -tubulin in PFOA-treated oocytes may be one of the causes of spindle defects and subsequent abnormal chromosomal alignments. Thus, our results suggest that PFOA treatment can interfere

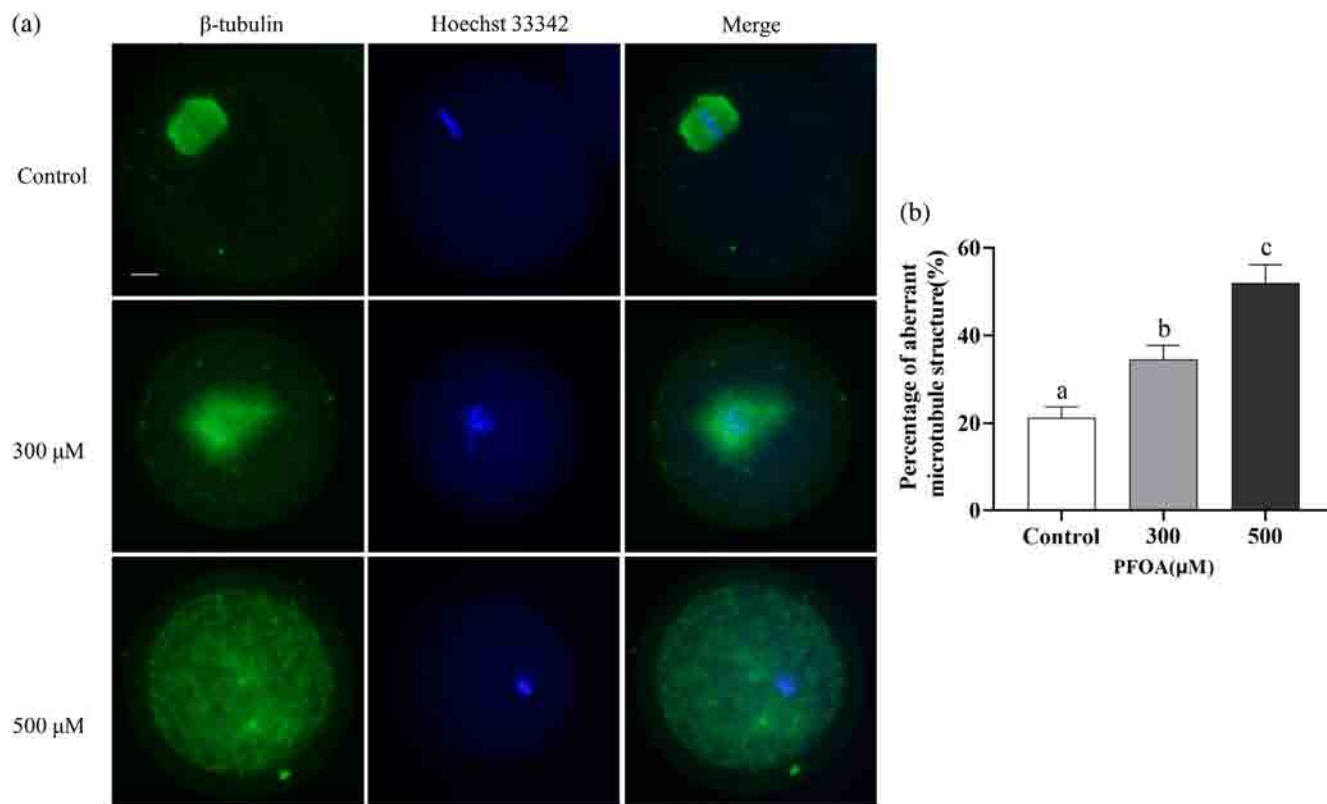


FIGURE 5 Effects of PFOA exposure during IVM on spindle morphogenesis and chromosome alignment. (a) Fluorescence images of oocytes stained with an antibody against β -tubulin and Hoechst 33342 from the PFOA-treated and control groups. Bar = 20 μ m.

(b) Percentage of oocytes with aberrant microtubule structure in the PFOA-treated and control groups (Con; $n = 50$, BP; $n = 50$). Data were obtained from three independent experiments, and the values are presented as the mean \pm SEM. The values marked by the different superscripts differ significantly ($p < .05$)

with spindle formation and abnormal chromosome alignment of oocytes.

In this study, it was found that treatment with $\leq 300 \mu$ M PFOA did not significantly decrease the oocyte maturation rate. However, PFOA $\geq 500 \mu$ M significantly increased oocyte mortality. Previous studies have reported that a PFOA concentration greater than 50μ M affects fetal mouse oocyte viability, and a concentration greater than 150μ M causes death (López-Arellano et al., 2019). The median lethal concentration (LC_{50}) of perfluorohexane sulfonate (PFHxS) to prepubertal porcine oocytes was 329.1μ M and the half-mature concentration (MIC_{50}) was 91.68μ M. The LC_{50} of PFOS for prepubertal porcine oocytes has been found to be 32μ M and the MIC_{50} was 22μ M (Domínguez et al., 2016). The LC_{50} of PFDA for prepubertal porcine oocytes was found to be 7.8μ M and the MIC_{50} was 3.8μ M (Domínguez et al., 2019). This indicates that different species, different ways of administration, and different kinds of PFCs have different toxicity. The toxic effects on the same species have also been shown to be different in different age periods; fetuses and young children are more likely to be affected

by the toxicity when compared to adults (Haug, Huber, Becher, & Thomsen, 2011). In this study, 6-week-old sexually mature mice were selected. The various organs of the its body gradually mature and have certain resistance, so the effective concentration of PFOA is higher. Furthermore, PFOA has a cumulative effect and a half-life as long as 3–4 years in humans and 16–22 day in mice (Li, Fletcher, et al., 2018; Wambaugh et al., 2009). Therefore, the toxic effects of PFOA should not be underestimated.

5 | CONCLUSION

This study evaluated the negative effects of PFOA on the maturation of mouse denuded oocytes in vitro. Our findings provide evidence that PFOA exposure during meiotic progression impairs oocyte quality by inducing ROS generation, aberrant mitochondrial distribution and functional impairment, DNA damage, defective spindle formation, abnormal chromosome alignment, and early apoptosis. These findings provide an opportunity to raise awareness regarding the toxicity of FPOA with respect to

oocyte maturation and to determine how PFOA detrimentally affects oocyte maturation. Further studies are needed to adequately characterize the molecular mechanisms underlying PFOA-mediated damage in mammalian oocytes.

ACKNOWLEDGMENTS

The authors thank the following grants that supported this work: The Natural Science Foundation of Guangdong Province (2020A1515010976); The Local Innovative and Research Teams Project of Guangdong Pearl River Talents Program (2019BT02N630); The Guangdong provincial promotion project on preservation and utilization of local breed of livestock and poultry (2018).

CONFLICT OF INTEREST

The authors declare no potential conflict of interest.

DATA AVAILABILITY STATEMENT

The data that support the findings of this study are available from the corresponding author upon reasonable request.

ORCID

Conghui Guo  <https://orcid.org/0000-0001-9213-453X>

REFERENCES

- Azoury, J., Verlhac, M. H., & Dumont, J. (2009). Actin filaments: Key players in the control of asymmetric divisions in mouse oocytes. *Biology of the Cell*, 101(2), 69–76. <https://doi.org/10.1042/bc20080003>
- Bach, C., Vested, A., Jørgensen, K. T., Bonde, J. P. E., Henriksen, T. B., & Toft, G. (2016). Perfluoroalkyl and polyfluoroalkyl substances and measures of human fertility: A systematic review. *Critical Reviews in Toxicology*, 46(9), 735–755.
- Bartell, S. M. (2017). Online Serum PFOA Calculator for Adults. *Environmental Health Perspectives*, 125(10), 10452(1)–10452(3). <https://doi.org/10.1289/EHP2820>
- Bennabi, I., Terret, M. E., & Verlhac, M.-H. (2016). Meiotic spindle assembly and chromosome segregation in oocytes. *Journal of Cell Biology*, 215(5), 611–619.
- Brevini, T. A. L., Vassena, R., Francisci, C., & Gandolfi, F. (2005). Role of adenosine triphosphate, active mitochondria, and microtubules in the acquisition of developmental competence of parthenogenetically activated pig oocytes. *Biology of Reproduction*, 72(5), 1218–1223.
- Chaparro-Ortega, A., Betancourt, M., Rosas, P., Vázquez-Cuevas, F., Chavira, R., Bonilla, E., ... Ducolomb, Y. (2018). Endocrine disruptor effect of perfluorooctane sulfonic acid (PFOS) and perfluorooctanoic acid (PFOA) on porcine ovarian cell steroidogenesis. *Toxicology in Vitro: An International Journal Published in Association with Bibra*, 46, 86–93.
- Chen, Y., Zhou, L., Xu, J., Zhang, L., Li, M., Xie, X., ... Yu, X. (2017). Maternal exposure to perfluorooctanoic acid inhibits luteal function via oxidative stress and apoptosis in pregnant mice. *Reproductive Toxicology*, 69, 159–166.
- Ding, Z. M., Jiao, X. F., Wu, D., Zhang, J. Y., Chen, F., Wang, Y. S., ... Huo, L. J. (2017). Bisphenol AF negatively affects oocyte maturation of mouse in vitro through increasing oxidative stress and DNA damage. *Chemico-Biological Interactions*, 278, 222–229.
- Ding, Z. M., Zhang, S. X., Jiao, X. F., Hua, L. P., Jamil, A. M., Wu, D., ... Meng, F. (2019). Doxorubicin exposure affects oocyte meiotic maturation through DNA damage-induced meiotic arrest. *Toxicological Ences*, 171(2), 359–368.
- Domínguez, A., Salazar, Z., Arenas, E., Betancourt, M., Ducolomb, Y., González-Márquez, H., ... Bonilla, E. (2016). Effect of perfluorooctane sulfonate on viability, maturation and gap junctional intercellular communication of porcine oocytes in vitro. *Toxicology in Vitro*, 35, 93–99.
- Domínguez, A., Salazar, Z., & Bonilla, E. (2019). Effect of perfluorodecanoic acid on pig oocyte viability, intracellular calcium levels and gap junction intercellular communication during oocyte maturation in vitro. *Toxicology In Vitro: An International Journal Published in Association with BIBRA*, 58, 224–229.
- Giesy, J. P., Kannan, K., & Jones, P. D. (2001). Global biomonitoring of Perfluorinated organics. *The scientific world Journal*, 1, 627–629.
- Guizhen, D., Jialei, H., Zhenyao, H., Huang, Z., Yu, M., Lu, C., ... Wu, D. (2018). Neonatal and juvenile exposure to perfluorooctanoate (PFOA) and perfluorooctane sulfonate (PFOS): Advance puberty onset and kisspeptin system disturbance in female rats. *Ecotoxicology & Environmental Safety*, 167, 412–421.
- Haug, L. S., Huber, S., Becher, G., & Thomsen, C. (2011). Characterisation of human exposure pathways to perfluorinated compounds — Comparing exposure estimates with biomarkers of exposure. *Environment International*, 37(4), 687–693.
- Huang, Q., Zhang, J., Martin, F. L., Peng, S., Tian, M., Mu, X., & Shen, H. (2013). Perfluorooctanoic acid induces apoptosis through the p53-dependent mitochondrial pathway in human hepatic cells: A proteomic study. *Toxicology Letters*, 223(2), 211–220.
- Jeong, P. S., Lee, S., Park, S. H., Kim, M. J., & Kim, S. U. (2020). Butylparaben is toxic to porcine oocyte maturation and subsequent embryonic development following in vitro fertilization. *International Journal of Molecular Ences*, 21(10), 3692.
- Kang, Q., Gao, F., Zhang, X., Wang, L., Liu, J., Fu, M., ... Hu, J. (2020). Nontargeted identification of per- and polyfluoroalkyl substances in human follicular fluid and their blood-follicle transfer. *Environment International*, 139, 105686. <https://doi.org/10.1016/j.envint.2020.105686>
- Koskela, A., Finnälä, M. A., Korkalainen, M., Spulber, S., Koponen, J., Håkansson, H., ... Viluksela, M. (2016). Effects of developmental exposure to perfluorooctanoic acid (PFOA) on long bone morphology and bone cell differentiation. *Toxicology and Applied Pharmacology*, 301, 14–21. <https://doi.org/10.1016/j.taap.2016.04.002>
- Lam, J., Koustas, E., Sutton, P., Johnson, P. I., Atchley, D. S., Sen, S., ... Woodruff, T. J. (2014). The navigation guide-evidence-based medicine meets environmental health: Integration of animal and human evidence for PFOA effects on fetal growth. *Environmental Health Perspectives*, 122(10), 1040–1051. <https://doi.org/10.1289/ehp.1307923>

- Li, X., Bao, C., Ma, Z., Xu, B., Liu, X., Ying, X., & Zhang, X. (2018). Perfluorooctanoic acid stimulates ovarian cancer cell migration, invasion via ERK/NF- κ B/MMP-2/-9 pathway. *Toxicology Letters*, 294, 44–50.
- Li, Y., Fletcher, T., Mucs, D., Scott, K., Lindh, C. H., Tallving, P., & Jakobsson, K. (2018). Half-lives of PFOS, PFHxS and PFOA after end of exposure to contaminated drinking water. *Occupational & Environmental Medicine*, 75(1), 46–51.
- López-Arellano, P., López-Arellano, K., Luna, J., Flores, D., Jiménez-Salazar, J., Gavia, G., ... Casas, E. (2019). Perfluorooctanoic acid disrupts gap junction intercellular communication and induces reactive oxygen species formation and apoptosis in mouse ovaries. *Environmental Toxicology*, 34(1), 92–98.
- Lunardi, D., Abelli, L., Panti, C., Marsili, L., Fossi, M. C., & Mancina, A. (2016). Transcriptomic analysis of bottlenose dolphin (*Tursiops truncatus*) skin biopsies to assess the effects of emerging contaminants. *Marine Environmental Research*, 114, 74–79. <https://doi.org/10.1016/j.marenvres.2016.01.002>
- Martínez-Quezada, R., González-Castañeda, G., Bahena, I., Domínguez, A., Domínguez-López, P., Casas, E., ... Bonilla, E. (2021). Effect of perfluorohexane sulfonate on pig oocyte maturation, gap-junctional intercellular communication, mitochondrial membrane potential and DNA damage in cumulus cells in vitro. *Toxicology in Vitro*, 70, 105011. <https://doi.org/10.1016/j.tiv.2020.105011>
- Noureddine, B., Branislav, V., Maria, G., Martine, C., & Vassilios, P. (2000). The peroxisome proliferator perfluorodecanoic acid inhibits the peripheral-type benzodiazepine receptor (PBR) expression and hormone-stimulated mitochondrial cholesterol transport and steroid formation in Leydig cells. *Endocrinology*, 9, 3137–3148.
- Pevny, S., Bitter, K., Krueger, E., & Thorsten, B. (2015). Perfluorooctanoic acid (PFOA) affects distinct molecular signaling pathways in human primary hepatocytes. *Toxicology: An International Journal Concerned with the Effects of Chemicals on Living Systems*, 333, 53–62.
- Rashid, F., Ramakrishnan, A., Fields, C., & Irudayaraj, J. (2020). Acute PFOA exposure promotes Epigenomic alterations in mouse kidney tissues. *Toxicology Reports*, 7, 125–132.
- Soto-Heras, S., & Paramio, M.-T. (2020). Impact of oxidative stress on oocyte competence for in vitro embryo production programs. *Research in Veterinary Science*, 132, 342–350. <https://doi.org/10.1016/j.rvsc.2020.07.013>
- Suyun, Z., Rongrong, T., Rui, P., Jianwei, X., Ying, T., Jie, W., & Ling, C. (2018). Association of Perfluoroalkyl and Polyfluoroalkyl Substances with Premature Ovarian Insufficiency in Chinese women. *Journal of Clinical Endocrinology & Metabolism*, 103(7), 2543.
- Tsuda, S., & Tsuda, S. (2016). Differential toxicity between perfluorooctane sulfonate (PFOS) and perfluorooctanoic acid (PFOA). *The Journal of Toxicological Ences*, 41(Special), SP27–SP36.
- Wambaugh, J. F., Lou, I., Lau, C., Hanson, R. G., Lindstrom, A. B., Strynar, M. J., ... Barton, H. A. (2009). Modeling single and repeated dose pharmacokinetics of PFOA in mice. *Reproductive Toxicology*, 27(3–4), 331.
- Wendan, X., Lingjun, L., Jingwen, S., Songyue, Z., Zhengjie, Y., Li, G., ... Caiping, M. (2018). Putrescine delays postovulatory aging of mouse oocytes by upregulating PDK4 expression and improving mitochondrial activity. *Aging*, 10(12), 4093–4106.
- Yang, C., Lim, W., Bazer, F. W., & Gwonhwa, S. (2018). Butyl paraben promotes apoptosis in human trophoblast cells through increased oxidative stress-induced endoplasmic reticulum stress. *Environmental Toxicology*, 33(4), 436–445.
- Yu, Y., Cui, Y., Niedernhofer, L. J., & Wang, Y. (2016). Occurrence, biological consequences, and human health relevance of oxidative stress-induced DNA damage. *Chemical Research in Toxicology*, 29(12), 2008–2039.

How to cite this article: Guo C, Zhao Z, Zhao K, et al. Perfluorooctanoic acid inhibits the maturation rate of mouse oocytes cultured in vitro by triggering mitochondrial and DNA damage. *Birth Defects Research*. 2021;113:1074–1083. <https://doi.org/10.1002/bdr2.1899>

谢社风, 韩贝贝, 高凤磊, 等. 猪催乳素的真核表达与生物活性验证 [J]. 华南农业大学学报, 2024, 45(2): 179-189.

XIE Shefeng, HAN Beibei, GAO Fenglei, et al. Eukaryotic expression and bioactivity verification of porcine prolactin[J]. Journal of South China Agricultural University, 2024, 45(2): 179-189.

猪催乳素的真核表达与生物活性验证

谢社风¹, 韩贝贝¹, 高凤磊², 马莹¹, 李莉¹, 张守全¹, 邹娴³, 卫恒习^{1,4}

(1 国家生猪种业工程技术研究中心/广东省农业动物基因组学与分子育种重点实验室/华南农业大学动物科学学院, 广东 广州 510642; 2 广东农工商职业技术学院 热带农林学院, 广东 广州 510507; 3 广东省农业科学院 动物科学研究所, 广东 广州 510640; 4 岭南现代农业科学与技术广东省实验室 茂名分中心, 广东 茂名 525000)

摘要:【目的】催乳素 (Prolactin, PRL) 具有广泛的生理调节作用, 但其多效性机制仍不清楚。为了更好地研究猪 PRL 的多效性, 本研究制备猪源 PRL 真核重组蛋白并验证其生物活性。【方法】利用分子克隆技术将猪 PRL 基因克隆到慢病毒表达载体 pCDH-CMV-MCS-EF1-GFP+Puro 中, 经慢病毒包装获得携带猪 PRL 基因的 PRL-慢病毒; 用浓缩的 PRL-慢病毒感染 CHO-K1 细胞, 经嘌呤霉素筛选后, 获得能够分泌 PRL 重组蛋白的阳性细胞系 CHO-K1-PRL; 利用镍柱亲和层析法对重组蛋白进行纯化并进行 LC-MS/MS 质谱鉴定, 利用 HC11 细胞体外培养体系验证 PRL 重组蛋白的生物活性。【结果】成功构建了携带猪 PRL 基因的 pCDH-CMV-6His-PRL-6His-EF1-GFP+Puro 慢病毒表达载体; 包装及浓缩后的 PRL-慢病毒滴度为 9.9×10^8 TU/mL, 其感染的 CHO-K1 细胞经嘌呤霉素筛选后得到阳性细胞系 CHO-K1-PRL; 从 CHO-K1-PRL 细胞培养液中成功纯化出重组蛋白, 质量浓度为 50 μ g/mL, LC-MS/MS 质谱分析的覆盖率达 94%, 鉴定为猪 PRL 重组蛋白; 重组 PRL 具有促进 HC11 细胞增殖及酪蛋白表达的生物活性。【结论】构建的细胞系 CHO-K1-PRL 可稳定表达具有生物活性的猪重组 PRL, 为猪 PRL 功能的研究和生产应用奠定了基础。

关键词: 猪; 催乳素; CHO-K1 细胞; 真核表达; 慢病毒载体; 重组蛋白

中图分类号: S828.2

文献标志码: A

文章编号: 1001-411X(2024)02-0179-11

Eukaryotic expression and bioactivity verification of porcine prolactin

XIE Shefeng¹, HAN Beibei¹, GAO Fenglei², MA Ying¹, LI Li¹, ZHANG Shouquan¹, ZOU Xian³, WEI Hengxi^{1,4}

(1 National Engineering Research Center for Breeding Swine Industry/Guangdong Provincial Key Laboratory of Agro-animal Genomics and Molecular Breeding/College of Animal Science, South China Agricultural University, Guangzhou 510642, China; 2 School of Tropical Agriculture and Forestry, College of Guangdong Agriculture Industry Business Polytechnic, Guangzhou 510507, China; 3 Institute of Animal Science, Guangdong Academy of Agricultural Sciences, Guangzhou 510640, China; 4 Maoming Branch, Guangdong Laboratory for Lingnan Modern Agriculture, Maoming 525000, China)

Abstract: 【Objective】Prolactin (PRL) has a wide range of physiological regulatory effects, but its pleiotropic mechanism is still unclear. In order to investigate the pleiotropy of porcine PRL, we obtain porcine PRL eukaryotic recombinant protein and verify its biological activity. 【Method】The porcine PRL gene was cloned

收稿日期: 2023-02-20 网络首发时间: 2023-12-16 11:42:53

首发网址: <https://link.cnki.net/urlid/44.1110.s.20231214.1910.002>

作者简介: 谢社风, 硕士研究生, 主要从事动物生殖生理与生物技术研究, E-mail: 2251078308@qq.com; 通信作者: 卫恒习, 副研究员, 博士, 主要从事动物繁殖与生物技术研究, E-mail: weihengxi@scau.edu.cn

基金项目: 广东省重点领域研发计划 (2022B0202110002); 广东省自然科学基金 (2020A1515010976); 广东省“珠江人才计划”本土创新科研团队项目 (2019BT02N630)

第 266 页, 共 307 页

into the lentiviral vector pCDH-CMV-MCS-EF1-GFP+Puro by molecular cloning technology, and the PRL-lentivirus carrying porcine *PRL* gene was obtained by lentivirus packaging. CHO-K1 cells were infected by the concentrated PRL-lentivirus solution, and the positive cell line named CHO-K1-PRL, which could secrete recombinant PRL protein, was obtained after puromycin screening. The recombinant protein was purified by nickel column affinity chromatography, and identified by LC-MS/MS mass spectrometry. The biological activity of recombinant PRL was verified by adding recombinant PRL into HC11 cell culture system *in vitro*. 【Result】 The recombinant expression vector pCDH-CMV-6His-PRL-6His-EF1-GFP+Puro carrying porcine *PRL* gene was successfully constructed. The titer of PRL-lentivirus after concentrating was 9.9×10^8 TU/mL, and the positive cell line CHO-K1-PRL was obtained after puromycin screening. The recombinant protein with the mass concentration of 50 $\mu\text{g/mL}$ was successfully purified from the supernatant of CHO-K1-PRL cells. The recombinant porcine PRL protein was identified as porcine PRL by LC-MS/MS mass spectrometry, and the coverage rate of recombinant PRL was 94%. The recombinant PRL had the biological activity of promoting the proliferation and casein expression of HC11 cells. 【Conclusion】 The cell line CHO-K1-PRL constructed in this study can stably express porcine recombinant PRL with biological activity, which lays a foundation for the functional research, production and application of porcine PRL.

Key words: Porcine; Prolactin; CHO-K1 cell; Eukaryotic expression; Lentiviral vector; Recombinant protein

催乳素 (Prolactin, PRL) 又称促乳素, 是由垂体前叶嗜酸性细胞合成与分泌的一种蛋白质激素, 广泛存在于多种组织器官, 在动物生殖、妊娠和哺乳、生长发育、内分泌和代谢、免疫调节、水电解质平衡、促进血管生成、行为和癌症等方面具有重要的调控作用^[1-2], 表现出广泛的生物多效性, 但其多效性机制仍不十分清楚。

PRL 作为经典的生殖激素可通过内分泌途径调控卵泡发育, 也可以作为细胞因子对卵泡发育起局部调控作用。在妊娠期或哺乳期时, PRL 的循环水平显著升高, 高水平的 PRL 会通过抑制下丘脑促性腺激素释放激素 (GnRH) 的分泌而降低垂体促性腺激素 (Gn) 的分泌, 进而抑制卵泡发育^[2-3]。PRL 在卵巢上可通过自分泌和旁分泌途径来调节卵巢功能^[4-5], PRL 通过与卵泡上的催乳素受体 (PRLR) 结合能够影响类固醇激素 (如 E_2 和 P_4) 的合成^[6], 从而影响发育卵泡的数量和排卵时间。垂体 PRL 的分泌受下丘脑、神经递质、激素、细胞因子、生殖生理状态、昼夜节律、应激等多种因素影响, 具有脉冲式波动的特点, 正常 PRL 脉冲性释放对泌乳和卵巢功能起到重要的调节作用^[7]。在临床上, PRL 抑制性调节的减弱可引发高催乳素血症 (Hyperprolactinemia, HPRL)^[8], 可造成女性月经不调甚至闭经、不孕不育、乳房肿大、溢乳和男性性功能障碍等^[9]。

PRL 是经产母猪卵巢卵泡功能的重要生理调控因子, 母猪断奶后 PRL 水平降低, 卵泡才能得到

继续发育, 在生产上通过调控母猪断奶后的 PRL 水平, 能够实现卵泡发育和发情的同步化^[10]。研究表明, PRL-PRLR 系统存在于猪卵泡中, 并且卵泡中的 PRL 可由颗粒细胞产生; PRL 作用于卵巢, 从而调节颗粒细胞 FSHR 和黄体细胞 LHR 的表达, 调节卵泡的发育和排卵与孕酮的合成, 此调节作用严格依赖于卵泡内 PRL 的激素水平^[10]。此外, 卵泡发育的一个关键过程是血管生成, PRL 可能作为局部调节因子影响卵泡血管内皮细胞生长^[11-12]。

PRL 具有显著的分子多态性, 包括不同百分比的糖基化形式, 这可能是 PRL 多效性的基础^[13]。PRL 的糖基化形式对生理学研究 and 潜在的临床应用非常重要, 然而, 当前市场上的重组 PRL 多为原核表达产物, 缺少糖基化修饰, 难以保证其生物活性, 这严重阻碍了 PRL 多效性的机制研究和临床应用。因此, 本研究利用真核表达载体系统构建能够稳定表达猪源 PRL 重组蛋白的中国仓鼠卵巢 (Chinese hamster ovary, CHO) 细胞系, 并验证猪源 PRL 重组蛋白的生物活性, 以期对猪 PRL 的功能研究及生产应用提供理论和参考依据。

1 材料与方法

1.1 试验材料

人胚肾细胞 (HEK-293T)、中国仓鼠卵巢细胞 (CHO-K1)、慢病毒表达载体 pCDH-CMV-MCS-

EF1-GFP+Puro 和辅助质粒 psPAX2、pMD2.G 均由华南农业大学动物科学学院动物繁殖研究室保存;小鼠乳腺上皮细胞 (HC11) 购自武汉普诺赛生命科技有限公司;DH5 α 感受态细胞和 Stbl3 感受态细胞购自擎科生物科技有限公司;母猪垂体组织采集自广东省农业科学院动物科学 (畜牧) 研究所三元杂商品母猪。

DMEM 高糖培养基、DMEM/F12 培养基、RPMI 1640 培养基、PBS 缓冲液、胎牛血清 (FBS)、胰酶-EDTA (含 2.5 g/L 胰酶)、青链霉素 (双抗) 购自 Gibco 公司;Premix TaqTM、DNA Loading Buffer、DNA Marker、pMD18-T、限制性内切酶 *EcoR* I 和 *Bam*HI 购自宝生物工程 (大连) 有限公司;T4 连接酶购自 Thermo Fisher 公司;慢病毒专用转染试剂 LentiFitTM 购自汉恒生物科技有限公司;HiScript[®] III 1st Strand cDNA Synthesis Kit (+gDNA wiper) 反转录试剂盒、HiScript[®] II Q RT SuperMix for qPCR (+gDNA wiper) 反转录试剂盒、ChamQTM Universal SYBR[®] qPCR Master Mix 购自南京诺唯赞生物有限公司;动物组织总 RNA 提取试剂盒、细胞总 RNA 提取试剂盒、无内毒素质粒小提中量试剂盒购自天根生化科技 (北京) 有限公司;凝胶 DNA 微量回收试剂盒购自广州美基生物科技有限公司;全蛋白提取试剂盒、BAC 蛋白含量检测试剂盒购自凯基生物技术股份有限公司;SDS-PAGE 凝胶配制试剂盒购自北京鼎国昌盛生物技术有限责任公司;嘌呤霉素、鼠源 His-Tag 单克隆抗体、兔源 α -tubulin 多克隆抗体、HRP-标记山羊抗小鼠 IgG、HRP-标记山羊抗兔 IgG、CCK-8 试剂盒购自碧云天生物技术有限公司;兔源 β -酪蛋白 (CSN2) 多克隆抗体购自博奥森生物技术有限公司;兔源 Cyclin D1 多克隆抗体购自正能生物技术有限公司;Western-blot Marker 购自 Fermentas 公司。引物由上海生工生物股份有限公司合成。

1.2 试验方法

1.2.1 *PRL* 基因的引物设计 根据 GenBank 数据库中猪 *PRL* 基因序列 (登录号 NM_213926.1), 使用 Premier 5.0 软件设计 1 对引物 Sus-PRL-F: 5'-ATCACCGCCATGGACAACAC-3', Sus-PRL-R: 5'-GACGTGGGCTTAGCAGTTGC-3', 扩增出含编码 *PRL* 蛋白 (CDs 序列) 的基因片段 (708 bp); 根据编码 *PRL* 蛋白的碱基序列再设计另 1 对引物 HPH-F-*EcoR* I: 5'-CGG/AATTCCGATGCATCATCA

AGA-3', HPH-R-*Bam*HI: 5'-CGG/GATCCCCGTTAATGGTGATGGTGATGATGCAGTTGCTGTCGTAGATGATTCGG-3', 分别在该引物中引入 6His-Tag、*EcoR* I 和 *Bam*HI 酶切位点 (注: 下划直线处分别为 *EcoR* I 和 *Bam*HI 酶切位点, 其中 "/" 为酶切识别位点; 下划波浪线处为 6His-Tag 序列), 以扩增含 *EcoR* I-6His-PRL-6His-*Bam*HI 的基因序列 (749 bp)。

1.2.2 pMD18-T-PRL 克隆载体的构建与鉴定 采集母猪垂体组织, 按照动物组织总 RNA 提取试剂盒说明书提取 RNA, 对 RNA 的浓度进行检测并按照 HiScript[®] III 1st Strand cDNA Synthesis Kit (+gDNA wiper) 反转录试剂盒说明书反转录成 cDNA。以猪垂体组织 cDNA 为模板, 用引物 Sus-PRL-F 和 Sus-PRL-R 扩增编码 *PRL* 蛋白的基因片段。扩增体系为: 20 μ L 2 \times Premix TaqTM, 4 μ L cDNA (500 ng/ μ L), 上、下游引物 (10 μ mol/L) 各 2 μ L, 12 μ L ddH₂O。PCR 反应程序为: 98 $^{\circ}$ C 预变性 30 s; 98 $^{\circ}$ C 变性 10 s, 57 $^{\circ}$ C 退火 30 s, 72 $^{\circ}$ C 延伸 1 min, 共 35 个循环; 72 $^{\circ}$ C 终延伸 2 min。将扩增产物回收纯化后连接到 pMD18-T 载体, 连接体系 (10 μ L): 4.5 μ L 目的基因, 0.5 μ L pMD18-T 载体, 5 μ L Solution I; 16 $^{\circ}$ C 连接 16 h。随后将连接产物转化到 DH5 α 感受态细胞, 经 PCR 鉴定为阳性的菌液送至上海生工生物股份有限公司进行测序, DNA 测序后序列比对正确的克隆载体命名为 pMD18-T-PRL。

1.2.3 pCDH-CMV-6His-PRL-6His-EF1-GFP+Puro 真核表达载体的构建 以 pMD18-T-PRL 克隆载体为模板, 用引物 HPH-F-*EcoR* I 和 HPH-R-*Bam*HI 扩增含 *EcoR* I 酶切位点-6His-PRL-6His-*Bam*HI 酶切位点序列的基因片段。扩增体系为: 20 μ L 2 \times Premix TaqTM, 4 μ L pMD18-T-PRL 克隆载体 (500 ng/ μ L), 上、下游引物 (10 μ mol/L) 各 2 μ L, 12 μ L ddH₂O。PCR 反应程序: 98 $^{\circ}$ C 预变性 30 s; 98 $^{\circ}$ C 变性 10 s, 72 $^{\circ}$ C 退火 30 s, 72 $^{\circ}$ C 延伸 1 min, 共 35 个循环; 72 $^{\circ}$ C 终延伸 2 min。将扩增产物回收纯化后, 通过内切酶 *EcoR* I 和 *Bam*HI 双酶切后将 6His-PRL-6His 基因连接到 pCDH-CMV-MCS-EF1-GFP+Puro 慢病毒表达载体中。双酶切体系: 1 μ L *EcoR* I, 1 μ L *Bam*HI, 2 μ L 10 \times K Buffer, 1000 ng cDNA 或质粒, 加入 ddH₂O 至 20 μ L, 37 $^{\circ}$ C 水浴酶切 2 h; 连接反应体系 (20 μ L): 2 μ L 10 \times T4 DNA Ligase Buffer, 0.2 μ L T4 DNA Ligase, 10 μ L 目的片

段 (40 ng/ μ L), 0.53 μ L 载体 (190 ng/ μ L), 加入 ddH₂O 至 20 μ L, 16 $^{\circ}$ C 连接 16 h。随后将连接产物转化到 Stbl3 感受态细胞, 经 PCR 鉴定为阳性的菌液送至上海生工生物股份有限公司进行测序, DNA 测序后序列比对正确的重组慢病毒表达载体命名为 pCDH-CMV-6His-PRL-6His-EF1-GFP+Puro。对序列正确的阳性菌进行扩培并按照无内毒素质粒小提中量试剂盒说明书抽提 pCDH-CMV-6His-PRL-6His-EF1-GFP+Puro 质粒, 并对其进行双酶切鉴定。

1.2.4 慢病毒的包装及滴度测定 取对数生长期的 HEK-293T 细胞接种于 T75 培养瓶中, 用完全培养基 (DMEM 基础培养基、FBS 和双抗的体积分数分别为 89%、10% 和 1%) 在 37 $^{\circ}$ C 培养箱中将细胞培养至生长密度达 70%~80%, 按照慢病毒专用转染试剂 LentiFit™ 说明书操作, 将 60 μ L 转染试剂与 16 μ g pCDH-CMV-6His-PRL-6His-EF1-GFP+Puro 重组质粒或 pCDH-CMV-MCS-EF1-GFP+Puro 空载质粒和 12 μ g psPAX2、8 μ g pMD2.G 辅助质粒充分混匀, 室温孵育 20 min 后转染 T75 培养瓶中的 HEK-293T 细胞, 培养 12 h 后更换为完全培养基, 继续培养 48 h 后, 收集细胞培养液, 并更换新的完全培养基, 72 h 继续收集细胞培养液; 收集的培养液过滤、离心浓缩得到 PRL-慢病毒浓缩液, 于 -80 $^{\circ}$ C 条件下保存。

将慢病毒浓缩液 10 倍梯度稀释, 连续做 6 个稀释度 (每个浓度梯度每 100 μ L 稀释液分别含病毒浓缩液 10、1、0.1、0.01、0.001 和 0.000 1 μ L), 吸弃 96 孔板内培养基, 分别加入 6 个浓度梯度的 100 μ L 慢病毒稀释液, 感染 96 孔板的 HEK-293T 细胞, 24 h 后更换完全培养液, 继续培养至 48 h 后观察绿色荧光蛋白 (GFP) 表达情况, 计数荧光比例约为 30% 的孔的细胞数, 按照以下公式算出病毒滴度: 病毒滴度 (TU/mL)=细胞数 \times 荧光百分比 $\times 10^3$ /病毒原液体积。

1.2.5 CHO-K1-PRL 阳性细胞的制备与鉴定 取对数生长期的 CHO-K1 细胞接种于 T25 培养瓶中, 用完全培养基 (DMEM/F12 基础培养基、FBS 和双抗的体积分数分别为 89%、10% 和 1%) 在 37 $^{\circ}$ C 培养箱中将细胞培养至生长密度达 50%~70%, 吸弃原培养基, 加入 2 mL DMEM/F12 完全培养基 (不含双抗)、12 μ L Polybrene 和 200 μ L 浓缩慢病毒液的混合液, 培养 4 h 后补齐培养液至 4 mL, 24 h 后更换为完全培养液, 48 h 后观察 GFP 表达效率, 并换成含有 6 μ g/mL 嘌呤霉素的完全培养液, 进行药

物筛选 7 d, 每 2~4 d 换液 1 次, 得到阳性细胞系, 命名为 CHO-K1-PRL。

分别提取上述药物筛选后的 CHO-K1-PRL 细胞、未感染慢病毒的 CHO-K1 细胞和感染空载体慢病毒的 CHO-K1 细胞的总 RNA 与总蛋白, 同时收集 CHO-K1-PRL 细胞、未感染慢病毒 CHO-K1 细胞和感染空载体慢病毒 CHO-K1 细胞的培养液。细胞总 RNA 反转录为 cDNA, 利用引物 HPH-F-*EcoR* I /HPH-R-*Bam* H I 进行 RT-PCR 检测 (β -*actin* 为内参基因, 引物 β -*actin*-F: 5'-CCACCATGTAC CCAGGCATT-3', β -*actin*-R: 5'-CGGACTCATCG TACTCCTGC-3'); 以鼠源 His-Tag 单克隆抗体 (用 TBST 缓冲液按照体积比 1:1 000 稀释) 为一抗, 再以 HRP-标记山羊抗小鼠 IgG (用 TBST 缓冲液按照体积比 1:1 000 稀释) 为二抗, 对细胞总蛋白及细胞培养液样品进行 Western blot 鉴定。

1.2.6 重组蛋白的纯化与鉴定 收集大量 CHO-K1-PRL 阳性细胞的培养液, 用 0.45 μ m 滤器过滤, 由重庆革兰氏生物科技有限责任公司利用镍柱亲和层析法对培养液通过 His-Tag 蛋白进行蛋白纯化; 对纯化蛋白用体积分数为 12% 的蛋白凝胶进行 SDS-PAGE 电泳检测, 并将目的条带切下, 送至深圳市微纳菲生物技术有限公司进行 LC-MS/MS 质谱分析鉴定。

1.2.7 重组 PRL 对 HC11 细胞增殖及酪蛋白表达的影响 参照田青等^[14-15]的方法, 取对数生长期的 HC11 细胞以每孔 1×10^4 的密度接种于 96 孔板, 或以每孔 2×10^5 的密度接种于 6 孔板, 先用完全培养基 (RPMI 1640、FBS 和双抗的体积分数分别为 89%、10% 和 1%) 将细胞培养至生长密度达 80% 左右, 再用无血清无激素含双抗的 RPMI 1640 培养基进行饥饿处理 16 h, 弃去旧培养基, 增殖试验 (96 孔板): 用含不同浓度重组 PRL 的激素诱导培养基 (RPMI 1640、FBS 和双抗的体积分数分别为 89%、10% 和 1%, 5 μ g/mL 胰岛素, 1 ng/mL 氢化可的松, 0/100/300/500 ng/mL 重组 PRL) 培养 20 h, 每孔加入 10 μ L CCK-8 试剂, 继续培养 4 h 后, 用酶标仪于 450 nm 波长测吸光度; 诱导酪蛋白表达试验 (6 孔板): 用含不同浓度重组 PRL 的激素诱导培养基 (同增殖试验) 培养 24 h 后收集细胞, 提取细胞的总 RNA 与总蛋白, 细胞总 RNA 反转录为 cDNA, qRT-PCR 检测 *PRLR*、*CSN1S1*、*CSN2*、*CSN3*、*Cyclin D1*、*PCNA* 等基因的相对表达量, *GAPDH* 为内参基因, 引物序列见表 1, 各基因的相对表达量用 $2^{-\Delta\Delta C_t}$ 值表示; 以兔源 β -酪蛋白

表 1 qPCR 引物序列
Table 1 Primer sequence for qPCR

基因 Gene	正向引物序列(5'→3') Forward primer sequence	反向引物序列(5'→3') Reverse primer sequence	产物大小/bp Product length
<i>GAPDH</i>	GAGCGAGACCCCACTAACATC	GCGGAGATGATGACCCTTTT	134
<i>PRLR</i>	GTGGAATCCTGGGTCAGATG	GGGCCACTGGTTTTGTAGTC	108
<i>CSN1S1</i>	CCTTTCCCCTTTGGGCTTAC	TGAGGTGGATGGAGAATGGA	193
<i>CSN2</i>	GCAATCCCGTCCCACAAAAC	GGGGCATCTGTTTGTGCTTG	138
<i>CSN3</i>	CCTTTTGTGCCGTGGTGAG	GGCTGGAGACCTAAGCAGAA	197
<i>Cyclin D1</i>	TGGCTAAACAAGGACCCCC	ATGTCCACATCTCGCACGTC	203
<i>PCNA</i>	AAAGATGCCGTCGGGTGAAT	TGGTTACCGCCTCCTCTTCT	179

(CSN2) 多克隆抗体或兔源 Cyclin D1 多克隆抗体(用 TBST 缓冲液按照体积比 1:1 000 稀释)为一抗,再以 HRP-标记山羊抗兔 IgG(用 TBST 缓冲液按照体积比 1:1 000 稀释)为二抗,对细胞总蛋白样品进行 Western blot 检测,并通过 ImageJ 软件进行灰度值分析,计算 CSN2 和 Cyclin D1 蛋白的相对表达水平。

细胞增殖试验设空白组(不加细胞,加培养液)、对照组(无激素)和试验组(100、300、500 ng/mL 重组 PRL),每组设 5 个重复,每个重复 1 个孔,试验重复 3 次,细胞相对增殖率(Relative growth rate, RGR)= $D_{450\text{ nm}}(\text{试验组})/D_{450\text{ nm}}(\text{对照组})$;诱导酪蛋白表达试验设对照组(无激素)和试验组(100、300、500 ng/mL 重组 PRL),每组设 3 个重复,每个重复 1 个孔,试验重复 3 次。

1.3 统计学分析

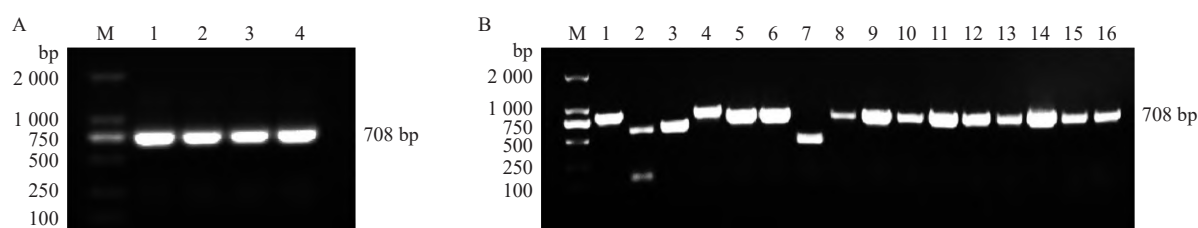
试验数据采用 SPSS22.0 进行单因素方差分析

(One-way ANOVA),采用 LSD 法进行多重比较分析,数据结果用平均值±标准误表示。

2 结果与分析

2.1 pMD18-T-PRL 克隆载体的构建与鉴定

以猪垂体 cDNA 为模板,用引物 Sus-PRL-F/Sus-PRL-R 扩增猪源 *PRL* 基因片段(图 1A),回收连接到 pMD18-T 载体后转化到 DH5 α 感受态细胞,菌液 PCR 鉴定结果如图 1B 所示,分别提取 5、6、9~16 号菌液质粒进行 DNA 测序鉴定,并将 DNA 测序结果经 Blast 比对发现 5、6、11 号菌液质粒插入片段均仅有 1 个碱基突变(A 突变为 G),导致三联密码改变(ATG 变为 GTG,成熟肽第 13 氨基酸 Met 变为 Val),而插入基因片段编码的 PRL 成熟肽段氨基酸序列与 PRL 亚型(XP_005665681.1)一致,pMD18-T-PRL 克隆载体构建成功。



A: *PRL* 基因的 PCR 产物, M 为 DL 2000 DNA Marker, 1~4 以母猪垂体组织 cDNA 为模板; B: pMD18-T-PRL 菌液 PCR 产物, M 为 DL 2000 DNA Marker, 1~16 分别以挑选的不同 pMD18-T-PRL 菌落的菌液为模板

A: PCR products of *PRL* gene, M is DL 2000 DNA Marker, 1~4 use sow pituitary tissue cDNA as template; B: PCR products of pMD18-T-PRL colonies, M is DL 2000 DNA Marker, 1~16 respectively use different pMD18-T-PRL colonies as template

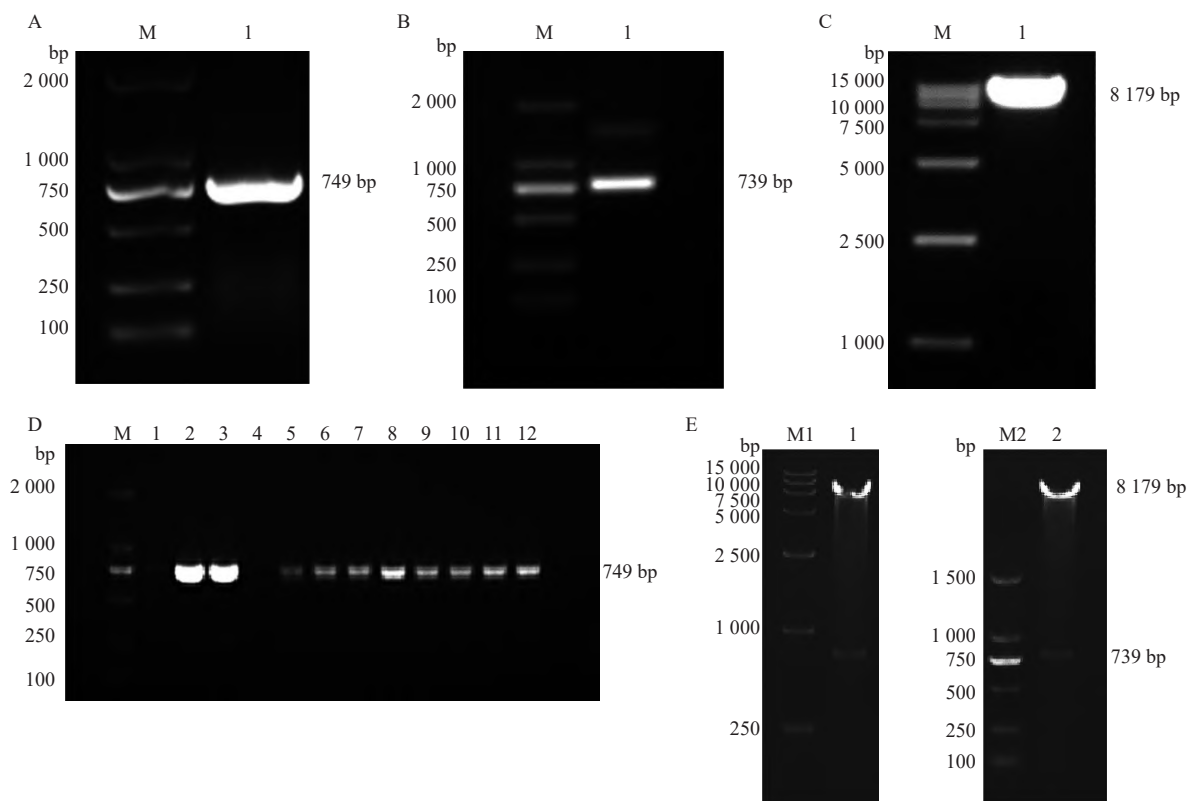
图 1 pMD18-T-PRL 克隆载体的构建与 PCR 鉴定

Fig. 1 Construction and PCR identification of pMD18-T-PRL cloning plasmid

2.2 pCDH-CMV-6His-PRL-6His-EF1-GFP+Puro 慢病毒表达载体的构建与鉴定

以 pMD18-T-PRL 克隆载体为模板,用引物 HPH-F-EcoR I/HPH-R-BamH I 扩增出 EcoR I-6His-

PRL-6His-BamH I 序列片段(图 2A);用 *EcoR* I 和 *BamH* I 内切酶分别对纯化回收的目的片段与 pCDH-CMV-MCS-EF1-GFP+Puro 慢病毒表达载体进行双酶切,分别得到 6His-PRL-6His 片段(图 2B)



A: *EcoRI*-6His-PRL-6His-*BamHI* 序列片段 PCR 产物, M 为 DL 2000 DNA Marker, 1 为 *EcoRI*-6His-PRL-6His-*BamHI* 序列片段; B: *EcoRI*-6His-PRL-6His-*BamHI* 序列片段双酶切产物, M 为 DL 2000 DNA Marker, 1 为 6His-PRL-6His 片段; C: pCDH-CMV-MCS-EF1-GFP+Puro 质粒双酶切产物, M 为 DL 15000 DNA Marker, 1 为 pCDH-CMV-MCS-EF1-GFP+Puro 线性片段; D: pCDH-CMV-6His-PRL-6His-EF1-GFP+Puro 菌液 PCR 产物, M 为 DL 2000 DNA Marker, 1~12 分别以挑选的不同单菌落的菌液为模板; E: 重组质粒 pCDH-CMV-6His-PRL-6His-EF1-GFP+Puro 的双酶切结果, M1 为 DL 15000 DNA Marker, M2 为 DL 2000 DNA Marker, 1 和 2 为重组质粒双酶切片段

A: PCR product of *EcoRI*-6His-PRL-6His-*BamHI* sequence fragment, M is DL 2000 DNA Marker, 1 is *EcoRI*-6His-PRL-6His-*BamHI* sequence fragment; B: Double digested product of *EcoRI*-6His-PRL-6His-*BamHI* sequence fragment, M is DL 2000 DNA Marker, 1 is 6His-PRL-6His sequence fragment; C: Double digested product of pCDH-CMV-MCS-EF1-GFP+Puro plasmid, M is DL 15000 DNA Marker, 1 is pCDH-CMV-MCS-EF1-GFP+Puro plasmid linear fragment; D: PCR products of pCDH-CMV-6His-PRL-6His-EF1-GFP+Puro colonies, M is DL 2000 DNA Marker, 1~12 respectively use selected bacterial solutions from different single colonies as templates; E: Double digested product of recombinant vector pCDH-CMV-MCS-EF1-GFP+Puro, M1 is DL 15000 DNA Marker, M2 is DL 2000 DNA Marker, 1 and 2 are double digested products of recombinant vector

图 2 pCDH-CMV-6His-PRL-6His-EF1-GFP+Puro 慢病毒表达载体的构建与 PCR 鉴定

Fig. 2 Construction and PCR identification of pCDH-CMV-6His-PRL-6His-EF1-GFP+Puro lentivirus expression plasmid

和线性化 pCDH-CMV-MCS-EF1-GFP+Puro 质粒片段 (图 2C), 并进行连接后转化到 *Stb13* 感受态细胞, 挑取单菌落进行菌液 PCR 鉴定 (图 2D), 阳性菌液 DNA 测序结果经 Blast 比对, 插入片段与 pMD18-T-PRL 中的测序序列一致; 对重组质粒进行双酶切后, 在约 739 bp 处有一条特异性条带, 与目的基因大小一致 (图 2E), 表明 pCDH-CMV-6His-PRL-6His-EF1-GFP+Puro 慢病毒表达载体构建成功。

2.3 慢病毒包装及滴度测定

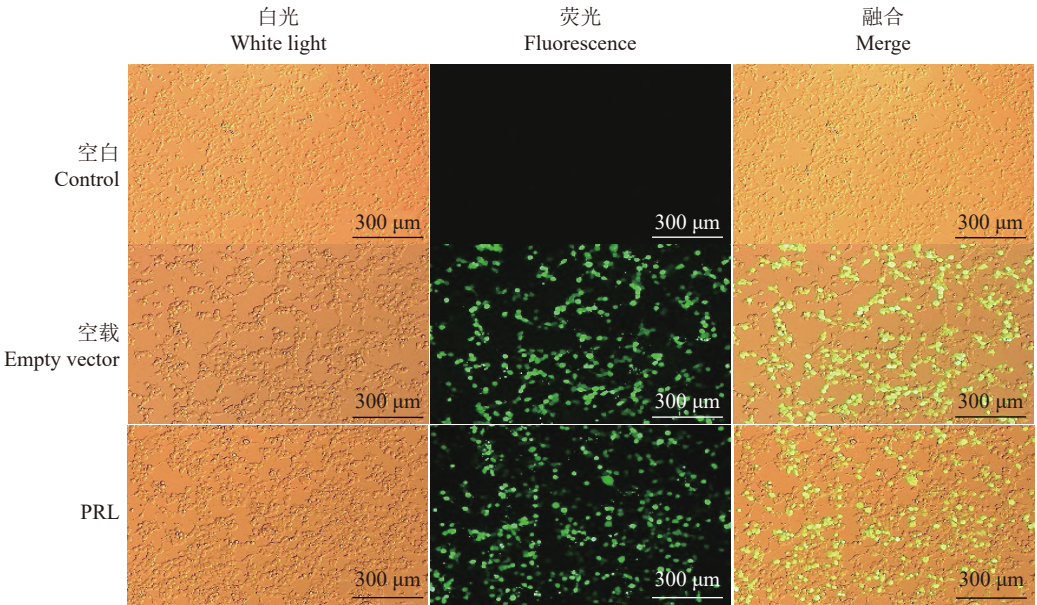
将慢病毒重组载体或空载体与辅助质粒共转染 293T 细胞, 包装含有 6His-PRL-6His 片段的 PRL-慢病毒, 共转染 24 h 后, 在荧光倒置显微镜下可见 293T 细胞中绿色荧光蛋白表达情况良好 (图 3), 转染效率为 30%~50%。对 PRL-慢病毒浓缩液进行滴度测定, 慢病毒滴度约为 9.9×10^8 TU/mL, 满足后续试验要求。

2.4 慢病毒感染 CHO-K1 细胞及阳性细胞系的筛选

用浓缩慢病毒液感染 CHO-K1 细胞 72 h 后, 在倒置荧光显微镜下观察到感染慢病毒的 CHO-K1 细胞中绿色荧光蛋白表达情况良好 (图 4), 感染效率达 30%~50%, 初步认定猪源 PRL 基因成功导入 CHO-K1 细胞中。PRL-慢病毒感染的 CHO-K1 细胞用嘌呤霉素进行连续 7 d 药物筛选后, 表达绿色荧光蛋白的细胞达 95% 以上, 获得阳性细胞系并命名为 CHO-K1-PRL。

2.5 CHO-K1-PRL 细胞的鉴定

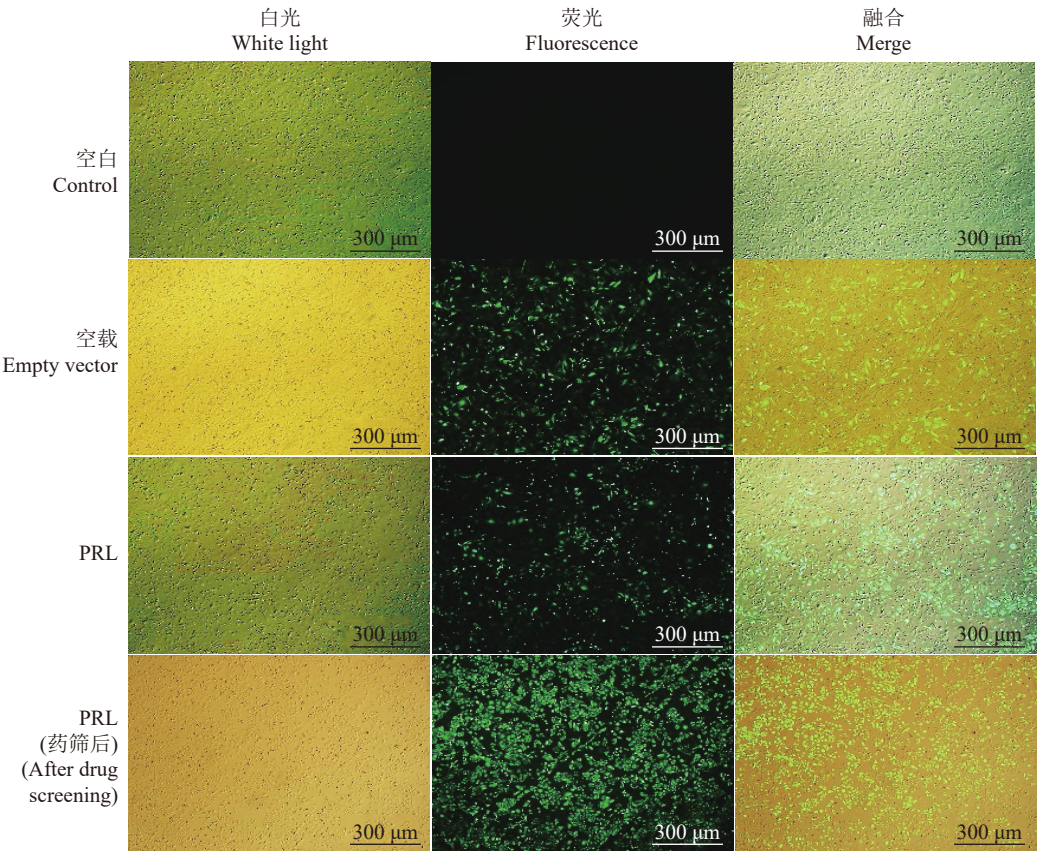
以未感染慢病毒的 CHO-K1 细胞和感染空载体慢病毒的 CHO-K1 细胞为对照, 对 CHO-K1-PRL 细胞进行 RT-PCR (β -actin 作为内参基因) 和 Western blot 鉴定。结果显示, 只有 CHO-K1-PRL 细胞能扩增出与预期相符的条带 (749 bp)



空白: 未做处理的 293T 细胞; 空载: 转染空慢病毒载体的 293T 细胞; PRL: 转染 pCDH-CMV-6His-PRL-6His-EF1-GFP+Puro 慢病毒表达载体的 293T 细胞
Control: Untreated 293T cells; Empty vector: 293T cells transfected with empty lentiviral vector; PRL: 293T cells transfected with pCDH-CMV-6His-PRL-6His-EF1-GFP+Puro lentiviral vector

图 3 慢病毒载体转染 293T 细胞 24 h 荧光表达情况

Fig. 3 Fluorescent expression of 293T cells transfected with lentivirus plasmid for 24 h



空白: 未做处理的 CHO-K1 细胞; 空载: 感染空载体慢病毒液的 CHO-K1 细胞; PRL: 感染 PRL-慢病毒液的 CHO-K1 细胞; PRL(药筛后): 感染 PRL-慢病毒液的 CHO-K1 细胞经嘌呤霉素药物筛选 7 d 后
Control: Untreated CHO-K1 cells; Empty vector: CHO-K1 cells infected by the concentrated empty lentivirus solution; PRL: CHO-K1 cells infected by the concentrated PRL-lentivirus solution; PRL (after drug screening): CHO-K1 cells infected with PRL-lentivirus solution and then screened by purinomycin for seven days

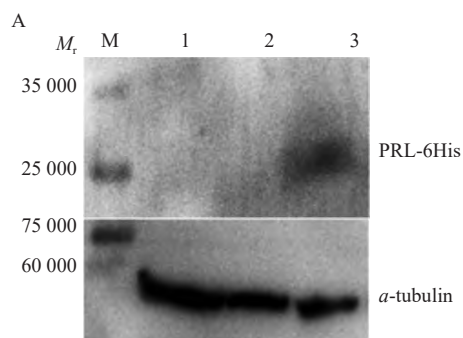
图 4 慢病毒浓缩液感染 CHO-K1 细胞 72 h 及药筛 7 d 后荧光表达情况

Fig. 4 Fluorescence expression of CHO-K1 cells infected with concentrated lentivirus solution for 72 h and seven days after drug screening

(图 5), 并且只有 CHO-K1-PRL 阳性细胞的细胞蛋白与培养液有且均有检测到 His-Tag 蛋白 (图 6), 相对分子质量约为 25 000 (猪 PRL 相对分子质量为 23 000)。

2.6 猪源 PRL 重组蛋白的纯化与 LC-MS/MS 质谱分析

收集 CHO-K1-PRL 细胞培养液, 利用镍柱亲和层析对培养液通过 His-Tag 进行纯化, 获得纯化的重组蛋白 (质量浓度为 50 $\mu\text{g/mL}$), 对纯化蛋白进行 SDS-PAGE (图 7), 并切取目的条带进行 LC-MS/MS 质谱分析, 经与蛋白质数据库比对分析, 重组蛋白与天然猪 PRL (XP_005665681.1) 比对覆盖率达 94%, 说明表达产物为猪源 PRL 重组蛋白。



A: 细胞裂解液; B: 细胞培养液; M 为 Western blot marker, 1 为未做处理的 CHO-K1 细胞, 2 为感染空载体慢病毒液的 CHO-K1 细胞, 3 为 CHO-K1-PRL; PRL-6His 重组蛋白和内参 α -tubulin 相对分子质量分别约为 25 000 和 55 000

A: Cell lysate; B: Cell culture fluid; M is Western blot marker, 1 is untreated CHO-K1 cells, 2 is CHO-K1 cells infected by the concentrated empty lentivirus solution, 3 is CHO-K1-PRL; The relative molecular weights of PRL-6His recombinant protein and α -tubulin are about 25 000 and 55 000 respectively

图 6 CHO-K1-PRL 细胞中 His-Tag 蛋白 Western blot 鉴定

Fig. 6 Western blot identification of His-Tag protein in CHO-K1-PRL cells

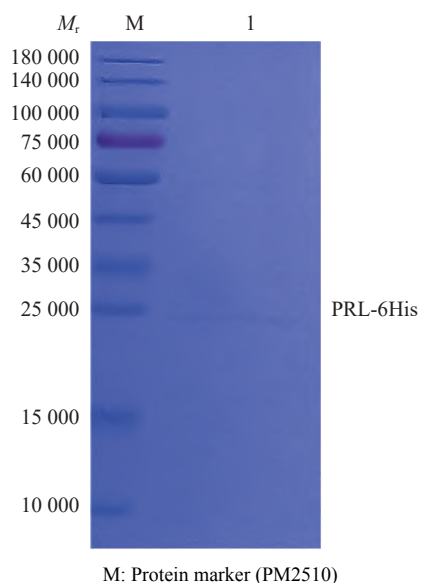
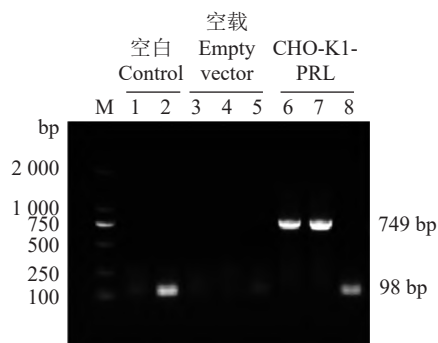


图 7 纯化猪源 PRL 重组蛋白的 SDS-PAGE 鉴定

Fig. 7 SDS-PAGE identification of purified porcine PRL recombinant proteins



M 为 DL 2000 DNA Marker; 1、3、4、6 和 7 为 749 bp 的 *EcoRI*-6His-PRL-6His-BamHI 片段; 2、5 和 8 为 98 bp 的 β -actin

M is DL 2000 DNA Marker; 1, 3, 4, 6 and 7 are the 749 bp *EcoRI*-6His-PRL-6His-BamHI fragments; 2, 5 and 8 are the 98 bp β -actin fragments

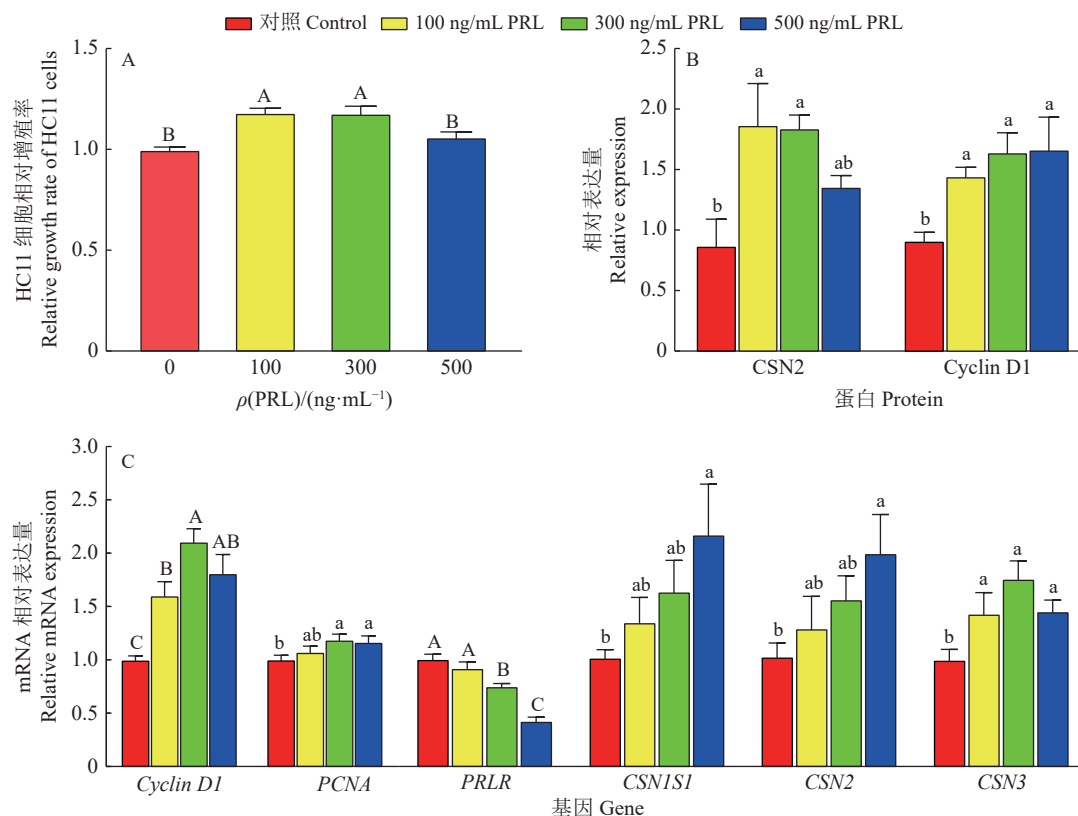
图 5 CHO-K1-PRL 细胞的 RT-PCR 鉴定

Fig. 5 RT-PCR identification of CHO-K1-PRL cells

2.7 猪源 PRL 重组蛋白对 HC11 细胞增殖及酪蛋白合成的影响

在 HC11 体外培养体系中分别加入不同质量浓度的重组 PRL (0、100、300、500 ng/mL) 处理 24 h 后, 发现添加重组 PRL 能促进 HC11 细胞增殖 ($P < 0.05$) (图 8A), 并且与细胞增殖相关的 *Cyclin D1*、*PCNA* 基因及 Cyclin D1 蛋白表达水平显著上升 ($P < 0.05$) (图 8B、8C、9A), 与细胞相对增殖率的结果相一致。

通过 qPCR 和 Western blot 检测, 结果显示, 添加 300、500 ng/mL 重组 PRL 极显著下调了 *PRLR* 的表达水平 ($P < 0.01$) (图 8C); 添加 100、300 ng/mL 重组 PRL 处理对 HC11 中 *CSN1S1*、*CSN2* 基因表达水平无显著影响, 而 *CSN3* 基因表达水平显著上调 ($P < 0.05$) (图 8C), 但 *CSN2* 蛋白表达水平显著高于对照组 ($P < 0.05$) (图 8B、9B); 添加 500 ng/mL 重组 PRL 显著上调了酪蛋白基因 (*CSN1S1*、



柱子上方 (图 A)、相同蛋白 (图 B) 或基因 (图 C) 柱子上的不同小写字母表示组间差异显著 ($P < 0.05$, LSD 法), 不同大写字母表示组间差异极显著 ($P < 0.01$, LSD 法)

Different lowercase letters on bars (figure A), or bars of the same protein (figure B) or gene (figure C) indicate significant differences among groups ($P < 0.05$, LSD method), different capital letters indicate highly significant differences among groups ($P < 0.01$, LSD method)

图 8 不同质量浓度重组 PRL 对 HC11 细胞增殖及酪蛋白表达的影响

Fig. 8 Different mass concentrations of recombinant PRL on proliferation and casein expressions of HC11 cells

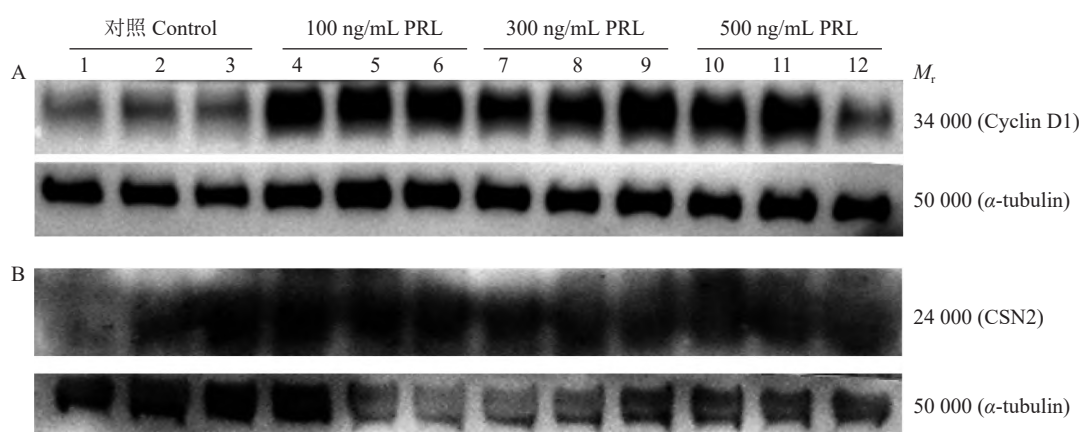


图 9 Western blot 检测不同质量浓度重组 PRL 对 HC11 细胞中 Cyclin D1、CSN2 蛋白表达的影响

Fig. 9 Effects of different mass concentrations of recombinant PRL on expressions of Cyclin D1 and CSN2 proteins in HC11 cells detected by western blot

CSN2、CSN3) 的表达水平 ($P < 0.05$) (图 8C), 而 CSN2 蛋白表达水平与对照组差异不显著 (图 8B、9B)。

3 讨论与结论

PRL 主要是由垂体前叶分泌的一类蛋白质激素, 具有广泛的生物活性。PRL 具有显著的分子多

态性, 包括不同百分比的糖基化形式, 这可能是 PRL 多效性的基础^[13]。当前市面上多为原核表达的 PRL 重组蛋白, 缺乏蛋白质翻译后修饰, 表达的蛋白既不能进行正确折叠, 也不能被糖基化, 并且通常由于二硫键错配而以包涵体形式存在^[16-17], 需要进一步溶解和复性, 蛋白质的生物活性难以保

证。为了获得与天然猪源 PRL 更相近的具有活性的重组蛋白,本研究利用 CHO 细胞真核表达系统体外表达了猪源 PRL 蛋白。

CHO 真核表达系统不仅具有蛋白质翻译后修饰功能,而且表达的蛋白质具有完整的生物学功能^[18];糖基化是蛋白质翻译后修饰的最重要形式之一,其直接影响重组蛋白的空间构象、稳定性、聚性和生物学活性以及体内特性(包括药物代谢动力学和免疫原性)^[19]。慢病毒载体是以慢病毒的基因组为基础,由目的基因取代部分病毒基因结构构成的一类载体^[20],能够携带大片段的外源基因,并且不容易诱发宿主的免疫反应,更重要的是其能够将目的基因高效整合到宿主细胞的染色体中,且不易引起插入突变,理论上能够在细胞内永久表达并在子代中稳定表达^[21];而且改造后的慢病毒是假病毒,没有复制能力,具备较好的生物安全性,是一种理想的基因转移载体^[22]。因此,我们选用慢病毒载体系统进行构建稳定表达猪源 PRL 重组蛋白的 CHO-K1-PRL 细胞系。

目前大多数慢病毒载体根据 HIV-1 基因组改装而来,慢病毒感染宿主细胞后,能够整合自身基因组到宿主细胞中,从而使外源基因能够在宿主细胞中实现长期稳定地表达。事实上,慢病毒载体已成功用于表达人的 PRL 重组蛋白^[23]。在本研究中,我们通过将猪 PRL 基因片段插入到 pCDH-CMV-MCS-EF1-GFP+Puro 慢病毒表达载体,经慢病毒包装获得含有猪 PRL 基因的 PRL-慢病毒液,其感染 CHO-K1 细胞并经过嘌呤霉素药物筛选后得到稳定的猪 PRL 表达系统,并利用镍柱亲和层析法纯化猪 PRL 重组蛋白。Western blot 鉴定发现该重组蛋白能与 His-Tag 抗体结合,条带的相对分子质量约为 25 000;此外,对纯化得到的猪 PRL 重组蛋白进行 LC-MS/MS 质谱分析,结果显示该重组蛋白与天然猪 PRL 蛋白对比的覆盖率达 94%,可以确定 CHO-K1-PRL 细胞培养液中含有猪源 PRL 蛋白。天然猪 PRL 相对分子质量为 23 000,而本研究表达的 PRL 蛋白携带 His-Tag 蛋白, PRL-6His 相对分子质量约为 25 000。信号肽通常位于新合成肽链的 N 端,一般由 15~30 个氨基酸残基组成,能够引导细胞内新合成的蛋白质转移到内质网并分泌到细胞;信号肽序列在不同蛋白质之间可以通用,优化蛋白质外源表达可通过选择高效引导蛋白质分泌表达的信号肽序列替换蛋白质本身的信号肽^[24]。本研究在构建慢病毒表达载体时,保留了 PRL 基因中的信号肽序列,在未经浓缩的 CHO-K1-PRL 阳性

细胞的培养液中难以检测到重组蛋白,而纯化得到的 PRL 重组蛋白质量浓度为 50 $\mu\text{g/mL}$,说明本研究的猪 PRL 表达系统蛋白表达量低,后续想要获得更高效的 PRL 表达系统,可以考虑通过替换 PRL 基因的信号肽序列进行优化。此外,由于在蛋白表达过程中,蛋白携带的 His-Tag 可能会被包裹在蛋白内部,可能是导致纯化的重组蛋白浓度低的原因之一^[25]。

PRL 以其促进乳腺的生长发育和泌乳而闻名^[26],PRL 与 PRLR 结合后,激活 PRL 介导的信号转导通路,刺激乳腺发育、乳蛋白的合成与分泌等^[27]。PRL 与乳腺分泌细胞膜上的 PRLR 结合,能够促进乳蛋白尤其是酪蛋白 mRNA 产生^[28],乳蛋白的合成与酪蛋白基因的表达式具有强相关性^[29]。本研究中,为验证 PRL 重组蛋白的生物活性,将其添加到 HC11 细胞的体外培养体系中,处理 24 h 后,检测分析细胞相对增值率和细胞中酪蛋白基因 (CSN1S1、CSN2、CSN3)mRNA 表达及 CSN2、Cyclin D1 蛋白的表达水平。试验结果表明,添加重组 PRL 蛋白能够显著促进 HC11 细胞的增殖,同时也上调了 HC11 细胞中 CSN1S1、CSN2、CSN3 mRNA 及 CSN2 蛋白的表达水平,说明重组 PRL 对乳腺细胞增殖和酪蛋白的表达具有显著的诱导作用。

综上,本研究利用真核表达系统成功表达了具有生物学活性的猪源 PRL 重组蛋白,为猪 PRL 的功能研究和生产应用奠定了基础。

参考文献:

- [1] MARANO R J, BEN-JONATHAN N. Minireview: Extrapituitary prolactin: An update on the distribution, regulation, and functions[J]. Molecular Endocrinology, 2014, 28(5): 622-633.
- [2] MACOTELA Y, TRIBEL J, CLAPP C. Time for a new perspective on prolactin in metabolism[J]. Trends in Endocrinology and Metabolism, 2020, 31(4): 276-286.
- [3] VILAR L, VILAR C F, LYRA R, et al. Pitfalls in the diagnostic evaluation of hyperprolactinemia[J]. Neuroendocrinology, 2019, 109(1): 7-19.
- [4] MELMED S, CASANUEVA F F, HOFFMAN A R, et al. Diagnosis and treatment of hyperprolactinemia: An Endocrine Society clinical practice guideline[J]. Journal of Clinical Endocrinology & Metabolism, 2011, 96(2): 273-288.
- [5] RATNER L D, GONZALEZ B, AHTIAINEN P, et al. Short-term pharmacological suppression of the hyperprolactinemia of infertile hCG-overproducing female mice persistently restores their fertility[J]. Endocrinology, 2012, 153(12): 5980-5992.
- [6] 何海迎,王泳,段春辉,等. 催乳素对绵羊颗粒细胞雌激素和孕酮分泌及相关基因表达的影响[J]. 中国兽医学报, 2020, 40(11): 2226-2233.
- [7] PHILLIPPS H R, YIP S H, GRATAN D R. Patterns of prolactin secretion[J]. Molecular and Cellular Endocrinology, 2020, 502: 110679.

- [8] SAMPERI I, LITHGOW K, KARAVITAKI N. Hyperprolactinemia[J]. Journal of Clinical Medicine, 2019, 8(12): 2203.
- [9] DI FILIPPO L, DOGA M, RWSMINI E, et al. Hyperprolactinemia and bone[J]. Pituitary, 2020, 23(3): 314-321.
- [10] BASINI G, BAIONI L, BUSSOLATI S, et al. Prolactin is a potential physiological modulator of swine ovarian follicle function[J]. Regulatory Peptides, 2014, 189: 22-30.
- [11] TRIEBEL J, BERTSCH T, BOLLHEIMER C, et al. Principles of the prolactin/vasoinhibin axis[J]. American Journal of Physiology Regulatory Integrative & Comparative Physiology, 2015, 309(10): R1193-R1203.
- [12] TRIEBEL J, ROBLES-OSORIO M L, GARCIA-FRANCO R, et al. From bench to bedside: Translating the prolactin/vasoinhibin axis[J]. Frontiers in Endocrinology, 2017, 8: 342.
- [13] SINHA Y N. Structural variants of prolactin: Occurrence and physiological significance[J]. Endocrine Reviews, 1995, 16(3): 354-369.
- [14] 田青, SPITZER A J, ZHAO F. PRL 对 HC11 细胞乳蛋白及其调节因子基因表达的影响[J]. 中国乳品工业, 2020, 48(12): 20-23.
- [15] 田青, 王洪荣. 胰岛素、催乳素和氢化可的松对奶牛乳腺上皮细胞增殖和凋亡的影响[J]. 中国饲料, 2013(2): 8-12.
- [16] NUC P, NUC K. Recombinant protein production in *Escherichia coli*[J]. Postepy Biochemii, 2006, 52(4): 448-456.
- [17] 邓春梅, 葛玉强, 刘丽, 等. 外源基因表达系统的研究进展[J]. 现代生物医学进展, 2010, 10(19): 3744-3746.
- [18] KIM J Y, KIM Y G, LEE G M. CHO cells in biotechnology for production of recombinant proteins: Current state and further potential[J]. Applied Microbiology and Biotechnology, 2012, 93(3): 917-930.
- [19] JAIN N K, BARKOWSLI-CLARK S, ALTMAN R, et al. A high density CHO-S transient transfection system: Comparison of Ex-piCHO and Expi293[J]. Protein Expression & Purification, 2017, 134: 38-46.
- [20] 孟凡荣, 陈琛, 万海粟, 等. 慢病毒载体及其研究进展[J]. 中国肺癌杂志, 2014, 17(12): 870-876.
- [21] COCKRELL A S, KAFRI T. Gene delivery by lentivirus vectors[J]. Molecular Biotechnology, 2007, 36(3): 184-204.
- [22] FOLLENZI A, SANTAMBROGIO L, ANNONI A. Immune responses to lentiviral vectors[J]. Current Gene Therapy, 2007, 7(5): 306-315.
- [23] ALARCON H, BONZON-KULICHENKO E, PEINADO R, et al. Generation of a lentiviral vector system to efficiently express bioactive recombinant human prolactin hormones[J]. Molecular and Cellular Endocrinology, 2020, 499: 110605.
- [24] 宋倩倩, 王文玲, 詹瑛, 等. 真核表达 MERS-CoV 刺突蛋白亚单位的信号肽序列优化研究[J]. 病毒学报, 2019, 35(1): 20-26.
- [25] 董金蓉, 毛树宝, 谢震渊, 等. 人巨细胞病毒 *gB/AD1* 基因在 CHO 细胞中的表达和纯化[J]. 生命科学研究, 2015, 19(5): 402-409.
- [26] FARMER C. Prolactin and the swine mammary gland[J]. Domestic Animal Endocrinology, 2022, 78: 106672.
- [27] FREEMAN M E, KANYICKSKA B, LERANT A, et al. Prolactin: Structure, function, and regulation of secretion[J]. Physiological Reviews, 2000, 80(4): 1523-1631.
- [28] AKERS R M. Major advances associated with hormone and growth factor regulation of mammary growth and lactation in dairy cows[J]. Journal of Dairy Science, 2006, 89(4): 1222-1234.
- [29] LEE G Y, KENNY P A, LEE E H, et al. Three-dimensional culture models of normal and malignant breast epithelial cells[J]. Nature Methods, 2007, 4(4): 359-365.

【责任编辑 庄 延】



冯美莹, 李桂焕, 徐振鹏, 等. 左旋肉碱对猪卵母细胞体外成熟、脂肪代谢和孤雌胚胎发育的影响[J]. 华南农业大学学报 2014 35(6):8-12.

左旋肉碱对猪卵母细胞体外成熟、脂肪代谢和孤雌胚胎发育的影响

冯美莹, 李桂焕, 徐振鹏, 白银山, 王文聪, 李莉, 张守全, 卫恒习

(华南农业大学 动物科学学院/国家生猪种业工程技术研究中心/广东省农业动物基因组学与分子育种重点实验室 广东 广州 510642)

摘要:【目的】探讨不同质量浓度的左旋肉碱对猪卵母细胞体外成熟、脂肪代谢和孤雌胚胎发育的影响。【方法】在成熟培养液中添加不同质量浓度左旋肉碱, 观察其对猪卵母细胞体外成熟和孤雌胚胎发育的影响, 并利用油红染色、三酰甘油定量试剂盒和定量 RT-PCR 技术检测其对卵母细胞脂肪代谢及其关键水解酶表达水平的影响。【结果和结论】在成熟液中添加 100 ng/mL 左旋肉碱能极显著促进猪卵母细胞的脂肪滴代谢 ($P < 0.001$), 并显著提高猪卵母细胞体外成熟率和孤雌激活囊胚发育率 ($P < 0.05$); 在胚胎培养液中添加 100 ng/mL 左旋肉碱能够显著提高猪孤雌胚胎卵裂率 ($P < 0.05$), 其囊胚率和囊胚质量均有提高的趋势; 通过定量 RT-PCR 进一步发现 100 ng/mL 左旋肉碱极显著降低猪卵母细胞中激素敏感脂肪酶基因 (HSL $P < 0.01$) 和三酰甘油水解酶基因 ($ATGL$ $P < 0.001$) 的 mRNA 表达水平, 表明左旋肉碱能够影响调控脂肪代谢关键酶基因的表达。试验结果表明, 左旋肉碱具有促进猪卵母细胞体外成熟和孤雌激活胚胎发育能力的作用, 其可能是通过调控脂肪代谢来实现的。

关键词:猪卵母细胞; 左旋肉碱; 孤雌激活; 脂肪代谢; 胚胎发育

中图分类号:S828

文献标志码:A

文章编号:1001-411X(2014)06-0008-05

Effects of *L*-carnitine on oocytes *in vitro* maturation, lipid metabolism and parthenogenetic embryos development in porcine

FENG Meiyong, LI Guihuan, XU Zhenpeng, BAI Yinshan, WANG Wencong,

LI Li, ZHANG Shouquan, WEI Hengxi

(College of Animal Science, South China Agricultural University/National Engineering Research Center for Breeding Swine Industry/
Guangdong Provincial Key Lab of Agro-animal Genomics and Molecular Breeding, Guangzhou 510642, China)

Abstract: 【Objective】This study was conducted to explore the effect of different concentrations of *L*-carnitine on the maturation of porcine oocytes, the development of parthenogenetic (PA) embryos *in vitro* and the lipid metabolism in pig oocytes. 【Method】Different concentrations of *L*-carnitine were added into mature medium to observe the influence on porcine oocytes maturation and parthenogenetic embryos development. Oil red staining, triacylglycerol kit and quantitative RT-PCR were used to detect the lipid metabolism and the key hydrolase expression level in oocytes. 【Result and conclusion】The rates of oocytes maturation and the subsequent PA blastocysts increased significantly when supplemented with 100 ng/mL *L*-carnitine to the IVM medium ($P < 0.05$), and the oocytes lipid metabolism also increased sig-

收稿日期:2014-02-20 优先出版时间:2014-10-03

优先出版网址: <http://www.cnki.net/kcms/detail/44.1110.S.20141003.1118.007.html>

作者简介:冯美莹(1989—),女,硕士研究生, E-mail:jony.ya@163.com;通信作者:卫恒习(1980—),男,副研究员, E-mail:weihengxi@163.com

基金项目:国家科技支撑计划(2011BAD19B03);广东省现代农业产业技术体系生猪创新团队(粤农(2009)380号);东莞市科技计划项目(201208102049)

nificantly ($P < 0.001$). The addition of 100 ng/mL *L*-carnitine into embryo culture medium significantly increased the cleavage rates ($P < 0.05$) and contributed to the PA blastocyst rates and qualities. Further analyses of quantitative RT-PCR revealed that the mRNA expression levels of adipose triglyceride lipase gene (*ATGL*) and hormone-sensitive triglyceride lipase gene (*HSL*) both decreased significantly with 100 ng/mL *L*-carnitine treatment, which indicated that the *L*-carnitine could affect the lipid metabolism by regulating the key lipases gene expression. In conclusion, these results demonstrated that *L*-carnitine can improve porcine oocytes maturation and enhance the PA embryos developmental ability through lipid metabolism regulation.

Key words: porcine oocytes; *L*-carnitine; parthenogenetic activation; lipid metabolism; embryo development

随着哺乳动物体细胞核移植、转基因和胚胎干细胞等高新生物技术的发展,人们对卵母细胞质量的要求越来越高。当前猪卵母细胞体外成熟(*In vitro* maturation, IVM)体系仍不完善,导致猪卵母细胞的体外成熟质量不高、胚胎发育受阻,这制约了其在科学研究和畜牧生产中的应用^[1-3]。研究发现,猪卵母细胞和早期胚胎中含有大量的脂肪滴,致使其对外界环境极为敏感,特别是低温条件会造成猪胚胎发育停止或死亡^[4]。同时这也造成了胚胎冷冻保存的困难。

左旋肉碱是脂肪代谢过程中的一种关键的分子,能够促进脂肪代谢。在细胞内,左旋肉碱作为载体把脂肪酸从线粒体膜外转运到线粒体膜内,促使脂肪酸在线粒体内氧化分解并释放出能量^[1,5-7]。研究还发现左旋肉碱能够有效促进卵子的体外成熟和胚胎发育^[4,5,8],但其在猪卵母细胞成熟和胚胎发育中的作用和机制尚不完全清楚。

本试验旨在研究不同质量浓度的左旋肉碱对猪卵母细胞的体外成熟、孤雌胚胎早期发育和囊胚质量的影响及其可能的作用途径,以期完善猪卵母细胞的体外培养体系,为提高猪卵母细胞和胚胎质量、促进猪胚胎冷冻保存技术的发展提供技术支持。

1 材料与方法

1.1 试验材料

DPBS(Dulbecco's phosphate buffered saline)、非必需氨基酸(MEM NEAA)、丙酮酸钠和谷氨酰胺为GIBCO公司产品,葡萄糖为Hyclone公司产品,其他试剂均为Sigma公司产品。

试验中所用的溶液主要成分如下:成熟培养液中含有TCM 199(Tissue culture medium 199)、体积分数为10%的猪卵泡液、10 ng/mL的表皮生长因子、10 IU/mL人绒毛膜促性腺激素、10 IU/mL孕马血清

促性腺激素和0.1 mg/mL的*L*-半胱氨酸,每组再根据试验要求添加一定质量浓度的左旋肉碱;采卵液(Polyvinyl alcohol-Dulbecco's phosphate buffered saline, PVA-DPBS)中含有DPBS和1 g/L的聚乙烯醇(Polyvinylalcohol PVA);电激活液中含有0.25 mol/L甘露醇、0.10 mmol/L CaCl_2 、0.10 mmol/L MgCl_2 、0.05 mmol/L 4-羟乙基哌嗪乙磺酸(HEPES)和0.1 g/L PVA;猪胚胎培养液(PZM-3, porcine zygote medium 3)中含有100.00 mmol/L NaCl、25.10 mmol/L NaHCO_3 、10.00 mmol/L KCl、0.35 mmol/L KH_2PO_4 、0.40 mmol/L $\text{MgSO}_4 \cdot 7\text{H}_2\text{O}$ 、2.00 mmol/L 乳酸钙、2.00 mmol/L 丙酮酸钠、1.00 mmol/L *L*-谷氨酰胺、5.00 mmol/L 亚牛磺酸、体积分数为2%必需氨基酸(BME EAA)、体积分数为1%非必需氨基酸(MEM NEAA)和3 g/L无脂肪酸牛血清白蛋白(BSA);油红染色液中含有0.15 g油红O、30 mL异丙醇和20 mL H_2O 。实时荧光定量RT-PCR检测所用的引物序列如表1所示。

表1 实时荧光定量PCR引物
Tab. 1 The primers of real-time fluorescent quantitative PCR

引物	引物序列(5'→3')	产物长度/bp
Hsl	TCCAAATCCCACGAGCCTTA GAGGAGACCGCAGTGCTTGA	159
Atgl	ATGGAGCCCACGGACCTG CTGCCTGCTGCTCCTTTATCC	179
Actb	AGGGCAGTAGCATCGCTTTAGT AAGGGGATTGTGATGGCTGA	118

1.2 试验方法

1.2.1 不同质量浓度左旋肉碱对猪卵母细胞体外成熟及其孤雌胚胎体外发育的影响 在无菌条件下收集卵巢表面直径3~8 mm卵泡中的卵母细胞,并在显微镜下挑选胞质均匀、颗粒细胞3层以上的卵丘-卵

母细胞复合体(Cumulus oocytes complexes, COCs). 然后将采集的猪卵母细胞随机分成4组, 分别在添加不同质量浓度(0、10、100、1 000 ng/mL)左旋肉碱的成熟液中(每100 μ L培养液培养20~30枚卵子)成熟培养42~46 h. 用透明质酸酶(1 mg/mL)脱去成熟培养后COCs的卵丘细胞, 在体视显微镜下检查卵母细胞第一极体排出情况. 之后, 分别给予100 V/cm、60 μ s的直流脉冲进行孤雌激活. 将电激后的卵母细胞转入PZM-3中培养, 分别于培养第2天和第7天检查胚胎卵裂和囊胚发育情况, 并利用5 μ g/mL Hoechst 33342对囊胚进行染色和细胞计数.

通过比较不同浓度左旋肉碱对猪卵母细胞体外成熟率(第一极体排出率)、卵裂率(卵裂数/激活卵数)、囊胚率(囊胚数/卵裂数)和囊胚细胞数的影响, 从而确定左旋肉碱对猪卵母细胞体外成熟的影响, 并筛选出其最佳添加质量浓度.

1.2.2 最佳成熟培养质量浓度左旋肉碱对卵母细胞脂肪代谢的影响 采用前期试验筛选的最佳左旋肉碱添加质量浓度, 以添加0 ng/mL作为对照组, 并对猪卵母细胞进行成熟培养. 然后分别收集成熟培养后的卵母细胞, 对其进行脂肪含量检测和脂肪代谢关键酶类的表达检测, 以期明确左旋肉碱对猪卵母细胞脂肪代谢的作用效果和作用途径.

首先, 用油红染色检测猪卵母细胞内脂肪滴的含量. 在各组中随机选择部分具有第一极体的成熟卵母细胞, 放入质量分数为4%多聚甲醛中固定20 min后, 用PVA-DPBS洗3遍. 用油红染色5~6 min后, 用含体积分数为50%乙醇的DPBS过夜洗涤. 第2天, 将卵母细胞放到含适量PVA-DPBS的载玻片上, 盖上盖玻片, 在倒置显微镜下观察并拍照.

然后, 用试剂盒检测卵母细胞的三酰甘油含量. 分别收集300个0和100 ng/mL左旋肉碱处理的成熟卵母细胞, 置于40 μ L含体积分数为1% Triton X-100的PBS中, 4 $^{\circ}$ C裂解40 min, 随后按照Dongou的三酰甘油测定试剂盒(浙江东瓯诊断产品有限公司)说明书

进行操作, 利用酶标仪(BIO RAD-680)测定各样品吸光度, 并计算三酰甘油含量. 试验重复3次.

最后, 用mRNA定量检测成熟卵母细胞中脂肪酶基因(*HSL*)和三酰甘油水解酶基因(*ATGL*)的表达. 分别收集100个0和100 ng/mL左旋肉碱处理的成熟卵母细胞, 按照Tiagen公司的RNAprep pure培养细胞/细菌总RNA提取试剂盒分别抽提这2组卵母细胞的总RNA, 用PrimeScript[®] 1st Strand cDNA Synthesis Kit试剂盒进行反转录, 合成cDNA第1链(40 μ L/管). 取1 μ L cDNA为模板, 以 β -actin为内参, 用实时荧光定量RT-PCR检测试验组与对照组间*HSL*和*ATGL*的mRNA表达水平. 试验均重复3次.

1.2.3 胚胎培养液中添加不同质量浓度左旋肉碱对猪孤雌胚胎体外发育的影响 在猪卵母细胞成熟培养液中不添加左旋肉碱而在早期胚胎体外培养液中添加不同质量浓度(0、10、100、1 000 ng/mL)的左旋肉碱, 通过48 h后胚胎卵裂率、7 d后的囊胚率和囊胚细胞数进行效果评价, 从而筛选出适合胚胎培养的最佳添加质量浓度.

1.2.4 统计分析 所有试验均重复3次以上, 统计数据用平均值 \pm 标准误差表示. 应用SPSS 17.0对试验数据进行单因素方差分析, 以 $P < 0.05$ 作为统计差异显著的标准.

2 结果与分析

2.1 在成熟培养液中添加不同质量浓度的左旋肉碱对猪卵母细胞的影响

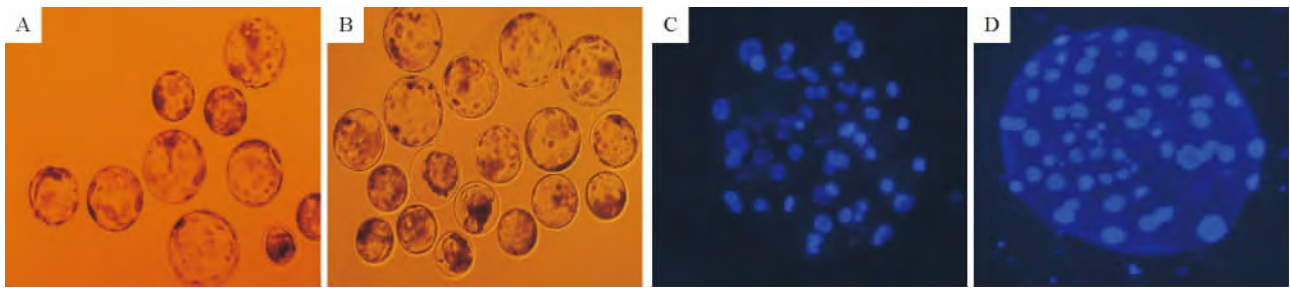
由表2可看出, 与对照组及1 000 ng/mL组对比, 添加100 ng/mL左旋肉碱可以显著提高卵母细胞的体外成熟率($P < 0.05$). 而在成熟液中添加左旋肉碱对卵裂率的影响不显著($P > 0.05$), 但以添加100 ng/mL组的最高, 并且其囊胚率和囊胚细胞数均较高(表2, 图1). 由此可以认为添加一定质量浓度的左旋肉碱能够提高卵母细胞的成熟率, 最佳的添加质量浓度为100 ng/mL.

表2 不同质量浓度左旋肉碱对猪卵母细胞体外成熟和孤雌激活胚胎发育的影响¹⁾

Tab. 2 Effects of different mass concentrations of L-carnitine on porcine oocytes maturation and PA embryos development *in vitro*

ρ (左旋肉碱) / (ng \cdot mL ⁻¹)	总卵数 / 枚	卵母细胞 成熟率 / %	电激卵数 / 枚	卵裂率 / %	囊胚率 / %	囊胚细 胞数 / 枚
0(对照)	193	56.65 \pm 1.68a	178	73.02 \pm 4.78a	17.60 \pm 4.44ab	33.67 \pm 11.79a
10	199	63.13 \pm 3.30ab	177	68.32 \pm 3.97a	21.35 \pm 6.22ab	43.67 \pm 9.94a
100	200	69.76 \pm 2.31b	188	77.37 \pm 4.11a	29.15 \pm 4.22b	40.33 \pm 3.71a
1 000	204	56.60 \pm 3.27a	189	66.05 \pm 5.70a	13.06 \pm 2.73a	27.67 \pm 6.69a

1) 同列数据后, 凡有一个相同小写字母者, 表示差异不显著($P > 0.05$, Duncan's 法).



A: 添加 0 ng/mL 左旋肉碱的囊胚 (100 ×); B: 添加 100 ng/mL 左旋肉碱的囊胚 (100 ×); C: 添加 0 ng/mL 左旋肉碱的囊胚细胞数 (200 ×); D: 添加 100 ng/mL 左旋肉碱的囊胚细胞数 (200 ×).

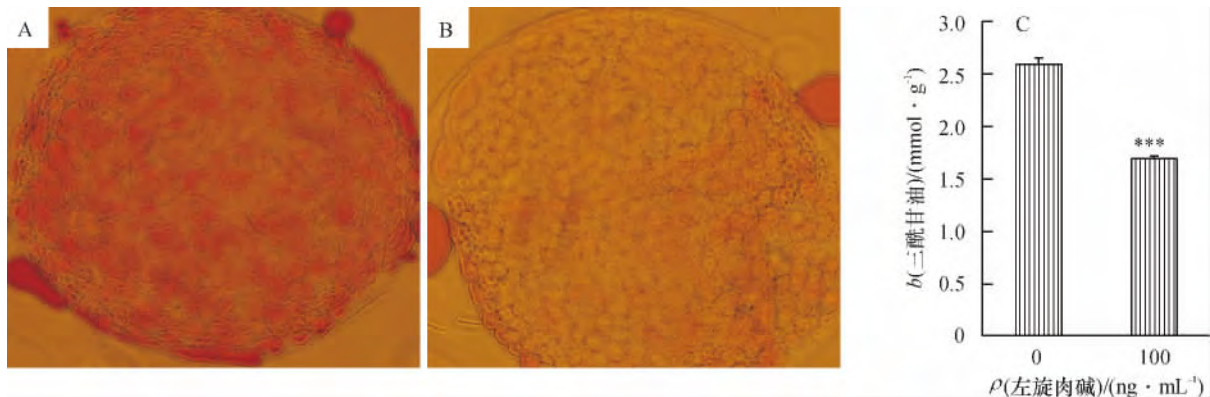
图1 成熟液中添加左旋肉碱对猪孤雌胚胎发育和囊胚质量的影响

Fig.1 The influence of blastocysts quality and developmental ability of PA embryos derived from IVM medium supplemented with *L*-carnitine

2.2 成熟后卵母细胞中脂肪含量和三酰甘油含量检测

如图2所示,通过比较油红O染色后卵母细胞的颜色发现,添加 100 ng/mL 左旋肉碱试验组的卵母细胞着色明显较浅,表明其脂肪含量相对较低。进一步对 0

和 100 ng/mL 组的成熟卵母细胞中三酰甘油含量进行检测,发现添加 100 ng/mL 左旋肉碱极显著降低了卵母细胞中三酰甘油的含量(图2),与油红O染色结果相一致,表明左旋肉碱能够促进三酰甘油分解,具有促进猪卵母细胞脂肪代谢的作用。



A: 添加 0 ng/mL 左旋肉碱的卵母细胞 (200 ×); B: 添加 100 ng/mL 左旋肉碱的卵母细胞 (200 ×); C: 卵母细胞中三酰甘油含量 (***) 表示在 0.001 水平上差异显著, Duncan's 法)。

图2 成熟后的猪卵母细胞油红O染色和三酰甘油含量检测

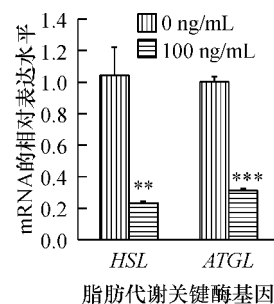
Fig.2 Fat staining by oil red O and triglycerides content detection of mature oocytes

2.3 左旋肉碱对猪卵母细胞中脂肪代谢关键酶 HSL 和 ATGL mRNA 表达水平的影响

实时荧光定量结果显示(图3),在成熟液中添加 100 ng/mL 的左旋肉碱后,其成熟卵母细胞中 HSL 和 ATGL 基因的 mRNA 表达水平均显著地低于对照组(0 ng/mL)。

2.4 在胚胎培养液中添加不同质量浓度的左旋肉碱对猪卵母细胞的影响

如表3所示,在胚胎培养液中添加一定质量浓度的左旋肉碱具有显著提高猪孤雌胚胎卵裂率的作用($P < 0.05$),且以添加 100 ng/mL 组的卵裂率和囊胚率最高。添加 10 ng/mL 左旋肉碱组的囊胚细胞数最多,但统计分析差异不显著($P > 0.05$)。



“**”表示在 0.01 水平上差异显著,“***”表示在 0.001 水平上差异显著(Duncan's 法)。

图3 左旋肉碱对猪卵母细胞 HSL 和 ATGL 基因 mRNA 表达水平的影响

Fig.3 Effects of *L*-carnitine supplementation on HSL and ATGL mRNA expression levels of porcine oocytes

表3 胚胎培养液中不同质量浓度左旋肉碱对猪孤雌激活后胚胎发育能力的影响¹⁾Tab.3 Effects of different concentrations of *L*-carnitine in embryo culture medium on porcine PA embryo development

ρ (左旋肉碱) / (ng · mL ⁻¹)	孤雌 胚数/枚	卵裂率/%	囊胚率/%	囊胚细胞数/枚
0	161	78.75 ± 1.88a	29.14 ± 8.70a	44.97 ± 3.19a
10	129	91.80 ± 2.16c	30.33 ± 4.44a	50.58 ± 2.18a
100	155	92.92 ± 1.23c	37.38 ± 5.66a	46.86 ± 0.69a
1 000	174	85.19 ± 0.44b	27.55 ± 6.37a	44.19 ± 2.10a

1) 同列数据后,凡有一个相同小写字母者,表示差异不显著($P > 0.05$, Duncan's 法)。

3 讨论与结论

研究发现,左旋肉碱为卵母细胞和胚胎利用脂肪酸提供了必不可少的辅助因子,在卵母细胞体外成熟和早期胚胎发育中加入时可以提高胚胎的产出^[5]。同时, Lonergan 等^[9]认为胚胎的发育能力是判定卵母细胞质量的指标, Soom 等^[10]认为囊胚内细胞数多少表明了胚胎的发育能力强弱。本试验通过在成熟液(或胚胎培养液)中添加不同质量浓度的左旋肉碱,发现左旋肉碱能够显著提高猪卵母细胞的体外成熟率、脂肪代谢以及孤雌激活卵裂率,并有助于提高猪孤雌激活胚胎的囊胚发育率和囊胚质量。

目前文献报道关于左旋肉碱对猪卵母细胞成熟培养和胚胎发育的影响浓度各不相同。Wu 等^[8]发现,在成熟液中添加不同质量浓度(0、0.25、0.50、1.00 mg/mL)的左旋肉碱对于成熟率影响不显著,添加 0.50 mg/mL 左旋肉碱显著提高囊胚率和减少囊胚细胞死亡数;而在胚胎培养液中添加不同质量浓度(0、0.25、0.50、1.00、2.00 mg/mL)的左旋肉碱对于猪孤雌胚胎卵裂率和细胞数目无显著影响。Somfai 等^[4]研究发现,在成熟液中添加质量浓度 0.6 ~ 5.0 mg/mL 的左旋肉碱可以显著提高卵母细胞的成熟率和卵裂率,但对于其囊胚率无显著性影响。而本研究发现,在成熟液中添加 100 ng/mL 左旋肉碱能够显著地提高猪卵母细胞的成熟率,但对于其卵裂率和囊胚率却没有显著影响;在胚胎培养液中添加 10、100 和 1 000 ng/mL 的左旋肉碱能显著地提高猪孤雌胚胎卵裂,添加不同质量浓度左旋肉碱对于猪囊胚的发育没有显著性影响。产生这种差异的原因可能是基础培养体系的不同造成的。

此外,本研究发现,左旋肉碱可以显著降低成熟猪卵母细胞中三酰甘油的含量。已有大量的研究证明左旋肉碱能够提高线粒体活力,通过增加 β -氧化作用来提高卵母细胞和胚胎的发育^[4-5]。左旋肉碱主要是在肉碱脂酰转移酶 I 的作用下,其 3-羟

基与脂酰 CoA 的酰基结合生成脂酰肉碱,随后在移位酶的作用下从细胞质进入到线粒体内部。在线粒体内部,肉碱脂酰基转移酶 II 催化其分开,重新形成的脂酰 CoA 可不断进行 β -氧化,进而促进脂肪代谢^[11]。脂肪的主要成分是三酰甘油,ATGL 只水解三酰甘油,对甘油二酯不起作用,而 HSL 水解甘油二酯的活性是三酰甘油的 10 倍^[12-13],因而三酰甘油水解的起始受 ATGL 限速。其主要过程是 ATGL 特异性地将三酰甘油分解为甘油二酯,产物进而被 HSL 水解为甘油一酯,随后在甘油一酯酶的作用下形成甘油和脂肪酸^[14]。本研究发现,在成熟培养液中添加 100 ng/mL 左旋肉碱,在降低猪成熟卵母细胞中三酰甘油含量的同时也显著降低了 HSL 和 ATGL 基因的 mRNA 表达水平,表明左旋肉碱促进三酰甘油代谢的作用并非是通过 HSL 和 ATGL 基因 mRNA 表达水平的升高实现的。据李玉成^[15]报道,脂肪细胞 ATGL 基因 mRNA 表达水平的升高并不伴随着 ATGL 表达蛋白的升高。本研究通过油红染色发现,在成熟液中添加左旋肉碱可以促进猪卵母细胞的脂肪代谢,从而影响卵母细胞的质量和胚胎发育能力,但其具体作用机制仍需要进一步研究。

参考文献:

- [1] 闫益波,吕善潮,叶绍辉. 猪卵母细胞体外成熟培养的主要影响因素[J]. 浙江畜牧兽医, 2007(6): 8-9.
- [2] 刘晓辉,曹阳,郎洪彦,等. 培养液对猪卵母细胞体外成熟及孤雌胚胎早期体外发育的影响[J]. 安徽农业科学, 2011(20): 12229-12230.
- [3] 徐小明,杨春荣,胡军和,等. 猪卵母细胞体外成熟及电激活后发育能力的研究[J]. 自然科学进展, 2006(3): 361-364.
- [4] SOMFAI T, KANEDA M, AKAGI S, et al. Enhancement of lipid metabolism with *L*-carnitine during *in vitro* maturation improves nuclear maturation and cleavage ability of follicular porcine oocytes[J]. Reprod Fertil Dev, 2011, 23(7): 912-920.

(下转第 18 页)

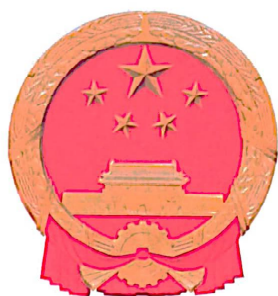
- tion, tissue distribution, metabolism and excretion of ormetoprim and sulphadimethoxine in Atlantic salmon (*Salmo salar*) after intravenous and oral administration of Romet³⁰ [J]. *Xenobiotics*, 1995, 25(11): 1169-1180.
- [17] 袁科平, 艾晓辉. 磺胺甲噁唑在罗非鱼体内的药代动力学及组织浓度研究[J]. *水利渔业*, 2008, 28(3): 25-27.
- [18] 孙玉增, 刘慧慧, 秦华伟, 等. 磺胺甲基异唑在大菱鲆体内的代谢动力学研究[J]. *渔业科学进展*, 2009, 30(11): 42-44.
- [19] 任利强, 王茂剑, 宫向红, 等. 磺胺甲噁唑在黑鲈肌肉中药代动力学及残留研究[J]. *海洋湖沼通报*, 2009(4): 143-145.
- [20] 范能全. 磺胺二甲嘧啶在鲫鱼体内的药代动力学研究[J]. *重庆师范大学学报: 自然科学版*, 2010, 27(3): 23-26.
- [21] 贺艳辉, 张红燕, 龚赞翀, 等. 我国罗非鱼养殖品种及养殖发展分析[J]. *水产养殖*, 2009(2): 12-13.
- [22] BAERT K, DE BAERE S, CROUBELS S, et al. Pharmacokinetics and oral bioavailability of sulfadiazine and trimethoprim in broiler chickens [J]. *Vet Res Commun*, 2003, 27: 301-309.
- [23] 艾晓辉, 刘长征, 周运涛. 不同水温和给药方式下磺胺甲噁唑在草鱼体内的药代动力学研究[J]. *水生生物学报*, 2005, 29(2): 210-214.
- [24] 林茂, 陈郑强, 纪荣兴, 等. 不同温度下氟苯尼考在鳊体内药代动力学比较[J]. *上海海洋大学学报*, 2013, 22(2): 226-230.
- [25] 祝艳蕾. 不同温度下麻保沙星在鲫鱼体内药物动力学及残留研究[D]. 武汉: 华中农业大学, 2008.
- [26] 李晶. 不同温度下芬苯达唑及其代谢产物在鲫鱼体内的药物动力学及残留研究[D]. 武汉: 华中农业大学, 2010.
- [27] 刘昌孝. 实用药物动力学[M]. 北京: 中国科技出版社, 2003: 7-10.
- [28] BUSHBY S R. Sulfonamide and trimethoprim combinations [J]. *J Am Vet Med Assoc*, 1980, 176(15): 1049-1053.
- [29] BATZIAS G, DELIS G, KOUTSOVITI-PAPADOPOULOU M. Bioavailability and pharmacokinetics of sulfadiazine, N4-acetyl sulfadiazine and trimethoprim following intravenous and intramuscular administration of a sulfadiazine/trimethoprim combination in sheep [J]. *Vete Res Commun*, 2005, 29(8): 699-712.
- [30] ABU-BASHA E A, GEHRING R, HANTASH T M, et al. Pharmacokinetics and bioavailability of sulfadiazine and trimethoprim following intravenous, intramuscular and oral administration in ostriches (*Struthio camelus*) [J]. *J Vet Pharmacol Ther*, 2009, 32(3): 258-263.
- [31] VAN DUIJKEREN E, ENSINK J M, MEIJER L A. Distribution of orally administered trimethoprim and sulfadiazine into noninfected subcutaneous tissue chambers in adult ponies [J]. *J Vet Pharmacol Ther*, 2002, 25(4): 273-277.
- [32] 林丽聪, 樊海平, 廖碧钗, 等. 磺胺嘧啶在欧洲鳊体内药代动力学研究[J]. *检验检疫学刊*, 2010, 20(4): 14-17.

【责任编辑 柴 焰】

(上接第12页)

- [5] DUNNING K R, ROBKER R L. Promoting lipid utilization with L-carnitine to improve oocyte quality [J]. *Anim Reprod Sci*, 2012, 134(1/2): 69-75.
- [6] 吴国权, 贾宝瑜, 李俊杰, 等. L-肉碱对猪卵母细胞体外成熟及孤雌激活早期胚胎发育能力的影响[C]//朱士恩, 冯建忠. 中国畜牧兽医学动物繁殖学分会第十五届学术研讨会论文集: 上册. 天津: 中国农业大学动物科技学院, 2010: 21-24.
- [7] 王玉萍, 谭训刚, 李翔太, 等. 肉碱的生理功能及其应用前景[J]. *生物技术通讯*, 2000(1): 65-67.
- [8] WU Guoquan, JIA Baoyu, LI Junjie, et al. L-carnitine enhances oocyte maturation and development of parthenogenetic embryos in pigs [J]. *Theriogenology*, 2011, 76(5): 785-793.
- [9] LONERGAN P, RIZOS D, GUTIERREZ-ADAN A, et al. Oocyte and embryo quality: Effect of origin, culture conditions and gene expression patterns [J]. *Reprod Domest Anim*, 2003, 38(4): 259-267.
- [10] VAN SOOM A, BOERJAN M L, BOLS P E, et al. Timing of compaction and inner cell allocation in bovine embryos produced *in vivo* after superovulation [J]. *Biol Reprod*, 1997, 57(5): 1041-1049.
- [11] 吕志伟, 马云霞, 孙泽. 脂肪代谢的调节因素及运动对脂肪代谢的影响[J]. *伊犁师范学院学报: 自然科学版*, 2010(1): 56-60.
- [12] HAEMMERLE G, ZIMMERMANN R, HAYN M, et al. Hormone-sensitive lipase deficiency in mice causes diglyceride accumulation in adipose tissue, muscle, and testis [J]. *J Biol Chem*, 2002, 277(7): 4806-4815.
- [13] ALI Y B, CARRIERE F, VERGER R, et al. Continuous monitoring of cholesterol oleate hydrolysis by hormone-sensitive lipase and other cholesterol esterases [J]. *J Lipid Res*, 2005, 46(5): 994-1000.
- [14] ZECHNER R, STRAUSS J G, HAEMMERLE G, et al. Lipolysis: Pathway under construction [J]. *Curr Opin Lipidol*, 2005, 16(3): 333-340.
- [15] 李玉成. ATGL 在 Leptin 介导脂解过程中的表达调控及其机理研究[D]. 杨凌: 西北农林科技大学, 2008.

【责任编辑 柴 焰】



广东省农业技术推广奖

获奖证书

为表彰在农业技术推广工作中做出贡献
的单位和个人，特颁发此证书，以资鼓励。

获奖项目：公猪高效繁育关键技术创新与推广应用

奖励等级：二等奖

奖励个人：卫恒习

奖励日期：2022年12月15日

证书号：2021-2-X12-R02





广东省农业技术推广奖

获奖证书

为表彰在农业技术推广工作中做出贡献
的单位和个人，特颁发此证书，以资鼓励。

获奖项目：种猪高效繁育关键技术创新与推广应用

奖励等级：二等奖

奖励个人：卫恒习

奖励日期：2023年12月21日

证书号：2022-2-X08-R03



证书号第7567819号



专利公告信息

发明专利证书

发明名称：一种鸡精液冷冻组合物、冷冻方法及去甘油方法

专利权人：华南农业大学;广东省农业科学院动物科学研究所

地址：510642 广东省广州市天河区五山路483号

发明人：卫恒习;方婷婷;邹娴;张守全;罗成龙;李莉

专利号：ZL 2024 1 1203811.1

授权公告号：CN 118716335 B

专利申请日：2024年08月30日

授权公告日：2024年11月29日

申请日时申请人：华南农业大学;广东省农业科学院动物科学研究所

申请日时发明人：卫恒习;方婷婷;邹娴;张守全;罗成龙;李莉

国家知识产权局依照中华人民共和国专利法进行审查，决定授予专利权，并予以公告。
专利权自授权公告之日起生效。专利权有效性及专利权人变更等法律信息以专利登记簿记载为准。

局长
申长雨

申长雨

2024年11月29日

证书号第 3717751 号



发明专利证书

发明名称：一种选育高繁殖性能种公猪的方法

发明人：卫恒习;张守全;陈预明;刘艳婷;高凤磊;李莉;孟立

专利号：ZL 2018 1 0614804.9

专利申请日：2018 年 06 月 14 日

专利权人：华南农业大学

地址：510642 广东省广州市天河区五山路 483 号

授权公告日：2020 年 03 月 17 日

授权公告号：CN 108835031 B

国家知识产权局依照中华人民共和国专利法进行审查，决定授予专利权，颁发发明专利证书并在专利登记簿上予以登记。专利权自授权公告之日起生效。专利权期限为二十年，自申请日起算。

专利证书记载专利权登记时的法律状况。专利权的转移、质押、无效、终止、恢复和专利权人的姓名或名称、国籍、地址变更等事项记载在专利登记簿上。



局长

申长雨

申长雨

2020 年 03 月 17 日

证书号 第 3717751 号

专利权人应当依照专利法及其实施细则规定缴纳年费。本专利的年费应当在每年 06 月 14 日前缴纳。未按照规定缴纳年费的，专利权自应当缴纳年费期满之日起终止。

申请日时本专利记载的申请人、发明人信息如下：

申请人：

华南农业大学

发明人：

卫恒习；张守全；陈预明；刘艳婷；高凤磊；李莉；孟立

证书号第 3870195 号



发明专利证书

发明名称：一种与种公猪繁殖性能密切相关的精子蛋白标记 IZUM02 及其应用

发明人：卫恒习;刘艳婷;高凤磊;张守全;李莉

专利号：ZL 2018 1 0614803.4

专利申请日：2018 年 06 月 14 日

专利权人：华南农业大学

地址：510642 广东省广州市天河区五山路 483 号

授权公告日：2020 年 07 月 03 日

授权公告号：CN 108840919 B

国家知识产权局依照中华人民共和国专利法进行审查，决定授予专利权，颁发发明专利证书并在专利登记簿上予以登记。专利权自授权公告之日起生效。专利权期限为二十年，自申请日起算。

专利证书记载专利权登记时的法律状况。专利权的转移、质押、无效、终止、恢复和专利权人的姓名或名称、国籍、地址变更等事项记载在专利登记簿上。



局长
申长雨

申长雨

2020 年 07 月 03 日

证书号第 3870195 号

专利权人应当依照专利法及其实施细则规定缴纳年费。本专利的年费应当在每年 06 月 14 日前缴纳。未按照规定缴纳年费的，专利权自应当缴纳年费期满之日起终止。

申请日时本专利记载的申请人、发明人信息如下：

申请人：

华南农业大学

发明人：

卫恒习；刘艳婷；高凤磊；张守全；李莉

证书号第 4447408 号



发明专利证书

发明名称：一种与种公猪繁殖性能密切相关的精子蛋白标记 SPACA4 及其应用

发明人：卫恒习;刘艳婷;高凤磊;张守全;孟立;李莉

专利号：ZL 2018 1 0613485. X

专利申请日：2018 年 06 月 14 日

专利权人：华南农业大学

地址：510642 广东省广州市天河区五山路 483 号

授权公告日：2021 年 05 月 28 日

授权公告号：CN 108872588 B

国家知识产权局依照中华人民共和国专利法进行审查，决定授予专利权，颁发发明专利证书并在专利登记簿上予以登记。专利权自授权公告之日起生效。专利权期限为二十年，自申请日起算。

专利证书记载专利权登记时的法律状况。专利权的转移、质押、无效、终止、恢复和专利权人的姓名或名称、国籍、地址变更等事项记载在专利登记簿上。



局长
申长雨

申长雨

2021 年 05 月 28 日

证书号 第 4447408 号

专利权人应当依照专利法及其实施细则规定缴纳年费。本专利的年费应当在每年 06 月 14 日前缴纳。未按照规定缴纳年费的，专利权自应当缴纳年费期满之日起终止。

申请日时本专利记载的申请人、发明人信息如下：

申请人：

华南农业大学

发明人：

卫恒习；刘艳婷；高凤磊；张守全；孟立；李莉

证书号第 8742650 号



实用新型专利证书

实用新型名称：一次性便携式抽卵仪

发 明 人：卫恒习;李笑艳;陶剑;张守全;孟立;李莉

专 利 号：ZL 2018 2 1004234.3

专利申请日：2018 年 06 月 27 日

专 利 权 人：华南农业大学

地 址：510642 广东省广州市天河区五山路 483 号

授权公告日：2019 年 04 月 19 日

授权公告号：CN 208762502 U

国家知识产权局依照中华人民共和国专利法经过初步审查，决定授予专利权，颁发实用新型专利证书并在专利登记簿上予以登记。专利权自授权公告之日起生效。专利权期限为十年，自申请日起算。

专利证书记载专利权登记时的法律状况。专利权的转移、质押、无效、终止、恢复和专利权人的姓名或名称、国籍、地址变更等事项记载在专利登记簿上。



局长
申长雨

申长雨



第 1 页 (共 2 页)

第 292 页，共 307 页

其他事项参见背面



证书号第8742650号



专利权人应当依照专利法及其实施细则规定缴纳年费。本专利的年费应当在每年06月27日前缴纳。未按照规定缴纳年费的，专利权自应当缴纳年费期满之日起终止。

申请日时本专利记载的申请人、发明人信息如下：

申请人：

华南农业大学

发明人：

卫恒习；李笑艳；陶剑；张守全；孟立；李莉

证书号第 3914545 号



发明专利证书

发明名称：一种畜禽场专用的驱蚊抑菌熏香

发明人：陶剑;张德隆;张守全;卫恒习;李莉;孟立

专利号：ZL 2018 1 0233344.5

专利申请日：2018 年 03 月 21 日

专利权人：华南农业大学

地址：510642 广东省广州市天河区五山路 483 号

授权公告日：2020 年 07 月 31 日

授权公告号：CN 108684739 B

国家知识产权局依照中华人民共和国专利法进行审查，决定授予专利权，颁发发明专利证书并在专利登记簿上予以登记。专利权自授权公告之日起生效。专利权期限为二十年，自申请日起算。

专利证书记载专利权登记时的法律状况。专利权的转移、质押、无效、终止、恢复和专利权人的姓名或名称、国籍、地址变更等事项记载在专利登记簿上。



局长
申长雨

申长雨

2020 年 07 月 31 日

证书号第 3914545 号

专利权人应当依照专利法及其实施细则规定缴纳年费。本专利的年费应当在每年 03 月 21 日前缴纳。未按照规定缴纳年费的，专利权自应当缴纳年费期满之日起终止。

申请日时本专利记载的申请人、发明人信息如下：

申请人：

华南农业大学

发明人：

陶剑；张德隆；张守全；卫恒习；李莉；孟立

证书号第 3106939 号



发明专利证书

发明名称：一种评定大白公猪受精能力的数学模型的建立方法

发明人：张守全；陈志林；冯美莹；卫恒习；李莉

专利号：ZL 2015 1 0431755.1

专利申请日：2015 年 07 月 21 日

专利权人：华南农业大学

地址：510642 广东省广州市天河区华南农业大学动物科学学院
新楼 408 房

授权公告日：2018 年 10 月 12 日

授权公告号：CN 105046083 B

本发明经过本局依照中华人民共和国专利法进行审查，决定授予专利权，颁发本证书并在专利登记簿上予以登记。专利权自授权公告之日起生效。

本专利的专利权期限为二十年，自申请日起算。专利权人应当依照专利法及其实施细则规定缴纳年费。本专利的年费应当在每年 07 月 21 日前缴纳。未按照规定缴纳年费的，专利权自应当缴纳年费期满之日起终止。

专利证书记载专利权登记时的法律状况。专利权的转移、质押、无效、终止、恢复和专利权人的姓名或名称、国籍、地址变更等事项记载在专利登记簿上。



局长
申长雨

申长雨



第 1 页 (共 1 页)

证书号第2879463号



发明专利证书

发明名称：一种评定长白公猪受精能力的数学模型及其建立方法

发明人：张守全；陈志林；陈预明；吴俊辉；卫恒习；李莉

专利号：ZL 2015 1 0431752.8

专利申请日：2015年07月21日

专利权人：华南农业大学

授权公告日：2018年04月10日

本发明经过本局依照中华人民共和国专利法进行审查，决定授予专利权，颁发本证书并在专利登记簿上予以登记。专利权自授权公告之日起生效。

本专利的专利权期限为二十年，自申请日起算。专利权人应当依照专利法及其实施细则规定缴纳年费。本专利的年费应当在每年07月21日前缴纳。未按照规定缴纳年费的，专利权自应当缴纳年费期满之日起终止。

专利书记载专利权登记时的法律状况。专利权的转移、质押、无效、终止、恢复和专利权人的姓名或名称、国籍、地址变更等事项记载在专利登记簿上。



局长
申长雨

申长雨



第1页(共1页)

第297页，共307页

证书号第 2995484 号



发明专利证书

发明名称：一种评定杜洛克公猪受精能力的数学模型及其建立方法

发明人：张守全;陈志林;张童;卫恒习;李莉

专利号：ZL 2015 1 0431777.8

专利申请日：2015 年 07 月 21 日

专利权人：华南农业大学

地址：510642 广东省广州市天河区华南农业大学动物科学学院
新楼 408 房

授权公告日：2018 年 07 月 10 日

授权公告号：CN 105095690 B

本发明经过本局依照中华人民共和国专利法进行审查，决定授予专利权，颁发本证书并在专利登记簿上予以登记。专利权自授权公告之日起生效。

本专利的专利权期限为二十年，自申请日起算。专利权人应当依照专利法及其实施细则规定缴纳年费。本专利的年费应当在每年 07 月 21 日前缴纳。未按照规定缴纳年费的，专利权自应当缴纳年费期满之日起终止。

专利书记载专利权登记时的法律状况。专利权的转移、质押、无效、终止、恢复和专利权人的姓名或名称、国籍、地址变更等事项记载在专利登记簿上。



局长
申长雨

申长雨



荣誉证书

卫恒习同志：

被评为华南农业大学“教书育人、
管理育人、服务育人”先进个人，特
发此证，以资鼓励。

华南农业大学委员会学
大
学

二〇一四年九月十日

荣誉证书

卫恒习同志：

在华南农业大学2022年“三育人”评选中，
被评为“教书育人”先进个人。

特发此证，以资鼓励。



荣誉证书

卫恒习 同志：

在2023年“七一表彰”中被评为华南农业大学动物科学学院

优秀共产党员

特发此证，以资鼓励。

中国共产党华南农业大学动物科学学院委员会

2023年5月31日



荣誉证书

卫恒习 同志：

被评为华南农业大学动物科学学院 2020 年度
“优秀班主任”。

特发此证，以资鼓励！



华南农业大学动物科学学院

2021 年 1 月 27 日

荣誉证书

卫恒习 同志：

被评为华南农业大学动物科学学院 2020 年度
“服务管理工作先进个人”。

特发此证，以资鼓励！



华南农业大学动物科学学院

2021 年 1 月 27 日

证书

卫恒习 同志：

经中国畜牧兽医学会动物繁殖学分会第十一届理事会选举，
您当选为本届理事会理事，任期四年（2021年至2025年）。

特发此证。



中国畜牧兽医学会动物繁殖学分会

2021年10月23日

河源市农村科技特派员 证书

编号: HYKTP2022052

实施乡村振兴战
略, 不忘初心、牢记使命,
心系群众、扎实肯
干, 努力做出无愧于时
代的业绩。

姓名: 卫恒习

单位: 华南农业大学动物科学学院

服务地区: 河源市

期限: 3年



聘 书
LETTER OF APPOINTMENT

兹聘请 卫恒习 为

广东省草食动物产业联盟
专家委员会特聘专家

广东省草食动物产业联盟
2019年3月16日

荣誉证书

卫恒习同志：

在2020—2021年度《华南农业大学学报》的评优活动中，荣获《华南农业大学学报》优秀审稿人。

特颁此证，以资鼓励

《华南农业大学学报》编辑部

二〇二四年三月